frontiers | Research Topics

Advances and controversies in skull base tumors: Implication for diagnosis, treatment and management

Edited by
Arianna Rustici, Diego Mazzatenta and Carlo Serra

Published in
Frontiers in Oncology
Frontiers in Neurology

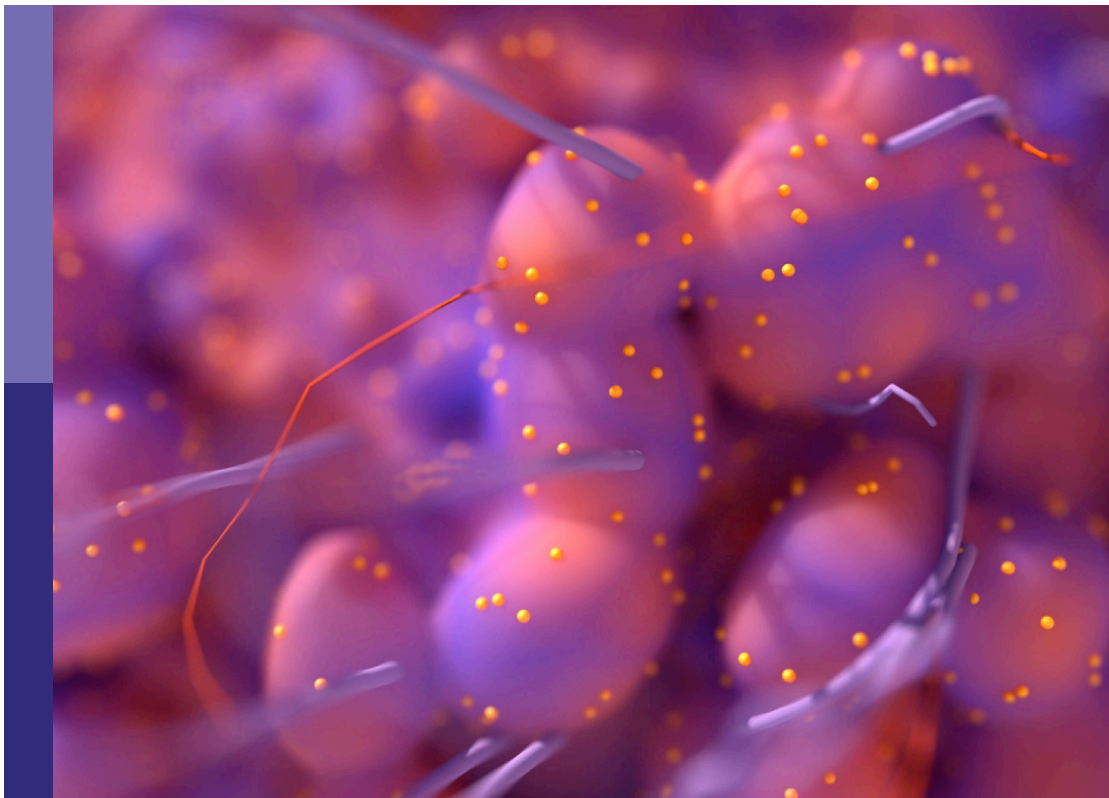

ISSN 1664-8714
ISBN 978-2-8325-4718-2
DOI 10.3389/978-2-8325-4718-2

About Frontiers

Frontiers is more than just an open access publisher of scholarly articles: it is a pioneering approach to the world of academia, radically improving the way scholarly research is managed. The grand vision of Frontiers is a world where all people have an equal opportunity to seek, share and generate knowledge. Frontiers provides immediate and permanent online open access to all its publications, but this alone is not enough to realize our grand goals.

Frontiers journal series

The Frontiers journal series is a multi-tier and interdisciplinary set of open-access, online journals, promising a paradigm shift from the current review, selection and dissemination processes in academic publishing. All Frontiers journals are driven by researchers for researchers; therefore, they constitute a service to the scholarly community. At the same time, the *Frontiers journal series* operates on a revolutionary invention, the tiered publishing system, initially addressing specific communities of scholars, and gradually climbing up to broader public understanding, thus serving the interests of the lay society, too.

Dedication to quality

Each Frontiers article is a landmark of the highest quality, thanks to genuinely collaborative interactions between authors and review editors, who include some of the world's best academicians. Research must be certified by peers before entering a stream of knowledge that may eventually reach the public - and shape society; therefore, Frontiers only applies the most rigorous and unbiased reviews. Frontiers revolutionizes research publishing by freely delivering the most outstanding research, evaluated with no bias from both the academic and social point of view. By applying the most advanced information technologies, Frontiers is catapulting scholarly publishing into a new generation.

What are Frontiers Research Topics?

Frontiers Research Topics are very popular trademarks of the *Frontiers journals series*: they are collections of at least ten articles, all centered on a particular subject. With their unique mix of varied contributions from Original Research to Review Articles, Frontiers Research Topics unify the most influential researchers, the latest key findings and historical advances in a hot research area.

Find out more on how to host your own Frontiers Research Topic or contribute to one as an author by contacting the Frontiers editorial office: frontiersin.org/about/contact

Advances and controversies in skull base tumors: Implication for diagnosis, treatment and management

Topic editors

Arianna Rustici — University of Bologna, Italy

Diego Mazzatenta — IRCCS Institute of Neurological Sciences of Bologna (ISNB), Italy

Carlo Serra — University Hospital Zürich, Switzerland

Citation

Rustici, A., Mazzatenta, D., Serra, C., eds. (2024). *Advances and controversies in skull base tumors: Implication for diagnosis, treatment and management*. Lausanne: Frontiers Media SA. doi: 10.3389/978-2-8325-4718-2

Table of contents

frontiers | Frontiers in Oncology

TYPE Editorial
PUBLISHED 25 March 2024
DOI 10.3389/fonc.2024.1377868

OPEN ACCESS

EDITED AND REVIEWED BY
David D. Eisenstat,
Royal Children's Hospital, Australia

*CORRESPONDENCE
Arianna Rustici
arianna.r87@gmail.com

RECEIVED 28 January 2024
ACCEPTED 04 March 2024
PUBLISHED 25 March 2024

CITATION
Mazzatenta D, Rustici A and Serra C (2024) Editorial: Advances and controversies in skull base tumors: implication for diagnosis, treatment and management.
Front. Oncol. 14:1377868.
doi: 10.3389/fonc.2024.1377868

Editorial: Advances and controversies in skull base tumors: implication for diagnosis, treatment and management

Diego Mazzatenta[1,2], Arianna Rustici[1,3]* and Carlo Serra[4]

[1]Department of Biomedical and Neuromotor Sciences (DIBINEM), University of Bologna, Bologna, Italy, [2]IRCCS Istituto delle Scienze Neurologiche di Bologna, Programma Neurochirurgia Ipofisi – Pituitary Unit, Bologna, Italy, [3]IRCCS Istituto delle Scienze Neurologiche di Bologna, UOSI Neuroradiologia – Ospedale Maggiore, Bologna, Italy, [4]Department of Neurosurgery, Clinical Neuroscience Center, University Hospital Zurich, University of Zurich, Zurich, Switzerland

KEYWORDS

skull base, advances and innovations in skull base, advanced therapies, endoscopic surgery, imaging biomarker, tumor, innovative surgical approaches

Editorial on the Research Topic
Advances and controversies in skull base tumors: implication for diagnosis, treatment and management

The skull base has long been regarded as one of the Pillars of Hercules of neurological pathologies. This is because, in addition to being a difficult surgical site, it is situated on the boundary between the nasal, paranasal, neck regions and the central nervous system. Moreover, it presents a number of vascular-nervous structures that have historically caused diagnostic challenges. In this anatomic region a huge number of pathological processes, including neoplasms ranging in nature from benign to malignant originating from each of the border regions that make up the base of the skull, as well as distant heteroplastic processes can be found.

This Research Topic focused on the Advances and Controversies in Skull Base Tumors: Implication for Diagnosis, Treatment and Management. Out of the 18 articles in this Research Topic, there are 8 original articles, 4 reviews, 2 systematic reviews, 3 case reports, and one opinion-based article.

Common skull base tumor pathologies and biomarkers

Although the most common pathologies are now well recognized, some of them should not be undervalued as they can resemble "common" skull base tumors. This is demonstrated in the publication by Bove et al. Furthermore, Ghezzi et al. showed in their case report that tumors that infrequently metastasize to the skull base region can also involve it, and thus a multidisciplinary team that takes into account both preoperative

imaging and postoperative histopathological findings is required in order to ensure better management for each patient.

Even though a preoperative diagnosis of certainty has not yet been questioned, Wijethilake et al. work offers a thorough summary of the noteworthy advancements in the fields of molecular biology and biochemical markers for skull base tumors. They explain the relationships between the histotypes of skull base tumors and growth-related parameters, such as grade, survival, growth/progression, recurrence, and treatment outcomes.

In another article published in this Research Topic, Righi et al. correlated a new protein mutation with clinicopathological parameters and survival outcomes in a group of poorly differentiated chordomas, which also included possible treatment suggestions.

However, the increasing need to guarantee an excellent outcome for patients has led to the identification of several preoperative biomarkers, some of which involve relatively simple preoperative execution. Takahara et al.'s retrospective series of Schwannomas serves as an example of this. Their study demonstrated a relationship between the preoperative neutrophil/lymphocyte ratio (NLR) and postoperative recurrence as well as treatment-free survival rate.

Current status of skull base surgery for major tumor pathologies

On the other hand, skull base surgery has seen a succession of historical phases, each differentially characterized in terms of objectives, techniques and problems, each inevitably influenced also in a broader perspective by the evolution of society and its needs and expectations, and the neurosurgeon is daily confronted with this challenge.

Where does skull base surgery stand today? Zhang et al. in an interesting review of scientometry on the state of research on meningiomas, indicate what Wang et al., Na et al. and Baussart et al. confirm for us in their clinical studies on the current, we would say consolidated, status of skull base neurosurgery with regard to pathologies of greater epidemiological significance in the neurosurgical field: meningiomas, craniopharyngiomas, pituitary adenomas and schwannomas.

Incorporating patient-specific factors into surgical planning

However, while the clinical studies comfort us and indicate that the possibility of more than satisfactory results can now be considered established in terms of tumor removal and surgical morbidity, Zhang et al. warns us of a change taking place, namely, of the need increasingly felt by both clinicians and, as we shall later see, patients, to try to understand pathology not only in terms of nosologic macrocategories but also in terms of the single, unique and, (exaggerating somewhat), unrepeatable pathology in the individual, and this yes, unrepeatable, patient.

In the case of the scientometry trend, this is expressed in the increasing focus of scientific literature and thus scientific research on more and more detailed molecular characterizations, which is nothing different than a reflection on the progress of medicine toward more and more personalized medicine. In other words, toward a possible future where artificial intelligence will help make sense of the huge amount of data that we are increasingly gathering about patients and patients' pathology.

The trend, however, can be seen in the clinical setting as well: this is now so true, and to such an extent, that neurosurgical practice can and must also be able to respond to n new needs of specific patient populations that are no longer the same as that with which the "noble fathers" of skull base neurosurgery in the 1970s and 1980s were confronted in their time. These are, at least in the Western world, patients who are on average increasingly frail and increasingly concerned with what is called "quality of life". The Tübingen group, on the strength of its experience and undisputed expertise in the microneurosurgery of schwannomas of the VII cranial nerve indicates to us on the one hand that advanced age is not a limitation even in surgeries once considered "high-risk", as vestibular schwannoma surgery might have been (Wang et al.), on the other hand how the focus should now be placed not only on the extent of resection but also if not especially on other indirect health parameters, such as mental health (Machetanz et al.) and obviously, as also suggested by Di Perna et al., on functional outcome. This is also seen, however, in the need to propose solutions, be they purely neurosurgical or interdisciplinary in nature, that can meet the needs of the individual case.

Optimizing surgical outcomes and safety, including endoscopy

Furthermore, current research efforts are also aimed at the optimization of the surgical results and safety during vestibular schwannoma resection. Vychopen et al., by the means of a systematic review, attempt to add evidence to the longstanding discussion of the patient positioning during these procedures, reporting that both the semisitting and the lateral position are safe, with a possible superiority of the first in the functional outcome of facial nerve. Concurrently, Yang et al. report their experience in the endoscopic assistance during microsurgical procedures, with good results. They add further corroborating evidence to this technique, which enhances the surgical view potentially improving the safety of the procedure and, ultimately, of the patient himself.

The endoscope itself could be considered as a cornerstone instrument in skull base neurosurgery. Its widespread diffusion, affordability and flexibility made it irreplaceable. In addition to its well – known use, for example for the management of sellar, parasellar and anterior skull base pathologies or for the exploration of the cerebello – pontine angle (as previously reported by Authors), surgeons and researchers are now pushing the boundaries further. Bai et al. describe in detail for the first time the endoscopic far lateral supracerebellar infratentorial approach,

which was successfully used *in vivo* for the resection of a posterior clinoid meningioma. The same authors complete their report with a systematic review focused on the treatment of this rare pathology. Furthermore, Yan et al. analyze their case series of endoport – assisted neuroendoscopic resection of lateral ventricle tumors. The endoscope will clearly retain its paramount role in skull base surgery, as the enhancement of the surgical view, by the means of advancing the "surgeon's eye" deep in the surgical field, is crucial to navigate and operate in anatomical areas full of delicate vascular and neural structures.

It should also be clear that surgery does not stand alone as the only treatment of skull base pathologies. Radiation therapy, by the means of conventional external beam radiotherapy or particle therapy, as extensively outlined by Iannalfi et al. is complementary to surgery, and should also always discussed in a multidisciplinary setting, with close collaboration between experts different as clearly stated by Carsuzaa et al.

A multidisciplinary management setting is also a key to provide the best treatment for olfactory neuroblastomas. This concept was clearly outlined by Tosoni et al., who extensively review and report the current knowledge and clinical practice concerning this uncommon clinical entity. While surgical resection with established skull base techniques and radiation therapy remains the mainstays of the treatment, the Authors analyze the possible role of chemotherapy protocols, which could be of the utmost importance especially in cases of advanced disease, while advocating also for forward - looking experimentation of targeted therapies basing on molecular profiling.

With the help of this Research Topic and the many articles it includes, one can obtain a comprehensive 360-degree view of the current debates surrounding the diagnosis and management of skull base pathologies. While the current guidelines for treating diseases of the skull base have been reaffirmed in this Research Topic, new developments in biomolecular, diagnostic, and surgical technologies have also been included to enhance patient outcomes. Because of their patient-centered approaches, the articles in this Research Topic provide a foundation for identifying the key areas of future research and development.

Author contributions

DM: Conceptualization, Data curation, Formal analysis, Investigation, Methodology, Project administration, Software, Supervision, Validation, Visualization, Writing – original draft, Writing – review & editing, Funding acquisition, Resources. AR: Conceptualization, Data curation, Formal analysis, Investigation, Methodology, Project administration, Software, Supervision, Validation, Visualization, Writing – original draft, Writing – review & editing. CS: Conceptualization, Data curation, Formal analysis, Investigation, Methodology, Project administration, Software, Supervision, Validation, Visualization, Writing – original draft, Writing – review & editing, Funding acquisition, Resources.

Conflict of interest

The authors declare that the research was conducted in the absence of any commercial or financial relationships that could be construed as a potential conflict of interest.

Publisher's note

frontiers | Frontiers in Oncology

TYPE Systematic Review
PUBLISHED 30 November 2022
DOI 10.3389/fonc.2022.1058329

OPEN ACCESS

EDITED BY
Arianna Rustici,
University of Bologna, Italy

REVIEWED BY
Alessandro Carretta,
University of Bologna, Italy
Kamil Krystkiewicz,
Copernicus Memorial Hospital, Poland
Matteo Zoli,
IRCCS Institute of Neurological Sciences of Bologna (ISNB), Italy

*CORRESPONDENCE
Kyu-Sun Choi
vertex-09@hanmail.net

†These authors have contributed equally to this work and share first authorship

SPECIALTY SECTION
This article was submitted to Neuro-Oncology and Neurosurgical Oncology, a section of the journal Frontiers in Oncology

RECEIVED 30 September 2022
ACCEPTED 02 November 2022
PUBLISHED 30 November 2022

CITATION
Na MK, Jang B, Choi K-S, Lim TH, Kim W, Cho Y, Shin H-G, Ahn C, Kim JG, Lee J, Kwon SM and Lee H (2022) Craniopharyngioma resection by endoscopic endonasal approach versus transcranial approach: A systematic review and meta-analysis of comparative studies.
Front. Oncol. 12:1058329.
doi: 10.3389/fonc.2022.1058329

Craniopharyngioma resection by endoscopic endonasal approach versus transcranial approach: A systematic review and meta-analysis of comparative studies

Min Kyun Na[1†], Bohyoung Jang[2†], Kyu-Sun Choi[1*], Tae Ho Lim[3], Wonhee Kim[4], Youngsuk Cho[4], Hyun-Goo Shin[3], Chiwon Ahn[5], Jae Guk Kim[4], Juncheol Lee[3], Sae Min Kwon[6] and Heekyung Lee[3]

[1]Department of Neurosurgery, College of Medicine, Hanyang University, Seoul, South Korea, [2]Department of Preventive Medicine, College of Korean Medicine, Kyung Hee University, Seoul, South Korea, [3]Department of Emergency Medicine, College of Medicine, Hanyang University, Seoul, South Korea, [4]Department of Emergency Medicine, College of Medicine, Hallym University, Chuncheon, South Korea, [5]Department of Emergency Medicine, College of Medicine, Chung-Ang University, Seoul, South Korea, [6]Department of Neurosurgery, Dongsan Medical Center, Keimyung University School of Medicine, Daegu, South Korea

Introduction: The transcranial approach (TCA) has historically been used to remove craniopharyngiomas. Although the extended endoscopic endonasal approach (EEA) to these tumors has been more commonly accepted in the recent two decades, there is debate over whether this approach leads to better outcomes. The goal of this systematic review and meta-analysis was to more comprehensively understand the benefits and limitations of these two approaches in craniopharyngioma resection based on comparative studies.

Methods: We conducted a systematic literature search in accordance with the Preferred Reporting Items for Systematic reviews and Meta-Analyses recommendations using MEDLINE, EMBASE, and the Cochrane Library. A total of 448 articles were screened. Data were extracted and analyzed using proportional meta-analysis. Eight comparative studies satisfied the inclusion criteria. The extent of resection, visual outcomes, and postoperative complications such as endocrine dysfunction and cerebrospinal fluid (CSF) leakage were compared.

Results and discussion: Eight studies, involving 376 patients, were included. Resection by EEA led to a greater rate of gross total resection (GTR) (odds ratio [OR], 2.42; p = 0.02; seven studies) with an incidence of 61.3% vs. 50.5% and a higher likelihood of visual improvement (OR, 3.22; p < 0.0001; six studies). However, TCA resulted in a higher likelihood of visual deterioration (OR, 3.68; p = 0.002; seven studies), and was related, though not significantly, to panhypopituitarism (OR, 1.39; p = 0.34; eight studies) and diabetes insipidus (OR, 1.14; p = 0.58; seven studies). Although TCA showed significantly lower likelihoods of CSF leakage (OR, 0.26; 95% confidence interval [CI], 0.10–0.71; p = 0.008; eight studies) compared to EEA, there

was no significant difference in meningitis (OR, 0.92; 95% CI, 0.20–4.25; p = 0.91; six studies) between the two approaches. When both approaches can completely resect the tumor, EEA outperforms TCA in terms of GTR rate and visual outcomes, with favorable results in complications other than CSF leakage, such as panhypopituitarism and diabetes insipidus. Although knowledge of and competence in traditional microsurgery and endoscopic surgery are essential in surgical decision-making for craniopharyngioma treatment, when both approaches are feasible, EEA is associated with favorable surgical outcomes.

Systematic review registration: http://www.crd.york.ac.uk/PROSPERO/, identifier CRD42021234801.

KEYWORDS

craniopharyngioma, endoscopic endonasal approach, transcranial approach, metaanalysis, systematic review

1 Introduction

Craniopharyngiomas are calcified embryonic tumors originating from the pituitary gland's anterior lobe, from epithelial remnants of squamous cell rests of Rathke's pouch (1, 2). Although craniopharyngiomas are histologically benign (World Health Organization grade I), their complete resection without neurological injury is challenging due to the tumor location (suprasellar, often superiorly extending into the third ventricle) and their relation to critical neurovascular structures, such as the pituitary gland, hypothalamus, infundibulum, ophthalmological systems, internal carotid artery and its branches, anterior cerebral artery-anterior communicating artery complex, basilar artery and its branches, and brain stem (3, 4). Symptoms are often related to surrounding structural compression or infiltration and may include visual disturbance, especially bitemporal hemianopsia, endocrine dysfunction, headache, and hydrocephalus (5).

The primary aims of treatment include tumor elimination; functional outcomes, such as visual, pituitary, and hypothalamic functions; favorable cognitive outcome; and quality of life. Traditionally, the transcranial approach (TCA) has been used to successfully remove these craniopharyngiomas. TCA procedures include the classical craniotomies such as pterional, orbitozygomatic, bifrontal interhemispheric, unilateral subfrontal, and supraorbital approaches (6). However, these approaches have a higher risk of visual impairment, stroke, and other neurologic complications from brain retraction and neurovascular structure manipulation (7, 8). Recently, it was shown that removing craniopharyngiomas in the retrochiasmatic space that extended superiorly into the third ventricle could be accomplished successfully using the purely extended endoscopic endonasal approach (EEA) through the transplanum transtuberculum corridor. Through a subchiasmatic corridor, this approach provides a wide surgical view and allows direct access to tumors without brain retraction and neurovascular structure manipulation (4). However, TCA has surgical advantages over EEA since it avoids damage to the nasal canal or traversing a contaminated field and provides a larger view of lateral tumor extension. The European Association of Neurosurgical Societies recommended the use of TCA for craniopharyngiomas presenting lateral extensions or that are purely intraventricular, whereas the use of EEA was recommended for purely intrasellar craniopharyngiomas (9).

The approach chosen is determined based on the tumor's location, pathology, consistency, and proximity to the pituitary stalk and optic chiasm; involvement of the third ventricle; history of prior surgeries; and the surgeon's inclination based on experience and feasibility. Although both approaches are expected to remain feasible options for the treatment of craniopharyngiomas based on presentation, a growing number of case-series reports have provided evidence indicating specific surgical complications that are unique to each approach. Although previous meta-analyses have analyzed each approach (10, 11), comparative studies between TCA and EEA on this topic are rare. Comparative studies provide precise clinical descriptions that can be compared in a meta-analysis. To our knowledge, no meta-analysis has dealt with cranipharyngioma outcomes. Thus, the goal of this systematic review and meta-analysis was to collect all currently accessible evidence, including solely comparative studies, and determine whether there are any differences in clinical outcomes between TCA and EEA used to treat craniopharyngiomas.

Abbreviations: CSF, Cerebrospinal fluid; DI, Diabetes insipidus; EEA, Endoscopic endonasal approach; EOR, Extent of resection; GTR, Gross total resection; OR, Odds ratio; OS, Observational studies; PICO, Population, intervention, comparison, and outcome; RE, Random-effects; STR, Sub-total resection; TCA, Transcranial approach.

2 Methods

2.1 Reporting guidelines and protocol registration

The guidelines of the Meta-analysis of Observational Studies in Epidemiology (MOOSE) (12) and the Preferred Reporting Items for Systematic Reviews and Meta-analysis guidelines were used in our investigation (13). The protocol was registered at http://www.crd.york.ac.uk/PROSPERO/ (CRD42021234801).

We developed a question that was based on population, intervention, comparison, and outcome (PICO). We conducted a critical evaluation based on the literature search and compiled the qualifying studies; their results were subsequently analyzed in a meta-analysis. The PICO question was as follows: Do patients with craniopharyngioma (population) treated surgically by EEA (intervention) compared to those treated by TCA (comparator) differ in surgical outcomes (outcome)?

2.2 Search strategy

Two expert reviewers (M. Na and B. Jang) conducted a literature search on July 28, 2020. The search included the MEDLINE and EMBASE databases *via* the Ovid interface, as well as the Cochrane library with no language restriction. Additionally, we manually searched the references of qualified studies to identify relevant research on July 30, 2022.

The following Medical Subject Headings terms were used to search all comparative studies in all logical permutations: "craniopharyngioma," and; "transcranial," or "craniotomy," and "endoscopic," or "endonasal" (Supplementary Table 1). We incorporated all publications that described prospective or retrospective cohort studies that addressed our PICO question.

2.3 Study selection

All studies from the literature search were registered into a reference management software, Endnote X8 (Clarivate Analytics, Philadelphia, United States). Two reviewers (M. Na and B. Jang) separately selected the studies based on predefined selection criteria after checking the title, abstract, and type of each article.

The exclusion criteria were as follows: inappropriate control in comparative studies, < 15 patients in the study, irrelevant results, duplicate data, letters, comments, editorials, case reports, reviews, or meta-analyses, and animal studies. After comparing the title, authors, and year of publication of all studies, we eliminated duplicate articles. On disagreement between the two reviewers, a third reviewer (K. Choi) intervened, and disagreements were debated until a consensus was reached. The full text of eligible publications was obtained after ineligible abstracts were removed and subjected to rigorous screening using the same inclusion and exclusion criteria.

2.4 Data extraction

Two reviewers (M. Na and B. Jang) independently extracted the pertinent patient data from the included studies. Disagreements between the reviewers were discussed till a consensus was reached. The following variables were extracted: the first author's name, country, year of publication, study design, inclusion period, number of patients, type of TCA, tumor size, preoperative symptoms, and operative outcomes (extent of resection [EOR], visual outcome, hormonal outcome, complication outcomes: endocrine disorders, cerebrospinal fluid [CSF] leak, and others).

2.5 Risk of bias in individual studies

The methodological quality of eight selected studies was examined separately by two reviewers (M. Na and B. Jang) who were blinded to the authorship and journal using the Risk of Bias Assessment Tool for Non-randomized Studies (14). Unresolved differences among reviewers were addressed through discussion or review by the third author.

2.6 Statistical analysis

For each relevant outcome, the mean difference and odds ratio (OR) were utilized as summary statistics. The results of interest were described as forest plots; the weighted mean difference or OR, 95% confidence interval (CI), and relative weightings were represented by the middle of the square, horizontal line, and relative size of the square, respectively. A random-effects model was utilized to estimate pooled outcome measures from individual data of included studies. I^2 statistics were used to determine the proportion of discrepancies between studies, with values of 25%, 50%, and 75% deemed as low, moderate, and high, respectively (15).

We used Review Manager version 5.4.1 (Cochrane Collaboration, Oxford, UK) to perform the statistical analysis for both main and sub-group analyses, and a P-value < 0.05 was considered statistically significant. Additionally, meta-regression was performed to analyze the gross total resection (GTR) rate in endocrinologic complication trends using web-r (http://www.web-r.org).

3 Results

3.1 Study selection and characteristics of included studies

Our literature search yielded eight eligible studies. On scanning the database, 447 records were found, and an additional study was identified from another source (Figure 1); 318 studies were assessed for eligibility after 130 duplicates were removed. Following this, 295 studies were eliminated after evaluating both titles and abstracts because of irrelevance to our study, leaving 23 potentially relevant studies. The full-text articles of these 23 studies were then obtained. We excluded 15 studies including systematic reviews (n = 9), those with irrelevant outcomes (n = 3), and non-comparative studies (n = 3), leaving eight studies (376 patients) to be included in the final meta-analysis (3, 4, 16–21).

The eight retrospective observational studies (OS) were published between 2008 and 2020 with an enrollment period that ranged from 2000–2019 (Table 1). All tumor resections were performed in a single institution in all studies. When reported, the overall cohort's mean age was 43.0 years, with a higher proportion of women (52%). The TCA group included a variety of methods, including pterional, orbitozygomatic, supraorbital, subfrontal, and transcallosal approaches. Although the descriptions in each article varied, intrasellar and significant laterally extended lesions were excluded, and tumors amenable to both approaches were included (Table 1). Therefore, we excluded 25 intrasellar tumors in one study (4) to reduce differences in inclusion criteria between the studies. Finally, the total number of patients was 401 and 376 in the systematic review and meta-analysis, respectively. Among 376 patients, 212 (56%) and 164 (44%) were surgically resected using EEA and TCA, respectively (Table 2). The most frequent presenting symptoms were visual disturbance (78%), hypopituitarism (48%), and headache (33%) (Figure 2).

3.2 Extent of resection

EOR was assessed in seven studies. We defined GTR as an event, and EEA demonstrated significantly higher likelihood of GTR (OR, 2.42; 95% CI, 1.13–5.17; p = 0.02; I^2 = 35%). The incidence of GTR was 80/130 (61.5%) and 149/193 (77.2%) in TCA and EEA, respectively (Figure 3).

3.3 Visual outcomes

When compared to TCA, EEA demonstrated significantly higher likelihood of visual improvement (OR, 3.22; CI, 1.87–5.53; p < 0.0001; I^2 = 0%; six studies); the incidence of visual

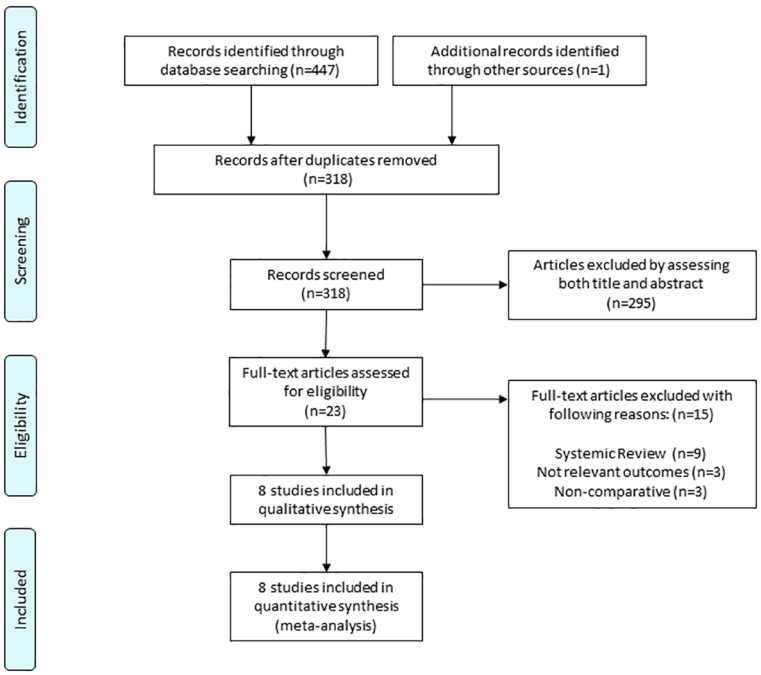

FIGURE 1
Flow diagram of identification of relevant studies.

TABLE 1 Characteristics of studies included in the systemic review.

Author, Year	Country	Study design	Study period	Number of patients	Male	Age (years)	Mean follow-up (months)	Transcranial type	Tumor location (Inclusion/Exclusion)
Fatemi, 2008 (18)	USA	R, 1 institution 1 surgeon	2000 - 2008	22	12	43.6	23.7	Supraorbital	Excluded parasellar lesions deemed unresectable by the endonasal route
Jeswani, 2016 (17)	USA	R, 1 institution NR	2000 - 2013	53	28	45.2	34.6	Bifrontal Pterional OZ transcallosal	Included midline suprasellar/ third ventricular lesions Excluded intrasellar lesions
Moussazadeh, 2016 (3)	USA	R, 1 institution surgeons	2000 - 2015	26	7	50.8	35.2	Pterional	Included suprasellar lesions whose lateral extent does not pass the carotid bifurcation
Wannemuehler, 2016 (16)	USA	R, 1 institution NR	2005 - 2015	21	13	50.1	10.5	Pterional OZ Bifrontal Transcallosal	Included tumors that were amenable to both approaches confirmed by another surgeon Excluded significant lateral extension
Ozgural, 2018 (15)	Austria	R, 1 institution surgeons	2013 - 2017	24	15	32.3	NR	Pterional OZ	Excluded intrasellar lesions
Li, 2018 (19)	China	R, 1 institution 4 surgeons	2011 - 2015	43	23	41.6	8.8	Pterional Supraorbital Subfrontal	Included only if the neurosurgeon confirmed that the tumor was amenable to both EEA and TCA
Marx, 2020 (20)	Germany	R, 1 institution 1 surgeon	2001 - 2018	30	14	41	90.6	Pterional Supraorbital Transcallosal	Excluded intrasellar lesions
*Lei, 2020 (4)	China	R, 1 institution NR	2013 – 2019	182	82	42.3	33	Pterion Subfrontal	*We excluded intrasellar lesions

R, retrospective; EEA, endoscopic endonasal approach; TCA, transcranial approach; OZ, orbitozygomatic; NR, not reported.
*We excluded 25 intrasellar type craniopharyngiomas in quantitative synthesis (meta-analysis) which were resected by EEA alone to reduce differences from inclusion criteria in other studies.

improvement was 34/104 (32.7%) and 108/178 (60.7%) in TCA and EEA, respectively (Figure 4A). When utilizing TCA compared to EEA, there was a significantly higher likelihood of visual deterioration (OR, 3.68; CI, 1.60–8.49; p = 0.002; I^2 = 0%; seven studies), with an incidence of 20/138 (14.5%) and 9/195 (4.6%) in TCA and EEA, respectively (Figure 4B).

3.4 Surgical complications

3.4.1 Endocrine disorders

There was no significant difference between TCA and EEA with respect to panhypopituitarism (OR, 1.37; 95% CI, 0.56–3.33; p = 0.49; I^2 = 46%; six studies), with an incidence of 55/103 (53.4%) and 43/94 (45.7%), respectively. In terms of diabetes insipidus (DI), there was no significant difference between TCA and EEA (OR, 1.18; 95% CI, 0.74–1.89; p = 0.48; I^2 = 0; six studies), with an incidence of 71/147 (48.3%) and 73/183 (39.9%), respectively (Figure 5).

3.4.2 CSF leakage and meningitis

When compared to EEA, TCA demonstrated a significantly lower likelihood of CSF leakage (OR, 0.26; 95% CI, 0.10–0.71; p = 0.008; I^2 = 0%; eight studies), with an incidence of 2/164 (1.2%) and 21/212 (9.9%) in TCA and EEA, respectively (Figure 5). When EEA patients were divided into two groups according to the start date of the study period, the CSF leakage rate was reduced from 16.7% (14/84, five studies) before 2010 to 5.5% (7/128, three studies) after 2010 (Supplementary Figure 1). In terms of meningitis, there was no significant difference between TCA and EEA (OR, 0.92; 95% CI, 0.20–4.25; p = 0.91; I^2 = 15%; six studies), with an incidence of 3/94 (3.2%) and 4/101 (4.0%), respectively (Figure 5).

3.5 Meta-regression analysis: Relationship between GTR and occurrence of endocrine disorders

Compared to EEA, TCA showed higher linear association between GTR and occurrence of panhypopituitarism (slope, 0.98; p = 0.048 vs. slope, 0.4; p=0.062) (Figure 6A). There was a linear association between GTR and occurrence of DI in TCA (slope, 0.69; p = 0.059), whereas an inverse association between GTR and occurrence of DI in EEA (slope, -0.12; p = 0.734) was observed (Figure 6B)

10.3389/fonc.2022.1058329

TABLE 2 Tumor size, pathology, and extent of resection in patients with craniopharyngioma.

.	Approach	Number of patients	Size		Extent of resection			Pathology		
			Volume, cm^3 mean (SD)	Length, mm mean (SD)	GTR, n (%)	NTR, n (%)	STR, n (%)	Adamantinomatous, n (%)	Papillary, n (%)	Mixed, n (%)
Fatemi, 2008 (18)	TCA	4	–	32 (14)	0	2	2	–	–	–
	EEA	18	–	31 (15)	3	9	6	–	–	–
Jeswani, 2016 (17)	TCA	34	9.5 (11.6)	–	–	–	–	23	9	2
	EEA	19	9 (9.8)	–	–	–	–	11	5	3
Moussazadeh, 2016 (3)	TCA	5	13.9 (7.8)	–	2	3	0	3	0	2
	EEA	21	8.5 (5.9)	–	19	2	0	7	3	11
Wannemuehler, 2016 (16)	TCA	12	7.8 (5)	–	7	0	5	11	1	0
	EEA	9	4.6 (4.7)	–	5	0	4	6	2	1
Ozgural, 2018 (15)	TCA	13	37.9 (22.4)		4	1	8	–	–	–
	EEA	11	24.6 (17.9)		9	0	2	–	–	–
Li, 2018 (19)	TCA	26	–	29.5 (9.5)	17	0	9	11	11	4
	EEA	17	–	25.2 (8.3)	11	0	6	6	8	3
Marx, 2020 (20)	TCA	13		–	43	11	3	–	–	–
	EEA	17	–	–	92	7	1	–	–	–
*Lei, 2020 (4)	TCA	57	–	–	7	0	6	–	–	–
	EEA	100	–	–	10	0	7	–	–	–

GTR, gross total resection; NTR, near total resection; STR, sub-total resection; TCA, transcranial approach; EEA, endoscopic endonasal approach; SD, standard deviation.

3.6 Risk of bias of the included studies

Using the Risk of Bias Assessment Tool for Non-randomized Studies system, the eight OS showed a low risk of bias in intervention measurement and blinding of outcome assessment and a high risk of bias in the selection of participants and confounding variables (Supplementary Figure S2A). Incomplete outcome data and selective outcome reporting were high risks of bias in two (20, 21) and four studies (Supplementary Figure S2B) (4, 16, 20, 21), respectively.

4 Discussion

This systematic review and meta-analysis examined surgical outcomes of craniopharyngiomas treated with EEA and TCA. To the best of our knowledge, this is the first meta-analysis providing direct comparison based on comparative studies. We found that compared to TCA, EEA showed favorable EOR and visual outcomes. EEA also showed less likelihood of endocrine disorders, although this was not statistically significant. Compared to EEA, TCA showed less likelihood of CSF

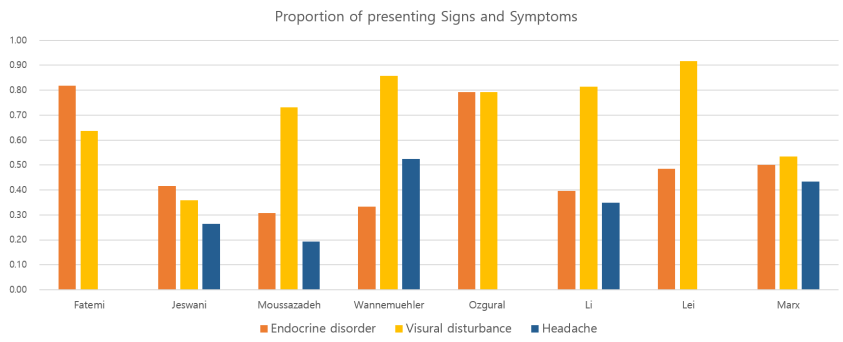

FIGURE 2
Bar plots representing the proportion of signs and symptoms in patients with craniopharyngioma in the included studies.

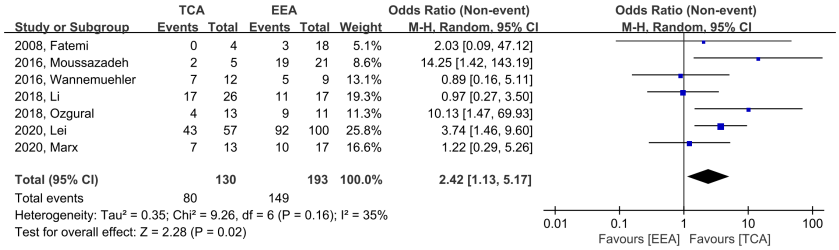

FIGURE 3
Forest plot comparing odd ratios (ORs) of extent of resection following TCA vs. EEA in craniopharyngioma patients. TCA, transcranial approach; EEA, endoscopic endonasal approach; CI, confidence interval; SD, standard deviation.

leakage, while the occurrence of meningitis was not significantly different between the approaches. These results suggest that when both approaches are feasible, EEA has favorable surgical outcomes.

Currently, the optimal management for treating patients with craniopharyngioma is controversial. GTR of craniopharyngioma was formerly considered to be challenging due to perioperative complications; therefore, sub-total resection (STR) followed by adjuvant radiotherapy was deemed as an alternative treatment option (7, 22). Although STR followed by adjuvant radiotherapy and GTR had comparable disease control rates, long-term complications after radiotherapy, such as hypopituitarism and cognitive impairment, have emerged (23). As a result, surgery remains the mainstay of treatment and offers radical resection, which maximizes the possibility of oncological cure (6, 8, 24, 25). The ability to accomplish GTR is an important factor in deciding surgical approaches. Liu et al. (6) emphasized the importance of a tailored approach for individual patients depending on the extent of the tumor and its proximity to neighboring structures in determining the optimal treatment strategy. TCA provides direct access to the parasellar compartments and is useful for tumors that extend laterally beyond the internal carotid artery bifurcation (3). However, EEA provides direct access to the anterior skull base and is appropriate for intrasellar lesions (26). In this study, EEA resulted in a significantly higher likelihood of GTR in lesions where both approaches are viable (77.2% vs 61.5%; OR, 2.24; p = 0.02). EEA allows for direct visualization and dissection of tumors and adhesive neurovascular structures, increasing the likelihood of complete resection.

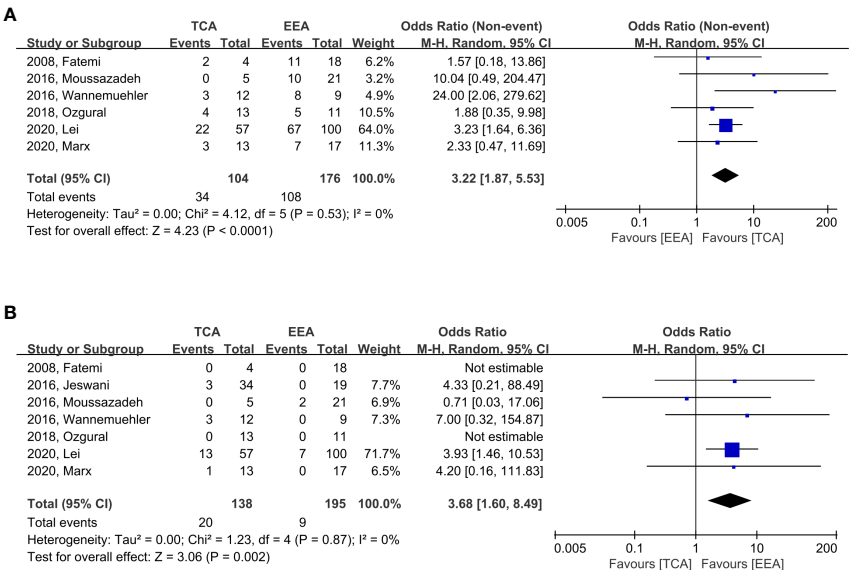

FIGURE 4
Forest plots comparing odd ratios (ORs) of visual outcomes following TCA vs. EEA in craniopharyngioma patients. **(A)** Visual improvement and **(B)** Visual deterioration. TCA, transcranial approach; EEA, endoscopic endonasal approach; CI, confidence interval; SD, standard deviation.

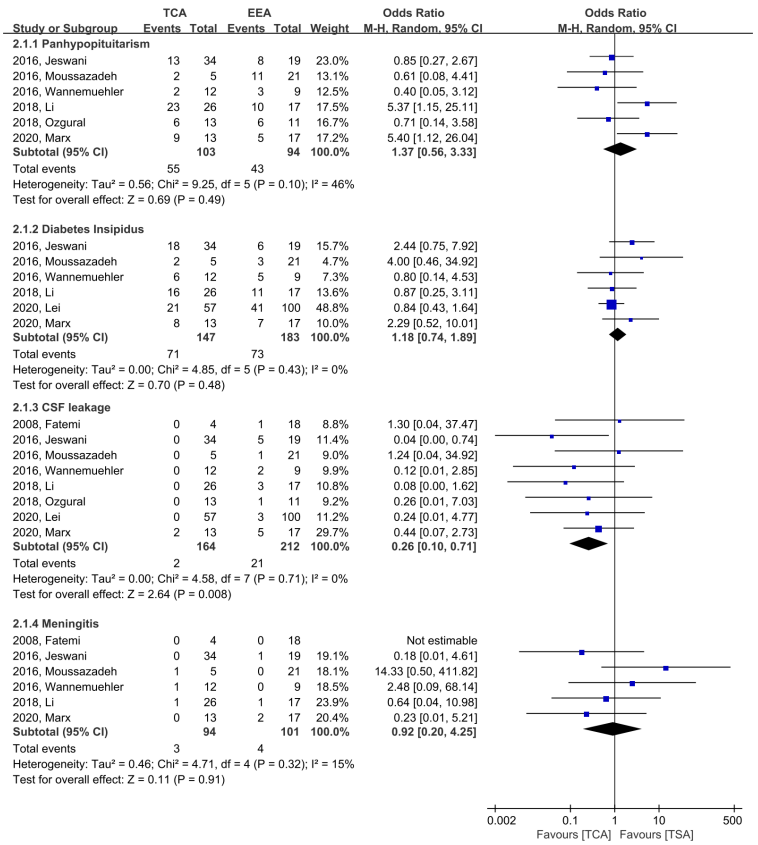

FIGURE 5
Forest plots comparing odd ratios (ORs) of complications following TCA vs. EEA in craniopharyngioma patients. TCA, transcranial approach; EEA, endoscopic endonasal approach; CI, confidence interval; SD, standard deviation; CSF, cerebrospinal fluid.

Endocrine dysfunction adversely affects health-related quality of life and seems inevitable after surgery (27–29). The pituitary stalk connects the pituitary gland to the hypothalamus and maintains the hypothalamic-pituitary function (2). The relationship between the tumor and stalk is critical for postoperative endocrine dysfunction, and the Kassam classification focused on this relationship (30). Dho et al. (2) reported that trans- and retro-infundibular tumors were associated more with endocrinological deterioration than pre-infundibular tumors according to the Kassam classification, and

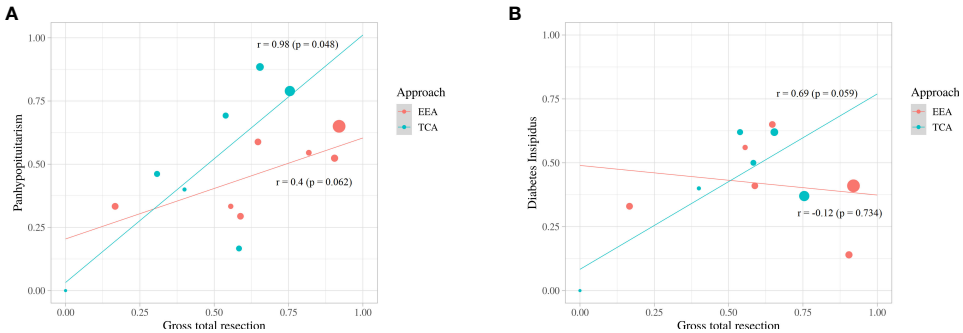

FIGURE 6
Scatter plot and linear-regression analysis between gross total resection and panhypopituitarism **(A)** and diabetes insipidus **(B)**.

centrally located tumors were significantly associated with endocrinological deterioration than peripherally located tumors. A previous meta-analysis found that patients treated with GTR had a considerably higher incidence of panhypopituitarism and DI than those treated with STR (27). In this study, there was no significant difference in the incidence of panhypopituitarism and DI between TCA and EEA. In a linear regression, the incidence of panhypopituitarism and DI increased significantly with increasing GTR ratio in TCA, whereas the incidence of panhypopituitarism increased slightly and DI showed a tendency to decrease with increasing GTR ratio in EEA. Compared to TCA, EEA allows for a more direct view of the skull base, allowing for early identification of the pituitary stalk and GTR while preserving the stalk. Chen et al. (31) reported that when craniopharyngiomas were resected *via* EEA, stalk preservation significantly lowered endocrine dysfunction without decreasing the rate of GTR and without increasing the rate of tumor recurrence.

We found that EEA resulted in a significantly higher likelihood of visual improvement when compared to TCA (60.7% vs. 32.7%, $p < 0.0001$), whereas TCA resulted in a significantly higher likelihood of visual deterioration when compared to EEA (14.5% vs. 4.6%, $p = 0.002$), and the results were comparable to those reported in a previous meta-analysis (11). These results support the evidence that EEA has an advantage over TCA by increasing visual improvement but reducing visual deterioration. Stefko et al. also demonstrated that EEA improves the visual field as well as visual accuracy (32). This is because EEA allows for early decompression of the optic apparatus without retraction and superior visualization of superior hypophyseal arteries originating from the internal carotid artery.

CSF leakage was shown to be statistically more prevalent in EEA compared to TCA (9.9% vs. 1.2%, $p = 0.008$). When EEA was originally introduced, the increased possibility of postoperative CSF leakage was a major complication. To access the tumors, EEA penetrates through the nasal cavity and deconstructs the anterior skull base due to the pathway of the approach. However, with the introduction of skull base reconstruction techniques using a pedicled vascularized nasoseptal flap, first introduced in 2006, this risk has been considerably decreased to approximately 5% (33, 34). In our study, it was confirmed that the CSF leakage rate was as low as 5.5% in the studies with a study period after 2010 (33, 34). The development of multi-layer skull base reconstruction techniques, including gasket-seal, artificial collagen dura mater, and artificial bone substitute, and increased surgeon experience are expected to further reduce the rate of CSF leakage.

4.1 Strengths and limitations

This meta-analysis adhered strictly to its selection criteria and the Preferred Reporting Items for Systematic Reviews and Meta-analysis guidelines. This study has several strengths. First, although direct comparative studies of craniopharyngioma resection using TCA vs. EEA are uncommon, we only incorporated this type of research to avoid intra-study variability which affects indirect comparisons, improve the validity of the results, and provide summary statistics. Second, we could reduce selection bias because most of the studies attempted to include tumors that were amenable to both approaches. Lei et al. (4) reported four types based on the location of the tumors, and we excluded the intrasellar type to avoid violating the inclusion criteria of other studies.

However, our study has some limitations. First, all included studies were retrospective in nature. Second, two of the eight studies reported incomplete outcome data and had selective outcome reporting, such as tumor size, pathology, and adjuvant radiotherapy. (Supplementary Figure 2B). However, missing data were not analyzed in this study and did not significantly impede the conclusions. Third, we were unable to analyze other complications such as hydrocephalus, nerve injury, cerebral infarction, cognitive dysfunction, and hemorrhage, as only a few studies have reported these parameters for their patients. Therefore, it is important to carefully interpret the results of this study, and a further well-designed study is warranted.

4.2 Conclusions

We found that when both approaches can completely resect the tumor, EEA outperforms TCA in terms of GTR rate and visual outcomes, as well as favorable results in terms of complications other than CSF leakage, such as panhypopituitarism and DI, considering the meta-regression results. Although knowledge of and competence in traditional microsurgery and endoscopic surgery are essential in surgical decision-making for craniopharyngioma treatment, when both approaches are viable, EEA is associated with favorable surgical outcomes.

Data availability statement

The original contributions presented in the study are included in the article/Supplementary Material. Further inquiries can be directed to the corresponding author.

Author contributions

K-SC contributed to the conceptualization, supervision, and project administration. MN, BJ, TL, WK, and YC contributed to the methodology, formal analysis, data curation, and writing the original draft. H-GS, CA, JK, JL, SK, and HL contributed to the validation, writing, review, and editing. All authors contributed to the article and approved the submitted version.

Funding

This work was supported by the Bio & Medical Technology Development Program of the National Research Foundation (NRF) funded by the Korean government (MSIT) (NRF-2019M3E5D1A01069356) and the National Research Foundation of Korea (NRF) grant funded by the Korea government (MSIT) (NRF-2022R1A5A1022977) to K-SC.

Conflict of interest

The authors declare that the research was conducted in the absence of any commercial or financial relationships that could be construed as a potential conflict of interest.

Publisher's note

Supplementary material

The Supplementary Material for this article can be found online at: https://www.frontiersin.org/articles/10.3389/fonc.2022.1058329/full#supplementary-material

References

1. Karavitaki N, Cudlip S, Adams CB, Wass JA. Craniopharyngiomas. *Endocr Rev* (2006) 27:371–97. doi: 10.1210/er.2006-0002

2. Dho YS, Kim YH, Se YB, Han DH, Kim JH, Park CK, et al. Endoscopic endonasal approach for craniopharyngioma: the importance of the relationship between pituitary stalk and tumor. *J Neurosurg* (2018) 129:611–9. doi: 10.3171/2017.4.JNS162143

3. Moussazadeh N, Prabhu V, Bander ED, Cusic RC, Tsiouris AJ, Anand VK, et al. Endoscopic endonasal versus open transcranial resection of craniopharyngiomas: a case-matched single-institution analysis. *Neurosurg Focus* (2016) 41:E7. doi: 10.3171/2016.9.FOCUS16299

4. Lei C, Chuzhong L, Chunhui L, Peng Z, Jiwei B, Xinsheng W, et al. Approach selection and outcomes of craniopharyngioma resection: a single-institute study. *Neurosurg Rev* (2021) 44:1737–46. doi: 10.1007/s10143-020-01370-8

5. Ordóñez-Rubiano EG, Forbes JA, Morgenstern PF, Arko L, Dobri GA, Greenfield JP, et al. Preserve or sacrifice the stalk? endocrinological outcomes, extent of resection, and recurrence rates following endoscopic endonasal resection of craniopharyngiomas. *J Neurol Surg* (2018) 131:1–9. doi: 10.3171/2018.6.JNS18901

6. Liu JK, Sevak IA, Carmel PW, Eloy JA. Microscopic versus endoscopic approaches for craniopharyngiomas: choosing the optimal surgical corridor for maximizing extent of resection and complication avoidance using a personalized, tailored approach. *Neurosurg Focus* (2016) 41:E5. doi: 10.3171/2016.9.FOCUS16284

7. Fernandez-Miranda JC, Gardner PA, Snyderman CH, Devaney KO, Strojan P, Suárez C, et al. Craniopharyngioma: A pathologic, clinical, and surgical review. *Head Neck* (2012) 34:1036–44. doi: 10.1002/hed.21771

8. Yaşargil MG, Curcic M, Kis M, Siegenthaler G, Teddy PJ, Roth P. Total removal of craniopharyngiomas. approaches and long-term results in 144 patients. *J Neurosurg* (1990) 73:3–11. doi: 10.3171/jns.1990.73.1.0003

9. Cossu G, Jouanneau E, Cavallo LM, Elbabaa SK, Giammattei L, Starnoni D, et al. Surgical management of craniopharyngiomas in adult patients: A systematic review and consensus statement on behalf of the EANS skull base section. *Acta Neurochir* (2020) 162:1159–77. doi: 10.1007/s00701-020-04265-1

10. Qiao N. Endocrine outcomes of endoscopic versus transcranial resection of craniopharyngiomas: A system review and meta-analysis. *Clin Neurol Neurosurg* (2018) 169:107–15. doi: 10.1016/j.clineuro.2018.04.009

11. Komotar RJ, Starke RM, Raper DM, Anand VK, Schwartz TH. Endoscopic endonasal compared with microscopic transsphenoidal and open transcranial resection of craniopharyngiomas. *World Neurosurg* (2012) 77:329–41. doi: 10.1016/j.wneu.2011.07.011

12. Stroup DF, Berlin JA, Morton SC, Olkin I, Williamson GD, Rennie D, et al. Meta-analysis of observational studies in EpidemiologyA proposal for reporting. *JAMA* (2000) 283:2008–12. doi: 10.1001/jama.283.15.2008

13. Liberati A, Altman DG, Tetzlaff J, Mulrow C, Gøtzsche PC, Ioannidis JP, et al. The PRISMA statement for reporting systematic reviews and meta-analyses of studies that evaluate health care interventions: explanation and elaboration. *PloS Med* (2009) 6:e1000100. doi: 10.1371/journal.pmed.1000100

14. Kim SY, Park JE, Lee YJ, Seo HJ, Sheen SS, Hahn S, et al. Testing a tool for assessing the risk of bias for nonrandomized studies showed moderate reliability and promising validity. *J Clin Epidemiol* (2013) 66:408–14. doi: 10.1016/j.jclinepi.2012.09.016

15. Higgins JP, Thompson SG. Quantifying heterogeneity in a meta-analysis. *Stat Med* (2002) 21:1539–58. doi: 10.1002/sim.1186

16. Ozgural OMD, Kahilogullari GMDP, Dogan I, Al-Beyati ESM, Bozkurt M, Tetik B. Single-center surgical experience of the treatment of craniopharyngiomas with emphasis on the operative approach: endoscopic endonasal and open microscopic transcranial approaches. *J Craniofac Surg* (2018) 29:e572–8. doi: 10.1097/SCS.0000000000004592

17. Wannemuehler TJ, Rubel KE, Hendricks BK, Ting JY, Payner TD, Shah MV, et al. Outcomes in transcranial microsurgery versus extended endoscopic endonasal approach for primary resection of adult craniopharyngiomas. *Neurosurg Focus* (2016) 41:E6. doi: 10.3171/2016.9.FOCUS16314

18. Jeswani S, Nuño M, Wu A, Bonert V, Carmichael JD, Black KL, et al. Comparative analysis of outcomes following craniotomy and expanded endoscopic endonasal transsphenoidal resection of craniopharyngioma and related tumors: A single-institution study. *J Neurosurg* (2016) 124:627–38. doi: 10.3171/2015.3.JNS142254

19. Fatemi N, Dusick JR, de Paiva Neto MA, Malkasian D, Kelly DF. Endonasal versus supraorbital keyhole removal of craniopharyngiomas and tuberculum sellae meningiomas. *Oper Neurosurg* (2009) 64:269–84; discussion 284-6. doi: 10.1227/01.NEU.0000327857.22221.53

20. Li X, Wu W, Miao Q, He M, Zhang S, Zhang Z, et al. Endocrine and metabolic outcomes after transcranial and endoscopic endonasal approaches for primary resection of craniopharyngiomas. *World Neurosurg* (2019) 121:e8–e14. doi: 10.1016/j.wneu.2018.08.092

21. Marx S, Tsavdaridou I, Paul S, Steveling A, Schirmer C, Eördögh M, et al. Quality of life and olfactory function after suprasellar craniopharyngioma surgery-a single-center experience comparing transcranial and endoscopic endonasal approaches. *Neurosurg Rev* (2021) 44:1569–82. doi: 10.1007/s10143-020-01343-x

22. Sughrue ME, Yang I, Kane AJ, Fang S, Clark AJ, Aranda D, et al. Endocrinologic, neurologic, and visual morbidity after treatment for craniopharyngioma. *J Neurooncol* (2011) 101:463–76. doi: 10.1007/s11060-010-0265-y

23. Kiehna EN, Merchant TE. Radiation therapy for pediatric craniopharyngioma. *Neurosurg Focus* (2010) 28:E10. doi: 10.3171/2010.1.FOCUS09297

24. Okada T, Fujitsu K, Ichikawa T, Miyahara K, Tanino S, Uriu Y, et al. Radical resection of craniopharyngioma: Discussions based on long-term clinical course and histopathology of the dissection plane. *Asian J Neurosurg* (2018) 13:640–6. doi: 10.4103/ajns.AJNS_258_16

25. Elliott RE, Hsieh K, Hochm T, Belitskaya-Levy I, Wisoff J, Wisoff JH. Efficacy and safety of radical resection of primary and recurrent craniopharyngiomas in 86 children. *J Neurosurg Pediatr* (2010) 5:30–48. doi: 10.3171/2009.7.PEDS09215

26. Gardner PA, Prevedello DM, Kassam AB, Snyderman CH, Carrau RL, Mintz AH. The evolution of the endonasal approach for craniopharyngiomas. *J Neurosurg* (2008) 108:1043–7. doi: 10.3171/JNS/2008/108/5/1043

27. Akinduro OO, Izzo A, Lu VM, Ricciardi L, Trifiletti D, Peterson JL, et al. Endocrine and visual outcomes following gross total resection and subtotal resection of adult craniopharyngioma: Systematic review and meta-analysis. *World Neurosurg* (2019) 127:e656–68. doi: 10.1016/j.wneu.2019.03.239

28. Crespo I, Santos A, Webb SM. Quality of life in patients with hypopituitarism. *Curr Opin Endocrinol Diabetes Obes* (2015) 22:306–12. doi: 10.1097/MED.0000000000000169

29. Cavallo LM, Frank G, Cappabianca P, Solari D, Mazzatenta D, Villa A, et al. The endoscopic endonasal approach for the management of craniopharyngiomas: A series of 103 patients. *J Neurosurg* (2014) 121:100–13. doi: 10.3171/2014.3.JNS131521

30. Kassam AB, Gardner PA, Snyderman CH, Carrau RL, Mintz AH, Prevedello DM. Expanded endonasal approach, a fully endoscopic transnasal approach for the resection of midline suprasellar craniopharyngiomas: A new classification based on the infundibulum. *J Neurosurg* (2008) 108:715–28. doi: 10.3171/JNS/2008/108/4/0715

31. Chen Z, Ma Z, He W, Shou X, Ye Z, Zhang Y, et al. Impact of pituitary stalk preservation on tumor recurrence/progression and surgically induced endocrinopathy after endoscopic endonasal resection of suprasellar craniopharyngiomas. *Front Neurol* (2021) 12:753944. doi: 10.3389/fneur.2021.753944

32. Stefko ST, Snyderman C, Fernandez-Miranda J, Tyler-Kabara E, Wang E, Bodily L, et al. Visual outcomes after endoscopic endonasal approach for craniopharyngioma: the Pittsburgh experience. *J Neurol Surg B Skull Base* (2016) 77:326–32. doi: 10.1055/s-0036-1571333

33. Kassam AB, Thomas A, Carrau RL, Snyderman CH, Vescan A, Prevedello D, et al. Endoscopic reconstruction of the cranial base using a pedicled nasoseptal flap. *Neurosurgery* (2008) 63:ONS44–52; discussion ONS52-3. doi: 10.1227/01.neu.0000297074.13423.f5

34. Hadad G, Bassagasteguy L, Carrau RL, Mataza JC, Kassam A, Snyderman CH, et al. A novel reconstructive technique after endoscopic expanded endonasal approaches: vascular pedicle nasoseptal flap. *Laryngoscope* (2006) 116:1882–6. doi: 10.1097/01.mlg.0000234933.37779.e4

frontiers | Frontiers in Oncology

TYPE Original Research
PUBLISHED 04 January 2023
DOI 10.3389/fonc.2022.1067312

OPEN ACCESS

EDITED BY
Carlo Serra,
University Hospital Zürich, Switzerland

REVIEWED BY
Filippo Flavio Angileri,
University of Messina, Italy
Ming Chen,
Shanghai Jiao Tong University, China
Teresa Somma,
Federico II University Hospital, Italy

*CORRESPONDENCE
Bertrand Baussart
bertrand.baussart@aphp.fr;
bertranbaussart@gmail.com

†These authors have contributed equally to this work and share first authorship

SPECIALTY SECTION
This article was submitted to Neuro-Oncology and Neurosurgical Oncology, a section of the journal Frontiers in Oncology

RECEIVED 11 October 2022
ACCEPTED 05 December 2022
PUBLISHED 04 January 2023

CITATION
Baussart B, Venier A, Jouinot A, Reuter G and Gaillard S (2023) Closure strategy for endoscopic pituitary surgery: Experience from 3015 patients.
Front. Oncol. 12:1067312.
doi: 10.3389/fonc.2022.1067312

Closure strategy for endoscopic pituitary surgery: Experience from 3015 patients

Bertrand Baussart[1,2*†], Alice Venier[3†], Anne Jouinot[2], Gilles Reuter[4] and Stephan Gaillard[1]

[1]Department of Neurosurgery, La Pitié-Salpêtrière University Hospital, Assistance Publique-Hôpitaux de Paris, Paris, France, [2]Université Paris Cité, Institut Cochin, CNRS, INSERM, Paris, France, [3]Department of Neurosurgery, Neurocenter of Southern Switzerland, Lugano, Switzerland, [4]Department of Neurosurgery, Centre Hospitalier Universitaire (CHU) de Liège, Bat B35, Domaine Universitaire du Sart-Tilman, Liège, Belgium

Introduction: Effective strategies are required to ensure optimal management of the crucial closure step in endoscopic pituitary surgery. Many surgical techniques have been reported but no significant consensus has been defined.

Methods: Between January 2006 and March 2022, 3015 adult patients with pituitary adenomas were operated on by a single expert neurosurgical team, using a mononostril endoscopic endonasal approach. Based of preoperative risk factors of and operative findings, a detailed closure strategy was used. Body mass index >40, sellar floor lysis, number of surgeries>2, large skull base destruction, prior radiotherapy were considered as preoperative risk factors for closure failure. All patients treated with an expanded endonasal approach were excluded.

Results: Patients were mostly women (F/M ratio: 1.4) with a median age of 50 (range: 18 −89). Intraoperative CSF leak requiring specific surgical management was observed in 319/3015 (10.6%) of patients. If intraoperative leak occurred, patients with predictive risk factors were managed using a Foley balloon catheter in case of sellar floor lysis or BMI>40 and a multilayer repair strategy with a vascularized nasoseptal flap in other cases. Postoperative CSF leak occurred in 29/3015 (1%) of patients, while meningitis occurred in 24/3015 (0.8%) of patients. In patients with intraoperative leak, closure management failed in 11/319 (3.4%) of cases.

Conclusion: Based on our significant 16-year experience, our surgical management is reliable and easy to follow. With a planned and stepwise strategy, the closure step can be optimized and tailored to each patient with a very low failure rate.

KEYWORDS

pituitary surgery, closure, skull base repair, endoscopy, strategy, nasoseptal flap

Introduction

Pituitary adenomas account for 15% of all intracranial neoplasms, making them the third most common pathology (1). Pituitary adenomas, recently renamed as pituitary neuroendocrine tumors (PitNETs) in the new classifications (2–4) are usually benign tumors, with a broad spectrum of biological and pathological characteristics (5–7). Surgery represents the first-line treatment for most pituitary adenomas (corticotroph, somatotroph and non-functional), except for most prolactinomas which are currently treated with dopamine agonists (8).

The transsphenoidal approach is the gold standard of surgical route for pituitary surgery (9–11), while the transcranial approach is considered only as a second-line surgical option, in well-selected patients with rare tumors extending anteriorly in the subfrontal area, laterally in the temporal fossa or encompassing the vessels (12, 13). The microscopic technique, initially developed by Cushing and successively taken forward by Dott, Guiot and Hardy (14–16), was progressively abandoned in most centers of excellence, leading to the transition towards the endoscopic technique in the late 1990s (10, 17–19). Nowadays, the endoscopic endonasal transsphenoidal approach is the mainstay in many centers worldwide, given its advantages in terms of quality of vision, tumor resection, endocrine outcome, sinus-nasal morbidity and length of hospital stay (17, 20, 21).

Despite advances in closure techniques, postoperative CSF (cerebrospinal fluid) leak remains the most common complication of the endoscopic endonasal transsphenoidal approach, occurring in around 10% of patients and requiring a specific second surgery. The rate of CSF leak-related meningitis is observed in approximately 5% of patients, increasing the length of hospital stay and medical costs (22, 23). Thus, a reconstruction strategy of the skull-base defect should be anticipated during preoperative planning and an accurate analysis of preoperative risk factors associated with CSF leak is essential. In previous studies, many preoperative risk factors have been reported such as BMI (body mass index) > 30, multiple surgeries, tumor size, extension and invasiveness, prior treatment with radiotherapy (24–29). In all these patients, the closure strategy should be rigorously considered before the sellar surgical step, in order to limit avoidable reconstruction failures (24, 30) and to modulate it according to the flow of the CSF leak observed during surgery (31–34).

Today, several protocols to reduce postoperative CSF leak have been proposed (33–40) but there is no consensus on the best closure strategy after endoscopic pituitary surgery. Moreover, a significant heterogeneity in the outcomes was reported (41). From the analysis of the first 1000 patients operated on with a mononostril endoscopic endonasal transsellar approach, we reported in 2014 a postoperative CSK leak rate <1% (18). Based on our substantial additional experience, we developed a gradual closure strategy that integrates individual preoperative risks of postoperative CSF leak with the operative findings.

The objective of the present study is to analyze the results of our closure strategy from a consecutive cohort of 3015 patients with pituitary adenomas, operated on by the same two senior expert neurosurgeons (S.G, B.B). The philosophy of this major surgical step is emphasized, highlighting the need to plan the closure step before entering the operative room.

Materials and methods

Patients

This is a French observational cohort of 3015 consecutive adult patients with pituitary adenomas operated on between January 2006 and March 2022.

Inclusion criteria were: (1) diagnosis of adenoma confirmed on histological examination; (2) adenoma patients treated with a mononostril endoscopic endonasal transsphenoidal approach, as described in the "endoscopic endonasal transsphenoidal surgery" section; (3) patients eligible for surgery selected at a multidisciplinary meeting with an endocrinologist, a neurosurgeon and a radiologist; (4) dedicated pituitary MRI performed for each patient before surgery. Exclusion criteria were: (1) adenoma patients treated with an expanded endoscopic approach - such as transtuberculum or transplanum approach; (2) patients under 18 years of age.

Prior medical therapy with dopamine agonists or somatostatin analogues was not considered an exclusion criterion. All patients with prior medical therapy were included in this series.

Predictive factors for closure failure

On the basis of previous studies (24, 25, 27–29, 42, 43), preoperative clinical and radiological assessment identified the following variables as preoperative risk factors for closure failure: severe obesity, number of surgeries > 2, focal sellar floor lysis, large skull base destruction due to invasive or giant pituitary adenomas and history of prior radiation therapy.

Intraoperative CSF leaks are often complex to treat in obese patients because of higher intracranial pressure (29). Furthermore, as previously published, the risk of symptomatic intracranial hypertension increases with increasing BMI. In patients with BMI>40, the risk of induced vision loss is well known (44). Based on this data, we have considered that patients with BMI>40 may be exposed to a higher risk of postoperative CSF leak due to increased intracranial pressure. Thus, this critical value was considered a risk factor of closure failure.

Endoscopic endonasal transsphenoidal surgery

The same two senior neurosurgeons (S.G, B.B) operated on all patients via a mononostril endoscopic endonasal transsphenoidal approach, as recently described by the present team (20). The patient was placed in a semi-sitting position. Care was taken to avoid any compression points. During patient positioning, the right thigh was prepared for musculoaponeurotic graft whenever needed. The head was deflected back by 30° to prevent jugular compression. 0° and 30° optic endoscopes (Karl Storz) were used. After lateralization of the middle turbinate, the mucosa of the anterior part of the sphenoid bone was coagulated with a luxation of the septum. The sellar floor was opened and the dura incised. The adenoma was removed for pathological analysis using standard curettes, dissecting instruments, and suction.

The crucial closure step was anticipated during the approach: the main objective was to preserve an optimal epidural space when the sellar floor was opened and the tumor was removed, in order to reconstruct an optimal sellar floor during the closure step. The sellar floor was opened is such a way that the bone opening was larger than the dural opening, in order to preserve the epidural space (Figure 1).

CSF leak evaluation

Once tumor was resected, the neurosurgeon had to determine the existence and intensity of a possible CSF leak. If a CSF leak was observed, the degree of CSF flow was assessed, as proposed by Esposito et al. (33). CSF leak was classified as follows: small leak without obvious diaphragm defect, defined as diaphragm oozing; low-flow leak with focal diaphragm defect; high-flow leak with large diaphragm or dural defect.

Closure stage: General considerations

The substantial experience gained since 2006 has allowed us to gradually establish a specific stepwise surgical strategy, based on a rigorous analysis of preoperative risk factors for closure failure and operative findings. The proposed closure strategy comes from a retrospective analysis of the authors' experience gained during the study period. Our current strategy used since 2014 for graded closure strategy in pituitary surgery has been provided in Figure 2.

Indeed, some nuances have been added from our initial operative technique. Until 2014 (n=1397 patients), a 5-day external lumbar drainage could be decided as a second surgical option in combination with the intrasellar muscular graft, in rare patients with failure of closure management. Since 2014 (n=1618 patients), external lumbar drainage has been abandoned and replaced by the Foley Catheter technique: a saline-inflate Foley catheter was applied inside the sphenoid sinus in order to constitute an abutment against the intrasellar muscular graft (in case of sellar floor lysis or BMI>40) or against the double pedicled nasoseptal flap (in case of number of surgeries > 2, large skull base destruction, giant tumors or prior radiotherapy). This change essentially resulted from an objective to improve clinical tolerance, to reduce the risk of complications due to lumbar drainage and to treat more complex patients with more complex adenomas.

If possible, no material was placed in the intrasellar compartment, so as not to interfere with the interpretation of the postoperative MRI and not to impact on tumor resection in any subsequent surgery. In the absence of CSK leak, an optimal standard bone sellar floor reconstruction was achieved, using an autologous bone from a sphenoid septation designed in a quadrangular shape and positioned by four corners in the epidural space (Figure 3). In case of patients with strong risk

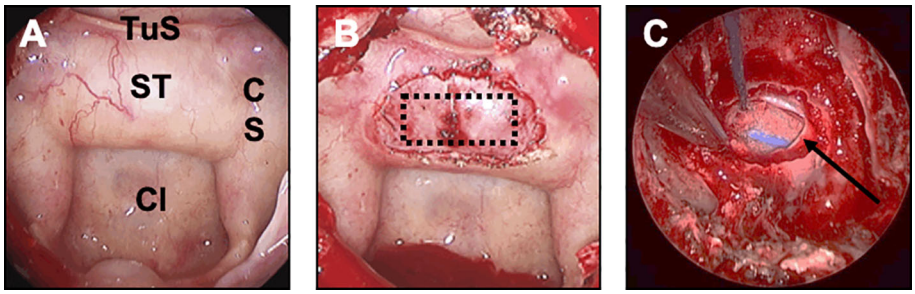

FIGURE 1
Preparation of the closure step during the endoscopic approach. This figure illustrates the concept that closure should be anticipated and planned for at each surgical step. **(A)** Sphenoid step. The main classic landmarks are identified: sella turcica (ST), tuberculum sellae (TuS), clivus (Cl), cavernous sinus (CS). **(B)** Sellar step. After opening the sellar floor, the dura has been carefully exposed and respected. The optimal rectangle shaped-dural opening is provided (dotted black rectangle). Note that the bone opening is oversized compared to the dural opening, in order to preserve the epidural space. **(C)** Sellar step after tumor resection. Note that the epidural space has been respected between the sellar floor and the dura mater (black arrow) for optimal closure.

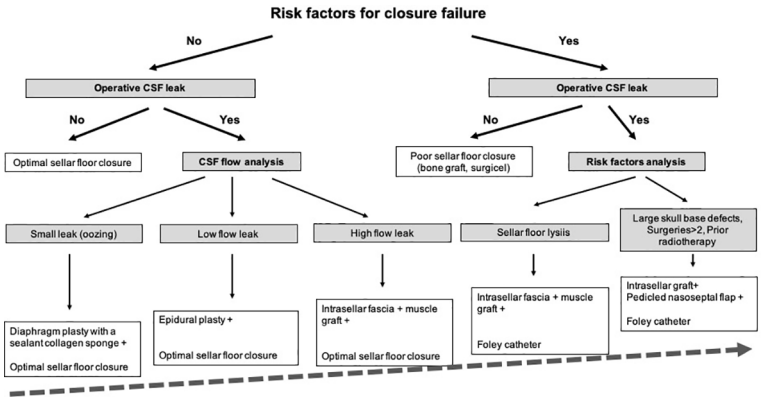

FIGURE 2
Closure strategy for pituitary surgery. Decision strategy.

factors of postoperative CSF leak (large skull base destruction due to invasive or giant pituitary adenomas, number of surgeries >2, history of prior radiotherapy), a multilayer reconstruction strategy was decided, using the double pedicled nasoseptal flap, as previously reported (45, 46).

Closure strategy

i. Patients with no risk factors of closure failure

In the absence of CSK leak, optimal bone sellar floor reconstruction was performed, as detailed above. In case of intraoperative CSF leak, the choice of the closure depended on the intensity of flow and the location of the leak.

In case of small leak due to diaphragm oozing, a collagen sponge coated with the human coagulation factors fibrinogen and thrombin (TachoSil®) was used. The sealant matrix was positioned in the intrasellar compartment, deployed, centered on the dural defect and applied against the diaphragm with the help of forceps holding a cottonoid and a suction tube (Figure 4A). The sellar floor was reconstructed and some biological glue was applied in the sphenoid sinus.

In case of focal low-flow leak, an epidural duraplasty was performed, using a dural substitute. After a right middle turbinectomy was performed, the mucosa of the turbinate was removed away from the bone. The mucosal graft from the middle turbinate was positioned in the epidural space, with the support of a bone graft or a PDS plate embedded in an epidural fashion (Figures 4A, B). With this technique, the mucosa should act as a seal. As previously described, biological glue was applied. In rare cases of focal diaphragm defect with a distended diaphragm bulging into the intrasellar

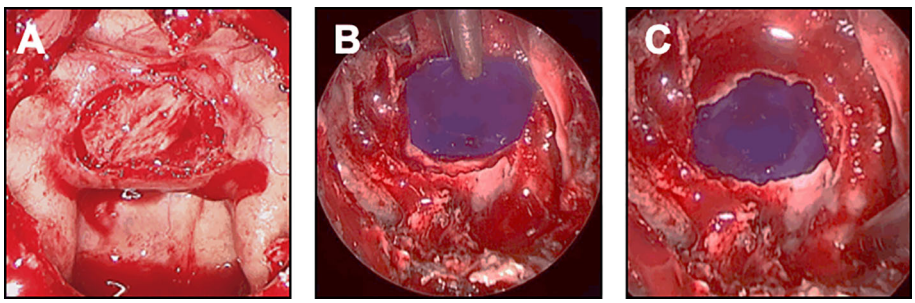

FIGURE 3
Closure strategy in patients with no CSF leak and no risk factor. For these patients, an optimal sellar floor closure should be achieved. **(A)** Sellar reconstruction with a bone graft. The piece of bone has been removed from the sphenoid rostrum or from a sphenoid septation, accurately designed and positioned in the previously prepared epidural space. **(B, C)** Sellar reconstruction with a synthetic polydioxanone (PDS) plate. **(B)** A synthetic polydioxanone (PDS) plate (in blue) has been shaped according to the sellar floor opening and introduced in the sphenoid sinus. The positioning always starts with the introduction of the two lower edges, the plate being held by a surgical forceps. **(C)** The two upper edges have been embedded so that the entire PDS plate was positioned in the epidural space.

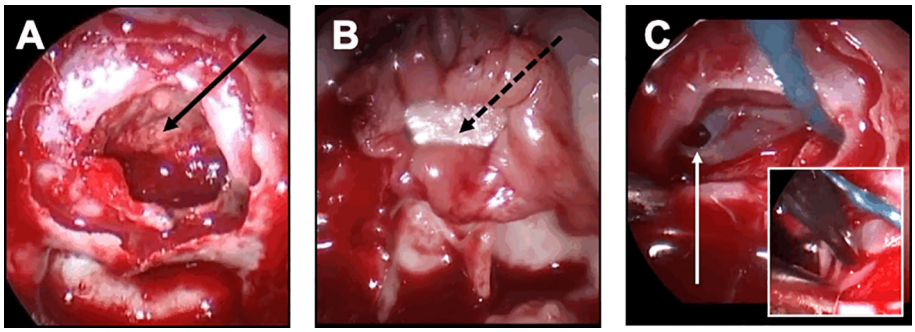

FIGURE 4
Closure strategy in patients with CSF leak and no risk factor. For these patients, the sella floor should be reconstructed and biological glue should be applied after the sealing has been achieved. **(A, B)** Minimal and diffuse flow diaphragm leak. **(A)** A sealant collagen sponge coated with the human coagulation factors fibrinogen and thrombin (black arrow) has been designed, positioned in the intrasellar compartment, deployed, centered on the dural defect and applied against the diaphragm with the help of a forceps holding a cottonoid and a suction tube. **(B)** An epidural duraplasty has been performed, using the mucosa of the right middle turbinate. After the mucosa has been embedded in the epidural space with a bone graft (black dotted arrow), the mucosa acts as a seal. **(C)** Focal low-flow leak. A unique focal defect is visualized on the right side of the diaphragm (white arrow). The sealing is achieved after coagulation of the dural defect using a bipolar forceps (insert).

space, watertight closure could be achieved by coagulating the edges of the transdiaphragmatic orifice with bipolar forceps (Figure 4C).

In case of diffuse of high-flow leak, an intrasellar packing technique was decided. Fascia and muscle grafts were taken from the right thigh. The fascia was introduced into the sella and applied superiorly to cover the entire defect, in order to recreate a new diaphragm. The muscle graft was then positioned within the intrasellar compartment. As previously described, the sellar floor was reconstructed with bone graft or PDS plate and biological glue was applied.

ii. Patients with risk factors of closure failure

BMI>40 with intact sellar floor, no intraoperative leak

A standard closure was performed, as previously described.

Focal sellar floor lysis and BMI<40, no intraoperative leak

A poor sellar closure was usually achieved, using a bone graft or PDS plate positioned by only two or three corners in the epidural space

Focal sellar floor lysis and BMI>40, no intraoperative leak

An additional Foley catheter technique was decided in order to avoid the migration of the poor sellar reconstruction. A two-way Foley balloon catheter technique was used: the balloon stent was positioned inside the sphenoid sinus against the sella turcica to reinforce the reconstruction and counter the effects of graft migration. Usually, we used a Foley urinary catheter from 8 to 12 French filled up with saline solution, inflating it to be in contact with the graft. The catheter was left in place for 4 to 5 days.

Focal sellar floor lysis and/or BMI>40, intraoperative leak

All patients were treated with an intrasellar fascia and muscle graft, combined with an additional Foley balloon catheter. Biological glue was always applied. Repeated lumbar punctures were performed on day 1 and day 2 after surgery

Large skull base destruction and/or number of surgeries >2 and/or prior radiotherapy

In complex cases of patients with strong risk factors of closure failure, the following strategy was decided, regardless the occurrence of an intraoperative leak: a multilayer repair strategy was chosen with combined intrasellar fascia and muscle grafts, optimal epidural closure if possible, and double pedicled mucosal nasoseptal flap (Figure 5). Each left and right mucosal flap was elevated from each side of the nasal bone septum and pedicled on the sphenopalatine artery. The pedicled flap was applied against the sella turcica and held in place with a Foley catheter for 5 days. Biological glue was always applied. Repeated lumbar punctures were performed on day 1 and day 2 after surgery. This multilayer strategy was also decided in case of patients with BMI>40.

Closure evaluation

Closure was considered as achieved if no postoperative CSF leak was observed 2 months after surgery. Failure of closure management was diagnosed when a postoperative CSF leak occurred despite the closure strategy applied because of an intraoperative CSF leak during the first procedure, requiring a second surgery.

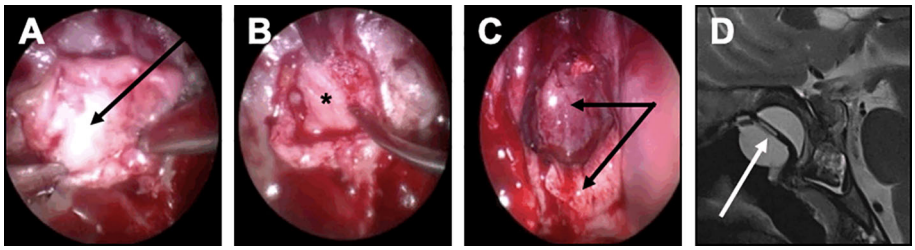

FIGURE 5
Closure strategy in patients with a risk factor. For these patients, a Foley urinary catheter is usually necessary and more complex multilayer closure strategies using a pedicled mucosal nasoseptal flap should be discussed. **(A-D)** Complex multilayer closure strategy for a patient with a recurrent pituitary adenoma treated with multiple surgery and radiotherapy. **(A)** After a muscle graft has been introduced in the intrasellar compartment, an autologous fascia lata graft has been positioned anterior to the sella turcica (black arrow). **(B)** After the fascia lata has been embedded in the epidural space with a bone graft (black asterisk), the primary sealing is obtained. **(C)** A vascularized mucosal nasoseptal flap is positioned and deployed in the sphenoid sinus (double black arrow), maintained using a Foley urinary catheter for 5 days. **(D)** Postoperative MRI showing the multilayer reconstruction and the Foley catheter (white arrow).

Data collection

The following variables were collected for each patient before, during, and after surgery.

i. Before surgery: age; sex; preoperative risk factors for closure failure.
ii. During surgery: intraoperative CSF leak; flow intensity and location of intraoperative CSF; type of closure strategy.
iii. After surgery: postoperative CSF leak; type of closure strategy; meningitis with bacteriological analysis if available.

Statistical analysis

Statistical analysis was performed using R statistical software (version 3.6.3). Descriptive statistics used median (range) for quantitative variables and raw numbers (%) for categorical variables.

Results

Characteristics of patients selected for surgery

The characteristics of 3015 patients operated on for an adenoma are provided in Table 1. Patients were mostly women (F/M ratio: 1.4), with a median age of 50 (range: 18 to 89). Hormone excess was observed in 1970/3015 (65.3%) of patients. Corticotroph adenomas with Cushing's disease, somatotroph adenomas with acromegaly, lactotroph adenoma, thyrotroph adenoma and non-secreting adenomas were diagnosed in 822/3015 (27.3%), 768/3015 (25.5%), 331/3015 (11%), 49/3015 (1.6%) and 1045/3015 (34.6%) of patients respectively.

Intraoperative CSF leak

Intraoperative CSF leak requiring a specific surgical management was observed in 319/3015 (10.6%) of patients.

No preoperative risk factor of closure failure was noted in 258/319 (80.9%) of these patients. Diaphragm oozing was noted in 32/258 (12.4%) of patients and was treated with collagen sponge (TachoSil® patch). Focal low-flow leak was noted in 83/258 (32.2%) of patients, mainly treated with epidural graft and more rarely with bipolar coagulation. Diffuse high-flow leak was observed in 143/258 (55.4%) of patients and was treated with intrasellar fascia and muscle graft technique in the vast majority of cases.

Preoperative factors of closure failure were observed in 61/319 (19.1%) of patients. Considering BMI>40 and/or sellar floor lysis, 39/61 (63.9%) of patients were treated with the Foley-catheter technique, while 6/61 (9.8%) were treated using collagen sponge, epidural graft or muscle graft. The 16/61(26.3%) patients with large skull base destruction and/or prior radiation therapy and/or number of surgeries >2 were treated with a multilayer repair strategy with nasoseptal flaps.

Postoperative CSF leak

Postoperative CSF leak requiring a second surgery was observed in 29/3015 (1%) of patients.

Among these patients, 18/29 (62.1%) had no intraoperative CSF leak. No risk factors for closure failure were noted in these

TABLE 1 Characteristics of 3015 adenoma patients treated with a mononostril endoscopic endonasal transsellar approach.

	Patients
Age, years	50 (18-89)
Sex ratio (F/M)	1.4
Type of secretion	
Cushing's disease	822/3015 (27.3%)
Acromegaly	768/3015 (25.5%)
Lactotroph adenoma	331/3015 (11%)
Thyrotroph adenoma	49/3015 (1.6%)
Non-secreting adenoma	1045/3015 (34.6%)
Intraoperative CSF leak requiring a specific surgical management	**319/3015 (10.6%)**
Intraoperative CSF leak with no risk factor of closure failure	**258/319 (80.9%)**
Diaphragm oozing treated with collagen sponge	32/258 (12.4%)
Focal low-flow leak treated	83/258 (32.2%)
treated by focal coagulation	6/83 (7.2%)
treated with an extrasellar epidural graft	77/83 (92.8%)
Diffuse high-flow leak treated with intrasellar fascia and muscle grafts	143/258 (55.4%)
treated with intrasellar fascia and muscle grafts	142/143 (99.3%)
treated with epidural graft	1/143 (0.7%)
Intraoperative CSF leak with a least one risk factor of closure failure	**61/319 (19.1%)**
BMI>40 and/or Sellar floor lysis treated with a Foley balloon Catheter	39/61 (63.9%)
BMI>40 and/or Sellar floor lysis treated with collagen sponge, epidural or muscle graft	6/61 (9.8%)
Large skull base destruction and/or prior radiotherapy and/or surgeries >2 treated with a mucosal nasoseptal flap	16/61 (26.3%)
Postoperative CSF leak requiring a second surgery	**29/3015 (1%)**
Patients with no intraoperative CSF leak	18/29 (62.1%)
Patients with intraoperative CSF leak	11/29 (37.9%)
Rate of failed closure management	**11/319 (3.4%)**
Meningitis requiring antibiotic therapy	**24/3015 (0.8%)**
Aseptic meningitis	14/24 (58.3%)
Septic meningitis	10/24 (41.7%)
Patients with intraoperative CSF leak	19/24 (79.2%)
Patients with no intraoperative CSF leak	5/24 (20.8%)

(Continued)

TABLE 1 Continued

	Patients
Patients with postoperative CSF leak	5/24 (20.8%)
Patients with no postoperative CSF leak	19/24 (79.2%)

Quantitative variables are expressed in median (range); qualitative variables are expressed in absolute numbers (proportion).

18 patients. In 2 patients, a postoperative leak occurred 5 and 6 days after surgery, in the context of nose blowing.

In contrast, 11/29 (37.9%) of patients had a well-identified intraoperative leak requiring a dedicated closure technique, as detailed in Table 2. The majority of these 11 patients had preoperative risk factors (n=7/11, 63.6%), mostly with BMI >40. Diaphragm oozing, low-flow leak and high-flow were identified in 2/11 (18.2%), 4/11 (36.4%) and 5/11 (45.4%) of patients respectively. All these 11 patients were reoperated on, using an intrasellar fascia and muscle graft combined with external lumbar drainage in 3 patients (before 2014) and Foley-catheter or mucosal flap in 2 patients (after 2014). A permanent lumboperitoneal shunt was needed in 2 patients. No difference in postoperative leak rate was observed after the change of our surgical strategy in 2014 (5 patients identified before 2014 and 6 patients identified after 2014). Considering the 11 patients with both intra and postoperative leak and all 319 patients with intraoperative leak, the rate of failed closure was 3.4%. The closure failure was mainly due to poor analysis of intraoperative CSF flow.

Postoperative meningitis

Meningitis occurred in 24/3015 (0.8%) of patients. Aseptic meningitis, diagnosed on the basis of fever, clinical symptoms and repeated CSF examinations (cells increase, low glucose, high protein), was found in 14/24 (58.3%) of patients, while septic meningitis with a well-documented bacteriological analysis was reported in 10/24 (41.7%) of patients. CSF examination revealed Gram-positive bacteria in 6 patients (Coagulase-negative staphylococci in 4 patients and Staphyloccocus aureus in 2 patients) and Gram-negative in 4 patients (Klebsiella pneumonia in 3 patients and Escherichia coli in 1 patient). All patients were treated with antibiotic therapy and had a favorable outcome.

Intraoperative leak was observed in 19/24 (79.2%) of patients with meningitis, while postoperative leak was observed in 5/24 (20.8%) of patients.

Discussion

This paper focuses on the evaluation of the closure step in pituitary surgery, based on a large series of 3015 adenoma patients treated with a mononostril endoscopic endonasal transsellar approach by the same expert surgical team. In PitNETs, invasion of the basal dura, cavernous sinus and/or diaphragm is encountered in up to 35% of patients (2), explaining the substantial occurrence of intraoperative leak requiring reliable watertight closure techniques. Initially the endoscopic technique was associated with high reported rates of postoperative CSF leak, ranging from 30 to 40% (47). With advances in endoscopic pituitary surgery and the development of new reconstruction techniques, optimized lower rates <10 % are currently reported (24, 40, 48–50). The present study demonstrates that our stepwise strategy is safe, reliable and effective. Applying our decision strategy, our rates of postoperative CSF leak and meningitis were 1% and 0.8% respectively, which compares favorably with the best rates previously reported (34, 51).

In pituitary surgery, the crucial step of closure should be anticipated. The neurosurgeon should keep in mind that the closure step already begins during the approach. Even if no intraoperative leak occurs, the overall concept is to preserve a good epidural space during the approach and to recreate a sellar floor whenever possible. Indeed, sellar floor closure is useful to identify bony landmarks in the event of a later second surgery and may limit the risk of postoperative CSF leak related to a secondary stall of the diaphragm during sneezing or blowing. During the approach, the sellar floor is opened is such a way that the bone opening is larger than the dural opening, in order to preserve the epidural space (34, 38, 52). When possible, an autologous bone graft is removed and preserved from the sphenoidal rostrum and/or one of a sphenoid sinus septation. If no bone graft is available, a synthetic resorbable polydioxanone (PDS) plate can be used with similar shaping and positioning (53). We choose to use the PDS material because of its stiffness, which is close to that of bone. We recommend the use of a resorbable sellar floor substitute to limit the risk of infectious complications.

In case of intraoperative CSF leak, our patients were divided into two groups on the basis of selected preoperative risk factors of closure failure (28, 29, 43). A specific gradual closure strategy was planned accordingly. Interestingly, other preoperative risk factors of closure failure have been reported recently by expert teams, such as suprasellar extension, chronic respiratory disease, type of sellar barrier, fibrous consistency, dumbbell-shape or

TABLE 2 Characteristics of the 11 patients with failed closure management despite a well-identified intraoperative CSF leak.

Patient	Age	Sex	Date of Surgery	Nb of surgeries	BMI>40	Lysis of sellar floor	Skull base destruction	Giant tumor	Prior radio-therapy	CSF Flow	First closure strategy	Meningitis	Second closure strat-egy	Hypothesis forclosure failure
1	57	M	2008	1	1	1	1	1	0	Oozing	Surgicel	0	Intrasellar graft	Poor material selection
2	42	M	2009	2	0	1	1	1	0	High	Intrasellar graft	1	Intrasellar graft + External lumbar drain Lumboperitoneal shunt	Poor graft design
3	43	M	2008	2	0	1	1	1	1	High	Intrasellar graft	0	Intrasellar graft + External lumbar drain Lumboperitoneal shunt	Poor graft design
4	68	M	2012	1	0	0	0	0	0	High	Epidural graft	0	Intrasellar graft + External lumbar drain	Poor choice of closure strategy
5	79	F	2013	1	0	0	0	0	0	Oozing	Tachosil	0	Intrasellar graft	Poor analysis of CSF flow
6	37	F	2015	1	1	0	0	0	0	Low	Epidural graft	0	Intrasellar graft	Poor analysis of CSF flow
7	51	F	2015	2	1	1	0	0	0	High	Intrasellar graft	0	Intrasellar graft + Foley catheter	Poor evaluation of predictive factor
8	43	F	2018	1	1	0	0	0	0	Low	Epidural graft	0	Intrasellar graft	Poor analysis of CSF flow
9	22	M	2019	2	0	0	0	0	0	Low	Epidural graft	1	Intrasellar graft	Poor analysis of CSF flow
10	59	M	2019	1	0	0	0	0	0	Low	Epidural graft	0	Intrasellar graft	Poor analysis of CSF flow
11	27	M	2019	1	1	1	1	1	0	High	Intrasellar graft	0	Intrasellar graft+ Mucosal flap	Poor evaluation of predictive factor

10.3389/fonc.2022.1067312

lobulated asymmetrical configuration (42). A comprehensive analysis of all these factors should allow surgical management to be tailored to the individual patient.

In patients with no risk factor, the objective is to achieve a watertight closure and reconstruct the sellar floor. Different materials have been proposed for the reconstruction of skull-base defects. Autologous materials have been proposed, such as mucosal grafts from middle turbinate, fat grafts from abdominal region, muscle graft from lateral thigh, fascia grafts from fascia lata, lateral thigh or temporal muscle (31, 32, 48, 53–58). Heterologous biologic dural substitutes have been used, such as equine pericardium sheet (59) or human-derived acellular dermal matrix (60). Heterologous synthetic dural substitutes have also been proposed, such as polyester-silicone (61), resorbable polyglactin acid sheet (62), polytetrafluoroethylene (63) or collagen matrix (64, 65). At the end of the closure procedure, fibrin glue should is usually applied inside the sphenoidal cavity to fill the dead spaces (66–68). In our strategy, the key objective was to minimize the risk of postoperative leak while minimizing the proportion of patients treated by packing the sella or sphenoid sinus. Indeed, packing the sellar area with additional fibrous scar tissue may impact on postoperative MRI analysis and alter the quality of surgical landmarks in case of repeated surgeries. The choice of the closure technique depends on the flow intensity and on the leak location, as proposed by Conger et al. (34). In case of minimal diaphragm oozing, a simple treatment with a collagen sponge can be chosen (64, 66, 69). Collagen sponge has the great advantage to be easy to use. However, if the CSF is underestimated, this closure technique will be insufficient and a postoperative CSF leak will occur, requiring a second surgery. We therefore recommend spending a lot of time analyzing the intensity of CSF flow and adopting a safer alternative reconstruction strategy when in doubt. Focal low-flow intraoperative leak requires a stronger closure strategy: although an adequate epidural graft is more complex to perform, this strategy is well suited in this case, with a high rate of watertight closure without intrasellar packing. An epidural duraplasty can be performed, using a dural substitute, such as mucosa from a middle turbinate or fascia lata, held in place by a rigid buttress, as previously reported under different names, such as the gasket seal technique (34, 52, 70). However, the surgeon should be aware that if part of this duraplasty is positioned inside the intradural intrasellar space, the strategy will not prevent a postoperative leak. In our experience, the graft will paradoxically have a "gutter effect" with an increased risk of postoperative leak. Of note, in rare cases of focal diaphragm defect with a distended diaphragm bulging into the intrasellar space, a watertight closure can be elegantly obtained by coagulating the edges of the transdiaphragmatic orifice with bipolar forceps. In case of high-flow leak, the objective is to achieve a strong and persistent watertight closure with an intrasellar packing. Some authors recommend to use intrasellar fat and glue (33, 57, 71–75) with low rates of postoperative leak. In our experience, we prefer to use a fascia and muscle graft to achieve a two-layer intrasellar repair: the fascia is introduced into the sella and applied superiorly to cover the entire defect, in order to recreate a new diaphragm; the muscle graft is then positioned in the intrasellar compartment. Special care must be taken in the design of the muscle graft to avoid significant mass effect with compression of the optic chiasma.

In patients with risk factors, more complex strategies should be decided. In case of sellar floor lysis, bone may be missing, which is why no solid epidural buttress can be performed. Solutions with a buttress positioned within the sphenoid sinus have been developed. Some authors proposed a fat buttress to pack the sphenoid sinus (33, 57, 76, 77). The disadvantage of this technique is that the counterpressure is not applied in a targeted manner against the sellar floor and the fibrous scarring may complicate the surgical approach if further intervention is required. For these reasons, we prefer to use a Foley balloon catheter inflated within the sphenoid sinus for a few days, as previously described (78). Thus, the transient buttress is directly applied against the sella floor until the intrasellar muscle graft can no longer move. In more complex patients with giant tumors and large dural defects, a multilayer strategy with mucosal flap is usually recommended. Vascularized grafts have been a surgical revolution in preventing postoperative CSF leak, especially in patients with risk factors (24, 25, 48, 49, 79, 80). Different types of vascularized grafts have been described: unilateral or bilateral mucosal flaps originating from nasal septum or inferior turbinate; pericranium or temporal fascia flaps (45, 46, 48, 53, 54, 56, 81, 82). The choice of using vascularized flaps involves more complex skull base reconstruction techniques with multilayered closure and should balance the risk of postoperative CSF leak versus the morbidity of the flap itself (30, 83–85).

All 29 patients with postoperative CSF leak were reoperated with a dedicated upgraded closure strategy. Our management has evolved over the time. Indeed, the use of external lumbar drainage in these patients is associated with a higher risk of complication (86, 87). Of note, as previously reported, there is a lack of statistically significant improvement between patients with lumbar drains and patients with no lumbar drains and graded reconstruction strategies without lumbar drainage have been proposed (39, 88–90). Today, external lumbar drainage has been abandoned for the overwhelming majority of our patients treated with simple transsellar approach.

Postoperative CSF leak occurred in 18 patients with no intraoperative CSF leak identified. In 2 patients, the postoperative leak was obviously caused by inappropriate postoperative nose blowing. In 16 patients, the complication may have been due to intraoperative surgical misinterpretation, related to unnoticed diaphragm oozing.

Despite of our closure strategy, surgery failed in 11 patients with a well-identified intraoperative CSF leak, leading to an

overall closure failure rate of 3.4%. Interestingly, most of the patients were treated before 2018, suggesting that this type of complication may decrease with endoscopic surgical experience, as previously proposed (91). Firstly, lack of experience with endoscopic techniques may have led to poor material selection or poor graft design, as previously reported (92–94). Secondly, the majority of these patients had at least one risk factor of closure failure. Thus, surgical failure was also explained by underestimated risk factors, such as severe obesity; BMI>40 is associated with increased intracranial pressure (44), which may affect the quality of closure (29). In patients with BMI>40 and focal sellar floor lysis, we now recommend the use of an additional Foley-catheter combined with repeated lumbar punctures, even if no CSF occurred during surgery. Closure failure was finally caused by poor operative conditions reducing the quality of vision and impacting on the analysis of CSF flow.

Our rate of postoperative meningitis was 0.8%, with a majority of aseptic meningitis. This result is in accordance with previous studies from pituitary centers of excellence (51, 95). In patients with no identified bacteria, antibiotic treatment was indicated on the basis of combined neurological symptoms (fever, meningeal syndrome) and analysis of repeated CSF examinations (cells increase, low glucose, high protein). These patients may have been overtreated. Nevertheless, all symptoms improved immediately after treatment was introduced, suggesting that a small bacterial inoculum was still present. In patients with septic meningitis, drug-sensitive Gram-positive positive organisms were predominant. All patients were treated by antibiotic therapy, with favorable outcome. Our results confirmed the data published by Jin et al. in a large retrospective study of 3242 patients (51). Interestingly, the vast majority of our patients (79.2%) with meningitis had a well-identified intraoperative leak, whereas a postoperative CSF leak was observed in only 20.8% of these patients. This result may suggest that the duration of CSF leak is not a strong predictor of postoperative meningitis. More data are needed to confirm this finding.

The main strength of this major study was the consecutive inclusion of all cases of adenoma patients treated with an endoscopic endonasal transsellar approach, reaching the substantial number of 3015 patients. Conversely, the inclusion of patients operated on by a single surgical team may be considered as a limitation. However, as mainly reported, the high expertise of surgical centers is essential (92, 96, 97). In this series, all patients were operated on by two experienced neurosurgeons treating >200 adenomas per year, after surgical indication was validated in a multidisciplinary meeting. If the expertise is not guaranteed, it can be hypothesized that outcome would become less favorable. Thus, at the beginning of the learning curve or if there is any doubt about a high-flow leak, safety should be paramount and intrasellar packing should be chosen. Due to the length of the study, our list of predictive factors is not exhaustive, which is a limitation of the present work. The main objective was to propose a graded closure strategy with excellent efficacy, based on our significant experience. Further studies with stronger decision-making paradigms, including more predictive factors, are needed in the future.

In conclusion, in pituitary surgery, the closure step should not be underestimated. By using a rigorous strategy, the postoperative leak rate can be reduced to 1% of patients. This crucial step must be planned before surgery and gently prepared during the surgical approach.

Data availability statement

The raw data supporting the conclusions of this article will be made available by the authors, without undue reservation.

Ethics statement

In accordance with the French legislation, patient consent was not needed for this retrospective non-interventional study evaluating a routine care. An agreement was obtained after ethical acceptance of the study by the General Register of the Assistance Publique des Hôpitaux de Paris - Sorbonne University (registered under “CLOSPIT” Study, N°: 202211210146).

Author contributions

BB, AV, and SG contributed to conception and design of the study. BB, AJ, and AV organized the database. BB and AJ performed the statistical analysis. AV wrote the first draft of the manuscript. BB, AV, AJ, GR, and SG wrote sections of the manuscript. BB, AJ, GR, and SG contributed to interpretation of data for work. All authors contributed to manuscript revision, read, and approved the submitted version

Acknowledgments

We thank Pr Paolo Cappabianca for his thoughtful and expert comments. We thank Dr Charlotte Bellamy for her useful grammar and spelling corrections.

Conflict of interest

The authors declare that the research was conducted in the absence of any commercial or financial relationships that could be construed as a potential conflict of interest.

Publisher's note

References

1. Ezzat S, Asa SL, Couldwell WT, Barr CE, Dodge WE, Vance ML, et al. The prevalence of pituitary adenomas: A systematic review. *Cancer* (2004) 101:613–9. doi: 10.1002/cncr.20412

2. Trouillas J, Jaffrain-Rea M-L, Vasiljevic A, Raverot G, Roncaroli F, Villa C. How to classify the pituitary neuroendocrine tumors (PitNET)s in 2020. *Cancers (Basel)* (2020) 12:E514. doi: 10.3390/cancers12020514

3. Asa SL, Casar-Borota O, Chanson P, Delgrange E, Earls P, Ezzat S, et al. From pituitary adenoma to pituitary neuroendocrine tumor (PitNET): An international pituitary pathology club proposal. *Endocr Relat Cancer* (2017) 24:C5–8. doi: 10.1530/ERC-17-0004

4. Laws ER, Penn DL, Repetti CS. Advances and controversies in the classification and grading of pituitary tumors. *J Endocrinol Invest* (2019) 42:129–35. doi: 10.1007/s40618-018-0901-5

5. Dekkers OM, Karavitaki N, Pereira AM. The epidemiology of aggressive pituitary tumors (and its challenges). *Rev Endocr Metab Disord* (2020) 21:209–12. doi: 10.1007/s11154-020-09556-7

6. Neou M, Villa C, Armignacco R, Jouinot A, Raffin-Sanson M-L, Septier A, et al. Pangenomic classification of pituitary neuroendocrine tumors. *Cancer Cell* (2020) 37:123–134.e5. doi: 10.1016/j.ccell.2019.11.002

7. Vroonen L, Daly AF, Beckers A. Epidemiology and management challenges in prolactinomas. *Neuroendocrinology* (2019) 109:20–7. doi: 10.1159/000497746

8. Melmed S, Casanueva FF, Hoffman AR, Kleinberg DL, Montori VM, Schlechte JA, et al. Diagnosis and treatment of hyperprolactinemia: An endocrine society clinical practice guideline. *J Clin Endocrinol Metab* (2011) 96:273–88. doi: 10.1210/jc.2010-1692

9. Cushing H. III. partial hypophysectomy for acromegaly: With remarks on the function of the hypophysis. *Ann Surg* (1909) 50:1002–17. doi: 10.1097/00000658-190912000-00003

10. Jane JA, Catalino MP, Laws ER. Surgical treatment of pituitary adenomas, in: *Endotext* (2000). South Dartmouth (MA: MDText.com, Inc. Available at: http://www.ncbi.nlm.nih.gov/books/NBK278983/ (Accessed May 9, 2021).

11. Liu JK, Weiss MH, Couldwell WT. Surgical approaches to pituitary tumors. *Neurosurg Clin N Am* (2003) 14:93–107. doi: 10.1016/s1042-3680(02)00033-5

12. Buchfelder M, Schlaffer S. Surgical treatment of pituitary tumours. *Best Pract Res Clin Endocrinol Metab* (2009) 23:677–92. doi: 10.1016/j.beem.2009.05.002

13. Youssef AS, Agazzi S, van Loveren HR. Transcranial surgery for pituitary adenomas. *Neurosurgery* (2005) 57:168–75. doi: 10.1227/01.neu.0000163602.05663.86

14. Guiot G, Derome P. Surgical approaches to hypophyseal adenomas. *Rev Otoneuroophtalmol* (1974) 46:337–46.

15. Hardy J. Transphenoidal microsurgery of the normal and pathological pituitary. *Clin Neurosurg* (1969) 16:185–217. doi: 10.1093/neurosurgery/16.cn_suppl_1.185

16. Patel SK, Husain Q, Eloy JA, Couldwell WT, Liu JK. Norman Dott, Gerard guiot, and Jules hardy: Key players in the resurrection and preservation of transsphenoidal surgery. *Neurosurg Focus* (2012) 33:E6. doi: 10.3171/2012.6.FOCUS12125

17. Li A, Liu W, Cao P, Zheng Y, Bu Z, Zhou T. Endoscopic versus microscopic transsphenoidal surgery in the treatment of pituitary adenoma: A systematic review and meta-analysis. *World Neurosurg* (2017) 101:236–46. doi: 10.1016/j.wneu.2017.01.022

18. Gaillard S. The transition from microscopic to endoscopic transsphenoidal surgery in high-caseload neurosurgical centers: The experience of foch hospital. *World Neurosurg* (2014) 82:S116–120. doi: 10.1016/j.wneu.2014.07.033

19. Eseonu CI, ReFaey K, Rincon-Torroella J, Garcia O, Wand GS, Salvatori R, et al. Endoscopic versus microscopic transsphenoidal approach for pituitary adenomas: Comparison of outcomes during the transition of methods of a single surgeon. *World Neurosurg* (2017) 97:317–25. doi: 10.1016/j.wneu.2016.09.120

20. Baussart B, Declerck A, Gaillard S. Mononostril endoscopic endonasal approach for pituitary surgery. *Acta Neurochir (Wien)* (2021) 163:655–9. doi: 10.1007/s00701-020-04542-z

21. Rotenberg B, Tam S, Ryu WHA, Duggal N. Microscopic versus endoscopic pituitary surgery: a systematic review. *Laryngoscope* (2010) 120:1292–7. doi: 10.1002/lary.20949

22. Asemota AO, Ishii M, Brem H, Gallia GL. Comparison of complications, trends, and costs in endoscopic vs microscopic pituitary surgery: Analysis from a US health claims database. *Neurosurgery* (2017) 81:458–72. doi: 10.1093/neuros/nyx350

23. Naunheim MR, Sedaghat AR, Lin DT, Bleier BS, Holbrook EH, Curry WT, et al. Immediate and delayed complications following endoscopic skull base surgery. *J Neurol Surg B Skull Base* (2015) 76:390–6. doi: 10.1055/s-0035-1549308

24. Fraser S, Gardner PA, Koutourousiou M, Kubik M, Fernandez-Miranda JC, Snyderman CH, et al. Risk factors associated with postoperative cerebrospinal fluid leak after endoscopic endonasal skull base surgery. *J Neurosurg* (2018) 128:1066–71. doi: 10.3171/2016.12.JNS1694

25. Karnezis TT, Baker AB, Soler ZM, Wise SK, Rereddy SK, Patel ZM, et al. Factors impacting cerebrospinal fluid leak rates in endoscopic sellar surgery. *Int Forum Allergy Rhinol* (2016) 6:1117–25. doi: 10.1002/alr.21783

26. Klatt-Cromwell CN, Thorp BD, Del Signore AG, Ebert CS, Ewend MG, Zanation AM. Reconstruction of skull base defects. *Otolaryngol Clin North Am* (2016) 49:107–17. doi: 10.1016/j.otc.2015.09.006

27. Patel PN, Stafford AM, Patrinely JR, Smith DK, Turner JH, Russell PT, et al. Risk factors for intraoperative and postoperative cerebrospinal fluid leaks in endoscopic transsphenoidal sellar surgery. *Otolaryngol Head Neck Surg* (2018) 158:952–60. doi: 10.1177/0194599818756272

28. Jahangiri A, Wagner J, Han SW, Zygourakis CC, Han SJ, Tran MT, et al. Morbidity of repeat transsphenoidal surgery assessed in more than 1000 operations. *J Neurosurg* (2014) 121:67–74. doi: 10.3171/2014.3.JNS131532

29. Dlouhy BJ, Madhavan K, Clinger JD, Reddy A, Dawson JD, O'Brien EK, et al. Elevated body mass index and risk of postoperative CSF leak following transsphenoidal surgery. *J Neurosurg* (2012) 116:1311–7. doi: 10.3171/2012.2.JNS111837

30. Peris-Celda M, Chaskes M, Lee DD, Kenning TJ, Pinheiro-Neto CD. Optimizing sellar reconstruction after pituitary surgery with free mucosal graft: Results from the first 50 consecutive patients. *World Neurosurg* (2017) 101:180–5. doi: 10.1016/j.wneu.2017.01.102

31. Mattavelli D, Schreiber A, Villaret AB, Accorona R, Turri-Zanoni M, Lambertoni A, et al. Complications and donor site morbidity of 3-layer reconstruction with iliotibial tract of the anterior skull base: Retrospective analysis of 186 patients. *Head Neck* (2018) 40:63–9. doi: 10.1002/hed.24931

32. Patel MR, Stadler ME, Snyderman CH, Carrau RL, Kassam AB, Germanwala AV, et al. How to choose? endoscopic skull base reconstructive options and limitations. *Skull Base* (2010) 20:397–404. doi: 10.1055/s-0030-1253573

33. Esposito F, Dusick JR, Fatemi N, Kelly DF. Graded repair of cranial base defects and cerebrospinal fluid leaks in transsphenoidal surgery. *Oper Neurosurg (Hagerstown)* (2007) 60:295–303. doi: 10.1227/01.NEU.0000255354.64077.66

34. Conger A, Zhao F, Wang X, Eisenberg A, Griffiths C, Esposito F, et al. Evolution of the graded repair of CSF leaks and skull base defects in endonasal endoscopic tumor surgery: trends in repair failure and meningitis rates in 509 patients. *J Neurosurg* (2018) 130:861–75. doi: 10.3171/2017.11.JNS172141

35. Patel KS, Komotar RJ, Szentirmai O, Moussazadeh N, Raper DM, Starke RM, et al. Case-specific protocol to reduce cerebrospinal fluid leakage after endonasal endoscopic surgery. *J Neurosurg* (2013) 119:661–8. doi: 10.3171/2013.4.JNS13124

36. Strickland BA, Lucas J, Harris B, Kulubya E, Bakhsheshian J, Liu C, et al. Identification and repair of intraoperative cerebrospinal fluid leaks in endonasal transsphenoidal pituitary surgery: surgical experience in a series of 1002 patients. *J Neurosurg* (2018) 129:425–9. doi: 10.3171/2017.4.JNS162451

37. CRANIAL Consortium. CSF rhinorrhoea after endonasal intervention to the skull base (CRANIAL) - part 1: Multicenter pilot study. *World Neurosurg* (2021) 149:e1077–89. doi: 10.1016/j.wneu.2020.12.171

38. Tabaee A, Anand VK, Brown SM, Lin JW, Schwartz TH. Algorithm for reconstruction after endoscopic pituitary and skull base surgery. *Laryngoscope* (2007) 117:1133–7. doi: 10.1097/MLG.0b013e31805c08c5

39. Ha C-M, Hong SD, Choi JW, Seol HJ, Nam D-H, Lee J-I, et al. Graded reconstruction strategy using a multilayer technique without lumbar drainage after endoscopic endonasal surgery. *World Neurosurg* (2021) 158:e451–8. doi: 10.1016/j.wneu.2021.11.003

40. Ogiwara T, Nagm A, Hasegawa T, Hanaoka Y, Ichinose S, Goto T, et al. Pitfalls of skull base reconstruction in endoscopic endonasal approach. *Neurosurg Rev* (2019) 42:683–9. doi: 10.1007/s10143-018-1006-5

41. Dorismond C, Santarelli GD, Thorp BD, Kimple AJ, Ebert CS, Zanation AM. Heterogeneity in outcome reporting in endoscopic endonasal skull base reconstruction: A systematic review. *J Neurol Surg B Skull Base* (2021) 82:506–21. doi: 10.1055/s-0040-1714108

42. Villalonga JF, Solari D, Cavallo LM, Cappabianca P, Prevedello DM, Carrau R, et al. The sellar barrier on preoperative imaging predicts intraoperative cerebrospinal fluid leak: a prospective multicenter cohort study. *Pituitary* (2021) 24:27–37. doi: 10.1007/s11102-020-01082-8

43. Staartjes VE, Zattra CM, Akeret K, Maldaner N, Muscas G, Bas van Niftrik CH, et al. Neural network-based identification of patients at high risk for intraoperative cerebrospinal fluid leaks in endoscopic pituitary surgery. *J Neurosurg* (2019), 21:1–7. doi: 10.3171/2019.4.JNS19477

44. Subramaniam S, Fletcher WA. Obesity and weight loss in idiopathic intracranial hypertension: A narrative review. *J Neuroophthalmol* (2017) 37:197–205. doi: 10.1097/WNO.0000000000000448

45. Baussart B, Racy E, Gaillard S. Double pedicled nasoseptal flap for skull base repair after endoscopic expanded endonasal approach. *Acta Neurochir* (2022) 164 (4):1111–4. doi: 10.1007/s00701-021-05094-6

46. Nyquist GG, Anand VK, Singh A, Schwartz TH. Janus flap: bilateral nasoseptal flaps for anterior skull base reconstruction. *Otolaryngol Head Neck Surg* (2010) 142:327–31. doi: 10.1016/j.otohns.2009.12.020

47. Kassam A, Carrau RL, Snyderman CH, Gardner P, Mintz A. Evolution of reconstructive techniques following endoscopic expanded endonasal approaches. *Neurosurg Focus* (2005) 19:E8.

48. Hadad G, Bassagasteguy L, Carrau RL, Mataza JC, Kassam A, Snyderman CH, et al. A novel reconstructive technique after endoscopic expanded endonasal approaches: Vascular pedicle nasoseptal flap. *Laryngoscope* (2006) 116:1882–6. doi: 10.1097/01.mlg.0000234933.37779.e4

49. Harvey RJ, Parmar P, Sacks R, Zanation AM. Endoscopic skull base reconstruction of large dural defects: a systematic review of published evidence. *Laryngoscope* (2012) 122:452–9. doi: 10.1002/lary.22475

50. Schuss P, Hadjiathanasiou A, Klingmüller D, Güresir Á, Vatter H, Güresir E. Transsphenoidal pituitary surgery: Comparison of two sellar reconstruction techniques and their effect on postoperative cerebrospinal fluid leakage. *Neurosurg Rev* (2018) 41:1053–8. doi: 10.1007/s10143-018-0949-x

51. Jin Y, Liu X, Gao L, Guo X, Wang Q, Bao X, et al. Risk factors and microbiology of meningitis and/or bacteremia after transsphenoidal surgery for pituitary adenoma. *World Neurosurg* (2018) 110:e851–63. doi: 10.1016/j.wneu.2017.11.125

52. Garcia-Navarro V, Anand VK, Schwartz TH. Gasket seal closure for extended endonasal endoscopic skull base surgery: efficacy in a large case series. *World Neurosurg* (2013) 80:563–8. doi: 10.1016/j.wneu.2011.08.034

53. Di Perna G, Penner F, Cofano F, De Marco R, Baldassarre BM, Portonero I, et al. Skull base reconstruction: A question of flow? a critical analysis of 521 endoscopic endonasal surgeries. *PloS One* (2021) 16:e0245119. doi: 10.1371/journal.pone.0245119

54. Hannan CJ, Kelleher E, Javadpour M. Methods of skull base repair following endoscopic endonasal tumor resection: A review. *Front Oncol* (2020) 10:1614. doi: 10.3389/fonc.2020.01614

55. Kimple AJ, Leight WD, Wheless SA, Zanation AM. Reducing nasal morbidity after skull base reconstruction with the nasoseptal flap: Free middle turbinate mucosal grafts. *Laryngoscope* (2012) 122:1920–4. doi: 10.1002/lary.23325

56. Reyes C, Mason E, Solares CA. Panorama of reconstruction of skull base defects: from traditional open to endonasal endoscopic approaches, from free grafts to microvascular flaps. *Int Arch Otorhinolaryngol* (2014) 18:S179–186. doi: 10.1055/s-0034-1395268

57. Roca E, Penn DL, Safain MG, Burke WT, Castlen JP, Laws ER. Abdominal fat graft for sellar reconstruction: Retrospective outcomes review and technical note. *Oper Neurosurg (Hagerstown)* (2019) 16:667–74. doi: 10.1093/ons/opy219

58. Sciarretta V, Mazzatenta D, Ciarpaglini R, Pasquini E, Farneti G, Frank G. Surgical repair of persisting CSF leaks following standard or extended endoscopic transsphenoidal surgery for pituitary tumor. *Minim Invasive Neurosurg* (2010) 53:55–9. doi: 10.1055/s-0029-1246161

59. Cavallo LM, Solari D, Somma T, Di Somma A, Chiaramonte C, Cappabianca P. Use of equine pericardium sheet (LYOMESH®) as dura mater substitute in endoscopic endonasal transsphenoidal surgery. *Transl Med UniSa* (2013) 7:23–8.

60. Gaynor BG, Benveniste RJ, Lieberman S, Casiano R, Morcos JJ. Acellular dermal allograft for sellar repair after transsphenoidal approach to pituitary adenomas. *J Neurol Surg B Skull Base* (2013) 74:155–9. doi: 10.1055/s-0033-1338263

61. Cappabianca P, Cavallo LM, Mariniello G, de Divitiis O, Romero AD, de Divitiis E. Easy sellar reconstruction in endoscopic endonasal transsphenoidal surgery with polyester-silicone dural substitute and fibrin glue: Technical note. *Neurosurgery* (2001) 49:473–5. doi: 10.1097/00006123-200108000-00042

62. Yano S, Tsuiki H, Kudo M, Kai Y, Morioka M, Takeshima H, et al. Sellar repair with resorbable polyglactin acid sheet and fibrin glue in endoscopic endonasal transsphenoidal surgery. *Surg Neurol* (2007) 67:59–64. doi: 10.1016/j.surneu.2006.05.049

63. Sherman JH, Pouratian N, Okonkwo DO, Jane JA, Laws ER. Reconstruction of the sellar dura in transsphenoidal surgery using an expanded polytetrafluoroethylene dural substitute. *Surg Neurol* (2008) 69:73–6. doi: 10.1016/j.surneu.2007.07.069

64. Jiménez Zapata HD, Rodríguez Berrocal V, Vior Fernández C, Sánchez FM, García Fernández A. Sellar diaphragm reconstruction with tachosil during endoscopic endonasal surgery: Technical note. *J Neurol Surg B Skull Base* (2020) 81:275–9. doi: 10.1055/s-0039-1688781

65. Shahein M, Montaser AS, Barbero JMR, Maza G, Todeschini AB, Otto BA, et al. Collagen matrix with mucoperiosteum graft as an effective fatless flapless reconstruction after endoscopic pituitary adenoma resection. *Oper Neurosurg (Hagerstown)* (2020) 19:E573–80. doi: 10.1093/ons/opaa212

66. Esposito F, Angileri FF, Kruse P, Cavallo LM, Solari D, Esposito V, et al. Fibrin sealants in dura sealing: A systematic literature review. *PloS One* (2016) 11: e0151533. doi: 10.1371/journal.pone.0151533

67. Cappabianca P, Esposito F, Magro F, Cavallo LM, Solari D, Stella L, et al. Natura abhorret a vacuo–use of fibrin glue as a filler and sealant in neurosurgical "dead spaces". *Tech Acta Neurochir (Wien)* (2010) 152:897–904. doi: 10.1007/s00701-009-0580-2

68. Dusick JR, Mattozo CA, Esposito F, Kelly DF. BioGlue for prevention of postoperative cerebrospinal fluid leaks in transsphenoidal surgery: A case series. *Surg Neurol* (2006) 66:371–6. doi: 10.1016/j.surneu.2006.06.043

69. Spitaels J, Moore J, Zaidman N, Arroteia IF, Appelboom G, Barrit S, et al. Fibrin-coated collagen fleece versus absorbable dural sealant for sellar closure after transsphenoidal pituitary surgery: a comparative study. *Sci Rep* (2022) 12:7998. doi: 10.1038/s41598-022-12059-x

70. Jane JA. "Gasket-seal" closure for cerebrospinal fluid leaks. *World Neurosurg* (2013) 80:491–2. doi: 10.1016/j.wneu.2011.10.007

71. Villalonga JF, Solari D, Guizzardi G, Scala MR, Campero A. Fat and fibrin glue: Quo vadis? *Turk Neurosurg* (2021) 31:238–46. doi: 10.5137/1019-5149.JTN.29712-20.2

72. Ahn S, Park J-S, Kim DH, Kim SW, Jeun S-S. Surgical experience in prevention of postoperative CSF leaks using abdominal fat grafts in endoscopic endonasal transsphenoidal surgery for pituitary adenomas. *J Neurol Surg B Skull Base* (2021) 82:522–7. doi: 10.1055/s-0040-1712179

73. Laws ER. Autograft fat in neurological surgery. *World Neurosurg* (2013) 80:489–90. doi: 10.1016/j.wneu.2012.11.006

74. Ziu M, Jimenez DF. The history of autologous fat graft use for prevention of cerebrospinal fluid rhinorrhea after transsphenoidal approaches. *World Neurosurg* (2013) 80:554–62. doi: 10.1016/j.wneu.2012.08.001

75. Cavallo LM, Solari D, Somma T, Cappabianca P. The 3F (Fat, flap, and flash) technique for skull base reconstruction after endoscopic endonasal suprasellar approach. *World Neurosurg* (2019) 126:439–46. doi: 10.1016/j.wneu.2019.03.125

76. Wei CC, Palmer JN. Planum, tubercular, sellar and clival defects. *Adv Otorhinolaryngol* (2013) 74:119–29. doi: 10.1159/000342288

77. Citardi MJ, Cox AJ, Bucholz RD. Acellular dermal allograft for sellar reconstruction after transsphenoidal hypophysectomy. *Am J Rhinol* (2000) 14:69–73. doi: 10.2500/105065800781602920

78. Cavallo LM, Messina A, Esposito F, de Divitiis O, Dal Fabbro M, de Divitiis E, et al. Skull base reconstruction in the extended endoscopic transsphenoidal approach for suprasellar lesions. *J Neurosurg* (2007) 107:713–20. doi: 10.3171/JNS-07/10/0713

79. Michael AP, Elbuluk O, Tsiouris AJ, Tabaee A, Kacker A, Anand VK, et al. The critical importance of a vascularized flap in preventing recurrence after endoscopic repair of spontaneous cerebrospinal fluid leaks and meningoencephaloceles. *J Neurosurg* (2021), 12:1–8. doi: 10.3171/2021.7.JNS211427

80. Reuter G, Bouchain O, Demanez L, Scholtes F, Martin D. Skull base reconstruction with pedicled nasoseptal flap: Technique, indications, and limitations. *J Craniomaxillofac Surg* (2019) 47:29–32. doi: 10.1016/j.jcms.2018.11.012

81. Boetto J, Labidi M, Watanabe K, Hanakita S, Bouazza S, Passeri T, et al. Combined nasoseptal and inferior turbinate flap for reconstruction of Large skull base defect after expanded endonasal approach: Operative technique. *Oper Neurosurg (Hagerstown)* (2019) 16:45–52. doi: 10.1093/ons/opy046

82. Liu JK, Schmidt RF, Choudhry OJ, Shukla PA, Eloy JA. Surgical nuances for nasoseptal flap reconstruction of cranial base defects with high-flow cerebrospinal fluid leaks after endoscopic skull base surgery. *Neurosurg Focus* (2012) 32:E7. doi: 10.3171/2012.5.FOCUS1255

83. Greig SR, Cooper TJ, Sommer DD, Nair S, Wright ED. Objective sinonasal functional outcomes in endoscopic anterior skull-base surgery: an evidence-based review with recommendations. *Int Forum Allergy Rhinol* (2016) 6:1040–6. doi: 10.1002/alr.21760

84. Shahangian A, Soler ZM, Baker A, Wise SK, Rereddy SK, Patel ZM, et al. Successful repair of intraoperative cerebrospinal fluid leaks improves outcomes in endoscopic skull base surgery. *Int Forum Allergy Rhinol* (2017) 7:80–6. doi: 10.1002/alr.21845

85. Sonnenburg RE, White D, Ewend MG, Senior B. Sellar reconstruction: is it necessary? *Am J Rhinol* (2003) 17:343–6.

86. Moza K, McMenomey SO, Delashaw JB. Indications for cerebrospinal fluid drainage and avoidance of complications. *Otolaryngol Clin North Am* (2005) 38:577–82. doi: 10.1016/j.otc.2005.01.001

87. Stokken J, Recinos PF, Woodard T, Sindwani R. The utility of lumbar drains in modern endoscopic skull base surgery. *Curr Opin Otolaryngol Head Neck Surg* (2015) 23:78–82. doi: 10.1097/MOO.0000000000000119

88. D'Anza B, Tien D, Stokken JK, Recinos PF, Woodard TR, Sindwani R. Role of lumbar drains in contemporary endonasal skull base surgery: Meta-analysis and systematic review. *Am J Rhinol Allergy* (2016) 30:430–5. doi: 10.2500/ajra.2016.30.4377

89. Eloy JA, Kuperan AB, Choudhry OJ, Harirchian S, Liu JK. Efficacy of the pedicled nasoseptal flap without cerebrospinal fluid (CSF) diversion for repair of skull base defects: incidence of postoperative CSF leaks. *Int Forum Allergy Rhinol* (2012) 2:397–401. doi: 10.1002/alr.21040

90. Mehta GU, Oldfield EH. Prevention of intraoperative cerebrospinal fluid leaks by lumbar cerebrospinal fluid drainage during surgery for pituitary macroadenomas. *J Neurosurg* (2012) 116:1299–303. doi: 10.3171/2012.3.JNS112160

91. Castelnuovo P, Mauri S, Locatelli D, Emanuelli E, Delù G, Giulio GD. Endoscopic repair of cerebrospinal fluid rhinorrhea: learning from our failures. *Am J Rhinol* (2001) 15:333–42. doi: 10.1177/194589240101500509

92. Mortini P, Nocera G, Roncelli F, Losa M, Formenti AM, Giustina A. The optimal numerosity of the referral population of pituitary tumors centers of excellence (PTCOE): A surgical perspective. *Rev Endocr Metab Disord* (2020) 21:527–36. doi: 10.1007/s11154-020-09564-7

93. Ciric I, Ragin A, Baumgartner C, Pierce D. Complications of transsphenoidal surgery: results of a national survey, review of the literature, and personal experience. *Neurosurgery* (1997) 40:225–36. doi: 10.1097/00006123-199702000-00001

94. Alobaid A, Dehdashti AR. Hemostasis in skull base surgery. *Otolaryngol Clin North Am* (2016) 49:677–90. doi: 10.1016/j.otc.2016.02.003

95. Pagliano P, Caggiano C, Ascione T, Solari D, Di Flumeri G, Cavallo LM, et al. Characteristics of meningitis following transsphenoidal endoscopic surgery: a case series and a systematic literature review. *Infection* (2017) 45:841–8. doi: 10.1007/s15010-017-1056-6

96. Ciric I, Zhao J-C, Du H, Findling JW, Molitch ME, Weiss RE, et al. Transsphenoidal surgery for cushing disease: experience with 136 patients. *Neurosurgery* (2012) 70:70–80. doi: 10.1227/NEU.0b013e31822dda2c

97. Frara S, Rodriguez-Carnero G, Formenti AM, Martinez-Olmos MA, Giustina A, Casanueva FF. Pituitary tumors centers of excellence. *Endocrinol Metab Clin North Am* (2020) 49:553–64. doi: 10.1016/j.ecl.2020.05.010

frontiers | Frontiers in Oncology

TYPE Case Report
PUBLISHED 04 January 2023
DOI 10.3389/fonc.2022.1059361

OPEN ACCESS

EDITED BY
Carlo Serra,
University Hospital Zürich, Switzerland

REVIEWED BY
Kamil Krystkiewicz,
Copernicus Memorial Hospital, Łódź, Poland
Domenico Solari,
Federico II University Hospital, Italy

*CORRESPONDENCE
Jessica Rossi
jessicarossi.mail@gmail.com

SPECIALTY SECTION
This article was submitted to Neuro-Oncology and Neurosurgical Oncology, a section of the journal Frontiers in Oncology

RECEIVED 01 October 2022
ACCEPTED 05 December 2022
PUBLISHED 04 January 2023

CITATION
Ghezzi A, Rossi J, Cavallieri F, Napoli M, Pascarella R, Rizzi R, Russo M, Salomone G, Romano A, Iaccarino C, Froio E, Serra S, Cozzi S, Giaccherini L, Valzania F and Pisanello A (2023) Case Report: Pituitary metastasis as a presenting manifestation of silent gastric cardia adenocarcinoma. *Front. Oncol.* 12:1059361. doi: 10.3389/fonc.2022.1059361

Case Report: Pituitary metastasis as a presenting manifestation of silent gastric cardia adenocarcinoma

Andrea Ghezzi[1], Jessica Rossi[2,3]*, Francesco Cavallieri[3], Manuela Napoli[4], Rosario Pascarella[4], Romana Rizzi[3], Marco Russo[3], Gaetano Salomone[3], Antonio Romano[5], Corrado Iaccarino[5], Elisabetta Froio[6], Silvia Serra[6], Salvatore Cozzi[7], Lucia Giaccherini[7], Franco Valzania[3] and Anna Pisanello[3]

[1]Department of Biomedical, Metabolic, and Neural Sciences, University of Modena and Reggio Emilia, Modena, Italy, [2]Clinical and Experimental Medicine PhD Program, University of Modena and Reggio Emilia, Modena, Italy, [3]Neuromotor & Rehabilitation Department, Neurology Unit, Azienda USL-IRCCS of Reggio Emilia, Reggio Emilia, Italy, [4]Neuroradiology Service, Department of Diagnostic Imaging and Laboratory Medicine, Azienda USL-IRCCS of Reggio Emilia, Reggio Emilia, Italy, [5]Neurosurgery Unit, Neuromotor and Rehabilitation Department, Azienda USL-IRCCS of Reggio Emilia, Reggio Emilia, Italy, [6]Pathological Anatomy Service, Oncology Department and Advanced Technologies, Azienda USL-IRCCS of Reggio Emilia, Reggio Emilia, Italy, [7]Radiation Oncology Unit, Oncological Department and Advanced Technologies, Azienda USL-IRCCS of Reggio Emilia, Reggio Emilia, Italy

Introduction: Pituitary metastases are very rare in cancer patients and often originate from lung or breast tumors. They usually occur in patients with known metastatic disease, but rarely may be the first presentation of the primary tumor.

Methods: We present the case of a 58 years-old-man who reported a three-month history of polyuria-polydipsia syndrome, generalized asthenia, panhypopituitarism and bitemporal hemianopsia. Brain-MRI showed a voluminous pituitary mass causing posterior sellar enlargement and compression of the surrounding structures including pituitary stalk, optic chiasm, and optic nerves.

Results: The patient underwent neurosurgical removal of the mass. Histological examination revealed a poorly differentiated adenocarcinoma of uncertain origin. A total body CT scan showed a mass in the left kidney that was subsequently removed. Histological features were consistent with a clear cell carcinoma. However, endoscopic examination of the digestive tract revealed an ulcerating and infiltrating adenocarcinoma of the gastric cardia. Total body PET/CT scan with 18F-FDG confirmed an isolated area of accumulation in the gastric cardia, with no hyperaccumulation at other sites.

Conclusion: To the best of our knowledge, there are no reports of pituitary metastases from gastric cardia adenocarcinoma. Our patient presented with symptoms of sellar involvement and without evidence of other body metastases. Therefore, sudden onset of diabetes insipidus and visual deterioration should lead to the suspicion of a rapidly growing pituitary mass, which may be the presenting manifestation of a primary extracranial adenocarcinoma. Histological investigation of the pituitary mass can guide the diagnostic workup, which must however be complete.

KEYWORDS

pituitary metastasis, gastroesophageal junction adenocarcinoma, diabetes insipidus - neurogenic/central, hypopituitarism, visual disturbance

Introduction

Pituitary metastasis (PM) represents only the 0.4% of cerebral metastases and up to the 3.6% of the pituitary tumors. The most frequent primary localizations include breast, lung, kidney, and prostate tumors (1). To the best of our knowledge, there are no reports on pituitary metastases from a gastroesophageal junction (GEJ) adenocarcinoma. GEJ adenocarcinoma arises from the mucosa between 5 cm above and 5 cm below the proximal ends of the gastric folds and is classified by Siewert's classification (2). Its incidence increased in the last decades, especially in western industrialized countries such as North America and Europe (especially in the Northern countries), whereas in Asia the incidence remains relatively low. This is probably due to lifestyle-related risk factors (3).

Here we describe the case of a patient in whom symptoms of pituitary metastasis represented the first manifestation of an occult GEJ adenocarcinoma.

Case description

A 59-year-old man came to our attention reporting a three-months history of progressive polyuria, polydipsia, fatigue, visual blurring, and dizziness. He was diagnosed with diabetes insipidus (DI) and panhypopituitarism and started replacement treatment with desmopressin, levothyroxine and cortisone acetate. His past medical history included the resection of multiple colic adenomas and a latent syphilis. He had no familiar history of cancer. He smoked cigarettes (47 pack/years) from the age of 12, and had an history of alcohol addiction, which he had quitted 15 years earlier. He underwent a brain MRI which showed a voluminous pituitary mass (18.5x19.5x15.5 mm diameter; Figure 1) involving the posterior lobe and the pituitary stalk with suprasellar invasion, causing posterior sellar enlargement, and compression of the surrounding structures including the optic chiasm and the optic tracts, with loss of neurohypophysis signal. These findings were consistent in first hypothesis with a primary pituitary tumor or craniopharyngioma.

An endoscopic endonasal multidisciplinary debulking surgery was performed by a combined approach with an otolaryngologist and a neurosurgeon. The procedure was performed under general anesthesia and preoperative antibiotics administration (cefazolin). Intraoperative magnetic neuronavigation with S7 StealthStation neuronavigation AxiEMTM ENT system (Medtronic, Inc.) is routinely used during this procedure. The patient's head is placed in a horseshoe headrest, slightly elevated, in extension, and slightly turned to the right (towards the operator). Following Povidon-Iodine disinfection, nasal infiltration with local anesthetic and adrenaline solution, with a rigid 0° endoscope (Karl Storz GmbH, Tuttlingen, Germany) a right middle turbinectomy is performed. A pedicled septal mucosa flap was prepared for final closure, and a large anterior sphenoidotomy and posterior septotomy was performed. After drilling planum sphenoidale, the optic carotid junction was exposed on both sides by high-speed drilling of the medial carotid optic processes.

Thus, through a "T shape" incision of the planum and sellar dura, the arachnoid was opened to gain access to the suprasellar lesion with a reddish gray fleshy appearance without any cleavage plane with the optic chiasm and the pituitary stalk. Several lesional samples were carried out suggesting the intraoperative diagnosis of probable metastatic malignant lesion. Therefore, a limited decompressive surgery of the optical pathways using an ultrasonic aspirator (CUSA) was decided as the main surgical strategy. Our closure technique is provided by a free flap of autologous abdominal fascia inlay and overlay of the previously prepared flap of the pedunculated septal mucosa.

Subsequent histologic examination showed a poorly differentiated HER-2-positive adenocarcinoma of uncertain origin (Figure 2). Neoplastic cells showed marked atypia, areas of necrosis and high mitotic index. At the immunohistochemical staining, the neoplasm was positive for CDX2, keratin 7, keratin 20, keratin 19, and negative for PAX8, p63, TTF1 and GATA 3.

A total-body CT scan showed a mass in the left kidney that was subsequently removed. Histological features were consistent with a clear cell carcinoma. However, endoscopic examination of the digestive tract revealed an ulcerating and infiltrating adenocarcinoma of the gastric cardia. Total body PET/CT scan with 18F-FDG confirmed an isolated area of accumulation in the gastric cardia, with no hyperaccumulation at other sites. The patient was discharged with an indication for oncology care. At the time of discharge, neurologic examination showed bitemporal hemianopsia and hyposmia, and Karnofsky Performance Status (KPS) score was 80.

One month later, the patient was readmitted because of visual symptoms worsening. A new brain MRI showed an extension of the post-surgical residual tumor, with compression of optic chiasma, hypothalamus, mammillary bodies, and third ventricle (Figure 3). Therefore, 36 days after surgery, adjuvant radiation therapy was started (single cycle of 5 sessions, 6 Gy for every session, total dose 30 Gy) on the post-surgical residual, followed by six cycles of chemotherapy with cisplatin (115 mg, started 9 days after the end of radiation therapy and converted to carboplatin 400 mg for the last three cycles after the nephrectomy), 5-fluorouracyle (4000 mg/m2) and trastuzumab (6 mg/m2). A follow-up MRI study was performed after 139 days that showed multifocal leptomeningeal dissemination in the posterior cranial fossa (Figure 4).

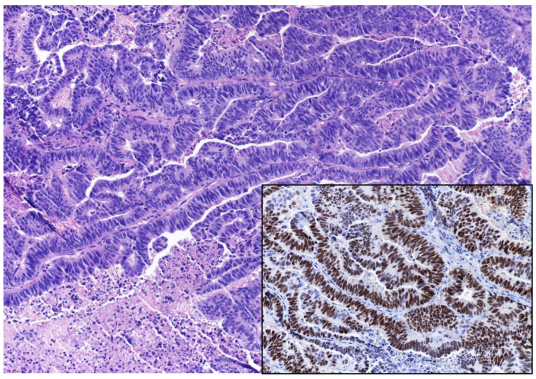

FIGURE 2
Histopathological examination of the sellar mass, consistent with a pituitary localization of an Adenocarcinoma, showing a pseudopapillary and glandular architectural pattern with necrosis and brisk mitotic activity (EE 20x). Insert: Immunostaining for CDX2 (20x).

The patient died 11 months after the onset of the symptoms because of the cranial dissemination of the tumor.

Discussion

Pituitary metastasis is a rare but increasing condition, as survival in patients with cancer has been improving in recent years. Common reported sites of primary tumors are breast (37.2%), lung (24.2%), renal cell (5%) and prostate (5%) (4).

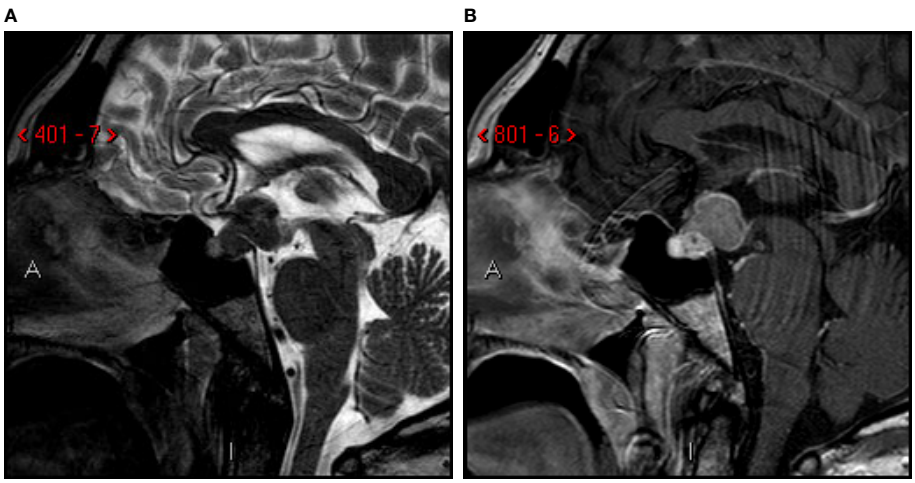

FIGURE 1
First MRI-scan. Sagittal T2-weighted **(A)** and post-contrast T1-weighted **(B)** images. Sellar and suprasellar mass involving posterior lobe and infundibulum of the pituitary gland, with low signal on T2-images. Compression of mammillary body, optic chiasm and tracts, third ventricle (infundibular recess).

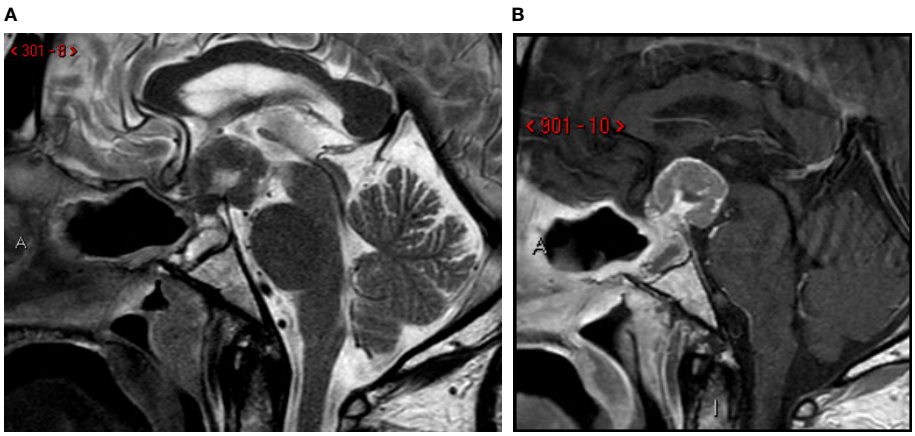

FIGURE 3
One-month follow-up MRI scan. Sagittal T2-weighted **(A)** and post-contrast T1-weighted **(B)** images. Post-surgical sellar modification with increase of the residual tumor in suprasellar spaces, third ventricle invasion and mammillary body compression and infiltration.

The most common sites of GEJ tumor metastasis are lung and liver (5). To the best of our knowledge, this is the first case of pituitary metastasis from gastroesophageal junction (GEJ) adenocarcinoma.

Moreover, whereas the main symptoms in patients with GEJ tumors are dysphagia and weight loss (6), our patient manifested signs of a rapid enlarging sellar mass, without any symptom of gastric or systemic involvement. Diabetes insipidus is one of the

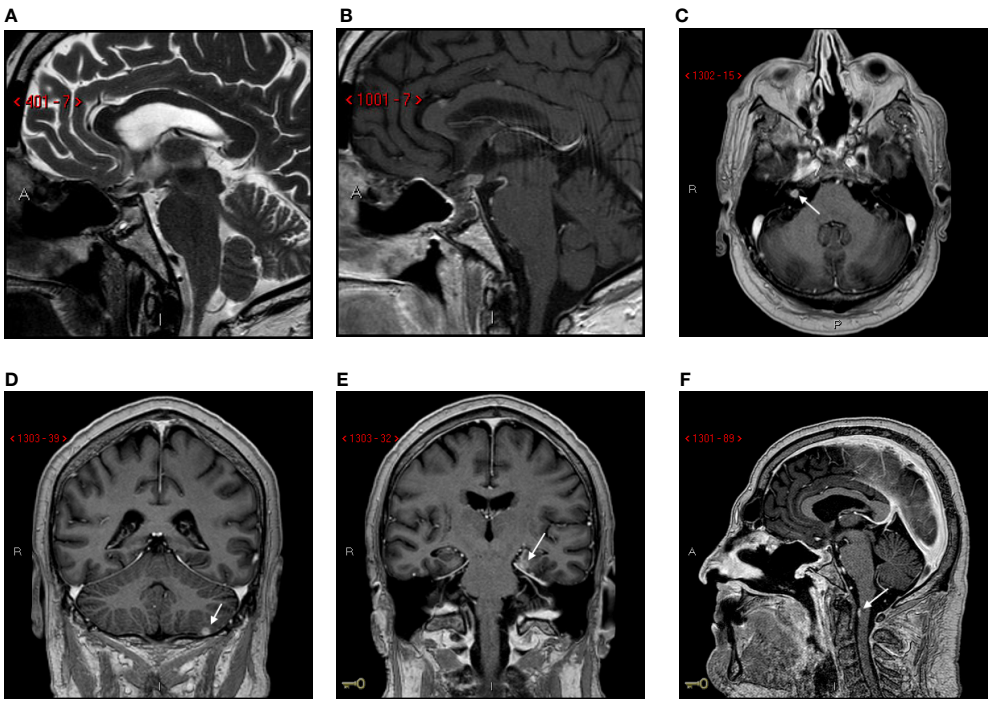

FIGURE 4
Follow-up MRI scan at 139 days. Sagittal T2-Weighted **(A)** and post-contrast T1-weighted **(B)** images. Post-surgical sellar modification with small residual tumor in suprasellar/infundibular region. Axial post-contrast T1-weighted images **(C–F)**: multifocal leptomeningeal dissemination (arrows).

most common symptoms in PM (27.4%), together with visual disturbance (generally bitemporal hemianopsia), fatigue, headache, cranial nerve palsies and anterior pituitary deficiencies such as hypothyroidism and hypocortisolism (7, 8). The frequency of diabetes insipidus in pituitary metastases reflects their predominance in the neurohypophysis, which is due to the lack of direct arterial blood supply to the adenohypophysis, that is nourished through the hypophyseal portal system (8, 9). Conversely, diabetes insipidus is found in only 1% of pituitary adenomas (9) making it a good sign to differentiate between PM and adenomas (9).

Radiologic findings of PM are mostly unspecific. The brain MRI usually shows an isointense or hypointense mass on T1w images and an hyperintense signal in T2w images, with a homogeneous contrast enhancement (9). A mass effect on the third ventricle might cause an hyperintense T2-weighted signal on adjacent brain parenchyma because of the vasogenic edema, as it was the case in our patient. Radiological differential diagnosis of intra- and suprasellar lesions includes: pituitary adenoma, lymphocytic hypophysitis, craniopharyngioma and pituicytoma (10). Lymphocytic hypophysitis in an idiopathic inflammation usually involving the anterior portion of pituitary gland or stalk and is more frequently observed in pregnant or postpartum females (10). Pituicytoma is a rare tumor arising from pituicyte, a specialized glial cell in neurohypophisis and infundibulum, and is difficult to be distinguished from a metastasis if primary tumor is unkown (10). In contrast to primitive pituitary tumors, in particular adenoma and craniopharyngioma, metastases can be distinguished through some characteristic features such a dumbbell shape, an indentation of the diaphragma sellae, sellar erosion without enlargement (due to the rapid growth of metastases versus the remodeling of slow-growing pituitary adenomas) and loss of the posterior bright spot (1, 9). However, radiological evaluation is generally not sufficient to distinguish PM from other lesions. Therefore, histologic examination is crucial, especially in doubtful cases, as in our patient, in whom instrumental investigations did not document other systemic metastases but confirmed the presence of a double pathology (a clear cell renal carcinoma and a gastric cardia adenocarcinoma). Prognosis of patients with PM is unfavorable and depend mostly on aggressiveness of the primary neoplasia (9). The mean overall survival is about 6–7 months (9), as in our case, although most patients die a few months after diagnosis.

We performed research in PubMed, looking for other cases of pituitary metastases and we found 107 cases between case series and single case reports (11–30-33). We found only 7 cases of pituitary metastasis originating from gastroenteric tract (12, 25, 29, 31, 32) and no cases of pituitary metastasis from gastro-esophageal junction adenocarcinoma (Supplementary Table 1).

Conclusions

The pituitary gland can be a site for metastases in patients with gastric cardia adenocarcinoma. Sudden onset of diabetes insipidus in a patient over 50 years of age should always raise the suspicion for PM, regardless of a malignancy history (9). In patients with limited metastatic disease, as well as double pathology, surgery and histological examination are essential to identify the primary tumor and better guide the definition of the prognosis and the most appropriate therapy.

Data availability statement

The original contributions presented in the study are included in the article/Supplementary Material. Further inquiries can be directed to the corresponding author.

Ethics statement

The studies involving human participants were reviewed and approved by the Ethics Committee of Area Vasta Emilia Nord. The patients/participants provided their written informed consent to participate in this study. Written informed consent was obtained from the individual(s) for the publication of any potentially identifiable images or data included in this article.

Author contributions

AG, JR and FC contributed to writing this article and to the literature review. MN and RP provided the neuroradiological images and descriptions. EF and SS provided the pathological images, descriptions and information regarding histological examination. RR, MR, GS, FV and AP contributed with information about the patient's clinical course. AR and CI furnished data regarding surgical procedures. SC and LG contributed with details on radiation therapy. All authors contributed to the article and approved the submitted version.

Funding

This study was partially supported by Italian Ministry of Health – Ricerca Corrente Annual Program 2023.

Conflict of interest

The authors declare that the research was conducted in the absence of any commercial or financial relationships that could be construed as a potential conflict of interest.

Publisher's note

All claims expressed in this article are solely those of the authors and do not necessarily represent those of their affiliated organizations, or those of the publisher, the editors and the reviewers. Any product that may be evaluated in this article, or claim that may be made by its manufacturer, is not guaranteed or endorsed by the publisher.

Supplementary material

The Supplementary Material for this article can be found online at: https://www.frontiersin.org/articles/10.3389/fonc.2022.1059361/full#supplementary-material

References

1. Kameda-Smith MM, Zhang E, Lannon M, Algird A, Reddy K, Lu JQ. Pituitary metastasis: From pathology to clinical and radiological considerations. *J Clin Neurosci* (2021) 93:231–40. doi: 10.1016/j.jocn.2021.09.016

2. Siewert JR, Stein HJ. Classification of adenocarcinoma of the oesophagogastric junction. *Br J Surg* (1998) 85(11):1457–9. doi: 10.1046/j.1365-2168.1998.00940.x

3. Bornschein J, Quante M, Jansen M. The complexity of cancer origins at the gastro-oesophageal junction. *Best Pract Res Clin Gastroenterol* (2021) 50-51:101729. doi: 10.1016/j.bpg.2021.101729

4. He W, Chen F, Dalm B, Kirby PA, Greenlee JD. Metastatic involvement of the pituitary gland: a systematic review with pooled individual patient data analysis. *Pituitary.* (2015) 18(1):159–68. doi: 10.1007/s11102-014-0552-2

5. van Vliet EP, Steyerberg EW, Eijkemans MJ, Kuipers EJ, Siersema PD. Detection of distant metastases in patients with oesophageal or gastric cardia cancer: a diagnostic decision analysis. *Br J Cancer.* (2007) 97(7):868–76. doi: 10.1038/sj.bjc.6603960

6. Chevallay M, Bollschweiler E, Chandramohan SM, Schmidt T, Koch O, Demanzoni G, et al. Cancer of the gastroesophageal junction: a diagnosis, classification, and management review. *Ann N Y Acad Sci* (2018) 1434(1):132–8. doi: 10.1111/nyas.13954

7. Habu M, Tokimura H, Hirano H, Yasuda S, Nagatomo Y, Iwai Y, et al. Pituitary metastases: current practice in Japan. *J Neurosurg* (2015) 123(4):998–1007. doi: 10.3171/2014.12.JNS14870

8. Henry A, Nugent A, Wallace IR, Oladipo B, Sheehy O, Johnston PC. Pituitary metastasis: a clinical overview. *Ulster Med J* (2021) 90(3):146–50.

9. Komninos J, Vlassopoulou V, Protopapa D, Korfias S, Kontogeorgos G, Sakas DE, et al. Tumors metastatic to the pituitary gland: case report and literature review. *J Clin Endocrinol Metab* (2004) 89(2):574–80. doi: 10.1210/jc.2003-030395

10. Osborn AG. *Diagnostic imaging: Brain. W.B.* Saunders (2004).

11. Lithgow K, Siqueira I, Senthil L, Chew HS, Chavda SV, Ayuk J, et al. Pituitary metastases: presentation and outcomes from a pituitary center over the last decade. *Pituitary.* (2020) 23(3):258–65. doi: 10.1007/s11102-020-01034-2

12. Schill F, Nilsson M, Olsson DS, Ragnarsson O, Berinder K, Edén Engström B, et al. Pituitary metastases: A nationwide study on current characteristics with special reference to breast cancer. *J Clin Endocrinol Metab* (2019) 104(8):3379–88. doi: 10.1210/jc.2019-00012

13. Gandhi GY, Fung R, Natter PE, Makary R, Balaji KC. Symptomatic pituitary metastasis as initial manifestation of renal cell carcinoma: Case report and review of literature. *Case Rep Endocrinol* (2020) 2020:8883864. doi: 10.1155/2020/8883864

14. Parthasarathy S, Lee DH, Levitt AH, Manavalan A. Pituitary metastasis presenting with central diabetes insipidus and panhypopituitarism. *AACE Clin Case Rep* (2021) 8(1):15–8. doi: 10.1016/j.aace.2021.06.006

15. Bailey D, Mau C, Zacharia B. Pituitary metastasis from urothelial carcinoma: A case report and review of the diagnosis and treatment of pituitary metastases. *Cureus.* (2021) 13(8):e17574. doi: 10.7759/cureus.17574

16. Oueslati I, Ayari S, Yazidi M, Bouali S, Khessairi N, Chihaoui M. Hypopituitarism secondary to a pituitary metastasis in a young woman with an invasive breast carcinoma. *Clin Case Rep* (2021) 9(6):e04175. doi: 10.1002/ccr3.4175

17. Liu CY, Wang YB, Zhu HQ, You JL, Liu Z, Zhang XF. Hyperprolactinemia due to pituitary metastasis: A case report. *World J Clin Cases.* (2021) 9(1):190–6. doi: 10.12998/wjcc.v9.i1.190

18. Watanabe M, Yasuda J, Ashida K, Matsuo Y, Nagayama A, Goto Y, et al. Masked diabetes insipidus hidden by severe hyponatremia: A case of pituitary metastasis of lung adenocarcinoma. *Am J Case Rep* (2020) 21:e928113. doi: 10.12659/AJCR.928113

19. El Habnouny J, Jandou I, Latrech H, Bourgon C. Pituitary metastasis of a breast ductal adenocarcinoma. *Ann Med Surg (Lond).* (2020) 60:380–3. doi: 10.1016/j.amsu.2020.10.054

20. Moon RDC, Singleton WGB, Smith P, Urankar K, Evans A, Williams AP. Slow-growing pituitary metastasis from renal cell carcinoma: Literature review. *World Neurosurg* (2021) 145:416–25. doi: 10.1016/j.wneu.2020.08.218

21. Ng S, Boetto J, Rigau V, Raingeard I, Crampette L, Favier V, et al. Pituitary metastasis of malignant melanoma misdiagnosed as pituitary adenoma: A case report and systematic review of the literature. *Neurochirurgie.* (2020) 66(5):383–90. doi: 10.1016/j.neuchi.2020.06.129

22. Ahmad S, Smeeton F, Hayhurst C, Lansdown A. Pituitary metastasis of prostate cancer presenting as a unilateral third nerve palsy. *BMJ Case Rep* (2020) 13 (6):e234550. doi: 10.1136/bcr-2020-234550

23. Du H, Jia A, Ren Y, Gu M, Li H, Sun M, et al. Endometrial adenocarcinoma metastatic to the pituitary gland: a case report and literature review. *J Int Med Res* (2020) 48(6):300060520924512. doi: 10.1177/0300060520924512

24. Sheahan KH, Huffman GC, DeWitt JC, Gilbert MP. Metastatic lung cancer presenting as monocular blindness and panhypopituitarism secondary to a pituitary metastasis. *Am J Case Rep* (2020) 21:e920948. doi: 10.12659/AJCR.920948

25. Estrada AJ, Sibley SD, Drake TC. Symptomatic pituitary mestastases: Two case reports with contrasting clinical presentations. *AACE Clin Case Rep* (2019) 5 (5):e294–7. doi: 10.4158/ACCR-2019-0207

26. Gao H, Wu S, Zhang X, Xie T. Minimally invasive follicular thyroid carcinoma mimicking pituitary adenoma: a case report. *Int J Clin Exp Pathol* (2019) 12(10):3949–52.

27. Nose K, Ogata T, Tsugawa J, Inoue T, Nabeshima K, Tsuboi Y. Pituitary metastasis of breast cancer mimicking IgG4-related hypophysitis. *eNeurologicalSci.* (2018) 14:13–5. doi: 10.1016/j.ensci.2018.11.014

28. Shen Z, Yang C, Bao X, Wang R. Giant sellar metastasis from renal cell carcinoma: A case report and literature review. *Med (Baltimore)* (2018) 97(47): e13376. doi: 10.1097/MD.0000000000013376

29. Javanbakht A, D'Apuzzo M, Badie B, Salehian B. Pituitary metastasis: a rare condition. *Endocr Connect.* (2018) 7(10):1049–57. doi: 10.1530/EC-18-0338

30. Souza Mota J, de Sá Caldas A, de Araújo Cortês Nascimento AGP, Dos Santos Faria M, Pereira Sobral CS. Pituitary metastasis of thyroid carcinoma: A case report. *Am J Case Rep* (2018) 19:896–902. doi: 10.12659/AJCR.909523

31. Castle-Kirszbaum M, Goldschlager T, Ho B, Wang YY, King J. Twelve cases of pituitary metastasis: a case series and review of the literature. *Pituitary.* (2018) 21 (5):463–73. doi: 10.1007/s11102-018-0899-x

32. Zhao Y, Lian W, Xing B, Feng M, Liu X, Wang R, et al. Diagnosis, therapy, and therapeutic effects in cases of pituitary metastasis. *World Neurosurg* (2018), 117:122–128. doi: 10.1016/j.wneu.2018.05.205

frontiers | Frontiers in Oncology

TYPE Original Research
PUBLISHED 17 January 2023
DOI 10.3389/fonc.2023.1033954

OPEN ACCESS

EDITED BY
Arianna Rustici,
University of Bologna, Italy

REVIEWED BY
Matteo Zoli,
IRCCS Institute of Neurological Sciences of Bologna (ISNB), Italy
Luigi Cirillo,
University of Bologna, Italy

*CORRESPONDENCE
Li Du
duliwh@whu.edu.cn

†First author

SPECIALTY SECTION
This article was submitted to Neuro-Oncology and Neurosurgical Oncology, a section of the journal Frontiers in Oncology

RECEIVED 01 September 2022
ACCEPTED 04 January 2023
PUBLISHED 17 January 2023

CITATION
Yang Z, Xiong X, Jian Z and Du L (2023) Analysis of the effect of neuroendoscopy-assisted microscopy in the treatment of Large (Koos grade IV) vestibular schwannoma. *Front. Oncol.* 13:1033954. doi: 10.3389/fonc.2023.1033954

Analysis of the effect of neuroendoscopy-assisted microscopy in the treatment of Large (Koos grade IV) vestibular schwannoma

Zhenxing Yang[1†], Xiaoxing Xiong[1], Zhihong Jian[1] and Li Du[2*]

[1]Department of Neurosurgery, Renmin Hospital of Wuhan University, Wuhan, Hubei, China, [2]Department of Anesthesiology, Renmin Hospital of Wuhan University, Wuhan, Hubei, China

Introduction: This article aimed to investigate the effects of the endoscopic-assisted microsurgery technique on the resection of large (Koos grade IV) vestibular schwannoma (VS) and provide a prognosis analysis of the patients.

Methods: A retrospective analysis of the use of the endoscopic-assisted microsurgery technique in 16 cases of large vestibular schwannoma surgery was carried out. Intraoperative nerve electrophysiological monitoring was conducted to explore the effect of neuroendoscopy on the resection of internal auditory canal tumors, protection of the facial nerve, and minimizing postoperative complications.

Results: Tumors were completely removed in all 16 cases, and the facial nerve was anatomically preserved in 14 cases (87.5%). There was no postoperative cerebrospinal fluid leakage and no intracranial infection complications occurred.Following the House-Brackmann (H-B) grading system, post-operative facial nerve function was grade I in 5 cases, grade II in 6 cases, grade III in 3 cases, and grade V in 2 cases. As a result, the preservation rate of facial nerve function (H-B grade I-II) was 68.8%. All 16 patients were followed up for 3 to 24 months, and no tumor recurrence was found on enhanced MRI.

Discussion: Using the endoscopic-assisted microsurgery technique in the retrosigmoid approach has many advantages over the microscopic-only approach. When compared to the microscopy-only approach, the endoscope can provide a wide-angle surgical field superior to that of a microscope in areas such as the internal auditory canal in the resection of large VS, minimize iatrogenic injuries, ensure complete removal of internal auditory canal tumors, and well as reducing postoperative complications such as cerebrospinal fluid leakage and the loss of facial and auditory nerve functions.

KEYWORDS

vestibular schwannoma, neuroendoscopy, internal auditory canal, facial nerve protection, hearing preservation

1 Introduction

Vestibular schwannomas (VS) are benign neoplasms arising from Schwann cells of the vestibulocochlear nerve (1), mostly from the vestibular part of the internal auditory canal. 75% of VS originate from the superior vestibular nerve, while the rest 25% originate from the cochlea. Accounting for about 90% of adult cerebellopontine angle tumors and 8% of intracranial tumors, VS is the most common benign tumor in the internal auditory canal and cerebellopontine angle (2). At present, more emphasis is being placed on total tumor resection, intraoperative nerve function preservation (facial and auditory nerves), postoperative complications reduction, and overall quality of life improvement using endoscopic-assisted techniques (3, 4). Due to the adult central neurons' lack of regenerative capacity and the irreversible nature of any cochlear and facial nerve damage sustained during acoustic neuroma removal, permanent facial paralysis and hearing loss result (5). In this article, we retrospectively analyzed the surgical outcomes of 16 cases of large vestibular schwannomas treated with endoscopic-assisted microsurgery *via* a retrosigmoid approach at Wuhan University's Renmin Hospital from May 2019 to July 2022. The report is as follows.

2 Methods

2.1 Patient and data collection

Electronic medical records were reviewed for patient demographic information, treatment, and audiometric data. The inclusion criteria for this study were: (1) an enhanced MRI scan diagnosed Vestibular schwannomas with a maximum diameter of more than 3 cm and tumor invasion into the internal auditory canal (Koos grade IV); (2) received operation treatment at the neurosurgery department; (3) a postoperative pathological examination confirmed Vestibular schwannomas. Patients who did not meet the above criteria were excluded from this study. The gender, age, clinical symptoms, hearing examination results, and facial nerve function evaluation results before and after surgery of patients meeting the above conditions were retrospectively analyzed.

2.2 Imaging and hearing examination

All 16 cases underwent a preoperative thin-slice CT scan of the skull base and a 3.0T MRI with gadolinium. Brainstem Auditory Evoked Potentials (BAEP) and pure tone threshold test dates were collected for these patients before the operation. 3 months after the operation, all the patients returned to our department for a Thin-slice CT scan of the skull base and 3.0T MRI with gadolinium, as well as a facial nerve function examination and hearing test. Follow-up inspection should be conducted every six months.

2.3 Surgical technique

This is a single-surgeon retrospective series in which all cases were performed by the same senior surgeon and assistants. After successful intubation under general anesthesia, the patient is placed in the park-bench position for a retrosigmoid approach. Compared with the semi-sitting or Jannetta position, this position is easy to place, and the surgery is more likely to expose tumors in the CPA area, which is convenient for our subsequent combined operation of microscope and neuroendoscope. Therefore, we routinely choose this surgical approach, the head is fixed by the frame, the root of the mastoid is at the highest point, the shoulder is retracted downward, and an arc incision is made behind the suboccipital sigmoid sinus behind the ear on the diseased side, up to the upper nuchal line 1.5 cm down to 2 cm below the level of the mastoid tip. Routinely sterilized drape, the skin and subcutaneous tissue are incised layer by layer, 125 ml of 20% mannitol is then rapidly infused intravenously to reduce intracranial pressure, drilled with an electric drill and the bone flap is milled off, the occipital dura is pulled downward to the skull base further exposing the area in front of the midline of the sigmoid sinus, up the transverse sinus, down to the lateral border of the foramen magnum. The bone window is about 4*3cm in size.

Microscopic resection of tumors in the cerebellopontine angle: German STORZ rigid endoscope was used during the operation, the rigid endoscope was 17 cm in length, 4.0 mm in diameter, and the angle was 30°. The endoscope was fixed with a Snake brand mechanical fixed arm, which could be adjusted in depth and angle at any time as needed. Under the microscope, the dura mater was cut along the sinus edge in an arc and retracted from the sinus edge to fully expose the cerebellopontine angle after releasing the cerebrospinal fluid (CSF) from the cisterna magna. The relationship between the tumor and the surrounding structures such as the trigeminal nerve, posterior cranial nerve, and blood vessels was first observed under the microscope, and the facial nerve monitoring response was observed by stimulating the tumor surface to confirm the location of the facial nerve. Then, the two layers of the arachnoid membrane along the tumor surface were separated under the microscope, the tumor capsule was cauterized and the tumor capsule was excised in pieces. When the tumor in the cerebellopontine angle has been separated to the deep part of the tumor after subtotal resection and decompression, a 30° endoscope is placed, the residual tumor and the brainstem surface, and the surrounding trigeminal nerve, trochlear nerve, petrosal vein, and supra cerebellum are carefully observed from multiple angles. The tumor capsule wall is peeled from the brainstem surface under the endoscope to avoid excessive stretching of the cerebellum and brainstem, and then the tumor and the facial nerve are carefully removed from the internal auditory canal opening. Attention should be paid to the principle of bidirectional separation. Stimulator stimulation helped identify the location of the facial nerve. After the tumor was removed at the cerebellopontine angle, the wound was covered with a gelatin sponge to protect the latter group's cranial nerves and blood vessels.

Treatment of residual tumors in the internal auditory canal: The lip of the internal auditory canal is where the tumor most closely adheres to the dura mater. The posterior lip of the internal auditory canal is removed with a small emery drill. Pay attention to continuous flushing and grinding at low speed to avoid excessive local temperature. When cauterizing the nerve in the internal auditory canal, the width and depth of the posterior wall should be enough to fully expose the tumor in the internal auditory canal, generally 5-6 mm. After incising the dura covering the internal auditory canal

with a hook knife, a 30° neuroendoscope was placed again to observe the relationship between the residual tumor and the nerve in the internal auditory canal. Almost always avoid blindly grasping and pulling the tumor with forceps. After the internal auditory canal tumor is completely removed, the facial, vestibular, and cochlear nerves can be distinguished under endoscopy, and the facial nerve is stimulated again to observe its function. The petrosal bone on the posterior wall of the internal auditory canal was examined to check whether the mastoid air cell was open, sealed with bone wax, packed with muscle fragments, and then fixed with biological protein glue to avoid leakage of CSF. After carefully achieving the hemostasis of the surgical field, the dura mater was sutured, the bone flap was fixed, and the muscle and skin were sutured in layers.

3 Result

Our review included 16 patients, 9 males, and 7 females; the age ranged from 33 - 75 years old, and the medical history was from 2 months to 15 years. There were 13 cases of tinnitus and partial hearing loss, 3 cases of complete hearing loss, 9 cases of dizziness, and 3 cases of limb ataxia; preoperative facial nerve function was classified according to House-Brackmann (6), as grade I in 8 cases, II in 6, III in 1 and IV in 1. hearing loss according to the WHO classification (7), as mild hearing loss in 2 cases, moderate hearing loss 3, moderately severe hearing loss 4, severe hearing loss 2, profound hearing loss 2, complete hearing loss 3 cases, respectively (Table 1). The tumor size (longest diameter of axial plane) was between 36 and 62 mm (average 43.6 mm). According to the Koos classification (8), all tumors were grade IV. The results of Brainstem Auditory Evoked Potentials (BAEP) and pure tone threshold test showed decreased hearing of varying degrees on the affected side, among which 3 cases had complete hearing loss.

Tumor tissue was collected from the 16 cases and sent to pathology for examination, and all of them were confirmed to be vestibular schwannoma by immunohistochemical staining. 16 cases achieved gross total resection, and the facial nerve was anatomically preserved in 14 cases (87.5%), The average length of bone resection of the internal auditory canal was 5.5 ± 0.5mm during the operation contrast the total length of the internal auditory canal was 10.7 ± 0.6mm (Figure 1). 5 cases of grade I, 6 cases of grade II, 3 cases of grade III, and 2 cases of grade V. 1 patient had developed delayed hemorrhage, but due to the small amount of bleeding, the hematoma was absorbed with conservative management, and was then discharged after recovery. As for postoperative hearing function, 11 patients had varying degrees of hearing loss, and 6 patients had complete hearing loss. There was no CSF leakage, wound infection, or hydrocephalus complications in this group of patients postoperatively. (Table 2). The 16 patients were followed up for 3 to 24 months after the operation, and no tumor recurrence was observed during the follow-up (Figure 2, 3).

TABLE 1 Clinical characters of patients.

No	Gender	Age	Ear	Main Symptoms	Max Diameter mm	Toumor Size Koos Grade	Facial Function (HB-grade)	Hearing Lose Grade
1	M	48	L	Tinnitus 5ys, HL 3ys	45	IV	I	MS
2	F	36	L	Vertigo with tinnitus 6ms	42	IV	I	Mild
3	F	52	R	Tinnitus 6ys, HL 3ys	46	IV	II	Severe
4	M	64	L	HL 3ys Vertigo 5ms	38	IV	II	Moderate
5	F	75	R	Deaf 15ys Ataxia 6ms	62	IV	II	deafness
6	F	56	R	Vertigo 8ms	38	IV	I	Moderate
7	M	46	L	HL 2ys	44	IV	II	MS
8	M	54	R	Deaf 3ys hoarseness 6ms	48	IV	III	deafness
9	M	62	R	Deaf 5ys FP 2 ms	49	IV	IV	deafness
10	F	33	L	Tinnitus 2ys	36	IV	I	Mild
11	F	70	R	HL5ys	52	IV	II	Profound
12	M	62	R	HL Tinnitus 3ys	38	IV	I	MS
13	M	58	L	Vertigo Ataxia 2 vs,	40	IV	II	Profound
14	F	49	R	HL2ys	44	IV	I	Moderate
15	M	51	L	HL 2ys Tinnitus 6ms	39	IV	I	MS
16	M	57	L	HL 3ys Ataxia 2 ms	54	IV	I	Severe

Maximum diameter of the tumor was measured from axial contrast-enhanced scan of the MRI; HL, hearing loss; ys, years; ms, months; FP, facial paralysis; MS moderately severe hearing lose.

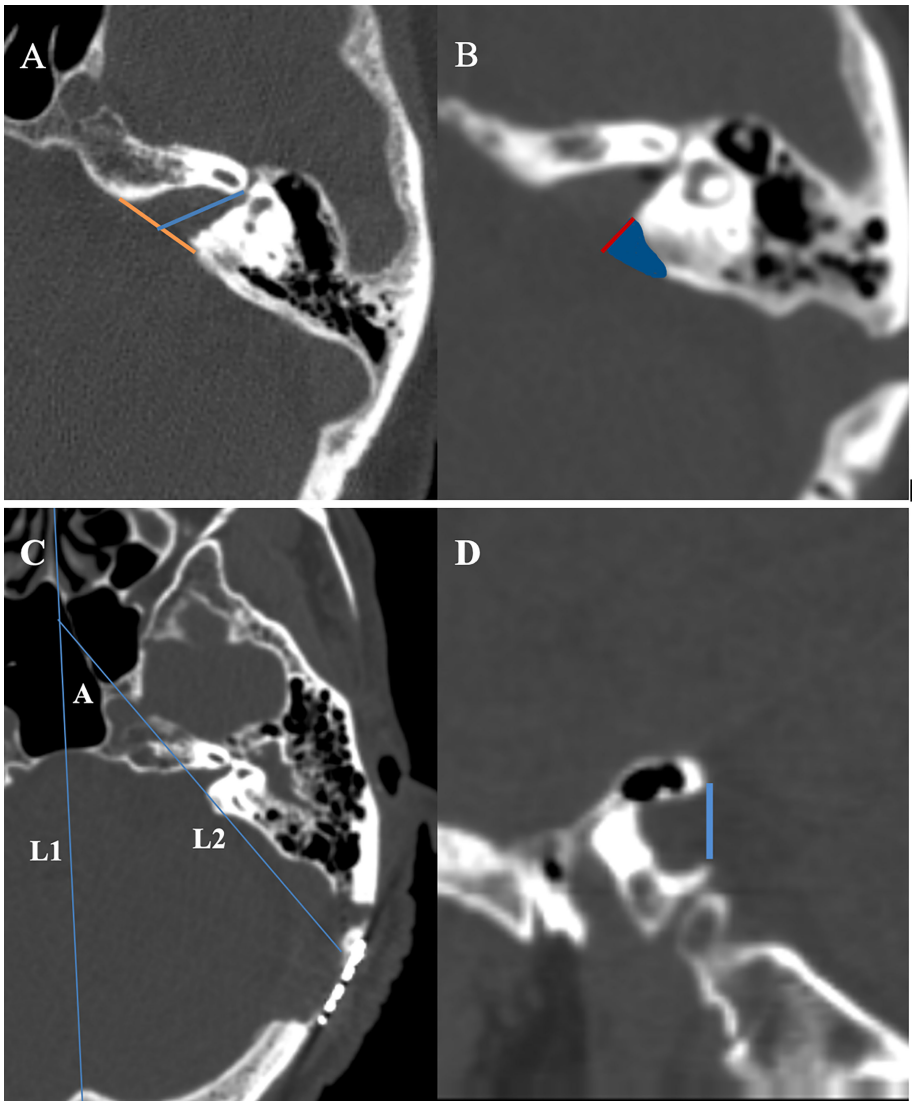

FIGURE 1
(A) Measurement of the absolute tumor extension into the internal auditory canal. On a thin slice CT scan, the slice with the most lateral extension of the tumor is selected for measurement. An auxiliary line (yellow) is drawn between the anterior and posterior lip of the porus acoustics. The length of absolute tumor extension is defined as the distance between the midpoint of the yellow line and the most lateral point of tumor extension. **(B)** We use Brainlab software to fuse the thin-slice CT scan images before and after surgery. The blue area shows the bone removal part of the internal auditory canal, and the length of the red line represents the exposure length of the internal auditory canal. **(C)** L1: the middle sagittal line at the axial plane; L2:the line of the bone removal plane of the posterior and lateral wall of the internal auditory canal at the axial plane; angle A the angle between L1 and L2 stands for the drilling angle. **(D)** The width of internal auditory canal exposure is defined as the distance as a blue line at the sagittal plane.

4 Discussion

Large VS are often closely adhered to the brain stem, facial nerve, glossopharyngeal nerve, vagus nerve, and cranial roots of the accessory nerve, they are closely related to the anterior inferior cerebellum, posterior inferior arteries, and petrosal veins. Variant degrees of hearing loss, facial nerve paralysis, brainstem injury, or even death are expected when such structures are damaged (9). An increase in tumor size can increase postoperative complications, due to the formation of more adhesion bands between tumor mass and other adjacent structures such as the brainstem, thus patients are at a higher risk of developing respiratory failure within 24 hours postoperatively (9). At present, an endoscopic-assisted technique for more complex cases of VS has been adopted widely by increasing numbers of neurosurgeons, due to the technological advancement of endoscopic-assisted microsurgery and improved intraoperative neurophysiological monitoring technology (10, 11). Endoscopic-assisted microsurgery has greatly reduced postoperative complications, significantly improved the tumor resection rate, and notably has improved the quality of life of patients (12, 13).

Using an endoscopic-assisted technique in internal auditory canal tumor resection can significantly reduce damage to the adjacent nerves and the residual internal auditory canal tumor, thus decreasing the chances of tumor recurrence (14–16). The vast majority of acoustic

TABLE 2 Surgical date and follow-up of the patients.

NO	LCA Length (mm)	LCA EL (mm)	Tumor Resection	Follow-up Time	FNF (HB-grade)	HF	Change of HF	Complication	Tumor Recurrence
1	12	5.6	TR	1 year	I	severe	↓	No	No
2	11.4	5.8	TR	6 months	II	MS	↓	No	No
3	12.3	6.2	TR	2 years	III	profound	↓	No	No
4	10.2	5.4	TR	2 years	II	severe	↓	No	No
5	11	5.3	TR	6 months	V	deafness	=	No	No
6	9.2	6	TR	1 year	I	severe	↓	No	No
7	10.3	5.8	TR	1 year	III	deafness	↓	No	No
8	9.4	6.4	TR	3 months	III	deafness	=	No	No
9	11	5.4	TR	1 year	II	deafness	=	No	No
10	9.8	4.8	TR	6 months	I	mild	=	No	No
11	10.2	6.2	TR	2 years	II	severe	=	delayed hematoma	No
12	9.5	5.2	TR	1 year	II	severe	↓	No	No
13	10.6	4.5	TR	6 months	V	deafness	↓	No	No
14	10.2	5.4	TR	3 months	I	MS	↓	No	No
15	11.2	4.8	TR	1 year	I	severe	↓	No	No
16	12.4	5.2	TR	2 years	II	deafness	↓	No	No

TR, Total resection; LCA EL, ICA Exposure Length; FNF, facial nerve function; HF, hearing function; CHF, Change of Hearing Function; ↓, Hearing Function worse than preoperation; = Hearing Function have no change compare to preoperation.

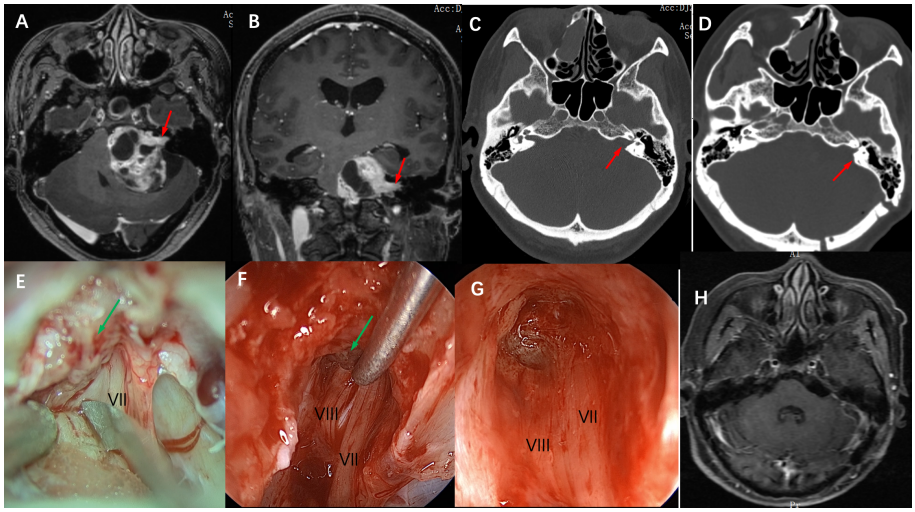

FIGURE 2
Imaging studies and intraoperative snapshots of a case of VS with an irregularly shaped tumor extending into the internal auditory canal. **(A)** The preoperative T1 MRI with contrast image revealed a giant vestibular schwannoma abutting the brainstem. The intracanalicular portion of the tumor was irregularly shaped as indicated by the red arrow (axial plane). **(B)** giant vestibular schwannoma abutting the brainstem and extension into the internal auditory canal as indicated by the red arrow (coronal plane) **(C)** Thin-section CT scan of the skull base showed that the ipsilateral internal auditory canal was significantly enlarged compared with the contralateral side (red arrow), and the mastoid air cells were well gasified. **(D)** A postoperative CT scan showed that the posterolateral part of the internal auditory canal bone was removed (red arrow), and the structure of the bony labyrinth and semicircular canal was intact. **(E)** Intra-operative microscopic view of the operation showed that after the tumor was removed in the CPA area, the internal auditory canal was opened and there were still a large number of tumor residues in the internal auditory canal (indicated by green arrow), and the VII nerve was located anterior and inferior to the internal auditory canal. **(F)** Intraoperative neuroendoscopy view showed tumor resection in the internal auditory canal, and the tumor was separated from the VII, and VIII nerves using a microscopic ball-tip dissection (green arrow). **(G)** Intraoperative neuroendoscopy view showed that after complete resection of the tumor in the internal auditory canal, the bottom structure of the internal auditory canal showed, and the VII and VIII nerves were intact. **(H)** Postoperative MRI review after 6 months showed complete tumor resection and no tumor recurrence.

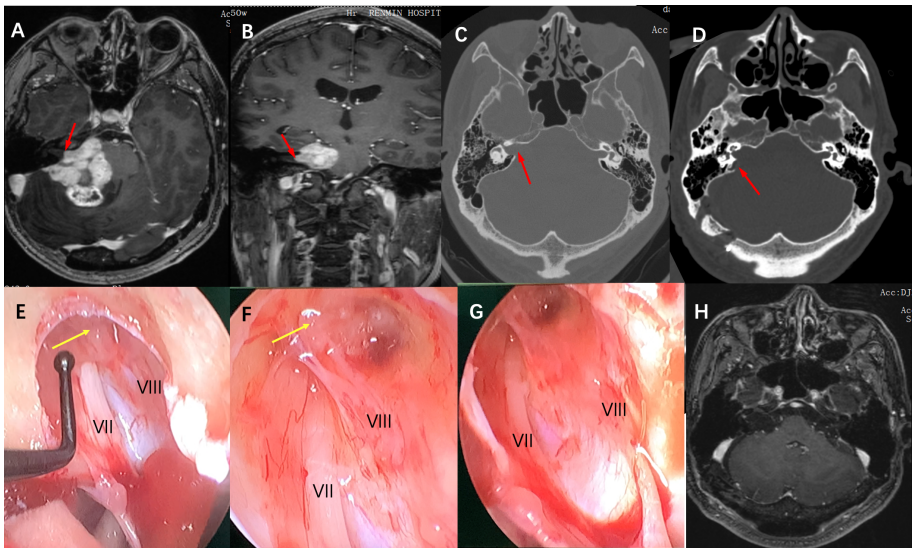

FIGURE 3
Imaging studies and intraoperative snapshots of a case of Grade IV VS extending into the internal auditory canal. **(A)** The preoperative T1 contrast image revealed a giant VS at the CPA area. The intracanalicular portion of the tumor was irregularly shaped as indicated by the red arrow (axial plane). **(B)** giant VA abutting the brainstem and extension into the internal auditory canal as indicated by the red arrow (coronal plane) **(C)** Thin-section CT scan of the skull base showed that the ipsilateral internal auditory canal was significantly enlarged compared with the contralateral side (red arrow), and the mastoid air cells were well gasified. **(D)** A postoperative CT scan showed that the posterolateral part of the internal auditory canal bone was removed (red arrow), and the structure of the bony labyrinth and semicircular canal was intact. **(E)** Intra-operative neuroendoscopy view of the operation showed that after the tumor was removed in the CPA area, the internal auditory canal was opened and there were tumor remnants in the internal auditory canal (yellow arrow), and nerves VII and VIII are located anterior and posterior inferior to the internal auditory canal respectively. **(F)** Intraoperative neuroendoscopy view showed after tumor resection, there were still tumor remnants at the bottom of the internal auditory canal adhering to the transverse crest (yellow arrow). **(G)** Intraoperative neuroendoscopy showed that after complete resection of the tumor in the internal auditory canal, the bottom structure of the internal auditory canal showed, and the VII and VIII nerves were intact. **(H)** Postoperative MRI review after 1 year showed complete tumor resection and no tumor recurrence.

neuromas originate from the vestibular nerve in the internal auditory canal and then grow outward into the cerebellopontine angle. Recurrence of acoustic neuromas is highly related to residual tumors in the internal auditory canal (12, 13). McKennan et al. were the first to use an endoscopic-assisted technique to explore the internal auditory canal, removing the portion of the VS in the internal auditory canal with preservation of facial nerve (17). Valtonenet al reported that in 78 cases of VS patients endoscope was permitted to identify and remove tumor residues at the bottom of the internal auditory canal in 11 (18). Other retrospective studies reported that the anatomical preservation rate of the facial nerve in VS was 73% to 93% (14–16). However, the anatomical preservation of the facial nerve is not an indicator of the integrity of the facial nerve function. Sobieski reported that a preservation rate of facial nerve function (H-B grade I to II) in of 53.4%, but for tumors with a diameter greater than 3 cm only 35.7% (15). Zhao et al. (19) reported that 33 cases of acoustic neuroma with a diameter of more than 3 cm had a facial nerve function preservation rate of 27.5%. Springborg (14) retrospectively analyzed 1244 cases of acoustic neuroma after surgery and found that the preservation rate of facial nerve function was only 55.6% with a tumor diameter greater than 25 mm. The anatomical preservation rate of our group of 16 patients was 87.5%, with a rate of 68.8% facial nerve function preservation rate (H-B grade I-II) postoperatively. We believe that this satisfactory preservation rate outcome of 68.8% may be related to the use of an endoscopic-assisted technique in our case series. After opening the internal auditory canal, the residual tumor in the internal auditory canal was observed under the endoscope. The endoscope's clear wide-angle view had a superior advantage over the microscope's viewing field, thus nerves passing along the tumor capsule can be identified more clearly. Therefore, in patients with preserved hearing functions, both the vestibular and the facial nerve could be identified and preserved throughout the removal of the internal auditory canal tumor. The utilization of endoscopic-assisted microsurgery can avoid nerve damage caused by the blind scraping of nerve dissections under the simple microscope field, and increase the probability of preserving facial and acoustic nerve function after surgery. Hearing loss occurs the most in patients undergoing VS surgery; thus, hearing preservation represents a difficult challenge. Many authors pointed out a correlation between tumor size and hearing preservation, suggesting that larger tumors are associated with poorer postoperative outcomes due to the resultant surgical complexity of these larger tumors (20–22). Good tonal audiometry can be achieved postoperatively with satisfactory results in selected patients with small tumors and good preoperative hearing. Postoperative hearing loss is thought to be related to the intraoperative direct impairment of the cochlear nerve and/or ischemia of nourishing vessels, which leads to cochlear nerve dysfunction (23). According to the results of our study, only 2 of the 16 patients had the same hearing preservation after surgery, 11 patients had varying degrees of hearing loss after the operation, and 6 patients had complete hearing loss.

In the process of microscopic surgery, to expand the surgical field and completely remove the tumor and particularly to expose the

lesions growing deep into the midline, it is often necessary to remove more bone, or even free the facial nerve, which may involve other structures such as jugular foramen, pontine triangle, internal carotid artery, high jugular bulb and other important structures that have a high surgical risk when we remove the bone of the internal auditory canal. The damage to the bony labyrinth and semicircular canal when the bony structure of the posterolateral internal auditory canal is removed is also one of the important factors affecting hearing preservation during surgery. Kouhi et al (24) studied the hearing preservation rate of 30 patients after VS surgery and concluded the impossibility of exposing the entire length from the lip to the bottom of the internal auditory canal without causing damage to the posterior semicircular canal. However, utilizing an endoscopic-assisted technique can reduce the extent of bony resection and help prevent intraoperative hearing loss. Ammirati et al. (25) reported that the most commonly damaged structures were: the common peduncle (52%), the posterior semicircular canal (23%), the vestibule (21%), and the superior semicircular canal (4%). Lui et al. (26) studied the safe resection area between the external lip of the internal auditory canal and the posterior semicircle in 120 patients. The maximum safe resection range of the posterior lip of the internal auditory canal was 7-9 mm, and the distance between the posterior superior wall of the internal auditory canal to the anterior edge of the jugular foramen was (3.94 ± 1.75) mm, moreover, the study showed that the length of the posterolateral wall of the internal auditory canal was 9.7 +/- 1.6 mm. Pillai et al. (27) reported the drilling angle (the angle between the drill bit and the posterolateral side of the petrous bone) is 43.3 +/- 6.0 degrees, and the length of the internal auditory canal posterior wall that can be ground without violating the integrity of the labyrinth is 7.2 +/- 0.9 mm. All these results showed that the extent of the safe resection zone varied widely, and the viewing angle and size of the craniotomy also greatly impacted the limit of exposure. Therefore, endoscopic assistance could further improve the intraoperative field of vision and illumination. According to our statistics, the use of the endoscopic-assisted technique in this group of cases showed that the grinding length of the posterior wall of the internal auditory canal in 16 patients was 5.5+/- 0.6 mm, the drilling angle was 42.3 +/- 5.8 degrees (axial plane), and the width of the internal auditory canal was 4.5 +/- 0.5 mm (sagittal plane) and all tumors were completely removed. Postoperative CT scans show no damage to the semicircular canal of all patients, which is superior to the data reported in the previous literature (28, 29). Our experience is that in the case of reducing the exposed length of the posterior of internal auditory canal walls, the width of the internal auditory canal bone resection can be appropriately increased by utilizing the good viewing field and angle of the endoscopy and the ductility of the microdissection device. All that was done to achieve a safer separation of the tumor from the facial auditory nerve under a good field of view as well as to reduce the probability of postoperative neurological damage.

At the same time, the use of the endoscopic-assisted technique can also reduce the incidence of postoperative complications of VS. The most common complications after VS surgery are cerebrospinal fluid leakage, wound infection, as well as postoperative delayed bleeding. The literature reports that the risk of postoperative CSF leakage is 0-17%, mainly caused by the opening of the mastoid air cells when the bone of the internal auditory canal is removed, or for injuries of the bone labyrinth (14, 29, 31). This can be favored by the blind view of the microscope, which failed to seal the open-air cell tightly with postoperative CSF leakage and possible meningitis (14, 29, 31). The 30° endoscope is convenient for close-up and wide-angle observation of tumor resection in the internal auditory canal, which can reduce the extent of opening of the posterior and lateral walls of the internal auditory canal, and at the same time, the opened mastoid air cells can be tightly sealed under a good viewing angle to reduce the risk of CSF leakage. Due to the large size of large acoustic neuromas, their tumors are often embedded in the medial side of the cerebellum and brainstem, they are also closely adhered to the trigeminal nerve, posterior cranial nerve, superior cerebellar artery, anterior inferior cerebellar artery, and petrosal vein. Endoscopic-assisted surgery expands the surgical field, with additional advantages such as overcoming the blind angle of some anatomical areas when only observed under the microscope, minimizing surgical traction, and improving visualization of the neurovascular structures (32, 33).

In addition, with the endoscopic-assisted microsurgery technique, none of the 16 patients in this group had cerebrospinal fluid leakage after surgery, and no serious complications such as death and disability occurred.

In the actual surgical operation, the use of endoscopic-assisted technique involves long-term training and accumulation of operating experience.

Unlike the operation under the 3D image under the microscope, endoscopic images are 2D, thus requiring specific surgical skills to achieve good surgical results. With the development of technology, the 3D endoscope has been gradually used in clinical practice, which will greatly help the application of neuroendoscope (34). At the same time, because this study is a retrospective analysis of the treatment of large VS, the number of cases is relatively small, and the individual differences of patients will inevitably lead to sample bias, which also requires us to further improve the work in the future.

5 Conclusion

With the rapid development of neurosurgery technologies, VS's better intraoperative and postoperative treatment goals are now more attainable. According to the experience of this group of cases, we believe that endoscopic-assisted microsurgery can give neurosurgeons a large and panoramic surgical field to remove VS, help to increase the rate of preserving the facial and acoustic nerves function, and reduce postoperative complications."

Data availability statement

The original contributions presented in the study are included in the article/supplementary material. Further inquiries can be directed to the corresponding author.

Ethics statement

The studies involving human participants were reviewed and approved by the ethics committee of Renmin Hospital of Wuhan University. Written informed consent for participation was not required for this study in accordance with the national legislation and the institutional requirements.

Author contributions

ZJ and LD supervised the project. Material preparation, data collection, and analysis were performed by XX, and the first draft of the manuscript was written by ZY and LD. All authors contributed to the article and approved the submitted version.

Conflict of interest

The authors declare that the research was conducted in the absence of any commercial or financial relationships that could be construed as a potential conflict of interest.

Publisher's note

All claims expressed in this article are solely those of the authors and do not necessarily represent those of their affiliated organizations, or those of the publisher, the editors and the reviewers. Any product that may be evaluated in this article, or claim that may be made by its manufacturer, is not guaranteed or endorsed by the publisher.

References

1. Kaul V, Cosetti MK. Management of vestibular schwannoma (including nf2): Facial nerve considerations. *Otolaryngol Clin North Am* (2018) 51:1193–212. doi: 10.1016/j.otc.2018.07.015

2. Ostrom QT, Cioffi G, Waite K, Kruchko C, Barnholtz-Sloan JS. Cbtrus statistical report: Primary brain and other central nervous system tumors diagnosed in the united states in 2014-2018. *Neuro Oncol* (2021) 23:iii1–105. doi: 10.1093/neuonc/noab200

3. Cheng CY, Qazi Z, Sekhar LN. Microsurgical and endoscope assisted resection of a right intracanalicular vestibular schwannoma two-dimensional operative video. *J Neurol Surg B Skull Base* (2019) 80:S288–9. doi: 10.1055/s-0038-1676840

4. Gerganov VM, Giordano M, Herold C, Samii A, Samii M. An electrophysiological study on the safety of the endoscope-assisted microsurgical removal of vestibular schwannomas. *Eur J Surg Oncol* (2010) 36:422–7. doi: 10.1016/j.ejso.2009.11.003

5. Lindsay SL, McCanney GA, Willison AG, Barnett SC. Multi-target approaches to cns repair: Olfactory mucosa-derived cells and heparan sulfates. *Nat Rev Neurol* (2020) 16:229–40. doi: 10.1038/s41582-020-0311-0

6. Jeong J, Lee JM, Cho YS, Kim J. Inter-rater discrepancy of the house-brackmann facial nerve grading system. *Clin Otolaryngol* (2022) 47(6):680–3. doi: 10.1111/coa.13956

7. Collaborators GBDHL. Hearing loss prevalence and years lived with disability, 1990-2019: Findings from the global burden of disease study 2019. *Lancet* (2021) 397:996–1009. doi: 10.1016/S0140-6736(21)00516-X

8. Won SY, Kilian A, Dubinski D, Gessler F, Dinc N, Lauer M, et al. Microsurgical treatment and follow-up of koos grade iv vestibular schwannoma: Therapeutic concept and future perspective. *Front Oncol* (2020) 10:605137. doi: 10.3389/fonc.2020.605137

9. Harris MS, Moberly AC, Adunka OF. Partial resection in microsurgical management of vestibular schwannomas. *JAMA Otolaryngol Head Neck Surg* (2017) 143:863–4. doi: 10.1001/jamaoto.2017.0293

10. Corrivetti F, Cacciotti G, Scavo CG, Roperto R, Stati G, Sufianov A, et al. Flexible endoscopic assistance in the surgical management of vestibular schwannomas. *Neurosurg Rev* (2021) 44:363–71. doi: 10.1007/s10143-019-01195-0

11. Bi Y, Ni Y, Gao D, Zhu Q, Zhou Q, Tang J, et al. Endoscope-assisted retrosigmoid approach for vestibular schwannomas with intracanalicular extensions: Facial nerve outcomes. *Front Oncol* (2021) 11:774462. doi: 10.3389/fonc.2021.774462

12. Przepiorka L, Kunert P, Rutkowska W, Dziedzic T, Marchel A. Surgery after surgery for vestibular schwannoma: A case series. *Front Oncol* (2020) 10:588260. doi: 10.3389/fonc.2020.588260

13. Samii M, Metwali H, Gerganov V. Microsurgical management of vestibular schwannoma after failed previous surgery. *J Neurosurg* (2016) 125:1198–203. doi: 10.3171/2015.8.JNS151350

14. Springborg JB, Fugleholm K, Poulsgaard L, Caye-Thomasen P, Thomsen J, Stangerup SE. Outcome after translabyrinthine surgery for vestibular schwannomas: Report on 1244 patients. *J Neurol Surg B Skull Base* (2012) 73:168–74. doi: 10.1055/s-0032-1301403

15. Sobieski C, Killeen DE, Barnett SL, Mickey BE, Hunter JB, Isaacson B, et al. Facial nerve outcomes after vestibular schwannoma microsurgical resection in neurofibromatosis type 2. *Otolaryngol Head Neck Surg* (2021) 164:850–8. doi: 10.1177/0194599820954144

16. Monfared A, Corrales CE, Theodosopoulos PV, Blevins NH, Oghalai JS, Selesnick SH, et al. Facial nerve outcome and tumor control rate as a function of degree of resection in treatment of large acoustic neuromas: Preliminary report of the acoustic neuroma subtotal resection study (ansrs). *Neurosurgery* (2016) 79:194–203. doi: 10.1227/NEU.0000000000001162

17. McKennan KX. Endoscopy of the internal auditory canal during hearing conservation acoustic tumor surgery. *Am J Otol* (1993) 14:259–62.

18. Valtonen HJ, Poe DS, Heilman CB, Tarlov EC. Endoscopically assisted prevention of cerebrospinal fluid leak in suboccipital acoustic neuroma surgery. *Am J Otol* (1997) 18:381–5.

19. Zhao F, Wang B, Yang Z, Zhou Q, Li P, Wang X, et al. Surgical treatment of large vestibular schwannomas in patients with neurofibromatosis type 2: Outcomes on facial nerve function and hearing preservation. *J Neurooncol* (2018) 138:417–24. doi: 10.1007/s11060-018-2812-x

20. Huo Z, Chen J, Wang Z, Zhang Z, Wu H. Prognostic factors of long-term hearing preservation in small and medium-sized vestibular schwannomas after microsurgery. *Otol Neurotol* (2019) 40:957–64. doi: 10.1097/MAO.0000000000002284

21. Preet K, Ong V, Sheppard JP, Udawatta M, Duong C, Romiyo P, et al. Postoperative hearing preservation in patients undergoing retrosigmoid craniotomy for resection of vestibular schwannomas: A systematic review of 2034 patients. *Neurosurgery* (2020) 86:332–42. doi: 10.1093/neuros/nyz147

22. Dowling EM, Patel NS, Lohse CM, Driscoll CLW, Neff BA, Van Gompel JJ, et al. Durability of hearing preservation following microsurgical resection of vestibular schwannoma. *Otol Neurotol* (2019) 40:1363–72. doi: 10.1097/MAO.0000000000002378

23. Roosli C, Linthicum FHJr., Cureoglu S, Merchant SN. Dysfunction of the cochlea contributing to hearing loss in acoustic neuromas: An underappreciated entity. *Otol Neurotol* (2012) 33:473–80. doi: 10.1097/MAO.0b013e318248ee02

24. Kouhi A, Zarch VV, Pouyan A. Risk of posterior semicircular canal trauma when using a retrosigmoid approach for acoustic neuroma surgery and role of endoscopy: An imaging study. *Ear Nose Throat J* (2018) 97:24–30. doi: 10.1177/0145561318097001-205

25. Ammirati M, Ma J, Cheatham ML, Maxwell D, Bloch J, Becker DP. Drilling the posterior wall of the petrous pyramid: A microneurosurgical anatomical study. *J Neurosurg* (1993) 78:452–5. doi: 10.3171/jns.1993.78.3.0452

26. Liu S, Tong D, Liu M, Lv D, Li Y. The safe zone of posterior semicircular canal resection in suboccipital retrosigmoid sinus approach for acoustic neuroma surgery. *J Craniofac Surg* (2013) 24:2103–5. doi: 10.1097/SCS.0b013e31829ad5cc

27. Pillai P, Sammet S, Ammirati M. Image-guided, endoscopic-assisted drilling and exposure of the whole length of the internal auditory canal and its fundus with preservation of the integrity of the labyrinth using a retrosigmoid approach: A laboratory investigation. *Neurosurgery* (2009) 65:53–59; discussion 59. doi: 10.1227/01.NEU.0000343521.88537.16

28. Ebner FH, Kleiter M, Danz S, Ernemann U, Hirt B, Lowenheim H, et al. Topographic changes in petrous bone anatomy in the presence of a vestibular schwannoma and implications for the retrosigmoid transmeatal approach. *Neurosurgery* (2014) 10 Suppl 3:481–6. doi: 10.1227/NEU.0000000000000454

29. Panara K, Hoffer M. *Anatomy, head and neck, ear internal auditory canal (internal auditory meatus, internal acoustic canal).* Treasure Island (FL: Statpearls (2022).

30. Zhang L, Galaiya D, Jackson CM, Tamargo RJ, Lim M, Carey J, et al. Bone cement internal auditory canal reconstruction to reduce csf leak after vestibular schwannoma retrosigmoid approach. *Otol Neurotol* (2021) 42:e1101–5. doi: 10.1097/MAO.0000000000003215

31. Hwa TP, Luu N, Henry LE, Naples JG, Kaufman AC, Brant JA, et al. Impact of reconstruction with hydroxyapatite bone cement on csf leak rate in retrosigmoid approach to vestibular schwannoma resection: A review of 196 cases. *Otol Neurotol* (2021) 42:918–22. doi: 10.1097/MAO.0000000000003072

32. Yang A, Folzenlogen Z, Youssef AS. Minimally invasive endoscopic-assisted approaches to the posterior fossa. *J Neurosurg Sci* (2018) 62:658–66. doi: 10.23736/S0390-5616.18.04474-0

33. Almeida JP, Gentili F. Endoscopic skull base surgery and the evolution of approaches to anterior cranial base lesions. *J Neurosurg Sci* (2021) 65:101–2. doi: 10.23736/S0390-5616.20.05209-1

34. Mevio N, Achena A, Pilolli F, Roncoroni L, Ormellese GL, Placentino A, et al. Eagle syndrome: 3d endoscope-assisted anterior tonsillar fossa approach to styloid process. *Am J Otolaryngol* (2021) 42:102979. doi: 10.1016/j.amjoto.2021.102979

frontiers | Frontiers in Oncology

TYPE Review
PUBLISHED 01 February 2023
DOI 10.3389/fonc.2023.1106819

OPEN ACCESS

EDITED BY
Arianna Rustici,
University of Bologna, Italy

REVIEWED BY
Alessandro Carretta,
University of Bologna, Italy
Kamil Krystkiewicz,
Copernicus Memorial Hospital, Poland

*CORRESPONDENCE
Johannes Wach
Johannes.wach@medizin.uni-leipzig.de

SPECIALTY SECTION
This article was submitted to Neuro-Oncology and Neurosurgical Oncology, a section of the journal Frontiers in Oncology

RECEIVED 24 November 2022
ACCEPTED 16 January 2023
PUBLISHED 01 February 2023

CITATION
Vychopen M, Arlt F, Güresir E and Wach J (2023) How to position the patient? A meta-analysis of positioning in vestibular schwannoma surgery *via* the retrosigmoid approach.
Front. Oncol. 13:1106819.
doi: 10.3389/fonc.2023.1106819

How to position the patient? A meta-analysis of positioning in vestibular schwannoma surgery *via* the retrosigmoid approach

Martin Vychopen, Felix Arlt, Erdem Güresir and Johannes Wach*

Department of Neurosurgery, University Hospital Leipzig, Leipzig, Germany

Objective: Patient positioning is a matter of ongoing debate in the surgical treatment of vestibular schwannoma (VS). Main endpoints of this discussion are preservation of facial nerve functioning, extent of resection, and complications. In this meta-analysis, we aim to investigate the impact of patient positioning on VS surgery *via* the retrosigmoid approach.

Methods: We searched for eligible comparative trials on PubMed, Cochrane library, and Web of Science. Positioning groups were compared regarding facial nerve outcome, extent of resection, postoperative hydrocephalus, postoperative CSF leaks, perioperative venous air embolism, and perioperative mortality. Two groups of positions were defined, and the following positions were allocated to those groups: (1) Semi-sitting and Sitting-position; (2) Lateral position, supine position with extensive head rotation, lateral oblique (=Fukushima/Three-quarter prone), and park-bench position.

Results: From 374 full-text screenings, 7 studies met the criteria and were included in our meta-analysis comprising 1640 patients. Our results demonstrate a significantly better long-term (≥6 months) outcome of the facial nerve after VS surgery in the semi-sitting positioning (OR: 1.49, 95%CI: 1.03-2.15, p = 0.03). Positioning did not influence the extent of resection, rate of postoperative CSF leaks, and the presence of a postoperative hydrocephalus. Overall incidence of venous air embolisms was significantly associated with VS surgery in sitting positioning (OR: 6.77, 95% CI: 3.66-12.54, p < 0.00001). Perioperative mortality was equal among both positioning groups.

Conclusion: Semi-sitting positioning seems to be associated with an improved facial nerve outcome after VS surgery *via* the retrosigmoid approach. Venous air embolisms are significantly more often observed among VS patients who underwent surgery in the sitting position, but the perioperative mortality is equal in both positioning groups. Both positioning groups are a safe procedure. Multicentric prospective randomized trials are needed to evaluate the risk-benefit ratio of each positioning in VS surgery *via* the retrosigmoid approach.

KEYWORDS

semi-sitting, lateral, positioning, vestibular schwannoma, venous air embolism, facial nerve, mortality

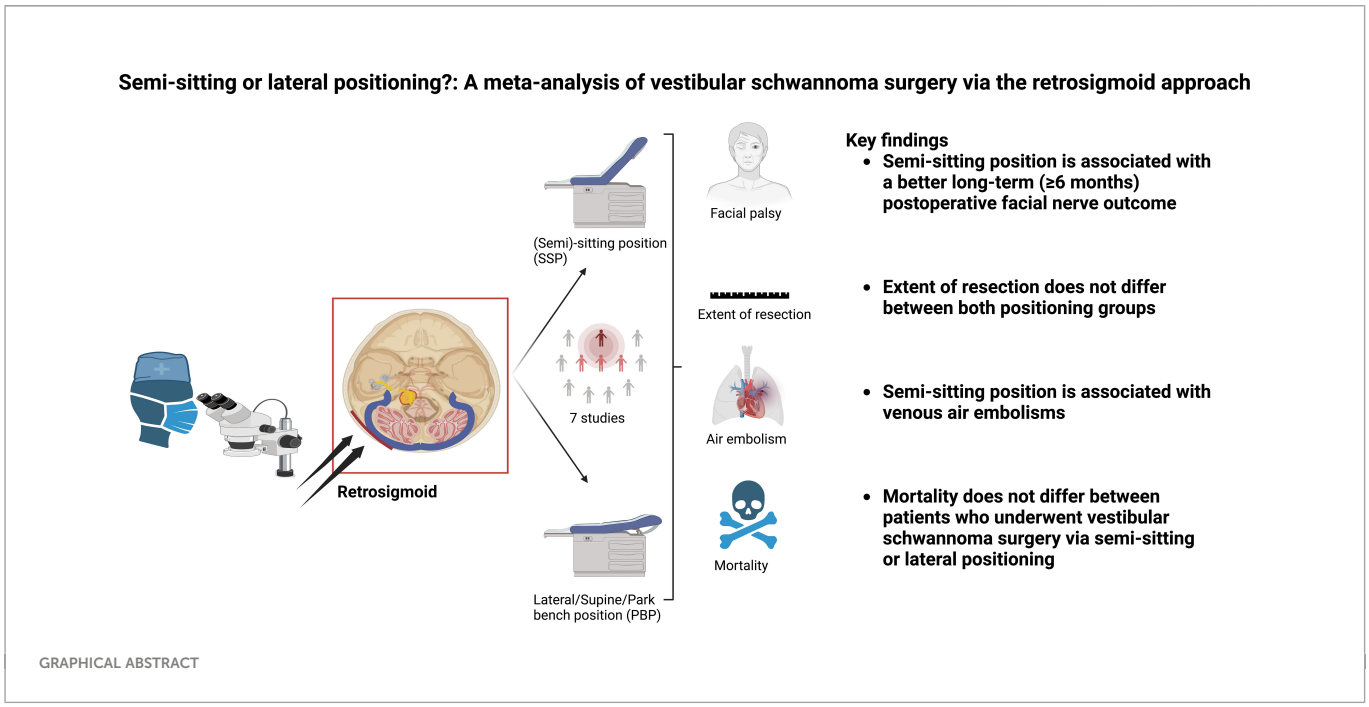

1 Introduction

Vestibular schwannoma (VS) is a benign neoplasm accounting for 75% of all tumors in the cerebellopontine angle, and it originates from the Schwann cells covering the vestibulocochlear nerve (1, 2). Gross total resection is suggested as the treatment of choice to achieve long-term tumor control (3). However, it is also of paramount importance to preserve the facial nerve. Furthermore, the perioperative mortality should be as low as possible in the context of a benign tumor disease. Due to the benign nature and slow growth rate, various therapy regimens have been introduced: watch and wait, radiotherapy or radiosurgery, and surgical resection (4, 5). The individual treatment of choice depends predominantly on the patient´s physical status, age at diagnosis, symptoms, and tumor size.

The retrosigmoid approach is the workhorse approach for enabling a microsurgical dissection in the Cerebellopontine angle. The positioning of VS patients during surgery *via* the retrosigmoid approach is highly debated. The lateral decubitus or supine positioning have been suggested for a long time as the benchmark positioning, whereas the semi-sitting positioning was underrepresented in most neurosurgical centers. The increased probability of a perioperative pulmonary air embolism and the preoperative logistical effort to perform a transesophageal echocardiogram in order to exclude a patent foramen ovale have been suggested as the major disadvantages of operating VS using the semi-sitting positioning (6). In contrast, recent monocentric comparative retrospective studies analyzing postoperative facial nerve functioning of VS patients who underwent either semi-sitting or lateral positioning found a potential superiority of the semi-sitting positioning regarding facial nerve outcome (7). To date, there is no high-level evidence (level 1 or 2) to support a general recommendation for of an individual preferred positioning for the retrosigmoid approach.

Against this backdrop, the present meta-analysis investigates comparative studies which analyzed lateral and semi-sitting positioning for VS surgery *via* the retrosigmoid approach. The primary aims of this meta-analysis are to identify the advantages and disadvantages of each kind of positioning regarding facial nerve outcome, incidence of pulmonary venous air embolism, extent of resection, and mortality.

2 Methods

For this systematic review we used the Cochrane Collaboration format (8) and the PRISMA checklist (9) were followed to conduct this systematic review.

2.1 Search strategy for identification of studies

We performed a systematic search of Pubmed database (http://www.ncbi.nlm.nih.gov/pubmed), Cochrane library, and Web of Science in September 2022. The search terms included "Vestibular Schwannoma" or "Acoustic Neuroma". The search was limited to "human studies" and "English". The inclusion criteria were formulated according to the PICOS (population, intervention, comparator, outcomes and study design) framework (10). These criteria were defined as follow: Subjects had undergone surgery for vestibular schwannoma; VS surgery was performed using the retrosigmoid approach; sitting/semi-sitting and lateral/lateral oblique/park-bench/supine positioning were compared; all results of the prespecified clinical endpoints are reported; and the studies were structured as comparative trials using those two defined positioning methods. The following kind of records were excluded: review articles, study protocols, conference abstracts, letters, unpublished manuscripts, animal experiments, and studies with insufficient data (e.g., clinical studies on the retrosigmoid approach in only one positioning group). All articles identified through the database search algorithm were evaluated for relevance according to a pre-

defined scheme: First, title screening was performed to search for articles focusing on vestibular schwannoma. Subsequently, abstract screening, and, in case of further uncertainty, full-text screening was performed independently by two authors (MV and JV). Any disagreement between the reviewers concerning study inclusion or exclusion was resolved by consensus of a third author (E.G.).

2.2 Types of studies and types of positioning

We included all comparative clinical trials reporting on two different positionings of the patients for the resection of vestibular schwannoma *via* the retrosigmoid approach. After harvesting all the available data, we conducted the meta-analysis for following outcomes: facial nerve function according to House-Brackmann (11) dichotomized into good (≤2) and poor (>2), gross total/near-total resection rates, cerebrospinal fluid leak/hydrocephalus rates requiring medical therapy, air embolism and mortality. From an intraoperative hemodynamic and ventilatory point of view, lateral positioning, supine positioning, lateral oblique (=three-quarter prone, Fukushima) position, and park-bench position are very similar to each other (12). Those kind of positionings are suggested to have the benefit of a reduced risk of venous air embolisms, whereas the sitting position or the semi-sitting (= modified sitting positioning) position are suggested to reduce intraoperative bleedings. Therefore, two general types of positions were considered and the following positions were allocated to those groups: (1) (Semi)-Sitting positioning: Semi-sitting, and Sitting-position; (2) Lateral position, supine position with extensive head rotation, lateral oblique (=Fukushima/Three-quarter prone), and park-bench position.

2.3 Statistics

Review Manager Web (Revman Web Version 5.4.1 from the Cochrane Collaboration) was used to conduct the statistical analysis. We investigated the statistical heterogeneity by x^2 and I^2 statistics. An I^2 value of 50% or more represented substantial heterogeneity. Weight of the relative contribution of the individual studies, based on the samples sizes, was included for the estimation of the treatment effects. Funnel plots were used to visually examine the publication bias of the included studies. Effect sizes were subsequently expressed as pooled odds ratio (OR) estimates in models using random effect.

3 Results

3.1 Literature search

In total, 16667 English records were screened for possible eligibility. After title, abstract, duplicate records, and full-text

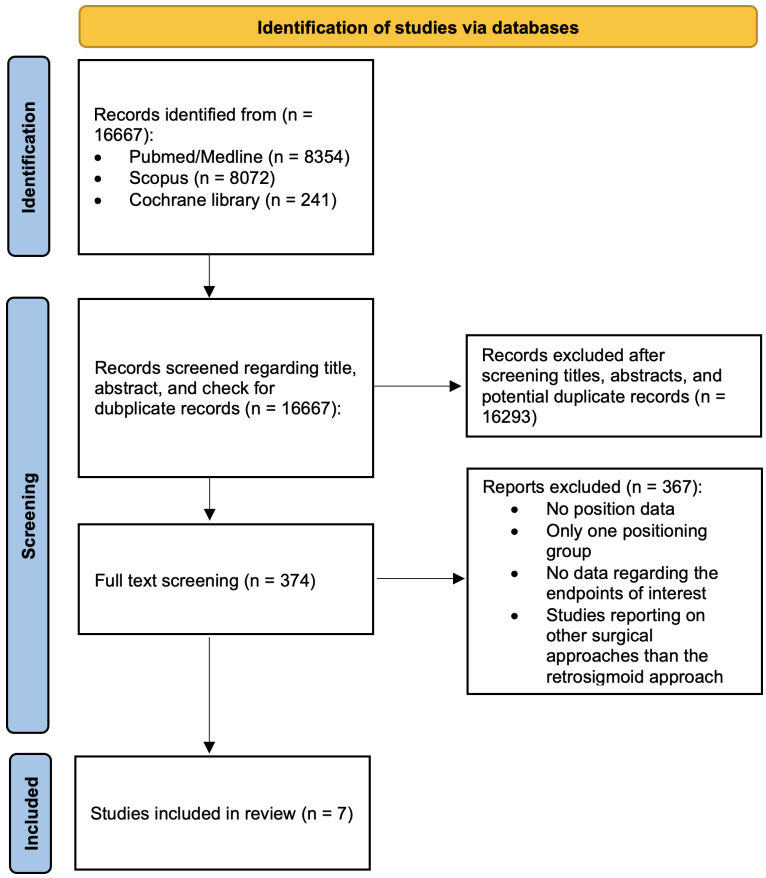

FIGURE 1
PRISMA flow chart illustrating the study selection of the present meta-analysis.

TABLE 1 Major characteristics of studies included in the present meta-analysis.

Name	Year	Study type	Types of postioing	Tumor size	Sample size (n)	Group 2: Lateral (n)	Group 1: Sitting/ Semi-Sitting (n)	Good facial nerve outcome (n)	Gross total resection (n)	CSF leak (n)	Hydrocephalus (n)	Venous air embolism (n)	Mortality (n)	Country
Song (13)	2021	R	Semi-sitting and lateral	Diameters (median): 3.9 cm (group 1) vs. 3.2 cm (group 2)	259	156	103	81/125 69/89	125/156 89/101	3/156 4/101	0/156 1/101	0/156 2/103	0%	China
Wach (14)	2020	R	Semi-sitting and lateral	Tumor size classes (1/2/3 = 0-2, 2-4, >4 cm) (not stratified by positioning)	118	86	32	29/41 20/24	60/86 23/32	NA	9/86 1/32	0/86 0/32	1/86 0/32	Germany
Schackert (15)	2020	R	Semi-sitting and lateral	Koos classification: 1: 16 2: 104 3: 164 4: 229 (not stratified by positioning)	544	381	163	54/68 134/163	363/381 150/163	2/68 14/ 163	0/68 2/163	0/68 7/163	0/68 1/163	Germany
Scheller (16)	2019	P	Semi-sitting and supine	Koos classification in group 1: 1: 1 2: 21 3: 25. 4: 9 Koos classification in group 2: 1: 1 2: 13 3: 16. 4: 11	97	41	56	31/41 48/56	30/41 52/56	2/41 1/56	0%	0/41 2/56	NA	Germany
Rössler (7)	2016	R	Semi-siting and lateral	Diameters (mean): 20.7 mm (group 1) vs. 24.9 mm (group 2)	60	30	30	12/30 19/30	26/30 26/30	3/30 1/30	NA	0/30 1/30	0%	Germany
Spektor (17)	2015	R	Sitting and lateral	Diameters (median): 30.88 mm (group 1) vs. 29.20 mm (group 2)	130	80	50	NA	58/80 41/50	3/80 1/50	1/80 0/50	NA	0%	Israel
Duke(6)	1998	R	Sitting and supine	Diameters (mean): 2.8 cm (group 1) vs. 2.2 cm (group 2)	432	210	222	NA	NA	NA	NA	11/210 63/222	0%	USA

NA, Not available; P, Prospective; R, Retrospective.

10.3389/fonc.2023.1106819

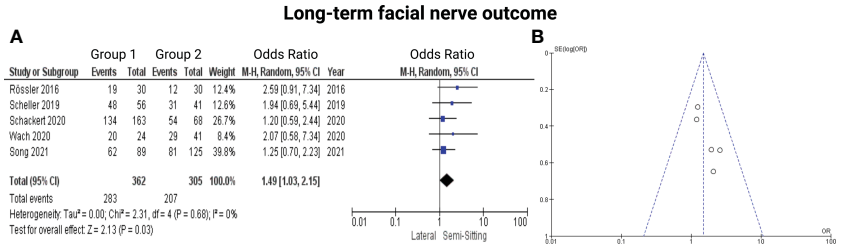

FIGURE 2
(A) Forrest Plots displaying OR and 95% CI estimates for facial nerve outcome comparison between Semi-Sitting and Lateral position and **(B)** Funnel plot showing no publication bias.

screenings, 16660 records were excluded. Finally, 7 original articles involving 1640 patients met the inclusion criteria. Figure 1 demonstrates the details of the literature search workflow.

3.2 Characteristics of included studies

The included studies were published from 1985 to 2022. Table 1 summarizes the details of the patient positioning groups and the reported outcomes of all 7 included trials. All patients of the included studies underwent surgery for VS *via* the retrosigmoid approach either in the positioning group 1 or in the positioning group 2. There was no multi-arm (≥3 arms) trial among the included studies. Reported outcome data were allocated to the patient positioning groups (lateral & semi-sitting position) to conduct the pairwise meta-analysis of the dichotomous endpoints.

3.3 Facial nerve

3.3.1 General outcome

Five of the 7 included studies reported on postoperative function of the facial nerve (7, 13–16). Positioning group 1 exclusively included patients who underwent VS surgery in the semi-sitting positioning. Reported data allowed us to dichotomize the results according to House-Brackmann score (10) into good (≤2) and poor (>2). Altogether, 667 patients were allocated to either semi-sitting positioning (n = 362) or positioning group 2 (n = 305). In the positioning group 2, 207 out of 305 patients (67.8%) showed good postoperative facial nerve function compared to 283 out of 362 (78.1%) in semi-sitting position. Facial nerve outcomes were assessed either at 6- or at 12-months postoperatively. The odds ratio (OR) for good postoperative outcome in the pooled analysis was 1.49 (95% CI: 1.03 – 2.15, p = *0.03*). I^2 of 0% showed no significant heterogeneity among the studies (*p=0.68*). The Funnel-plot analysis showed no publication bias. For detailed information, see Figure 2.

Subsequently, we divided the studies according to the time of evaluation of the postoperative facial nerve outcome into 6-months outcome and 12-months outcome and analyzed the results accordingly:

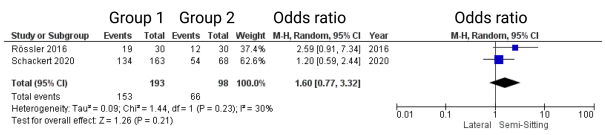

FIGURE 3
Forrest Plots displaying OR and 95% CI estimates for facial nerve outcome comparison between positioning group 1 (exclusively semi-sitting positioning) and positioning group 2 at 6 months postoperatively.

3.3.2 Outcome at 6-months after surgery for vestibular schwannoma

Two out of 7 studies report on facial nerve outcome at 6-months after surgery for VS (7, 15). Reported data allowed us to dichotomize the results according to House-Brackman score (10) into good (≤2) and poor (>2). Altogether, 291 patients were allocated to either semi-sitting positioning (n = 193) or positioning group 2 (n = 98). In positioning group 2, 66 out of 98 (67.3%) showed good outcome at 6-months postoperatively compared to 153 out of 193 patients (79.2%) in semi-sitting position. The odds ratio (OR) for good postoperative outcome in the pooled analysis was 1.60 (95% CI: 0.77 – 3.32, p = *0.21*). I^2 of 30% showed no significant heterogeneity among the studies (*p=0.23*). For detailed information, see Figure 3.

3.3.3 Outcome at 12 months postoperatively

Three out of 7 studies reported on facial nerve outcome at 12-months after VS surgery (13, 14, 16). Reported data allowed us to dichotomize the results according to House-Brackman score (10) into good (≤2) and poor (>2). Altogether, 376 patients were allocated to either semi-sitting positioning (n = 207) or positioning group 2 (n = 169). In positioning group 2, 141 out of 207 patients (68.1%) showed good outcome 6-months postoperatively compared to 130 out of 169 (76.9%) in semi-sitting positioning group. The odds ratio (OR) for good postoperative outcome in the pooled analysis was 1.47 (95% CI: 0.92 – 2.35, p = *0.11*). I^2 of 0% showed no significant heterogeneity among the studies *(p=0.65)*. For detailed information, see Figure 4.

3.4 Extent of resection – Gross total resection

Six of the 7 included studies reported on the rates of gross total resection in surgery for VS (7, 13–17). Two studies further reported on the rates of near total resection (13, 16). Three studies reported on the frequencies of patients who did not underwent a gross total

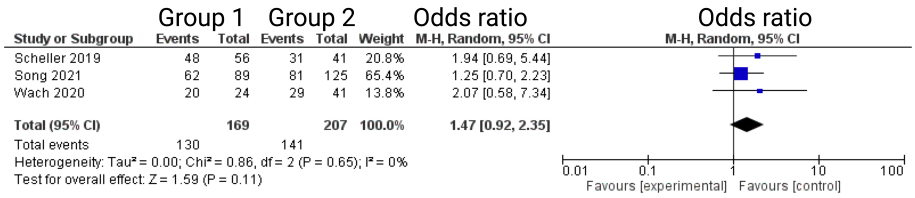

FIGURE 4
Forrest Plots displaying OR and 95% CI estimates for facial nerve outcome comparison between positioning group 1 (exclusively semi-sitting positioning) and positioning group 2 at 12 months postoperatively.

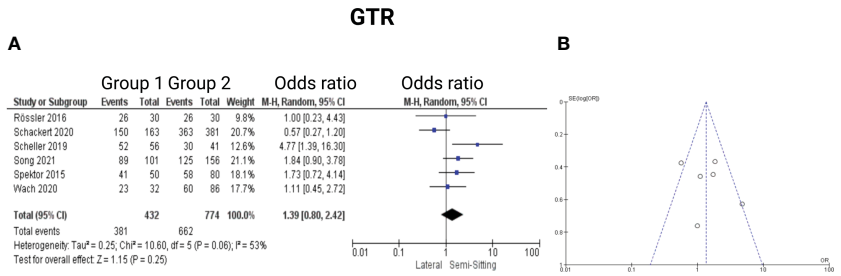

FIGURE 5
(A) Forrest Plots displaying OR and 95% CI estimates for gross total resection. **(B)** Funnel plot showing publication bias.

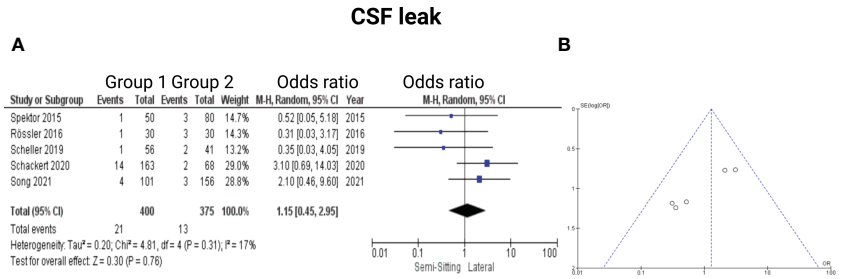

FIGURE 6
(A) Forrest Plots displaying OR and 95% CI estimates for CSF leak. **(B)** Funnel plot showing publication bias.

resection (7, 14, 15). Spektor et al. (17) reported data on patients who underwent a complete resection, subtotal resection, and partial resection, respectively. Reported data allowed us to dichotomize the results into gross totally and incompletely resected VS patients. Altogether, 1206 patients were allocated to either positioning group 1 (n = 432) or positioning group 2 (n = 774). In lateral position, 662 out of 774 patients (85.5%) underwent a gross total resection (GTR, whereas 381 out of 432 (88.2%) underwent GTR in sitting or semi-sitting position. The odds ratio (OR) for GTR in the pooled analysis was 1.39 (95% CI: 0.80 – 2.42, $p = 0.25$). I^2 of 53% showed moderate, but not statistically significant heterogeneity among the studies *(p=0.06)*. For detailed information, see Figure 5.

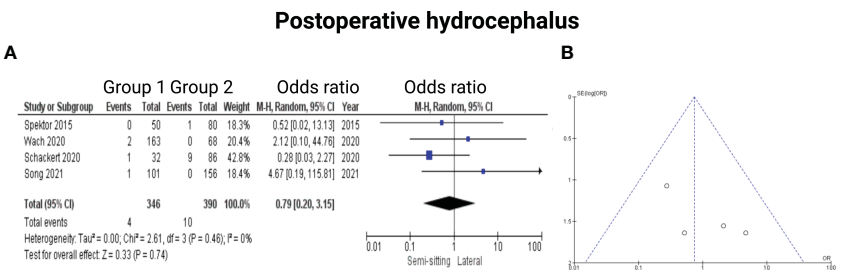

FIGURE 7
(A) Forrest Plots displaying OR and 95% CI estimates for Hydrocephalus. **(B)** Funnel plot showing publication bias.

3.5 CSF leak and postoperative hydrocephalus

3.5.1 CSF leak

Five of the 7 included studies reported on CSF leak (7, 13, 15–17). Timepoints of the exact occurrence of postoperative CSF fistula were not given. All patients underwent a secondary treatment for CSF fistula (lumbar drain or revision surgery). Rössler et al. (7) stated that all CSF leak patients underwent a revision surgery. Reported data allowed us to dichotomize the results according to presence of CSF leak. Altogether, 775 patients were allocated to either positioning group 1 (n = 400) or positioning group 2 (n = 375). In positioning group 2, 13 out of 375 patients (4.9%) had CSF leaks compared to 21 out of 400 (5.3%) in sitting or semi-sitting position. The odds ratio (OR) for the presence of CSF leak in the pooled analysis was 1.15 (95% CI: 0.45 – 2.95, $p = 0.76$). I^2 of 17% showed no significant heterogeneity among the studies *(p=0.31)*. For detailed information, see Figure 6.

3.5.2 Postoperative hydrocephalus

Four of the 7 included studies reported on hydrocephalus (13–15, 17). Reported data allowed us to dichotomize the results according to presence of postoperative hydrocephalus. Altogether, 736 patients were allocated to either sitting or semi-sitting (n = 346) or positioning group 2 (n = 390). In positioning group 2, 10 out of 390 patients (2.6%) showed hydrocephalus compared to 4 out of 346 (1.6%) in the sitting or semi-sitting position. The odds ratio (OR) for the presence of hydrocephalus in the pooled analysis was 0.79 (95% CI: 0.20 – 3.15, $p = 0.74$). I^2 of 0% showed no significant heterogeneity among the studies *(p=0.46)*. For detailed information, see Figure 7.

3.6 Venous air embolism

Five of the 7 included studies reported on venous air embolism (6, 7, 13, 15, 16). Reported data allowed us to dichotomize the results according to overall incidence of venous air embolism. Altogether, 1079 patients were allocated to either sitting/semi-sitting (n = 574) or positioning group 2 (n = 505). In positioning group 2, 11 out of 505 patients (2.2%) showed venous air embolism compared to 75 out of 574 (13.1%) in sitting or semi-sitting position. The odds ratio (OR) for the presence of venous air embolism in the pooled analysis was 6.77 (95% CI: 3.66 – 12.54, $p < 0.00001$). This effect was mainly based on the findings of the study by Duke et al. (6) in which patients of positioning group 1 underwent surgery in the sitting position. I^2 of 0% showed no significant heterogeneity among the studies *(p=0.98)*. Funnel plot analysis showed no significant publication bias. For detailed information, see Figure 8.

3.7 Mortality

Two of the 7 included studies reported on mortality (14, 15). Reported data allowed us to dichotomize the results. Altogether, 349 patients were allocated to either positioning group 1 (n = 195) or positioning group 2 (n = 154). In positioning group 2, 1 out of 154 patients (0.6%) deceased compared to 1 out of 194 (0.5%) in the sitting or semi-sitting position. The odds ratio (OR) for the mortality in the pooled analysis was 1.05 (CI 95%: 0.11 – 10.27), $p = 0.96$. I^2 of 0% showed no significant heterogeneity among the studies *(p=0.87)*. For detailed information, see Figure 9.

4 Discussion

In the present meta-analysis, we have summarized the evidence from comparative studies investigating lateral and semi-sitting positioning for VS surgery using the retrosigmoid approach. Our main results can be summarized as follows: (1) The postoperative long-term (≥6 months) facial nerve outcome was significantly better in the patients who underwent VS surgery *via* the retrosigmoid approach in the semi-sitting position; (2) Extent of resection is not influenced by the patient positioning; (3) The rate of CSF leaks or hydrocephalus is equal among both positioning groups; (4) Pulmonary venous air embolism was significantly associated with sitting positioning; (5) Perioperative mortality is not influenced by the positioning and both methods are safe for the retrosigmoid approach.

Immediate worsening of the facial nerve functioning in the first weeks after surgery is a frequently observed dysfunction after VS surgery. Despite a preservation of the anatomical and electrophysiological continuity of the facial nerve, immediate worsening after surgery can often not be avoided. Predictors for postoperative facial nerve functioning are the extent of resection, neuropathological characteristics (e.g., MIB-1 index, macrophage density), intraoperative electrophysiological threshold and the proximal-to-distal amplitude ratio (14, 18–20). Postoperative 7th nerve palsy can promote many serious side effects. Often, additional surgeries to treat facial nerve palsy induced comorbidities are necessary (e.g., hypoglossal-facial nerve anastomosis (21), treatment of eye and tear dysfunctions). To date, the retrosigmoid approach is the workhose for

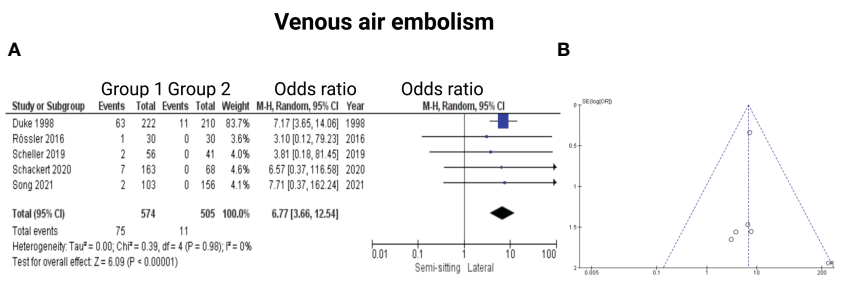

FIGURE 8
(A) Forrest Plots displaying OR and 95% CI estimates for venous air embolism. **(B)** Funnel plot for publication bias.

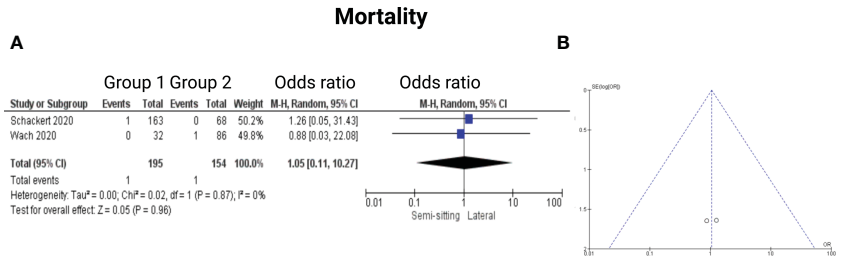

FIGURE 9
(A) Forrest Plots displaying OR and 95% CI estimates for mortality. **(B)** Funnel plot for publication bias.

surgery of vestibular schwannomas in the cerebellopontine angle (22). Large tumors (classified according to Koos as T3 or T4) can be challenging and necessitate extensive surgical interventions (23). Facilitating surgery by placing the VS patients into the semi-sitting position reduces the use of surgical aspirators in the resection cavity by enhancing the venous drainage and irrigation fluid keeps the cavity clear during surgery. Hence, the surgeon might have an improved setting regarding the use of both hands and can work bimanually with a straight and direct view of the operating field at the stage of nerve structure preparation. The identification of the facial nerve can be very challenging and in giant VSs the facial nerve can be stretched around the schwannoma. Hence, a clear surgical view is of paramount importance to identify the nerve structures. The semi-sitting position might enable surgery with less bleeding, brain swelling, and reduced intracranial pressure due to the improved venous drainage of the cerebral blood flow (24). Furthermore, gravity enables an operating field free from blood and CSF (24). The continuous irrigation during semi-sitting surgery facilitates the bimanual dissection technique. Furthermore, Schackert et al. (14) showed that the intraoperative blood loss is significantly lower in patients who underwent VS surgery using the semi-sitting positioning. Hence, those favorable intraoperative physiological mechanisms in the semi-sitting VS patients seem to support a more ergonomic work of the neurosurgeon which reduces the factors resulting in surgical manipulations of the facial nerve.

We found no significant association between the patient positioning and the probability of a gross total resection in our meta-analysis. Extent of resection is of paramount importance regarding the long-term tumor control and patients who underwent a complete resection have a lower risk of recurrence (25). However, there is also evidence that subtotal resection with subsequent irradiation of tumor remnants is also a feasible method to provide a nearly equal result with regard to the probability of progression-free survival (25, 26). Nevertheless, a total tumor resection results in a 30-50% risk of a facial nerve dysfunction (27–31). Hence, there is a stringent need for each VS patient regarding the creation of a tailored treatment and follow-up schedule. Preserving cranial nerve functioning is the primary goal and precedes the goal of achieving maximal cytoreductive surgery.

The positioning of the VS patients in the retrosigmoid approach was not found to have a role in the frequency of postoperative CSF leaks. The incidence of CSF leaks after surgery for vestibular schwannoma *via* the retrosigmoid approach is reported with a broad range from 0% to 27% (32, 33). Hence, there is no optimum positioning to potentially reduce the patient's risk of a secondary surgery to repair a CSF leak. Hydrocephalus is found in 3.7-42% of patients with a VS (34–37). Despite total tumor removal, hydrocephalus sometimes does not improve because of obstruction of the arachnoid granulations by proteins or hemorrhage (37, 38). In the present meta-analysis, we could not identify a role of the positioning regarding the development of a persistent hydrocephalus. Tumor size, increased age at diagnosis, and cystic tumor appearance are suggested as the main predictors of persistent postoperative hydrocephalus necessitating therapy (39).

Due to the inconsistency of reported data, we were not able to statistically examine the effect of the positioning on the surgery duration (see supplementary Table 1). The most consistent data was reported on skin-to-skin time. Schackert (15) and Roessler (7) show significantly shorter mean duration if surgery was performed in semi-sitting position. On the other hand, Spektor (17) favors lateral positioning with mean difference of 163.8 minutes. The possible explanation for these discrepancies might be the change of the surgical workflow over the course of the years demonstrated by Schackert et al. (15). In the analysis of surgery duration, Schackert shows the tendency towards skin-to-skin time reduction between 1991 and 2019, mainly for T3 and T4 tumors. Furthermore, semi-sitting positioning significantly reduced the skin-to-skin time in larger T3-4 tumors, whereas no influence on skin-to-skin time was observed in T 1-2 tumors (15).

These facts would theoretically support the sitting position for giant VSs because of the emerging availability of radiosurgical therapy for T1 and T2 VS. Most of the VS surgeries are indicated because of the mass effect on the brainstem and are caused by giant VSs of the T3-4 category, in which the semi-sitting position seems to significantly shorten the length of the procedure (15)."

The most feared adverse event in patients who underwent VS surgery *via* the retrosigmoid approach using sitting or semi-sitting positioning is venous air embolism. We found that semi-sitting positioning is significantly associated with an increased risk of venous air embolism. However, this finding has to be interpreted with caution because the severity of the venous air embolisms was not homogeneously classified (e.g., hemodynamic instability, length of stay in ICU) in the individual studies which did not allow a more detailed analysis. Venous air embolism can cause pulmonary edema, acute respiratory distress syndrome and acute right ventricular failure (40). The literature provides data with a wide range between 5.6-21% regarding the risk of venous air embolism (41–43). However, this wide range might be caused by the heterogeneous intraoperative monitoring techniques to detect a venous air embolism (e.g., transesophageal echocardiography, transthoracic doppler, capnography, mass spectrometry). For instance, it is known that a

transesophageal echocardiography identifies significantly more venous air embolism events compared to a transthoracic doppler, but the incidence of clinically relevant venous air embolisms (drop in end-tidal carbon dioxide above 3 mmHg) using the transthoracic doppler is much higher (24). Hence, the majority of the venous air embolisms were found to be non-significant, and the patients had no clinically relevant sequelae (24, 44). This finding is also reaffirmed by our meta-analysis which found no association regarding the perioperative mortality and patient positioning in VS surgery *via* the retrosigmoid approach. Consequently, both methods seem to be safe and pulmonary venous air embolism in the semi-sitting positioning can be prevented and managed in an experienced interdisciplinary team. Indeed, a patent foramen ovale is considered to be an exclusion criterion for the semi-sitting position. In those cases, the patient should not underwent VS surgery in the semi-sitting positioning and they should be operated on in the prone, supine or lateral position. Nevertheless, the German Society of Anaesthesiology and Intensive Care approves semi-sitting positioning in neurosurgical patients if the benefits outrank the risks (45). The presence of a giant vestibular schwannoma with an increased risk of a new postoperative facial nerve palsy might be a potential indication for this tailored interdisciplinary teamwork using a semi-sitting positioning. The main strategy is to prevent venous air embolisms, and not the detection. Operating in the semi-sitting position necessitates a continuous communication and interdisciplinary teamwork with the neuroanesthesiologists. For instance, electrophysiological monitoring, intermittent bilateral jugular compression to identify venous leaks, moving the VS patients into "head down-feet up", and hemodynamic management using continuous fluid administration to increase the central venous pressure are essential intraoperative steps which have to be communicated and decided interdisciplinary by the neurosurgeon and the neuroanesthesiologist. Against the background of equivalent perioperative mortality among semi-sitting or lateral positioning in VS surgery *via* the retrosigmoid approach, semi-sitting positioning should be strongly considered in the setting of an experienced interdisciplinary team if it is preoperatively known that the patients have no patent foramen ovale.

The major limitation of our meta-analysis of comparative trials investigating semi-sitting and lateral positioning is the retrospective design of the included studies. Moreover, we could not include the duration of the surgery in a reliable statistical analysis because of relevant differences regarding the definition of duration as well as the reported outcome data (e.g., median, mean values, lack of standard deviation). Furthermore, there are heterogeneous definitions of the venous air embolisms. Furthermore, six of seven studies reported the rates of complete VS resection but further analysis of the rates of near total resection was limited to only two studies. Moreover, the tumor size might be a potential confounder in the analysis of the facial nerve outcome. Heterogeneous measurements and definitions of tumor size did not allow an inclusion of this variable in our meta-analysis approach. However, the meta-analysis showed that the perioperative safety regarding mortality is equal among both positioning methods and the facial nerve might have a better outcome in the semi-sitting group. An ongoing prospective randomized controlled trial comparing semi-sitting and lateral position in vestibular schwannoma surgery might give some further essential insights into this interesting debate (Chinese Clinical Trial Registry: ChiCTR1900027550) (46).

5 Conclusion

Semi-sitting positioning seems to be associated with an improved facial nerve outcome after VS surgery *via* the retrosigmoid approach. The incidence of venous air embolisms is significantly higher among the patients who underwent VS surgery in the semi-sitting position, but there is no difference regarding perioperative mortality between semi-sitting or lateral positioning. Further multicentric prospective randomized trials with a homogeneous intraoperative neuroanesthesiological monitoring setup are needed to provide a detailed assessment of the risk and benefits of each positioning in the retrosigmoid approach.

Author contributions

Data acquisition was performed by JW; MV, and EG performed the data interpretation. Writing and creation of figures were performed by JW, MV, and EG Proof reading was done by FA, and EG. All authors contributed to the article and approved the submitted version

Acknowledgments

The graphical abstract in this article was created using BioRender.

Conflict of interest

The authors declare that the research was conducted in the absence of any commercial or financial relationships that could be construed as a potential conflict of interest.

Publisher's note

Supplementary material

The Supplementary Material for this article can be found online at: https://www.frontiersin.org/articles/10.3389/fonc.2023.1106819/full#supplementary-material

References

1. Ammar MB, Piccrillo E, Topsakal V, Taibah A, Sanna M. Surgical results and technical refinements in translabyrinthine excision of vestibular schwannomas: the gruppo otologico experience. *Neurosurgery* (2012) 70:1481–91. doi: 10.1227/NEU.0b013e31824c010f

2. Wach J, Güresir A, Borger V, Schuss P, Becker A, Coch C, et al. Elevated basline c-reactive protein levels predict poor progression-free survival in sporadic vestibular schwannoma. *J Neurooncol* (2022) 156(2):365–75. doi: 10.1007/s11060-021-03918-0

3. Samii M, Gerganov VM, Samii A. Functional outcome after complete surgical removal of giant vestibular schwannomas. *J Neurosurg* (2010) 112:860–7. doi: 10.3171/2009.7.JNS0989

4. Torres Maldonado S, Naples JG, Fathy R, Eliades SJ, Lee JYK, Brant JA, et al. Recent trends in vestibular schwannoma management: an 11-year analysis of the national cancer database. *Otolaryngol Head Neck Surg* (2019) 161:137–43. doi: 10.1177/0194599819835495

5. Leon J, Trifiletti DM, Waddle MR, Vallow L, Ko S, May B, et al. Trends in initial management of vestibular schwannoma in the united states. *J Clin Neurosci* (2019) 68:174–8. doi: 10.1016/j.jocn.2019.07.002

6. Duke DA, Lynch JJ, Harner SG, Faust RJ, Ebersold MJ. Venous air embolism in sitting and supine patients undergoing vestibular schwannoma resection. *Neurosurgery* (1998) 42:1282–6. doi: 10.1097/00006123-199806000-00047

7. Roessler K, Krawagna M, Bischoff B, et al. Improved postoperative facial nerve and hearing function in retrosigmoid vestibular schwannoma surgery significantly associated with semisitting position. *World Neurosurg* (2016) 87:290–7. doi: 10.1016/j.wneu.2015.11.089

8. Higgins JPT, Thomas J, Chandler J, Cumpston M, Li T, Page MJ, Welch VA (editors). *Cochrane Handbook for Systematic Reviews of Interventions version 6.3 (updated February 2022)*. Cochrane (2022). Available from www.training.cochrane.org/handbook.

9. Moher D, Liberati A, Tetzlaff J, Altman DG. Preferred reporting items for systematic reviews and meta-analyses: the PRISMA statement. *PloS Med* (e1000097) 2009):6. doi: 10.1371/journal.pmed.1000097

10. Schardt C, Adams MB, Owens T, Keitz S, Fontelo P. Utilization of the PICO framcework to improve searching PubMed for clinical questions. *BMC Med Inform Decis Mak* (2007) 7:16. doi: 10.1186/1472-6947-7-16

11. House JW, Brackmann DE. Facial nerve grading system. *Otolaryngol Head Neck Surg* (1985) 93(2):146–7. doi: 10.1177/019459988509300202

12. Velho V, Naik H, Bhide A, Bhople L, Gade P. Lateral semi-sitting position: A novel method of patient´s head positioning in suboccipital retrosigmoid approaches. *Asian J Neurosurg* (2019) 14(1):82–6. doi: 10.4103/ajns.AJNS_203_17

13. Song G, Liu D, Wu X, Wang X, Zhou Y, Li M, et al. Outcomes after semisitting and lateral positioning in large vestibular schwannoma surgery: A single-center comparison. *Clin Neurol Neurosurg* (2021) 207:106768. doi: 10.1016/j.clineuro.2021.106768

14. Wach J, Brandecker S, Güresir A, Schuss P, Vatter H, Güresir E. The impact of the MIB-1 index on facial nerve outcomes in vestibular schwannoma surgery. *Acta Neurochir (Wien)* (2020) 162(5):1205–13. doi: 10.1007/s00701-020-04283-z

15. Schackert G, Ralle S, Martin KD, Reiss G, Kowalski M, Sobottka SB, et al. Vestibular schwannoma surgery: Outcome and complications in lateral decubitus position versus semi-sitting position-a personal learning curve in a series of 544 cases over 3 decades. *World Neurosurg* (2021) 148:e182–91. doi: 10.1016/j.wneu.2020.12.107

16. Scheller C, Rampp S, Tatagiba M, Gharabaghi A, Ramina KF, Ganslandt O, et al. A critical comparison between the semisitting and the supine positioning in vestibular schwannoma surgery: subgroup analysis of a randomized, multicenter trial. *J Neurosurg* (2019) 133(1):1–8. doi: 10.3171/2019.1.JNS181784

17. Spektor S, Fraifeld S, Margolin E, Saseedharan S, Eimerl D, Umansky F. Comparison of outcomes following complex posterior fossa surgery performed in the sitting versus lateral position. *J Clin Neurosci* (2015) 22(4):705–12. doi: 10.1016/j.jocn.2014.12.005

18. Graffeo CS, Perry A, Raghunathan A, Kroneman TN, Jentoft M, Driscoll CL, et al. Macrophage density predicts facial nerve outcome and tumor growth after subtotal resection of vestibular schwannoma. *J Neurol Surg B Skull Base* (2018) 79(5):482–8. doi: 10.1055/s-0038-1627474

19. Sobottka SB, Schackert G, May SA, Wiegleb M, Reiss G. Intraoperative facial nerve monitoring (IFNM) predicts facial nerve outcome after resection of vestibular schwannoma. *Acta Neurochir (Wien)* (1998) 140:235–42. doi: 10.1007/s007010050090

20. Acioly MA, Liebsch M, de Aguiar PH, Tatagiba M. Facial nerve monitoring during cerebellopontine angle and skull base tumor surgery: a systematic review from description to current success on function prediction. *World Neurosurg* (2013) 80:e271–300. doi: 10.1016/j.wneu.2011.09.026

21. Han JH, Suh MJ, Kim JW, Cho HS, Moon IS. Facial reanimation using hypoglossal-facial nerve anastomosis after schwannoma removal. *Acta Otolaryngol* (2017) 137:99–105. doi: 10.1080/00016489.2016.1212398

22. Jackler RK, Pitts LH. Selection of surgical approach to acoustic neuroma. *Neurosurg Clin N Am* (1992) 19:217–38. doi: 10.1016/j.nec.2008.02.010

23. Erickson NJ, Schmalz PGR, Agee BS, Fort M, Walters BC, McGrew BM, et al. Koos classification of vestibular schwannomas: A realiability study. *Neurosurgery* (2019) 85 (3):409–14. doi: 10.1093/neuros/nyy409

24. Günther F, Frank P, Nakamura M, Hermann EJ, Palmaers T. Venous air embolism in the sitting position in cranial neurosurgery: incidence and severity according to the used monitoring. *Acta Neurochir (Wien)* (2017) 159(2):339–46. doi: 10.1007/s00701-016-3034-7

25. Park HH, Park SH, Oh HC, Jung HH, Chang JH, Lee KS, et al. The behavior of residual tumors following incomplete surgical resection for vestibular schwannomas. *Sci Rep* (2021) 11(1):4665. doi: 10.1038/s41598-021-84319-1

26. Iwai Y, Ishibashi K, Watanabe Y, Uemura G, Yamanaka K. Functional preservation after planned partial resection followed by gamma knife radiosurgery for large vestibular schwannomas. *World Neurosurg* (2015) 84:292–300. doi: 10.1016/j.wneu.2015.03.012

27. Sughrue ME, Kaur R, Rutkowski MJ, Kane AJ, Kaur G, Yang I, et al. Extent of resection and the long-term durability of vestibular schwannoma surgery. *J Neurosurg* (2011) 114:1218–23. doi: 10.3171/2010.11.JNS10257

28. Jung S, Kang SS, Kim TS, Kim HJ, Jeong SK, Kim SC, et al. Current surgical results of retrosigmoid approach in extralarge vestibular schwannomas. *Surg Neurol* (2000) 53 (4):370–7. doi: 10.1016/S0090-3019(00)00196-8

29. Lanman TH, Brackmann DE, Hitselberger WE, Subin B. Report of 190 consecutive cases of large acoustic tumors (vestibular schwannoma) removed via the translabyrinthine approach. *J Neurosurg* (1999) 90:617–23. doi: 10.3171/jns.1999.90.4.0617

30. Zhang X, Fei Z, Chen YJ, Fu LA, Zhang JN, Liu WP, et al. Facial nerve function after excision of large acoustic neuromas via the suboccipital retrosigmoid approach. *J Clin Neurosci* (2005) 12(4):405–8. doi: 10.1016/j.jocn.2004.03.042

31. Nakatomi H, Jacob JT, Carlson ML, Tanaka S, Tanaka M, Saito N, et al. Long-term risk of recurrence and regrowth after gross-total and subtotal resection of sporadic vestibular schwannoma. *J Neurosurg* (2017) 19:1–7. doi: 10.3171/2016.11.JNS16498

32. Hoffmann RA. Cerebrospinal fluid leak following acoustic neuroma removal. *Laryngoscope* (1994) 104(1 Pt 1):40–58. doi: 10.1288/00005537-199401000-00009

33. Bentivoglio P, Cheeseman AD, Symon L. Surgical management of acoustic neuromas during the last five years. part I. *Surg Neurol* (1988) 29:197–204. doi: 10.1016/0090-3019(88)90006-7

34. Tanaka Y, Kobayashi S, Hongo K, Tada T, Sato A, Takasuna H. Clinical and neuroimaging characteristics of hydrocephalus associated with vestibular schwannoma. *J Neurosurg* (2003) 98:1186–93. doi: 10.3171/jns.2003.98.6.1188

35. Fukuda M, Oishi M, Kawaguchi T, Watanabe M, Takao T, Tanaka R, et al. Etiopathological factors related to hydrocephalus associated with vestibular schwannoma. *Neurosurgery* (2007) 61:1186–93. doi: 10.1227/01.neu.0000306096.61012.22

36. Briggs RJ, Shelton C, Kwartler JA, Hitselberger W. Management of hydrocephalus resulting from acoustic neuromas. *Otolaryngol Head Neck Surg* (1993) 109:1020–4. doi: 10.1177/019459989310900608

37. Gerganov VM, Pirayesh A, Nouri M, Hore N, Ludemann WO, Oi S, et al. Hydrocephalus associated with vestibular schwannomas: management options and factors predicting the outcome. *J Neurosurg* (2011) 114:1209–15. doi: 10.3171/2010.10.JNS1029

38. Jeon CJ, Kong DS, Nam DH, Lee JI, Park K, Kim JH. Communicating hydrocephalus associated with surgery or radiosurgery for vestibular schwannoma. *J Clin Neurosci* (2010) 17:862–4. doi: 10.1016/j.jocn.2009.12.004

39. Shin DW, Song SW, Chong S, Kim YH, Cho YH, Hong SH, et al. Treatment outcome of hydrocephalus associated with vestibular schwannoma. *J Clin Neurol* (2021) 17(3):455–62. doi: 10.3988/jcn.2021.17.3.455

40. Wong AY, Irwin MG. Large Venous air embolism in the sitting position despite monitoring with transoesophageal echocardiography. *Anesthesia* (2005) 60:811–3. doi: 10.1111/j.1365-2044.2005.04237.x

41. Breun M, Nickl R, Perez J, Hagen R, Löhr M, Vince G, et al. Vestibular schwannoma resection in a consecutive series of 502 cases via the retrosigmoid approach: technical aspects, complications, and functional outcome. *World Neurosurg* (2019) 129:e114–27. doi: 10.1016/j.wneu.2019.05.056

42. Tonn JC, Schlake HP, Goldbrunner R, Milewski C, Helms J, Roosen K. Acoustic neuroma surgery as an interdisciplinary approach: a neurosurgical series of 508 patients. *J Neurol Neurosurg Psychiatry* (2000) 69:161–6. doi: 10.1136/jnnp.69.2.161

43. Saladino A, Lamperti M, Mangraviti A, Legnani FG, Prada FU, Casali C, et al. The semisitting position: analysis of the risks and surgical outcomes in a contemporary series of 425 adult patients undergoing cranial surgery. *J Neurosurg* (2017) 127:867–76. doi: 10.3171/2016.8.JNS16719

44. Feigl GC, Decker K, Wurms M, Krischek B, Ritz R, Unertl K, et al. Neurosurgical procedures in the semisitting position: evaluation of the risk of paradoxical venous air embolism in patients with a patent foramen ovale. *World Neurosurg* (2014) 81:150–64. doi: 10.1016/j.wneu.2013.01.003

45. Fritz G, von Gösseln HH, Linstedt U, Suhr D. Perioperatives management bei neurochirurgischen operationen in sitzender oder halbsitzender position – empfehlungen des wissenschaftlichter arbeitskreis neuroanästhesie der DGAI. *Anaesth Intensivmed* (2008) 49:47–51. https://www.ai-online.info/images/ai-ausgabe/2008/01-2008/047-051_ak_neuro.pdf.

46. Wu X, Wang X, Song G, Li M, Hou C, Chen G, et al. The effects of different surgical positions (semi-sitting and lateral position) on the surgical outcomes of large vestibular schwannoma: study protocol for a randomized controlled trial. *Trials* (2022) 23(1):492. doi: 10.1186/s13063-022-06437-z

frontiers | Frontiers in Oncology

TYPE Original Research
PUBLISHED 10 February 2023
DOI 10.3389/fonc.2023.1099384

OPEN ACCESS

EDITED BY
Arianna Rustici,
University of Bologna, Italy

REVIEWED BY
Liemei Guo,
Shanghai Jiao Tong University, China
Gianluca Ferini,
Rem Radiotherapy, Italy

*CORRESPONDENCE
Ryota Tamura
moltobello-r-610@hotmail.co.jp

SPECIALTY SECTION
This article was submitted to Neuro-Oncology and Neurosurgical Oncology, a section of the journal Frontiers in Oncology

RECEIVED 15 November 2022
ACCEPTED 30 January 2023
PUBLISHED 10 February 2023

CITATION
Takahara K, Tamura R, Kuranari Y, Karatsu K, Akiyama T and Toda M (2023) Prognostic significance of preoperative neutrophil-to-lymphocyte ratio in surgically resected schwannomas. *Front. Oncol.* 13:1099384. doi: 10.3389/fonc.2023.1099384

Prognostic significance of preoperative neutrophil-to-lymphocyte ratio in surgically resected schwannomas

Kento Takahara[1], Ryota Tamura[1]*, Yuki Kuranari[2], Kosuke Karatsu[1], Takenori Akiyama[1] and Masahiro Toda[1]

[1]Department of Neurosurgery, Keio University School of Medicine, Tokyo, Japan, [2]Department of Neurosurgery, Kawasaki Municipal Hospital, Kawasaki-ku, Kanagawa, Japan

Objective: The goal of schwannoma resection is to control the tumor while preserving neurological function. Schwannomas have a variable postoperative growth pattern, therefore preoperative prediction of a schwannoma's growth pattern is favorable. This study aimed to examine the relationship between preoperative neutrophil-to-lymphocyte ratio (NLR) and postoperative recurrence and retreatment in patients with schwannoma.

Methods: We retrospectively examined 124 patients who underwent schwannoma resection in our institution. Associations between preoperative NLR, other patient and tumor characteristics, and tumor recurrence and retreatment were analyzed.

Results: Median follow-up was 2569.5 days. Postoperative recurrence occurred in 37 patients. Recurrence that required retreatment occurred in 22. Treatment-free survival (TFS) was significantly shorter in patients with NLR ≥2.21 (P = 0.0010). Multivariate Cox proportional hazards regression showed that NLR and neurofibromatosis type 2 were independent predictors of retreatment (P = 0.0423 and 0.0043, respectively). TFS was significantly shorter in patients with NLR ≥2.21 in the following subgroups: sporadic schwannoma, primary schwannoma, schwannoma ≥30 mm in size, subtotal resection, vestibular schwannoma, and postoperative recurrence.

Conclusions: Preoperative NLR ≥2.21 before surgery was significantly associated with retreatment after schwannoma resection. NLR may be a novel predictor of retreatment and assist surgeons in preoperative surgical decision making.

KEYWORDS

schwannoma, neutrophil-to-lymphocyte ratio, neurofibromatosis type 2, prognostic factor, retreatment

Introduction

Schwannomas are benign tumors that originate from Schwann cells of the cranial and peripheral nerves, and have a variable growth pattern (1). Clinical outcome after their surgical resection is related to extent of removal (2–6), which in the future could be assisted by new imaging modalities besides classic magnetic resonance imaging (MRI) (7). The goal of schwannoma resection is to control the tumor while preserving neurological function (8–11). Accurate preoperative prediction of a schwannoma's growth pattern might assist surgeons with clinical decision making regarding aggressiveness of resection and need for adjuvant radiotherapy. Ki-67 is a commonly used proliferative marker for several types of tumors; however, it cannot be evaluated before surgery and its significance in schwannoma is controversial (3, 5).

Inflammation promotes tumor development throughout all stages of tumorigenesis (12). Systemic inflammation and immune system activation is broadly reflected by the neutrophil-to-lymphocyte ratio (NLR), an inexpensive, easily measured, and readily available blood test. A high NLR has been associated with worse overall survival in many solid malignant tumors (13–17). A relationship between NLR and refractory intracranial benign tumor has also been demonstrated in other studies (18–22). In a previous study, we showed that preoperative NLR ≥2.6 was significantly associated with shorter progression-free survival in all grades of meningioma, including World Health Organization grade I (22). This study aimed to examine the relationship between preoperative NLR and postoperative recurrence and retreatment in patients with schwannoma.

Methods

Study design and clinical data

We retrospectively reviewed 270 patients who underwent surgical schwannoma resection in our institution from February 2010 to February 2018. The study received institutional review board approval (reference number, 20050002) and all patients provided written informed consent. Patients who received steroids or immunosuppressive drugs before preoperative laboratory testing, those with systemic infection, and with a history of malignancy were excluded. We also excluded those with incomplete clinical, laboratory, or radiological data.

The following data were obtained from the medical records: age at time of surgery, sex, neurofibromatosis 2 (NF2) status, tumor origin, primary/recurrent tumor, solid/cystic tumor, brain compression, neurological symptoms, and extent of removal. Tumor origin was determined using gadolinium-enhanced T1-weighted MRI. Extent of removal was determined using MRI after surgery.

MRI was performed every 6 to 12 months after surgery. In patients who underwent gross total resection (GTR), tumor recurrence was defined as the appearance of new tumor at the surgical site. In patients who underwent subtotal resection (STR), recurrence was defined as residual tumor growth ≥2 mm. Recurrence-free survival (RFS) was defined as the time from the date of surgery to the date of tumor recurrence or last imaging follow-up. Because not all schwannoma recurrences require treatment, treatment-free survival (TFS), a relatively new measure of disease control (23), was also evaluated. TFS was defined as the time from the date of surgery to the date of retreatment decision or last follow-up.

Laboratory data

Absolute neutrophil, lymphocyte, monocyte, and platelet counts and concentrations of albumin, C-reactive protein, and fibrinogen were routinely obtained before surgery and the following inflammatory parameters calculated (24–29): NLR, lymphocyte-to-monocyte ratio (LMR), platelet-to-lymphocyte ratio (PLR), and prognostic nutritional index (PNI). PNI was calculated using the following formula: (10 × albumin concentration) + (0.005 × lymphocyte count).

Statistical analysis

Statistical analyses were performed using JMP 16 software (SAS Institute, Cary, NC, USA). Continuous variables are expressed as means with standard deviation and were compared using the Mann–Whitney U test. Categorical variables are expressed as numbers with percentage and were compared using Fisher's exact test. RFS and TFS were estimated using the Kaplan–Meier method and compared using the log-rank test. Univariate and multivariate Cox proportional hazards regression were used to evaluate the influence of variables on RFS and TFS. Receiver operating characteristic (ROC) curves were constructed to determine optimal cut-off values for each variable. $P < 0.05$ was considered significant.

Results

Patient characteristics and laboratory data

After excluding 146 patients based on criteria, 124 patients were included for analysis. Median follow-up was 2569.5 days. Postoperative recurrence occurred in 37 patients; recurrence that required retreatment occurred in 22. ROC curves were constructed for each variable using two outcomes, recurrence and retreatment. The optimal NLR cut-off value for recurrence and retreatment was 2.03 and 2.21, respectively. The area under the curve for recurrence and retreatment was 0.6039 and 0.7273, respectively (Supplementary Figure 1). Table 1 and Supplementary Table 1 show patient and tumor characteristics overall and with patients stratified by NLR cut-off value. The stratified groups were similar except for extent of resection. As shown in Figure 1, NLR value was significantly higher in younger patients and those with NF2 and tumor size ≥30 mm. NLR value was significantly higher in the retreatment group than the no recurrence and the recurrence but no retreatment groups. This suggests that NLR might be an important predictor of retreatment. NLR did not significantly differ between the no recurrence and the recurrence but no retreatment groups (Figure 2).

10.3389/fonc.2023.1099384

TABLE 1 Patient and tumor characteristics.

Clinical feature	All cases	Baseline NLR		P value
		<2.21	≧2.21	
		No.(%)	No.(%)	
Patient number	124	75 (60.5)	49 (39.5)	
Age (means ± SD)		49.8 ± 12.9	47.0 ± 14.8	0.2694
Sex				0.2689
Male	55	30 (54.5)	25 (45.5)	
Female	69	45 (65.2)	24 (34.8)	
NF2				0.1104
+	11	4 (36.4)	7 (63.6)	
-	113	71 (62.8)	49 (37.2)	
Tumor status				>0.9999
primary	109	66 (60.6)	43 (39.4)	
recurrent	15	9 (60.0)	6 (40.0)	
Tumor origin				0.2212
CN 8	91	52 (57.1)	39 (42.8)	
non CN 8	33	23 (69.7)	10 (30.3)	
Neurological symptoms				0.5629
+	110	65 (59.1)	45 (40.9)	
-	14	10 (71.4)	4 (28.6)	
Tumor size (mm)		24.8 ± 13.0	29.1 ± 12.0	0.0713
Brain compression				0.3416
+	79	45 (57.0)	34 (43.0)	
-	45	30 (66.7)	15 (33.3)	
Tumor cyst				0.3610
+	59	33 (55.9)	26 (44.1)	
-	65	42 (64.6)	23 (35.4)	
Removal rate				**0.0228**
GTR	46	34 (73.9)	12 (26.1)	
non-GTR	78	41 (52.6)	37 (47.4)	

NLR, neutrophil-to-lymphocyte ratio; SD, standard deviation; NF2, neurofibromatosis type 2; CN, cranial nerve; GTR, gross total resection.
Factors which made statistically significant differences are shown in bold.

Survival analysis

As shown in Supplementary Figure 2, RFS was significantly shorter in patients with NF2 than in patients without NF2 (p <0.0001); RFS did not significantly differ between patients stratified by NLR using a cut-off value of 2.03 (p = 0.088). TFS was significantly shorter in patients with NF2 and in those who underwent STR (p <0.0001 and p = 0.0040, respectively; Figure 3A, B). TFS was significantly shorter in patients with NLR ≥2.21 (p = 0.0010; Figure 3C).

Univariate and multivariate analyses

Because NLR was associated with TFS but not RFS, univariate and multivariate Cox proportional hazards regression was performed to investigate the influence of variables on TFS (Tables 2, 3). Although LMR was also associated with shorter TFS, NLR had a higher statistical power than LMR. The multivariate analysis showed that NF2 and NLR ≥2.21 were independent predictors of retreatment (P = 0.0043 and 0.0423, respectively).

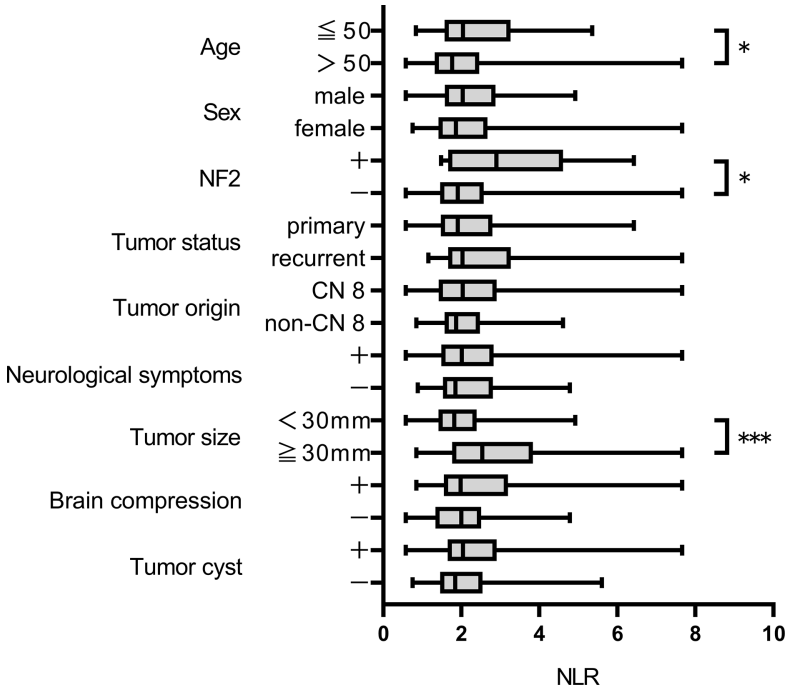

FIGURE 1
NLR value according to clinical characteristics *p < 0.05, ***p < 0.001.

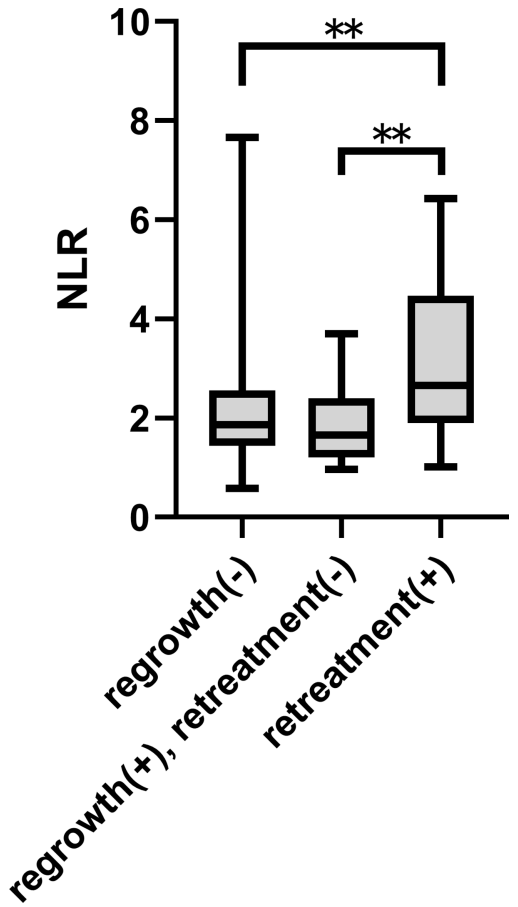

FIGURE 2
NLR value according to postoperative outcome **p < 0.01.

10.3389/fonc.2023.1099384

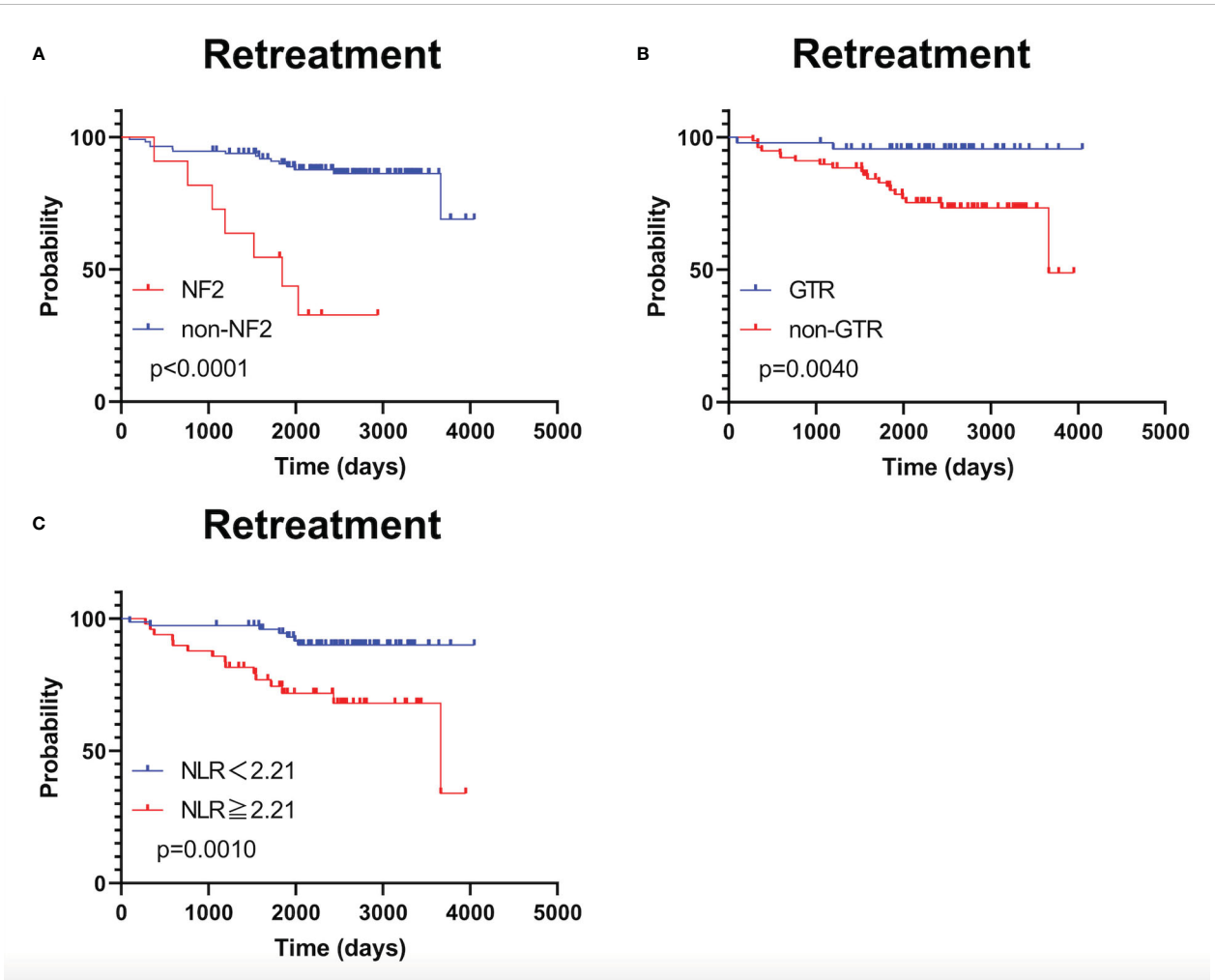

FIGURE 3
Kaplan–Meier treatment-free survival curves with patients stratified according to neurofibromatosis type 2 status **(A)**, extent of tumor removal **(B)**, and optimal neutrophil-to-lymphocyte ratio cut-off value **(C)**.

TABLE 2 Univariate Cox proportional hazards regression analysis.

Variables	HR	95% CI	p value
Age (>50)	0.60	0.25-1.49	0.2719
Sex (male)	0.86	0.37-2.01	0.7271
NF2 (+)	**7.02**	**2.80-17.60**	**<0.0001**
Tumor status (recurrent)	1.66	0.56-4.92	0.3598
Origin (CN 8)	0.77	0.31-1.90	0.5707
Neurological symptoms (+)	0.57	0.19-1.69	0.3082
Tumor size (≧30mm)	**3.08**	**1.31-7.25**	**0.0098**
Brain compression (+)	1.96	0.72-5.33	0.1863
Cyst (+)	**2.49**	**1.01-6.12**	**0.0467**
Removal rate (non-GTR)	**6.40**	**1.50-27.40**	**0.0123**
PLT (>227000/μL)	0.51	0.22-1.19	0.1196
CRP (>0.025 mg/dL)	0.74	0.27-2.05	0.5657

(Continued)

TABLE 2 Continued

Variables	HR	95% CI	p value
Fibrinogen (>274mg/dL)	1.97	0.62-6.21	0.2495
NLR (≧2.21)	**4.07**	**1.65-10.02**	**0.0023**
LMR (<4.11)	**3.29**	**1.39-7.75**	**0.0065**
PLR (≧116.2)	2.51	0.84-7.45	0.0988
PNI (≧52.7)	1.64	0.60-4.43	0.3304

NF2, neurofibromatosis type 2; CN, cranial nerve; GTR, gross total resection; WBC, white blood cell; PLT, platelet; CRP, C-reactive protein; NLR, neutrophil-to-lymphocyte ratio; LMR, lymphocyte-to-monocyte ratio; PLR, platelet-to lymphocyte ratio; PNI, prognostic nutritional index.
Factors which made statistically significant differences are shown in bold.

Subgroup analysis

As shown in Figure 4, TFS was significantly shorter in patients with NLR ≥2.21 in the following subgroups: sporadic schwannoma, primary schwannoma, schwannoma ≥30 mm in size, STR, vestibular schwannoma, and postoperative recurrence. Subgroup analysis of NF2 patients was not performed because the sample size was small.

Discussion

In this study, preoperative NLR was an independent predictor of postoperative schwannoma recurrence that required retreatment. It was also applicable to a subgroup of vestibular schwannomas. Ki-67, S100, p53, microvessel density, and macrophage colony stimulating factor have been previously reported as biomarkers with prognostic value in schwannoma (5, 30–32). Histological inflammation and angiogenesis play a role in growth of sporadic and NF2-related vestibular schwannoma (33). CD163+ tumor-associated macrophages in particular have a supportive effect on schwannoma growth (31, 34–36). However, histopathological biomarkers cannot be evaluated preoperatively and therefore cannot contribute to early surgical decision making. In contrast, NLR can be easily calculated using preoperative blood testing. Although a few previous studies have evaluated serum and radiological prognostic factors associated with inflammatory status, only one has demonstrated that NLR is an important predictor of the natural history in schwannomas (18). However, this study did not examine postoperative growth pattern in surgical cases. Although dynamic positron emission tomography can predict inflammation in schwannomas (37), routine use of such a specialized and expensive imaging modality before surgery is not practical.

Based on the natural history of schwannomas, a subset of schwannomas do not exhibit growth after diagnosis (38–40). Similarly, some schwannomas grow slowly or transiently after surgery, while others grow rapidly and require retreatment. It is important to evaluate continuous tumor growth needing active treatment strategies such as surgery and radiotherapy. TFS, which is survival without the need of treatment for recurrence, may allow us to identify distinct prognostic group of schwannomas. Preoperative identification of those with a shorter TFS would assist surgeons and clinicians with treatment decision making. Our findings suggest that preoperative NLR ≥2.21 is a predictor of shorter TFS after surgery and that STR without adjuvant radiotherapy may be enough for those with a lower NLR. This surgical strategy has a merit in preserving neurological function (8). NLR may be essential in order to provide an evidence-based treatment recommendation for the patient with schwannomas.

This study has several limitations. It was retrospective in design and histopathological analysis was not performed. In addition, the relationship between serum inflammatory parameters and histopathological inflammatory status has not been fully elucidated, and our previous study found no association between NLR and histopathological inflammatory cell infiltration in meningioma (22). Moreover, we did not evaluate NLR after surgery, which may also be a useful predictor of recurrence and retreatment. All the cases were benign schwannomas, therefore the relationship between NLR and malignant schwannoma was not assessed. Future prospective studies are warranted to confirm our findings and investigate further.

TABLE 3 Multivariate Cox proportional hazards regression analysis.

Variables	HR	95% CI	p value
NF2 (+)	**4.94**	**165-14.78**	**0.0043**
Tumor size (≧30mm)	0.89	0.30-2.70	0.8411
Cyst (+)	2.29	0.83-6.31	0.1093
Removal rate (non-GTR)	3.15	0.69-14.38	0.1380
Adjuvant radiotherapy (+)	1.56	0.42-5.82	0.5045
NLR (≧2.21)	**2.82**	**1.04-7.68**	**0.0423**

NF2, neurofibromatosis type 2; GTR, gross total resection; NLR, neutrophil-to-lymphocyte ratio.
Factors which made statistically significant differences are shown in bold.

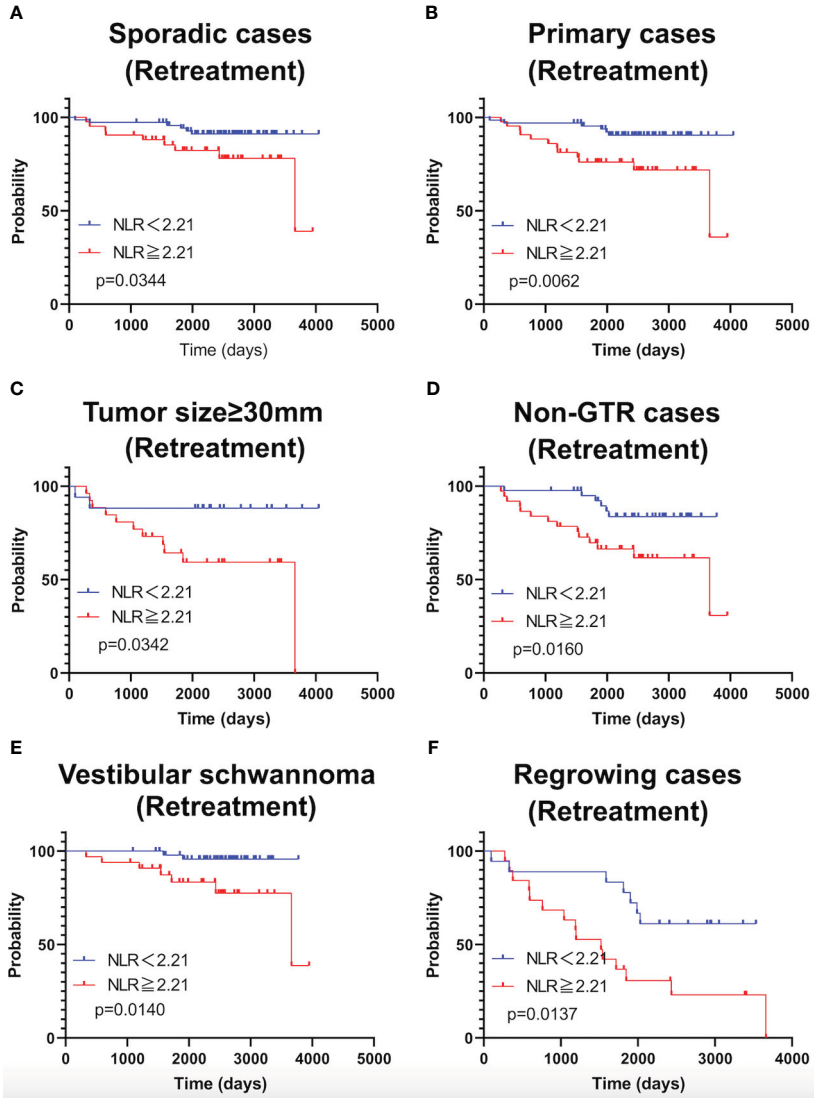

FIGURE 4
Kaplan-Meier curves of TFS related to sporadic cases **(A)**, primary cases **(B)**, large tumor (≥30mm) **(C)**, Non-GTR cases **(D)**, cases with vestibular schwannomas **(E)**, and growing cases **(F)** are shown.

Conclusions

Preoperative NLR ≥2.21 before surgery was significantly associated with retreatment after schwannoma resection. NLR may be a novel predictor of retreatment and assist surgeons in preoperative surgical decision making.

Data availability statement

The raw data supporting the conclusions of this article will be made available by the authors, without undue reservation.

Ethics statement

The studies involving human participants were reviewed and approved by Keio University Hospital. Written informed consent to participate in this study was provided by the participants' legal guardian/next of kin.

Author contributions

KT and RT conceptualized, designed, and performed the study and wrote the manuscript. YK and KK assisted in the acquisition of data. TA and MT assisted with discussion and review of the manuscript. All authors contributed to the article and approved the submitted version.

Acknowledgments

The authors thank Dr. Noboru Tsuda at the Department of Pathology, Keio University School of Medicine for technical assistance and Edanz (https://jp.edanz.com/ac) for editing a draft of this manuscript.

Conflict of interest

The authors declare that the research was conducted in the absence of any commercial or financial relationships that could be construed as a potential conflict of interest.

Publisher's note

All claims expressed in this article are solely those of the authors and do not necessarily represent those of their affiliated organizations, or those of the publisher, the editors and the reviewers. Any product that may be evaluated in this article, or claim that may be made by its manufacturer, is not guaranteed or endorsed by the publisher.

Supplementary material

The Supplementary Material for this article can be found online at: https://www.frontiersin.org/articles/10.3389/fonc.2023.1099384/full#supplementary-material

SUPPLEMENTARY FIGURE 1
Receiver operating characteristic curves for recurrence and retreatment

SUPPLEMENTARY FIGURE 2
Kaplan–Meier recurrence-free survival curves with patients stratified according to neurofibromatosis type 2 status and optimal neutrophil-to-lymphocyte ratio cut-off value

References

1. Bin-Alamer O, Bhenderu LS, Palmisciano P, Balasubramanian K, Upadhyay P, Ferini G, et al. Tumors involving the infratemporal fossa: A systematic review of clinical characteristics and treatment outcomes. *Cancers (Basel).* (2022) 14(21):5420. doi: 10.3390/cancers14215420

2. Fieux M, Zaouche S, Rabaste S, Riche B, Maucort-Boulch D, Tringali S. MRI Monitoring of residual vestibular schwannomas: Modeling and predictors of growth. *Otol Neurotol* (2020) 41(8):1131–9. doi: 10.1097/MAO.0000000000002742

3. Li J, Deng X, Ke D, Cheng J, Zhang S, Hui X. Risk factors for progression in vestibular schwannomas after incomplete resection: A single center retrospective study. *Front Neurol* (2021) 12:778590. doi: 10.3389/fneur.2021.778590

4. Park HH, Park SH, Oh HC, Jung HH, Chang JH, Lee KS, et al. The behavior of residual tumors following incomplete surgical resection for vestibular schwannomas. *Sci Rep* (2021) 11(1):4665. doi: 10.1038/s41598-021-84319-1

5. Fukuda M, Oishi M, Hiraishi T, Natsumeda M, Fujii Y. Clinicopathological factors related to regrowth of vestibular schwannoma after incomplete resection. *J Neurosurg* (2011) 114(5):1224–31. doi: 10.3171/2010.11.JNS101041

6. Lee WJ, Lee JI, Choi JW, Kong DS, Nam DH, Cho YS, et al. Optimal volume of the residual tumor to predict long-term tumor control using stereotactic radiosurgery after facial nerve-preserving surgery for vestibular schwannomas. *J Korean Med Sci* (2021) 36 (16):e102. doi: 10.3346/jkms.2021.36.e10

7. Umana GE, Ferini G, Harikar MM, Venkataram T, Costanzo R, Scalia G, et al. Detection of "Incidentalomas" on brain and body ^{68}Ga-DOTATOC-PET scans: A retrospective study and case illustration. *Anticancer Res* (2022) 42(12):5867–73. doi: 10.21873/anticanres.16095

8. Chen Z, Prasad SC, Di Lella F, Medina M, Piccirillo E, Taibah A, et al. The behavior of residual tumors and facial nerve outcomes after incomplete excision of vestibular schwannomas. *J Neurosurg* (2014) 120(6):1278–87. doi: 10.3171/2014.2.JNS131497

9. Arlt F, Kasper J, Winkler D, Jähne K, Fehrenbach MK, Meixensberger J, et al. Facial nerve function after microsurgical resection in vestibular schwannoma under neurophysiological monitoring. *Front Neurol* (2022) 13:850326. doi: 10.3389/fneur.2022.850326

10. Iwai Y, Ishibashi K, Watanabe Y, Uemura G, Yamanaka K. Functional preservation after planned partial resection followed by gamma knife radiosurgery for Large vestibular schwannomas. *World Neurosurg* (2015) 84(2):292–300. doi: 10.1016/j.wneu.2015.03.012

11. Palmisciano P, Ferini G, Watanabe G, Conching A, Ogasawara C, Scalia G, et al. Surgical management of craniovertebral junction schwannomas: A systematic review. *Curr Oncol* (2022) 29(7):4842–55. doi: 10.3390/curroncol29070384

12. Grivennikov SI, Greten FR, Karin M. Immunity, inflammation, and cancer. *Cell* (2010) 140(6):883–99. doi: 10.1016/j.cell.2010.01.025

13. Prabawa IPY, Bhargah A, Liwang F, Tandio DA, Tandio AL, Lestari AAW, et al. Pretreatment neutrophil-to-Lymphocyte ratio (NLR) and platelet-to-Lymphocyte ratio (PLR) as a predictive value of hematological markers in cervical cancer. *Asian Pac J Cancer Prev* (2019) 20(3):863–8. doi: 10.31557/APJCP.2019.20.3.863

14. Duan J, Pan L, Yang M. Preoperative elevated neutrophil-to-lymphocyte ratio (NLR) and derived NLR are associated with poor prognosis in patients with breast cancer: A meta-analysis. *Med (Baltimore).* (2018) 97(49):e13340. doi: 10.1097/MD.0000000000013340

15. Amaral SR, Casal Moura M, Carvalho J, Chaves A, Jesus E, Sousa G. 6P prognostic significance of neutrophil-to-lymphocyte ratio (NLR) and platelet-to-lymphocyte ratio (PLR) in non-small cell lung cancer (NSCLC) treated with immune checkpoint inhibitors. *Ann Oncol* (2019) 30(suppl 1). doi: 10.1093/annonc/mdz027.004

16. Stojkovic Lalosevic M, Pavlovic Markovic A, Stankovic S, Stojkovic M, Dimitrijevic I, Radoman Vujacic I, et al. Combined diagnostic efficacy of neutrophil-to-Lymphocyte ratio (NLR), platelet-to-Lymphocyte ratio (PLR), and mean platelet volume (MPV) as biomarkers of systemic inflammation in the diagnosis of colorectal cancer. *Dis Markers.* (2019) 2019:6036979. doi: 10.1155/2019/6036979

17. Jung MR, Park YK, Jeong O, Seon JW, Ryu SY, Kim DY, et al. Elevated preoperative neutrophil to lymphocyte ratio predicts poor survival following resection in late stage gastric cancer. *J Surg Oncol* (2011) 104(5):504–10. doi: 10.1002/jso.21986

18. Kontorinis G, Crowther JA, Iliodromiti S, Taylor WA, Locke R. Neutrophil to lymphocyte ratio as a predictive marker of vestibular schwannoma growth. *Otol Neurotol* (2016) 37(5):580–5. doi: 10.1097/MAO.0000000000001026

19. Zhang J, He M, Liu Z, Song Y, Wang Y, Liang R, et al. Impact of neutrophil-lymphocyte ratio on long-term outcome in patients with craniopharyngioma. *Med (Baltimore).* (2018) 97(37):e12375. doi: 10.1097/MD.0000000000012375

20. Hu W, Yu J, Huang Y, Hu F, Zhang X, Wang Y. Lymphocyte-related inflammation and immune-based scores predict prognosis of chordoma patients after radical resection. *Transl Oncol* (2018) 11(2):444–9. doi: 10.1016/j.tranon.2018.01.010

21. Marques P, de Vries F, Dekkers OM, van Furth WR, Korbonits M, Biermasz NR, et al. Pre-operative serum inflammation-based scores in patients with pituitary adenomas. *Pituitary* (2021) 24(3):334–50. doi: 10.1007/s11102-020-01112-5

22. Kuranari Y, Tamura R, Tsuda N, Kosugi K, Morimoto Y, Yoshida K, et al. Prognostic significance of preoperative neutrophil-to-Lymphocyte ratio in patients with meningiomas. *Front Oncol* (2020) 10:592470. doi: 10.3389/fonc.2020.592470

23. Regan MM, Werner L, Rao S, Gupte-Singh K, Hodi FS, Kirkwood JM, et al. Treatment-free survival: A novel outcome measure of the effects of immune checkpoint inhibition-a pooled analysis of patients with advanced melanoma. *J Clin Oncol* (2019) 37 (35):3350–8. doi: 10.1200/JCO.19.00345

24. Templeton AJ, McNamara MG, Šeruga B, Vera-Badillo FE, Aneja P, Ocaña A, et al. Prognostic role of neutrophil-to-lymphocyte ratio in solid tumors: a systematic review and meta-analysis. *J Natl Cancer Inst* (2014) 106(6):dju124. doi: 10.1093/jnci/dju124

25. Nishijima TF, Muss HB, Shachar SS, Tamura K, Takamatsu Y. Prognostic value of lymphocyte-to-monocyte ratio in patients with solid tumors: A systematic review and meta-analysis. *Cancer Treat Rev* (2015) 41(10):971–8. doi: 10.1016/j.ctrv.2015.10.003

26. Guo W, Lu X, Liu Q, Zhang T, Li P, Qiao W, et al. Prognostic value of neutrophil-to-lymphocyte ratio and platelet-to-lymphocyte ratio for breast cancer patients: An updated meta-analysis of 17079 individuals. *Cancer Med* (2019) 8(9):4135–48. doi: 10.1002/cam4.2281

27. Chan AW, Chan SL, Wong GL, Wong VW, Chong CC, Lai PB, et al. Prognostic nutritional index (PNI) predicts tumor recurrence of very Early/Early stage hepatocellular carcinoma after surgical resection. *Ann Surg Oncol* (2015) 22(13):4138–48. doi: 10.1245/s10434-015-4516-1

28. Hirahara N, Tajima Y, Fujii Y, Kaji S, Yamamoto T, Hyakudomi R, et al. Preoperative prognostic nutritional index predicts long-term surgical outcomes in patients with esophageal squamous cell carcinoma. *World J Surg* (2018) 42(7):2199–208. doi: 10.1007/s00268-017-4437-1

29. Sun K, Chen S, Xu J, Li G, He Y. The prognostic significance of the prognostic nutritional index in cancer: a systematic review and meta-analysis. *J Cancer Res Clin Oncol* (2014) 140(9):1537–49. doi: 10.1007/s00432-014-1714-3

30. Li B, Li J, Miao W, Zhao Y, Jiao J, Wu Z, et al. Prognostic analysis of clinical and immunohistochemical factors for patients with spinal schwannoma. *World Neurosurg* (2018) 120:e617–27. doi: 10.1016/j.wneu.2018.08.135

31. de Vries M, Briaire-de Bruijn I, Malessy MJ, de Bruïne SF, van der Mey AG, Hogendoorn PC. Tumor-associated macrophages are related to volumetric growth of vestibular schwannomas. *Otol Neurotol* (2013) 34(2):347–52. doi: 10.1097/MAO.0b013e31827c9fbf

32. de Vries WM, Briaire-de Bruijn IH, van Benthem PPG, van der Mey AGL, Hogendoorn PCW. M-CSF and IL-34 expression as indicators for growth in sporadic vestibular schwannoma. *Virchows Arch* (2019) 474(3):375–81. doi: 10.1007/s00428-018-2503-1

33. Hannan CJ, Lewis D, O'Leary C, Donofrio CA, Evans DG, Roncaroli F, et al. The inflammatory microenvironment in vestibular schwannoma. *Neurooncol Adv* (2020) 2(1): vdaa023. doi: 10.1093/noajnl/vdaa023

34. Mantovani A, Marchesi F, Malesci A, Laghi L, Allavena P. Tumour-associated macrophages as treatment targets in oncology. *Nat Rev Clin Oncol* (2017) 14(7):399–416. doi: 10.1038/nrclinonc.2016.217

35. Solinas G, Germano G, Mantovani A, Allavena P. Tumor-associated macrophages (TAM) as major players of the cancer-related inflammation. *J Leukoc Biol* (2009) 86 (5):1065–73. doi: 10.1189/jlb.0609385

36. Tamura R, Morimoto Y, Sato M, Kuranari Y, Oishi Y, Kosugi K, et al. Difference in the hypoxic immunosuppressive microenvironment of patients with neurofibromatosis type 2 schwannomas and sporadic schwannomas. *J Neurooncol* (2020) 146(2):265–73. doi: 10.1007/s11060-019-03388-5

37. Lewis D, Roncaroli F, Agushi E, Mosses D, Williams R, Li KL, et al. Inflammation and vascular permeability correlate with growth in sporadic vestibular schwannoma. *Neuro Oncol* (2019) 21(3):314–25. doi: 10.1093/neuonc/noy177

38. Stangerup SE, Caye-Thomasen P. Epidemiology and natural history of vestibular schwannomas. *Otolaryngol Clin North Am* (2012) 45(2):257–2. doi: 10.1016/j.otc.2011.12.008

39. Carlson ML, Habermann EB, Wagie AE, Driscoll CL, Van Gompel JJ, Jacob JT, et al. The changing landscape of vestibular schwannoma management in the united states–a shift toward conservatism. *Otolaryngol Head Neck Surg* (2015) 153(3):440–6. doi: 10.1177/0194599815590105

40. Reznitsky M, Cayé-Thomasen P. Systematic review of hearing preservation in observed vestibular schwannoma. *J Neurol Surg B Skull Base*. (2019) 80(2):165–8. doi: 10.1055/s-0039-1679894

frontiers | Frontiers in Oncology

TYPE Case Report
PUBLISHED 13 February 2023
DOI 10.3389/fonc.2023.1089002

OPEN ACCESS

EDITED BY
Arianna Rustici,
University of Bologna, Italy

REVIEWED BY
Kamil Krystkiewicz,
Copernicus Memorial Hospital, Poland
Paolo Palmisciano,
University of Cincinnati, United States

*CORRESPONDENCE
Sizhe Feng
fengsizhe@sohu.com
Guobiao Liang
liangguobiao6708@vip.163.com

†These authors have contributed equally to this work

SPECIALTY SECTION
This article was submitted to Neuro-Oncology and Neurosurgical Oncology, a section of the journal Frontiers in Oncology

RECEIVED 03 November 2022
ACCEPTED 30 January 2023
PUBLISHED 13 February 2023

CITATION
Bai Y, Han S, Sun X, Liu X, Li X, Feng S and Liang G (2023) Endoscopic far-lateral supracerebellar infratentorial approach for resection of posterior clinoid meningioma: Case report and literature review. *Front. Oncol.* 13:1089002. doi: 10.3389/fonc.2023.1089002

Endoscopic far-lateral supracerebellar infratentorial approach for resection of posterior clinoid meningioma: Case report and literature review

Yang Bai[1†], Song Han[1†], Xiaoyu Sun[1], Xuantong Liu[2], Xinning Li[1], Sizhe Feng[1*] and Guobiao Liang[1*]

[1]Department of Neurosurgery, General Hospital of Northern Theater Command, Shenyang, Liaoning, China, [2]Department of Pathology, General Hospital of Northern Theater Command, Shenyang, Liaoning, China

Introduction: The surgery of posterior clinoid meningioma (PCM) remains one of the most formidable challenges for neurosurgeons because of its location at great depth in the cranium and proximity to vital neurovascular structures. Herein, we aim to describe the technique and feasibility of a novel approach, the purely endoscopic far-lateral supracerebellar infratentorial approach (EF-SCITA), for resection of this extremely rare entity.

Case description: A 67-year-old women presented with gradually deteriorating vision in right eye for 6 months. Imaging examinations revealed a right-sided PCM, and the EF-SCITA approach was attempted for tumor resection. Tentorium incision allowed a working corridor toward the PCM in the ambient cistern through the supracerebellar space. During surgery, the infratentorial part of the tumor was found to compress the CN III and posterior cerebral artery medially and encase the CN IV laterally. Following debulking of the infratentorial tumor, the supratentorial part could be exposed and then excised, which had dense adhesions to the ICA and the initial part of the basal vein in front. After total tumor removal, its dural attachment was detected at the right posterior clinoid process and then coagulated under direct vision. The patient on follow-up at 1 month had improvement in visual acuity in right eye, with no restriction of extra-ocular movements.

Discussion: EF-SCITA approach combines advantages of the posterolateral approach and endoscopic technique, allowing access to PCMs with seemingly low risks of postoperative morbidity. It would be a safe and effective alternative for resection of lesions in the retrosellar space.

KEYWORDS

posterior clinoid meningioma, supracerebellar infratentorial approach, endoscope, surgical approach, case report

Introduction

Posterior clinoid process (PCP) is an uncommon site for the origin of meningiomas, which have only been reported in 18 cases as yet (1–8). Surgical excision of posterior clinoid meningiomas (PCM) presents neurosurgeons with a special challenge since it is deeply nested in the center of cranial base and surrounded by critical neurovascular structures. The complications of surgery for this extremely rare entity are unpredictable, ranging from none to severe disabling neurological deficits. A variety of surgical approaches, including anterolateral, lateral, and posterolateral routes, have been described to access PCM (5). However, the optimal approach to minimize approach-related morbidity and improve the extent of resection still remains to be explored.

Extreme-lateral supracerebellar infratentorial (ELSI) approach remains one of the most versatile approaches in neurosurgery with respect to its ability to address various anatomical regions, especially the posterolateral midbrain and tentorial region (9). In the last few years, the rapid development of endoscopic neurosurgery has brought a great opportunity for the improvement of this approach. Recently, Xie et al. first described the technique of the purely endoscopic far-lateral SCITA (EF-SCITA) for treatment of petroclival region meningiomas (10). We further tested the feasibility of this approach in resection of retroinfundibular craniopharyngioma (CP) in the suprasellar region. Under endoscopy, the retrosellar region and PCP could be clearly exposed through the ambient cistern after tentorium incision (11). This successful experience motivated us to use the same technique for PCM resection.

Herein, we report a case of EF-SCITA in total removal of PCM, with specific emphasis on technical surgical nuances. In the discussion, we summarize breakthroughs and insights on operative approaches for the treatment of PCM, and analyze the operation essentials, and strengths and weaknesses of each passage from the perspective of surgery. In this report, we also review the previous relevant publications within PubMed and abstracts from international conference literature concerning PCM according to the PRISMA guideline. The literature review found a total of 18 cases which was listed in Table 1.

Case description

A 67-year-old female presented with progressively worsening vision in her right eye for approximately 6 months. On ophthalmological examination, she had mild bilateral peripheral visual field defects, which was severer in right eye. The visual acuity was 0.4 in right eye and 0.8 in left eye. The extraocular muscles were intact and no other neurological deficit was found. Routine laboratory investigations, including endocrinological studies, were normal. No specific past, medical, family and psycho-social history was reported.

Computed tomography (CT) scans revealed a hyperdense lesion on the right side of suprasellar region. The mass grew into the ambient cistern, lying medially close to the medial temporal lobe and displacing the midbrain posteriorly (Figure 1A). Magnetic resonance imaging (MRI) examinations showed a homogeneously enhancing tumor centering over the PCP (Figures 1B–E). On CT angiography, the tumor was displacing the ICA anteriorly and encasing the right P1 segment of posterior cerebral artery posteriorly (Figure 1F). Owing to the mass effect, the right-sided optic chiasma was up-elevated and the pituitary stalk (PS) was slightly displaced to the contralateral side (Figure 1E). Based on these clinico-radiological features, PCM was proposed as the most likely diagnosis, and the EF-SCITA approach was attempted for tumor resection (Video 1).

Surgery was performed in left lateral position after placement of a continuous lumbar CSF drainage system. The head was placed in upper flexion and backward rotation to allow gravity retraction of the cerebellum. As described before, a C-shaped retroauricular incision was performed to obtain adequate exposure of the suboccipital region and the mastoid bone. Then, the entire transverse sinus, the transverse-sigmoid junction, and the proximal part of the sigmoid sinus were revealed through suboccipital craniotomy (11). The surgical position, together with intraoperative drainage, facilitated endoscopic explorations in the lateral superior cerebellar space (Figure 2A).

After opening the tentorium cerebelli, the tumor could be identified in the ambient cistern. Anatomically, it was located in front of the midbrain and was divided by the tentorial incisura into the supratentorial and infratentorial parts. The tumor was found to encase and compress the CN IV towards the tentorial incisura (Figure 2B). Then, the infratentorial part was excised in a piecemeal fashion. After stepwise tumor reduction, the CN III and the P1 segment located medially to the lesion were identified and the tumor capsule was gently dissected away. In addition, the supratentorial part descended to the surgery field owing to gravity as well as surgical retraction (Figures 2C, D). During resection of the supratentorial tumor, we observed that the tumor had dense adhesions to the ICA and the initial part of the basal vein (BV) in front, which were carefully dissected from the tumor (Figure 2E). Intraoperatively, the tumor was grayish, soft, and moderately vascular. Total tumor removal was achieved, with all neighboring blood vessels and cranial nerves preserved. Finally, its dural attachment could be detected at the right PCP and adjacent petrous apex, which was coagulated under direct vision (Figure 2F).

The postoperative course was uneventful and the patient was discharged on 7th postoperative day. Postoperative MRI demonstrated complete excision of the lesion (Figures 3A–C). Histopathological examinations demonstrated findings consistent with a meningioma of meningothelial type (Figure 3D). The patient on follow-up at 1 month had improvement in visual acuity (0.8) in right eye, with no restriction of extra-ocular movements observed (Figure 3E).

Discussion

Clinical and radiological features of PCM

Due to their rarity and ambiguous terminologies, the true identity of PCMs has only been recognized by Horiguchi et al. in 2008 (2).

Abbreviations: ACM, anterior clinoid meningioma; BV, basal vein; CP, craniopharyngioma; CT, computed tomography; DS, dorsum sellae; EF-SCITA, endoscopic far-lateral supracerebellar infratentorial approach; ELSI, extreme-lateral supracerebellar infratentorial approach; FTOZ, frontotemporo-orbito-zygomatic orbitozygomatic approach; MRI, magnetic resonance imaging; PCM, posterior clinoid meningioma; PCP, posterior clinoid process; PS, pituitary stalk.

TABLE 1 Summary of reported cases of posterior clinoid meningiomas.

Authors	Age (years)	Sex	Symptoms	Surgical approach	Extent of excision	Complications	Pathology
Horiguchi et al. N = 5 (2)	N/D	N/D	N/D	N/D	Simpson G3 (3) Simpson G4 (2)	Permanent hemiparesis (2), permanent CN palsy (4), thalamic dementia (1), perforating artery infarction (3)	N/D
Goto et al. N = 5 (1)	Mean age = 51.6	M (3) F (2)	N/D	Presigmoidal transpetrosal (4) Combined transpetrosal and FTOZ (1)	Total (3) Near total (1) Partial (1)	None	N/D
Ohba et al. N = 1 (8)	60	M	CN III palsy	Transzygomatic	Subtotal	Hemiparesis, hydrocephalus, brainstem infarction	Clear cell
Shukla et al. N = 2 (3)	50	F	HA, diplopia (CN III)	Transzygomatic subtemporal	Total	None	Transitional
	41	F	HA, diplopia (CN III)	Transzygomatic subtemporal	Partial	Hemiparesis, hemianopsia, partial CN III palsy, ACho infarction	Atypical
Sodhi et al. N = 1 (4)	48	F	HA, VD, HH	FTOZ	Near total	Transient ptosis	Meningothelial
Takase et al. N = 2 (5)	54	F	Ophthalamalgia	FT	Near total	None	Meningothelial
	62	F	Akinesia, amnesia, VD, HH	FTOZ	Subtotal	Transient hemiparesis, LSA infarction	Meningothelial
Nanda et al. N = 1 (7)	66	F	Facial pain	Retrosigmoid	Total	Transient hemiparesis	N/D
Young et al. N = 1 (6)	53	F	N/D	Orbitozygomatic transpetrosal	Near total	Mild CN III and IV palsy	N/D
Present case N = 1	67	F	VD	EF-SCITA	Total	None	Meningothelial

ACho, anterior choroidal artery; CN, cranial nerve; EF-SCITA, endoscopic far-lateral supracerebellar infratentorial approach; FT, frontotemporal craniotomy; FTOZ, frontotemporo-orbito-zygomatic craniotomy; HA, headache; HH, homonymous hemianopia; ICA, Internal carotid artery; LSA, lenticulostriate artery; N/D, not described; VD, visual deterioration.

Later, Sodhi et al. clarified the terminology of lesions in the region of dorsum sellae (DS) and separated PCMs (eccentrically placed meningiomas centering on PCPs) from DS or upper clival meningiomas (centrally located meningiomas between PCPs) (4). On the basis of this definition, there have been only 19 reported cases of PCMs including this study. These patients had a mean age of 54 at the time of diagnosis and most of them were female (71.4%) (Table 1).

Anatomically, the PCP is a bony prominence at the superolateral aspect of the DS. Anteromedial to the PCP is the PS. Anterolateral to this process is the posterior edge of the cavernous sinus. The ICA ascends into the posterior aspect of the cavernous sinus where the posterior bend is formed lateral to the PCP. The bifurcation of basilar artery lies posterior to the PCP and DS. The CN III enters the edge of the tentorial dura lateral to the PCP in the oculomotor triangle (12, 13). Thus, meningiomas arising from PCP usually compress the PS anteriorly and the CN III laterally or infero-laterally, and encase the C1-2 segment of the ICA or its branches. The optic chiasm can be even shifted superiorly or antero-superiorly as the tumor expands anteriorly. Therefore, headache, visual disturbance, and diplopia are common presenting symptoms. Huge PCMs also cause facial pain or akinesia if the CN V or ICA perforators is involved (14).

The diagnosis of PCM can be challenging. Radiologically, the "dural tail" sign is seldom detected since the tumor attachment at PCP is very small. Owing to clinical and radiological similarities, some PCMs are preoperatively misinterpreted as DS or upper clival meningiomas, and may be even confused with anterior clinoid meningiomas (ACM) and parasellar meningiomas. The direction of ICA displacement may help in differentiating PCM from ACM, since the ICA is often shifted posteriorly in the case of ACM but anteriorly in the case of PCM (15).

Like most PCMs, the tumor in this case grew upwardly and forwardly beyond the tentorial incisura and up-elevated the right optic chiasma, which could account for progressively visual loss in right eye. However, this case is unique in the tumor site presented unlike those reported in previous studies. Intraoperatively, the tumor was located between CN III and CN IV in the mediolateral direction. Correspondingly, the origin of PCM was found to occupy the junction of the PCP and petrous apex. Thus, the protection of CN IV should also be emphasized during surgery.

Current surgical strategies for PCM

The principles of PCM surgery are early devascularization of tumor and careful dissection of tumor from ICA perforators, cranial nerves, PS, and even hypothalamus (1). Several approaches have been

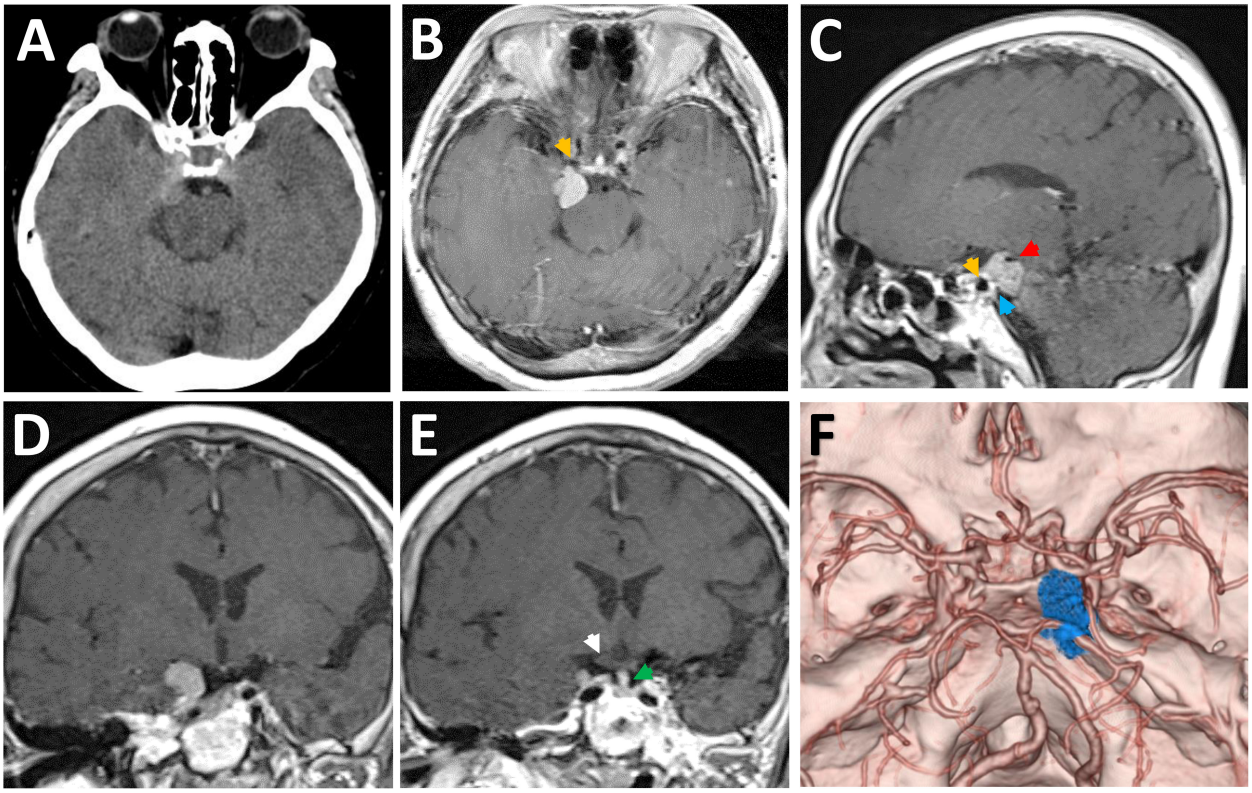

FIGURE 1
Radiological evaluation of the retrosellar lesion preoperatively. **(A)** Preoperative CT image showing a hyperdense lesion on the right-sided of posterior clinoid process. **(B-E)** Post-contrast (gadolinium-enhanced) axial **(B)**, sagittal **(C)**, and coronal **(D, E)** MRI images showing the thick enhancement of the lesion as well as the relative position to surrounding neural structures. **(F)** Preoperative CT angiography images demonstrating the relative location of tumor to the Willis' circle and the dorsum sellae. The yellow arrows denote the posterior bend of caveronous carotid artery. The red arrow indicates the posterior cerebral artery. The white arrow denotes the up-elevated right optic chiasma. The green arrow indicates the pituitary stalk. The blue arrow indicates the dural detachment of the tumor on the posterior clinoid process.

implemented to treat this lesion with acceptable risks, and many of them represent variations of the classical pterional, subtemporal, or presigmoid routes with modifications in bone resection. According to surgical directions accessing the PCP, they could be classified into anterolateral, lateral, posterolateral, and complex routes (Figure 4).

The transcavernous-transsellar approach was proposed for PCM resection by Dr. Dolenc in 2003. During surgery, the sphenoid wing, ACP, and the lateral wall of the optic canal are excised extradurally. Then, with additional resection of the PCP and DS, the PCM could be devascularized at the attachment and then excised (15). The classical pterional approach allows early identification of ICA perforators and renders direct access to the tumor through the optico-carotid and carotico-oculomotor corridors. Common disadvantages for these anterolateral routes include hindrance of direct approach to tumor by anteriorly shifted ICA and risks to ICA perforators during devascularization and debulking of the tumor through the narrow spaces between them (5, 15). In addition, early detection of CN III is difficult in the transcavernous-transsellar approach (15). Hence, only soft or small PCMs might be treated with these approaches. So far, only one case of reported PCM has been resected *via* fronto-temporal craniotomy with wide splitting of the Sylvian fissure (5).

The inherent drawbacks of anterolateral approaches could be circumvented by lateral or posterolateral approaches. In 2013, Shukla et al. firstly reported two cases of PCM excision *via* transzygomatic subtemporal approach (3). This lateral approach is technically the simplest approach for exposure of tentorial notch and upper clivus. A further incision of the tentorium may be required for a wider exposure. It is a better choice for early devascularization and debulking, and allows for direct access to the PCP between the CN III and posterior communicating artery after resection of small compartment around these structures. Major disadvantages of this approach are temporal retraction and injury to the vein of Labbe, which might be avoided by placing a lumbar drain preoperatively (3).

In 2009, Goto et al. described their experience with five cases of PCM resected *via* presigmoid transpetrosal approach. This posterolateral route guarantees earliest coagulation of feeding arteries of the PCM. Tracing the CN III from the normal proximal side in the interpeduncular cistern to the involved distal side could prevent unexpected injury of the nerve. This approach also enables safe dissection of the antero-superiorly displaced ICA under direct vision and provides direct exposure to the inferior surface of the optic chiasm, PS, and hypothalamus from the posterolateral side. However, burdensome bone drilling with related risks to hearing and facial nerve function as well as cerebrospinal fluid leakage makes it somewhat less desirable surgical choice. Operational complexity also restricts the popularization of this technique (1). In 2017, Nanda et al. reported a case of resection of a large PCM with obvious brainstem compression *via* retrosigmoid approach.

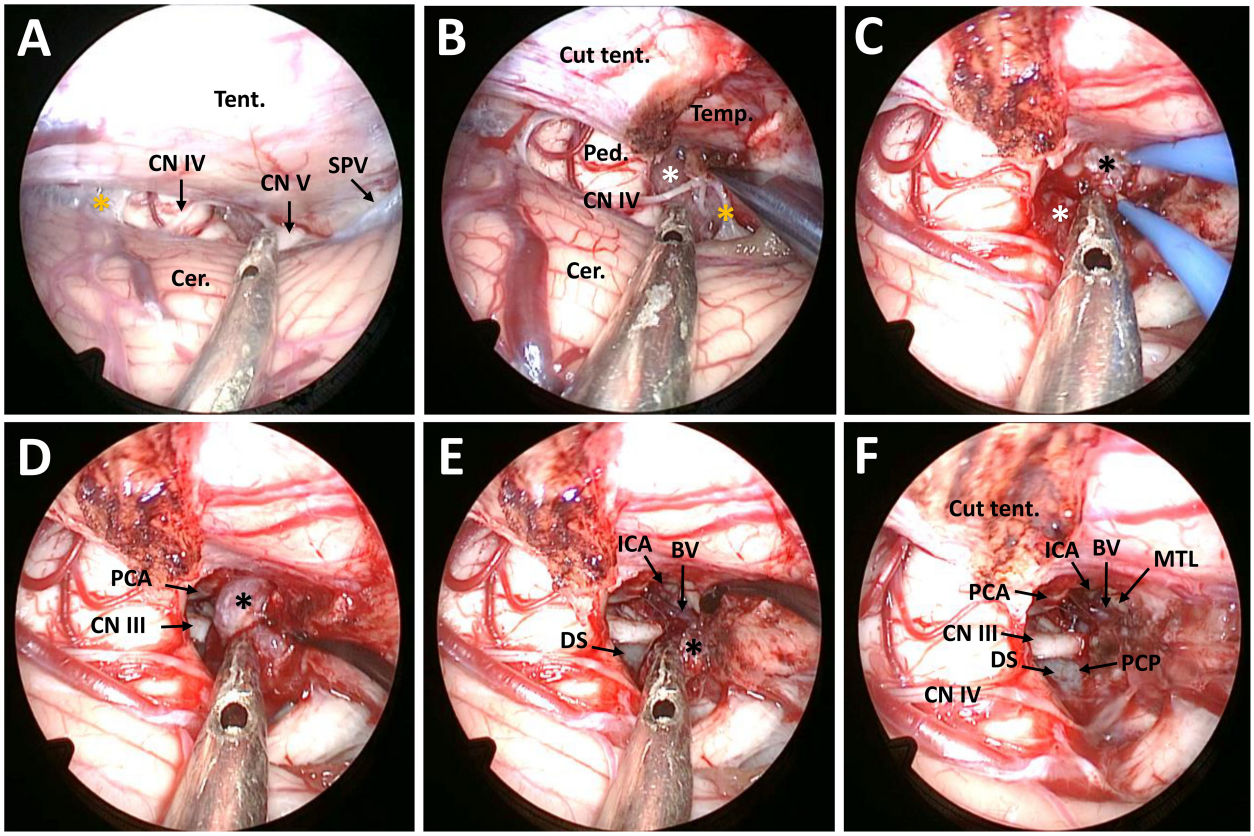

FIGURE 2
Surgical procedure and nuances of the EF-SCITA approach for resection of posterior clinoid meningioma. **(A)** Endoscopic explorations in the lateral supracerebellar infratentorial space and the exposure of CN IV after opening the arachnoid in the ambient cistern. **(B)** The exposure of the infratentorial part of the tumor in the ambient cistern after incision of the tentorium cerebelli. **(C)** The exposure of the supratentorial tumor after up-elevating the tentorium cerebelli. **(D)** The exposure of the PCA and CN III as well as the supratentorial tumor after debulking of the infratentorial tumor. **(E)** Dissection of the supratentorial tumor from the ICA and the initial part of BV and the exposure of DS during tumor resection. **(F)** The exposure of PCP after total tumor removal. BV, basal vein of Rosenthal (the initial part); Cer., cerebellum; CN III, oculomotor nerve; CN IV, trochlear nerve; CN V, trigeminal nerve; DS, dorsum sellae; ICA, internal carotid artery; MTL, medial temporal lobe; PCA, posterior cerebral artery; PCP, posterior clinoid process; Ped., pedunculus cerebri; PS, pituitary stalk; SPV, superior petrosal vein; Tent., tentorium cerebelli. The black asterisks indicate the supratentorial part of the tumor, the white asterisk denotes the infratentorial part of the tumor, and the yellow asterisks indicate the arachnoid in the ambient cistern.

Although the most amazing finding was the extent of visualization around the PCP region gained through this approach, the narrow width and great depth of this working corridor pose significant risks of neurovascular injury (7).

Size, consistency, and tumor micromorphology are the most important determinants of the extent of resection and outcome of PCM. Small, soft, and well-delineated tumors can be excised totally with any of the above approaches without significant neurological sequelae, while tumors with large size, hard texture, rich vascularity, and multiple micro-lobules encasing perforators often result in incomplete resection (3). Among the 19 reported PCM cases, total resection was achieved in 9 patients (47.4%) (Table 1). It is worth noting that removal of far anterior extension of PCM could not be realized through lateral and posterolateral routes. Under this condition, a basal frontotemporo-orbito-zygomatic orbitozygomatic (FTOZ) approach with wide Sylvian fissure splitting has been recommended. Compared with the classical frontotemporal craniotomy, this approach provides additional anterior temporal or subtemporal route. This surgical trajectory allows direct access to the PCP posterior to the perforating vessels for tumor devascularization and debulking without temporal retraction. Thereafter, the devascularized tumor could be removed through the transsylvian route (4, 5). For extremely huge and complex PCMs, a combined and multi-staged surgical approach could be options of tailor-made surgical strategy. In one reported case, a presigmoid transpetrosal approach was recommended for the first stage combined with an orbitozygomatic transsylvian approach for devascularized residual tumor in the second stage (1).

EF-SCITA for suprasellar/retrosellar lesions

The ELSI approach was firstly described by Spetzler et al. in 2000 as a distinct variant of the median SCITA approach for accessing the posterolateral mesencephalon (16). Later, it proved its versatility and clinical practicality in treating tumors residing in centrally-located intra-axial structures like the splenium, pulvinar, brainstem, and mesial temporal lobe as well as skull base extra-axial tumors like petroclival meningiomas (9). With the rapid development of neuroendoscopy, the infratentorial space has been recognized as another optimal endoscopic operating area. Earlier anatomic studies have addressed the possibility of endoscope-assisted or purely

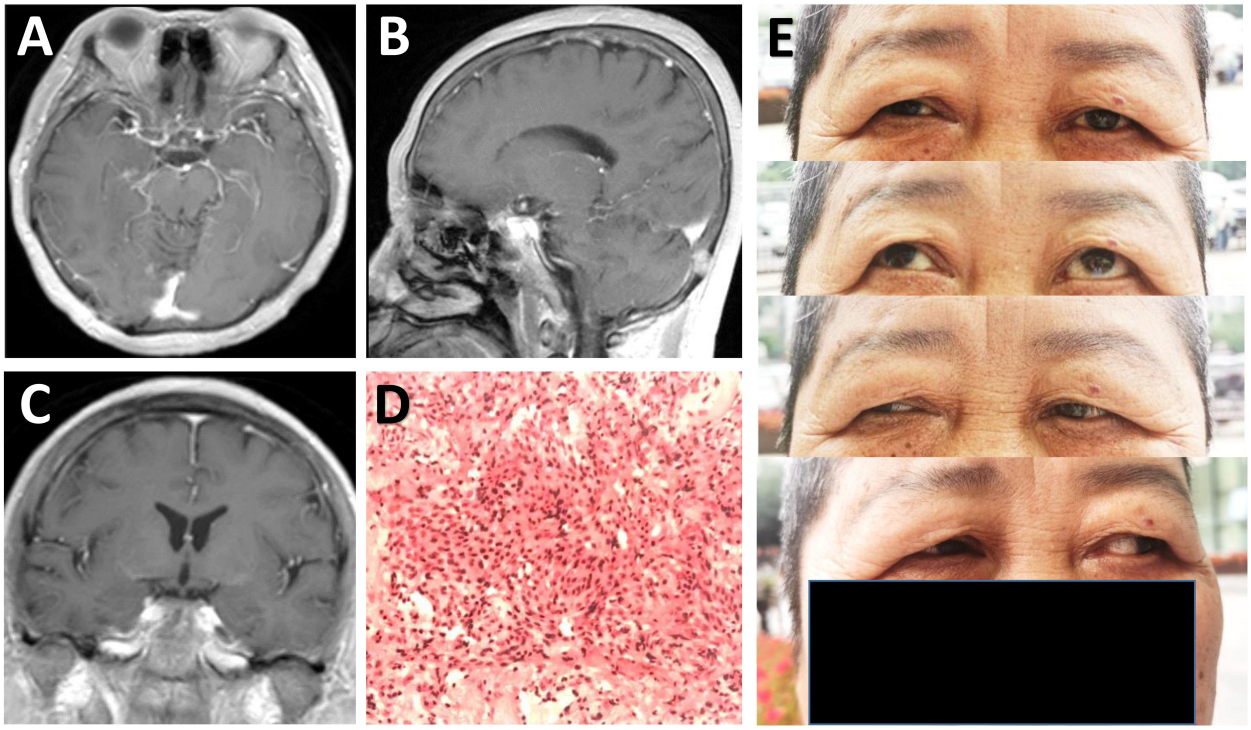

FIGURE 3
Radiological and pathological evaluation of the lesion postoperatively. **(A-C)** Postoperative post-contrast axial **(A)**, sagittal **(B)**, and coronal **(C)** MRI scans performed one month after surgery showing total removal of the lesion. **(D)** Photomicrograph of hematoxylin-eosin staining showing typical features of meningothelial meningioma. **(E)** Physical examinations at one month follow-up indicating no limitation in eye movements.

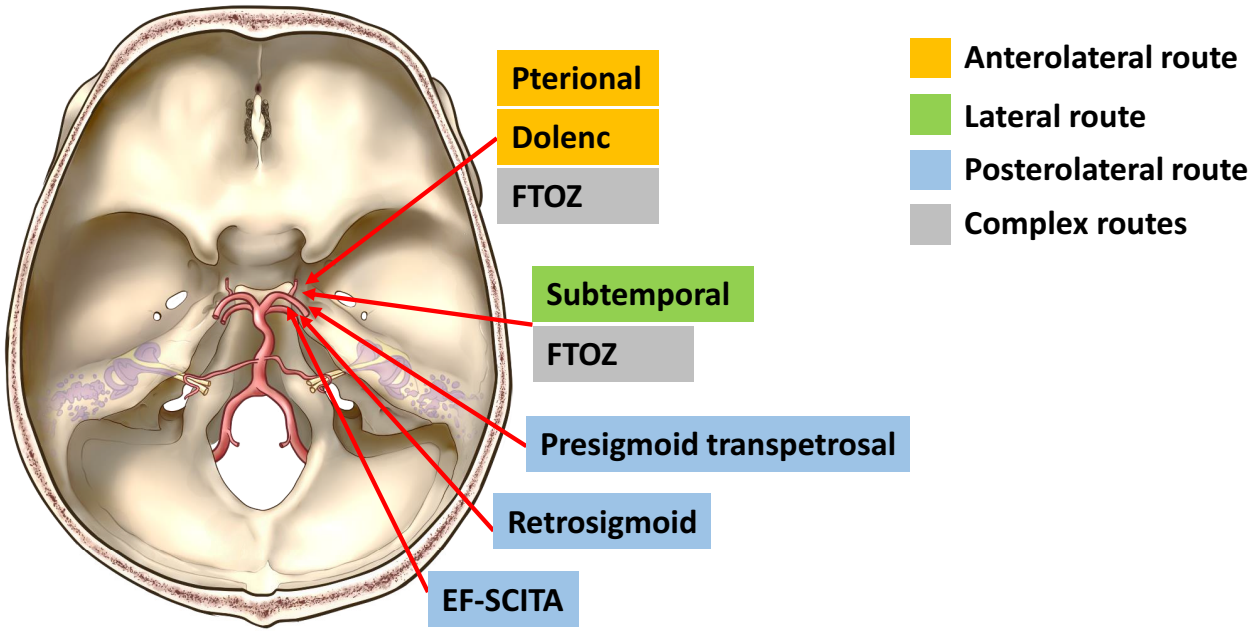

FIGURE 4
Schematic diagram of surgical approaches for resection of posterior clinoid meningiomas. Current approaches for resection of posterior clinoid meningiomas include anterolateral approaches (the classical pterional approach and the Dolenc approach), the lateral approach (the subtemporal approach), posterolateral approaches (the presigmoid transpetrosal approach, the retrosigmoid approach, and the EF-SCITA approach), and the complex route (the FTOZ approach). FTOZ: frontotemporo-orbito-zygomatic orbitozygomatic approach; EF-SCITA: endoscopic far-lateral supracerebellar infratentorial approach.

endoscopic ELSI for accessing the posterior and posterolateral incisural space (17–19). Clinically, endoscope-assisted or purely endoscopic ELSI has been used for removal of supratentorial lesions, such as cavernous malformation in the posteromedial temporal lobe and petroclival meningiomas extending into the middle fossa, with the aid of tentorium incision (10, 20). Based on these studies, we attempted to treat central skull base lesions through this novel approach and have succeed in resection of retroinfundibular CP in a recently reported case (11). Herein, we represented a case of PCM resected *via* the EF-SCITA approach. Despite with the longest working distance, endoscopy extends our eye to see the central skull base and our hands to excise lesions centering over the PCP.

This posterolateral approach necessitates tentorial disconnection to traverse the tentorial incisura and arrive at the retrosellar space, and requires working between neural structures for PCM removal in the ambient cistern. The decompression of infratentorial tumor facilitates the exposure and resection of the part in the supratentorial space. As with transpetrosal approach, this approach allows tracing the natural trajectory of CN III and IV for nerve protection. Based on our prior experience in resection of retroinfundibular CP, this approach also provides direct exposure to the branches of ICA (including the PCA and anterior choroidal artery), optic chiasm and PS from the posterolateral side (11). Thus, this novel approach might be a promising alternative approach for resection of suprasellar or retrosellar lesions.

Compared with the retrosigmoid view, the supracerebellar view supplies the corridor from the medial to cranial nerves and significantly reduces the manipulation of neurovascular complex (21). By exploiting the natural infratentorial space, this corridor is devoid of cortex retraction seen in frontotemporal craniotomy. This approach also avoids other inherent shortcomings of above-mentioned anterolateral, lateral, and posterolateral routes, such as hearing loss, damage to the central skull-base bone, and injury of the Labbe vein. In addition, this technique simplifies craniotomy procedures, with a small incision that does not affects the appearance of patients (11). Another important advantage of this approach is high-definition wide-angle visualization and close-up observation endowed with endoscopy, which further minimize injury especially to various neurovascular structures behind the DS. Concerning the small size of the tumor, only a forward viewing endoscope was utilized in this case. The adoption of angled endoscope will allow visualization of anatomical structures out of the axis of the telescope and minimize the chance of tumor remnants under the condition of large PCMs.

Despite these merits, we are clearly aware that it is not without flaws. Firstly, endoscopy technique has difficulties when handling deep bleeding and necessitates a steep learning curve. Secondly, it is not entirely risk free because it may endanger the brainstem and cerebellum, and has inherent shortcomings of suboccipital craniotomy such as injury to the cerebrovenous system (including the petrosal venous, transverse sinus, and sigmoid sinus). Thirdly, unlike lateral and other posterolateral routes, tumor devascularization could only be achieved after tumor removal owing to the final exposure of PCP. Thus, bleeding control should be stressed especially in resection of massive or easily bleeding tumors. Last but not least, this case represented resection of a small PCM. Considering the surgical corridor, it would be an ideal approach for PCMs with lateral extension to the temporal lobe or posterolateral extension to the petroclival region, but may not be enough for complex PCMs with extreme suprasellar extensions. In this situation, microscopic FTOZ craniotomy may be needed either as an add-on or instead of the EF-SCITA. We believe multi-corridor hybrid surgery *via* combined EF-SCITA and microsurgical middle fossa approach might be an ultimate piece of the surgeon's armamentarium to improve outcomes in patient with complex DS lesions.

Conclusion

To the best of our knowledge, this is the first case report describing the EF-SCITA approach in the treatment of meningiomas situated over PCP. Overall, this posterolateral approach is technically simple and appears to be associated with less morbidity, which provides neurosurgeons with a viable alternative to traditional approaches to this kind of extremely rare lesions. However, the efficacy of this approach for larger PCMs awaits further verifications.

Data availability statement

The raw data supporting the conclusions of this article will be made available by the authors, without undue reservation.

Ethics statement

Written informed consent was obtained from the individual(s) for the publication of any potentially identifiable images or data included in this article.

Author contributions

SF, GL, YB and SH have been involved in the operation and management of the patient. SF and GL designed the report. YB and SH reviewed the literature, drafted the article and prepared the figures. XTL and XNL provided important academic inputs during surgery as well as during the revision of this manuscript. All authors contributed in editing of the manuscript and approved its final version. All authors contributed to the article and approved the submitted version.

Funding

This research was supported by Science & Technology Plan of Liaoning Province (grant No. 2021JH2/10300116 to SF and 2022020775-JH2/1015 to SH) and National Natural Science Foundation of China (grant No. 82101318 to YB and No. 81971133 to GL).

Conflict of interest

The authors declare that the research was conducted in the absence of any commercial or financial relationships that could be construed as a potential conflict of interest.

Publisher's note

Supplementary material

The Supplementary Material for this article can be found online at: https://www.frontiersin.org/articles/10.3389/fonc.2023.1089002/full#supplementary-material

SUPPLEMENTARY VIDEO 1

Video legend This video shows technical specification of endoscopic far-lateral supracerebellar infratentorial approach for resection of posterior clinoid meningioma. Firstly, endoscopic explorations in the lateral supracerebellar space are facilitated by disconnection of the draining vein with bipolar coagulator. Then, the ambient cistern could be exposed by opening ambient cistern arachnoid membranes, and the CN IV and CN V could be revealed in this process. Next, the tumor in the ambient cistern was exposed with the aid of tentorium cerebelli incision, with special attention paid to CN IV protection. The tumor was found to be divided into two parts by the tentorium cerebelli: the infratentorial part and the supratentorial part. Before infratentorial tumor debulking, tumor adhesions to residual ambient cistern arachnoid membranes and the tentorial incisura were separated and removed. The CN IV was found to be encased and compressed towards the tentorial incisura, which was carefully separated from the tumor. In addition, the CN III and the P1 segment of posterior cerebral artery located medially to the lesion were identified, and the tumor capsule was gently dissected away. Along with tumor decompression of the infratentorial part, the supratentorial part descended to the surgery field. During resection of the supratentorial tumor, dense adhesions of this part to the internal carotid artery and the initial part of the basal vein (BV) in front were found, which were carefully dissected from these vital neurovascular structures. Finally, its dural attachment could be detected at the right PCP and adjacent petrous apex after removal of residual tumor, and the dural attachment was coagulated under direct vision.

References

1. Goto T, Ohata K. *Posterior clinoidal meningiomas*. Lee JH, editor. Meningiomas London: Springer (2009) p. 399–402.

2. Horiguchi T, Yoshida K, Kawase T. *Posterior clinoid meningioma*. AANS (2008). Available at: http://www.aans.org/Media/Article.aspx?ArticleId=51587.

3. Shukla D, Gangadharan J, Kakati A, Devi BI. Posterior clinoid process meningioma. *Clin Neurol neurosurgery* (2013) 115(8):1517–9. doi: 10.1016/j.clineuro.2012.12.007

4. Sodhi HB, Singla N, Gupta SK. Posterior clinoid meningioma: A case report with discussion on terminology and surgical approach. *Surg Neurol Int* (2015) 6:21. doi: 10.4103/2152-7806.151261

5. Takase H, Kawasaki T, Tateishi K, Yokoyama TA, Murata H, Kawahara N. Characteristics and surgical strategies for posterior clinoid process meningioma: Two case reports and review of the literature. *Neurosurgical Rev* (2017) 40(1):163–9. doi: 10.1007/s10143-016-0774-z

6. Young IM, Yeung J, Glenn C, Teo C, Sughrue ME. Aggressive progression of a WHO grade I meningioma of the posterior clinoid process: An illustration of the risks associated with observation of skull base meningiomas. *Cureus* (2021) 13(3):e14005. doi: 10.7759/cureus.14005

7. Nanda A, Patra DP, Savardekar A, Maiti TK, Kalakoti P. Resection of posterior clinoid meningioma through retrosigmoid approach: Concepts and nuances. *Neurosurgical Focus* (2017) 43(VideoSuppl2):V5. doi: 10.3171/2017.10.FocusVid.17325

8. Ohba S, Sasaki H, Kimura T, Ikeda E, Kawase T. Clear cell meningiomas: Three case reports with genetic characterization and review of the literature. *Neurosurgery* (2010) 67 (3):E870–1; discussion E1. doi: 10.1227/01.NEU.0000374857.06732.CD

9. Giammattei L, Starnoni D, Benes V, Froelich S, Cossu G, Borsotti F, et al. Extreme lateral supracerebellar infratentorial approach: Surgical anatomy and review of the literature. *World neurosurgery* (2021) 147:89–104. doi: 10.1016/j.wneu.2020.12.042

10. Xie T, Wang Y, Zhang X, Shao N, Lu W, Yang Q, et al. Endoscopic far-lateral supracerebellar infratentorial approach for petroclival region meningioma: Surgical technique and clinical experience. *Operative Neurosurg (Hagerstown Md)* (2022) 22 (5):290–7. doi: 10.1227/ons.0000000000000126

11. Bai Y, Sun X, Li X, Han S, Liang G, Feng S, et al. Case report and literature review: Resection of retroinfundibular craniopharyngioma *via* endoscopic far-lateral supracerebellar infratentorial approach. *Front Oncol* (2022) 28(12):976737. doi: 10.3389/fonc.2022.976737

12. Youssef AS, van Loveren HR. Posterior clinoidectomy: Dural tailoring technique and clinical application. *Skull base* (2009) 19(3):183–91. doi: 10.1055/s-0028-1096196

13. Chanda A, Nanda A. Anatomical study of the orbitozygomatic transsellar-transcavernous-transclinoidal approach to the basilar artery bifurcation. *J neurosurgery* (2002) 97(1):151–60. doi: 10.3171/jns.2002.97.1.0151

14. Nakamura M, Samii M. Surgical management of a meningioma in the retrosellar region. *Acta neurochirurgica* (2003) 145(3):215–9; discussion 9-20. doi: 10.1007/s00701-002-1053-z

15. Dolenc V. *Microsurgical anatomy and surgery of the central skull base* Vol. 212-6. . New York: Springer (2003).

16. Vishteh AG, David CA, Marciano FF, Coscarella E, Spetzler RF. Extreme lateral supracerebellar infratentorial approach to the posterolateral mesencephalon: Technique and clinical experience. *Neurosurgery* (2000) 46(2):384–8; discussion 8-9. doi: 10.1097/00006123-200002000-00022

17. Akiyama O, Matsushima K, Gungor A, Matsuo S, Goodrich DJ, Tubbs RS, et al. Microsurgical and endoscopic approaches to the pulvinar. *J neurosurgery* (2017) 127 (3):630–45. doi: 10.3171/2016.8.JNS16676

18. Zaidi HA, Elhadi AM, Lei T, Preul MC, Little AS, Nakaji P. Minimally invasive endoscopic supracerebellar-infratentorial surgery of the pineal region: Anatomical comparison of four variant approaches. *World neurosurgery* (2015) 84(2):257–66. doi: 10.1016/j.wneu.2015.03.009

19. Rehder R, Luiz da Costa MP, Al-Mefty O, Cohen AR. Endoscope-assisted microsurgical approach to the posterior and posterolateral incisural space. *World neurosurgery* (2016) 91:210–7. doi: 10.1016/j.wneu.2016.04.017

20. Kalani MY, Lei T, Martirosyan NL, Oppenlander ME, Spetzler RF, Nakaji P. Endoscope-assisted supracerebellar transtentorial approach to the posterior medial temporal lobe for resection of cavernous malformation. *Neurosurgical Focus* (2016) 40 Video Suppl 1:15465. doi: 10.3171/2016.1.FocusVid.15465

21. Jittapiromsak P, Little AS, Deshmukh P, Nakaji P, Spetzler RF, Preul MC. Comparative analysis of the retrosigmoid and lateral supracerebellar infratentorial approaches along the lateral surface of the pontomesencephalic junction: A different perspective. *Neurosurgery* (2008) 62(5 Suppl 2):ONS279–87: discussion ONS87-8. doi: 10.1227/01.neu.0000326008.69068.9a

frontiers | Frontiers in Oncology

TYPE Opinion
PUBLISHED 28 February 2023
DOI 10.3389/fonc.2023.1130040

OPEN ACCESS

EDITED BY
Diego Mazzatenta,
IRCCS Institute of Neurological Sciences of Bologna (ISNB), Italy

REVIEWED BY
Kamil Krystkiewicz,
Copernicus Memorial Hospital, Poland

*CORRESPONDENCE
Florent Carsuzaa
florent.carsuzaa@gmail.com

†These authors have contributed equally to this work

SPECIALTY SECTION
This article was submitted to Neuro-Oncology and Neurosurgical Oncology, a section of the journal Frontiers in Oncology

RECEIVED 22 December 2022
ACCEPTED 20 February 2023
PUBLISHED 28 February 2023

CITATION
Carsuzaa F, Favier V, Ferrari M, Turri-Zanoni M, Ingargiola R, Camarda AM, Seguin L, Contro G, Orlandi E and Thariat J (2023) Need for close interdisciplinary communication after endoscopic endonasal surgery to further personalize postoperative radiotherapy in sinonasal malignancies.
Front. Oncol. 13:1130040.
doi: 10.3389/fonc.2023.1130040

Need for close interdisciplinary communication after endoscopic endonasal surgery to further personalize postoperative radiotherapy in sinonasal malignancies

Florent Carsuzaa[1*†], Valentin Favier[2†], Marco Ferrari[3], Mario Turri-Zanoni[4], Rossana Ingargiola[5], Anna Maria Camarda[5], Lise Seguin[1], Giacomo Contro[3], Ester Orlandi[5] and Juliette Thariat[6]

[1]Department of Otorhinolaryngology – Head and Neck Surgery, University Hospital of Poitiers, Poitiers, France, [2]Department of Otorhinolaryngology – Head and Neck Surgery, University Hospital of Montpellier, Montpellier, France, [3]Section of Otorhinolaryngology – Head and Neck Surgery, University of Padova, "Azienda Ospedale Università di Padova", Padova, Italy, [4]Division of Otorhinolaryngology – Head and neck surgery, Department of Biotechnology and Life Sciences, University of Insubria, ASST Sette Laghi University Hospital, Varese, Italy, [5]Radiation Oncology, Clinical Department, National Center for Oncological Hadrontherapy (CNAO), Pavia, Italy, [6]Radiation Oncology, Centre François Baclesse: ARCHADE, Caen, France

KEYWORDS

sinonasal malignancies, radiotherapy, surgery, skull base tumors, interdisciplinary

Introduction

Sinonasal malignancies represent 3% of the head and neck cancers and have an incidence of 1/100,000 persons a year. Numerous epithelial and non-epithelial histologic subtypes are described in this localization: squamous cell carcinomas in 50% of sinonasal tumors, intestinal-type adenocarcinomas (ITAC) in 13%, mucosal melanomas in 7%, olfactory neuroblastomas in 7%, adenoid cystic carcinomas in 7%, undifferentiated carcinomas in 3%, and other very rare histologies in 13% (1–3). Most sinonasal malignancies are locally aggressive diseases. Five-year survival rates vary between 30–60%, with local recurrence as the main cause of death. Oncologic outcomes indeed vary widely with histological subtype: 5-year overall survival rates are 50-66.2% for squamous cell carcinomas, 60.0-72.7% for ITAC, 30.0%-35.7% for melanomas, 70.0-94.0% for olfactory neuroblastomas, 35.0-82.2% for undifferentiated carcinomas, and 87.7% for adenoid cystic carcinoma (4).

The management of sinonasal malignancies has undergone several changes in recent years. Surgery was initially performed through open approaches with complication rates of 33–42% and 4% of mortality. It has evolved toward minimally-invasive endoscopic surgery. Such strategy has allowed non-inferior oncological local control (LC) and lower morbidity

(about 7% of complications, overall) (5, 6). Endoscopic surgery is now the mainstay of treatment in most sinonasal tumors. Radiotherapy (RT) is often necessary as an adjuvant modality, with or without chemotherapy, following surgery to optimize local control. Such key decisions for the patients should be made at multidisciplinary staff meetings before each important step (surgery, radiotherapy, etc).

When a tumor involves the skull base and paranasal sinuses, surgeons and radiation oncologists faced with several anatomical challenges: 1) most of the anatomical landmarks are difficult to identify on an CT imaging basis due to a soft-tissue CT density (but also on MRI) and a combination of invasion and compression/displacement of normal anatomical structures; 2) sinonasal tumors are often pedicled, with a larger "polyp-like" intraluminal compartment (i.e.: the portion of tumor which is growing in the sinonasal air spaces) which is not invasive for surrounding structures; 3) postoperatively, most of the anatomical landmarks are removed (e.g.: turbinates, sinuses walls, crista galli…); 4) during RT administration, some changes in the mucosal thickness and modification of collected fluid can contribute to the amount of aeration inside the paranasal sinuses with a significant impact on dose distribution on target volumes and organs at risk (7). Of course, structures adjacent to sinonasal regions are also at risk and need to be preserved. However, it is necessary to guarantee the effectiveness of the treatment allowing good LC. Orbital preservation best represents the compromise made to achieve acceptable oncological results while maximizing functional outcomes (8). Therefore, sinonasal tumors are indeed an example of multidisciplinarity and should be best performed at high volume centers (9), a statement that of course is challenged by the rarity of these tumors and their variable presentations and histologies.

Interdisciplinary communication

Endoscopic surgery is a major change for radiation oncologists. To that extent, it should be well documented and understood to ensure tumor control. Mutual understanding of endoscopic surgery might also be a great opportunity to not only reduce surgical morbidity but also radiation-induced morbidity.

Planning post-operative radiotherapy (PORT) in sinonasal malignancies is a complex task. It is inherently interdisciplinary, requiring mutual understanding of the various reports made during the course of treatment: the imaging report should be well understood by the surgeon; in particular, MRI has been reported to overestimate tumor extensions, suggesting that the surgeons should be able to discuss with radiologists before surgery (10). It also allows feedback from surgeons to radiologists based on perioperative observations as a way to make imaging reports more usable by the practicing surgeons, recognizing the implications of imaging reports. Perioperative observations could be enriched by neuronavigation images to correlate tumor areas with radiologist's assessment and also with radiation oncologists to transpose operate findings onto postoperative the PORT planning CT scanner.

Endoscopic endonasal resection led to tumor disassembling into smaller tissue fragments, which may measure a few centimeters only. Each of these fragments is typically annotated and oriented by the surgeon (11). Standardization of oriented surgical sampling and the way the anatomical areas are resected is key. Operative reports may either refer to a graphical or textual list of the resected anatomical structures. They are the basis for a common language for all specialties involved in the management of patients with sinonasal tumors. The pathologist can locate safe tissue fragments, tumor sub-volumes, and can report on the quality of tumor margins and additional surgical margins. Their analysis is essential to qualify the quality of margins and further the dose defined by the radiation oncologists.

Finally, historadiological correlations are needed to further locate each fragment onto the successive planar images of the planning radiotherapy scanner. The volumes to be irradiated are usually determined from the imaging performed pre-operatively, the operative and pathological reports and knowledge of anatomical extensions. At the era of endoscopic surgery, communication between the surgeon and radiation oncologist is critical to accurate RT volume and dose definitions so as to ensure local tumor control (12).

The whole process requires continuous interdisciplinary communication. This is a strong prerequisite to further optimize RT in a way that could reduce irradiation volumes, as local failure cannot be an option when customizing treatments toward less morbidity from RT.

Toward a better use of scheme and navigation

A schematic anatomic 3D drawing was designed by Bastier and de Gabory and validated as a tool to help clinicians to report the surgical and pathological results of sinonasal malignancy removal (11). Those not familiar with this figure may also use the corresponding list table of anatomical fragments that is necessarily report on the pathology report following surgical minimally-invasive and annotated resection. It indicates the extension of the surgical resection and locates all the histological specimens. It helps in understanding the position and relationship between each sample, which is very helpful since many fragments are removed from the same anatomical structure during the surgery for sinonasal malignancies. It demonstrates tumor invasion within the resected structures and shows the free margins. The use of this scheme makes it possible to improve the communication between the various stakeholders and in particular the pathologist's understanding of the position of the various tumor portions and the radiation oncologist's understanding of the areas most at risk of relapse. However, this scheme is a fragmented view of the sinonasal anatomical spaces, which can make it difficult to represent tumors especially in the borderline areas.

Advances in in-room imaging using surgical navigation systems can help surgeons intraoperatively and might further improve the rate of safe margins and may further improve oncologic outcomes (13). The accuracy of new generation navigation systems is now < 1 mm (14). Given the complex anatomical structures that lie in close proximity to critical structures such as optic nerves, orbits and

their content, optic chiasm, pituitary gland, internal carotid artery, cranial nerves and brain, this tool helps to reduce morbidity of the surgery. The use of surgical navigation also allows the surgeon to combine the macroscopic view with a precise CT/MRI location as well as to better understand the tumor implantation area. In the future, data acquired during intraoperative navigation could be coupled with the pre- and postoperative imaging to enhance accuracy. The surgeon could then contour the area of the tumor implantation during the surgery with a navigated pointer and this contouring could automatically be transferred to the postoperative imaging in order to facilitate understanding of the volumes at risk by the radiation oncologist.

Radiotherapy planning

The low morbidity of endoscopic sinonasal surgeries can be combined with modern irradiation modalities to promote minimally invasive and maximally effective therapeutic options. PORT planning of sinonasal malignancies, in its delineation step, requires virtual geolocation transfer of sinonasal tumor from preoperative views to postoperative axial CT in RT practice. This is of pivotal importance not only for optimal delineation of the initial macroscopical disease, but also for the selection, along with histopathological data, target volumes at risk of harboring microscopic disease.

Given that toxicities are cumulative between surgery and RT, these findings point the opportunity to improve patient care and avoid therapeutic escalation. Two trials are currently investigating de-escalation in high-dose volumes. The French "SinocaRT" randomized phase II trial compares dose-painting intensity-modulated radiation therapy (IMRT) versus standard IMRT. The GORTEC 2016-02 phase III SANTAL trial NCT02998385, investigates the use of cisplatin in addition to PORT; it includes an arm with proton therapy. Accrual will end in 2023 with more than 260 patients. An American trial (NCT01586767) currently investigates the efficacy of proton therapy on local control rate and the toxicity compared to IMRT in the treatment of locally advanced sinonasal malignancy. Such precision RT includes other constraints. Using minimally-invasive endoscopic technique, the resected tumor and surrounding anatomical structures are small and characterized by a complex shape. Therefore the dose distribution may be geometrically complex with areas of steep dose gradients (in the order of 1-2 Gy/mm). Complex dose geometry requires quality assurance processes that consists in assessing whether an optimally planned radiotherapy can indeed be delivered accurately as planned. Moreover, the resected sinonasal areas have complex air-soft tissues/mucosae-bone interfaces (regardless of the type of surgery). These interfaces may change from day to day because sinonasal cavities are variably filled in with secretions. Secretions can change in quantity and density over the treatment course along the beam paths and might result in inaccurate dose delivery.

Improvements to facilitate dose-painting RT might come from optimized reporting during the endoscopic surgery procedure. The surgical navigation system using a digital pointer on CT images may be exploited further by radiation oncologists when planning PORT. If images and pointing information can be stored, these images may be co-registered and transferred on postoperative radiotherapy planning CT. 3D tumor reconstruction and printing might also be another intriguing option. At present, it has been used only for educational purposes with students or as some information aid for patients (15, 16). It could provide a postoperative basis to improve understanding of positive margins on the tumor anatomy preoperatively. However, it is time consuming for the surgeons and pathologists, and this may be selected for complex cases until automated solutions will be available.

The sinonasal structures are anatomically complex and small and therefore difficult to precisely delineate on CT by the radiation oncologist. Due to the lack of specific sinonasal atlases identifying endoscopic resection fragments, the anatomic uncertainties and the level of confidence of using histosurgical mapping by radiation oncologists may limit the use of dose-painting IMRT in daily practice (17). Even more, this could be limiting for proton therapy due to the sharp dose profiles usually achieved and a higher sensitivity to uncertainties compared to IMRT, requiring caution to avoid unintended hot spots. It is therefore necessary to create tools allowing radiation oncologists to better navigate in postoperative imaging. Researches in this area should focus on automatization of tumor and sinonasal anatomy representation (e.g.: automatic recognition of anatomical spaces and segmentation on CT/MRI images).

Conclusion

As surgery-related morbidity has been reduced over the years by the contribution of endoscopic-assisted endonasal surgery, an attempt should be made to limit postoperative sequelae of RT and improve oncological outcomes by more precise targeting of areas at risk of tumor extension. RT is associated with severe middle- and long-term toxicities, suggesting efforts should be made by the scientific community to reduce its morbidity. The first major challenge, although there are no clinical studies on this point, is to be able to reduce the irradiated volumes to reduce radiation-induced morbidity and without taking an additional risk of local relapse. Closer communication between surgeons, pathologists and radiation oncologists, with the help of specifically designed tools, is mandatory to achieve the next step in sinonasal malignancy management. This may allow a better personalization of postoperative treatment to improve LC and reduce the morbidity of combined surgical and RT.

Author contributions

Conceptualization: FC, VF, JT. Original writing: FC, VF, JT. Reviewing original manuscript: all authors. All authors contributed to the article and approved the submitted version.

Conflict of interest

The authors declare that the research was conducted in the absence of any commercial or financial relationships that could be construed as a potential conflict of interest.

Publisher's note

References

1. Gore M, Zanation A. Survival in sinonasal melanoma: A meta-analysis. *J Neurol Surg B* (2012) 73(03):157–62. doi: 10.1055/s-0032-1301400

2. Thariat J, Moya Plana A, Vérillaud B, Vergez S, Régis-Ferrand F, Digue L, et al. Diagnostic, pronostic et traitement des carcinomes nasosinusiens (hors mélanomes, sarcomes et lymphomes). *Bull du Cancer* (2020) 107(5):601–11. doi: 10.1016/j.bulcan.2020.02.013

3. Slevin F, Pan S, Mistry H, Denholm M, Shor D, Oong Z, et al. A multicentre UK study of outcomes for locally advanced sinonasal squamous cell carcinoma treated with adjuvant or definitive intensity-modulated radiotherapy. *Clin Oncol* (2021) 33(10):e450–61. doi: 10.1016/j.clon.2021.05.012

4. Ferrari M, Mattavelli D, Tomasoni M, Raffetti E, Bossi P, Schreiber A, et al. The MUSES∗: a prognostic study on 1360 patients with sinonasal cancer undergoing endoscopic surgery-based treatment: ∗MUlti-institutional collaborative study on endoscopically treated sinonasal cancers. *Eur J Cancer* (2022) 171:161–82. doi: 10.1016/j.ejca.2022.05.010

5. Ganly I, Patel SG, Singh B, Kraus DH, Bridger PG, Cantu G, et al. Craniofacial resection for malignant paranasal sinus tumors: Report of an international collaborative study. *Head Neck* (2005) 27(7):575–84. doi: 10.1002/hed.20165

6. Meccariello G, Deganello A, Choussy O, Gallo O, Vitali D, De Raucourt D, et al. Endoscopic nasal versus open approach for the management of sinonasal adenocarcinoma: A pooled-analysis of 1826 patients: Endoscopic surgery for sinonasal adenocarcinoma. *Head Neck* (2016) 38(S1):E2267–74. Eisele DW. doi: 10.1002/hed.24182

7. Fukumitsu N, Ishikawa H, Ohnishi K, Terunuma T, Mizumoto M, Numajiri H, et al. Dose distribution resulting from changes in aeration of nasal cavity or paranasal sinus cancer in the proton therapy. *Radiother Oncol* (2014) 113(1):72–6. doi: 10.1016/j.radonc.2014.08.024

8. Turri-Zanoni M, Lambertoni A, Margherini S, Giovannardi M, Ferrari M, Rampinelli V, et al. Multidisciplinary treatment algorithm for the management of sinonasal cancers with orbital invasion: A retrospective study. *Head Neck* (2019) 41(8):2777–88. doi: 10.1002/hed.25759

9. Teitelbaum JI, Issa K, Barak IR, Ackall FY, Jung SH, Jang DW, et al. Sinonasal squamous cell carcinoma outcomes: Does treatment at a high-volume center confer survival benefit? *Otolaryngol Head Neck Surg* (2020) 163(5):986–91. doi: 10.1177/0194599820935395

10. Fierens S, Moya-Plana A, Vergez S, Bénard A, Gallard R, Molinier-Blossier S, et al. Do practitioners assess sinonasal adenocarcinoma extension similarly? interdisciplinary concordance in 21 cases. *Clin Otolaryngol* (2021) 46(3):665–9. doi: 10.1111/coa.13708

11. Bastier PL, de Gabory L. Design and assessment of an anatomical diagram for sinonasal malignant tumour resection. *Rhin* (2016) 54(4):361–7. doi: 10.4193/Rhino15.355

12. Paré A, Blanchard P, Rosellini S, Aupérin A, Gorphe P, Casiraghi O, et al. Outcomes of multimodal management for sinonasal squamous cell carcinoma. *J Cranio-Maxillofacial Surg* (2017) 45(8):1124–32. doi: 10.1016/j.jcms.2017.05.006

13. Vicaut E, Bertrand B, Betton JL, Bizon A, Briche D, Castillo L, et al. Use of a navigation system in endonasal surgery: Impact on surgical strategy and surgeon satisfaction. a prospective multicenter study. *Eur Ann Otorhinolaryngol Head Neck Dis* (2019) 136(6):461–4. doi: 10.1016/j.anorl.2019.08.002

14. Grauvogel TD, Engelskirchen P, Semper-Hogg W, Grauvogel J, Laszig R. Navigation accuracy after automatic- and hybrid-surface registration in sinus and skull base surgery. *PloS One* (2017) 12(7):e0180975. doi: 10.1371/journal.pone.0180975

15. Sander IM, Liepert TT, Doney EL, Leevy WM, Liepert DR. Patient education for endoscopic sinus surgery: Preliminary experience using 3D-printed clinical imaging data. *J Funct Biomater 7 avr* (2017) 8(2):13. doi: 10.3390/jfb8020013

16. Molinari G, Emiliani N, Cercenelli L, Bortolani B, Gironi C, Fernandez IJ, et al. Assessment of a novel patient-specific 3D printed multi-material simulator for endoscopic sinus surgery. *Front Bioeng Biotechnol* (2022) 10:974021. doi: 10.3389/fbioe.2022.974021

17. Leleu T, Bastit V, Doré M, Kammerer E, Florescu C, Alfonsi M, et al. Histosurgical mapping of endoscopic endonasal surgery of sinonasal tumours to improve radiotherapy guidance. *Cancer Radiother* (2022) 26(3):440–4. doi: 10.1016/j.canrad.2021.06.014

frontiers | Frontiers in Oncology

TYPE Review
PUBLISHED 08 March 2023
DOI 10.3389/fonc.2023.1112018

OPEN ACCESS

EDITED BY
Diego Mazzatenta,
IRCCS Institute of Neurological Sciences of Bologna (ISNB), Italy

REVIEWED BY
Junya Fukai,
Wakayama Medical University, Japan
Warren Boling,
Loma Linda University, United States
Promod Pillai,
Loma Linda University Health Care, United States

*CORRESPONDENCE
Kui Liu
kuiliu3009@126.com
Zheng Liu
liuzheng@znhospital.com

†These authors have contributed equally to this work and share first authorship

SPECIALTY SECTION
This article was submitted to Neuro-Oncology and Neurosurgical Oncology, a section of the journal Frontiers in Oncology

RECEIVED 30 November 2022
ACCEPTED 21 February 2023
PUBLISHED 08 March 2023

CITATION
Zhang T, Feng Y, Liu K and Liu Z (2023) Advances and trends in meningioma research over the last decade: A scientometric and visual analysis. *Front. Oncol.* 13:1112018. doi: 10.3389/fonc.2023.1112018

Advances and trends in meningioma research over the last decade: A scientometric and visual analysis

Tingbao Zhang†, Yu Feng†, Kui Liu* and Zheng Liu*

Department of Neurosurgery, Zhongnan Hospital of Wuhan University, Wuhan, China

Objective: We conducted a scientometric and visual analysis of meningioma studies in the past ten years and discussed the current status and trends of meningioma research to provide a reference basis for conducting relevant clinical practice or research.

Method: A search of the topic of meningioma in the Web of Science Core Collection database was conducted for January 2012-December 2021. The scientometric tools CiteSpace (version 5.8.R3), VOS viewer (version 1.6.17), and the Bibliometrix package of R software (version 4.2.1) were used to visualize and analyze the country of publication, institution, author, keywords, and cited literature of meningioma.

Results: A total of 10,397 documents related to meningioma were collected, of which 6,714 articles were analyzed. The annual analysis shows an increase in published articles, with an annual growth rate of 8.9%. 26,696 authors from 111 countries or regions were involved in publishing relevant studies. The country with the highest number of publications was the United States (1671), and the institution with the highest number of publications was the University of California, San Francisco (242). The keyword clustering of current studies can be grouped into five groups: meningioma characteristics and basic research, surgical treatment, radiation therapy, stereotactic radiosurgery, and management of complications. Keyword trend analysis shows that meningioma classification and molecular characteristics are emerging hotspots for meningioma research in recent years.

Conclusion: The scientometric and visual analysis demonstrated the research status and trends of meningioma. Over the past decade, meningioma research has focused on managing meningiomas with a predominance of surgical treatment and radiation therapy. At the same time, meningioma classification and molecular characteristics are emerging as current and possible research hotspots in the coming period.

KEYWORDS

meningioma, scientometric, treatment, classification, molecular characteristics

Introduction

Meningioma is one of the most common central nervous system tumors, accounting for more than 30% of primary intracranial tumors in adults, second only to glioma, and relatively rare in children and adolescents (0.4% to 4.6%) (1, 2). Meningiomas originate from the arachnoid cap cells in the dura mater's inner layer and grow more slowly; most of them are grade WHO I tumors (2, 3). Meningioma management is primarily surgical resection and most patients with gross total resection have a good prognosis (4). As a result, meningioma research has not received enough attention in the past compared to more malignant gliomas. Until the last decade, there has been a growing interest in the study of meningiomas, as evidenced by many studies and review articles on the subject. For instance, many attractive new therapeutic targets have been identified in the last decade (5). Various anti-angiogenic drugs, genomic-targeted drugs, and immunotherapies have performed exceptionally well in early trials (6, 7). However, a comprehensive scientometric review of the latest research on meningiomas is lacking. There are a few previous scientometric articles on meningioma, including an analysis of the top 100 most cited papers (8) and an analysis of stereotactic radiotherapy for meningioma (9). Although these studies provide a preliminary understanding of meningioma research, a more comprehensive scientometric analysis of meningiomas is not available in the literature.

The scientometric analysis is an emerging tool to quickly explore the structure and trends of a topic or domain through statistical methods and visualization (10–12). It can extract useful information from a large amount of literature by identifying relevant nodes. Currently, commonly used scientometric software includes CiteSpace (13), VOS viewer (14), bibliometrix package of R software (15), Science of Science (SCI2) and HistCite, etc. (16). Among them, CiteSpace and VOS viewer are the most popular ones due to their convenience and authority. CiteSpace is a scientometric software developed by Professor Chaomei Chen, a leading informatics expert at Drexel University, based on citation analysis theory and using the Java language (17). It enables researchers to find the most relevant topics and scientific literature in their field of knowledge and to understand the most critical valid information. Moreover, it clarifies the field's development process and identifies current research frontiers and trends. VOS viewer is a software application for visual analysis of scientific literature developed by Leiden University in the Netherlands to create, visualize and explore information maps based on web data (18). VOS viewer is based on a clustering analysis algorithm to realize scientific knowledge mapping, showing the structure, evolution, cooperation and other relationships in the knowledge domain. Moreover, its outstanding feature is its graphic solid display capability and suitability for large-scale data.

In this study, we used CiteSpace and VOS viewer in combination with the bibliometrix package of R software for scientometric and visual analysis of meningioma studies in the past 10 years. Meanwhile, we used artificial statistical screening to analyze keywords for meningioma classification, treatment, and molecular characteristics based on scientometric analysis. The combination of scientometric analysis and historical review will identify key evidence and highlight emerging meningioma research trends.

Materials and methods

Given that the Web of Science Core Collection (WoSCC), the most commonly used database for scientific or scientometric analysis, contains all the essential information used for the analysis, we chose WOS as our data source (19). We use WoSCC as our data source. All data were retrieved from WoSCC on October 01, 2022, to avoid possible bias due to continuous database updates. We used "meningioma*" as a subject search term and set the period from 2012 to 2021, limiting the type of literature to articles. The detailed search and analysis process is shown in Figure 1.

First, the collected data were scientometric analyzed using the bibliometrix package of R software (version 4.2.1), including overall characteristics, annual publications, topographic maps of national collaborations, and trend maps of authors and keywords. Combined with the scientometric results, bar charts of publications and citations by country/region, institutions, authors and journals were created using Origin 2022. Also, the H/G/M index was added to the journal bar chart to analyze the scientometric results on journal impact comprehensively. Then, a network graph of country collaboration, a keyword co-citation trend graph and a cluster analysis graph were visually analyzed using VOS viewer (version 1.6.17). Different colors indicate the clusters in the graph, and the collaboration or co-citation connecting lines are indicated. The size of the circles indicates the number of documents, references or keywords. Finally, a literature citation node analysis was performed using CiteSpace (version 5.8. R3).to find the most cited keywords. The parameter settings included time slices (2012-2021) and selection criteria (cited more than 50). In addition, we performed artificial statistical analysis of keywords based on scientometric results to filter out the top 10 most cited keywords in different directions and visualized and analyzed them using Origin 2022.

Results

General characteristics and annual analysis

From 2012 to 2021, 10,397 documents were published on "meningioma", including 6,714 articles (Figure 2A). These articles were published in 1217 journals by 26696 authors, with an average of 6.94 co-authors per article; 87 of these articles were independently authored, and another 17.32% were published in international collaboration. 96,905 references were cited in these articles, with an average of 11.99 citations per article. In addition, these articles have been cited 80,501 times, with an average of 11.99 citations per article.

The annual number of publications in the last decade tended to increase each year, especially from 2016 to 2017 (Figure 2B); the annual number of publications increased nearly 1-fold from 483 in

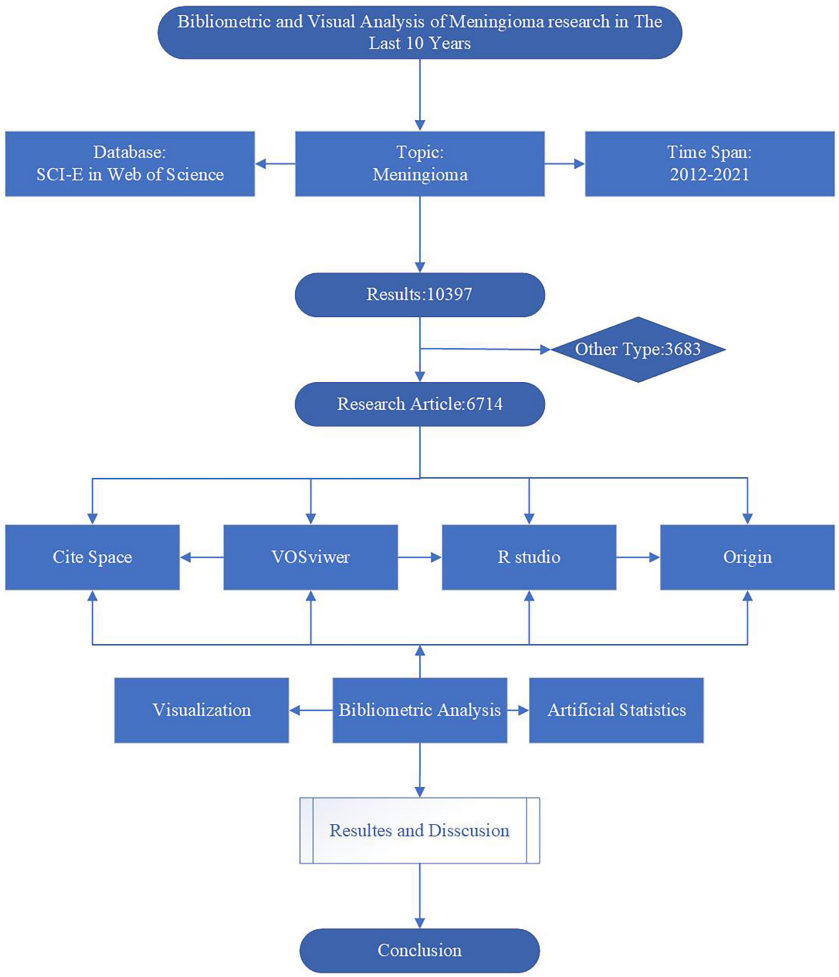

FIGURE 1
Flowchart of Scientometric and Visual Analytics.

2012 to 935 in 2021, with an average annual growth rate of 8.91%. Each country's annual publication volume also shows a yearly performance increase. The United States has the highest number of publications (1671), with more than 1000, followed by China with 928, Japan with 496, Germany with 489, and Italy with 339 (Figure 2C). Some countries, such as South Korea and France, have concentrated their publications in the early years. In contrast, others have concentrated in recent years, such as Denmark, Egypt, and Saudi Arabia.

Analysis of the influence of countries/regions and cooperation

A total of 111 countries/regions were involved in meningioma-related research, and their differences in impact were related to the volume of articles published (Figure 2D). The overall citation volume of country articles was ranked the same as the volume of publications, with the top five being the United States (27674), China (8427), Germany (8293), Japan (4368), and Italy (4033). However, the number of citations of a single article in different countries shows varying levels. Switzerland has the highest number of citations for a single article, with 22.64, followed by the UK with 17.96 and Germany with 18.86. Although the US and China rank first and second in total citations, they rank 4th and 14th in citations for a single article, with 16.56 and 9.08. The articles published in collaboration between different institutions are mainly domestic but also partially (17.32%) international (Figures 2E, F). The most significant inter-country collaborations were in the United States, with China, Germany, and Canada as the leading collaboration countries.

Analysis of institutions, authors, and journals

These articles originated from 4835 institutions, with the top 10 publishing more than 100 articles (Figure 3A). Three of the top five institutions are from the United States: The University of

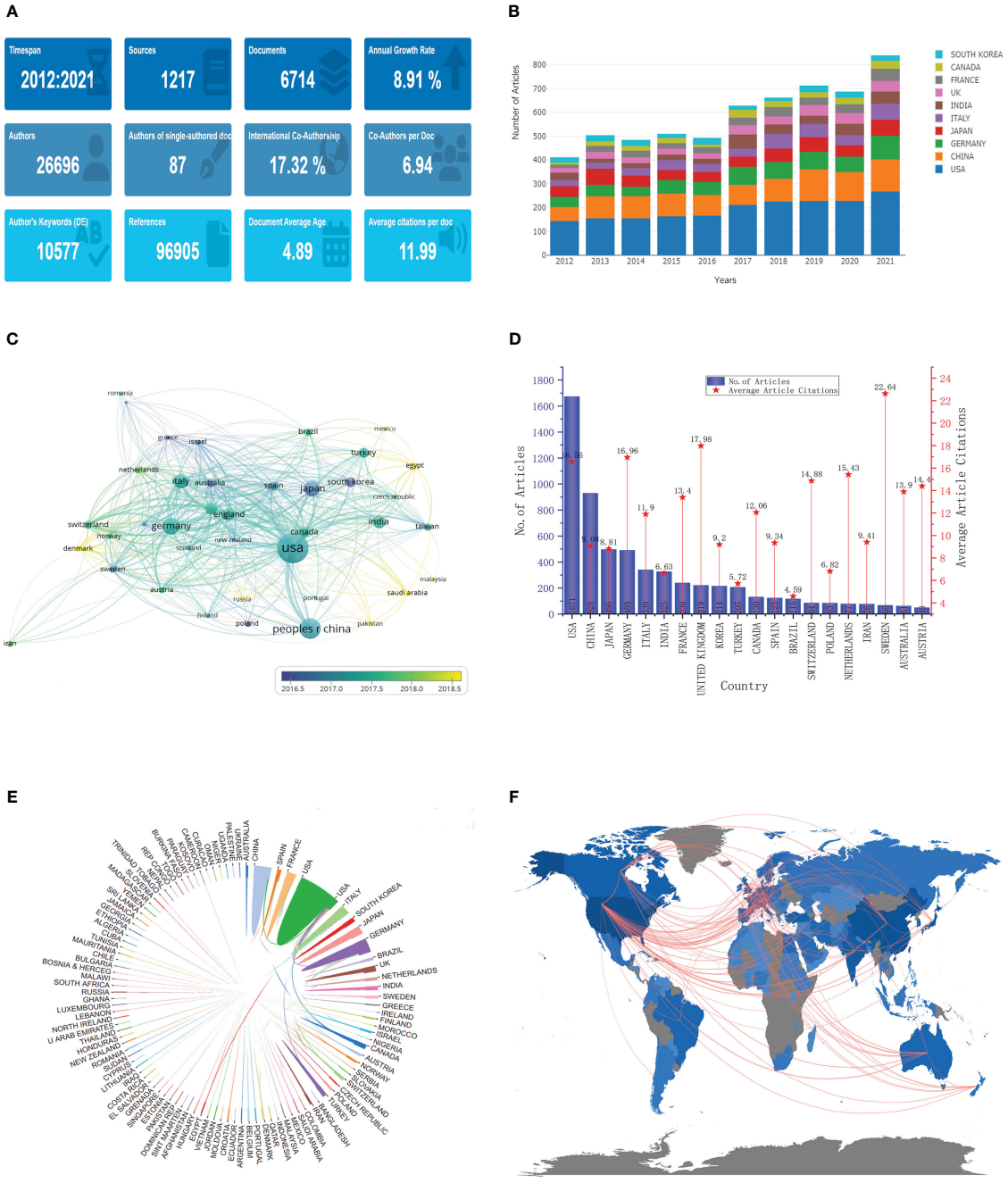

FIGURE 2
General characteristics and annual, country and cooperation analysis. **(A)** General characteristics; **(B)** Annual analysis; **(C)** Publication volume and trends in various countries; **(D)** Number of articles published and average number of articles cited in various countries; **(E, F)**. Cooperation between the various countries.

California (242 articles), Mayo Clinic (208 articles), and Ohio State University (178 articles); the other two institutions are from China: Capital Medical University (205 articles) and Fudan University (172 articles). The top 10 authors are shown in Figure 3B, mainly from China (4), the United States (3), and Germany (2), with the highest number of publications coming from WM (46), followed by DF from the United States and MC from Germany (45). The distribution of the top 20 authors in terms of publication volume is shown in Figure 3C. From the figure, it can be seen that these authors have published at least one article almost every year in the last ten years, with the highest number of articles published in 2019.

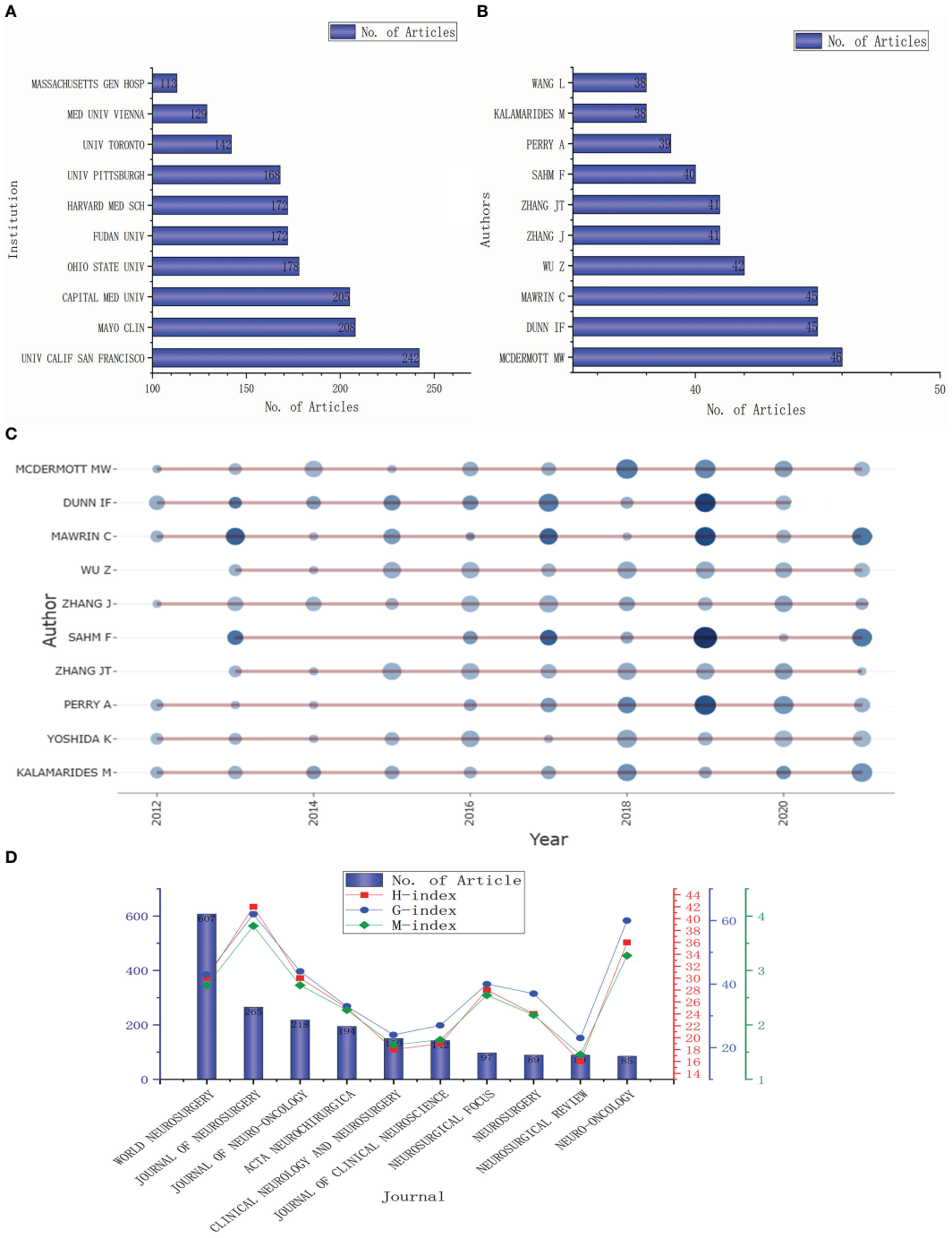

FIGURE 3
Analysis of institutions, authors and journals. **(A, B)**. The top 10 institutions and authors by published volume; **(C)** The time distribution of the first ten authors' published volume; **(D)** The number of articles published in the top 10 journals and their influence.

The top 10 journals with the most articles related to meningioma are listed in Figure 3D. The most published journal is WORLD NEUROSURGERY (607 articles), accounting for about one-tenth of the total number of articles, followed by the JOURNAL OF NEUROSURGERY (265 articles) and JOURNAL OF NEURO-ONCOLOGY (218 articles). The journals with more than 100 articles also include ACTA NEUROCHIRURGICA (194 articles), CLINICAL NEUROLOGY AND NEUROSURGERY (150 articles), and JOURNAL OF CLINICAL NEUROSCIENCE (142 articles). However, the impact of these journals is not proportional to their number of publications. H-index, g-index, and m-index are the highest for JOURNAL OF NEUROSURGERY with 42, 62, and 3.818, respectively. Followed by NEURO-ONCOLOGY (36, 60, and 3.273)

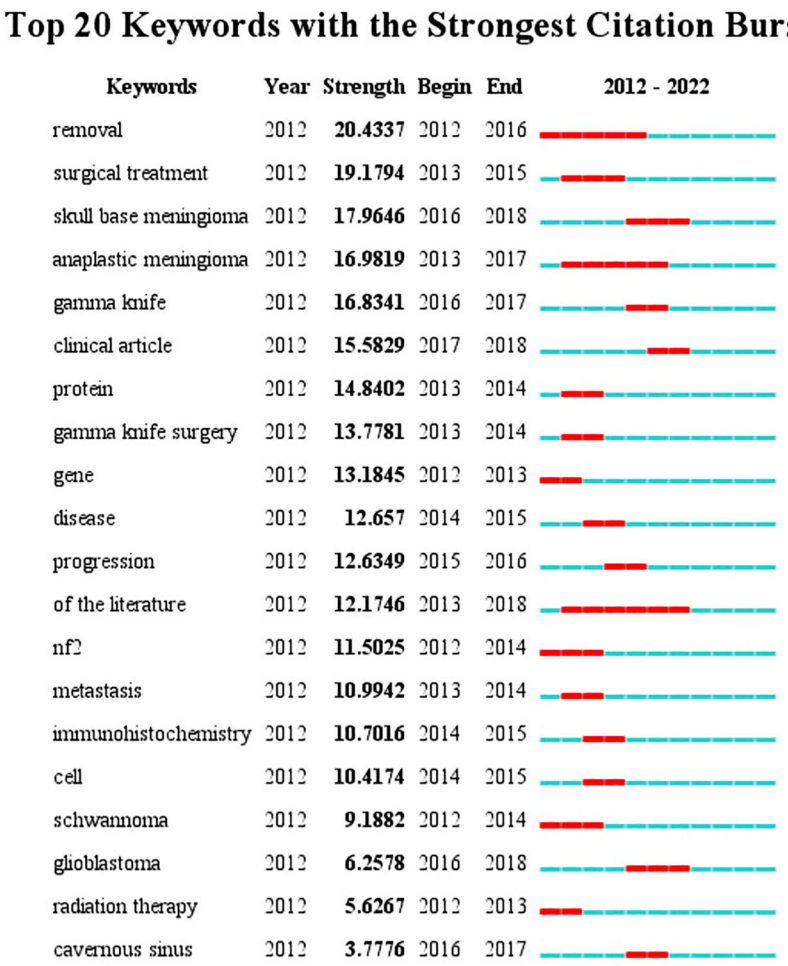

FIGURE 4
Top 20 keywords with the strongest citation bursts.

Keyword clustering and trending analysis

The top 20 most frequently used keywords in this literature are shown in Figure 4. As can be seen from the chart, the two most used keywords are related to surgical resection, which are "resection" and "surgical treatment"; the top 5 keywords are also "skull base meningioma", "mesenchymal meningioma", and "gamma knife". Regarding period, the three keywords with the largest span were "resection", "mesenchymal meningioma", and "literature". The keywords at the time of WOS inclusion were displayed according to the utilization size (see Figure 5A). From the word cloud, it can be seen that the top 5 most recorded keywords are: "tumor", "surgery", "management", "meningioma", and "cancer", in that order. VOS viewer was used for co-occurring keywords, and it was found that "classification" became a prominent new keyword around 2018 (Figure 5B). A temporal distribution of keywords using citations shows that keywords related to tumor surgery, such as "surgery", "resection", and "management", have been used (Figure 5C). In addition, it can be seen that the focus keywords used in the last 3 years, such as "cell", "microRNA expression", and "ewelmer", are related to basic research and molecular characteristics of tumors. It indicates that the research hotspots of meningioma in recent years have gradually favored basic research.

At the same time, we also performed cluster analysis on the keywords. The keywords with more than 50 citations were clustered using VOS viewer (Figure 5D). We could see that these keywords were clustered into 5 categories: (i) the red part with "meningioma" as the main keyword was mainly related to the general characteristics and basic research of meningioma; (ii)the green part with "surgery" as the main keyword was mainly related to the surgical resection treatment of meningioma; (iii)the yellow part with "recurrence" and "radiotherapy" as the primary keywords is mainly related to the radiotherapy treatment of meningioma. (iv) the purple part with "stereotactic radiosurgery" as the main keyword is mainly related to stereotactic radiosurgery for meningioma; (v)the blue part with "intracranial meningioma" as the main keyword is mainly related to brain edema and other related complications.

In addition, we listed all keywords with more than 20 citations and performed the artificial statistical analysis. First, considering that "classification" became the most used keyword in 2018, we screened the keywords related to meningioma classification (Figure 5E). The figure shows that the main classifications include those based on tumor site and pathological type. Secondly, the keywords related to meningioma management were screened and

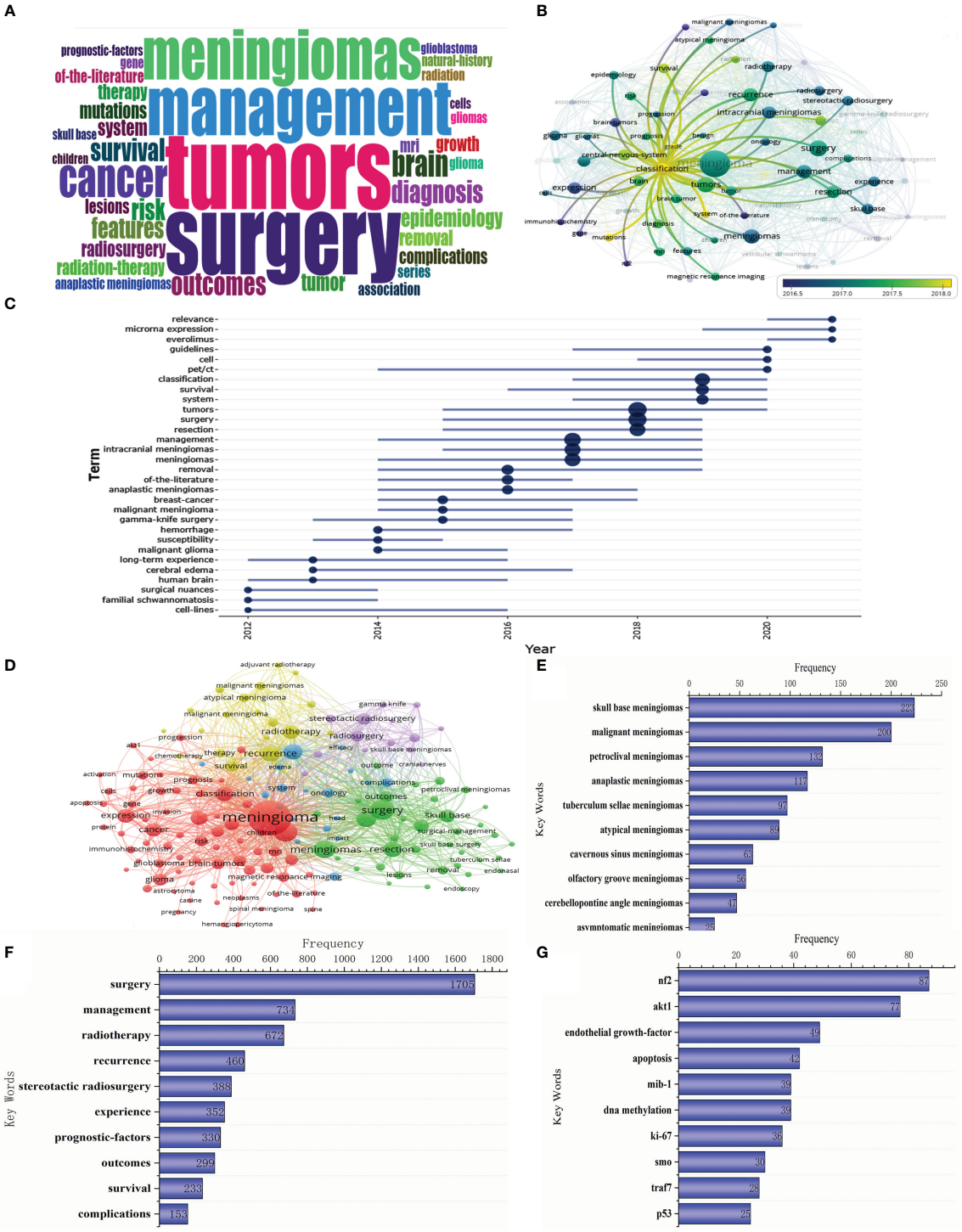

FIGURE 5
Keyword clustering, trend analysis and manual analysis. **(A)** Keyword Cloud; **(B, C)** Keyword trend analysis; **(D)** Keyword clustering analysis; **(E)** Keywords related to meningioma classification; **(F)** Keywords related to meningioma treatment; **(G)** Keywords related to meningioma molecular characteristics.

summarized, and the first 10 keywords in the list are shown in Figure 5F. As we can see from the figure, the primary treatment modalities include surgical resection and radiotherapy or stereotactic radiosurgery. The main content of the study is about survival after treatment and its impact factors. Finally, considering that meningioma molecular characteristics research has gradually become a hot spot in meningioma research in the past 3 years, we screened the related keywords (Figure 5G). It can be seen that the hot molecules in basic meningioma research include nf2, akt1, and endothelial growth factor.

Discussion

Major findings

From the results of the scientometric analysis of the last 10 years in this paper, it can be seen that: (i) in recent years, meningioma-related research has increased annually and received attention from various countries, with close cooperation among the countries or regions involved in the research; (ii) some scholars and journals have continued to focus on meningioma-related research and achieve specific results and influence, but the influence is not entirely consistent with the total number of articles issued; (iii) in the last decade, the focus of related studies has been gradually refined, with a shift from studies related to meningioma management with surgical resection and radiation therapy as the theme to a shift focusing on tumor differentiation and molecular characteristics studies. In the following, we discuss three aspects of meningioma classification, treatment, and molecular characteristics, combining the results of this study with related literature.

Meningioma classification

We can see from the scientometric results that in the keyword trend analysis, "classification" was widely cited as a keyword in the period centered on 2018. We believe this may be related to the publication of the fourth edition of the WHO classification of central nervous system tumors in 2016 (3). In this version of the classification, the diagnostic terminology of "integration" with histological and molecular information has been introduced to improve the accuracy of diagnosis and patient treatment, which is an essential guideline for the clinical diagnosis and treatment of meningioma (20, 21). In the recent 2021 update of the WHO Classification of CNS Tumors, the applicability of pathologic histologic features to the staging of meningiomas was continued, while the importance of biological markers for the classification of different grades of meningiomas was emphasized (2). Therefore, in our keyword trend analysis, we can see that meningioma-related molecular characteristics have become a hot research topic in recent years (see " Meningioma Related Molecular Characteristics" below).

We conducted an artificial screening and statistical analysis of keywords related to meningioma classification. The results showed that these keywords were mainly divided into two categories. One of them is the anatomical classification, including skull base meningioma (22), petroclival meningioma (23, 24), tuberculum sellae meningioma (25), cavernous sinus meningioma (26), olfactory groove meningioma (27) and cerebellopontine keratoma (28), etc. The surgical approach and operative details of meningiomas at different anatomic sites are also different. These clinical studies mainly discuss the most suitable surgical approach and operation for meningiomas in a particular anatomic site to obtain better surgical prognosis for patients (29). The other classification relates mainly to pathological features, including malignant meningioma (30), atypical meningioma (31), anaplastic meningioma (32), and asymptomatic meningioma (33), etc. This classification is primarily associated with treatment modalities and prognosis, such as atypical and anaplastic meningiomas, which tend to have a poor prognosis and require postoperative adjuvant therapy (34, 35).

Meningioma treatment

The latest guidelines suggest that asymptomatic meningiomas without occupying effects can be awaited by annual magnetic resonance imaging (MRI) (4). However, growing or symptomatic meningiomas with occupying effects should be treated by maximum safe resection. Moreover, asymptomatic meningiomas managed by observation usually show rapid growth, requiring a shift in management to surgical resection to reduce the occupancy effect. Most patients have a favorable outcome with maximal resection to reduce the occupancy effect. However, the possibility of recurrence exists for patients with incomplete resection or high-grade meningiomas. And the higher the grade of meningioma, with higher recurrence rates and worse survival rates (36). For instance, compared to benign meningiomas, the 5-year recurrence rate of total tumor excision for atypical meningiomas is 35% to 38%, and the risk of recurrence is 7 to 8 times higher than that of benign meningiomas (33). Therefore, postoperative adjuvant radiotherapy or stereotactic radiosurgery should be considered for this group of patients (34, 37).

As seen in the scientometric results of this study, meningioma management occupies the most significant portion of meningioma research in the last decade (38). Most studies related to meningioma resection include surgery details, the extent of resection, management of postoperative complications, and prognostic factors influencing prognosis. Secondly, radiation therapy and stereotactic radiosurgery are the other two primary management modalities after surgical meningioma resection. Related studies have included adjuvant therapy for specific types of meningiomas (e.g., atypical meningioma and mesenchymal meningioma) and their outcomes (5). In addition, we identified many studies on novel drug treatments for meningiomas in our artificial screening and statistical analysis of keywords. These drug treatments for meningiomas are usually considered experimental and are used as remedial treatments without further local treatment options (39–41). For example, targeted drugs such as anti-angiogenic drugs are used in the remedial treatment of meningiomas (42).

Meningioma molecular characteristics

We can see from our analysis of keyword trends that some keywords related to meningioma molecular characteristics are gradually increasing, such as NF2 and AKT1. The trends may be related to the significant progress in research on meningioma molecular characteristics in recent years. Studies have shown that NF2 variants, including shift mutations, allelic inactivation, and missense mutations, could be detected in approximately 60% of meningiomas (2, 43). In addition to NF2, mutations were found in TRAF7, SMO, KLF4, PI3K and AKT1 (44). Non-NF2 variants of

meningiomas are more complex and include Hedgehog signaling pathway variants (SMO, SUFU, PRKAR1A, PTCH1/2, etc.), phosphatidylinositol 3-kinase (PI3K) signaling pathway variants (PTEN, AKT1, PIK3CA, PIK3R1, etc.), chromosome remodeling complex variants (SMARCB1, SMARCE1, ARID1A, PBRM1, etc.) and other gene variants (KLF4, BAP1, POLR2A, DMD, etc.) (43).

Some molecular characteristics are associated with histological subtypes of meningioma. For example, TRAF7 and KLF4 mutations are molecular biological markers of secretory meningioma (43), RAF7, POLR2A, and ATK1 mutations are markers of endothelial meningioma (43, 45), SMARCE1 mutations are markers of clear cell meningioma (46), and BAP1 and PBRM1 mutations are markers of rhabdoid and papillary meningioma (47–49). Another part is related to the degree of tumor malignancy, such as the deletion of histone H3 K27me3 expression is closely associated with meningioma recurrence (50–52), TERT promoter mutation and CDKN2A/B pure deletion are molecular biological markers of CNS WHO grade 3 meningioma (53, 54). In addition, changes in DNA methylation levels or expression of specific genes (e.g., NRDG2, MEG3, PDGFR, etc.) are also closely associated with the development of meningiomas (46, 55). Based on DNA methylation characteristics, meningiomas can be subtyped, with differences in anatomic sites, driver genes, and clinical prognosis among subtypes (56). The study of meningioma molecular characteristics is beneficial for further typing of meningiomas and diagnosing and treating tumors. It has been gradually becoming a hot issue in meningioma research.

Conclusion

A scientometric and visual analysis of meningioma research over the last decade demonstrates its current status and trends to some extent. The main research direction is meningioma management based on surgical resection, radiotherapy, or stereotactic radiosurgery. In recent years, with the progress of basic meningioma research, meningioma classification and molecular characteristics studies have gradually become hot spots for research. In the future, research related to meningioma molecular characteristics may further increase and significantly influence molecular diagnosis and precision treatment of meningioma.

Author contributions

TZ, KL, and ZL contributed to conception and design of the study. TZ and YF organized the database. TZ performed the statistical analysis. YF wrote the first draft of the manuscript. TZ, YF, KL, and ZL wrote sections of the manuscript. All authors contributed to manuscript revision, read, and approved the submitted version.

Conflict of interest

The authors declare that the research was conducted in the absence of any commercial or financial relationships that could be construed as a potential conflict of interest.

Publisher's note

References

1. Ostrom QT, Cioffi G, Gittleman H, Patil N, Waite K, Kruchko C, et al. Cbtrus statistical report: Primary brain and other central nervous system tumors diagnosed in the united states in 2012-2016. *Neuro Oncol* (2019) 21:V1–100. doi: 10.1093/neuonc/noz150

2. Louis DN, Perry A, Wesseling P, Brat DJ, Cree IA, Figarella-Branger D, et al. The 2021 who classification of tumors of the central nervous system: A summary. *Neuro Oncol* (2021) 23:1231–51. doi: 10.1093/neuonc/noab106

3. Louis DN, Perry A, Reifenberger G, von Deimling A, Figarella-Branger D, Cavenee WK, et al. The 2016 world health organization classification of tumors of the central nervous system: A summary. *Acta Neuropathol* (2016) 131:803–20. doi: 10.1007/s00401-016-1545-1

4. Goldbrunner R, Stavrinou P, Jenkinson MD, Sahm F, Mawrin C, Weber DC, et al. Eano guideline on the diagnosis and management of meningiomas. *Neuro Oncol* (2021) 23:1821–34. doi: 10.1093/neuonc/noab150

5. Mair MJ, Berghoff AS, Brastianos PK, Preusser M. Emerging systemic treatment options in meningioma. *J Neurooncol* (2022). doi: 10.1007/s11060-022-04148-8

6. Belanger K, Ung TH, Damek D, Lillehei KO, Ormond DR. Concomitant temozolomide plus radiotherapy for high-grade and recurrent meningioma: A retrospective chart review. *BMC Cancer.* (2022) 22:367. doi: 10.1186/s12885-022-09340-7

7. Kaley TJ, Wen P, Schiff D, Ligon K, Haidar S, Karimi S, et al. Phase ii trial of sunitinib for recurrent and progressive atypical and anaplastic meningioma. *Neuro Oncol* (2015) 17:116–21. doi: 10.1093/neuonc/nou148

8. Almutairi O, Albakr A, Al-Habib A, Ajlan A. The top-100 most-cited articles on meningioma. *World Neurosurg* (2017) 107:1025–32. doi: 10.1016/j.wneu.2017.08.021

9. Kondziolka D. Citation measures in stereotactic radiosurgery: Publication across a discipline. *Stereotact Funct Neurosurg* (2011) 89:56–61. doi: 10.1159/000322277

10. Ma W, Xu D, Zhao L, Yuan M, Cui YL, Li Y. Therapeutic role of curcumin in adult neurogenesis for management of psychiatric and neurological disorders: A scientometric study to an in-depth review. *Crit Rev Food Sci Nutr* (2022) 28:1–13. doi: 10.1080/10408398.2022.2067827

11. Xu D, Wang YL, Wang KT, Wang Y, Dong XR, Tang J, et al. A scientometrics analysis and visualization of depressive disorder. *Curr Neuropharmacol.* (2021) 19:766–86. doi: 10.2174/1570159X18666200905151333

12. Wei N, Xu Y, Li Y, Shi J, Zhang X, You Y, et al. A bibliometric analysis of t cell and atherosclerosis. *Front Immunol* (2022) 13:948314. doi: 10.3389/fimmu.2022.948314

13. Hua N, Tan X, He Y, Sun M, Wang X. Medical decision-making for adolescents with depression: A bibliometric study and visualization analysis via citespace. *Int J Ment Health Nurs* (2022). doi: 10.1111/inm.13085

14. Xie L, Chen Z, Wang H, Zheng C, Jiang J. Bibliometric and visualized analysis of scientific publications on atlantoaxial spine surgery based on web of science and vosviewer. *World Neurosurg* (2020) 137:435–42. doi: 10.1016/j.wneu.2020.01.171

15. Yin H, Zhang F, Yang X, Meng X, Miao Y, Noor Hussain MS, et al. Research trends of artificial intelligence in pancreatic cancer: A bibliometric analysis. *Front Oncol* (2022) 12:973999. doi: 10.3389/fonc.2022.973999

16. Wang M, Ho Y, Fu H. Global performance and development on sustainable city based on natural science and social science research: a bibliometric analysis. *Sci total Environ.* (2019) 666:1245–54. doi: 10.1016/j.scitotenv.2019.02.139

17. Chen C. Searching for intellectual turning points: progressive knowledge domain visualization. *Proc Natl Acad Sci USA* (2004) 101 Suppl 1:5303–10. doi: 10.1073/pnas.0307513100

18. van Eck NJ, Waltman L. Software survey: Vosviewer, a computer program for bibliometric mapping. *Scientometrics* (2010) 84:523–38. doi: 10.1007/s11192-009-0146-3

19. Falagas ME, Pitsouni EI, Malietzis GA, Pappas G. Comparison of pubmed, scopus, web of science, and google scholar: Strengths and weaknesses. *FASEB J Off Publ Fed Am Soc. Exp Biol* (2008) 22:338–42. doi: 10.1096/fj.07-9492LSF

20. DeWitt JC, Mock A, Louis DN. The 2016 who classification of central nervous system tumors: What neurologists need to know. *Curr Opin Neurol* (2017) 30:643–9. doi: 10.1097/WCO.0000000000000490

21. Fuller CE, Jones DTW, Kieran MW. New classification for central nervous system tumors: Implications for diagnosis and therapy. *Am Soc Clin Oncol Educ book. Am Soc Clin Oncol Annu Meeting.* (2017) 37:753–63. doi: 10.1200/EDBK_175088

22. Seaman SC, Ali MS, Marincovich A, Li L, Walsh JE, Greenlee JDW. Minimally invasive approaches to anterior skull base meningiomas. *J neurol. surg. Part B Skull base.* (2022) 83:254–64. doi: 10.1055/s-0040-1716671

23. Jean WC, Yang Y, Srivastava A, Tai AX, Herur-Raman A, Kim HJ, et al. Study of comparative surgical exposure to the petroclival region using patient-specific, petroclival meningioma virtual reality models. *Neurosurg Focus* (2021) 51:E13. doi: 10.3171/2021.5.FOCUS201036

24. Guinto G, Hernández E, Estrada E, Gallardo D, Kageyama M, Aréchiga N, et al. Petroclival meningiomas: A simple system that could help in selecting the approach. *Operat Neurosurg (Hagerstown Md.)* (2021) 21:225–34. doi: 10.1093/ons/opab224

25. Godano U. Transcranial approaches for tuberculum sellae meningiomas in the endoscopic era. *J Neurosurg Sci* (2021) 65:457–9. doi: 10.23736/S0390-5616.20.05115-2

26. Pikis S, Mantziaris G, Samanci Y, Peker S, Nabeel AM, Reda WA, et al. Stereotactic radiosurgery for incidentally discovered cavernous sinus meningiomas: A multi-institutional study. *World Neurosurg* (2022) 158:e675–80. doi: 10.1016/j.wneu.2021.11.037

27. Liu JK, Hattar E, Eloy JA. Endoscopic endonasal approach for olfactory groove meningiomas: Operative technique and nuances. *Neurosurg Clin N Am* (2015) 26:377–88. doi: 10.1016/j.nec.2015.03.009

28. Steiert C, Masalha W, Grauvogel TD, Roelz R, Klingler JH, Heiland DH, et al. Piezosurgery for safe and efficient petrous bone cutting in cerebellopontine angle and petroclival meningioma surgery. *J Clin Neurosci Off J Neurosurg. Soc Australasia.* (2021) 89:319–28. doi: 10.1016/j.jocn.2021.05.021

29. Al Abdulsalam HK, Aldahish AK, Albakr A, Hussain S, Alroqi A, Alromaih S, et al. Endoscopic transnasal resection of midline skull base meningiomas: tumor consistency and surgical outcomes. *J neurol. surg. Part B Skull base.* (2021) 82:500–5. doi: 10.1055/s-0040-1714111

30. Yeung J, Yaghoobi V, Miyagishima D, Vesely MD, Zhang T, Badri T, et al. Targeting the csf1/csf1r axis is a potential treatment strategy for malignant meningiomas. *Neuro Oncol* (2021) 23:1922–35. doi: 10.1093/neuonc/noab075

31. Buttrick S, Shah AH, Komotar RJ, Ivan ME. Management of atypical and anaplastic meningiomas. *Neurosurg Clin N Am* (2016) 27:239–47. doi: 10.1016/j.nec.2015.11.003

32. Masalha W, Heiland DH, Delev D, Fennell JT, Franco P, Scheiwe C, et al. Survival and prognostic predictors of anaplastic meningiomas. *World Neurosurg* (2019) 131:e321–8. doi: 10.1016/j.wneu.2019.07.148

33. Näslund O, Skoglund T, Farahmand D, Bontell TO, Jakola AS. Indications and outcome in surgically treated asymptomatic meningiomas: A single-center case-control study. *Acta Neurochir (Wien).* (2020) 162:2155–63. doi: 10.1007/s00701-020-04244-6

34. Chen WC, Perlow HK, Choudhury A, Nguyen MP, Mirchia K, Youngblood MW, et al. Radiotherapy for meningiomas. *J Neurooncol* (2022), 160(2):505-515. doi: 10.1007/s11060-022-04171-9

35. Patel B, Desai R, Pugazenthi S, Butt OH, Huang J, Kim AH. Identification and management of aggressive meningiomas. *Front Oncol* (2022) 12:851758. doi: 10.3389/fonc.2022.851758

36. Moreau JT, Hankinson TC, Baillet S, Dudley R. Individual-patient prediction of meningioma malignancy and survival using the surveillance, epidemiology, and end results database. *NPJ Digit Med* (2020) 3:12. doi: 10.1038/s41746-020-0219-5

37. Zhu H, Bi WL, Aizer A, Hua L, Tian M, Den J, et al. Efficacy of adjuvant radiotherapy for atypical and anaplastic meningioma. *Cancer Med* (2019) 8:13–20. doi: 10.1002/cam4.1531

38. Brastianos PK, Galanis E, Butowski N, Chan JW, Dunn IF, Goldbrunner R, et al. Advances in multidisciplinary therapy for meningiomas. *Neuro Oncol* (2019) 21:i18–31. doi: 10.1093/neuonc/noy136

39. Chamberlain MC, Barnholtz-Sloan JS. Medical treatment of recurrent meningiomas. *Expert Rev Neurother.* (2011) 11:1425–32. doi: 10.1586/ern.11.38

40. Preusser M, Berghoff AS, Hottinger AF. High-grade meningiomas: New avenues for drug treatment? *Curr Opin Neurol* (2013) 26:708–15. doi: 10.1097/WCO.0000000000000035

41. Suppiah S, Nassiri F, Bi WL, Dunn IF, Hanemann CO, Horbinski CM, et al. Molecular and translational advances in meningiomas. *Neuro Oncol* (2019) 21:i4–17. doi: 10.1093/neuonc/noy178

42. Hou J, Kshettry VR, Selman WR, Bambakidis NC. Peritumoral brain edema in intracranial meningiomas: The emergence of vascular endothelial growth factor-directed therapy. *Neurosurg Focus.* (2013) 35:E2. doi: 10.3171/2013.8.FOCUS13301

43. Birzu C, Peyre M, Sahm F. Molecular alterations in meningioma: Prognostic and therapeutic perspectives. *Curr Opin Oncol* (2020) 32:613–22. doi: 10.1097/CCO.0000000000000687

44. Clark VE, Erson-Omay EZ, Serin A, Yin J, Cotney J, Ozduman K, et al. Genomic analysis of non-nf2 meningiomas reveals mutations in traf7, klf4, akt1, and smo. *Science* (2013) 339:1077–80. doi: 10.1126/science.1233009

45. Cordova C, Kurz SC. Advances in molecular classification and therapeutic opportunities in meningiomas. *Curr Oncol Rep* (2020) 22:84. doi: 10.1007/s11912-020-00937-4

46. Sievers P, Sill M, Blume C, Tauziede-Espariat A, Schrimpf D, Stichel D, et al. Clear cell meningiomas are defined by a highly distinct dna methylation profile and mutations in smarce1. *Acta Neuropathol.* (2021) 141:281–90. doi: 10.1007/s00401-020-02247-2

47. Williams EA, Wakimoto H, Shankar GM, Barker FGN, Brastianos PK, Santagata S, et al. Frequent inactivating mutations of the pbaf complex gene pbrm1 in meningioma with papillary features. *Acta Neuropathol.* (2020) 140:89–93. doi: 10.1007/s00401-020-02161-7

48. Prasad RN, Gardner UG, Yaney A, Prevedello DM, Koboldt DC, Thomas DL, et al. Germline bap1 mutation in a family with multi-generational meningioma with rhabdoid features: A case series and literature review. *Front Oncol* (2021) 11:721712. doi: 10.3389/fonc.2021.721712

49. Shankar GM, Abedalthagafi M, Vaubel RA, Merrill PH, Nayyar N, Gill CM, et al. Germline and somatic bap1 mutations in high-grade rhabdoid meningiomas. *Neuro Oncol* (2017) 19:535–45. doi: 10.1093/neuonc/now235

50. Nassiri F, Wang JZ, Singh O, Karimi S, Dalcourt T, Ijad N, et al. Loss of h3k27me3 in meningiomas. *Neuro Oncol* (2021) 23:1282–91. doi: 10.1093/neuonc/noab036

51. Ammendola S, Rizzo PC, Longhi M, Zivelonghi E, Pedron S, Pinna G, et al. The immunohistochemical loss of h3k27me3 in intracranial meningiomas predicts shorter progression-free survival after stereotactic radiosurgery. *Cancers (Basel).* (2022) 14:1718. doi: 10.3390/cancers14071718

52. Katz LM, Hielscher T, Liechty B, Silverman J, Zagzag D, Sen R, et al. Loss of histone h3k27me3 identifies a subset of meningiomas with increased risk of recurrence. *Acta Neuropathol.* (2018) 135:955–63. doi: 10.1007/s00401-018-1844-9

53. Sievers P, Hielscher T, Schrimpf D, Stichel D, Reuss DE, Berghoff AS, et al. Cdkn2a/b homozygous deletion is associated with early recurrence in meningiomas. *Acta Neuropathol.* (2020) 140:409–13. doi: 10.1007/s00401-020-02188-w

54. Spiegl-Kreinecker S, Lotsch D, Neumayer K, Kastler L, Gojo J, Pirker C, et al. Tert promoter mutations are associated with poor prognosis and cell immortalization in meningioma. *Neuro Oncol* (2018) 20:1584–93. doi: 10.1093/neuonc/noy104

55. Paramasivam N, Hubschmann D, Toprak UH, Ishaque N, Neidert M, Schrimpf D, et al. Mutational patterns and regulatory networks in epigenetic subgroups of meningioma. *Acta Neuropathol.* (2019) 138:295–308. doi: 10.1007/s00401-019-02008-w

56. Sahm F, Schrimpf D, Stichel D, Jones D, Hielscher T, Schefzyk S, et al. Dna methylation-based classification and grading system for meningioma: A multicentre, retrospective analysis. *Lancet Oncol* (2017) 18:682–94. doi: 10.1016/S1470-2045(17)30155-9

frontiers | Frontiers in Neurology

TYPE Case Report
PUBLISHED 24 April 2023
DOI 10.3389/fneur.2023.1149858

OPEN ACCESS

EDITED BY
Arianna Rustici,
University of Bologna, Italy

REVIEWED BY
Roberto Colasanti,
University Hospital of Padua, Italy
Mahmoud Messerer,
Centre Hospitalier Universitaire Vaudois (CHUV), Switzerland

*CORRESPONDENCE
Ilaria Bove
ilariabove90@gmail.com

RECEIVED 23 January 2023
ACCEPTED 27 March 2023
PUBLISHED 24 April 2023

CITATION
Bove I, Franca RA, Ugga L, Solari D, Elefante A, De Caro MLDB and Cavallo LM (2023) The "chameleon" sellar lesions: a case report of unexpected sellar lesions.
Front. Neurol. 14:1149858.
doi: 10.3389/fneur.2023.1149858

The "chameleon" sellar lesions: a case report of unexpected sellar lesions

Ilaria Bove[1]*, Raduan Ahmed Franca[2], Lorenzo Ugga[3], Domenico Solari[1], Andrea Elefante[3], Maria Laura Del Basso De Caro[2] and Luigi Maria Cavallo[1]

[1]Division of Neurosurgery, Department of Neurosciences, Reproductive and Odontostomatological Sciences, Università degli Studi di Napoli "Federico II", Naples, Italy, [2]Department of Advanced Biomedical Sciences, Pathology Section, University of Naples "Federico II", Naples, Italy, [3]Department of Advanced Biomedical Sciences, University of Naples "Federico II", Naples, Italy

Introduction: The sellar region and its boundaries represent a challenging area, harboring a variety of tissues of different linings. Therefore, a variety of diseases can arise or involve in this area (i.e., neoplastic or not). A total of three challenging cases of "chameleon" sellar lesions treated via EEA were described, and the lesions mimicked radiological features of common sellar masses such as craniopharyngiomas and/or pituitary adenomas, and we also report a literature review of similar cases.

Methods: A retrospective analysis of three primary cases was conducted at the Università degli Studi di Napoli Federico II, Naples, Italy. Clinical information, radiological examinations, and pathology reports were illustrated.

Results: A total of three cases of so-called "chameleon" sellar lesions comprising two men and one woman were reported. Based on the intraoperative finding and pathological examination, we noticed that case 1 had suprasellar glioblastoma, case 2 had a primary neuroendocrine tumor, and case 3 had cavernous malformation.

Conclusion: Neurosurgeons should consider "unexpected" lesions of the sellar/suprasellar region in the preoperative differential diagnosis. A multidisciplinary approach with the collaboration of neurosurgeons, neuroradiologists, and pathologists plays a fundamental role. The recognition of unusual sellar lesions can help surgeons with better preoperative planning; so an endoscopic endonasal approach may represent a valid surgical technique to obtain decompression of the optic apparatus and vascular structures and finally a pathological diagnosis.

KEYWORDS

sellar region, oncology, neuroimaging, endoscopic endonasal surgery, pathology

1. Introduction

The sellar and the suprasellar regions represent a very complex area, harboring a remarkable variety of tissues of different linings, and many diseases can arise from or involve these areas, with a majority of them from hypophysis, both neoplastic or not (1). Over 90% of sellar tumors are pituitary adenomas that are recently redefined as pituitary neuroendocrine tumors (PitNETs) to underline their unpredictable behavior (2, 3). In nearly 10% of cases, other etiologies are responsible for the mass effect in the sellar region including gliomas, meningiomas, craniopharyngiomas, and Rathke's cysts, and vascular

lesions like aneurysms and cavernous angiomas may also be rarely encountered in the sellar region (1). Rapid recognition of the sellar masses is crucial to determine prognostic outcomes and therefore guide management (4). Over the past century, we have assisted a vivid development of endoscopic skull base surgery, along with advances in diagnostic imaging techniques: The endoscopic endonasal approach allows access to the multiple and various lesions of the sellar–suprasellar areas that were previously accessible only via the transcranial routes (5). The main advantage of the endoscopic endonasal approach (EEA) lies in the possibility of obtaining a close-up view of the neurovascular structures, reducing overall tissue manipulation (6–8). The most common lesions arising from this region have a distinctive radiological appearance; however, in some cases, "unexpected" masses may mimic the radiological characteristics typical of common sellar pathologies. Neuroradiological detection of complex sellar–suprasellar lesions can sometimes be extremely difficult. In recent years, the advancement of neuroimaging has been investigated in order to provide information to improve diagnostic accuracy, including a description of tumor cell biology, cerebral blood perfusion, and vascular proliferation characteristics. In this context, radiomics has become an interesting and continuously evolving technique. It represents a tool capable of building decision support models based on conventional or functional imaging, thanks to the extraction of large quantities of image features and quantitative data analysis (9).

Herein, we report three challenging cases of "chameleon" sellar lesions treated via EEA that mimicked radiological features of common lesions such as craniopharyngiomas and/or pituitary adenomas, with the literature review of similar cases.

2. Illustrative cases

2.1. Case 1. Suprasellar glioblastoma

A 46-year-old man was admitted to our department with a frontal headache and vomiting. Bitemporal hemianopsia, spatial–temporal disorientation, and memory loss were detected upon hospital admission. Laboratory examination revealed an increase in the level of PIVKA (75 n.v.16–48 AU/mL). In 1996 and later in 2006, the patient underwent left and then right orchidectomy for testicular seminoma. Brain MRI showed a huge mass located in the median and paramedian portion of the hypothalamus–chiasmatic region (Dmax 50 cm), with irregular margins infiltrating the uncus–amygdaloid complex in the hypothalamus region and the floor of the third ventricle; the lesion presented a central colliquative necrotic component, and its signal was relatively homogenous with slightly hypointense images in T1 and hyperintense on T2-weighted images, with significant heterogenous post-Gad enhancement. Signs of supratentorial hydrocephalus were noticed. The first radiological impression was compatible with a case of craniopharyngioma. An extended suprasellar endoscopic endonasal approach was run for tumor removal: Upon dural opening, the lesion appeared diffusely infiltrating the infundibulum and third ventricle, and it presented as a grayish-yellow tissue and was highly vascularized (Figure 2). Intraoperative histological examination revealed the presence of a malignant glial cell tumor. Further resection of the tumor was not performed because the tumor adhered tenaciously to surrounding structures. During the postoperative course, due to the presence of supratentorial hydrocephalus, a biventricular peritoneal shunt with a 130 cm H_2O Codman programmable valve was positioned in a second surgery. A path report revealed an IDH1-wild-type glioblastoma. Adjuvant radio and concomitant chemotherapy treatment were started immediately as per the STUPP protocol. The patient died 1 year after the surgery due to the progression of the disease (Figure 1).

2.2. Case 2. Sellar primary neuroendocrine tumor

A 50-year-old woman with a history of cervix adenocarcinoma was admitted to our department with a headache and visual disturbance. MRI with enhancement post-contrastographic revealed the presence of suprasellar mass (Dmax 3.9 cm) with the third ventricle involvement with heterogenous contrast enhancement compressing the optic chiasm. A *transtuberculum/transplanum* endoscopic endonasal approach was performed. A fibro-elastic and infiltrating lesion was partially removed in order to obtain optic nerve decompression. Intraoperative histological examination showed the presence of atypical cells with a plasmacytoid appearance (Figure 2). The lesion appeared very firmly adherent to surrounding structures, so, after decompression of the optic chiasm, a small residual mass of the tumor was left in place. Histology and immunohistochemical staining ultimately confirmed the diagnosis of a primary neuroendocrine tumor (Figure 3). Laboratory examination revealed an increase in the level of neuron-specific enolase NSE (68.7 mcg/L; v.n. <18.3). During the postoperative course, the patient reported an improvement in visual acuity. Follow-up ^{18}F-FDG-PET/CT revealed the absence of any localization of the disease, while MRI showed the decompression of the optic apparatus despite a large intra-suprasellar residual lesion.

2.3. Case 3. Suprasellar cavernous malformations

A 21-year-old man was admitted to our department with a headache and sudden visual loss. Ophthalmological examination revealed 1/30 in RE with diffuse reduction of light sensitivity and bitemporal hemianopia in LE. Endocrinological assessment and lab essays revealed central hypercortisolism. Brain computed tomography imaging demonstrated hyperdense large sellar and suprasellar mass with extension into the third ventricle cavity with the presence of calcifications. MRI showed a heterogenous low signal in T1 images, an intermediate high signal in T2 images, and cystic with calcific components of the suprasellar lesion. It measured ~3 × 2, 4 × 3, and 3 cm in anteroposterior, cephalocaudal, and transverse dimensions, respectively.

An extended endoscopic endonasal approach was performed. During surgery, the evacuation of the intralesional blood component of the neoformation localized inside the optic chiasm and infundibulum of the third ventricle was performed, which

10.3389/fneur.2023.1149858

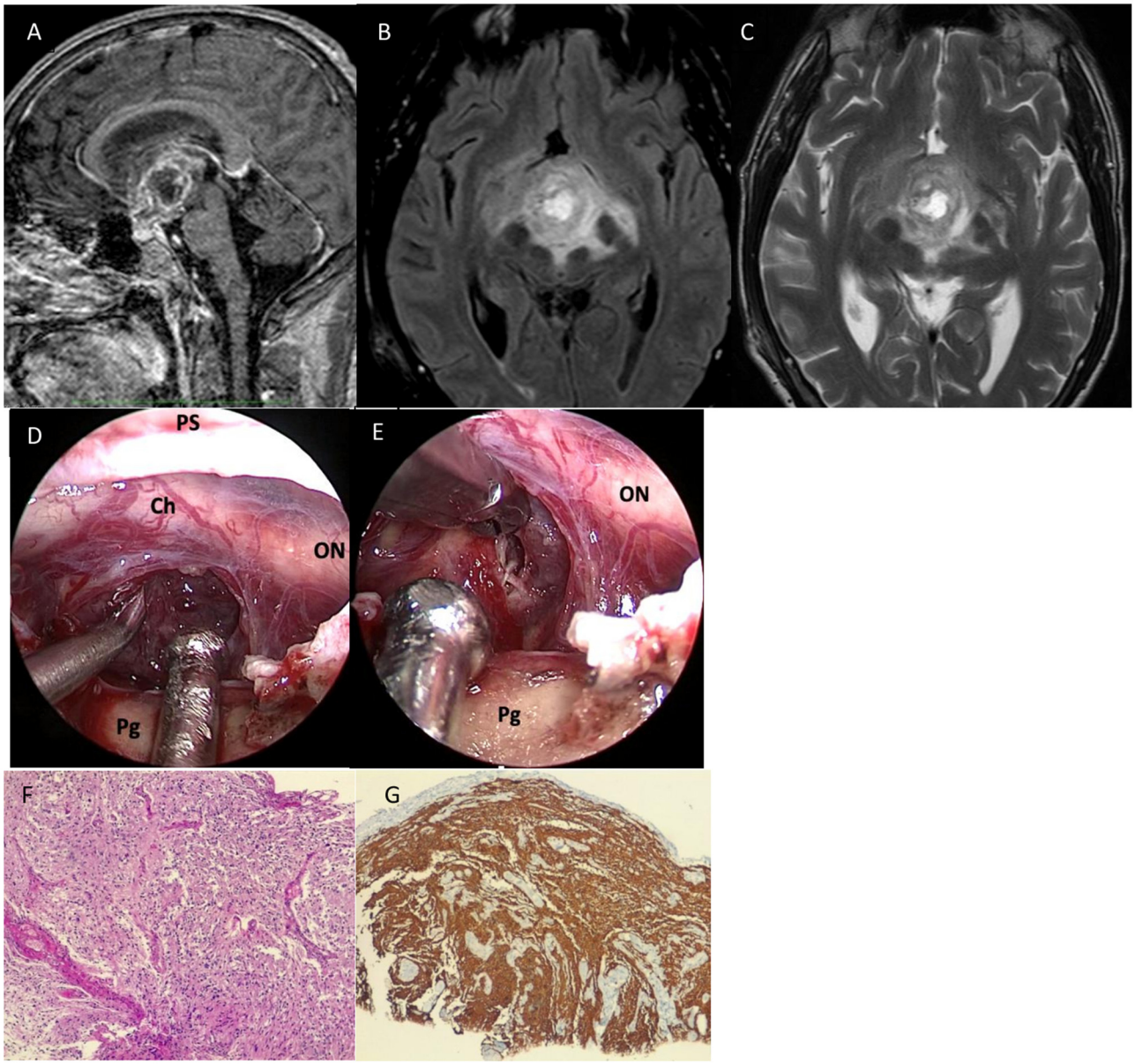

FIGURE 1
Preoperative sagittal **(A)**, axial **(B)** T2, and axial **(C)** T2-fluid-attenuated inversion recovery (FLAIR) sequences showed a huge mass located in the median and paramedian portion of the hypothalamus-chiasmatic region (Dmax 50 cm), with irregular margins infiltrating the uncus-amygdaloid complex in the hypothalamus region and the floor of the third ventricle; the lesion presented central colliquative necrotic component and its signal was relatively homogenous with slightly hypointense in T1 and hyperintense on T2-weighted images, with significant heterogenous post-Gad enhancement and peripherical vasogenic edema. **(D)** After dural opening, the lesion appeared diffusely infiltrating the infundibulum and third ventricle, and it presented as a grayish-yellow tissue and was highly vascularized. **(E)** Further resection of the tumor was not performed because the tumor adhered tenaciously to surrounding structures. **(F)** Histological examination revealed a highly cellular neoplasm having a fibrillary background, composed of pleomorphic, medium-sized cells. Necrosis and microvascular proliferation were also seen (*hematoxylin-eosin, original magnification 10x*). **(G)** On immunohistochemistry, tumor cells were GFAP positive (*immunoperoxidase staining, original magnification 10x*). IDH1 immunostaining was negative (not shown in the figure). ON, optic nerve; Ch, chiasm; T, tumor; Pg, pituitary gland.

appeared dislocated below; at the end of the procedure a yellowish granulomatous formation was removed in fragments, of dubious vascularization, but suspected of a possible, already site of previous bleeding and adhering to the ventricular walls. Considering its high vascularity and the difficulty of dissection from the adjacent structures, a subtotal resection of the lesion aiming at optic nerve decompression was achieved (Figure 4). Histopathological examination was consistent with cavernous malformation.

The patient's visual acuity improved on postoperative day 3, and MRI showed decompression of the optic apparatus despite a large intra-suprasellar residual lesion. A second-stage surgery was proposed to the patient to obtain a more radical excision, but he refused. The neuro-oncological multidisciplinary team meeting

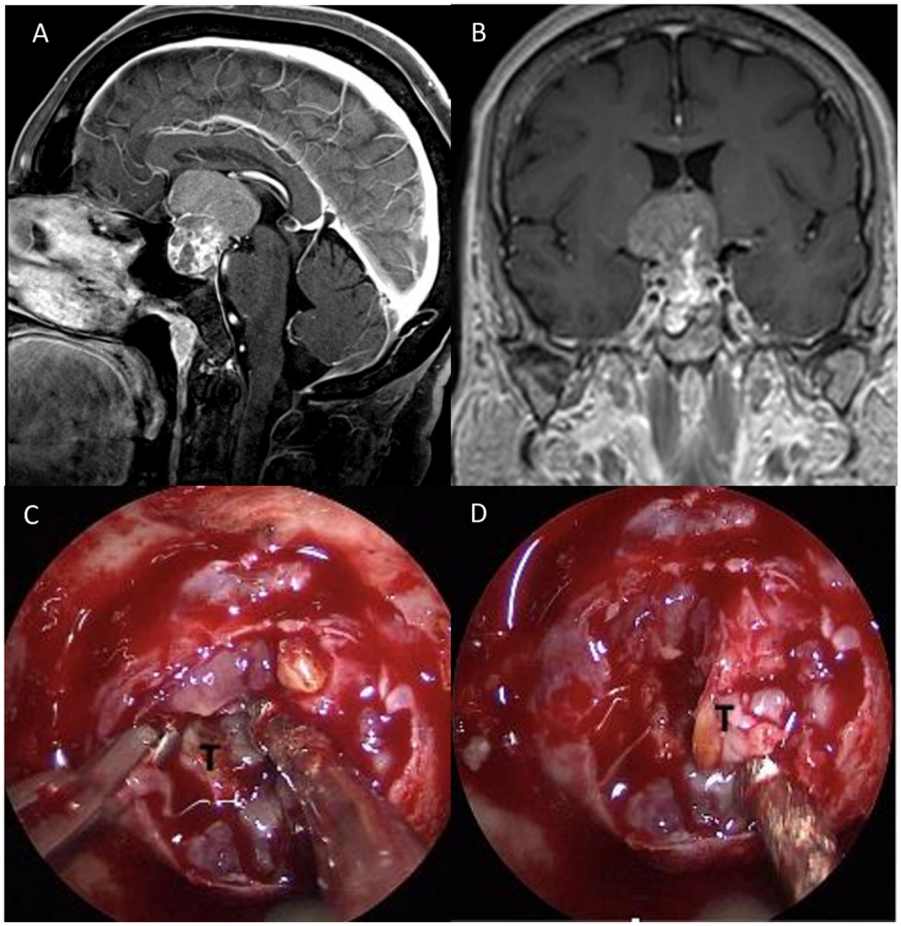

FIGURE 2
Preoperative sagittal **(A)** and coronal **(B)**, post-gadolinium MRI scan showing a suprasellar mass (Dmax 3.9 cm) with the third ventricle involvement and heterogenous contrast enhancement compressing the optic chiasm. **(C)** After dural opening, **(D)** a fibro-elastic and infiltrating lesion was partially removed in order to obtain optic nerve decompression.

discussed the case, and considering the patient's decision, the patient underwent stereotactic radiosurgery. At the follow-up visit after 6 and 12 months, the residual lesion is stable, and the patient did not develop any new neurological signs maintaining the visual improvement.

3. Discussion

Tumors of the sellar region account for ∼10–15% of all brain tumors, and a large variety of non-neoplastic, inflammatory, vascular, or developmental lesions can be found in this region (10, 11).

Pituitary adenomas constitute over 90% of sellar masses, while the remaining 10% of the lesions includes pituitary-origin tumors, such as craniopharyngiomas, Rathke's cleft cysts, and astrocytomas, and non-pituitary origin lesions, such as meningiomas, germ cell tumors, chondrosarcomas/chordomas, giant cell tumors, epidermoid cysts, and metastatic lesions (12).

According to previous data, rare sellar lesions represent a heterogeneous group of non-adenomatous lesions that deserve special care regarding their surgical and clinical management (1, 13). A total of 2,452 consecutive patients were operated on via an endoscopic endonasal approach for the removal of a sellar/parasellar lesion at the Division of Neurosurgery of the Università degli Studi di Napoli Federico II, Naples, between January 1997 and January 2023; of them, a total of 118 rare sellar lesions were identified (4.8%). Somma et al. (1) affirmed how several signs (i.e., DI and ophthalmoplegia) and neuroradiological features (i.e., intense and homogeneous contrast enhancement, invasive aspect of the lesion) should induce suspicion of non-adenomatous diseases. In the three cases reported, the suspicion of rare/unexpected sellar lesions was low due to the non-pathognomonic clinical presentation and radiological appearance.

Brain MRI is routinely adopted for diagnosis and proper identification of sellar lesions details and features; however, MRI appearance of different sellar/parasellar lesions can be very similar though misleading (14, 15). The differentiation between several tumor types based on radiological features can sometimes be difficult on conventional radiological examinations because of the overlapping MRI findings (16). Based on recent studies, MRI imaging can provide information on the

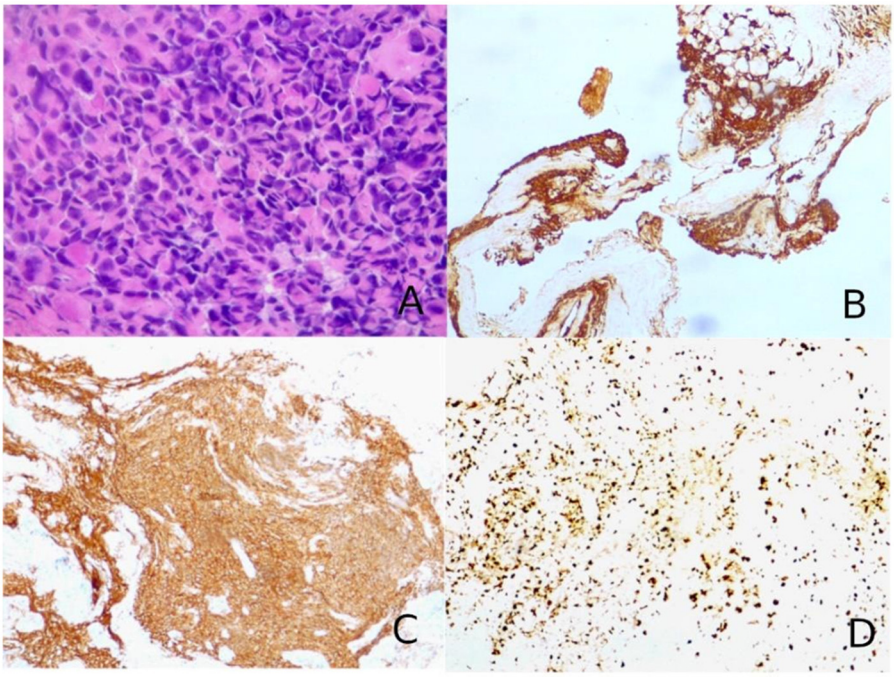

FIGURE 3
(A) Hematoxylin–eosin slides showed a hypercellular tumor composed of large, epithelioid, often nucleolated cells, with abundant cytoplasm, arranged in a "vertebral-like" fashion (*hematoxylin–eosin, original magnification 40x*). **(B)** Tumor cells were positive for pancytokeratin (AE1/AE3; *immunoperoxidase staining, original magnification 10x*). **(C)** Neuroendocrine markers were consistently positive, as for synaptophysin shown in the figure (*immunoperoxidase staining, original magnification 10x*). **(D)** The cellular proliferation index Ki67 was nearly 70–80% (*immunoperoxidase staining, original magnification 10x*).

consistency of macroadenomas, craniopharyngiomas, and germ cell tumors (17); Khant et al. (18) demonstrated how the TSE-ADC images may aid to differentiate craniopharyngioma from pituitary adenomas, and DWI sequences should distinguish craniopharyngiomas from germ cell tumors. Other imaging modalities, such as somatostatin receptor scintigraphy, can help in the differential diagnosis (19). Although the presence of unusual sellar masses is rare, suspicion should always be based on the history, clinical presentation, and radiological appearance. The diagnostic workup and management in these cases should require a specialized multidisciplinary team including neurosurgeons, neuroradiologists, endocrinologists, oncologists, and pathologists.

3.1. Glioma

Glioblastoma (GBM) is the most common adult brain tumor, occurring in the subcortical white matter of the cerebral hemispheres (20). From the literature review, only five cases of sellar and suprasellar GBM have been reported. In all cases, sellar GBM mimicked common sellar lesions, such as pituitary macroadenoma and/or craniopharyngioma; four cases underwent surgery via endoscopic endonasal surgery, and two cases underwent transcranial surgeries. Lemm et al. (21) reported two cases with preoperative suspect of craniopharyngiomas; Mahta et al. (22) and Anvari et al. (23) reported in both cases the preoperative workup pointed toward the suspicion of a pituitary macroadenoma. The case reported by Deng et al. (24) was a 42-year-old woman with an intra- and suprasellar not well-defined lesion, presenting headache, amenorrhea, diabetes insipidus, visual loss, and visual field defect. In five of six cases, including our case (Case 1), the sellar GBM originated from the hypothalamic/pituitary axis and from the pituitary gland. Thus, the onset symptoms were endocrinological abnormalities and visual and cognitive disturbances.

Sellar and/or suprasellar gliomas are usually low-grade glioma, i.e., optic nerve pilocytic astrocytoma associated with neurofibromatosis NF-1 (25). Appearance on MRI may vary; glial lesions can appear hypodense or isodense and, in some cases, hyperdense. The presence of calcifications is rare; in these cases, the lesion appears isointense on T1 and lacks a cystic component (26). The rarity of malignant gliomas lies in uncommon localization in this region and in their heterogeneous presentation on neuroimaging, making this diagnosis very challenging before obtaining the tissue for histological analysis. Radiographically, craniopharyngioma is characterized by heterogeneous solid tissue, cystic regions, and calcification. In T2-weighted images, the cysts are predominantly hyperintense, and the solid components present a heterogeneous signal. Post-contrast, there is a heterogeneous increase in contrast of the solid portions, as well as of the walls of the cysts (27). The presence of protein, cholesterol, and/or

10.3389/fneur.2023.1149858

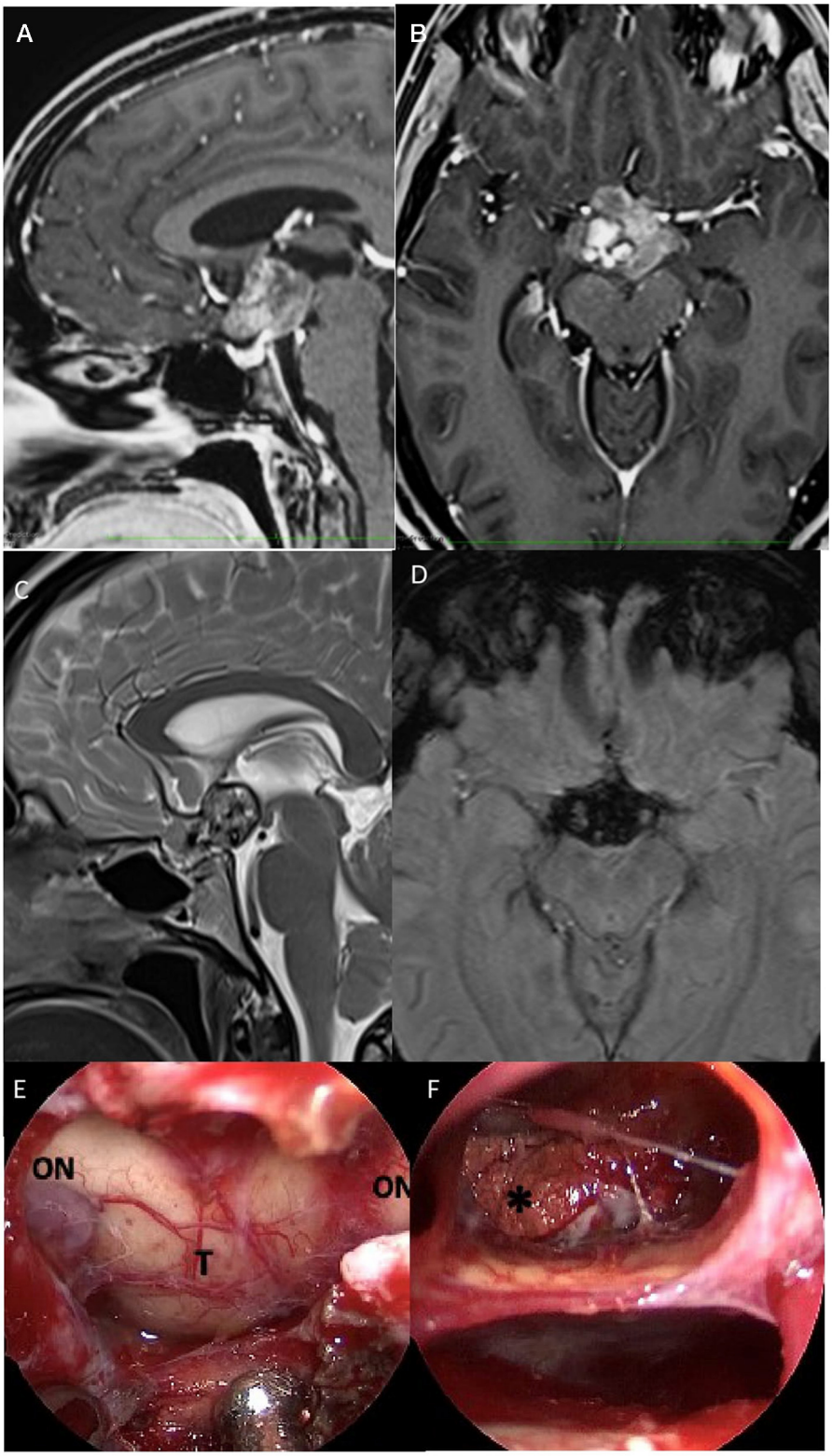

FIGURE 4
Preoperative sagittal **(A)** axial **(B)** post-gadolinium, and sagittal **(C)** T2 MRI scan demonstrated a suprasellar mass with heterogenous low signal in T1 images and an intermediate high signal in T2 images, with cystic and calcific components of the lesion. Axial **(D)** susceptibility-weighted imaging (SWI) showed signal dropout (hypointensity) in the sellar region. The lesion measured ~3 × 2,4 × 3, and 3 cm on anteroposterior, cephalocaudal, and transverse dimensions. **(E)** After dura opening**,** the evacuation of the intralesional hemorrhagic component localized inside the optic chiasm and infundibulum of the third ventricle was performed, which appeared dislocated below; **(F)** at the end of the procedure, a yellowish granulomatous formation was removed in fragments of dubious vascularization but suspected of a possible, already site of previous bleeding and adhering to the ventricular walls. ON, optic nerve; T, tumor. *Calcification.

methemoglobin may determine a high signal, which would be more likely encountered in craniopharyngioma.

Albeit gadolinium enhancement MRI is observed in both craniopharyngioma and high-grade gliomas, the latter are less likely to present cystic degeneration and calcifications (28). In the differential diagnosis of lesions with central necrosis, the presence of a brain abscess is also included. In this case, correlation with clinical status, i.e., the presence of infectious signs like fever and increased inflammatory indices together with diffusion-weighted imaging (DWi), with diffusion restriction in the abscess, may help in the differential diagnosis between these two rare entities.

3.2. Primary neuroendocrine tumor

Neuroendocrine tumor (NET) arises from the neoplastic transformation of enterochromaffin cells (29). These epithelial cells are usually found in all human organs, especially in the gastrointestinal tract and respiratory system (29, 30). According to the recent literature, two cases of sellar primary intracranial NET have been reported (31, 32). Liu et al. (31) reported a case of sellar/suprasellar NET. This is a case of a patient who underwent a single nostril transsphenoidal approach to obtain a gross tumor removal. The pathological diagnosis revealed the presence of high-grade small cell NET, and the patient died after 3 months of extensive metastases. Nasi et al. (32) reported a successful case; after a subtotal resection by an endoscopic endonasal approach, the patient underwent fractioned stereotactic radiotherapy (total irradiation dose 43.1 Gy) and polychemotherapy (cisplatin, ifosfamide, and etoposide). Four years later, the follow-up MRI showed a stable residual disease without any neurological complications.

Usually, patients with NET do not have specific clinical features, but in presence of functional tumors, they may develop endocrine symptoms from secreting one or more hormones, while non-functional tumors may affect pituitary gland function leading hypopituitarism (33). In our case, the lesion invaded the suprasellar region with compression of the optic chiasm and third ventricle involvement, without endocrine dysfunction.

CT and MRI are not specific radiological investigations for these tumors; as demonstrated by our case, NET presents MRI findings similar and compatible with other more common pathologies of the sellar region, such as pituitary adenoma, meningioma, and metastases (34). It is known as NETs express somatostatin receptor subtypes type 2 and 5; therefore, in these cases, it would be useful for diagnostic purposes to perform a somatostatin receptor scintigraphy. Scintigraphy may aid in the differential diagnosis, as well as staging and monitoring of this tumor (31, 33). It has been shown that a PET scan with 11C-5-hydroxytryptophan can be effective in tracing small NETs, with a significantly higher detection rate than somatostatin receptor scintigraphy in most cases (30, 31, 34). On the contrary, since NET is characterized by low cellular proliferative activity and high differentiation rate, positron emission tomography scanning with 18F-labeled fluorodeoxyglucose is not a technique to detect this tumor (35).

3.3. Cavernous malformation

The cavernous malformation (CM) can affect any cerebral region, but it is more frequent as it tends to affect the subcortical areas of the frontal and temporal lobes, while in the posterior fossa, it tends to involve the pons and the cerebellar hemispheres, however, medulla involvement is uncommon (36). However, in rare cases, the sellar region is involved (37). Impaired vision and/or cranial nerve palsies are common clinical findings, but all of these manifestations cannot aid in differentiation since they are usually present in other common pathologies (e.g., pituitary adenomas, meningiomas, craniopharyngiomas, and Schwannomas) (38). However, in the literature, some MRI features have been reported that could raise the suspicion of CM of the sellar region. Indeed, the presence of a hyperintense signal in T2 sequences associated with delayed centripetal contrast enhancement on MRI images could raise suspicion (39). Due to the high vascularity and profuse bleeding of the lesion during surgical removal, a subtotal resection to obtain neurovascular decompression followed by radiotherapy might be considered the most effective strategy of treatment.

To date, only 16 operated cases were reported in the current literature, and total resection was achieved in two cases (37, 40–44). Multiple surgical approaches have reportedly been utilized including pterional and subfrontal craniotomies or sublabial, transseptal, and endoscopic endonasal transsphenoidal approaches.

Maximally safe resection should be performed, including decompression of the optic apparatus and cavernous sinus. Therefore, considering the nature of the lesion and its anatomical extension, an endoscopic endonasal approach (EEA), which allows easier access and feasible debulking of sellar masses, is advocated (38, 45–52). In case of preoperatively suspected and intraoperative confirmation of sellar CM via frozen section, partial resection should be attempted, paying particular attention to obtain complete hemostasis. Additional treatments, such as stereotaxic radiosurgery, should be considered for the management of the residual lesion, after histological confirmation, in order to avoid further morbidity (25). Radiation therapy has been used successfully both before and after surgery and is recently considered an effective treatment with an average 54% reduction in tumor volume (53). Given the excellent results of radiotherapy treatment and the low possibility of obtaining a total resection, surgery remains a controversial treatment modality, if not for biopsy.

4. Future perspectives

The recent advancement of the radiological technique is increasingly used by the surgeon, to plan the type of approach and the best treatment modality. Recent studies highlight how machine learning can provide additional information to support clinical decisions for neuroradiologists and neurosurgeons (40, 41). Histogram analysis, as part of quantitative plot analysis, evaluates the internal structure of tumors by analyzing the distribution of pixels or voxels in the image, which may not be visually perceptible to the human eye. Recent evidence suggests that it can be used to predict, for example, the histopathological and genomic characteristics of tumors and the response to treatment; it helps to evaluate the consistency and therefore be able to identify the tumor

before histological evaluation (41). The possible clinical application of machine learning and radiomics of the sellar masses and other brain neoplasms, in general, should be adapted in a clinical model. Two systematic reviews performed by Saha et al. (54) and Qiao (55) summarize the application of machine learning in imaging analysis of the sellar lesion but only in pituitary adenomas. However, further research is necessary to understand the correct model that is most effective for the differential diagnosis and characterization of sellar lesions.

Neurosurgeons should consider the "unexpected" lesions of the sellar/suprasellar region in the preoperative differential diagnosis. The multidisciplinary approach with the collaboration of neurosurgeons, neuroradiologists, and pathologists plays a fundamental role. The proper diagnostic assessment of the sellar masses may help surgeons with better preoperative and postoperative planning, and in this scenario, the endonasal endoscopic approach could represent a fundamental surgical technique to obtain both a proper neurovascular structures decompression and a pathological diagnosis.

5. Conclusion

The presence of unusual sellar and suprasellar lesion features at the MRI associated with a rapidly worsening clinical course, altered hormonal profile, and cognitive disturbances should raise the suspicion of uncommon sellar lesions. From a radiological standpoint, the possibility of a malignant tumor diagnosis should be considered in case of evidence of invasion and infiltration of the surrounding tissues. Progress in imaging studies may help differentiate among the variety of possible lesions involving the suprasellar area. Further research and case series should be carried out in order to improve diagnosis and provide a proper strategy to ameliorate outcomes and ensure the overall survival of these patients.

Data availability statement

The raw data supporting the conclusions of this article will be made available by the authors, without undue reservation.

Ethics statement

Ethical review and approval was not required for the study on human participants in accordance with the local legislation and institutional requirements. The patients/participants provided their written informed consent to participate in this study. Written informed consent was obtained from the individual(s) for the publication of any potentially identifiable images or data included in this article. Written informed consent was obtained from the participant/patient(s) for the publication of this case report.

Author contributions

IB: concept and design. IB, RF, and LU: data collection. IB and DS: original draft preparation. DS and AE: reviewing and editing. MD, DS, and LC: study supervision. All authors read and approved the final manuscript.

Conflict of interest

The authors declare that the research was conducted in the absence of any commercial or financial relationships that could be construed as a potential conflict of interest.

Publisher's note

Supplementary material

The Supplementary Material for this article can be found online at: https://www.frontiersin.org/articles/10.3389/fneur.2023.1149858/full#supplementary-material

SUPPLEMENTARY VIDEO 1
Intraoperative video of case 1 demonstrating an endoscopic endonasal approach for resection of suprasellar glioblastoma.

SUPPLEMENTARY VIDEO 2
Intraoperative video of case 2 demonstrating an endoscopic endonasal approach for resection of sellar primary neuroendocrine tumor.

SUPPLEMENTARY VIDEO 3
Intraoperative video of case 3 demonstrating an endoscopic endonasal approach for resection of suprasellar cavernous malformations.

References

1. Somma T, Solari D, Beer-Furlan A, Guida L, Otto B, Prevedello D, et al. Endoscopic endonasal management of rare sellar lesions: Clinical and surgical experience of 78 cases and review of the literature. *World Neurosurg.* (2017) 100:369–80. doi: 10.1016/j.wneu.2016.11.057

2. Asa SL, Casar-Borota O, Chanson P, Delgrange E, Earls P, Ezzat S, et al. From pituitary adenoma to pituitary neuroendocrine tumor (PitNET): An International Pituitary Pathology Club proposal. *Endocr Relat Cancer.* (2017) 24:C5–8. doi: 10.1530/ERC-17-0004

3. Asa SL, Mete O, Perry A, Osamura RY. Overview of the 2022 WHO classification of pituitary tumors. *Endocr Pathol.* (2022) 33:6–26. doi: 10.1007/s12022-022-09703-7

4. Mete O, Lopes MB. Overview of the 2017 WHO classification of pituitary tumors. *Endocr Pathol.* (2017) 28:228–43. doi: 10.1007/s12022-017-9498-z

5. de Divitiis E, Cappabianca P, Cavallo LM. Endoscopic transsphenoidal approach: Adaptability of the procedure to different sellar lesions. *Neurosurgery.* (2002) 51:699–705. doi: 10.1097/00006123-200209000-00016

6. Cappabianca P, Cavallo LM, Solari D, Stagno V, Esposito F, de Angelis M. Endoscopic endonasal surgery for pituitary adenomas. *World Neurosurg.* (2014) 82:S3–11. doi: 10.1016/j.wneu.2014.07.019

7. Solari D, Villa A, De Angelis M, Esposito F, Cavallo LM, Cappabianca P. Anatomy and surgery of the endoscopic endonasal approach to the skull base. *Transl Med UniSa.* (2012) 2:36–46.

8. Cavallo LM, de Divitiis O, Aydin S, Messina A, Esposito F, Iaconetta G, et al. Extended endoscopic endonasal transsphenoidal approach to the suprasellar area: Anatomic considerations–Part 1. *Neurosurgery.* (2008) 62(6Suppl.3):1202–12. doi: 10.1227/01.NEU.0000333786.98596.33

9. Koong K, Preda V, Jian A, Liquet-Weiland B, Di Ieva A. Application of artificial intelligence and radiomics in pituitary neuroendocrine and sellar tumors: A quantitative and qualitative synthesis. *Neuroradiology.* (2022) 64:647–68. doi: 10.1007/s00234-021-02845-1

10. Ezzat S, Asa SL, Couldwell WT, Barr CE, Dodge WE, Vance ML, et al. The prevalence of pituitary adenomas: A systematic review. *Cancer.* (2004) 101:613–9. doi: 10.1002/cncr.20412

11. Daly AF, Rixhon M, Adam C, Dempegioti A, Tichomirowa MA, Beckers A. High prevalence of pituitary adenomas: A cross-sectional study in the province of Liege, Belgium. *J Clin Endocrinol Metab.* (2006) 91:4769–75. doi: 10.1210/jc.2006-1668

12. Fatemi N, Dusick JR, de Paiva Neto MA, Kelly DF. The endonasal microscopic approach for pituitary adenomas and other parasellar tumors: A 10-year experience. *Neurosurgery.* (2008) 63(4Suppl.2):244–56. doi: 10.1227/01.NEU.0000327025.03975.BA

13. Cossu G, Brouland J-P, Rosa SL, Camponovo C, Viaroli E, Daniel RT, et al. Comprehensive evaluation of rare pituitary lesions: A single tertiary care pituitary center experience and review of the literature. *Endocr Pathol.* (2019) 30:219–36. doi: 10.1007/s12022-019-09581-6

14. Corsello SM, Paragliola RM. Differential diagnosis of pituitary masses at magnetic resonance imaging. *Endocrine.* (2017) 58:1–2. doi: 10.1007/s12020-017-1230-8

15. Ugga L, Franca RA, Scaravilli A, Solari D, Cocozza S, Tortora F, et al. Neoplasms and tumor-like lesions of the sellar region: Imaging findings with correlation to pathology and 2021 WHO classification. *Neuroradiology.* (2023) 2023:1. doi: 10.1007/s00234-023-03120-1

16. Kachhara R, Nair S, Gupta AK, Radhakrishnan VV, Bhattacharya RN. Infrasellar craniopharyngioma mimicking a clival chordoma: A case report. *Neurol India.* (2002) 50:198–200.

17. Kinoshita Y, Yamasaki F, Tominaga A, Ohtaki M, Usui S, Arita K, et al. Diffusion-weighted imaging and the apparent diffusion coefficient on 3T MR imaging in the differentiation of craniopharyngiomas and germ cell tumors. *Neurosurg Rev.* (2016) 39:207–13. doi: 10.1007/s10143-015-0660-0

18. Khant ZA, Azuma M, Kadota Y, Hattori Y, Takeshima H, Yokogami K, et al. Evaluation of pituitary structures and lesions with turbo spin-echo diffusion-weighted imaging. *J Neurol Sci.* (2019) 405:116390. doi: 10.1016/j.jns.2019.07.008

19. Iglesias P, Cardona J, Díez JJ. The pituitary in nuclear medicine imaging. *Eur J Intern Med.* (2019) 68:6–12. doi: 10.1016/j.ejim.2019.08.008

20. van den Bent MJ, Weller M, Wen PY, Kros JM, Aldape K, Chang S, et al. clinical perspective on the 2016 WHO brain tumor classification and routine molecular diagnostics. *Neuro Oncol.* (2017) 19:614–24. doi: 10.1093/neuonc/now277

21. Lemm D, de Oliveira FH, Bernays R-L, Kockro RA, Kollias S, Fischer I, et al. Rare suprasellar glioblastoma: Report of two cases and review of the literature. *Brain Tumor Pathol.* (2012) 29:216–20. doi: 10.1007/s10014-012-0086-0

22. Mahta A, Buhl R, Huang H, Jansen O, Kesari S, Ulmer S. Sellar and supra-sellar glioblastoma masquerading as a pituitary macroadenoma. *Neurol Sci.* (2013) 34:605–7. doi: 10.1007/s10072-012-1110-1

23. Anvari K, Samini F, Faraji M, Khooei A, Ghiasi T, Dehghan P. Pituitary glioblastoma: A case report. *Iran J Cancer Prev.* (2015) 8:e3436. doi: 10.17795/ijcp-3436

24. Deng S, Liu L, Wang D, Tong D, Zhao G. Small cell glioblastoma of the Sella Turcica region: Case report and review of the literature. *World Neurosurg.* (2018) 110:174–9. doi: 10.1016/j.wneu.2017.11.038

25. Alshail E, Rutka JT, Becker LE, Hoffman HJ. Optic chiasmatic-hypothalamic glioma. *Brain Pathol.* (1997) 7:799–806. doi: 10.1111/j.1750-3639.1997.tb01065.x

26. Kornreich L, Blaser S, Schwarz M, Shuper A, Vishne TH, Cohen IJ, et al. Optic pathway glioma: Correlation of imaging findings with the presence of neurofibromatosis. *Am J Neuroradiol.* (2001) 22:1963–9.

27. Laws ER, Weiss MH, White WL. Craniopharyngioma. *Skull Base.* (2003) 13:55–8. doi: 10.1055/s-2003-37554

28. Bommakanti K, Panigrahi M, Yarlagadda R, Sundaram C, Uppin MS, Purohit AK. Optic chiasmatic-hypothalamic gliomas: Is tissue diagnosis essential? *Neurol India.* (2010) 58:833–40. doi: 10.4103/0028-3886.73738

29. Faggiano A, Mansueto G, Ferolla P, Milone F, de Caro MLdB, Lombardi G, et al. Diagnostic and prognostic implications of the World Health Organization classification of neuroendocrine tumors. *J Endocrinol Invest.* (2008) 31:216–23. doi: 10.1007/BF03345593

30. Sirsath NT, Babu KG, Das U, Premlatha CS. Paranasal sinus neuroendocrine carcinoma: A case report and review of the literature. *Case Rep Oncol Med.* (2013) 2013:728479. doi: 10.1155/2013/728479

31. Liu H, Wang H, Qi X, Yu C. Primary intracranial neuroendocrine tumor: Two case reports. *World J Surg Oncol.* (2016) 14:138. doi: 10.1186/s12957-016-0887-4

32. Nasi D, Perano D, Ghadirpour R, Iaccarino C, Servadei F, Romano A. Primary pituitary neuroendocrine tumor: Case report and literature review. *Surg Neurol Int.* (2017) 8:101. doi: 10.4103/sni.sni_450_16

33. Ibrahim M, Yousef M, Bohnen N, Eisbruch A, Parmar H. Primary carcinoid tumor of the skull base: Case report and review of the literature. *J Neuroimaging.* (2010) 20:390–2. doi: 10.1111/j.1552-6569.2008.00317.x

34. Porter DG, Chakrabarty A, McEvoy A, Bradford R. Intracranial carcinoid without evidence of extracranial disease. *Neuropathol Appl Neurobiol.* (2000) 26:298–300. doi: 10.1046/j.1365-2990.2000.00257.x

35. Hood B, Bray E, Bregy A, Norenberg M, Weed D, Morcos JJ. Primary carcinoid tumor of the cavernous sinus. *World Neurosurg.* (2014) 81:202.e9–13. doi: 10.1016/j.wneu.2013.06.009

36. Cortés Vela JJ, Concepción Aramendía L, Ballenilla Marco F, Gallego León JI, González-Spínola San Gil J. Cerebral cavernous malformations: Spectrum of neuroradiological findings. *Radiologia.* (2012) 54:401–9. doi: 10.1016/j.rxeng.2011.09.004

37. Buonaguidi R, Canapicci R, Mimassi N, Ferdeghini M. Intrasellar cavernous hemangioma. *Neurosurgery.* (1984) 14:732–4. doi: 10.1227/00006123-198406000-00014

38. Al-Sharydah AM, Al-Suhibani SS, Al-Jubran SA, Al-Abdulwahhab AH, Al-Bar M, Al-Jehani HM, et al. Endoscopic management of Atypical sellar cavernous hemangioma: A case report and review of the literature. *Int J Surg Case Rep.* (2018) 42:161–4. doi: 10.1016/j.ijscr.2017.12.006

39. Pan X, Shen J, Ma Y, Lou H, Weng Y, Zhan R. Imaging characteristics of Intrasellar cavernous hemangioma: A case report. *Medicine.* (2020) 99:e23405. doi: 10.1097/MD.0000000000023405

40. Al-Saiari S, Al-Orabi K, Farag A, Brinji Z, Azzouz A, Mohammed T, et al. Intrasellar cavernous hemangiomas: A case report with a comprehensive review of the literature. *Surg Neurol Int.* (2021) 12:58. doi: 10.25259/SNI_622_2020

41. Kamrin RB, Buchsbaum HW. Large vascular malformations of the brain not visualized by serial angiography. *Arch Neurol.* (1965) 13:413–20. doi: 10.1001/archneur.1965.00470040079013

42. Sansone ME, Liwnicz BH, Mandybur TI. Giant pituitary cavernous hemangioma: Case report. *J Neurosurg.* (1980) 53:124–6. doi: 10.3171/jns.1980.53.1.0124

43. Mitsuhashi T, Hashimoto R, Nagahama S, Nagata Y. Intrasellar cavernous angioma in neurofibromatosis. *Hum Pathol.* (1991) 22:623–4. doi: 10.1016/0046-8177(91)90244-J

44. Chhang WH, Khosla VK, Radotra BD, Kak VK. Large cavernous haemangioma of the pituitary fossa: A case report. *Br J Neurosurg.* (1991) 5:627–9. doi: 10.3109/02688699109002886

45. Lombardi D, Giovanelli M, de Tribolet N. Sellar and parasellar extra-axial cavernous hemangiomas. *Acta Neurochir.* (1994) 130:47–54. doi: 10.1007/BF01405502

46. Cobbs CS, Wilson CB. Intrasellar cavernous hemangioma. Case report. *J Neurosurg.* (2001) 94:520–2. doi: 10.3171/jns.2001.94.3.0520

47. Chibbaro S, Cebula H, Ganau M, Gubian A, Todeschi J, Lhermitte B, et al. Multidisciplinary management of an intra-sellar cavernous hemangioma: Case report and review of the literature. *J Clin Neurosci.* (2018) 52:135–8. doi: 10.1016/j.jocn.2018.03.021

48. Jeon SCYJ, Yang JH, Lee I. Intrasellar cavernous hemangioma. *J Korean Neurosurg Soc.* (2004) 36:163–5.

49. Zhou BY, Cai BW, Liu YH, Fan YJ. Cavernous sinus but not intrasellar cavernous hemangioma. *Neurol India.* (2013) 61:442–3. doi: 10.4103/0028-3886.117603

50. Ma LC, Li WY, Chen WQ, Wu YK. Intrasellar cavernous hemangioma. *Neurol India.* (2014) 62:95–6. doi: 10.4103/0028-3886.128352

51. Das S, Ang LC, Ramsay D. Intrasellar cavernous hemangioma presenting as pituitary adenoma: A report of two cases and review of the literature. *Clin Neuropathol.* (2018) 37:64–7. doi: 10.5414/NP301012

52. Chuang CC, Jung SM, Yang JT, Chang CN, Pai PC. Intrasellar cavernous hemangioma. *J Clin Neurosci.* (2006) 13:672–5. doi: 10.1016/j.jocn.2005.08.017

53. Poorthuis MHF, Rinkel LA, Lammy S, Al-Shahi Salman R. Stereotactic radiosurgery for cerebral cavernous malformations: A systematic review. *Neurology 11.* (2019) 93:e1971–9. doi: 10.1212/WNL.0000000000008521

54. Saha A, Tso S, Rabski J, Sadeghian A, Cusimano MD. Machine learning applications in imaging analysis for patients with pituitary tumors: A review of the current literature and future directions. *Pituitary.* (2020) 23:273–93. doi: 10.1007/s11102-019-01026-x

55. Qiao N. A systematic review on machine learning in sellar region diseases: Quality and reporting items. *Endocr Connect.* (2019) 8:952–60. doi: 10.1530/EC-19-0156

frontiers | Frontiers in Oncology

TYPE Systematic Review
PUBLISHED 25 April 2023
DOI 10.3389/fonc.2023.1131013

OPEN ACCESS

EDITED BY
Arianna Rustici,
University of Bologna, Italy

REVIEWED BY
Felix Ehret,
Charité University Medicine
Berlin, Germany
Claudia Godi,
San Raffaele Hospital (IRCCS), Italy
Yan Ren,
Fudan University, China

*CORRESPONDENCE
Navodini Wijethilake
navodini.wijethilake@kcl.ac.uk

SPECIALTY SECTION
This article was submitted to Neuro-Oncology and Neurosurgical Oncology, a section of the journal Frontiers in Oncology

RECEIVED 24 December 2022
ACCEPTED 27 March 2023
PUBLISHED 25 April 2023

CITATION
Wijethilake N, MacCormac O, Vercauteren T and Shapey J (2023) Imaging biomarkers associated with extra-axial intracranial tumors: a systematic review.
Front. Oncol. 13:1131013.
doi: 10.3389/fonc.2023.1131013

Imaging biomarkers associated with extra-axial intracranial tumors: a systematic review

Navodini Wijethilake[1]*, Oscar MacCormac[1,2], Tom Vercauteren[1] and Jonathan Shapey[1,2]

[1]School of Biomedical Engineering and Imaging Sciences, King's College London, London, United Kingdom, [2]Department of Neurosurgery, King's College Hospital NHS Foundation Trust, London, United Kingdom

Extra-axial brain tumors are extra-cerebral tumors and are usually benign. The choice of treatment for extra-axial tumors is often dependent on the growth of the tumor, and imaging plays a significant role in monitoring growth and clinical decision-making. This motivates the investigation of imaging biomarkers for these tumors that may be incorporated into clinical workflows to inform treatment decisions. The databases from Pubmed, Web of Science, Embase, and Medline were searched from 1 January 2000 to 7 March 2022, to systematically identify relevant publications in this area. All studies that used an imaging tool and found an association with a growth-related factor, including molecular markers, grade, survival, growth/progression, recurrence, and treatment outcomes, were included in this review. We included 42 studies, comprising 22 studies (50%) of patients with meningioma; 17 studies (38.6%) of patients with pituitary tumors; three studies (6.8%) of patients with vestibular schwannomas; and two studies (4.5%) of patients with solitary fibrous tumors. The included studies were explicitly and narratively analyzed according to tumor type and imaging tool. The risk of bias and concerns regarding applicability were assessed using QUADAS-2. Most studies (41/44) used statistics-based analysis methods, and a small number of studies (3/44) used machine learning. Our review highlights an opportunity for future work to focus on machine learning-based deep feature identification as biomarkers, combining various feature classes such as size, shape, and intensity.

Systematic Review Registration: PROSPERO, CRD42022306922

KEYWORDS

extra-axial, intracranial, biomarker, marker, imaging, growth, tumor neoplasms

1 Introduction

Extra-axial brain tumors occur at anatomical sites external to the brain parenchyma and account for approximately half of all adult intracranial neoplasms (1). The main anatomical locations from which these tumors most commonly arise include the supratentorial dural region, cerebellopontine angle (CPA) region, sellar and suprasellar regions, pineal region, and intraventricular region (2).

Neoplasms identified as extra-axial brain tumors include meningiomas, metastases, vestibular schwannomas, solitary fibrous tumors, and pituitary tumors. Meningiomas are the most common supratentorial dural-based masses and most frequently arise from the meninges overlying the cerebral convexities. Dural-based metastases from other primary malignancies can also occur, although they are much rarer. Vestibular schwannomas (VS) are the most common tumor type found within the CPA. Meningiomas and metastases also develop less frequently in the CPA region. Pituitary adenoma is the most common tumor found in the sellar region, and macroadenomas often extend into the suprasellar region. Meningiomas are also found in the sellar region, originating from the tuberculum sellae, although these are much less common (2). Out of all primary brain and other central nervous system (CNS) tumors, 39.2% arise from the meninges, while 18.1% arise from the pituitary and craniopharyngeal ducts (1). Thus, extra-axial tumors comprise over half of all brain and CNS tumors in the USA, and behaviorally, most extra-axial tumors are non-malignant (1).

Meningioma is the most common extra-axial intracranial neoplasm, and 81.2% of meningiomas are located in the cerebral meninges. Meningiomas are most common found in children aged 0–14 years, and incidence increases with age. This tumor type is most common among adults over 65. Furthermore, meningiomas are also more common in females compared to males and are thought to arise from the arachnoid cap cells in the arachnoid layer of the meninges (1). In the 5th edition of the WHO CNS tumor classification, meningiomas are grouped into three main grade categories (WHO grades 1–3) that involve 15 different histological subtypes (3). However, a wide range of histological patterns can be seen in meningiomas, and some exhibit mixed patterns. WHO grade 1 tumors are generally slow-growing, whereas grade 2 meningiomas typically demonstrate a higher rate of growth and recurrence following resection (4). WHO Grade 3 meningiomas are the most aggressive, accounting for about 1.2% of meningiomas in the US (5).

Pituitary region tumors are the second most commonly reported brain and CNS tumor histology, with an incidence of 4.36 per 100,000 people. These tumors are also more frequently reported in females than in males. Neoplasms located in pituitary and craniopharyngeal ducts are the most common tumor among children and adolescents (age 0–19 years) (1). Pituitary tumors are not categorized into the WHO grading system; however, the WHO has classified pituitary tumors (most of which are pituitary adenomas) into subtypes based on the immunohistochemistry of pituitary hormones and other molecular and pathological markers. The transcription factors PIT-1, T-PIT, and SF-1 that are involved in the development of pituitary tumors are closely assessed for their characterizations (6). Importantly, these subtypes do not characterize the invasion, recurrence, or aggressiveness of adenomas. Nevertheless, the tumor size and its invasion into the cavernous sinus demonstrated on imaging are considered indicators of recurrence and aggressiveness. In addition, other subtypes that have been shown to be more aggressive (known as high-risk adenomas) include sparsely granulated somatotroph adenomas (growth hormone-releasing tumors) and lactotroph adenomas (prolactin-releasing tumors) in males (7).

Nerve sheath tumors are the third most common non-malignant brain and CNS tumors, of which 75% occur in the CPA (1). VSs arise from Schwann cells in the vestibulocochlear nerve and have unpredictable clinical behavior (8). Approximately 95% of VSs are sporadic unilateral tumors. Bilateral tumors are typically caused by a neurofibromatosis type 2 (NF2) genetic alteration (9). However, the NF2 mutations can also cause increased growth patterns in the sporadic VSs and can be considered a marker of VS tumor growth (10).

Solitary fibrous tumor/hemangiopericytoma (SFT/HPC) are rare intracranial extra-axial tumor types. These two types have different origins and prognoses, with the SFT phenotype having benign behavior while the HPC phenotype having a higher recurrence rate and malignant behavior (11). However, the fifth edition of the WHO Classification of Tumors of the Central Nervous System (CNS) introduces a single term ('solitary fibrous tumor') for both, rather than SFT/HPC, and a three-class CNS grading scheme based on histological phenotype and mitotic activity (3). Classic SFT phenotypes are considered WHO grade 1, and HPC phenotypes are considered grades 2 and 3 (12).

A biomarker is an indicator that can be either qualitative or quantitative and can depict an underlying biological process, a disease condition, the severity of the condition, or a response to a therapeutic intervention (13). Traditionally, biomarkers are obtained using molecular-level analysis of the disease. However, in the past couple of decades, advancements in medical imaging have enabled the obtainment of anatomic, functional, metabolic, and physiological measurements that can reflect such molecular substrates of diseases. These measurements are called imaging biomarkers—the features or characteristics that can be determined using medical images such as magnetic resonance imaging (MRI), diffusion-weighted imaging (DWI), perfusion-weighted imaging (PWI), positron emission tomography (PET), etc. (14).

Recently, there has been a growing interest in identifying imaging biomarkers related to oncology due to the rising emphasis on personalized cancer management, also called *precision cancer medicine* (90 14). Imaging is used widely, from tumor detection to staging, monitoring therapy, surgical planning, and surveillance. Imaging biomarkers can therefore play a pivotal role in optimizing patient management and outcomes. The non-invasive behavior of imaging biomarkers has a great potential to provide a comprehensive measurement over the other invasive biomarkers, which only reflect a fragment of a spatially or temporally heterogeneous tumor. Systematic reviews had been conducted to explore the imaging biomarkers of various brain tumors, including gliomas and neuro-oncology (15, 16). But to the best of our knowledge, this is the first systematic review to focus on intracranial extra-axial brain tumors.

This review guides the design of future studies looking at imaging features or biomarkers that may be used as tools for developing personalized treatments for extra-axial brain tumors. Early medical

imaging research used basic statistical analysis to investigate associations with tumor prognostic factors. Laterally, interest has moved towards using machine learning and deep learning algorithms for tumor segmentation and prognosis analysis (17, 18). This motivated us to look at the imaging and analysis techniques used to evaluate extra-axial tumors and how this work has evolved over time to incorporate methodological advancements.

In this review, we summarize the imaging biomarkers associated with the growth or poor prognosis of intracranial extra-axial neoplasms.

2 Methods

The Preferred Reporting Items for Systematic Reviews and Meta-Analyses (PRISMA) Statement and 2020 updated guidance were used for the preparation of this manuscript (19). The study was registered on PROSPERO, an international prospective register of systematic reviews (CRD42022306922)[1].

2.1 Search strategy

A structured search was performed on the Pubmed, Web of Science, Embase, and Medline databases and included studies from 1 January 2000 to 7 March 2022. The following boolean search criteria were applied:

1. ('dural-based mass' OR 'extra-axial brain tumor' OR meningiomas OR 'brain metastasis' OR neurofibroma OR 'peripheral nerve sheath tumors' OR schwannoma OR 'solitary fibrous tumor' OR 'hemangiopericytoma' OR epidermoid OR 'pituitary adenoma' OR 'pituitary macroadenoma' OR 'pituitary microadenoma' OR 'pituitary tumor') AND
2. (imaging OR radiomics) AND
3. (biomarker OR marker) AND
4. (growth OR prognosis OR risk)

2.2 Study selection

The articles included in this systematic review were written in English and were peer-reviewed. The eligibility criteria included:

1. the study must not be a case study or a review; and
2. an imaging technique was utilized; and
3. all the subjects used in the study had extra-axial tumors; and
4. the study used imaging feature(s); and
5. the study has assessed the association with growth or growth-related factor.

Full articles were obtained by the first author (NW) and further assessed for eligibility by two independent reviewers (NW and OM). Any discrepancy was resolved through mutual review with the senior author (JS). Covidence was used as a supporting tool throughout the filtering process[2].

In total, 811 studies were filtered by searching databases. After the removal of duplicates, 589 studies were screened by going through the titles and abstracts. This was followed by full-text screening of 49 studies. Six studies were excluded after applying the eligibility criteria. A total of 43 studies satisfied the inclusion criteria and were included in the descriptive analysis 1 (Figure 1).

In addition, we defined the outcomes the study should analyze. Since our main aim of the study was to identify growth-related imaging biomarkers, we defined the outcomes we included at the eligibility stage. Studies that assessed imaging biomarkers related to growth related molecular, histopathological, and other markers were considered. Moreover, studies with tumor size monitored before and after treatment, where other pre-treatment imaging biomarkers were assessed, were included. Studies with outcomes not related to growth were excluded.

2.3 Data extraction

The included studies were descriptively analyzed based on two main, predefined categories:

1. type of neoplasm,
2. imaging tool used.

In the *Results* section, we discuss our observations in detail.

2.4 Quality assessment

The Quality Assessment of Diagnostic Accuracy Studies-2 tool (QUADAS-2) was used to assess the methodological quality of all included studies (20). A quality assessment was performed by the first

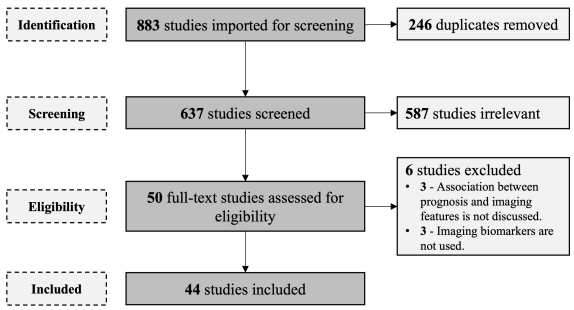

FIGURE 1
PRISMA flow diagram for the article selection.

1 https://www.crd.york.ac.uk/prospero.

2 https://www.covidence.org.

author (NW). The risk of bias and applicability concerns were assessed. The risk of bias assessment was performed using four QUADAS-2 criteria: i) patient selection; ii) index test; iii) reference standard; and iv) flow and timing. All criteria were scored as 'low risk,' 'high risk,' or 'unclear.' Studies that failed to comment on the criteria or partially commented on the criteria were considered 'unclear.'

- For patient selection criteria to be 'low' risk, patient samples should have been consecutively or randomly selected, and inappropriate exclusions should have been avoided; otherwise, studies were considered 'high' risk.
- For the index test, we considered imaging biomarker extraction. If feature extraction was performed blinded to the reference standard, the index test was assessed as 'low' risk. If not blinded, the risk of bias is considered 'high.'
- For the reference standard, we considered outcome-related measurements. In our study, this included histopathological details such as tumor grade and mitotic index. We assessed if this reference standard was acquired while blinded to the index test. Studies fulfilling the criteria were assigned a 'low' risk, while those that did not fulfill the criteria were assigned a 'high' risk.
- For the flow and timing criteria, we assessed if all the patients who went through the index test received the reference standard and whether they received the same reference standard. Studies fulfilling the criteria were assigned a 'low' risk, while those that did not fulfill the criteria were assigned a 'high' risk.

Study applicability was assessed on three criteria: (i) patient selection, (ii) index test, and (iii) reference standard. The studies were assigned 'low,' 'high,' or 'unclear' based on the conduct or interpretation of each criteria related to the review question we addressed (can be related, not related, or unclear).

3 Results

The imaging biomarkers of the included studies were extracted using four main imaging tools: conventional MRI, DWI, PWI, and PET. Further, the included studies have conducted the corresponding analysis on three main tumor neoplasms: meningiomas, pituitary tumors, and VSs, as we identified after the data extraction. In this section, we explicitly describe the included studies in relation to the two aspects mentioned above. Table 1 summarizes the included studies.

3.1 Imaging tools used in neuro-oncology

In this section, we discuss the imaging tools used in the studies we included. Conventional MRI was often used, as it is also used routinely in the clinical workflow of extra-axial brain tumor management. Additionally, other tools such as DWI, PWI, and PET were used in the studies we included.

3.1.1 Conventional MRI

MRI is considered the workhorse of brain tumor imaging. MRI can provide macro-structural anatomical information for basic diagnosis and screening of tumors and is routinely used for conventional MRI sequences: T1-weighted MRI (T1) and T2-weighted MRI (T2). Spin echo, fast-field echo, and turbo spin echo are the main techniques used to acquire the above sequences (65). Fluid-attenuated inversion recovery (FLAIR) is the third most commonly used sequence, an inversion recovery sequence with a long inversion time.

T1-weighted MRI may also be acquired after gadolinium contrast agent injection. Contrast-enhanced MRI depicts certain attributes related to the pathophysiology of the tumor by enhancing morphological details within the tumor and also provides basic indications of response to therapy treatments (66). However, contrast agents also carry certain (albeit small) risks associated with patient safety and are also costly compared to imaging without contrast agents.

This imaging tool does not expose the patient to ionizing radiation, posing a low risk. Due to its high sensitivity, MRI is frequently used in brain tumor diagnosis and assessment. In particular, FLAIR is used to detect tumor infiltration beyond the limits of the identified mass (66).

Some advanced MRI techniques, such as DWI and PWI, provide precise, visually differentiable information on microstructural, biophysical, and cellular processes that are also quantitative compared to conventional MRI sequences.

As mentioned above, the routine usage of MRI in clinical workflow is the key motivation behind using conventional MRI in most of the included studies (30). Conventional MRI is more feasible than other advanced imaging techniques (36), and the clear tissue differentiation seen with conventional MRI can provide a region of interest for feature extraction from other co-registered sequences such as DWI (55).

3.1.2 Diffusion-weighted imaging

DWI is extensively used to provide insight into the microscopic tissue structure in neuro-oncology using qualitative and quantitative measures. DWI measures the Brownian motion of water molecules between the intracellular and extracellular spaces, as well as within the extracellular space. Thus, it is sensitive to fine physiological changes that occur in the tissues (67). DWI does not require the administration of contrast agents and utilizes the conventional spin-echo T2 imaging sequence, in which two additional gradient pulses are applied. When water molecules are in low motion, DWI generates a high signal; this is known as a restriction. The parameter controlling the diffusion sensitivity of DWI, known as the "b value," depends on the gradient amplitude, duration of the applied gradient, and time gap between two gradients. DWI is useful in tumor detection as it can differentiate tumors as they are more cellular than normal tissue, causing diffusion reduction/impairment (68).

The apparent diffusion coefficient (ADC) map provides a measure of the diffusion magnitude from the DWI by eliminating T2 weighting. ADC maps are frequently used as a visual, qualitative measure. In addition, ADC values can be extracted for specific regions of interest from the ADC map as a quantitative measure. The microstructural information about cellular density is reflected in the ADC measurements and has proven to be useful for

TABLE 1 Summary of the included studies.

Study	Imaging Tool					Feature Class				Tool		Associated clinical features					
	Conventional MRI	DWI	PWI (DCE-MRI, DSC-MRI)	PET	Other	Intensity/first order statistics	Heterogeneity and texture	Size, Shape, location and Volume	Peritumoral radiomics	Statistical Analysis	Learning Model	Histopathology/ Molecular markers	Grade/ agressiveness	Survival/Prognosis/Growth	Recurrence	Treatment outcome	Other
Meningiomas																	
Takeda et al. (21)					×	×				×		×					
Ginat et al. (22)			×			×				×		×					
Tang et al. (23)		×				×				×		×					
Seystahl et al. (24)				×		×				×			×	×			
Shi et al. (25)			×			×				×		×					
Gihr et al. (26)		×				×	×			×		×	×				
Gihr et al. (27)	×					×	×			×			×				
Keil et al. (28)			×			×				×		×					
Bashir et al. (29)				×		×				×				×			
Chen et al. (30)	×						×				×		×				
Loewenstern et al. (31)	×							×	×	×				×			
Lu et al. (32)		×				×				×		×					
Bashir et al. (33)				×		×				×		×					
Bashir et al. (34)				×		×				×		×					
Hess et al. (35)	×					×		×		×		×					
Park et al. (36)	×							×		×			×				
Sun et al. (37)	×							×		×			×				
Yu et al. (38)	×	×				×		×	×	×			×				
Bozdağ et al. (39)		×				×			×	×		×	×				
Buizza et al. (40)		×				×				×			×			×	
Feraco et al. (41)																	
Gill et al. (42)	×								×	×				×			
Pituitary tumors																	
Pan et al. (43)	×							×		×		×					
Mahmoud et al. (44)	×	×				×				×		×					
Zhang et al. (45)	×					×		×		×							×
Heck et al. (46)	×					×		×		×			×				
Ceccato et al. (47)	–	–	–	–	–			×		×			×				

(Continued)

10.3389/fonc.2023.1131013

TABLE 1 Continued

Study	Imaging Tool					Feature Class				Tool		Associated clinical features					
	Conventional MRI	DWI	PWI (DCE-MRI, DSC-MRI)	PET	Other	Intensity/first order statistics	Heterogeneity and texture	Size, Shape, location and Volume	Peritumoral radiomics	Statistical Analysis	Learning Model	Histopathology/ Molecular markers	Grade/ agressiveness	Survival/Prognosis/Growth	Recurrence	Treatment outcome	Other
Tamrazi et al. (48)		×				×				×							×
Alhambra-Expósito et al. (49)	×					×				×							×
Galm et al. (50)	×					×				×				×	×		
Park et al. (51)	×							×		×		×					
Fan et al. (52)	×					×	×				×					×	
Hasanov et al. (53)	×							×		×		×					×
Ugga et al. (54)	×					×	×			×		×					
Conficoni et al. (55)	×	×				×		×		×		×					
Park et al. (56)	×					×	×			×							×
Swanson et al. (57)	×					×		×		×							×
Lewis et al. (58)	×					×				×					×		
Zhang et al. (59)	×					×	×	×			×				×		
Vestibular schwannomas																	
de Vries et al. (60)	×							×		×		×					
Lewis et al. (61)			×	×		×				×				×			
Lewis et al. (62)			×			×				×				×			
Solitary fibrous tumor																	
Mama et al. (63)	×	×				×				×			×				
Li et al. (64)			×			×				×				×			

10.3389/fonc.2023.1131013

histologic differentiation of meningiomas over conventional MRI (69). This has been a key reason for using ADC maps for analyzing meningioma-related grading and histopathologies in several included studies (23, 26, 32, 39).

Diffusion anisotropy is unequal directional diffusion that occurs due to the organization of cells and tissues and can be assessed using DWI. This measurement helps clinicians identify the invasion of the tumor to adjacent structures (e.g., white matter tracts) and the malignancy of the tumor as the heterogeneity within the tumor causes the diffusion to become isotropic (70, 71).

However, DWI has limitations, including a lack of standardization in assessing and analyzing diffusion metrics. For instance, most commercial software used in clinical practice does not allow pre-processing of DWI by image registration and noise filtration, which can significantly affect quantitative measurements. In addition, post-processed DWI sequences might cause an overlap between the ADC values of malignant and non-malignant tissues (72).

3.1.3 Perfusion-weighted imaging

Perfusion refers to the delivery of blood to the end organ at the level of the capillaries. PWI is a non-invasive MRI tool capable of measuring cerebral perfusion using specific hemodynamic parameters. Three types of PWI approaches have been developed to acquire this information using both plain and contrast-enhanced sequences. Dynamic susceptibility contrast (DSC-MRI) and dynamic contrast enhanced (DCE-MRI) are the two types that use contrast agents, while arterial spin-labeling (ASL) does not require administration of exogenous contrast agents as it uses blood as an endogenous tracer (73).

DSC-MRI is more specifically used in brain imaging, unlike the other two types. This technique involves the rapid intravenous injection of a bolus of a paramagnetic contrast agent while obtaining a serial measurement of the signal change of the T2- or T2*-weighted MRI. Subsequently, concentration time curves are obtained that lead to the calculation of quantitative maps that depict cerebrovascular hemodynamic parameters such as cerebral blood volume and flow rate. Low spatial resolution and signal loss artifacts due to the metallic surgical implants and other abnormalities such as calcification and dense bones are several disadvantages associated with DSC-MRI (74).

DCE-MRI is a standardized PWI technique that requires the administration of a contrast agent; T1-weighted MRI images are acquired dynamically before, during, and after the injection of the bolus of contrast agent. The information obtained is interpreted as permeability characteristics of the tissues based on tracer kinetic modeling principles. These extracted features from regions of DCE-MRI, such as K_{trans}, K_{ep}, V_e, and V_p, can describe the vascular micro-environment, including angiogenesis in brain tumors. Angiogenesis plays a pivotal role in the growth of sporadic VS, and that has been the reason for using DCE-MRI in two of the three included VS studies (61, 62). In high-flow lesions, including meningiomas, the kinetic parameter K_{trans} is permeability-limited (28). Therefore, several included studies used DCE-MRI kinetic parameters to analyze meningioma molecular markers (22, 25, 28).

ASL is a PWI technique that uses magnetically labeled arterial blood as an endogenous diffusible tracer to measure cerebral blood flow. Thus, ASL is recognized as a completely noninvasive and safe imaging tool that does not require the administration of contrast agents and can be repeated for frequent assessments. This imaging technique has limitations related to methodological shortcomings and artifacts when imaging the posterior fossa (75).

3.1.4 Positron emission tomography

PET is an imaging tool where *in vivo* biochemical and physiological processes, such as metabolism and blood flow, are visualized using radioactive substances known as PET tracers, providing unique functional information about the tumor (76). PET tracers have been used on specific molecular targets during the past few decades, but few have been demonstrated to be clinically relevant. PET tracer traditionally used in tumor imaging is 18F-2-fluoro-2-deoxy-D-glucose (18F-FDG). This tracer is use to distinguish recurrent tumors from radiation necrosis (77). It is a glucose analog that is actively transported into the metabolically active cells, phosphorylated, and trapped intracellularly. Malignant cells have an increased energy demand, resulting in high glucose consumption and an upregulation of glucose transport compared to other cells, resulting in increased accumulation of FDG (78). However, FDG has shown limitations in brain tumor imaging due to the high glucose consumption of the surrounding healthy brain parenchyma, thus decreasing PET imaging sensitivity (78). Another known PET tracer for brain tumor imaging is a nucleoside analog called 3'-deoxy-3'-fluorothymidine (18F-FLT) (77). This tracer can limit the uptake of 18F-FLT by healthy brain tissues. Several included studies used 18F-FLT to find associations with the progression of tumors. In meningiomas, a correlation was found between the uptake of 18F-FLT and the Ki-67 molecular marker, in addition to the association with the progression of the tumor reported by Bashir et al. (33); Bashir et al. (29).

Consequently, amino acid PET tracers, such as 11C-methyl-L-methionine (11C-MET), O-(2-[18F]fluoroethyl)-L-tyrosine (18F-FET), and 3,4-dihydroxy-6-[18F]-fluoro-L-phenylalanine (18F-FDOPA), have been used due to their high uptake in neoplastic tissue and relatively low uptake in healthy brain tissues (78). Amino acid PET has been used in several scenarios, including the detection and precise delineation of neoplastic tissue when conventional MRI is inconclusive and the determination of the post-radiation treatment effects that yield progression and/or recurrence. Since meningiomas have a strong expression of somatostatin receptor subtype 2, PET with somatostatin receptor ligands (68Ga-DOTATOC, 68Ga-DOTATATE) is used (78). In a few studies, the uptake of 68Ga-DOTATOC was found to be related to treatment outcomes and the VEGF molecular marker in meningiomas (24, 34). This PET is reported to be useful for differentiating the normal pituitary tissue from the pituitary adenomas (79).

Standard uptake value (*SUV*) is a common metric taken from PET imaging that depicts a relative measure of radiotracer uptake (80). Other metrics, such as the tumor-to-blood ratio (TBR), that correlate to the metabolic rate of the radiotracer, are used to

overcome shortcomings such as time dependence and susceptibility to errors caused by dose calibration and the scanner in the *SUV* metric.

SPECT is a similar nuclear imaging technique to PET, but it is less expensive and uses radiotracers. SPECT measures gamma-rays, whereas PET uses positrons to measure the decay of the specific radiotracers. PET is considered a more sensitive nuclear imaging technique than SPECT (81).

3.2 Imaging biomarkers of different tumors

In this section, we discuss imaging biomarkers we identified through this systematic review, categorized based on tumor neoplasm.

3.2.1 Meningiomas

3.2.1.1 Imaging biomarkers associated with molecular and histopathological markers

VEGF is a histopathological marker that correlates with tumor vascularity, vascular permeability, malignancy, progression-free survival, and overall survival of meningiomas (82–84). Hence, non-invasive imaging tools such as SPECT, DSC-MRI, and DCE-MRI have been used to find imaging biomarkers associated with the VEGF marker. Takeda et al. (21) identified significant differences in the Thallium-201 (Tl) uptake index of Thallium-201 chloride single-photon emission CT (Tl SPECT) between VEGF weakly and strongly positive tumors. In their study, they calculated the Tl uptake index by dividing the mean value obtained from the tumor region by the mean value extracted from the non-tumor region. Similarly, the association between the VEGF biomarker and a cerebral blood volume (CBV) marker extracted from dynamic susceptibility-weighted contrast-enhanced perfusion MRI (DSC-MRI) was assessed for meningiomas by Ginat et al. (22). This study extracted the maximum CBV manually from the tumor region, excluding areas containing necrosis, cysts, hemorrhage, large vessels, or calcification. A relative CBV (rCBV) value was computed as a ratio between the intratumoral maximum CBV value and contralateral cerebral white matter CBV, which provides the highest inter-/intra-observer reproducibility (85). They observed a significantly positive correlation between rCBV and VEGF scores. Keil et al. (28) assessed the ability to use the DCE-MRI kinetic parameters for predicting the VEGF marker *via* linear regression analysis. However, their results did not demonstrate a reliable prediction of VEGF, concluding that the DCE-MRI-derived kinetic parameters may not be able to be used as an imaging biomarker for meningioma. In recent studies, research has focused on finding associations with the PET-related metrics, and Bashir et al. (34) demonstrated that the [68Ga]Ga-DOTA-TOC PET metrics, the SUV_{mean} and SUV_{max}, all positively correlate with VEGF in meningiomas.

Ki-67/MIB-1 labeling index is a biomarker used to distinguish proliferating and quiescent cells, with an elevated Ki-67 index typically associated with a less favorable clinical outcome in many tumors (86, 87). Tang et al. (23) used ADC values extracted from DWI to find a correlation with the Ki-67 proliferation index in meningiomas. Regions of interest were annotated on the ADC maps, excluding the cystic and necrotic areas, which were identified using conventional MRI, and then the mean ADC values were extracted. The observations suggest that the ADC value inversely correlates with the Ki-67 index and, thus, can be used to differentiate the aggressiveness of meningiomas. Later, this was further proved by the work done by Lu et al. (32). Bozdağ et al. (39) also demonstrated the negative correlation between ADC and the Ki-67, additionally stating that meningiomas with necrosis have a lower ADC compared to non-nectrotic meningiomas. However, Lu et al. (32) found a positive correlation between ADC extracted from the edema region and Ki-67. Moreover, Gihr et al. (26) have assessed the correlation between the additional parameters extracted from the ADC histogram profile and the Ki-67. A positive correlation is identified between the entropy and the Ki-67, revealing the entropy as a promising imaging biomarker for presurgical grading. Takeda et al. (21) recognized a correlation between the delayed Tl uptake index and the MIB-1 labeling index with $p<0.0001$. In addition to these imaging tools, PET imaging has been used to find a relation to the Ki-67 proliferation index. Bashir et al. (33) have identified a correlation with the 3'-deoxy-3'-[18F] fluorothymidine (18F-FLT) PET/MRI metrics, SUV_{max} and SUV_{mean}.

Microvessel density (MVD) is a surrogate marker used to measure the angiogenesis and blood vessel formation of tumors. Due to the rapid growth of malignant tumors, microvessel formation is relatively low due to ischemia and hypoxia. Hence, an association between MVD and prognosis has been analyzed in many studies for different intracranial tumor types, including meningiomas, gliomas, and pituitary tumors (88, 89). Jensen and Lee (84) did not observe any statistical difference in MVD between high- and low-grade meningiomas. However, contrary to this study, Shi et al. (25) showed a significantly higher MVD value in benign meningiomas compared to malignant meningiomas. Additionally, they assessed the association of various PWI parameters with MVD in meningiomas, demonstrating a statistically significant positive correlation between rCBV and MVD.

Fibrotic tumor vessels (FTV) are another marker related to the vessel environment and were identified to have associations with the recurrence of tumors, vessel density, and VEGF in a study conducted by Hess et al. (35). They further recognized FTV to have associations with morphological characteristics on T1 post-contrast MRI, disruption of the arachnoid layer, and irregular shape in tumors, speculating that these imaging biomarkers might serve as predictors of underlying histopatological markers of meningiomas.

3.2.1.2 Imaging biomarkers associated with meningioma grades

In addition to finding associations between imaging markers and the different invasive histopathological or gene markers such as Ki-67 and VEGF, in the past decade research has been conducted to find the association of imaging markers with different meningioma grades, reflecting meningioma prognosis. Gihr et al. (26) used histogram profiling of ADC maps to distinguish low- and high-

grade meningiomas. In this study, they obtained the following set of first and second order features: mean ADC, max ADC, min ADC, percentile 10, 25, 75, and 90 ADC, median ADC, skewness, kurtosis, and entropy, from the histogram profile of the ADC map of the whole tumor. The results demonstrate that the percentile, mean, and median ADC values are significantly lower in high-grade meningiomas compared to those in the low-grade group. This observation was further proved in later studies (38, 39). However, the entropy was significantly higher in high-grade meningiomas compared to low-grade meningiomas. More recently, Buizza et al. (40) demonstrated that several other features extracted from DWI, such as median ADC, water intrinsic diffusivity and radius, cell volume fraction, and apparent cellularity, are significantly different between high-grade (WHO grades 2 and 3) and low-grade (WHO grade 1) meningiomas.

Later, Gihr et al. (27) extended their initial study (26) on meningiomas to assess the ability to use post-contrast T1 instead of DWI. They did not observe any significant difference in first order characteristics between low and high grade meningiomas, according to previous studies. However, they did observe a subtle difference in second-order characteristics, such as entropy and skewness, between both groups and suggested future research with a larger patient cohort to achieve statistical significance. Park et al. (36) assessed features that might explain complexity of structures to predict meningioma grades using post-contrast T1. They demonstrate that the fractal dimension may be used as an imaging biomarker to predict the grade of meningiomas. Sun et al. (37) analyzed tumor location on post-contrast T1 MRI to differentiate the biological characteristics of meningiomas. Their observations indicate that the grade 2 and 3 meningiomas present a strong predominance in the frontal structures compared to the grade 1 meningiomas. Subsequently, Yu et al. (38) also assessed conventional T1 and T2 characteristics for different meningioma grades. They observed that WHO grade 3 tumors have a large maximum tumor diameter and a high area of peritumoral edema compared to the lower grades (1 and 2). In addition, the enhancement degree and patterns (homogeneous or heterogeneous), lobulation (shape of the tumor), flowing voids (blood flow as a signal on MRI), and dural tail (indicating the thickening of the dura adjacent to the tumor) were significantly different between any two grades. In contrast to this study, Bozdağ et al. (39) found no significant difference between the presence of peritumoral edema on conventional MRI in low- and high-grade meningiomas. Additionally, they also observed no significant difference in the irregularity of the tumor margin and the presence of bone invasion.

Recently, a machine-learning-based study has used imaging features to classify meningioma grades. Chen et al. (30) extracted texture features from post-contrast T1.

3.2.1.3 Imaging biomarkers associated with clinical outcomes

Apart from assessing the grade of meningiomas, some studies have also considered clinical outcomes such as complications, operative time, tumor recurrence, and functional status [using the Karnofsky Performance Status scoring system (90)] to develop or identify imaging biomarkers. Loewenstern et al. (31) evaluated the relationship between peritumoral edema and clinical outcomes quantitatively using conventional MRI, T1, and T2 MRI. They obtained a measurement called the Edema Index, by dividing the peritumoral edema volume by the whole tumor volume. This index shows an association with functional decline after surgery in older patients. This research group has extended this work by assessing the association between the Edema Index and mutational burden (42), observing that tumor edema is associated with brain invasion and reduced overall survival. Subsequently, Bashir et al. (29) used TBR metrics from the (18F-FLT) PET, observing increased (18F-FLT) uptake in progressive asymptotic meningiomas.

Clinical outcomes of treatments such as proton therapy have also been examined in the past few years. Buizza et al. (40) utilized DWI to recover markers of tumor microstructure by longitudinal analysis pre- and post-treatment. The increment in the values for median ADC, water intrinsic diffusivity, and radius and the decrement in the values for cell volume fraction and apparent cellularity are observed in the post-treatment DWI for high-risk meningiomas. Feraco et al. (41) also conducted similar research, where they used the relative ADC mean (rADCm) to assess longitudinal volume changes. Their results indicated a statistically significant difference in rADCm between pre- and post-proton therapy treatment, with significant, progressively increasing rADCm values at each time point. Subjects that showed 20% or more volume reduction after treatment had significantly lower pre-treatment rADCm values.

Seystahl et al. (24) conducted a study to find the outcomes of the somatostatin-receptor (SSTR)-targeted radionuclide therapy treatment for meningiomas using the 68Ga-DOTATOC PET/CT. The results demonstrate that the SUV_{mean} and SUV_{max} is significantly low in WHO grade 2 tumors, which had shown progression after 6 months of the treatment. The multivariate regression analysis has shown the high grade and the low SUV_{mean} are associated with the progression at 6 months, and higher uptake is associated with longer progression-free survival.

3.2.2 Pituitary tumors

3.2.2.1 Imaging biomarkers associated with molecular and histopathological markers

Similar to the case of meningiomas described in the previous section, biomarkers such as VEGF, MVD, and Ki-67/MIB-1 may also depict pituitary tumor progression and outcomes (88). In an earlier study, Pan et al. (43) performed an analysis in which a significantly higher Ki-67 was observed in the presence of invasion on post-contrast T1 MRI compared to non-invasive pituitary adenomas. Similar observations have been made in other studies (53), with a higher Ki-67 index seen in invasive pituitary adenomas. In recent studies, more imaging tools have been used to investigate associations with the Ki-67 index. Conficoni et al. (55) utilized conventional MRI and DWI to predict the Ki-67 index. They observed a negative correlation between the enhancement ratio, the ratio between the signal intensity in post-contrast T1 and pre-contrast T1 within the solid region of the tumor, and the Ki-67

index. Nonetheless, the mean ADC value showed a negative correlation with the Ki-67 index. In other recent studies, the Ki-67 labeling index was predicted using 1,128 quantitative imaging features extracted from preoperative T2-weighted MRI (54). These features include both first-order histograms and high-order textural features, with and without various filters such as wavelets to derive hidden textural features. However, Mahmoud et al. (44) have not found a significant correlation between the ADC values and the MIB-1 labeling index in pituitary adenomas; Tamrazi et al. (48) have determined an inverse correlation between mean ADC values and the MIB-1 labeling index in pituitary macroadenomas.

Pan et al. (43) also demonstrated higher MVD present in invasive adenomas compared to non-invasive adenomas, which has been confirmed later in other published research (45). Studies also reveal that the invasion of adenomas is associated with VEGF expression, another marker of less favorable outcomes for tumors (43).

3.2.2.2 Imaging biomarkers associated with functioning/non-functioning pituitary adenomas

Pituitary adenomas are also categorized based on various hormone secretory functions. Mahmoud et al. (44) used conventional T1 and T2 MRI along with DWI to differentiate these different tumor categories. They observed a significantly lower mean and minimum signal intensity on T2-weighted MRI for growth hormone-secreting adenomas compared to others. Park et al. (51) demonstrated significantly high ratios of tumor width/anteroposterior diameter on conventional MRI in non-functioning adenomas with hyperprolactinemia. These hormone-secreting pituitary adenomas are typically considered benign based on histology, but there is an underlying significant morbidity due to direct mass effects such as defects in visual fields and/or hypersecretion of hormones, which results in a shortened lifespan (91, 92).

According to the literature, sparsely granulated adenomas are comparatively more aggressive, and therefore imaging biomarkers related to granulation have also been analyzed in the past decade. A higher T2 intensity was identified in sparsely granulated adenomas compared to densely or intermediately granulated adenomas (46). This observation has been confirmed in more recent studies (57, 58). Swanson et al. (57) also demonstrated size increment and invasive behavior in sparsely granulated adenomas. Park et al. (56) recently developed a machine-learning-based model to predict the granulation pattern in growth hormone-secreting pituitary adenomas using shape and first- and second-order features extracted from the post-contrast T1 and T2 weighted MRI.

3.2.2.3 Imaging biomarkers associated with clinical outcomes

Simultaneously, research has been conducted to find the imaging biomarkers that can correlate with treatment responses, recurrence, and outcomes. Heck et al. (46) have reported homogeneity within the adenoma on the T2 MRI as a marker of tumor size reduction after the somatostatin analog treatment. Galm et al. (50) have extracted textural features, namely the mean, median, maximum, and minimum intensities of the tumor region; skewness; measure of asymmetry of the intensity distribution; kurtosis; and degree of peaking in the intensity distribution, from the T1-weighted MRI. Cox proportional hazards regression analysis subsequently showed that the mean, median, minimum, and maximum pixel values of pituitary adenomas were all associated with recurrence and progression following surgery. Fan et al. (52) have used T1, T2, and post-contrast T1-weighted MRI to predict the responses to radiotherapeutic treatments for acromegaly patients. They extracted 1,561 imaging features from the tumor region, including first-order, textural, wavelet features, size, and shape features. The final radiomic signature developed for response prediction includes one shape, two textural, and three wavelet features, selected using the leave-one-out cross-validation technique. In another recent study by Zhang et al. (59), the same radiomic features were extracted from post-contrast T1 MRI and machine learning was used to predict the recurrence of pituitary macroadenoma within 5 years. They concluded that the combination of clinicopathological features and images is useful for recurrence prediction and is superior to prediction using only clinical features.

Ceccato et al. (47) observed that radiological invasion is typically present in aggressive pituitary adenomas. Hasanov et al. (53) demonstrated that invasion of the cavernous sinus is associated with recurrence. Thus, these studies verify that tumor invasion can be considered an imaging biomarker in pituitary tumors related to prognosis. Some studies have also searched for other imaging biomarkers associated with the invasiveness characteristic of pituitary tumors. Alhambra-Expósito et al. (49) also demonstrated that hyperintense adenomas are more invasive than hypointense adenomas.

3.2.3 Vestibular schwannoma

3.2.3.1 Imaging biomarkers associated with molecular and histopathological markers

The study of imaging biomarkers in VS has included the evaluation of biological processes such as cell proliferation and vessel density, including Ki-67 and microvessel density markers. de Vries et al. (60) obtained size measurements (the largest tumor diameter), an evaluation of tumor density (homogeneous, inhomogeneous, and cystic), and a tumor growth index (maximal tumor diameter/age of the patient) using post-contrast T1 and T2 images. They reported no relation between these features and the Ki-67 index. In their results, MVD shows a significantly positive correlation with tumor size and tumor growth index.

3.2.3.2 Imaging biomarkers associated with tumor growth

Some studies identified imaging biomarkers associated with tumor growth. Lewis et al. (61) utilized both PET with the 11C-(R)-PK11195 tracer and DCE-MRI to investigate the relationship between inflammation and tumor growth in sporadic VS. The results demonstrated the binding potential of 11C-(R)-PK11195, and that values were significantly higher in growing tumors relative to static ones. In another study, Lewis et al. (62) assessed the relationship between diffusion metrics (e.g., mean diffusivity and

fractional anisotropy) extracted from the DCE-MRI and tumor growth rates in both NF2 and sporadic VS. They demonstrated that and tissue extravascular–extracellular space v_e, increased with the increasing tumor size in both types.

3.2.4 Solitary fibrous tumors

The identification of imaging biomarkers has been conducted, focusing on the phenotypes and the grading of SFT. Grade 2 and 3 SFTs are classified based on mitotic activity, and thus, the studies have been conducted to predict the grade before surgery using imaging biomarkers. Therefore, the imaging features associated with the Ki-67 index have been assessed in several studies. Lu et al. (32) identified a statistically significant negative correlation between the ADC of the lesion and the Ki-67 in grade 2 SFT. This was also later observed by Li et al. (64). Moreover, Lu et al. (32) found a significantly positive correlation between ADC extracted from the edema region and Ki-67. These observations were on par with their observations of meningiomas in the same study.

Mama et al. (63) have identified imaging features related to the HPC phenotype using conventional MRI and ADC maps. They observed that the grade 2 HPCs had higher ADC values, whereas the grade 3 values (which were more aggressive and malignant than the grade 2 HPCs) were slightly lower. Li et al. (64) also verified these observations, with significantly different ADC values between grade 2 and 3 SFTs.

4 Discussion

4.1 Critical assessment of the included studies

There were certain biases in patient selection in the included studies. Most of the studies used relatively small datasets, usually because of the limited availability of clinical data, likely resulting in selection bias (29, 30). Consequently, the sample populations and the target populations varied significantly, which may limit the ability to generalize the observations and findings from these studies. For example, Ugga et al. (54) excluded patients with extensively necrotic and hemorrhagic lesions from the study. Furthermore, 75% of the included studies did not clearly mention if patients were selected consecutively. Approximately 12% of the studies were considered to have a 'high' risk of bias as they did not mention the time period in which patients were enrolled, the exclusion criteria, or whether a consecutive or random sample was used. Approximately 14% of the included studies clearly mentioned all the above factors and satisfied the criteria. Those were considered to have a 'low' risk of bias in patient selection.

Hasanov et al. (53) extracted tumor size from the MRIs but did not clearly mention the feature extraction process or whether it was done automatically or performed manually by an expert. This made it unclear whether the index test had caused a risk of bias. Yu et al. (38) extracted MRI characteristics to find associations with the WHO grades of meningiomas. However, they did not mention if the feature extraction and the labeling of WHO grades were done by independent experts, which made the risk of bias unclear. Similarly, 50% of the included studies did not mention the independent and blinded extraction of the features, i.e., the index test, and were thus considered to have an 'unclear' risk of bias. Ceccato et al. (47) mentioned that they used radiological images but did not specify which imaging type was used and were thus excluded, leading to reporting biases in the index test. Lewis et al. (61) clearly mentioned that their study was unblinded. Therefore, both of those studies (6.8% of the included studies) were considered to have a 'high' risk of bias in the index test. Approximately 43% of the included studies interpreted the index test results without knowledge of the results of the reference standard.

In this review, we considered several types of adverse outcome-related factors, such as molecular and histopathological markers, progression, invasiveness, recurrence, and grading of tumors. For these different outcomes, the studies used appropriate reference standards to categorize the patients. Bashir et al. (29) used the trial end-point criteria from the Response Assessment of Neuro-Oncology (RANO) workgroup (93) and considered the tumor to be progressing when there is a 25% increment in the product of two maximal perpendicular diameters (2D) of the tumor in comparison to the baseline. Therefore, the standard reference interprets the target condition, i.e., progression, appropriately. Similarly, appropriate and standardized reference standards were used in 38% of the included studies, which were interpreted without the knowledge of the index test.

The concerns regarding applicability were low, with almost all the included studies aligning with the review question we address.

Details of the QUADAS-2 assessment are summarized in Figure 2.

4.2 Overall assessment

In this systematic review, we identified studies that investigated imaging biomarkers of extra-axial intracranial tumors. Included studies predominantly focused on the association and correlation of imaging biomarkers with tumor growth. Others relate to the association of imaging biomarkers with molecular or histopathological tumor markers.

With the advancement of high-throughput technologies during the past decade, research was conducted to find the molecular markers of all types of tumors. Acquisition of molecular markers requires biological samples obtained using an invasive approach (biopsy or surgery). Surgical biopsy always provides the most definitive means of diagnosis, but it is associated with surgical risk and additional costs. Heterogeneity within the tumor also means that different areas may yield different molecular results. However, for diagnosis and screening, imaging tests such as MRI that are already obtained as part of the routine clinical workflow present an opportunity to recognize underlying molecular markers without the need for an invasive biopsy. Moreover, imaging biomarkers can also overcome the intra-tumor heterogeneity, providing consistent predictions. This can lead clinicians to take critical decisions at the right time, ultimately optimizing the personalized management of tumors.

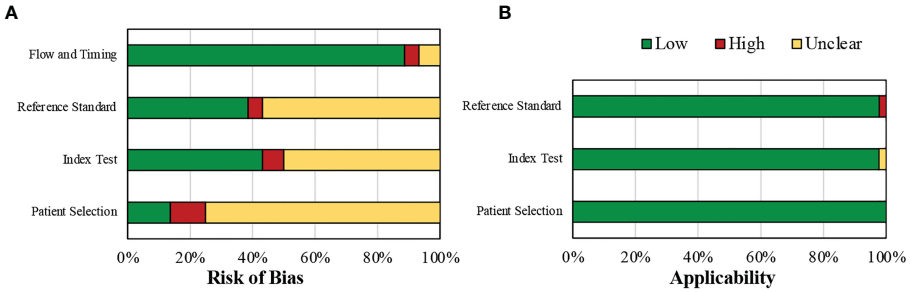

C

Study	Risk of Bias				Applicability		
	Patient Selection	Index Test	Reference Standard	Flow and Timing	Patient Selection	Index Test	Reference Standard
Takeda et al., 2011	☺	☺	☺	☺	☺	☺	☺
Ginat et al., 2012	?	☺	☺	☺	☺	☺	☺
Tang et al., 2014	?	?	?	☺	☺	☺	☺
Seystahl et al., 2016	☺	?	?	☺	☺	☺	☺
Shi et al., 2016	?	?	?	☺	☺	☺	☺
Gihr et al., 2018a	?	?	?	☺	☺	☺	☺
Gihr et al., 2018b	?	?	?	☺	☺	☺	☺
Keil et al., 2018	☹	?	?	☺	☺	☺	☺
Bashir et al., 2020a	?	☺	☺	☺	☺	☺	☺
Chen et al., 2019	?	☺	?	☺	☺	☺	☺
Loewenstern et al., 2019	☺	☺	☺	☺	☺	☺	☺
Lu et al., 2019	?	?	?	☺	☺	☺	☺
Bashir et al., 2020b	☺	☺	☺	☺	☺	☺	☺
Bashir et al., 2020c	☺	☺	☺	☺	☺	☺	☺
Hess et al., 2020	?	☺	☺	☺	☺	☺	☺
Park et al., 2020a	?	☺	?	☺	☺	☺	☺
Sun et al., 2020	☺	?	?	☺	☺	☺	☺
Yu et al., 2020	?	☺	?	☺	☺	☺	☺
Bozdag et al., 2021	?	☺	☺	☺	☺	☺	☺
Buizza et al., 2021	?	?	?	☺	☺	☺	☺
Feraco et al., 2021	?	?	?	☹	☺	☺	☺
Gill et al., 2021	☹	☺	☺	☺	☺	☺	☺
Pan et al., 2005	?	?	☺	☺	☺	☺	☺
Mahmoud et al., 2011	?	☺	☺	☺	☺	☺	☺
Zhang et al., 2011	?	?	☺	☺	☺	☺	☺
Heck et al., 2016	☹	?	?	☺	☺	☺	☺
Ceccato et al., 2018	?	☹	☹	?	☺	☺	☹
Tamrazi et al., 2017	?	?	?	☺	☺	☺	☺
Alhambra-Exposito et al., 2018	?	?	?	☺	☺	☺	☺
Galm et al., 2018	?	☺	☺	☺	☺	☺	☺
Park et al., 2018	?	?	?	☺	☺	☺	☺
Fan et al., 2019	?	☺	☺	☺	☺	☺	☺
Hasanov et al., 2019	?	?	?	☺	☺	?	☺
Ugga et al., 2019	☹	☺	☺	?	☺	☺	☺
Conficoni et al., 2020	?	?	?	☺	☺	☺	☺
Park et al., 2020b	?	☺	?	☺	☺	☺	☺
Swanson et al., 2021	?	?	?	☹	☺	☺	☺
Lewis et al., 2022	?	☺	☺	☺	☺	☺	☺
Zhang et al., 2022	☺	☺	☺	☺	☺	☺	☺
deVries et al., 2012	?	?	?	☺	☺	☺	☺
Lewis et al., 2019	☹	☹	☹	☺	☺	☺	☺
Lewis et al., 2021	?	?	?	☺	☺	☺	☺
Mama et al., 2014	?	?	?	?	☺	☺	☺
Li et al., 2021	?	☹	?	☺	☺	☺	☺

☹ High Risk ☺ Low Risk ? Unclear

FIGURE 2
Summary of the QUADAS-2 assessments of the included studies. **(A)** Graphical representation of included studies (in percentages) in each key domain in terms of the risk of bias. **(B)** A graphical representation of the included studies (in percentages) in each key domain in terms of the concerns regarding their applicability. **(C)** A tabular representation of the assessments assigned for each included study. QUADAS-2: Quality Assessment of Diagnostic Accuracy Studies-2.

For meningiomas, the majority of studies assessed imaging biomarkers that depict the underlying molecular or histopathological biomarkers such as MVD, Ki-67 index, and VEGF. Since the WHO has given a grading system based on aggressiveness and histopathology, several other included studies have assessed imaging biomarkers that relate to the grade or aggressiveness of the meningioma.

In addition, we observed PET imaging metrics showing relationships to different underlying molecular markers with different PET tracers for meningiomas. Bashir et al. (33) demonstrated a correlation between Ki-67 and 18F-FLT PET/MRI metrics, while in another study by Bashir et al. (34), where he used the [68Ga]Ga-DOTA-TOC PET tracer, no correlation with Ki-67 was found. Furthermore, in Bashir et al. (34), they found a correlation between [68Ga]Ga-DOTA-TOC PET metrics and VEGF, but this was not observed with the 18F-FLT PET tracer.

For pituitary tumors, most studies focused on the correlation between the tumor invasion of surrounding structures and the

underlying histopathology. In particular, aggressiveness is often correlated to how invasive the lesion is found to be, either intra-operatively or on diagnostic imaging (47). The fourth edition of the World Health Organization (WHO) classification of pituitary tumors recommends evaluation of tumor proliferation and invasion to identify aggressiveness (94). Zhang et al. (45) further distinguish the invasive adenomas as having significantly greater tumor diameters and volumes. In pituitary adenomas (PA), invasiveness has been shown to be the main contributing factor to recurrence and poor prognosis (95). Most of the early studies focused on using the invasiveness of the lesion as an imaging marker for prognosis; however, subsequent to this, other imaging biomarkers that can be extracted from more modern imaging techniques were assessed with increasing interest.

An imaging-based grading system based on the invasion of pituitary tumors was proposed by Knosp et al. (96). In this grading system, grades 0 and 1 mean no invasion, grade 2 is assigned when there is a probable invasion, and grades 3 and 4 indicate a cavernous sinus invasion. The majority of studies that assessed invasion as an imaging biomarker used this grading system (43, 58). As well as the Knosp system, a scoring system proposed by Cottier et al. (97) has also been used in a few studies (45). This scoring system assesses the percentage of the intra-cavernous internal carotid artery encased by the adenoma.

For VS, there were a very limited number of studies that assessed imaging biomarkers. Conventional MRI was used only in a single study where they found an association with histopathological markers of VS (60). Limited availability of patient cases with serial MRI scans restricted them from analyzing imaging biomarkers associated with the tumor growth in depth.

To clearly distinguish between two and three SFTs, surgery is necessary. Since both of these types are also malignant, research has been conducted to identify the tumor grade using pre-operative medical images, which can allow clinicians to formulate personalized treatment plans. However, the number of patients used in all the included studies on SFTs is limited due to the low incidence rate.

4.3 Future directions

Considering the included extra-axial brain tumor studies, the majority of the studies extracted features by determining the region of interest manually (54, 59). This is a time-consuming task that requires clinical experts. Future work can focus on automating the segmentation task using deep learning. This will lead to more deep feature extraction and analysis. Moreover, automated feature extraction, unlike manual feature extraction, is likely to result in reduced inter-observer variability. In the future, such techniques may be adapted to analyze the growth or progression of extra-axial tumors too. This has the potential for more personalized and standardized management of extra-axial tumors. To assess the impact of such automated methods, it would be worthwhile to test their use in simulated clinical workflows before assessing their effectiveness in the clinic.

4.4 Limitations

As we recognized through this review, the major limitation is the limited usage of machine learning, and in particular deep learning. The major reason behind this may be the lack of large-scale annotated datasets. Most of the included studies used private single-institutional datasets (27, 30; 612 59). These datasets could be made public for common use. This might lead to better reproducible and transparent research. Further, multi-institutional datasets will produce more persistent results.

The present systematic review was limited by various factors. Firstly, given the variety of ways data were presented and the relatively small number of available studies, it was not possible to perform a meta-analysis and quantitatively analyze the data. Consequently, we could not draw any firm conclusions concerning the effectiveness of the described imaging techniques and biomarkers. Secondly, the studies were of mixed methodological quality, reporting a variety of imaging biomarkers, limiting our discussion to qualitative and narrative discussion.

5 Conclusions

A limited number of studies have assessed imaging biomarkers related to intracranial extra-axial tumors. Future work should focus on using serial images and longitudinal patient data to develop composite imaging and clinical imaging biomarkers capable of predicting tumor behavior and growth. Such work would be particularly beneficial for the management of extra-axial tumors, pathologies that are typically benign and where surveillance management is commonly employed. This review provides a guide to the features researchers can utilize for developing reproducible and standardized imaging biomarkers.

Data availability statement

The original contributions presented in the study are included in the article/supplementary material. Further inquiries can be directed to the corresponding author.

Author contributions

NW conceived the manuscript. NW and OM performed the systematic literature search. NW drafted the initial manuscript. JS and TV reviewed the final manuscript. All authors contributed to the article and approved the submitted version.

Funding

NW was supported by the UK Medical Research Council [MR/N013700/1] and the King's College London MRC Doctoral

Training Partnership in Biomedical Sciences. This work was supported by core funding from the Wellcome Trust (203148/Z/16/Z) and EPSRC (NS/A000049/1) funding. TV is also supported by a Medtronic/Royal Academy of Engineering Research Chair (RCSRF1819/7/34). For the purpose of open access, the authors have applied a CC BY public copyright licence to any Author Accepted Manuscript version arising from this submission.

Conflict of interest

JS and TV are co-founders and shareholders of Hypervision Surgical. The remaining authors declare that the research was conducted in the absence of any other commercial or financial relationships that could be construed as a potential conflict of interest.

Publisher's note

References

1. Ostrom QT, Cioffi G, Waite K, Kruchko C, Barnholtz-Sloan JS. Cbtrus statistical report: primary brain and other central nervous system tumors diagnosed in the united states in 2014–2018. *Neuro-oncology* (2021) 23:iii1–iii105. doi: 10.1093/neuonc/noab200

2. Drevelegas A. Extra-axial brain tumors. *Eur Radiol* (2005) 15:453–67. doi: 10.1007/s00330-004-2557-0

3. Louis DN, Perry A, Wesseling P, Brat DJ, Cree IA, Figarella-Branger D, et al. The 2021 who classification of tumors of the central nervous system: a summary. *Neuro-oncology* (2021) 23:1231–51. doi: 10.1093/neuonc/noab106

4. Mawrin C, Perry A. Pathological classification and molecular genetics of meningiomas. *J neuro-oncol* (2010) 99:379–91. doi: 10.1007/s11060-010-0342-2

5. Kshettry VR, Ostrom QT, Kruchko C, Al-Mefty O, Barnett GH, Barnholtz-Sloan JS. Descriptive epidemiology of world health organization grades ii and iii intracranial meningiomas in the united states. *Neuro-oncology* (2015) 17:1166–73. doi: 10.1093/neuonc/nov069

6. Burcea IF, Năstase VN, Poiană C. Pituitary transcription factors in the immunohistochemical and molecular diagnosis of pituitary tumoursâ€"a systematic review. *Endokrynologia Polska* (2021) 72:53–63. doi: 10.5603/EP.a2020.0090

7. Laws E, Penn D, Repetti C. Advances and controversies in the classification and grading of pituitary tumors. *J Endocrinological Invest* (2019) 42:129–35. doi: 10.1007/s40618-018-0901-5

8. Carlson ML, Link MJ. Vestibular schwannomas. *New Engl J Med* (2021) 384:1335–48. doi: 10.1056/NEJMra2020394

9. Niknafs YS, Wang AC, Than KD, Etame AB, Thompson BG, Sullivan SE. Hemorrhagic vestibular schwannoma: review of the literature. *World Neurosurg* (2014) 82:751–6. doi: 10.1016/j.wneu.2013.02.069

10. Lassaletta L, Torres-Martín M, Peña-Granero C, Roda JM, Santa-Cruz-Ruiz S, Castresana JS, et al. Nf2 genetic alterations in sporadic vestibular schwannomas: clinical implications. *Otol Neurotol* (2013) 34:1355–61. doi: 10.1097/MAO.0b013e318298ac79

11. Schiariti M, Goetz P, El-Maghraby H, Tailor J, Kitchen N. Hemangiopericytoma: long-term outcome revisited. *J Neurosurg* (2011) 114:747–55. doi: 10.3171/2010.6.JNS091660

12. Macagno N, Vogels R, Appay R, Colin C, Mokhtari K, Consortium FCS, et al. Grading of meningeal solitary fibrous tumors/hemangiopericytomas: analysis of the prognostic value of the m arseille g rading s ystem in a cohort of 132 patients. *Brain Pathol* (2019) 29:18–27. doi: 10.1111/bpa.12613

13. Kessler LG, Barnhart HX, Buckler AJ, Choudhury KR, Kondratovich MV, Toledano A, et al. The emerging science of quantitative imaging biomarkers terminology and definitions for scientific studies and regulatory submissions. *Stat Methods Med Res* (2015) 24:9–26. doi: 10.1177/0962280214537333

14. Dregely I, Prezzi D, Kelly-Morland C, Roccia E, Neji R, Goh V. Imaging biomarkers in oncology: basics and application to MRI. *J Magnetic Resonance Imaging* (2018) 48:13–26. doi: 10.1002/jmri.26058

15. Waldman AD, Jackson A, Price SJ, Clark CA, Booth TC, Auer DP, et al. Quantitative imaging biomarkers in neuro-oncology. *Nat Rev Clin Oncol* (2009) 6:445–54. doi: 10.1038/nrclinonc.2009.92

16. Booth TC, Williams M, Luis A, Cardoso J, Ashkan K, Shuaib H. Machine learning and glioma imaging biomarkers. *Clin Radiol* (2020) 75:20–32. doi: 10.1016/j.crad.2019.07.001

17. Wijethilake N, Meedeniya D, Chitraranjan C, Perera I, Islam M, Ren H. Glioma survival analysis empowered with data engineeringâ€"a survey. *IEEE Access* (2021) 9:43168–91. doi: 10.1109/ACCESS.2021.3065965

18. Wijethilake N, Kujawa A, Dorent R, Asad M, Oviedova A, Vercauteren T, et al. (2022). Boundary distance loss for intra-/extra-meatal segmentation of vestibular schwannoma, in: *Machine Learning in Clinical Neuroimaging: 5th International Workshop, MLCN 2022, Held in Conjunction with MICCAI 2022*, Singapore, September 18, 2022. pp. 73–82, Proceedings (Springer).

19. Page MJ, Moher D, Bossuyt PM, Boutron I, Hoffmann TC, Mulrow CD, et al. Prisma 2020 explanation and elaboration: updated guidance and exemplars for reporting systematic reviews. *BMJ* (2021) 372. doi: 10.1136/bmj.n160

20. Whiting PF, Rutjes AW, Westwood ME, Mallett S, Deeks JJ, Reitsma JB, et al. Quadas-2: a revised tool for the quality assessment of diagnostic accuracy studies. *Ann Internal Med* (2011) 155:529–36. doi: 10.7326/0003-4819-155-8-201110180-00009

21. Takeda T, Nakano T, Asano K, Shimamura N, Ohkuma H. Usefulness of thallium-201 spect in the evaluation of tumor natures in intracranial meningiomas. *Neuroradiology* (2011) 53:867–73. doi: 10.1007/s00234-010-0822-2

22. Ginat DT, Mangla R, Yeaney G, Schaefer PW, Wang H. Correlation between dynamic contrast-enhanced perfusion MRI relative cerebral blood volume and vascular endothelial growth factor expression in meningiomas. *Acad Radiol* (2012) 19:986–90. doi: 10.1016/j.acra.2012.04.006

23. Tang Y, Dundamadappa SK, Thangasamy S, Flood T, Moser R, Smith T, et al. Correlation of apparent diffusion coefficient with ki-67 proliferation index in grading meningioma. *AJR Am J Roentgenol* (2014) 202:1303–8. doi: 10.2214/AJR.13.11637

24. Seystahl K, Stoecklein V, Schüller U, Rushing E, Nicolas G, Schäfer N, et al. Somatostatin receptor-targeted radionuclide therapy for progressive meningioma: benefit linked to 68ga-dotatate/-toc uptake. *Neuro-oncology* (2016) 18:1538–47. doi: 10.1093/neuonc/now060

25. Shi R, Jiang T, Si L, Li M. Correlations of magnetic resonance, perfusion-weighed imaging parameters and microvessel density in meningioma. *J BUON* (2016) 21:709–13.

26. Gihr GA, Horvath-Rizea D, Garnov N, Kohlhof-Meinecke P, Ganslandt O, Henkes H, et al. Diffusion profiling via a histogram approach distinguishes low-grade from high-grade meningiomas, can reflect the respective proliferative potential and progesterone receptor status. *Mol Imaging Biol* (2018) 20:632–40. doi: 10.1007/s11307-018-1166-2

27. Gihr GA, Horvath-Rizea D, Kohlhof-Meinecke P, Ganslandt O, Henkes H, Richter C, et al. Histogram profiling of postcontrast t1-weighted MRI gives valuable insights into tumor biology and enables prediction of growth kinetics and prognosis in meningiomas. *Trans Oncol* (2018) 11:957–61. doi: 10.1016/j.tranon.2018.05.009

28. Keil VC, Pintea B, Gielen GH, Hittatiya K, Datsi A, Simon M, et al. Meningioma assessment: kinetic parameters in dynamic contrast-enhanced MRI appear independent from microvascular anatomy and vegf expression. *J Neuroradiol.* (2018) 45:242–8. doi: 10.1016/j.neurad.2018.01.050

29. Bashir A, Vestergaard MB, Marner L, Larsen VA, Ziebell M, Fugleholm K, et al. PET imaging of meningioma with 18F-FLT: a predictor of tumour progression. *Brain* (2020) 143:3308–17. doi: 10.1093/brain/awaa267

30. Chen C, Guo X, Wang J, Guo W, Ma X, Xu J. The diagnostic value of radiomics-based machine learning in predicting the grade of meningiomas using conventional magnetic resonance imaging: a preliminary study. *Front Oncol* (2019) 9:1338. doi: 10.3389/fonc.2019.01338

31. Loewenstern J, Aggarwal A, Pain M, Barthélemy E, Costa A, Bederson J, et al. Peritumoral edema relative to meningioma size predicts functional outcomes after resection in older patients. *Operative Neurosurg* (2019) 16:281–91. doi: 10.1093/ons/opy107

32. Lu Z, You Z, Xie D, Wang Z. Apparent diffusion coefficient values in differential diagnosis and prognostic prediction of solitary of fibrous tumor/hemangiopericytoma

(whoii) and atypical meningioma. *Technol Health Care* (2019) 27:137–47. doi: 10.3233/THC-181447

33. Bashir A, Binderup T, Vestergaard MB, Broholm H, Marner L, Ziebell M, et al. *In vivo* Imaging of cell proliferation in meningioma using 3'-deoxy-3'-[18f] fluorothymidine PET/MRI. *Eur J Nucl Med Mol Imaging* (2020) 47:1496–509. doi: 10.1007/s00259-020-04704-2

34. Bashir A, Vestergaard MB, Binderup T, Broholm H, Marner L, Ziebell M, et al. Pharmacokinetic analysis of [68ga] ga-DOTA-TOC PET in meningiomas for assessment of in vivo somatostatin receptor subtype 2. *Eur J Nucl Med Mol Imaging* (2020) 47:2577–88. doi: 10.1007/s00259-020-04759-1

35. Hess K, Spille DC, Adeli A, Sporns PB, Zitta K, Hummitzsch L, et al. Occurrence of fibrotic tumor vessels in grade i meningiomas is strongly associated with vessel density, expression of vegf, plgf, igfbp-3 and tumor recurrence. *Cancers* (2020) 12:3075. doi: 10.3390/cancers12103075

36. Park YW, Kim S, Ahn SS, Han K, Kang SG, Chang JH, et al. Magnetic resonance imaging–based 3-dimensional fractal dimension and lacunarity analyses may predict the meningioma grade. *Eur Radiol* (2020) 30:4615–22. doi: 10.1007/s00330-020-06788-8

37. Sun C, Dou Z, Wu J, Jiang B, Iranmanesh Y, Yu X, et al. The preferred locations of meningioma according to different biological characteristics based on voxel-wise analysis. *Front Oncol* (2020) 10:1412. doi: 10.3389/fonc.2020.01412

38. Yu J, Chen Ff, Zhang Hw, Zhang H, Luo Sp, Huang Gd, et al. Comparative analysis of the MRI characteristics of meningiomas according to the 2016 who pathological classification. *Technol Cancer Res Treat* (2020) 19:1533033820983287. doi: 10.1177/1533033820983287

39. Bozdağ M, Er A, Ekmekçi S. Association of apparent diffusion coefficient with ki-67 proliferation index, progesterone-receptor status and various histopathological parameters, and its utility in predicting the high grade in meningiomas. *Acta Radiologica* (2021) 62:401–13. doi: 10.1177/0284185120922142

40. Buizza G, Paganelli C, Ballati F, Sacco S, Preda L, Iannalfi A, et al. Improving the characterization of meningioma microstructure in proton therapy from conventional apparent diffusion coefficient measurements using monte carlo simulations of diffusion MRI. *Med Phys* (2021) 48:1250–61. doi: 10.1002/mp.14689

41. Feraco P, Scartoni D, Porretti G, Pertile R, Donner D, Picori L, et al. Predict treatment response by magnetic resonance diffusion weighted imaging: a preliminary study on 46 meningiomas treated with proton-therapy. *Diagnostics* (2021) 11:1684. doi: 10.3390/diagnostics11091684

42. Gill CM, Loewenstern J, Rutland JW, Arib H, Pain M, Umphlett M, et al. Peritumoral edema correlates with mutational burden in meningiomas. *Neuroradiology* (2021) 63:73–80. doi: 10.1007/s00234-020-02515-8

43. Pan Lx, Chen Zp, Liu Ys, Zhao Jh. Magnetic resonance imaging and biological markers in pituitary adenomas with invasion of the cavernous sinus space. *J neuro-oncol.* (2005) 74:71–6. doi: 10.1007/s11060-004-6150-9

44. Mahmoud OM, Tominaga A, Amatya VJ, Ohtaki M, Sugiyama K, Sakoguchi T, et al. Role of propeller diffusion-weighted imaging and apparent diffusion coefficient in the evaluation of pituitary adenomas. *Eur J Radiol* (2011) 80:412–7. doi: 10.1016/j.ejrad.2010.05.023

45. Zhang Y, He N, Zhou J, Chen Y. The relationship between MRI invasive features and expression of emmprin, galectin-3, and microvessel density in pituitary adenoma. *Clin Imaging* (2011) 35:165–73. doi: 10.1016/j.clinimag.2010.06.002

46. Heck A, Emblem KE, Casar-Borota O, Bollerslev J, Ringstad G. Quantitative analyses of t2-weighted MRI as a potential marker for response to somatostatin analogs in newly diagnosed acromegaly. *Endocrine* (2016) 52:333–43. doi: 10.1007/s12020-015-0766-8

47. Ceccato F, Regazzo D, Barbot M, Denaro L, Emanuelli E, Borsetto D, et al. Early recognition of aggressive pituitary adenomas: a single-centre experience. *Acta neurochirurgica* (2018) 160:49–55. doi: 10.1007/s00701-017-3396-5

48. Tamrazi B, Pekmezci M, Aboian M, Tihan T, Glastonbury CM. Apparent diffusion coefficient and pituitary macroadenomas: pre-operative assessment of tumor atypia. *Pituitary* (2017) 20:195–200. doi: 10.1007/s11102-016-0759-5

49. Alhambra-Expósito MR, Ibáñez-Costa A, Moreno-Moreno P, Rivero-Cortés E, Vázquez-Borrego MC, Blanco-Acevedo C, et al. Association between radiological parameters and clinical and molecular characteristics in human somatotropinomas. *Sci Rep* (2018) 8:1–10. doi: 10.1016/j.trsl.2019.07.013

50. Galm BP, Martinez-Salazar EL, Swearingen B, Torriani M, Klibanski A, Bredella MA, et al. MRI Texture analysis as a predictor of tumor recurrence or progression in patients with clinically non-functioning pituitary adenomas. *Eur J Endocrinol* (2018) 179:191–8. doi: 10.1530/EJE-18-0291

51. Park SS, Kim JH, Kim YH, Lee JH, Dho YS, Shin CS. Clinical and radiographic characteristics related to hyperprolactinemia in nonfunctioning pituitary adenomas. *World Neurosurg* (2018) 119:e1035–40. doi: 10.1016/j.wneu.2018.08.068

52. Fan Y, Jiang S, Hua M, Feng S, Feng M, Wang R. Machine learning-based radiomics predicts radiotherapeutic response in patients with acromegaly. *Front Endocrinol* (2019) 10:588. doi: 10.3389/fendo.2019.00588

53. Hasanov R, Aydoğan Bİ, Kiremitçi S, Erden E, Güllü S. The prognostic roles of the ki-67 proliferation index, p53 expression, mitotic index, and radiological tumor invasion in pituitary adenomas. *Endocrine Pathol* (2019) 30:49–55. doi: 10.1007/s12022-018-9563-2

54. Ugga L, Cuocolo R, Solari D, Guadagno E, D'Amico A, Somma T, et al. Prediction of high proliferative index in pituitary macroadenomas using MRI-based radiomics and machine learning. *Neuroradiology* (2019) 61:1365–73. doi: 10.1007/s00234-019-02266-1

55. Conficoni A, Feraco P, Mazzatenta D, Zoli M, Asioli S, Zenesini C, et al. Biomarkers of pituitary macroadenomas aggressive behaviour: a conventional MRI and DWI 3t study. *Br J Radiol* (2020) 93:20200321. doi: 10.1259/bjr.20200321

56. Park YW, Kang Y, Ahn SS, Ku CR, Kim EH, Kim SH, et al. Radiomics model predicts granulation pattern in growth hormone-secreting pituitary adenomas. *Pituitary* (2020) 23:691–700. doi: 10.1007/s11102-020-01077-5

57. Swanson AA, Erickson D, Donegan DM, Jenkins SM, Van Gompel JJ, Atkinson JL, et al. Clinical, biological, radiological, and pathological comparison of sparsely and densely granulated somatotroph adenomas: a single center experience from a cohort of 131 patients with acromegaly. *Pituitary* (2021) 24:192–206. doi: 10.1007/s11102-020-01096-2

58. Lewis D, Roncaroli F, Kearney T, Coope DJ, Gnanalingham K. Quantitative magnetic resonance-derived biomarkers as predictors of function and histotype in adenohypophyseal tumours. *Neuroendocrinology* (2022) 112:276–86. doi: 10.1159/000516823

59. Zhang Y, Luo Y, Kong X, Wan T, Long Y, Ma J. A preoperative MRI-based radiomics-clinicopathological classifier to predict the recurrence of pituitary macroadenoma within 5 years. *Front Neurol* (2021) 12. doi: 10.3389/fneur.2021.780628

60. de Vries M, Hogendoorn PC, Briaire-de Bruyn I, Malessy MJ, van der Mey AG. Intratumoral hemorrhage, vessel density, and the inflammatory reaction contribute to volume increase of sporadic vestibular schwannomas. *Virchows Archiv* (2012) 460:629–36. doi: 10.1007/s00428-012-1236-9

61. Lewis D, Roncaroli F, Agushi E, Mosses D, Williams R, Li Kl, et al. Inflammation and vascular permeability correlate with growth in sporadic vestibular schwannoma. *Neuro-oncology* (2019) 21:314–25. doi: 10.1093/neuonc/noy177

62. Lewis D, Donofrio CA, O'Leary C, Li Kl, Zhu X, Williams R, et al. The microenvironment in sporadic and neurofibromatosis type ii–related vestibular schwannoma: the same tumor or different? a comparative imaging and neuropathology study. *J Neurosurg* (2020) 134:1419–29. doi: 10.3171/2020.3.JNS193230

63. Mama N, Abdallah AB, Hasni I, Kadri K, Arifa N, Ladib M, et al. Mr Imaging of intracranial hemangiopericytomas. *J Neuroradiol.* (2014) 41:296–306. doi: 10.1016/j.neurad.2013.10.007

64. Li S, Zhou Q, Zhang P, Ma S, Xue C, Deng J, et al. The relationship between the apparent diffusion coefficient and the ki-67 proliferation index in intracranial solitary fibrous tumor/hemangiopericytoma. *Neurosurgical Rev* (2021) 45:1–9. doi: 10.21203/rs.3.rs-903739/v1

65. Ferda J, Ferdová E, Hes O, Mraček J, Kreuzberg B, Baxa J. PET/MRI: multiparametric imaging of brain tumors. *Eur J Radiol* (2017) 94:A14–25. doi: 10.1016/j.ejrad.2017.02.034

66. Essig M, Weber MA, von Tengg-Kobligk H, Knopp MV, Yuh WT, Giesel FL. Contrast-enhanced magnetic resonance imaging of central nervous system tumors: agents, mechanisms, and applications. *Topics Magnetic Resonance Imaging* (2006) 17:89–106. doi: 10.1097/01.rmr.0000245464.36148.dc

67. Padhani AR, Liu G, Mu-Koh D, Chenevert TL, Thoeny HC, Takahara T, et al. Diffusion-weighted magnetic resonance imaging as a cancer biomarker: consensus and recommendations. *Neoplasia* (2009) 11:102–25. doi: 10.1593/neo.81328

68. Baehring JM, Fulbright RK. Diffusion-weighted MRI in neuro-oncology. *CNS Oncol* (2012) 1:155–67. doi: 10.2217/cns.12.28

69. Nagar V, Ye J, Ng W, Chan Y, Hui F, Lee C, et al. Diffusion-weighted mr imaging: diagnosing atypical or malignant meningiomas and detecting tumor dedifferentiation. *Am J Neuroradiol.* (2008) 29:1147–52. doi: 10.3174/ajnr.A0996

70. Inoue T, Ogasawara K, Beppu T, Ogawa A, Kabasawa H. Diffusion tensor imaging for preoperative evaluation of tumor grade in gliomas. *Clin Neurol Neurosurg* (2005) 107:174–80. doi: 10.1016/j.clineuro.2004.06.011

71. Hernando CG, Esteban L, Cañas T, Van den Brule E, Pastrana M. The role of magnetic resonance imaging in oncology. *Clin Trans Oncol* (2010) 12:606–13. doi: 10.1007/s12094-010-0565-x

72. Koh DM, Padhani AR. Diffusion-weighted MRI: a new functional clinical technique for tumour imaging. *Br J Radiol* (2006) 79:633–5. doi: 10.1259/bjr/29739265

73. Jahng GH, Li KL, Ostergaard L, Calamante F. Perfusion magnetic resonance imaging: a comprehensive update on principles and techniques. *Korean J Radiol* (2014) 15:554–77. doi: 10.3348/kjr.2014.15.5.554

74. Arrigoni F, Calloni S, Huisman TA, Chiapparini L. Conventional MRI. *Handb Clin Neurol* (2018) 154:219–34. doi: 10.1016/B978-0-444-63956-1.00013-8

75. Pollock JM, Tan H, Kraft RA, Whitlow CT, Burdette JH, Maldjian JA. Arterial spin-labeled mr perfusion imaging: clinical applications. *Magnetic Resonance Imaging Clinics North America* (2009) 17:315–38. doi: 10.1016/j.mric.2009.01.008

76. Wong TZ, van der Westhuizen GJ, Coleman RE. Positron emission tomography imaging of brain tumors. *Neuroimaging Clinics* (2002) 12:615–26. doi: 10.1016/S1052-5149(02)00033-3

77. Sharma A, McConathy J. Overview of PET tracers for brain tumor imaging. *PET Clinics* (2013) 8:129–46. doi: 10.1016/j.cpet.2013.02.001

78. Galldiks N, Langen KJ, Pope WB. From the clinician's point of view-what is the status quo of positron emission tomography in patients with brain tumors? *Neuro-oncology* (2015) 17:1434–44. doi: 10.1093/neuonc/nov118

79. Wang H, Hou B, Lu L, Feng M, Zang J, Yao S, et al. PET/MRI in the diagnosis of hormone-producing pituitary microadenoma: a prospective pilot study. *J Nucl Med* (2017) 59:523–8. doi: 10.2967/jnumed.117.191916

80. Kinahan PE, Fletcher JW. Positron emission tomography-computed tomography standardized uptake values in clinical practice and assessing response to therapy. *Semin Ultrasound CT MRI* (2010) 31:496–505. doi: 10.1053/j.sult.2010.10.001

81. Karpuz M, Silindir-Gunay M, Ozer AY. Current and future approaches for effective cancer imaging and treatment. *Cancer biother. radiopharmaceuticals* (2018) 33:39–51. doi: 10.1089/cbr.2017.2378

82. Provias J, Claffey K, delAguila L, Lau N, Feldkamp M, Guha A, et al. Meningiomas: role of vascular endothelial growth factor/vascular permeability factor in angiogenesis and peritumoral edema. *Neurosurgery* (1997) 40:1016–26. doi: 10.1097/00006123-199705000-00027

83. Lamszus K, Lengler U, Schmidt NO, Stavrou D, Ergün S, Westphal M. Vascular endothelial growth factor, hepatocyte growth factor/scatter factor, basic fibroblast growth factor, and placenta growth factor in human meningiomas and their relation to angiogenesis and malignancy. *Neurosurgery* (2000) 46:938–48.

84. Jensen R, Lee J. Predicting outcomes of patients with intracranial meningiomas using molecular markers of hypoxia, vascularity, and proliferation. *Neurosurgery* (2012) 71:146–56. doi: 10.1227/NEU.0b013e3182567886

85. Wetzel SG, Cha S, Johnson G, Lee P, Law M, Kasow DL, et al. Relative cerebral blood volume measurements in intracranial mass lesions: interobserver and intraobserver reproducibility study. *Radiology* (2002) 224:797–803. doi: 10.1148/radiol.2243011014

86. Maiuri F, De Caro MDB, Esposito F, Cappabianca P, Strazzullo V, Pettinato G, et al. Recurrences of meningiomas: predictive value of pathological features and hormonal and growth factors. *J neuro-oncol.* (2007) 82:63–8. doi: 10.1007/s11060-005-9078-9

87. Menon SS, Guruvayoorappan C, Sakthivel KM, Rasmi RR. Ki-67 protein as a tumour proliferation marker. *Clinica chimica Acta* (2019) 491:39–45. doi: 10.1016/j.cca.2019.01.011

88. Vidal S, Kovacs K, Horvath E, Scheithauer BW, Kuroki T, Lloyd RV. Microvessel density in pituitary adenomas and carcinomas. *Virchows Archiv* (2001) 438:595–602. doi: 10.1007/s004280000373

89. Flynn JR, Wang L, Gillespie DL, Stoddard GJ, Reid JK, Owens J, et al. Hypoxia-regulated protein expression, patient characteristics, and preoperative imaging as predictors of survival in adults with glioblastoma multiforme. *Cancer* (2008) 113:1032–42. doi: 10.1002/cncr.23678

90. Schag CC, Heinrich RL, Ganz PA. Karnofsky performance status revisited: reliability, validity, and guidelines. *J Clin Oncol* (1984) 2:187–93. doi: 10.1200/JCO.1984.2.3.187

91. Dekkers O, Biermasz N, Pereira A, Romijn J, Vandenbroucke J. Mortality in acromegaly: a metaanalysis. *J Clin Endocrinol Metab* (2008) 93:61–7. doi: 10.1210/jc.2007-1191

92. Clayton R, Raskauskiene D, Reulen R, Jones P. Mortality and morbidity in cushing's disease over 50 years in stoke-on-trent, uk: audit and meta-analysis of literature. *J Clin Endocrinol Metab* (2011) 96:632–42. doi: 10.1210/jc.2010-1942

93. Huang RY, Bi WL, Weller M, Kaley T, Blakeley J, Dunn I, et al. Proposed response assessment and endpoints for meningioma clinical trials: report from the response assessment in neuro-oncology working group. *Neuro-oncology* (2019) 21:26–36. doi: 10.1093/neuonc/noy137

94. Nishioka H, Inoshita N. New who classification of pituitary adenomas: assessment of pituitary transcription factors and the prognostic histological factors. *Brain Tumor Pathol* (2018) 35:57–61. doi: 10.1007/s10014-017-0307-7

95. Zhou Y, Fu X, Zheng Z, Ren Y, Zheng Z, Zhang B, et al. Identification of gene co-expression modules and hub genes associated with the invasiveness of pituitary adenoma. *Endocrine* (2020) 68:377–89. doi: 10.1007/s12020-020-02316-2

96. Knosp E, Steiner E, Kitz K, Matula C. Pituitary adenomas with invasion of the cavernous sinus space: a magnetic resonance imaging classification compared with surgical findings. *Neurosurgery* (1993) 33:610–8. doi: 10.1227/00006123-199310000-00008

97. Cottier JP, Destrieux C, Brunereau L, Bertrand P, Moreau L, Jan M, et al. Cavernous sinus invasion by pituitary adenoma: Mr imaging. *Radiology* (2000) 215:463–9. doi: 10.1148/radiology.215.2.r00ap18463

frontiers | Frontiers in Oncology

TYPE Original Research
PUBLISHED 05 June 2023
DOI 10.3389/fonc.2023.1153698

OPEN ACCESS

EDITED BY
Arianna Rustici,
University of Bologna, Italy

REVIEWED BY
Konstantinos Gousias,
University of Münster, Germany
Julius Höhne,
University Medical Center Regensburg, Germany

*CORRESPONDENCE
Sophie Shih-Yüng Wang
sophie.wang@med.uni-tuebingen.de

†These authors have contributed equally to this work

RECEIVED 30 January 2023
ACCEPTED 02 May 2023
PUBLISHED 05 June 2023

CITATION
Wang SS-Y, Machetanz K, Ebner F, Naros G and Tatagiba M (2023) Association of extent of resection on recurrence-free survival and functional outcome in vestibular schwannoma of the elderly. *Front. Oncol.* 13:1153698. doi: 10.3389/fonc.2023.1153698

Association of extent of resection on recurrence-free survival and functional outcome in vestibular schwannoma of the elderly

Sophie Shih-Yüng Wang[1*], Kathrin Machetanz[1], Florian Ebner[2], Georgios Naros[1†] and Marcos Tatagiba[1†]

[1]Department of Neurosurgery and Neurotechnology, Eberhard Karls University Tübingen, Tübingen, Germany, [2]Department of Neurosurgery, Alfried Krupp Hospital, Essen, Germany

Background: Despite the ongoing debate on the risk–benefit ratio of vestibular schwannoma (VS) treatment options, watchful observation and radiation are usually favored in the elderly (>65 years). If surgery is inevitable, a multimodal approach after deliberate subtotal resection has been described as a valid option. The relationship between the extent of resection (EOR) of surgical and functional outcomes and recurrence-free survival (RFS) remains unclear. This present study aims to evaluate the functional outcome and RFS of the elderly in relation to the EOR.

Methods: This matched cohort study analyzed all consecutive elderly VS patients treated at a tertiary referral center since 2005. A separate cohort (<65 years) served as a matched control group (young). Clinical status was assessed by the Charlson Comorbidity Index (CCI), the Karnofsky Performance (KPS), and the Gardner and Robertson (GR) and House & Brackmann (H&B) scales. RFS was evaluated by Kaplan–Meier analysis using contrast-enhanced magnetic resonance imaging to identify tumor recurrence.

Results: Among 2,191 patients, 296 (14%) patients were classified as elderly, of whom 133 (41%) were treated surgically. The elderly were characterized by a higher preoperative morbidity and worse gait uncertainty. Postoperative mortality (0.8% and 1%), morbidity (13% and 14%), and the functional outcome (G&R, H&B, and KPS) did not differ between the elderly and the young. There was a significant benefit in regard to the preoperative imbalance. Gross total resection (GTR) was accomplished in 74% of all cases. Lower grades of the EOR (subtotal and decompressive surgery) raised the incidence of recurrence significantly. Mean time to recurrence in the *surg*ELDERLY was 67.33 ± 42.02 months and 63.2 ± 70.98 months in the *surgCONTROL*.

Conclusions: Surgical VS treatment aiming for complete tumor resection is feasible and safe, even in advanced age. A higher EOR is not associated with cranial nerve deterioration in the elderly compared to the young. In contrast, the EOR determines RFS and the incidence of recurrence/progression in both study

cohorts. If surgery is indicated in the elderly, GTR can be intended safely, and if only subtotal resection is achieved, further adjuvant therapy, e.g., radiotherapy, should be discussed in the elderly, as the incidence of recurrence is not significantly lower compared to the young.

KEYWORDS

acoustic neuroma, neuro-oncology, skull base, geriatric, elderly, vestibular schwannoma

Introduction

Among benign nerve sheath tumors, the vast majority are vestibular schwannomas (VSs) with a reported incidence rate of 1.52 per 100,000 (1, 2). They account for 80%–90% of all tumors in the cerebellopontine angle and approximately 6%–8% of all primary intracranial neoplasms (3, 4). Historically, surgical removal has been an appreciated treatment of choice as complete resection represents maximal tumor control (5). However, due to the anatomical relationship of the VS to multiple cranial nerves (CNs), a great deal of precision and delicacy is required in surgical management (1, 6). Several studies have documented severe clinical consequences of postoperative CN function decline for VS patients (1, 7). Thus, other treatment options including watchful observation (i.e., wait-and-scan, WaS) and radiation (i.e., stereotactic radiosurgery, SRS) have been claimed (8). Ever since, there is an ongoing debate on the risk–benefit ratio of these treatment options on tumor control and function preservation considering different factors such as tumor size, initial CN function, and/or patient's age (9).

In contrast to other patient cohorts, there seems to be a general agreement that watchful observation and radiation treatment should be favored in the elderly (>65 years of age) assuming a higher operative morbidity and lower life expectancy (10, 11). However, surgical intervention is sometimes inevitable, even in this patient cohort (e.g., large VS compressing the brainstem). In these particular cases, a multimodal therapy approach [i.e., deliberate subtotal resection (STR) with adjuvant SRS] has been suggested as a valid option recently in order to reduce perioperative morbidity (9). The level of evidence, however, is remarkably low (9).

However, creating clinical evidence in VS management, the *elderlies* (>65 years of age) is of paramount importance, as an incidence peak is described in this specific patient group (9). In detail, there are three evidence gaps for the elderly patient cohort. Firstly, the few existing small-sized studies on surgical morbidity in the elderly describe the outcome of surgeries performed several decades ago (10–12) and surgical techniques have evolved reducing surgery time and improving functional outcome since then (8, 13). Thus, it remains unclear whether the surgical morbidity of the elderly differs from the young in the environment of contemporary neurosurgery. Second, as deliberate STR or decompressive surgery (DS) could be a valid option in this specific subgroup, the relation of surgical morbidity to the extent of resections (EORs) in the elderly should be investigated. Third, there is no data on the relation between the EOR on tumor control as in long-term recurrence-free-survival (RFS) (i.e. progress-free-survival in subtotal resection) in the elderly. Notably, most studies provide follow-up data of <5 years (10, 11).

Thus, the aim of this study is to evaluate (1) the patterns of VS management in a tertiary neurosurgical center, (2) the onco-functional outcome, and (3) the incidence of recurrence in relation to the EOR in a large cohort of elderly patients compared to a matched-control cohort.

Abbreviations: CCI, Charlson Comorbidity Index; CDC, Clavien–Dindo Classification; DS, decompression surgery; ENT, ear, nose, and throat; EOR, extent of resection; G&R, Gardner and Robertson; H&B, House and Brackmann; IAC, internal auditory canal; GTR, gross total resection; KPS, Karnofsky Performance Score; MRI, magnetic resonance imaging; N/A, not applicable; SRS, stereotactic radiosurgery; STR, subtotal resection; VS, vestibular schwannoma.

Methods

Study design and patient cohort

This retrospective blinded cohort study analyzed all consecutive (elderly) patients (>65 years) with unilateral VS treated at a German academic, tertiary referral center between April 2005 and October 2020. Patients were referred to non-surgical (i.e., WaS, stereotactic radiosurgery; *nonsurg*ELDERLY) or surgical treatment (*surg*ELDERLY) depending on tumor size, the presence of hydrocephalus, clinical presentation, and a patient's individual preference. A separate cohort of patients with <65 years of age, who underwent elective VS surgery, served as a matched control group (*surgCONTROL*) to specifically compare surgical treatment in the elderly and the young (Figure 1). Pairing was based on the *EOR*, surgical approach (semi-sitting or prone position), gender, and tumor size (closest match). All patients were treated by the retrosigmoid approach with intraoperative neurophysiological monitoring. Large VS (e.g., Koos °III–°IV) were generally treated in the semi-sitting position, while small VS (e.g., Koos °I–°II) in the prone position (14). VS associated with neurofibromatosis was systematically excluded from this study. Same was applied to the previously treated VS (by surgery or radiotherapy). All histopathological examinations of *surg*ELDERLY and *surgCONTROL* were graded as schwannoma by a board-certified neuropathologist. The study population was

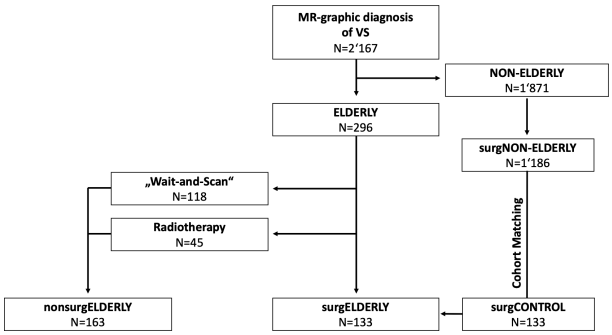

FIGURE 1
Flow chart on the study population.

identified through a prospective registry. The local ethics committee approved data collection and *post-hoc* analyses.

Data collection

Medical records of each patient were reviewed, and various demographic, tumor, and treatment variables were recorded. Magnetic resonance images (MRIs) were retrospectively analyzed to determine the tumor size according to the Koos grading system in a blinded fashion (14). The EOR was determined by postoperative MRI (3 months postoperatively) and classified by gross total resection (GTR), STR (i.e., residual tumor exclusively in the internal auditory canal), and DS (i.e., residual tumor beyond the internal auditory canal) (Figure 2). MR-graphic tumor progression/recurrence was defined as tumor progress or new tumor recurrence during MR-graphic surveillance with gadolinium contrast. Symptom-affected everyday-life dependency was acquired with the Karnofsky Performance Score (KPS) (15). Pre- and postoperative symptoms were recorded including tinnitus, functional hearing loss in Gardner–Robertson (GR) classes (16), gait uncertainty, vertigo, trigeminal affection (neuralgia or hypesthesia), double vision, swallowing deficit, headache, gustatory deficit, hydrocephalus, and facial palsy. Facial nerve function was reported using the House and Brackmann (H&B) scale pre- and postoperatively, as well as after a follow-up of 3 months and 1 year (17). Recorded patient comorbidities were assessed using the Charlson Comorbidity Index (CCI) (18). Adverse postoperative events were classified according to the Clavien–Dindo Classification (CDC) (19).

Statistical analysis

Statistical analysis was performed in R Studio (Version 1.2) using descriptive statistics. To compare nonnumeric parameters of both groups, the chi-square test and Fisher's exact test were applied. For numeric parameters, Welch's two-sample *t*-test was used. Recurrence-free and overall survival were estimated using the Kaplan–Meier method and compared between cases and controls using a log-rank test. The length of follow-up for recurrence-free survival was calculated from the date of surgical intervention to the date of either recurrence or the last clinical visit. Significance was defined as the probability of a two-sided type 1 error being <5% ($p < 0.05$). Data are presented as mean ± standard deviation (SD) if not indicated otherwise. Due to the low incidence of complications and perioperative morbidity, for its analysis and comparison dependent on the EOR, DS and STR were grouped together.

Results

Study cohorts

Among 2,167 patients with VS, 296 patients (14%) were of >65 years of age at date of diagnosis and classified as elderly (Figure 1). Mean age was 71.1 ± 5.0 [range 65–89] years in all elderly patients. Tumor size was equally distributed across Koos grades (°I: 69/296, 23%; °II: 86/296, 29%; °III: 80/296, 27%; °IV: 61/296. 21%). The majority of elderly patients (163/296, 55%) was managed non-surgically (*nonsurg*ELDERLY) by either SRS (45/163, 28%) or watchful observation (118/163, 72%). 133/296 (45%) of elderly patients were treated microsurgically (*surg*ELDERLY) *via* a retrosigmoid approach. A separate cohort of patients younger than 65 years (N = 133) served as a matched control group (*surgCONTROL*). The mean age of the *surgCONTROL* cohort was 46.3 ± 11.9 years (Table 1).

The most common initial symptom in the elderly was functional hearing loss in 172/296 (58%) cases, followed by vertigo in 117/296 (40%) patients. Tinnitus and gait uncertainty were similarly common with 84/296 (28%) cases and 85/296 (29%) cases, respectively. Facial

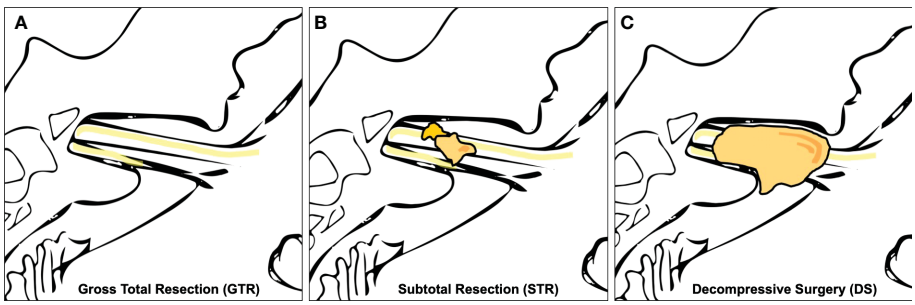

FIGURE 2
Extent of resection (EOR). **(A)** shows gross total resection (GTR), **(B)** subtotal resection (STR), and **(C)** shows a schematic representation of decompressive surgery (DS) with no decompression of the tumor in the internal auditory canal.

TABLE 1 Patient demographics, tumor characteristics, and initial clinical presentation.

	nonsurgELDERLY	surgELDERLY	surgCONTROL	p-value**
No. of cases	163	133	133	N/A
Demographics				
Age	71.9 ± 5.1	70.2 ± 4.6	46.3 ± 11.9	**0.002/<0.001***
Female	95 (58)	72 (54)	61 (46)	0.717/0.220
Tumor size				
Koos°I	67 (41)	2 (2)	2 (2)	**<0.001*/1**
Koos°II	64 (39)	22 (16)	22 (16)	**<0.001*/1**
Koos°III	27 (17)	53 (40)	53 (40)	**<0.001*/1**
Koos°IV	5 (3)	56 (42)	56 (42)	**<0.001*/1**
MR-graphic tumor progression	30 (18)	31 (23)	25 (19)	0.371/0.081
Cystic tumor	5 (3)	12 (9)	8 (6)	0.052/0.486
KPS score	82.9 ± 10.2	81.1 ± 8.4	85.4 ± 6.5	0.105/**<0.001***
Initial neurological symptoms				
Facial palsy	6 (4)	21 (16)	10 (8)	**<0.001***/0.056
Tinnitus	45 (28)	39 (29)	59 (44)	0.840/**0.016***
Functional hearing loss	71 (53)	93 (70)	101 (76)	**<0.001***/0.334
Gait uncertainty	33 (20)	52 (39)	18 (14)	**<0.001*/<0.001***
Vertigo	62 (38)	55 (41)	40 (30)	0.644/0.073
Trigeminal affection	4 (2)	20 (15)	22 (17)	**<0.001***/0.867
Swallowing deficit	0 (0)	5 (4)	3 (2)	**0.041***/0.719
Headache	0 (0)	1 (1)	0 (0)	N/A/0.316
Other	0 (0)	0 (0)	2 (2)	N/A/0.478
Comorbidities				
Charlson Index	0.45 ± 0.90	0.6 ± 1.11	0.1 ± 0.44	0.176/**<0.001***
0	123 (75)	94 (70)	126 (94)	0.360/**<0.001***
1	18 (11)	13 (10)	2 (2)	0.870/**0.045***
2	12 (7)	16 (12)	4 (3)	0.243/**0.011***
>3	10 (7)	10 (8)	1 (1)	0.646/**0.014***

(**) p-values indicate significant differences comparing (i) nonsurgELDERLY vs. surgELDERLY and (ii) surgELDERY vs. surgCONTROL cohorts. Values are presented as the number of patients (%) unless indicated otherwise. Significant p-values (<0.05) are highlighted in bold. p-values are indicated as *nonsurgELDERLY* vs. *surgELDERLY/surgELDERLY* vs. *surgCONTROL*.
N/A = Not applicable. "*" signifies a statistical significant value.

palsy was a leading initial symptom in only 27/296 (9%) cases in the elderly. Trigeminal affection and swallowing deficits were very rare clinical symptoms with 24/296 (8%) and 5/296 (2%) cases, respectively. No patient presented with double vision (Table 1).

When comparing *surg*ELDERLY with the younger *surgCONTROL* cohort, they presented with a worse initial KPS (81.1 ± 8.4 and 85.4 ± 6.5, respectively; $p < 0.001$) poorer preoperative comorbidity status (e.g., the incidence of myocardial infarction, congestive heart failure, diabetes, and malignant tumors), yielding in a significantly higher CCI in the *surg*ELDERLY compared to the *surgCONTROL* group (0.6 ± 1.1 and 0.1 ± 0.4, respectively; $p < 0.001$) (Tables 1, 2). However, there was no significant difference in the following VS-associated morbidities: initial incidence of facial palsy, functional hearing loss, vertigo, trigeminal affection, swallowing deficit, headache, gustatory deficit, and hydrocephalus. *surg*ELDERLY had a higher incidence of preoperative gait uncertainty ($p < 0.001$), but complained of less tinnitus than their controlled matches ($p = 0.016$).

Non-surgical vestibular schwannoma management in the elderly

The *surg*ELDERLY and *nonsurg*ELDERLY cohort did not differ in age, gender, the clinical status in KPS. The incidence of cystic

TABLE 2 Patients' comorbidities (*surgELDERLY vs. surgCONTROL*).

Comorbidities	surgELDERLY	surgCONTROL	p-value
Myocardial infarction	9 (7)	0 (0)	**0.007**
Congestive heart failure	6 (5)	0 (0)	**0.039**
Peripheral vascular disease	1 (1)	0 (0)	0.316
Cerebrovascular disease	8 (6)	3 (2)	0.218
Dementia	1 (1)	0 (0)	0.316
Peptic ulcer disease	1 (1)	0 (0)	0.316
Mild liver disease	2 (2)	0 (0)	0.478
Diabetes, uncomplicated	6 (5)	0 (0)	**0.039**
Hemiplegia	1 (1)	1 (1)	1
Renal disease	2 (2)	0 (0)	0.478
Tumor without metastasis	15 (11)	4 (3)	**0.017**
Metastatic tumor	3 (2)	0 (0)	0.245

Values are presented as the number of patients (%) unless indicated otherwise. Significant p-values (<0.05) are highlighted in bold.

morphology and MR-graphic progression was higher in the surgically treated but did not reach statistical significance in this cohort. However, non*surg*ELDERLY were characterized by a significant smaller tumor size ($p < 0.001$). The non*surg*ELDERLY cohort had less initial severe CN deficits (facial palsy, functional hearing loss, gait uncertainty, trigeminal affection) than *surg*ELDERLY. The CCI was not significantly different in both cohorts (Table 1).

Surgical vestibular schwannoma management in the elderly

The *surgCONTROL* was younger than the *surgELDERLY* cohort but did not differ in other patient demographics or tumor characteristics (Table 1). *surg*ELDERLY presented with a worse initial KPS then their younger *surgCONTROL* cohort (81.1 ± 8.4 and 85.4 ± 6.5, respectively; $p < 0.001$). There were no significant group difference in the initial incidence of facial palsy, functional hearing loss, vertigo, trigeminal affection, swallowing deficit, headache, gustatory deficit and hydrocephalus in a matched control comparison ("*surg*ELDERLY" vs. "*surgCONTROL*"). Remarkably, *surgELDERLY* had a higher incidence of gait uncertainty but complained of less tinnitus than their controlled matches. Additionally, *surg*ELDERLY had a poorer preoperative comorbidity status (e.g., the incidence of myocardial infarction, congestive heart failure, diabetes, and malignant tumors), yielding in a significantly higher CCI in the *surg*ELDERLY compared to the *surgCONTROL* group (0.6 ± 1.1 and 0.1 ± 0.4, respectively; $p < 0.001$) (Tables 1, 2).

Surgical data and surgical complications

Surgery was performed by a retrosigmoid craniotomy in all cases using either a semi-sitting (221/266, 83%) or prone position (45/266, 17%) in both surgical study groups. Mean operating time (skin to skin) was noted similarly at 248.0 ± 75.2 minutes in the *surg*ELDERLY and 240.0 ± 82.1 minutes in the *surgCONTROL* ($p = 0.398$).

The incidence of perioperative complication was comparable in the *surg*ELDERLY (17/133, 13%) and *surgCONTROL group (19/133, 14%)* ($p=0.858$). Larger tumors (Koos °III and °IV) more often yielded in postoperative complications (*surg*ELDERLY: °II: N = 3; °III: N = 2; °IV: N = 12 and *surgCONTROL*: °I: N = 1; °II: N = 2; °III: N = 8; °IV: N = 8). Postoperative hemorrhage, venous thrombosis and symptomatic pneumoncephalon occurred more frequently in the *surg*ELDERLY, but this did not reach any statistical significance. In contrast, younger patients were more prone to postoperative CSF leakage. Overall, the complication rate in the *surg*ELDERLY cohort was not significantly raised. One patient suffered a postoperative hemorrhage and treatment was terminated after the patient's presumed will, yielding in a mortality rate of N = 1 (Table 3). The CDC Index of complication severity is summarized in Table 4. Discharge modality (home, rehab, and other hospital) was significantly indifferent in both groups.

Functional outcome

Postoperative KPS did not differ between *surg*ELDERLY and *surgCONTROL* patients (78.1 ± 9.3 and 78.8 ± 4.9; $p = 0.409$). There was no significant difference in discharge modality ($p = 0.377$). Impeccable facial function (H&B = 1) was completely unaffected by the surgery in 38/112 (34%) and 53/123 (43%) in *surg*ELDERLY and *surgCONTROL*, respectively ($p = 0.096$). After surgery-related deterioration, facial function recovered to a favorable outcome (i.e., H&B°I and H&B°II) in 45/75 (60%) and 46/70 (65%) *surg*ELDERLY and *surgCONTROL* patients, respectively (Table 5). Therefore, overall favorable facial function outcome after 1 year was 70% (93/133) in the elderly and 76% (102/133) in the young. Hearing preservation was insignificantly better in *surg*ELDERLY at 84% (27 out of 32 with functional hearing) than in

TABLE 3 Incidence of perioperative complication surgELDERLY and surgCONTROL.

Incidence of complications following VS surgery	surgELDERLY	surgCONTROL	p-value
Mortality	1 (0.8)	0 (0)	0.316
Postoperative neurological complications (including secondary to infarction or hemorrhage)	4 (3)	0 (0)	0.131
Hydrocephalus	4 (3)	1 (1)	0.366
CSF otorrhea/rhinorrhea	7 (5)	15 (11)	0.119
Ventriculostomy placement	2 (1)	1 (1)	0.562
Facial nerve reconstruction	4 (3)	1 (1)	0.366
Symptomatic pneumencephalon	3 (2)	0 (0)	0.245
Sinus thrombosis	1 (1)	3 (2)	0.614

Values are presented as the number of patients (%) unless indicated otherwise.

surgCONTROL at 71% (28 out of 39 with functional hearing) with p = 0.164. New trigeminal deficit was observed in 2%. Of the 20 patients suffering from preoperative trigeminal affection (hypesthesia or neuralgia), 17 patients recovered clinically in the *surg*ELDERLY group (85%); the same was observed in 20/22 patients (90%) in the *surgCONTROL* group (p = 0.277). New postoperative gait uncertainty was observed in N = 4 in the *surg*ELDERLY but none in the younger *surgCONTROL* group. Postoperative recovery of symptomatic gait uncertainty was observed in 71% (37/52) and 76% (12/16) of the *surg*ELDERLY and *surgCONTROL*, respectively (p = 0.382). The recovery of vertigo symptoms was observed in N = 40/55 (71%) of all *surg*ELDERLY presenting with preoperative vertigo; this rate was higher in the *surgCONTROL* cohort with N = 37/40 (90%) (p = 0.013). The incidence of new postoperative vertigo was N = 0 (0%) in *surg*ELDERLY but N = 8/91 (9%) in its control cohort. Considering new postoperative tinnitus, the incidence was higher in the young (N = 1 in *surgELDERLY* and N = 9 in *surgCONTROL)*, whereas the postoperative improvement of known tinnitus was similar at 14% and 16%, respectively (*surg*ELDERLY and *surgCONTROL*) (p = 0.585).

Extent of resection and recurrence-free survival

GTR was achieved in the majority of *surg*ELDERLY cases (99/133, 74%). When taking the EOR into account, there was no significantly higher postoperative CN affection (facial, trigeminal, and vestibulocochlear) in *surg*ELDERLY associated with GTR and STR/DS (Table 6). However, the rate of permanent facial deterioration within patients treated with GTR remained significantly higher in the *surg*ELDERLY compared to the *surgCONTROL* (p = 0.035). Additionally, within the *surgCONTROL* group, STR/DS was associated with a significantly higher incidence of permanent facial deterioration (p = 0.036) compared to GTR.

STR/DS was significantly associated with the incidence of recurrence compared to GTR in both subgroups (*surg*ELDERLY: p = 0.015; *surgCONTROL*: p = 0.003). The incidence of recurrence was statistically insignificant in *surg*ELDERLY compared to *surgCONTROL*, when treated with GTR (p = 0.621). Mean time for surveillance was 38 ± 36 months in *surgCONTROL* (median: 25 months) and 31 ± 37 months (median: 34 months) in

TABLE 4 Complication severity according to the Clavien–Dindo Classification.

Clavien–Dindo Classification	surgELDERLY	surgCONTROL	p-value
0	116 (87)	114 (86)	0.685
1	1 (1)	1 (1)	1
2	1 (1)	3 (2)	0.290
3	14 (11)	14 (11)	1
3a	5 (36)	10 (71)	0.065
3b	9 (64)	4 (29)	
4	0 (0)	1 (1)	0.158
4a	0 (0)	1 (100)	0.158
4b	0 (0)	0 (0)	
5	1 (1)	0 (0)	0.301
Total incidence	17 (13)	19 (14)	0.858

Values are presented as the number of patients (%) unless indicated otherwise. Significant p-values (<0.05) are highlighted in bold.

10.3389/fonc.2023.1153698

TABLE 5 Functional outcome.

	surgELDERLY	surgCONTROL	p-value
KPS at discharge	78.05 (± 9.25)	78.79 (± 4.93)	0.409
Shunt dependency	8 (6)	2 (2)	0.104
Tumor recurrence	5 (4)	10 (8)	0.288
Initial House–Brackmann	1.28 (± 0.74)	1.14 (± 0.55)	0.075
H&B I	112 (84)	123 (92)	
H&B II	10 (8)	5 (4)	
H&B III	8 (6)	3 (2)	
H&B IV	1 (1)	1 (1)	
H&B V	2 (1)	1 (1)	
H&B VI	0 (0)	0 (0)	
Postoperative House–Brackmann	2.64 (± 1.37)	2.39 (± 1.44)	0.150
H&B I	38 (29)	53 (40)	
H&B II	27 (20)	28 (21)	
H&B III	26 (20)	13 (10)	
H&B IV	31 (23)	26 (19)	
H&B V	9 (7)	12 (9)	
H&B VI	2 (1)	1 (1)	
House–Brackmann 1 Year follow-up	1.98 (± 1.29)	1.71 (± 1.11)	0.061
H&B I	73 (55)	88 (66)	
H&B II	20 (15)	14 (10)	
H&B III	16 (12)	19 (14)	
H&B IV	18 (13)	10 (8)	
H&B V	5 (4)	2 (2)	
H&B VI	1 (1)	0 (0)	
Initial Gardner–Robertson Grade			
I–II (serviceable)	32 (24)	39 (29)	0.209
III–IV (non-serviceable)	101 (76)	94 (71)	
Postoperative Gardner–Robertson Grade			
I–II (serviceable)	27 (20)	28 (21)	0.843
III–IV (non-serviceable)	106 (80)	105 (79)	
Discharge to			
Home	126 (95)	131 (98)	0.376
Rehab	3 (2)	1 (1)	
Other hospital	3 (2)	1 (1)	
Death	1 (1)	0 (0)	

Values are presented as the number of patients (%) unless indicated otherwise. Significant p-values (<0.05) are highlighted in bold.

*surg*ELDERLY. The overall incidence for recurrence was 5/133 (4%) and 10/133 (8%) after neurosurgical tumor resection in the *surg*ELDERLY and *surgCONTROL*, respectively, with no statistical significance (p = 0.143). Mean time to recurrence was 67.33 ± 42.02 months in *surg*ELDERLY and 63.2 ± 70.98 months in *surgCONTROL*. Kaplan–Meier analysis on RFS depending on the EOR is shown in Figure 3. The EOR was significantly associated with RFS in both *surg*ELDERLY and *surgCONTROL* cohorts (p <

TABLE 6 Comparison between the extent of resection.

	GTR (N = 99) [surgELDERLY/surgCONTROL]	STR & DS (N = 34) [surgELDERLY/surgCONTROL]	p-value [surgELDERLY/surgCONTROL]
Recurrence	1 (1)/3 (3)	4 (12)/7 (21)	**0.015*/0.003**
Complications	13 (13)/14 (14)	4 (12)/4 (12)	1/1
Hearing loss	4 (4)/10 (10)	0 (0)/1 (3)	0.572/0.288
New tinnitus	1 (1)/8 (8)	0 (0)/1 (3)	1/0.447
Temporary facial deterioration	24 (24)/30 (30)	10 (29)/8 (24)	0.649/0.515
Permanent facial deterioration	33 (34)/19 (19)	8 (24)/13 (38)	0.389/**0.036**

Values are presented as the number of patients (%) unless indicated otherwise. Significant p-values (<0.05) are highlighted in bold.

0.001). Mean time to recurrence in *surg*ELDERLY was 67 ± 53 months and 79 ± 71 months in *surgCONTROL*.

Discussion

The present study aimed to evaluate the management of VS in the elderly (>65 years) in a tertiary neurosurgical center and to assess the oncological and functional outcome of this particular cohort in comparison to matched young controls and in regard to the EOR. The elderly represented approx. 14% of all VS patients in our cohort. The majority was eligible for non-surgical treatment. Patients were allocated for surgical treatment due to large tumor size affecting the brainstem and worse preoperative clinical symptomatology (e.g., the presence of vertigo and imbalance). In comparison to a matched-control cohort, elderly selected for surgery were characterized by a worse preoperative clinical condition (KPS and CCI). Despite this, postoperative mortality, morbidity and functional outcome did not differ between both surgical groups. These data suggest that the retrosigmoid approach for VS resection is safe in the elderly >65 years of age. Patients significantly benefit in regard to preoperative imbalance. GTR was accomplishable in the majority of patients. Notably, the EOR determined RFS.

Patterns of care and clinical characteristics

In the present population of surgically treated elderly (*surg*ELDERLY), preoperative CN deficits (facial function, hearing, gait, and trigeminal affection) were distinctively more severe than in the conservatively managed (*nonsurg*ELDERLY). Same was described in a nationwide registry study in Sweden with 58 elderly patients and by a series of surgically managed elderly patients by Samii et al. (12, 20). When comparing the nuances of clinical deficits, *surg*ELDERLY rarely presented with tinnitus but suffered from gait uncertainty more often than their matched and younger cohort. Interestingly, preoperative functional hearing was similar in both groups and not decreased in the elderly, even though presbyacusis is a common phenomenon in the general elderly population (21). This observation suggests that symptoms leading to the diagnosis of VS most likely are not hearing function but other vestibulocochlear (gait and vertigo), facial, or trigeminal symptoms.

Microsurgical care

Microsurgical tumor resection of VS by a retrosigmoid craniotomy was safe and did not yield in a higher risk for postoperative CN deficits in the elderly in comparison to the matched *surgCONTROL* cohort. Even with a highly significant incidence of relevant comorbidity (i.e., higher CCI and worse KPS), perioperative complication rates and morbidity are statistically comparable. Perioperative complications in the elderly have been described by current literature from 20% to 57% (1, 3, 10). In contrast, the present population showed an incidence of perioperative complication of 13% and 14% in the elderly and the

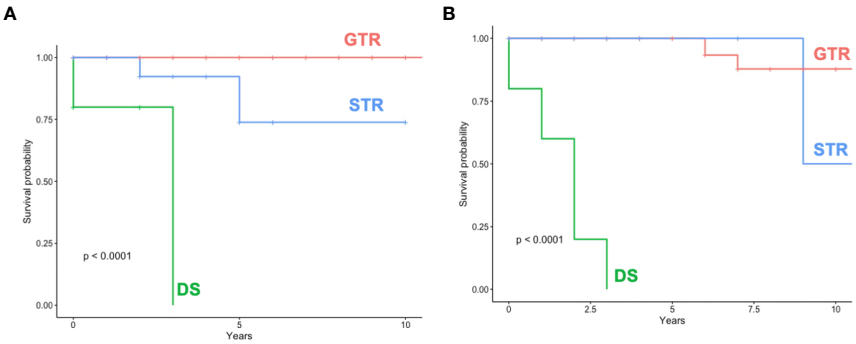

FIGURE 3
Recurrence/Progression-free-survival (RFS) **(A)** shows RFS dependent on the EOR in *surg*ELDERLY and **(B)** surg*CONTROL*. GTR, gross total resection; STR, subtotal resection; DS, decompressive surgery.

young, respectively. Due to a higher case load of elderly VS patients in the past 15 years (i.e., nine cases per year) in comparison to previous studies (approx. two to three per year) (3, 10), our department was able to acquire and develop a surgical routine and protocols for VS surgery in this patient cohort. The operative experience of the surgical team has been described as an important factor affecting onco-functional outcome in VS management, and therefore, treatment in high-volume centers has been recommended (9). The distribution of complications is different in both cohorts with a higher prevalence of CSF leakage and venous thrombosis in the younger population, while the elderly more often suffered from postoperative hemorrhage and symptomatic pneumocephalus, which has been described in the literature before (1, 10, 12, 22). Previous studies have mixed surgical approaches (translabyrinthine, middle fossa, and retrosigmoid) (23). This is the first comparative series to describe a large elderly cohort treated exclusively by a microsurgical, retrosigmoid approach. Thus, lower perioperative morbidity of the present study might be partially attributed by differences in the surgical approach.

Postoperative functional outcome

There were no differences in general functional outcome or the independency score (KPS) comparing the *surg*ELDERLY to the *surgCONTROL*. In contrast, the *surg*ELDERLY cohort showed a significant improvement of gait/vertigo after surgery. Tinnitus was improved in 13%–14% of all surgically treated. Postoperative hearing loss was not worse but significantly better in the *surg*ELDERLY. In approx. 60% of the patients, facial function normalized within 3 months, making postoperative functional deterioration temporary. There was no difference in facial nerve outcome between the *surg*ELDERLY and the *surgCONTROL* group. While observing a remarkable transient functional deterioration right after surgery, of which the majority recovers, these numbers should not be compared to direct results after other non-surgical treatment options (e.g., radiotherapy or radiosurgery). The rate of permanent facial deterioration was significantly higher in *surg*ELDERLY compared to *surgCONTROL* in the GTR group suggesting decreased postoperative rehabilitation potential in facial function with advanced age (24).

The explanation for the inversely proportional relationship of permanent facial deterioration and GTR vs. STR/DS in the elderly (more facial deterioration in GTR) and the young (more facial deterioration in STR/DS) could be attributed to the actual intention-to-treat. In the young, we usually intend GTR unless there is a deterioration of the intraoperative neuromonitoring (e.g., facial motor–evoked potentials). This approach explains the GTR rate of 74% in the present study. However, in a larger cohort of the same group, GTR was even higher with approx. 93% (25). This fact shows that we are more aggressive in the young than in the elderly to achieve GTR explaining the higher rate of unfavorable rates in the Young STR/DS subcohort. In turn, the present analysis has shown that surgical management strategy in the elderly is more careful compared to the young.

Long-term results should be chosen to compare functional outcome between such different treatment modalities as radiosurgery and microsurgery, e.g., in hearing outcome. Watchful observation ("WaS") abandons CN function (hearing and vestibular, more prominently then facial and trigeminal function) to the natural history of VS and tumor dynamic. Thus, it has been shown that 12% lose functional hearing in the course of the VS natural history (26). In line with this, SRS has been shown to result in a long-term hearing preservation of only 35%–51% (27) and therefore similarly to surgical treatment. Additionally, it is well known that hearing function dramatically decreases within the first decade after SRS (8, 13, 27). Additionally, tinnitus and imbalance are shown to increase and facial nerve dysfunction (e.g., hemispasm) might appear after SRS (28). Finally, little is known about radiation-associated tumor malignization (11, 29). The present study design, however, does not allow a direct comparison of functional outcome between radiotherapy and surgery.

It is not to be forgotten that functional outcome, as physicians and/or treating surgeons may define it, does not necessarily transfer to quality-of-life in the patients' eyes in a proportional way. Leaving residual tumor behind or treating the tumor by non-invasive treatments such as SRS can impact mental health or illness perception (30).

Extent of resection and recurrence-free survival

Due to the study design (matched by tumor size and the EOR), this analysis does not allow any general statement considering the frequency of the achieved EOR in the elderly compared to the young alone. However, when put into context with another series published and treated by the same group and institution with N = 572 primary VS patients, the rate of GTR was significantly higher among a general VS patient cohort of any age. Therefore, we can assume that the management of elderly patients with VS is carried out more conservatively—even in regard to the surgical EOR (25).

Mean time to recurrence was >5 years in both groups, proposing that long-term follow-up in VS patients should be carried out regardless of age. Still, the overall incidence of and mean time to recurrence were statistically insignificant in the elderly compared to the young concordant to previous matched cohort studies with distinctly smaller patient numbers (3, 10). In large VS, where surgery is inevitable, tumor mass reduction with SRS or observation could be suggested to avoid functional deterioration (9). In our cohort, microsurgical care followed by observation was the only treatment (no adjuvant SRS) carried out. Even though the number of STR- and DS-resected patients was low, the risk for tumor recurrence within 5 years was significantly increased in STR and DS. Thus, a deliberate DS as a standard treatment strategy in VS must be critically analyzed, especially in a setting of DS with observation alone (9). Therefore, if DS is inevitable, adjuvant therapy, e.g. SRS, should be evaluated for long-term tumor control. However, our study design does not allow any direct comparison between surgical GTR and DS plus SRS. This issue has yet to be investigated. Still, our results imply that if surgery is indicated in VS—even in patients with advanced age—GTR (or

near-total tumor resection) should be the intention of surgery to ensure maximal tumor control. Also, our data imply that subtotal VS resection without adjuvant therapy is not recommended.

The EOR is significantly associated with RFS in both groups independent of age with noted early tumor recurrence in DS compared to STR and GTR. Pre-existing data show that the volume of residual tumor correlates with the incidence of recurrence (31, 32). GTR—whenever safely feasible—should be the primary intention-to-treat, and this study confirms the beneficial aspect in the tumor control of GTR compared to STR/DS even in an elderly cohort. We reckon the fact that STR is defined more strictly (minimal residual only in the IAC and complete removal of the tumor in the CPA) in this presented study than in previously published studies by other groups. Therefore, we suggest that the EOR must be defined homogenously to truly convey this observed relationship of the EOR, recurrence, and functional outcome to clinical day-to-day care in the form of intention-to-resect to patients' benefit.

A definite statement on surgical treatment of VS is generally very difficult to acquire due to several reasons: (1) the level of evidence: there are no published randomized controlled clinical trials or even prospective studies on surgical resection in the current literature (11), (2) heterogenicity in surgical modality (e.g., approaches) by a heterogenous groups of specialists (neurosurgery and ENT), and 3) the lack of agreement of an EOR classification. To address these issues, an interdisciplinary network should be encouraged and a clinically relevant EOR classification should be enforced (including GTR, NTR, STR, and DS) to homogenously evaluate RFS and perioperative morbidity in larger multicenter settings. Such detailed distinction between the EOR might appear overelaborate, however, as tumor recurrence has shown to be dependent on the residual tumor, the idea of exact EOR classification has shown promise in other brain tumor entities already (33, 34).

Limitations of this study

It is apparent that the retrospective nature of this study bears its limitations and biases. Firstly, this is a single-center study. Therefore, the generalizability and reproducibility of the results may be limited to specialized centers with a comparative caseload in VS. Furthermore, although the number of patients classified as elderly may be regarded as the largest cohort compared to previously published studies (3, 10), still, the patient number and its value have to be put into its statistical context. Moreover, detailed subgroup analysis cannot be carried out (e.g., tumor size and cystic morphology) due to this cohort size.

Conclusion

The evidence level of VS management is remarkably low, and the debate on the risk–benefit ratio of surgical treatment is still ongoing, especially in the elderly. The present matched-cohort study shows that the microsurgical tumor resection of VS is safe and does not bear additional perioperative morbidity or worse functional outcome in the elderly as compared to a young control group. The overall incidence and of recurrence was statistically insignificant in the elderly compared to the young. When treating with surgery alone, the EOR determines RFS and the incidence of recurrence/progression in both study cohorts. For maximal tumor control, GTR should be intended. As incidence of recurrence is not significantly lower compared to the young. Postoperative follow-up should be carried out as mean time to recurrence was > 5 years in both groups. If leaving relevant tumor residual is inevitable, adjuvant therapy, e.g. SRS, should be evaluated in the Elderly.

Data availability statement

The raw data supporting the conclusions of this article will be made available by the authors, without undue reservation.

Ethics statement

Ethical review and approval were not required for the study on human participants in accordance with the local legislation and institutional requirements. Written informed consent from the participants was not required to participate in this study in accordance with the national legislation and the institutional requirements.

Author contributions

SW contributed to the acquisition, analysis, interpretation of data, conception and design, and writing the first draft. KM and FE contributed to interpretation of the data and critical review of the final manuscript. GN contributed to data analysis, interpretation of the data, and reviewing the final manuscript. MT contributed to the interpretation of the data and critical review of the manuscript. All authors contributed to the article and approved the submitted version.

Conflict of interest

The authors declare that the research was conducted in the absence of any commercial or financial relationships that could be construed as a potential conflict of interest.

Publisher's note

References

1. McClelland S3rd, Guo H, Okuyemi KS. Morbidity and mortality following acoustic neuroma excision in the united states: analysis of racial disparities during a decade in the radiosurgery era. *Neuro Oncol* (2011) 13(11):1252–9. doi: 10.1093/neuonc/nor118

2. Ostrom QT, Price M, Neff C, Cioffi G, Waite KA, Kruchko C, et al. CBTRUS statistical report: primary brain and other central nervous system tumors diagnosed in the united states in 2015-2019. *Neuro Oncol* (2022) 24(Suppl 5):v1–v95. doi: 10.1093/neuonc/noac202

3. Jiang N, Wang Z, Chen W, Xie Y, Peng Z, Yuan J, et al. Microsurgical outcomes after gross total resection on vestibular schwannoma in elderly patients: a matched cohort study. *World Neurosurg* (2017) 101:457–65. doi: 10.1016/j.wneu.2017.01.120

4. Hoffman S, Propp JM, McCarthy BJ. Temporal trends in incidence of primary brain tumors in the united states, 1985-1999. *Neuro Oncol* (2006) 8(1):27–37. doi: 10.1215/S1522851705000323

5. Nakatomi H, Jacob JT, Carlson ML, Tanaka S, Tanaka M, Saito N, et al. Long-term risk of recurrence and regrowth after gross-total and subtotal resection of sporadic vestibular schwannoma. *J Neurosurg* (2017) 133(4):1–7. doi: 10.3171/2016.11.JNS16498

6. Carlson ML, Link MJ. Vestibular schwannomas. *N Engl J Med* (2021) 384 (14):1335–48. doi: 10.1056/NEJMra2020394

7. Bederson JB, von Ammon K, Wichmann WW, Yasargil MG. Conservative treatment of patients with acoustic tumors. *Neurosurg* (1991) 28(5):646–50; discussion 50-1. doi: 10.1097/00006123-199105000-00002

8. Kondziolka D, Mousavi SH, Kano H, Flickinger JC, Lunsford LD. The newly diagnosed vestibular schwannoma: radiosurgery, resection, or observation? *Neurosurg Focus* (2012) 33(3):E8. doi: 10.3171/2012.6.FOCUS12192

9. Goldbrunner R, Weller M, Regis J, Lund-Johansen M, Stavrinou P, Reuss D, et al. EANO guideline on the diagnosis and treatment of vestibular schwannoma. *Neuro Oncol* (2020) 22(1):31–45. doi: 10.1093/neuonc/noz153

10. Van Abel KM, Carlson ML, Driscoll CL, Neff BA, Link MJ. Vestibular schwannoma surgery in the elderly: a matched cohort study. *J Neurosurg* (2014) 120 (1):207–17. doi: 10.3171/2013.6.JNS122433

11. Wolbers JG, Dallenga AH, Mendez Romero A, van Linge A. What intervention is best practice for vestibular schwannomas? a systematic review of controlled studies. *BMJ Open* (2013) 3(2). doi: 10.1136/bmjopen-2012-001345

12. Samii M, Tatagiba M, Matthies C. Acoustic neurinoma in the elderly: factors predictive of postoperative outcome. *Neurosurg* (1992) 31(4):615–9; discussion 9-20. doi: 10.1227/00006123-199210000-00001

13. Kondziolka D, Lunsford LD, McLaughlin MR, Flickinger JC. Long-term outcomes after radiosurgery for acoustic neuromas. *N Engl J Med* (1998) 339 (20):1426–33. doi: 10.1056/NEJM199811123392003

14. Koos WT, Day JD, Matula C, Levy DI. Neurotopographic considerations in the microsurgical treatment of small acoustic neurinomas. *J Neurosurg* (1998) 88(3):506–12. doi: 10.3171/jns.1998.88.3.0506

15. Schag CC, Heinrich RL, Ganz PA. Karnofsky performance status revisited: reliability, validity, and guidelines. *J Clin Oncol* (1984) 2(3):187–93. doi: 10.1200/JCO.1984.2.3.187

16. Gardner G, Robertson JH. Hearing preservation in unilateral acoustic neuroma surgery. *Ann Otol Rhinol Laryngol* (1988) 97(1):55–66. doi: 10.1177/000348948809700110

17. Yen TL, Driscoll CL, Lalwani AK. Significance of house-brackmann facial nerve grading global score in the setting of differential facial nerve function. *Otol Neurotol* (2003) 24(1):118–22. doi: 10.1097/00129492-200301000-00023

18. Charlson M, Szatrowski TP, Peterson J, Gold J. Validation of a combined comorbidity index. *J Clin Epidemiol* (1994) 47(11):1245–51. doi: 10.1016/0895-4356(94)90129-5

19. Clavien PA, Barkun J, de Oliveira ML, Vauthey JN, Dindo D, Schulick RD, et al. The clavien-dindo classification of surgical complications: five-year experience. *Ann Surg* (2009) 250(2):187–96. doi: 10.1097/SLA.0b013e3181b13ca2

20. Bartek JJr., Forander P, Thurin E, Wangerid T, Henriksson R, Hesselager G, et al. Short-term surgical outcome for vestibular schwannoma in Sweden: a nation-wide registry study. *Front Neurol* (2019) 10:43. doi: 10.3389/fneur.2019.00043

21. Disease GBD, Injury I, Prevalence C. Global, regional, and national incidence, prevalence, and years lived with disability for 310 diseases and injuries, 1990-2015: a systematic analysis for the global burden of disease study 2015. *Lancet* (2016) 388 (10053):1545–602. doi: 10.1016/S0140-6736(16)31678-6

22. Machetanz K, Leuze F, Mounts K, Trakolis L, Gugel I, Grimm F, et al. Occurrence and management of postoperative pneumocephalus using the semi-sitting position in vestibular schwannoma surgery. *Acta Neurochirurgica* (2020) 162 (11):2629–36. doi: 10.1007/s00701-020-04504-5

23. Ansari SF, Terry C, Cohen-Gadol AA. Surgery for vestibular schwannomas: a systematic review of complications by approach. *Neurosurg Focus* (2012) 33(3):E14. doi: 10.3171/2012.6.FOCUS12163

24. Verdu E, Ceballos D, Vilches JJ, Navarro X. Influence of aging on peripheral nerve function and regeneration. *J Peripher Nerv Syst* (2000) 5(4):191–208. doi: 10.1111/j.1529-8027.2000.00026.x

25. Tatagiba M, Ebner FH, Nakamura T, Naros G. Evolution in surgical treatment of vestibular schwannomas. *Curr Otorhinolaryngol Rep* (2021) 9(4):467–76. doi: 10.1007/s40136-021-00366-2

26. Pennings RJ, Morris DP, Clarke L, Allen S, Walling S, Bance ML. Natural history of hearing deterioration in intracanalicular vestibular schwannoma. *Neurosurg* (2011) 68(1):68–77. doi: 10.1227/NEU.0b013e3181fc60cb

27. Watanabe S, Yamamoto M, Kawabe T, Koiso T, Yamamoto T, Matsumura A, et al. Stereotactic radiosurgery for vestibular schwannomas: average 10-year follow-up results focusing on long-term hearing preservation. *J Neurosurg* (2016) 125(Suppl 1):64–72. doi: 10.3171/2016.7.GKS161494

28. Tolisano AM, Hunter JB. Hearing preservation in stereotactic radiosurgery for vestibular schwannoma. *J Neurol Surg B Skull Base* (2019) 80(2):156–64. doi: 10.1055/s-0039-1677680

29. Shin M, Ueki K, Kurita H, Kirino T. Malignant transformation of a vestibular schwannoma after gamma knife radiosurgery. *Lancet* (2002) 360(9329):309–10. doi: 10.1016/S0140-6736(02)09521-1

30. Carlson ML, Barnes JH, Nassiri A, Patel NS, Tombers NM, Lohse CM, et al. Prospective study of disease-specific quality-of-Life in sporadic vestibular schwannoma comparing observation, radiosurgery, and microsurgery. *Otol Neurotol* (2021) 42(2): e199–208. doi: 10.1097/MAO.0000000000002863

31. Vakilian S, Souhami L, Melancon D, Zeitouni A. Volumetric measurement of vestibular schwannoma tumour growth following partial resection: predictors for recurrence. *J Neurol Surg B Skull Base* (2012) 73(2):117–20. doi: 10.1055/s-0032-1301395

32. Seol HJ, Kim CH, Park CK, Kim CH, Kim DG, Chung YS, et al. Optimal extent of resection in vestibular schwannoma surgery: relationship to recurrence and facial nerve preservation. *Neurol Med Chir (Tokyo)* (2006) 46(4):176–80; discussion 80-1. doi: 10.2176/nmc.46.176

33. Simpson D. The recurrence of intracranial meningiomas after surgical treatment. *J Neurol Neurosurg Psychiatry* (1957) 20(1):22–39. doi: 10.1136/jnnp.20.1.22

34. Brown TJ, Brennan MC, Li M, Church EW, Brandmeir NJ, Rakszawski KL, et al. Association of the extent of resection with survival in glioblastoma: a systematic review and meta-analysis. *JAMA Oncol* (2016) 2(11):1460–9. doi: 10.1001/jamaoncol.2016.1373

frontiers | Frontiers in Oncology

TYPE Review
PUBLISHED 07 June 2023
DOI 10.3389/fonc.2023.1161752

OPEN ACCESS

EDITED BY
Arianna Rustici,
University of Bologna, Italy

REVIEWED BY
Kamil Krystkiewicz,
Copernicus Memorial Hospital, Poland
Alessandro Carretta,
University of Bologna, Italy

*CORRESPONDENCE
Alberto Iannalfi
alberto.iannalfi@cnao.it

†These authors have contributed equally to this work and share first authorship

RECEIVED 08 February 2023
ACCEPTED 19 May 2023
PUBLISHED 07 June 2023

CITATION
Iannalfi A, Riva G, Ciccone L and Orlandi E (2023) The role of particle radiotherapy in the treatment of skull base tumors. *Front. Oncol.* 13:1161752. doi: 10.3389/fonc.2023.1161752

The role of particle radiotherapy in the treatment of skull base tumors

Alberto Iannalfi*†, Giulia Riva†, Lucia Ciccone† and Ester Orlandi†

Radiation Oncology Unit, Clinical Department, National Center for Oncological Hadrontherapy (CNAO), Pavia, Italy

The skull base is an anatomically and functionally critical area surrounded by vital structures such as the brainstem, the spinal cord, blood vessels, and cranial nerves. Due to this complexity, management of skull base tumors requires a multidisciplinary approach involving a team of specialists such as neurosurgeons, otorhinolaryngologists, radiation oncologists, endocrinologists, and medical oncologists. In the case of pediatric patients, cancer management should be performed by a team of pediatric-trained specialists. Radiation therapy may be used alone or in combination with surgery to treat skull base tumors. There are two main types of radiation therapy: photon therapy and particle therapy. Particle radiotherapy uses charged particles (protons or carbon ions) that, due to their peculiar physical properties, permit precise targeting of the tumor with minimal healthy tissue exposure. These characteristics allow for minimizing the potential long-term effects of radiation exposure in terms of neurocognitive impairments, preserving quality of life, and reducing the risk of radio-induced cancer. For these reasons, in children, adolescents, and young adults, proton therapy should be an elective option when available. In radioresistant tumors such as chordomas and sarcomas and previously irradiated recurrent tumors, particle therapy permits the delivery of high biologically effective doses with low, or however acceptable, toxicity. Carbon ion therapy has peculiar and favorable radiobiological characteristics to overcome radioresistance features. In low-grade tumors, proton therapy should be considered in challenging cases due to tumor volume and involvement of critical neural structures. However, particle radiotherapy is still relatively new, and more research is needed to fully understand its effects. Additionally, the availability of particle therapy is limited as it requires specialized equipment and expertise. The purpose of this manuscript is to review the available literature regarding the role of particle radiotherapy in the treatment of skull base tumors.

KEYWORDS

particle radiotherapy, proton radiotherapy, carbon ion radiotherapy, skull base tumors, pediatric tumors, sellar tumors

Introduction

The skull base is an anatomically complex and functionally critical area. Because of their anatomical location, the management of skull base tumors is challenging for both neurosurgeons and radiation oncologists.

Surgery is often the first step in therapeutic management to obtain pathologic sampling, improvement of symptoms, and cytologic reduction. Due to the proximity of critical vasculo-nervous structures, total removal of the tumor is often not possible or could be achieved at the price of potentially life-threatening complications (1, 2).

Maximum safe surgical resection, usually followed by radiation therapy (RT), represents the standard of care for many skull base tumor histologies, both malignant and benign.

Improvements in RT technology, such as intensity-modulated radiotherapy (IMRT) or volumetric arc therapy (VMAT), have allowed precise delivery of RT doses to skull base lesions.

However, due to the proximity to some organs at risk (OARs), such as the brainstem and the optic pathways, and the need to deliver very high doses (even over about 70 Gy) for radioresistant histologies, RT with photons may not be sufficient to obtain good control of disease without side effects.

Particle radiotherapy (PRT) using protons or heavy ions is probably currently the most advanced form of RT and offers new opportunities for improving cancer care and research.

Protons and heavy ions, such as carbon ions, can potentially improve dose sparing of normal tissues through the exploitation of the Bragg peak phenomenon, resulting in an increase in energy deposition with penetration depth up to a sharp maximum followed by a rapid decrease at the end of the penetration range (3). These features permit more precise and conformal dose localization to the target compared with conventional photon RT (Figure 1).

Moreover, considering carbon ions, other biological advantages are provided in addition to the improved physical dose distribution, owing to the high relative biological effectiveness (RBE) of radiation with high linear energy transfer (LET) (4).

RBE is the parameter that expresses quantitatively the biological effect of PRT, which is the ratio between the reference photon radiation and the PRT that produces the same biological effect.

Because carbon ion beams have a high LET, they can create clusters of DNA damage that cannot be repaired. Carbon ions are more effective than protons and photons for the treatment of hypoxic cells, with fewer variations in radiosensitivity related to the cell cycle.

Currently, according to the Particle Therapy Co-Operative Group (PTCOG) website, there are 115 particle therapy facilities clinically active: 101 proton centers, eight carbon ion centers, and six centers with both carbon ions and protons (5).

This review summarizes published literature and assesses the present status regarding the role of proton (PT) and carbon ion (CIRT) therapy in skull base tumors.

Chordomas

Chordomas are rare primary bone tumors arising from notochord remnants, with an incidence of 0.8–1 case per 1 million population/year (6). These tumors arise mostly in the axial skeleton, with the midline clivus involved in approximately one-third of cases.

Currently, the World Health Organization (WHO) histologically defines three types of chordoma: conventional chordoma, dedifferentiated chordoma, and poorly differentiated chordoma (7). Chordoma is immunopositive for epithelial markers such as cytokeratins (CKs) and endothelial membrane antigen (EMA) and can also be positive for S-100 and vimentin (8). Brachyury was recognized as the diagnostic hallmark for chordoma staining to discriminate chordomas from histological entities with similar morphological characteristics (7). In poorly differentiated chordomas, tumor cells are positive for broad-spectrum CKs and brachyury; they show loss of SMARCB1/INI1, and the S100 protein is rarely expressed (9).

Chordomas are locally aggressive and invasive and generally slow-growing; therefore, they are often clinically silent until the late stages of the disease. Clinically, patients mostly present with headache and cranial nerve deficits (especially diplopia, vision impairment, and trigeminal neuralgia), sensorimotor deficits, pituitary dysfunction, and hydrocephalus (10). Metastases are rare at the time of diagnosis and can occur in the lung, liver, bone, lymph nodes, and other sites, but the prognosis is more related to the local aggressiveness of chordoma than to its potential to metastasize.

The large tumor burden at the time of diagnosis and the surrounding critical structures, such as the brainstem, cavernous sinus, and optic apparatus, could often preclude a gross total resection (GTR). Surgery should aim towards maximum tumor resection combined with preservation of neurological function and quality of life, decompressing the brainstem and optic pathway, and reducing the volume of disease to enhance the effectiveness of subsequent RT (11–13).

Due to the low radiosensitivity of chordomas, different studies have reported that a dose escalation to at least 70 Gy is needed to improve tumor control rate, even though these doses are often difficult to achieve with conventional photons due to directly adjacent vital structures (14, 15).

Advances in RT technology with the introduction of PRT have led to higher doses of radiation delivered to the target volume with minimal injury to the surrounding tissue and improved radiobiological effects (7).

Both PT and CIRT have been successfully used in the treatment of skull base chordoma, and good results have been reported with limited severe acute and late toxicity and a high probability of local control (LC). Because protons have a longer treatment history and have been applied in multiple centers over the past 25 years, their series are larger than carbon ions (16–23) (Table 1).

Five-year LC ranged between 59% and 84%, whereas 5-year overall survival (OS) rates ranged from 72% to 83%. The largest published study reported 10-year LC and OS rates of 54% and 75%, respectively (18).

Some prognostic factors for LC have consistently been reported to be of predictive value, whereas others have only been sporadically discussed. Regarding the influence of residual tumor volume after surgery, many series have reported the residual tumor volume to be a prognostic factor for LC, with different cut-off points ranging from 10 cc to 75 cc (18–22, 24).

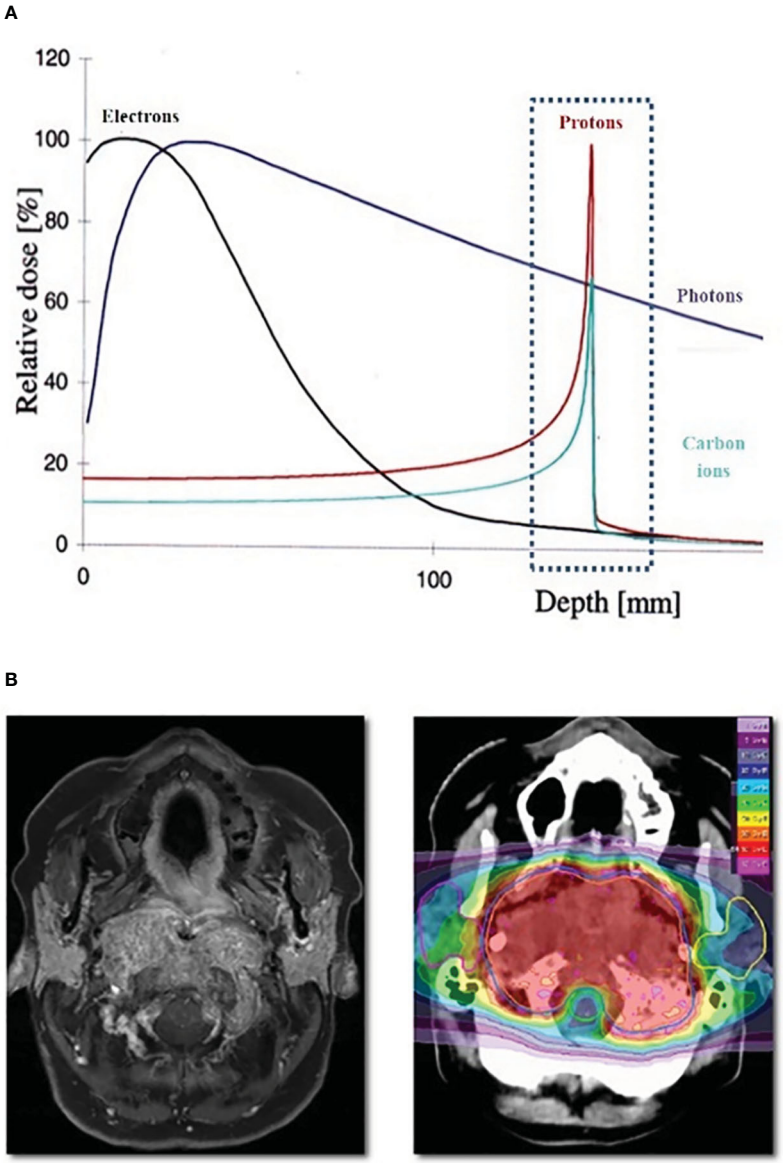

FIGURE 1
(A) Bragg Peak Curve Plot; **(B)** Example of particle radiotheraphy plan for skull base tumor.

Furthermore, the presence of low-dose regions and dose inhomogeneity within the gross tumor volume (GTV) is a primary reason for local recurrence. The underdosing of a tumor's portion may increase the risk of local recurrence, but on the other hand, some portions of the target are underdosed to meet constraints on critical normal structures; this critical situation is intrinsically due to the occurrence of disease in very close proximity to or involving brainstem or optic pathways (22). The prognostic factors emphasize the importance of the combination strategy of maximally safe resection followed by PRT, which permits high biologically effective doses. In the event that that the surgeon determines that a maximally safe resection is not feasible, a debulking "space" surgery that creates distance between tumor and organ at risk should be considered to favor the delivery of a high RT dose in the most optimal way by PRT. In this perspective, the sharing of combined treatment planning strategies between the surgeon and radiation oncology is crucial to obtaining the most favorable clinical outcomes within the framework of the network, which includes highly specialized centers for the management of skull base tumors.

Although Munzenrider et al. raised the issue of female patients having decreased local control rates (17), this data was not confirmed by other series, and, according to a recent retrospective analysis of 238 patients with skull base chordomas, sex was not found to have a predictive value (24).

Moreover, except for Jahangiri and colleagues, who identified tumor localization in the middle and lower third of the clivus as other risk factors for recurrence, no relation between the site of residual tumor and LC was reported in other series (25).

TABLE 1 Patients and treatment description of chordomas irradiated with proton or carbon ion (selected series).

Study	Particle	Patients (number)	Follow-up (months)	RT Dose (GyRBE)	LC (%)	OS (%)	Severe late toxicity
Hug, 1999 (16)	P	33	33 (median)	TD: 65–79 Dpf: 1.8–2	5-y: 59	5-y: 79	7%
Munzenrider, 1999 (17)	P + ph	169	41 (median)	TD: 66–83 Dpf: 1.8–1.9	5-y: 73 10-y: 54	5-y: 80 10-y: 54	Disaggregated data not reported or limited cohort followed-up for toxicity outcomes
Uhl, 2014 (18)	C	155	72 (median)	TD: 60 (median) Dpf: 3	5-y: 72	5-y: 85	0%
Weber, 2016 (19)	P	151	50 (mean)	TD: 72.5 (mean) Dpf: 1.8–2	7-y: 70.9	7-y: 72.9	8%
Fung, 2018 (20)	P + ph	106	61 (mean)	TD: 8.4–73.8 Dpf: 1.8	5-y: 75	5-y: 88	7%
Koto, 2019 (21)	C	34	108 (median)	TD: 60.8 (median) DpF: 3.8 (median)	5-y: 77	5-y: 93	11%
Iannalfi, 2020 (22)	P	135	49 (median) whole series	TD: 74 (median) Dpf: 1.8–2	5-y: 84	5-y: 83	12% (2% expected for tumor very close to optic nerve and/or pre-existing severe deficit). No G3 brain necrosis.
Iannalfi, 2020 (22)	C	65	49 (median) whole series	TD: 70,4 Dpf: 4.4	5-y: 71	5-y: 82	12% (2% expected for tumor very close to optic nerve and/or pre-existing severe deficit). No G3 brain necrosis.
Mattke, 2022 (23)	P	36	36 (median)	TD: 74 (median) Dpf: 1.8-2	5-y: 61	5-y: 92	13% (cumulative rates of brain injury) G3 toxicity reported, but disaggregated data for G3 not reported
Mattke, 2022 (23)	C	111	52 (median)	TD: 66	5-y: 65	5-y: 83	13% (cumulative rates of brain injury) G3 toxicity reported, but disaggregated data for G3 not reported

P, proton; C, carbon; RT, radiotherapy; TD, total dose; Dpf, dose per fraction; LC, local control; y, years; OS, overall survival.

In primary PRT, the target volume delineation should be primarily based on the concept of risk-based volumes, considering preoperative disease extension, potential dissemination ways, data emerging from a detailed surgical report (as dural infiltration), and post-operative changes (12, 22).

Loco-regional relapse is a relatively common pattern of recurrence following initial treatment of chordoma patients and includes progression of the treated primary tumor, lesions recurring near surgical margins, or lesions developing because of iatrogenic seeding along a biopsy or surgical tract (26, 27). Salvage treatment choices represent a major clinical challenge and can include surgery and/or RT, balancing morbidity and expected disease control.

The choice of the best treatment strategy between surgery alone, surgery plus RT, and RT alone must be based on an individual case evaluation. Potential eligible patients for a complete surgical re-intervention are patients presenting isolated disease, a long disease-free interval, good performance status, and a reasonable likelihood of acceptable morbidity (26).

Uhl et al. (27) reported outcomes regarding reirradiation (re-RT) with carbon ions performed on 25 patients with locally recurrent skull base chordoma (n = 20) or chondrosarcoma (n = 5). Fourteen of the patients underwent PRT (CIRT/PT) as previous RT, with a median dose of 60 GyE (range: 42–72 GyE), while 11 of them had photon therapy with a median dose of 66 Gy. The median applied total dose of re-RT with carbon ions was 51 GyE (range: 45–60 GyE) in five to six fractions of 3 GyE per week, and it was reported as correspondence to a median equivalent dose of 63.8 GyE (range: 56.2–75 GyE) calculated for a fraction dose of 2 Gy (EQD2 Gy) and an alpha/beta ratio of 2. The 2-year local progression-free survival (PFS) probability was 79.3%. Five cases of recurrence occurred in chordomas, but only one in chondrosarcomas. A planning tumor volume (PTV) of <100 ml or a total dose of >51 GyE was correlated with an improved LC rate. Low acute toxicity was described: one patient developed grade (G) 2 mucositis during therapy, while three patients had hypoacusis related to a new onset of temporary middle ear effusion (G2). Furthermore, five patients developed an asymptomatic temporal lobe reaction after treatment without the need for surgical intervention (G1). Only one patient had a G3 osteoradionecrosis in the treatment area 1 month after irradiation, which required surgery. In 84% (21/25) of patients, the tumor-associated symptoms were stable or had decreased after therapy (27).

In the case of recurrent disease after previous RT, a re-RT can be indicated only in the following situations: re-RT can be delivered without exceeding the estimated dose tolerance limits on OARs, and appropriate dose coverage of target volumes can be obtained. Conversely, other treatment strategies should be preferred. Currently, the cumulative dose tolerance for the most critical OARs and the degree of recovery of healthy tissue receiving radiation dose after the first course of RT and its potentially protective role are still widely preliminary and very difficult to estimate (26, 28).

In the case where a complete macroscopic resection of a recurrent lesion cannot be likely obtained and proximity to critical structures does not permit adequate RT coverage of target volumes, debulking "space" surgery may be an adequate solution to create a distance between the critical structures and the residual recurrent tumor, thereby allowing delivery of a tolerable radiation dose (26).

The radiation oncologist must be develop the radiation plans based on an accurate reconstruction of the previous RT dose distribution and taking into account expected morbidity of second radiation. If a re-RT can be delivered without exceeding the estimated dose constraints on OARs, the patient should be treated with the same intent and approach as a RT naïve recurrence. When this goal is not achievable, sufficient data are not available to recommend an optimal dose and fractionation scheme for radiation in this setting and radiation oncologists should develop a treatment plan for obtaining the best balance between the higher RT dose with adequate target volume coverage and respecting dose constraints (26).

In cases of tumor seeding in the surgical pathway, the site of recurrence is often "out of field" regarding the previously irradiated volume, and the relapsed site can be adequately and easily treated by RT at higher curative doses. Low-dose re-RT with palliative intent can be appropriate in selected cases, but only if it can be performed with a negligible risk of toxicity. The use of high-LET radiation, such as CIRT, may be estimated as a more effective option against the radioresistant clones that may have been selected by the first treatment (26).

Due to the lack of sufficient data to assess dose tolerance in relation to toxicity in the re-RT of chordomas, the dose/fractionation schemes for re-RT cases have remained heterogeneous and based primarily on qualitative evaluation of the prior treatment plan. Caution is warranted in re-irradiating the carotid artery because of life-threatening complications such as carotid blowout (CBO) syndrome that have been reported in patients treated with re-RT for head and neck cancer (28).

In a recently published review, it emerged that a higher risk of CBO is likely awaited when a higher cumulative dose than 120 Gy is delivered to the carotid artery in received RT courses (28). The risk of CBO represents consequently a critical concern, often limiting the indication of the re-RT option for skull base chordomas, considering the high dose required in radiation treatment of chordomas in both primary RT and re-RT settings (26).

When re-RT, especially with carbon ions, represents the required main salvage treatment option, in the case of high-risk patients for threatened or impending CBO in the current practice, the multidisciplinary team should carefully evaluate the best preventive strategy for CBO (surgical ligation, stenting, or occlusion), similarly to how much is suggested for head and neck tumors (28).

In RT treatment of chordomas located in the lower third of the skull base and extended to the cervical spine, metal implants (e.g., for cranio-cervical stabilization) can make RT delivery more complicated by creating artifacts in radiological imaging and interfering with precise delineation of target and OAR, especially in the spinal canal. Furthermore, these artifacts affect the range calculation for PRT, determining additional uncertainty in the delivered dose (12, 26). Theoretically, the presence of metal implants should be considered a critical factor in deciding not to deliver curative RT or in deciding to deliver it with photons, which are less sensitive to artifacts compared to particles.

Especially in the setting of patients with newly diagnosed skull base chordomas invading the cranio-spinal junction and extending to the cervical spine, a multidisciplinary assessment involving a surgeon and radiation oncologist is mandatory to plan a better combined strategy. In many cases, this problem can be resolved in the current practice by sharing the best geometric arrangement of craniocervical metal implants and screw fixation to obtain stabilization and be compatible with the particle beam geometry assessment estimated based on disease extension on pre-surgery imaging. In other cases, the shared decision by surgeons and radiation oncologists to postpone stabilization after PRT can represent the best option.

In the case of treatment of recurrent disease with metal implants previously positioned, especially if a debulking or separating surgery is planned, the possibility of modifying, removing, or substituting metal implants with non-metal implant devices (carbon fiber devices) should be considered to enable radiation with potentially curative intent; however, this represents an appropriate choice only in very well selected cases after an accurate multidisciplinary evaluation (26). It is important to underline that in craniocervical junctions, in current practice, the required curvature of bars is very often not compatible with the availability of carbon fibers (or other non-metal based) devices.

Chondrosarcomas and other sarcomas

Chondrosarcomas are a heterogeneous group of slow-growing neoplasms originating from cartilage-producing cells in enchondral ossification areas, with an incidence of 0.2 per 100,000 cases (29). At the base of the skull, common sites of involvement are usually represented by the temporo-occipital junction, parasellar area, spheno-ethmoidal complex, and clivus.

WHO grading of chondrosarcomas is essential and useful in predicting histological behavior. Chondrosarcomas are divided into three grades based upon their histopathology: grade I, considered to be low-grade and usually indolent with minimal malignant potential regardless of their location and presentation; grade II; and grade III (30). A fourth group considered grade IV, makes up

10% of all chondrosarcomas and, by definition, is a high-grade neoplasm with an inferior prognosis (31).

Histological subtypes include the following: classical/conventional (85% of all chondrosarcomas), mesenchymal, clear cell, and dedifferentiated (10, 31).

Skull base chondrosarcomas are slow-growing tumors that gradually progress at the base of the skull structures from abutting or encasing them to subsequently invading critical organs. Most patients are asymptomatic or develop symptoms at a later stage of the disease as a result of infiltration and compression of the surrounding neural structures (headache, diplopia secondary to abducens nerve palsy, lower cranial nerve deficits) (32).

The dominant failure pattern after treatment for a skull base chondrosarcoma is local recurrence, and surgery is the cornerstone of the primary management of this disease. However en bloc resection/GTR with sufficient surgical margin is universally challenging due to the complexity of the anatomy. In 2009, a systematic literature review demonstrated a significant reduction in the 5-year rate of local recurrence from 44% after surgery alone to 9% after RT (29).

However, to achieve adequate LC, high radiation doses are necessary due to relatively high radioresistance. Given the need for high doses and the sparing of the OARs, PRT has been used in the treatment of skull base chondrosarcomas to accomplish this goal.

The review by Amichetti et al. reported 5-year and 10-year LC rates after PRT in patients with chondrosarcomas of the skull base of 75% to 99% and 98%, respectively (33).

In Table 2, clinical outcomes of the largest series of skull base chondrosarcoma treated with PRT are summarized (16, 34–36).

Chondrosarcoma is perhaps the most common histotype of sarcoma starting at the skull base, but it is not the only one. Literature on the use of PRT for the treatment of the base of skull sarcomas other than chordoma and chondrosarcoma, which are usually more aggressive, is scarce (37, 38).

Few data concerning other types of skull base sarcomas are reported in case series or in inclusive studies of different sarcomatous histologies, such as the study by Yang and colleagues published in 2020. In this study, the authors reported the clinical outcomes of 62 patients with skull base bone or soft-tissue sarcomas (chordoma excluded) treated with PRT (both proton and carbon ion) as primary RT or re-RT for relapse (38).

Among the 45 radiation-naïve patients in this study, 2-y PFS and OS were 62.9% and 80.2%, respectively (38).

However, for a rare condition such as skull base sarcoma, it will be difficult to perform prospective randomized trials concerning PRT for each histological subtype of the disease because patients' treatment in terms of surgery and chemotherapy varies substantially.

Meningiomas

Meningiomas are the most common primary intracranial tumor, with an incidence rate of 37.6% (39).

The WHO 2021 classifies meningiomas into three different histopathological types: grade I (benign), which has a low recurrence rate and accounts for 80% of cases; grade II (atypical), which comprises 20%–30% of patients and has a recurrence rate of 30%–40%; and grade III (anaplastic), which is found in 1%–2% of patients and almost surely recurs (40).

The diagnosis of meningioma is most common in middle and old age. The frequency increases with age, and women are twice as likely to be diagnosed as men (39, 41, 42).

The occurrence risk of a meningioma is linked to previous cranial exposure to ionizing radiation and previous brain RT in childhood. Furthermore, the risk is associated with a genetic condition called type 2 neurofibromatosis (NF2). In fact, NF2 patients are more likely to develop WHO 2–3 or multiple meningiomas (39).

Finally, growing data suggest an association between the prolonged exposure of women to endogenous or exogenous sex hormones and meningioma. An association with breast cancer and a higher incidence in reproductive age (increasing during pregnancy and decreasing after delivery) and in menopause is reported. Progesterone receptor expression may be involved in the occurrence of meningiomas (43).

With the increase in neuroimaging availability, incidental meningioma diagnoses have increased. The 1% of the general

TABLE 2 Patients and treatment description of chondrosarcomas irradiated with proton or carbon ion (selected series).

Study	Particle	Patients (number)	Follow-up (months)	RT Dose (GyRBE)	LC (%)	OS (%)	Severe late toxicity
Hug, 1999 (16)	P	25	33 (median)	TD: 69.3 (mean) Dpf: 1.8	5-y: 75	5-y: 100	7%
Weber, 2016 (34)	P	77	69.2 (mean)	TD: 70.0 (mean) Dpf: 1.8–2	8-y: 89.7	8-y: 93.5	8%
Mattke, 2018 (35)	P	22	30.7 (median)	70 (median)	4-y: 100	4-y: 100	0%
Mattke, 2018 (35)	C	79	43.7 (median)	60 (median)	4-y: 90.5	4-y: 92.9	0%
Riva, 2021 (36)	P	32	31 (median)	TD: 74 (median) Dpf: 2	3 y LC: 100%	–	6%
Riva, 2021 (36)	C	16	66 (median)	70.4 Dpf: 4.4	3 y LC: 94%	–	12%

P, proton; C, carbon, RT, radiotherapy; TD, total dose; Dpf, dose per fraction; LC, local control; y, years; OS, overall survival.

population that undergoes a brain magnetic resonance imaging (MRI) presents an incidental meningioma (39).

Surgically accessible meningiomas that can be safely removed have indications for surgical resection. The cornerstone of symptomatic or growing meningiomas is maximal surgical resection, minimizing morbidity and preserving neurological functions. However, as happens with skull base tumors located close to the cavernous sinus, total removal is rarely achieved without a planned subtotal resection. Incomplete surgical removal is associated with an increased risk of progression. Afterward, according to grade, residual meningioma can be monitored or treated with postoperative RT. The interval from surgery to progression can be long, and the timing of RT after incomplete surgery or when meningioma relapses remains questioned (2).

External beam RT improves LC, and new advanced radiation techniques can provide excellent target dose coverage, precise target localization, and accurate dose delivery. Photon-based RT is usually recommended as adjuvant therapy or as the primary treatment for meningioma. Several RT techniques have been developed: IMRT, VMAT, and stereotactic irradiation modalities (i.e., Gamma Knife, CyberKnife) (39, 44).

PRT is an option in meningioma management as an alternative to photon RT. PT is the most common PRT used in clinical practice (40, 42). Another option is represented by CIRT, whose use is reserved especially for re-RT after disease progression (41).

PT has a radiobiological superior advantage over photon RT due to the capability to deposit most of the particle energy at the end of their trajectory with a very little exit dose beyond the target, sparing surrounding healthy tissues. Furthermore, PRT is characterized by a RBE equal to 1.1 and 1.5–3.0 for proton and ion-carbon, respectively (45).

Consequently, for patients with potentially long-term survival, PT may be proposed for skull base meningiomas, especially in cases of complex shapes and larger volumes.

Moreover, a better profile of dose distribution decreases the risk of treatment-related side effects (i.e., radionecrosis and neurocognitive impairment) and the risk of potential radiation-induced secondary malignancy (2). In the dedicated paragraph below, selection criteria for PRT in low-grade skull base tumors are discussed. In a smaller portion of the patients, the meningiomas with skull base location present higher-grade types (WHO II–III), which required a higher dose level. For this reason, the achievement of the most favorable ratio between optimal coverage of treatment volume with a therapeutic higher dose and the sparing of tolerance dose to critical structures can further represent a critical advantage of PT in the treatment of higher-grade skull base meningiomas, especially in cases with the closest proximity of tumors with brainstem and/or optic pathways.

PT is successfully utilized for meningioma (skull base and other localizations) treatment, with both a good achievement of LC and a few reports of acute and severe toxicities. Characteristics of the principal studies of PT for meningioma are summarized in Table 3 (46–54).

Meningiomas often recur over time, regardless of the initial extent of surgery, and repeating surgery with/without the use of adjuvant therapeutic options may be necessary. PT may be a treatment option when surgery is not feasible. In fact, due to its higher RBE, it is feasible to treat more radioresistant diseases, such as a recurrence of pre-irradiated meningioma, with a lower burden of side effects.

Champeaux-Depond et al. reviewed 193 cases of recurrence or progression of meningioma that underwent PT (55).

Five-year PFS was 71.5% (95% CI 64.4–79.4), 55.6% (95% CI 32.5–95), and 35.6% (95% CI 12.8–98.9) for WHO G1, G2, and G3 meningiomas, respectively. Five-year OS rates were 93% (95% CI 88.7–97.4), 76.4% (95% CI 51.4–100), and 44.4% (95% CI 16.7–100) for WHO G1, G2, and G3 meningiomas, respectively (55). Recurrences after RT in patients with meningiomas generally represent a very challenging clinical situation: prior RT has often completely saturated the margin of radiation tolerance of critical organs, and for this reason any additional RT must be performed using highly advanced RT modalities. Skull base location represents a very critical feature, which further contributes to the high degree of difficulty in performing effective re-RT. In terms of treatment alternatives, the risk of neurosurgical intervention can be associated with high rates of treatment-related sequelae.

El Shafie et al. (56) published the results of 42 patients treated with PRT for recurrent intracranial meningioma after previous irradiation. The location was the skull base in 73.8% of patients. Concerning dose received in previous RT, the median dose was 52.9 Gy (range 12.1–62.4 Gy) for IMRT (n = 16 patients), while the median dose for 3-dimensional conformal RT (n = 16 patients) was 54 Gy (range 50.5–55.8 Gy); seven patients received stereotactic radiosurgery (SRS) at a median dose of 12.1 Gy (range 12.0–17.0 Gy), and one patient received fractionated stereotactic RT (FSRT) at a cumulative dose of 58.8 Gy. One patient had previously received radiopeptide therapy with Y-90 DOTATATE at 4.39 GBq, corresponding to an approximated local dose of 10 Gy, whereas another patient previously received previous CIRT due to tumor progression. The patients were treated with PT in 19% of cases (n = 8) and CIRT in 81% of cases (n = 34). The median total dose of PRT was 51 Gy (RBE) [range 15–60 Gy (RBE)]. Four patients received bimodal treatment with a carbon ion boost and a photon base plan: 15 Gy (RBE) (n = 1) or 18 Gy (RBE) (n = 3), applied after 50–52 Gy of photon irradiation. For CIRT, most commonly, a dose per fraction of 3 Gy (RBE) was applied, as well as a dose per fraction of 3.3 Gy in one case. For PT, smaller doses per fraction, such as 1.8 Gy (RBE) or 2 Gy (RBE), were used. Different fractional schemes of PRT were applied depending on the previous treatment dosimetry, and the goal was to deliver a dose upward of 50 Gy (RBE) for WHO-1 tumors and upward of 54 Gy (RBE) for higher-grade tumors. The PFS after 12 months accounted for 71% and 56.5% after 24 months, and the OS was 89.6 and 71.4%, respectively. Histology impacted PFS significantly for high WHO G2/G3 tumors; the median PFS was 25.7 months, while the median PFS was not reached for WHO 1 tumors due to a limited number of events. No significant difference in PFS could be detected between WHO G2 and G3 meningiomas. Notably, it is relevant that the tumor volume treated was large: the mean GTV was 51.3 ml, while the median GTV was 18.1 cc. The OS after re-RT was 89.6% after 12 months and 71.4% after 24 months, with a median OS of 61 months (95% CI 34.2–87.7). The WHO grading had a relevant effect, as the

TABLE 3 Patients and treatment description of meningiomas irradiated with proton or carbon ion (selected series).

Study	Site	WHO grade	Particle	Patient (number)	Follow up (Month)	RT dose (GyRBE)	LC (%)	OS (%)	Toxicity
Gudjonsson, 1999 (46)	Skull base	15 (G1) 4 (Unknown)	P	19	36 (at least)	TD: 24 DpF: 6	3-y: 100	/	No severe toxicity
Vernimmen, 2001 (47)	Skull base	23 (G1)	P	23	40 (mean)	TD: 54-61.1 Dpf: 16-27	5-y: 88	/	Late toxicity (any grade): 11%
Weber,2004 (48)	Skull base + Other sites	11 (G1) 2 (G2)	P	13	34 (median)	TD: 56 (median) Dpf: 1.8-2	3-y: 100	3-y: 84	Late toxicity (any grade): 19%
Halasz, 2011 (49)	Skull base + Other sites	50 (G1)	P	50	32 (median)	TD: 13 DpF: 13	3-y: 94	/	/
Weber, 2012 (50)	Skull base + Other sites	23 (G1) 9 (G2) 2 (G3) 5 (Unknown)	P	39	54.8 (median)	TD: 56 (median) Dpf: 1.8–2	5-y: 84.6	5-y: 82	Late toxicity (any grade): 41% Severe late toxicity: 13%
Combs, 2013 (51)	Skull base	71 (G1) 36 (G2-3)	P ± C boost	107	12 (median)	TD P: 52.2–57.6 TD C: 18	LC at the end of FUP WHO G1: 100 2-y WHO G2–3: 33%	3-y: 100	/
Murray, 2017 (52)	Skull base + Other sites	61 (G1) 35 (G2–3)	P	96	56.9 (median)	TD WHO G1: 54 (median) TD WHO G2-3: 62 Dpf: 1.8–2	5-y WHO G1: 95 5-y WHO G2: 69	5-y WHO G1: 92 5-y WHO G2: 80	Late toxicity (any grade): 45% Severe late toxicity: 10%
Vlachogiannis,2017 (53)	Skull base + Other sites	170 (G1)	P	170	84	TD: 14–46 Dpf: 3–8	5-y: 93	/	Late toxicity (any grade): 9%
El Shafie, 2018 (54)	Skull base	60 (G1) 7 (G2) 1 (G3) 42 (Unknown)	P +/- C boost	110	46.8 (median)	TD P: 54 TD P+C: 50 P + 18 C	5-y: 96.6	5-y: 96.2	Severe late toxicity: 3.6%

WHO, World Health Organization; P, proton; C, carbon; RT, radiotherapy; TD, total dose; Dpf, dose per fraction; LC, local control, y, years, OS, overall survival.

median OS for low-risk patients was not reached, whereas for high-risk patients it was 45.5 months. Treatment was performed safely without interruption, and no G4 or G5 toxicities were observed. In total, three patients developed radiation necrosis; two required surgeries (G3), and one was treated with corticosteroid administration (G1) (56).

Imber et al. (57) reported a review of 16 patients who received PT re-RT for recurrent meningiomas. The location was the skull base in 69%. At diagnosis, 44%, 50%, and 6% of patients presented WHO G1, G2, and G3 tumors, respectively. The median dose received with prior RT was a median of 54 Gy (range 13–65.5). The median time between the prior RT and the PT re-RT was 5.8 years (range 0.7–18.7). The median PT dose was 60 Gy (RBE) (range 30–66.6), and the median PTV was 76 cm^3 (range 8–249). The median follow-up was 18.8 months. At the last follow-up (range 1.2–41.5 months), 44% of intracranial recurrences and 19% of disease-related deaths were found. The median cohort PFS was 22.6 months, with 1- and 2-year PFS of 80% and 43%, respectively. Median OS was not achieved, with 1- and 2-year OS of 94% and 73%, respectively; all deaths were attributed to being related to meningioma. Patients with initially WHO G1 tumors presented significantly improved PFS versus higher grades with 1- and 2-year PFS estimates of 100% versus 71% and 75% versus 29%, respectively. Longer intervals between prior RT and PT also predicted improved PFS (P = .03) and OS (P = .049). Overall, the late G ≥3 toxicity rate was five out of 16 patients. The most common post-treatment complication was new or worsening hydrocephalus in three patients. A review of the imaging acquired to plan PT re-RT suggested that all three patients had some degree of baseline radiological evidence of ventriculomegaly. Two patients (13%) developed radionecrosis at 6 and 16 months after PT; only one was symptomatic (57).

Craniopharyngiomas

Craniopharyngiomas (CPs) are rare, histopathologically neuroepithelial tumors arising from the embryological remnants of the primitive craniopharyngeal duct, or Rathke's pouch. Despite

their histopathologically low-grade classification, these patients frequently experience profound disabilities that affect their quality of life and instrumental daily activities. CPs present two classically distinct subtypes in adults: adamantinomatous (ACP) and papillary (PCP). In children, ACP is nearly total. The overall incidence of CPs is reported as 0.13–0.16 in 100,000, constituting 5%–10% of pediatric and 1%–4% of adult brain tumors, respectively (58).

The age distribution was bimodal, with one peak in 5- to 9-year-olds and another in 55- to 69-year-olds. Compared with ACP, PCP only represents 5.5% of the histologically diagnosed CPs in 0- to 29-year-olds (58).

Primarily in children affected by CPs, several studies supported the idea that the pre-operative hypothalamic involvement should address treatment strategy towards a conservative surgical approach followed by RT aimed at hypothalamic damage sparing (59–64).

In a recent consensus paper regarding surgical management of CPs in adult patients published by EANS (European Association of Neurosurgical Societies), it was recommended performing a GTR when there is no infiltration of the hypothalamus, while performing subtotal resection (STR) coupled with adjuvant RT when hypothalamic infiltration is confirmed (hypothalamic-sparing resection). Furthermore, the authors recommended the use of traditional endonasal trans-sphenoidal approaches for purely intrasellar CPs and suggested performing an expanded endonasal trans-sphenoidal approach as a first-line surgical approach for midline and retro-chiasmatic CPs without lateral extension (65).

The endoscopic endonasal approach (EEA) series can achieve high rates of GTR (68.9%) and satisfactory clinical outcomes: 64.3%–78.9% GTR rates for purely infra-diaphragmatic CPs and 66.3% GTR rates in lesions involving the supradiaphragmatic space (66). The main advantage of endoscopic EEA has been observed in more complex supradiaphragmatic lesions, which can be treated effectively and safely with this approach (67). When both approaches are feasible, the endoscopic endonasal approach has been found to be significantly associated with better surgical outcomes compared with transcranial approaches in terms of GTR rates and visual outcomes. Furthermore, favorable results for EEA have been related, though not significantly, to complications such as panhypopituitarism and diabetes insipidus. No significant rates of meningitis have been recorded between the two surgical approaches, although TCA showed a significantly lower risk of CSF leakage (68).

Furthermore, the endoscopic endonasal can be an effective approach for midline CPs in children (69). The largest adult CP meta-analysis reviewing 22 unique studies providing data for 759 cases with 68.9-month average follow-up, reported recurrence rates among adult CPs of 17% after GTR, 27% after STR + RT, and 45% after STR. The risk of recurrence after GTR vs STR + RT did not reach significance (70).

In their systematic review, Clark et al. found that also in pediatric CPs, there is no difference in 1- or 5-year PFS between the groups who underwent GTR and STR combined with radiation (5-year PFS: 77 vs 73%, respectively) (71).

Hypothalamic damage presents a detrimental impact on long-term co-morbidities, even to a severe degree, potentially impacting long-term survival and quality of life (62, 72). Hypothalamic preservation represents an important goal in driving surgical management and a comprehensive treatment strategy both for adults and children (60, 62, 65).

In patients with hypothalamic involvement, it is generally recommended a treatment strategy based on the combination of maximal resection with hypothalamic sparing and following radiotherapy on residual disease (60, 62, 65).

RT can be delivered as postoperative treatment in cases of residual disease or recurrence, and depending on the surgical strategy based on pre-operative hypothalamic involvement. Many advanced radiation techniques are available nowadays: SRS/hypofractionated stereotactic RT (HFSRT), FSRT, IMRT, and PT. LC rates ranged from 65% to 100%, with the same efficacy expected in terms of LC across different advanced radiation modalities adopted, with a range between different series due mainly to the prevalent retrospective nature of published series and the wide heterogeneity of their populations (73–82).

For example, the presence of cystic disease negatively impacts tumor control. Greenfield et al. for pediatric series with IMRT reported 5- and 10-year cystic disease PFS rates of 70.2% and 65.2%, while the 5- and 10-year solid disease PFS were the same at 90.7% (79).

Bishop et al. for pediatric series treated with IMRT or PT reported that 3-year cystic failure-free survival (CFFS) and nodular failure-free survival (NFFS) rates for the entire group were 75.5% and 95.0%, respectively, with no significant differences for disaggregated analysis for two different techniques (75). The doses adopted were 11–13 Gy in radiosurgical series and 45–54 Gy in conventionally fractionated series (1.8–2 Gy per fraction) (73–82).

The choice of RT dose schedule comes before the choice of radiotherapy modality/technique, as we will discuss widely in the paragraph below on selection criteria for PRT in low-grade skull base tumors. In CPs, the choice of fractionation depends first on the distance of the tumors from the optic pathways (76).

Conventional fractionation is adopted in cases of tumors very close (within 3 mm) or touching/compressing optic pathways, while the radiosurgical/hypofractionated schedule requests at least 3 mm of tumor distance from optic pathways. Furthermore, the larger volume (>3 cm) and complex shape of the tumor, especially in the case of cystic tumors, can influence the choice of conventional fractionation. Regardless of the patients' age, the PT in patients affected by CP is usually delivered with conventional fractionation of dose (1.8–2 Gy per fraction, 45–30 fractions, total dose 45–54 Gy) (75, 80–82). PT represents an elective option for children and adolescents with brain tumors to spare cognitive function and adaptive performance and ultimately to preserve quality of life (8, 83–93).

Particularly, CPs represent one of the pediatric brain tumor types historically most investigated, related to, and most indicated for treatment with PT (8, 83–85, 93). Dosimetric studies in CPs have shown significant better sparing of healthy tissues, especially brain volumes involved in cognitive performance as hippocampi, comparing PT with photon RT, especially delivered with the IMRT modality (83–85). Furthermore, studies with diffusion tensor imaging (DTI) have been conducted because of its sensitivity to RT-induced alterations in the structural integrity of white matter.

Uh et al. found that in patients with CPs, deep white matter structures developed an early decline during the first year after PT but subsequently recovered, and that surgical defects observed in the corpus callosum before irradiation seemed to prevent complete recovery. These findings can be considered in RT planning to enhance the recovery of white matter (94).

In the second study, the authors found that below-average baseline neurocognitive performance in patients with CPs before PT seems to be related to structural degradation of white matter tracts. Surgery, obstructive hydrocephalus, and preoperative hypothalamic involvement seem to be the main features of these degradations. Longitudinal DTI showed improving trends over 5 years after PT in global integrity and efficiency measures, particularly in children in whom a smaller brain volume was irradiated (95).

In an old clinical series of patients treated with protons, LC rates were 93% at 5 years (96, 97).

Fitzek et al. delivered combined photo-proton RT in 15 patients with a median dose of 56.9 cobalt Gy equivalent (CGE; 1 proton Gy 1⁄4 1.1 CGE) (96). The median PT dose component was 26.9 CGE.

Luu et al. treated 16 patients entirely with PT with a daily dose of 1.8 CGE for a total CGE of 50.4 to 59.4 (97).

In these old-dated series, higher radiation therapeutic doses than those currently adopted and considerations useful for current practice cannot be drawn (96, 97).

Nevertheless, Fitzek et al. reported no treatment-related neurocognitive deficits were recorded within the follow-up period, and functional status, academic skills, and professional abilities were unaltered after PT (96).

In Table 4, we summarized selected published series of patients affected by craniopharyngiomas and treated with PT (75, 80–82).

Recently, Jimenez et al. published a series on 77 patients affected by CP and treated with PT (from 2002 to 2018) with a median RT dose of 52.2 Gy. Of 77 patients, 76 (97%) received passively scattered protons and 1 (1%) received pencil beam scanning protons, which represent the current standard in PT delivery. The median age at radiation was 9.6 years. The most common presenting symptoms before were headache (58%), visual impairment (55%), and endocrinopathy (40%). Patients underwent a median of two surgical interventions (range, 1–7) before PT. At a median of 4.8 years from RT (range, 0.8–15.6), six local failures were observed, and the 5-year local failure estimate was 9.9%, while the 5-year OS was 97.7%. Only 4% developed acute G3 toxicity. Concerning visual function, the authors observed no patients with new cases of visual impairment after PT. The majority (68%) of patients with pre-existing visual impairments presented stability, with 10% improving and 10% worsening. Among those patients with worsening vision after treatment, six out of the eight patients presented documented pre-treatment poor vision, including three who presented defect severity compatible with blindness. This finding suggests that pre-treatment impairments may make patients more susceptible to additional damage, and specific attention should be focused on these patients to minimize any additional radiation exposure to the optic chiasm and optic nerves. Concerning cognitive function, the Full Scale Intelligence Quotient, Processing Index, and verbal and visual memory scores were stable and did not significantly change. Only adaptive skills showed a statistically significant decrease in mean score at follow-up compared with baseline, but clinically, this decrease was not considered significant as scores remained within the average range for patients. Five patients out of 77 (6%) developed moyamoya syndrome. New endocrinopathies were reported in 7%; among pre-

TABLE 4 Patients and treatment description of craniopharyngiomas irradiated with proton radiotherapy (selected series).

Study	Patient characteristics (number and age group)	Follow up (Months/Years)	RT dose (GyRBE)	LC (%)	Late Toxicity
Bishop, 2014 (75)	21 (children, median age 9.1 y)	33 months median	TD: 50.4–54 Dpf: 1.8	3-y NFFS rates: 91.7% 3-y CFFS rates: 67.0%	10% vascular toxicity 5% vision toxicity 19% hypothalamic morbidity 76% endocrinopathy
Ajithkumar, 2018 (82)	16 (13 patients <18 y; median age 10.2 y	32.6 months median	TD: 54 Dpf: 1.8	94%	No high grade toxicity
Rutenberg, 2020 (81)	14 (adults, median age 28 y	29 months median (clinical) 26 months median (radiographic)	TD: 52.2–54 Dpf: 1.8	100% at 3 years	Endocrinopathy G2 (29%) Insomnia G2 (7%) No high grade toxicity No vision loss or Optic neuropathy
Jimenez, 2021 (80)	77 (median age 8.6 y)	4.8 years	TD: 54 (median) Dpf: 1.8	92%	Visual impairment: (no new cases; worsened: 10%) No cognitive changes; moyamoya syndrome: 6% Endocrinopathy (new cases: 7% worsened: 47%)

RT, radiotherapy; TD, total dose; Dpf, dose per fraction; LC, local control; y, years; cystic failure-free survival (CFFS) rates; nodular failure-free survival (NFFS) rates.

existing cases, they worsened in 47%, were stable in 49%, and improved in 4%. Notably, diabetes insipidus was reduced from 36% pre-PT to 12% post-RT (80).

Bishop et al. reported the outcomes of a clinical comparison study between PT (n = 21) and IMRT (n = 31) in children. The clinical outcomes measured in terms of LC, cyst dynamics after RT, and late toxicity did not show statistically significant differences between the two techniques. Nevertheless, the main parameters testing the critical differences between these radiation modalities were not investigated: the RT dose-volume parameters for supratentorial brain and hippocampi and the neurocognitive outcomes. The 3-year CFFS and NFFS rates for the entire group were 75.5% and 95.0%: 3-year CFFS rates were 67.0% for PT and 76.8% for IMRT, but the biological significance of cyst growth is undefined; 3-year NFFS rates were 91.7% for PT vs. 96.4% for IMRT. The 3-year OS rate was 96% (94.1% PT vs. 96.8% IMRT). The proton cohort presented the following late toxicity profile: 10% of vascular morbidity (versus 10% in the IMRT cohort), 5% of vision morbidity (versus 13% in the IMRT cohort), 19% of hypothalamic obesity (versus 29% in the IMRT cohort), and 76% of endocrinopathy (versus 77% in the IMRT cohort) (75).

In a mixed series with pediatric and adult patients, Ajithkumar et al. reported the early clinical outcomes of 13 children of 16 patients included in a registry study. The control rate was 93%: five patients remained in complete remission, four were in partial remission, and seven had stable disease. There were no treatment-related grade 3 toxicities (82).

Endocrinopathy is a very common clinical morbidity in all patients with CPs, regardless of age, due to disease or treatment. Endocrine outcomes of protons series are comparable with those of other RT techniques considered relevant, with differences in reporting this outcome between different published reports (75, 80).

In the evaluation of the endocrine toxicity rates of the RT series, it should be considered that the pituitary gland is included within the target volume for these tumors. Vascular morbidity and moyamoya syndrome represent a serious concern for the treatment of CPs, especially in children, with 6%–10% rates reported in the above-mentioned proton series (75, 80). Recent studies have reviewed 644 pediatric patients at a single institution to estimate the rate of and identify risk factors for vasculopathy after PT in pediatric patients with central nervous system and skull base tumors (98). The three most common histologies were craniopharyngioma (n = 135), ependymoma (n = 135), and low-grade glioma (n = 131). The authors found the 3-year cumulative rates of any vasculopathy and serious vasculopathy were 6.4% and 2.6%, respectively, and that a maximum dose exceeding or equal to 54 CGE to the optic chiasm was significantly associated with the development of any vasculopathy (13.1% vs 2.2%; P <.001) and serious vasculopathy (3.8% vs 1.7%; P <.05). Interestingly, Lucas et al. found in their phase II prospective study that postsurgical, pre-PT vasculopathy, and PT dose to unperturbed vessels were predictive of vascular stenosis, while the effect of PT on stenosis was negligible within the surgical corridor (99). In the radiation treatment of CPs, the cystic dynamic represents a frequent and critical point in the clinical management of patients during treatment and follow-up. The cyst growth was observed in 13%–40% of cases; adaptive replanning was necessary because cyst growth was beyond the original treatment fields in 12%–24% of cases (75, 80, 100). Bishop et al. observed immediately after RT that 17 patients (33%) had cyst growth (transient in 14) and 27% experienced late cyst growth, with intervention required in 40%. Bishop et al. recommend that if there is asymptomatic early cyst growth immediately after RT, interventions should be avoided and the patients closely monitored. They emphasize the need for close observation and intervention for continued cyst expansion. Bishop et al. reported that cyst growth was related to visual and hypothalamic toxicity (P = 0.009 and 0.04) (75).

Winkfield et al. recommend surveillance imaging be performed at least every 2 weeks during PT to avoid marginal failure, while cases with large cystic components or enlargement during treatment might require weekly imaging (100). Regarding adults affected by CPs, the potential range of applications for PT is more selective. Rutenberg et al. reported in their series of 14 patients with exclusion that 3-year LC and OS rates were 100%. There were no G3 or greater acute or late radiotherapy-related side effects. There was no RT-related vision loss or optic neuropathy. No patients required intervention or treatment replanning due to tumor changes during RT (81). Ajithkumar et al. reported a series of 16 CPs treated with PT, on which three were adults. The patients received 54 Gy (RBE) of PT and a follow-up of 25 months. The three patients exhibited a complete radiological response (82).

In adult patients, the PT finds its potential application in patients not suitable for SRS and requiring conventional fractionation for larger/giant tumor volumes (maximum diameter >3 cm) and tumors with proximity to or involvement (abutting/compression) of optic pathways. The PT should be chosen among available high-precision radiotherapy modalities (such as intensity modulated techniques and fractionated stereotactic radiotherapy) that permit treatment with conventional dose fractionation when this schedule should be preferred, as discussed widely in the paragraph dedicated to clinical selection criteria for PT in skull base low-grade tumors.

Pituitary adenomas

Pituitary adenomas are usually low-grade tumors but have a significant impact on the daily quality of life of patients and health care systems. Increased availability of MRI has resulted in an increase in incidentally found pituitary lesions and clinically relevant pituitary adenomas.

Epidemiologic studies show that pituitary adenomas are increasing in incidence (between 3.9 and 7.4 cases per 100,000 per year) and prevalence (76 to 116 cases per 100,000 population) in the general population (approximately one case per 1,000 of the general population) (101).

Approximately 50% are microadenomas (<10 mm); the remaining are macroadenomas (≥10 mm) and giant adenomas (≥40 mm). Pituitary carcinomas with distant metastases are rare, occurring in 0.1% to 0.2% of cases. About two-thirds of pituitary adenomas may secrete excess hormones (102).

In 2022, the 5th Edition of the WHO Classification of Endocrine and Neuroendocrine Tumors was published. Regarding

the section dedicated to the pituitary gland, the new classification clearly distinguishes the anterior lobe (adeno-hypophysis) from posterior lobe (neuro-hypophysis) and hypothalamic tumors. In the anterior lobe, tumors were well-differentiated adenohypophyseal tumors that are now classified as pituitary neuroendocrine tumors (PitNETs; formerly known as pituitary adenomas). The routine use of immunohistochemistry for pituitary transcription factors (PIT1, TPIT, SF1, GATA3, and ERα) is included in this classification. The major PIT1, TPIT, and SF1 lineage-defined PitNET types and subtypes have distinct morphologic, molecular, and clinical differences. The "null cell" tumor, which is a diagnosis of exclusion, is reserved for PitNETs with no evidence of adenohypophyseal lineage differentiation. The term "metastatic PitNET" is advocated to replace the previous terminology of "pituitary carcinoma" (103). The treatment options include trans-sphenoidal surgery, medical therapies, and radiotherapy. Trans-sphenoidal surgical resection of adenomas represents the initial treatment option for all tumors except prolactinomas, for which medical therapy represents the first-line option (103).

Endoscopic transsphenoidal surgery in comparison with microscopic trans-sphenoidal surgery is associated with a higher GTR, no significant effect on the risk of cerebrospinal fluid leak, a reduction in the risk of diabetes insipidus, and a significantly reduced risk of septal perforation (104). SRS represents an effective treatment option regardless of the fractionation dose schedule adopted for both non-functioning and secreting pituitaries with residual or recurrent disease post-surgery or with refractory disease after medical therapy (105). Based on available data, there is no evidence supporting the superiority of SRS over FSRT for the treatment of patients with pituitary adenomas. The dose and fractionation schedules are usually prescribed based on the size and position of the pituitary adenomas (105). The single-fraction SRS may represent an appropriate approach for patients with small and medium-sized pituitary adenomas far at least 2 mm from the optic chiasm or optic nerves, while FSRT is more indicated over SRS for lesions >2.5–3 cm in size and/or involving optic pathways (105).

Some series suggest that multi-fraction SRS may be an adequate option in patients with tumors in proximity to the optic apparatus (106–109).

Recent systematic reviews and meta-analyses regarding the role of stereotactic radiosurgery in pituitary adenomas have been published by the International Stereotactic Radiosurgery Society (110, 111).

In SRS for non-functioning tumors, the following results have been reported (110). The 5-year random effects LC estimate after SRS was 94% and 97.0% after HSRT. The 10-year local control random effects estimate after SRS was 83.0%. Post-SRS hypopituitarism was the most common treatment-related toxicity observed, with a random effect estimate of 21.0%, while visual dysfunction or other cranial nerve injuries were uncommon (range: 0%–7%). The authors recommended a prescription dose of 14–16 Gy for patients treated in the definitive setting and patients with residual or recurrent disease. Hypofractionated RT (21 Gy in three fractions, 20 Gy in four fractions, or 25 Gy in five fractions) can be considered for patients with larger adenomas (>2–3 cm) or close to the optic apparatus, but it should be carefully considered due to the acknowledged lack of long-term tumor control data (110).

In SRS for secreting tumors, the following results have been reported in a systematic review published by Mathieu et al. (111).

Random effects meta-analysis estimates for crude tumor control rate, crude endocrine remission rate, and any new hypopituitarism rates ranged 92%–97%, 28%–48%, and 12–21%, respectively (111). Mean margin doses reported ranged from 13.2% to 35%, and new neurological or visual deficit rates ranged between 0% and 17%. No minimal margin dose was shown to definitively lead to better endocrine cure rates (111). Several authors supported the use of doses >30–40 Gy (112–114).

Mathieu et al. recommend that higher margin doses can be used, provided dose constraints safely protect surrounding structures at risk (optic pathways, brainstem) (111).

The FSRT achieves local control rates ranging from 91 to 100% and prescribed doses range from 45 to 54 Gy (1.8–2 Gy/fractions). Visual toxicity ranged from 0 to 7.5% and hypopituitarism ranged from 3 to 48% (105).

The published PT series included three series adopting protons with radiosurgical schedules (115–117) and one series treating patients exclusively with conventional fractionation schedules (118).

In Table 5, we summarized a selected published series of patients affected by pituitary adenomas and treated with PT (115–118).

The proton radiosurgical series adopted a dose of 20 Gy (RBE) and obtained the following results in terms of disease control outcomes. Wattson et al. reported in 165 mixed functional adenomas 98% of local control and 59% of 5-year hormonal normalization rates (117). Petit reported that in 38 ACTH-secreting adenomas, complete remission (CR) occurred in 52% of patients with Cushing disease, and the median time to complete remission was 14 months (range 5–49). Actuarial rates of CR at 5 years were 55%. Complete remission was obtained in all patients with Nelson's disease (115). Petit reported in 22 patients, with an acromegaly complete response achieved in 13 patients (59%). Among patients with CR, the median time to CR was 42 (range, 6–62) months (116).

In these series, new pituitary deficits were reported in the range of 38%–62% (115–117).

Ronson et al. reported outcomes of fractionated PT with 54 Gy CGE for treatment of pituitary adenomas: 100% of LC with 29.3% partial tumor regression and 24.4% complete tumor regression at last follow-up, while 85.7% had normalized or decreased hormone levels at last follow-up. New hypopituitarism cases were observed in 11 patients. In this series, seven patients developed minor visual deficits, and two patients developed major visual deficits that consisted of a new quadrantanopsia and bilateral optic nerve atrophy. Both patients had Cushing's disease, and the authors hypothesize that the long-term effects of hypercortisolism make the optic chiasm microvasculature of Cushing's patients susceptible to radiation injury. Furthermore, dose fractionation permits treatment of larger target volumes that may be adjacent to or

TABLE 5 Patients and treatment description of pituitary adenomas irradiated with proton radiotherapy (selected series).

Study	Patient characteristics (number and age group)	Follow up (Months/ Years)	RT dose schedule (GyRBE)	Disease Control	Late Toxicity
Ronson, 2006 (118)	47 (51% no functional) -	47 mo.	PFRT: TD: 54 median Dpf: 1.8–2	**Whole series:** Complete Tumor Regression: 24.4% Partial Tumor Regression: 29.3% Tumor Stabilization: 46.3% **Functional adenomas:** biochemical control: 85.7% CR: 38.1% PR: 47.6%	No visual worsening: 76.7% Minor visual complications: 23% Major visual complications: 4.6% New pituitary defect: 29.7% Developed panhypopituitarism: 5.4% Brain injury: one patient
Petit 2007 (116)	22 with acromegaly	6.3 y Median	**PRS** TD: 20 Dpf: 20	CR rates: 59%	No evidence of visual complications, seizure, or brain injury New pituitary deficit: 38%
Petit, 2008 (115)	38 patients 33 (CD) (range 19–60 y) 5 (NS) (range 29–53 y)	62 mo. Median	**PRS** TD: 20 Dpf: 20	(CD): CR rates: 52% 5-y CR: 55% (NS): CR rates: 100%	No evidence of optic nerve damage, seizure, or brain injury New pituitary deficit: 53%
Wattson, 2014 (117)	165 mixed Functional adenomas	4.3 y median	PRS (92%): TD: 20 Dpf: 20 PFRT (8%): TD: 50.4 Dpf: 1.8	5-y CR: 59% LC: 98%	5-y new pituitary deficit: 62% Seizures: 2% (4/165)

RT, radiotherapy; PRS, Proton Radiosurgery; PFRT, Proton Fractionated Radiotherapy; TD, total dose; Dpf, dose per fraction; LC, local control; y, years; mo, months; CR, Complete Response (biochemical); PR, Partial Response (biochemical); CD, Cushing's disease; NS, Nelson's syndrome.

even compress the optic pathways,resulting in a higher risk of injury. In these patients, particular caution is requested in radiation treatment planning, especially if additional risk factors for radiation damage are present (118).

The radiosurgical dose schedule can usually be indicated when the tumor presents at least 3 mm of distance from the optic pathways, and this condition favors fewer visual complications. In the most challenging cases of patients with optic pathways directly involved by tumors with an abutment or compression pattern, the conventional fractionated schedule is more indicated to preserve residual visual function and minimize visual worsening as much as possible. In these situations, the visual function is often variously compromised by previous radiotherapy, and this condition subjectively enhances the susceptibility to radio-induced visual worsening. For these biased pre-treatment conditions in radiation treatment delivered with conventional fractionation, we can observe more cases of visual complications. Generally, in published series, minimal neurological toxicity has been recorded (115–118).

Nowadays, the PT in the treatment of pituitary adenomas can find a real perspective of clinical application when a conventional fractionated dose schedule is required: in cases with larger-sized/ giant tumor volumes and cases with tumor in very close proximity or involving optic pathways by abutting or compressing. The issue of selection criteria for low-grade skull base tumors is discussed in a dedicated paragraph.

Vestibular schwannomas

Vestibular schwannomas (VS, formerly termed acoustic neuromas) are usually benign tumors derived from Schwann cells. VS develops from the nerve sheath of the vestibular division of the vestibulocochlear nerve (VIII cranial nerve) at the internal auditory meatus (119).

VSs represent the third most common intracranial non-malignant tumor entity; incidence rates range between 1.1 and 1.9 per 100,000, and usually a diagnosis is made in the third to fifth decades of life (120–122).

The majority of VSs occur unilaterally and sporadically. The most well-documented risk factor for VS development is NF2, 4%–6% of VS are associated with NF2. These patients typically develop bilateral disease as well as multiple other tumors (120, 121).

The diagnosis is made with contrast-enhanced magnetic resonance imaging. Patients often present with unilateral sensorineural hearing loss, tinnitus, and vertigo with gait disorders. Large tumors may cause neuropathies (trigeminal and facial nerves) as well as brainstem compression and hydrocephalus (120).

Furthermore, VS may be found incidentally on imaging examinations; the increased use of MRI imaging has also led to an increase in the diagnosis of smaller VSs.

Koos grading scale (KGS) (120, 122, 123) is a score frequently used for VS. KGS is designed to stratify tumors and is divided into

four grades based on extra-meatal extension and compression of the brainstem:

- Grade I = small intracanalicular tumor.
- Grade II = small tumor with protrusion into the cerebellopontine angle (CPA); no contact with the brainstem.
- Grade III = tumor occupying the cerebellopontine cistern with no brainstem displacement.
- Grade IV = large tumor with brainstem and cranial nerve displacement.

Standard management of VS includes observation, surgery, SRS, or conventional RT (120). The type of treatment is typically based on tumor size and its impact on adjacent brain structures (120, 122, 123).

Due to the slow progression of VS, the "watch and wait strategy" can be a legitimate treatment option for selected patients (120).

Surgical management of VS should be based on tumor size and morphology, symptoms, comorbidities, and patient preferences (120, 122, 123). Surgical resection offers excellent local tumor control but has been associated with a significant risk of injury to the V, VII, and VIII cranial nerves. In VS of Koos grade IV, surgery should be the primary treatment to remove a symptomatic lesion or potentially life-threatening mass effect (120). Surgery may also be considered for smaller tumors with cystic degeneration or if the cure is the primary goal of treatment (120).

RT can be delivered through several modalities, including SRS, which uses a single high-dose fraction, and conventionally fractionated RT (FRT), which uses smaller daily doses typically delivered in 28 to 32 fractions (119, 120, 124–128).

SRS defines the delivery of high-dose irradiation with high conformity and precision in a single fraction and is commonly used for small to medium-sized VSs. SRS can be performed using GammaKnife or CyberKnife at doses ranging from 11 to 14 Gy (120, 128).

SRS is used as a noninvasive approach for definitive treatment of small to medium-sized or recurrent tumors as it offers excellent rates of local control and better functional outcome and quality of life (QOL) compared to surgery (119, 120, 128).

SRS and FRT with modern techniques can achieve similar results in terms of local control and hearing function, although FRT can be used when surgery is not feasible or when a patient has larger VSs (Koos grades 3–4) in close proximity to the brainstem (119, 120, 127, 128).

Fractionated proton radiotherapy (FPT) for VS achieves high tumor control rates, equivalent to photon FRT techniques. Furthermore, FPT has peculiar physical properties that allow it to give more radiation energy to the target, sparing the surrounding normal tissues and thus having the potential to reduce treatment-associated toxicities (120, 124, 125, 127, 128). To date, there are few data points on PT for VSs.

In Table 6, we summarize selected published series of patients affected by pituitary adenomas and treated with PT (119, 124–127).

A retrospective cohort study investigated proton-beam stereotactic radiosurgery for VS. It was reported that there was a 5-year tumor control rate of 93.6% and a dose dependency for facial neuropathy (126).

Barnes et al. prospectively investigated efficacy and toxicity rates in 94 patients who underwent FPT for VS. FPT at a daily dose of 1.8 Gy (RBE) was employed (125). Patients were treated with one of three total dose options: 59.4 Gy (RBE), 54 Gy (RBE), or 50.4 Gy (RBE). Five-year local control rates for the 59.4 Gy (RBE), 54 Gy (RBE), and 50.4 Gy (RBE) groups were 95%, 97%, and 92%, respectively; the overall 10-year control rate was 90%. These data demonstrated a dose-dependent risk for hearing deterioration of 36% to 56% at doses from 50.4 to 54 Gy (RBE), while the risk for damage to other cranial nerves was 5%. FPT of 50.4 Gy (RBE) offers excellent LC rates with minimal cranial nerve toxicities (125).

Zhu and colleagues reported a retrospective case series of 14 patients who received 50.4 Gy (RBE) in 28 fractions of 1.8 Gy (RBE)/fraction (124). The 3-year LC rate was 85%, with no cranial nerve V or VII injuries. Twenty-one percent of patients had a radiographic tumor regression on MRI after a median of 26 months. No acute toxicity of G3 or above was reported.

Eichkorn et al. analyzed 45 patients who underwent FPT with a median total dose of 54 Gy (RBE) at 1.8 Gy (RBE)/fraction (127). It was reported that there was 100% local control in a median follow-up period of 3.6 years, and MRI revealed 93.3% of stable disease and 6.7% of partial regression. There was no case of progressive disease. New or worsening cranial nerve dysfunction (G1–2) was found in 20.0% of all patients. In 16% of cases, radiation-induced contrast enhancements (RICEs) were detected after a median of 14 months. RICEs were asymptomatic (71%) or transiently symptomatic (G2; 29%). No G3 or G4 toxicities were observed.

Küchler and colleagues reported a retrospective exploratory analysis to evaluate differences in tumor control, symptoms, and quality of life in VS patients after SRS/HFSRT, FRT, and FPT (119). For SRS/HFSRT, the median fraction dose applied was 12 Gy. For FRT and FPT, the median doses applied were 57.6 Gy and 54 Gy (RBE), respectively. FRT and FPT used single median doses of 1.8 Gy (RBE). Local control was 99.5% at 12 months after RT, with no statistical difference between treatment groups. SRS/HFSRT, FRT, and FPT for VS show similar functional outcomes. Cranial nerve impairment rates vary, potentially due to selection bias with larger VS in the FRT and FPT groups (119).

The hearing preservation rate varies among these cases because of the heterogeneity of treatments administered. Weber et al. evaluated proton-beam stereotactic radiosurgery with a hearing preservation rate of 79.1% and 21.9% at the 2 and 5-year follow-up, respectively (126).

In Barnes et al., 43% of 54-Gy-group patients maintained functional hearing during a median follow-up time of 58.2 months, with a median time to onset of the unserviceable hearing status of 14.8 months. Instead, 64% of the 50.4-Gy group maintained functional hearing with a median follow-up time of 42.7 months. The median time to hearing loss in patients who did not preserve useful hearing was 12 months. The difference in serviceable hearing between the 50.4-Gy and 54-Gy groups at 24 months and 48 months was not statistically significant (125).

Zhu et al. described the outcome of conventional FPT for VSs: the retained serviceable hearing in patients with baseline serviceable hearing was 33% (two patients) with a median follow-up of 70 months (124). Eichkorn et al. did not highlight acute or late hearing

TABLE 6 Patients and treatment description of vestibular schwannomas irradiated with proton radiotherapy (selected series).

Study	Patient characteristics (number and age groups)	Follow up (Month)	RT dose (GyRBE)	LC (%)	Late Toxicity
Weber, 2003 (126)	88 (median age 69.2y)	38.7	Median prescribed dose: 12 CGE (10–18) Median maximal tumor dose: 17.1 CGE (13.3–20) Isodose line percentage prescription: 70% (70–108) No. of fractions: 3 (2–4)	2-y: 95.3% 5-y: 93.6%	Permanent facial nerve dysfunction (HB Grade 3–4: 4 patients) Permanent "significant" trigeminal nerve dysfunction: two patients
Barnes, 2018 (125)	95 (median age 56 y) 43 (Group: 50.4 Gy) 34 (Group: 54.0 Gy) 19 (Group: 59.4 Gy)	4.3 y (Group: 50.4 Gy) 7.4 y (Group: 54.0 Gy) 6.6 y (Group: 59.4 Gy)	TD: Group: 50.4 Gy Group: 54.0 Gy Group: 59.4 Gy Dpf: 1.8 Gy	5-y LC: 92% (Group: 50.4 Gy) 95% (Group: 54.0 Gy) 97% (Group: 59.4 Gy) Overall 10-y: 90%.	No high grade toxicity
Zhu, 2018 (124)	14 (median age 60 y)	68	TD: 50.4 Gy Dpf: 1.8 Gy	3-y: 85%.	No high grade toxicity
Eichkorn, 2021 (127)	45 (median age 55 y)	42	TD: 54 Gy Dpf: 1.8 Gy	100%	No high grade toxicity. Radiation-induced contrast enhancements (seven patients,16%): G1–G2
Küchler, 2022 (119)	261	38	SRS/HFSRT (TD:12 Gy, single fraction; TD 18 Gy, Dpf 6 Gy) FRT (TD: 57.6 Gy; Dpf: 1.8 Gy) FPT (TD: 54GyRBE), Dpf: 1.8/GyRBE).	1 y: 99.5%; 3 y: 93.7%; 6y: 90.8%; No statistical difference between treatment groups (p = 0.19)	No high grade toxicity.

RT, radiotherapy; CGE, cobalt Gray equivalents; TD, total dose; Dpf, dose per fraction; LC, local control; y, years; HB, House-Brackmann; SRS/HFSRT, stereotactic radiosurgery/hypofractionated stereotactic radiotherapy; FRT, fractionated radiotherapy; FPT, fractionated proton therapy.

loss after PT (127). Küchler et al. reported a hearing preservation rate of 97.1%, 94.2%, and 87.1% at 12, 24, and 60 months in patients with useful hearing before treatment. Hearing deterioration was underlined in 17.8% and 16.7% of patients treated with fractionated radiotherapy (photon and PT, respectively) and in 3.6% of patients treated with SRS/HFSRT (119).

Regarding identifying patients affected by VS, cases requiring conventional FRT in an elective way can potentially be indicated for particle radiotherapy (and especially proton radiotherapy), as discussed widely in a dedicated paragraph regarding selection criteria for particle therapy in low-grade skull base tumors.

Low grade skull base tumors: considerations on selection criteria for PRT

Low-grade skull base tumors include WHO-G1 meningiomas (or presumed WHO-G1 in cases with an exclusive radiological diagnosis), craniopharyngiomas, pituitary adenomas, and vestibular schwannomas. For these types of tumors, lower levels of effective radiation doses are required. Consequently, high local control rates and the same efficacy obtained by PRT in comparison with advanced photon RT techniques are expected for these low-grade tumor types.

The selection criteria for PRT compared with photon radiotherapy are mainly based on the evaluation of the achievement of the goal represented by toxicity minimization and functional preservation.

Many advanced modalities and techniques are available for photon RT (SRS techniques and IMRT modalities), and for PT, the delivery techniques have been refined, evolving from passive scattering to active scanning technology, which represents the current standard for PRT (51, 52, 54, 80–82, 105, 128–131).

Among PRT options, carbon ions are not suitable as primary radiation treatment for patients affected by low-grade tumor types due to their high RBE and consequent overtreatment in terms of therapeutic ratio, and only PT is indicated in this subset of patients.

When recurrent previously irradiated low-grade tumors switch towards more aggressive biological behavior or a higher histology grade, CIRT can be re-considered, especially if valid and effective therapeutic alternatives are not available. In these cases, we are faced with *de facto* radioresistance, regardless of histological type, and CIRT is particularly indicated in cases of radioresistant tumors (56, 132, 133).

As previously introduced, in the treatment of low-grade skull base tumors, considering the wide availability of precise RT options and the lower effective radiation dose required, the same high probability of disease control and low toxicity rates are reasonably expected with either proton or photon RT advanced techniques and the same treatment volume identification criteria across RT techniques, are adopted (51, 52, 54, 73–75, 80, 81, 105, 115–119, 128–130, 134).

A competitive approach between different radiation technical modalities does not help in the choice of a better radiation option.

In making the decision-process of each clinical case, the evaluation and choice of the most suitable fractionation radiation dose schedule based on tumor volume and spatial relationship with the organ at risk represents the first step, and the choice of the radiation modality and technique represents a secondary step (54, 76, 105, 119, 120, 127–130, 135, 136).

Regardless of tumor histology, low-grade skull base tumors with small-medium size or at most larger volumes with a maximum diameter of 3–3.5 cm and at least 3 mm distance from the brainstem and optic pathways are typically suitable cases for radiosurgical schedules (up to a multi-session schedule with five fractions) with different technology delivery options (GammaKnife, CyberKnife, or other LINAC machines with radiosurgical equipment, proton radiosurgery) (76, 105, 115–117, 119, 120, 128, 129, 135, 136).

In several cases, a conventional fractionation schedule (1.8–2 Gy/fraction) is more indicated in skull base low-grade tumors considering the critical location represented by the skull base: very large or giant tumors; tumors closely involving the brainstem and/or optic pathways by abutting, compressing and enveloping these structures. In these cases, conventional fractionation has been well recognized as preferable to minimize toxicity in the brainstem, optic pathways, and other cranial nerves (54, 74, 76, 81, 105, 118–120, 127–131, 135–140).

The IMRT techniques (tomotherapy, VMAT) represent a photon RT option for very large/giant, and complex-shaped tumors with conventional fractionation, but compared with this option, the PT can more effectively spare neurocognitive function by minimizing dose delivered to hippocampi and brain (84, 85, 141).

Especially in patients with low-grade tumors and a favorable long-term prognosis, PT significantly reduces the risk of radio-induced malignancy (142, 143).

The sparing of neuro-cognitive function represents a major concern in the irradiation of intracranial tumors, both in children and adults. Neurocognitive impairment negatively affects the quality of life and instrumental activities of daily living (86, 144, 145).

The cause of neurocognitive decline in patients with intracranial tumors is multifactorial. The further RT, several factors are associated with impairment in neurocognitive factors: the tumor itself and its features (size, location, type, and grade; initial versus recurrent disease); medical treatment as corticosteroids and anticonvulsants; metabolic/endocrine dysfunction; the impact of surgery; the number of surgeries; the ventriculoperitoneal shunt; postoperative complications; and many others. The extent of the contribution of radiotherapy relative to other factors is not known or quantifiable. Multiple pathophysiological mechanisms have been suggested to explain the brain injuries and consequent cognitive impairment induced by RT, including impairment of neurogenesis (145–150).

Hippocampi represent a relevant region for neurocognitive function outcomes, but several other regions in the brain and various healthy cerebral tissues are potentially involved in the pathophysiology of cognitive impairment, as, for example, cerebral white matter, cerebral cortex, and subventricular zones (145, 146, 151, 152).

The impact of several RT dose parameters on neurocognitive function reported in the literature supports the idea that reduction of radiation dose–volume relationships between hippocampi and brain volume can positively affect the preservation of neurocognitive functions. Particularly considering the important role of the hippocampus in terms of cognitive function, hippocampal-sparing approaches in cranial radiation treatment have been developed in recent years (87, 88, 145, 146, 151–159).

As above-mentioned, PT permits significantly reduced radiation dose-volume delivery to the brain volume and hippocampi, and consequently, this dosimetric advantage can determine better outcomes in terms of neurocognitive sparing, as supported also by normal tissue complication probability (NTCP) modeling studies (84–90, 141, 160–164).

In children, adolescents, and young adults, the role of PT as an elective radiation modality, especially in brain tumors, has been increasingly supported in recent years (8, 83–93).

Summarizing, the PT could represent the elective radiation modality for patients affected by low-grade skull base tumors with indications for conventionally fractionated radiotherapy and cases not suitable for a radiosurgical schedule: larger-sized and/or complex-shaped tumors; tumors with proximity and involving brainstem and/or optic pathways. Furthermore, PT should be considered the first option among radiation modalities for these patients.

Conclusions

PRT represents an effective and safe therapeutic option for skull base tumors.

In radioresistant skull base tumors such as chordomas and sarcomas, the PRT permits higher dose levels required with optimal dose coverage and higher local control probability while minimizing dose to the critical organs and toxicity.

Furthermore, in radioresistant tumor types and recurrent tumors previously irradiated, carbon ions have an intrinsic and peculiarly higher RBE and are more capable of overcoming radioresistance compared with protons, regardless of features such as hypoxia, cell phases, and dose schedule fractionation.

Due to the prognostic factors affecting disease control, in these tumors, the combination of maximally safe surgical resection and high-dose PRT should be the goal of the treatment strategy.

In cases not amenable to attempted gross total/near total removal, the combination of debulking surgery providing space between tumor and brainstem and/or optic pathways followed by PRT should be evaluated.

Considering the critical location represented by the skull base, these patients should be referred to highly specialized centers for skull base surgery.

Furthermore, close and continuous cooperation between surgeons and particle radiation oncologists should favor the planning of a shared optimal combined treatment strategy.

In the skull base location of low-grade tumors, protons are the particle currently adopted.

In low-grade tumors, patients are potentially eligible for PT when the cases require a preferentially conventionally fractionated dose schedule, and if they are not amenable to SRS/HFSRT:

a) tumors with very close proximity or direct involvement (compression or abutment) of the brainstem and/or optic pathways

b) larger, giant sized, and/or very complex-shaped tumors.

Primarily, the dose sparing of brain volumes and subvolumes, such as hippocampi, is correlated with neuro-cognitive function, as well as the minimization of secondary tumor risk, strongly supporting the use of PT when fractionated radiation dose is preferentially indicated in comparison with IMRT techniques.

Even in high-grade meningiomas, a conventional fractionation radiation schedule is required as recommended in EANO guidelines (39) and the above-mentioned considerations for low-grade tumors have amplified implications considering the higher dose required in these tumor types (44, 165). Regardless of skull base location, systematic reviews support the role of PRT in terms of efficacy, local control, and survival rates in high-grade meningiomas, considering that PRT allows for more targeted treatment plans that may limit excess radiation damage for tumors generally considered difficult to manage (166, 167).

In children, adolescents, and young adults, PT should be the preferred option, when available, for the radiation treatment of low-grade skull base tumors.

Considering the critical location of skull base tumors, high-quality and advanced pretreatment MRI imaging and a careful, highly detailed, and comprehensive evaluation in the process of treatment target volume delineation are closely required and represent a crucial point to perform an optimal and high-quality assured radiation treatment (134).

Multi-institutional and collaborative efforts will be important to further increase our knowledge of the management and treatment of skull base tumors.

Author contributions

All authors listed have made a substantial, direct, and intellectual contribution to the work and approved it for publication. All authors have read and approved the final manuscript.

Conflict of interest

The authors declare that the research was conducted in the absence of any commercial or financial relationships that could be construed as a potential conflict of interest.

Publisher's note

References

1. Hug EB, Pelak M, Frank SJ, Fossati P. A review of particle therapy for skull base tumors: modern considerations and future directions. *Int J Part Ther* (2021) 8(1):168–78. doi: 10.14338/IJPT-20-00083

2. Noel G, Gondi V. Proton therapy for tumors of the base of the skull. *Chin Clin Oncol* (2016) 5(4):51. doi: 10.21037/cco.2016.07.05

3. Mizumoto M, Oshiro Y, Tsuboi K. Proton beam therapy for intracranial and skull base tumors. *Transl Cancer Res* (2013) 2(2):87–96. doi: 10.3978/j.issn.2218-676X.2013.04.08

4. Loeffler J, Durante M. Charged particle therapy–optimization, challenges and future directions. *Nat Rev Clin Oncol* (2013) 10:411–24. doi: 10.1038/nrclinonc.2013.79

5. Particle Therapy Co-Operative Group. Available at: https://www.ptcog.ch/index.php/facilities-in-operation-restricted (Accessed January 2023).

6. Smoll NR, Gautschi OP, Radovanovic I, Schaller K, Weber DC. Incidence and relative survival of chordomas: the standardized mortality ratio and the impact of chordomas on a population. *Cancer* (2013) 119(11):2029–37. doi: 10.1002/cncr.28032

7. Walcott BP, Nahed BV, Mohyeldin A, Coumans JV, Kahle KT, Ferreira MJ. Chordoma: current concepts, management, and future directions. *Lancet Oncol* (2012) 13(2):e69–76. doi: 10.1016/S1470-2045(11)70337-0

8. Hess CB, Indelicato DJ, Paulino AC, Hartsell WF, Hill-Kayser CE, Perkins SM, et al. An update from the pediatric proton consortium registry. *Front Oncol* (2018) 8:165. doi: 10.3389/fonc.2018.00165

9. Ulici V, Hart J. Chordoma. *Arch Pathol Lab Med* (2022) 146(3):386–95. doi: 10.5858/arpa.2020-0258-RA

10. Mercado CE, Holtzman AL, Rotondo R, Rutenberg MS, Mendenhall WM. Proton therapy for skull base tumors: a review of clinical outcomes for chordomas and chondrosarcomas. *Head Neck* (2019) 41(2):536–41. doi: 10.1002/hed.25479

11. Cavallo LM, Mazzatenta D, d'Avella E, Catapano D, MM F, Locatelli D, et al. The management of clival chordomas: an Italian multicentric study. *J Neurosurg* (2020) 4:1–10. doi: 10.3171/2020.5.JNS20925

12. Stacchiotti S, Sommer JChordoma Global Consensus Group. Building a global consensus approach to chordoma: a position paper from the medical and patient community. *Lancet Oncol* (2015) 16(2):e71–83. doi: 10.1016/S1470-2045(14)71190-8

13. Samii A, Gerganov VM, Herold C, Hayashi N, Naka T, Mirzayan MJ, et al. Chordomas of the skull base: surgical management and outcome. *J Neurosurg* (2007) 107(2):319–24. doi: 10.3171/JNS-07/08/0319

14. Pahwa B, Medani K, VM Lu, Elarjani T. Proton beam therapy for skull base chordomas: a systematic review of tumor control rates and survival rates. *Neurosurg Rev* (2022) 45(6):3551–63. doi: 10.1007/s10143-022-01880-7

15. Mizoe JE. Review of carbon ion radiotherapy for skull base tumors (especially chordomas). *Rep Pract Oncol Radiother* (2016) 21(4):356–60. doi: 10.1016/j.rpor.2015.01.008

16. Hug EB, Loredo LN, Slater JD, DeVries A, Grove RI, Schaefer RA, et al. Proton radiation therapy for chordomas and chondrosarcomas of the skull base. *J Neurosurg* (1999) 91(3):432–9. doi: 10.3171/jns.1999.91.3.0432

17. Munzenrider JE, Liebsch NJ. Proton therapy for tumors of the skull base. *Strahlenther Onkol* (1999) 175 Suppl 2:57–63. doi: 10.1007/BF03038890

18. Uhl M, Mattke M, Welzel T, Roeder F, Oelmann J, Habl G, et al. Highly effective treatment of skull base chordoma with carbon ion irradiation using a raster scan technique in 155 patients: first long-term results. *Cancer* (2014) 120(21):3410–7. doi: 10.1002/cncr.28877

19. Weber DC, Malyapa R, Albertini F, Bolsi A, Kliebsch U, Walser M, et al. Long term outcomes of patients with skull-base low-grade chondrosarcoma and chordoma patients treated with pencil beam scanning proton therapy. *Radiother Oncol* (2016) 120 (1):169–74. doi: 10.1016/j.radonc.2016.05.011

20. Fung V, Calugaru V, Bolle S, Mammar H, Alapetite C, Maingon P, et al. Proton beam therapy for skull base chordomas in 106 patients: a dose adaptive radiation protocol. *Radiother Oncol* (2018) 128(2):198–202. doi: 10.1016/j.radonc.2017.12.017

21. Koto M, Ikawa H, Kaneko T, Hagiwara Y, Hayashi K, Tsuji H. Long-term outcomes of skull base chordoma treated with high-dose carbon-ion radiotherapy. *Head Neck* (2020) 42(9):2607–13. doi: 10.1002/hed.26307

22. Iannalfi A, D'Ippolito E, Riva G, Molinelli S, Gandini S, Viselner G, et al. Proton and carbon ion radiotherapy in skull base chordomas: a prospective study based on a dual particle and a patient-customized treatment strategy. *Neuro Oncol* (2020) 22 (9):1348–58. doi: 10.1093/neuonc/noaa067

23. Mattke M, Ohlinger M, Bougatf N, Harrabi S, Wolf R, Seidensaal K, et al. Proton and carbon ion beam treatment with active raster scanning method in 147 patients with skull base chordoma at the Heidelberg ion beam therapy center-a single-center experience. *Strahlenther Onkol* (2022) 199(2):160–8. doi: 10.1007/s00066-022-02002-4

24. Wang L, Wu Z, Tian K, Wang K, Li D, Ma J, et al. Clinical features and surgical outcomes of patients with skull base chordoma: a retrospective analysis of 238 patients. *J Neurosurg* (2017) 127(6):1257–67. doi: 10.3171/2016.9.JNS16559

25. Jahangiri A, Jian B, Miller L, IH E-S, Aghi MK. Skull base chordomas: clinical features, prognostic factors, and therapeutics. *Neurosurg Clin N Am* (2013) 24(1):79–88. doi: 10.1016/j.nec.2012.08.007

26. Stacchiotti S, Gronchi A, Fossati P, Akiyama T, Alapetite C, Baumann M, et al. Best practices for the management of local-regional recurrent chordoma: a position paper by the chordoma global consensus group. *Ann Oncol* (2017) 28(6):1230–42. doi: 10.1093/annonc/mdx054

27. Uhl M, Welzel T, Oelmann J, Habl G, Hauswald H, Jensen A, et al. Active raster scanning with carbon ions: reirradiation in patients with recurrent skull base chordomas and chondrosarcomas. *Strahlenther Onkol* (2014) 190(7):686–91. doi: 10.1007/s00066-014-0608-2

28. Alterio D, Turturici I, Volpe S, Ferrari A, Russell-Edu SW, Vischioni B, et al. Carotid blowout syndrome after reirradiation for head and neck malignancies: a comprehensive systematic review for a pragmatic multidisciplinary approach. *Crit Rev Oncol Hematol* (2020) 155:103088. doi: 10.1016/j.critrevonc.2020.103088

29. Bloch OG, Jian BJ, Yang I, Han SJ, Aranda D, Ahn BJ, et al. A systematic review of intracranial chondrosarcoma and survival. *J Clin Neurosci* (2009) 16:1547–51. doi: 10.1016/j.jocn.2009.05.003

30. Evans HL, Ayala AG, Romsdahl MM. Prognostic factors in chondrosarcoma of bone: a clinicopathologic analysis with emphasis on histologic grading. *Cancer* (1977) 40(2):818–31. doi: 10.1002/1097-0142(197708)40:2<818::aid-cncr2820400234>3.0.co;2-b

31. van Praag Veroniek VM, Rueten-Budde AJ, Ho V, Dijkstra PDSStudy group Bone and Soft tissue tumours (WeBot), , Fiocco M, et al. Incidence, outcomes and prognostic factors during 25 years of treatment of chondrosarcomas. *Surg Oncol* (2018) 27(3):402–8. doi: 10.1016/j.suronc.2018.05.009

32. Patel S, Nunna RS, Ryoo JS, Ansari D, Chaudhry NS, Mehta AI. Outcomes and patterns of care in adult skull base chondrosarcoma patients in the united states. *World Neurosurg* (2021) 150:71–83. doi: 10.1016/j.wneu.2021.03.097

33. Amichetti M, Amelio D, Cianchetti M, RM E, Minniti G. A systematic review of proton therapy in the treatment of chondrosarcoma of the skull base. *Neurosurg Rev* (2010) 33(2):155–65. doi: 10.1007/s10143-009-0235-z

34. Weber DC, Badiyan S, Malyapa R, Albertini F, Bolsi A, AJ L, et al. Long-term outcomes and prognostic factors of skull-base chondrosarcoma patients treated with pencil-beam scanning proton therapy at the Paul scherrer institute. *Neuro Oncol* (2016) 18(2):236–43. doi: 10.1093/neuonc/nov154

35. Mattke M, Vogt K, Bougatf N, Welzel T, Oelmann-Avendano J, Hauswald H, et al. High control rates of proton-and carbon-ion–beam treatment with intensity-modulated active raster scanning in 101 patients with skull base chondrosarcoma at the Heidelberg ion beam therapy center. *Cancer* (2018) 124:2036–44. doi: 10.1002/cncr.31298

36. Riva G, Cavallo I, Gandini S, Ingargiola R, Pecorilla M, Imparato S, et al. Iannalfi a. particle radiotherapy for skull base chondrosarcoma: a clinical series from Italian national center for oncological hadrontherapy. *Cancers (Basel)* (2021) 13(17):4423. doi: 10.3390/cancers13174423

37. Demizu Y, Mizumoto M, Onoe T, Nakamura N, Kikuchi Y, Shibata T, et al. Proton beam therapy for bone sarcomas of the skull base and spine: a retrospective nationwide multicenter study in Japan. *Cancer Sci* (2017) 108(5):972–7. doi: 10.1111/cas.13192

38. Yang J, Hu W, Guan X, Hu J, Gao J, Qiu X, et al. Particle beam radiation therapy for skull base sarcomas. *Front Oncol* (2020) 16:1368. doi: 10.3389/fonc.2020.01368

39. Goldbrunner R, Stavrinou P, Jenkinson MD, Sahm F, Mawrin C, Weber DC, et al. EANO guideline on the diagnosis and management of meningiomas. *Neuro Oncol* (2021) 23(11):1821–34. doi: 10.1093/neuonc/noab150

40. Weber DC, Bizzocchi N, Bolsi A, Jenkinson MD. Proton therapy for intracranial meningioma for the treatment of Primary/Recurrent disease including re-irradiation. *Front Oncol* (2020) 10:558845. doi: 10.3389/fonc.2020.558845

41. Li JY, Li JW, Jin YC, Li MX, Guo LP, Bing ZT, et al. The efficacy and safety of carbon ion radiotherapy for meningiomas: a systematic review and meta-analysis. *Front Oncol* (2021) 11:620534. doi: 10.3389/fonc.2021.620534

42. Sato H, Mizumoto M, Okumura T, Sakurai H, Sakamoto N, Akutsu H, et al. Long-term outcomes of patients with unresectable benign meningioma treated with proton beam therapy. *J Radiat Res* (2021) 62(3):427–37. doi: 10.1093/jrr/rrab017

43. Hoisnard L, Laanani M, Passeri T, Duranteau L, Coste J, Zureik M, et al. Risk of intracranial meningioma with three potent progestogens: a population-based case-control study. *Eur J Neurol* (2022) 29(9):2801–9. doi: 10.1111/ene.15423

44. Vagnoni L, Aburas S, Giraffa M, Russo I, Chiarella V, Paolini S, et al. Radiation therapy for atypical and anaplastic meningiomas: an overview of current results and controversial issues. *Neurosurg Rev* (2022) 45(5):3019–33. doi: 10.1007/s10143-022-01806-3

45. Matsumoto Y, Fukumitsu N, Ishikawa H, Nakai K, Sakurai H. A critical review of radiation therapy: from particle beam therapy (Proton, carbon, and BNCT) to beyond. *J Pers Med* (2021) 11(8):825. doi: 10.3390/jpm11080825

46. Gudjonsson O, Blomquist E, Nyberg G, Pellettieri L, Montelius A, Grusell E, et al. Stereotactic irradiation of skull base meningiomas with high energy protons. *Acta Neurochir (Wien)* (1999) 141(9):933–40. doi: 10.1007/s007010050399

47. Vernimmen FJ, Harris JK, Wilson JA, Melvill R, Smit BJ, Slabbert JP. Stereotactic proton beam therapy of skull base meningiomas. *Int J Radiat Oncol Biol Phys* (2001) 49(1):99–105. doi: 10.1016/s0360-3016(00)01457-7

48. Weber DC, Lomax AJ, Rutz HP, Stadelmann O, Egger E, Timmermann B, et al. Spot-scanning proton radiation therapy for recurrent, residual or untreated intracranial meningiomas. *Radiother Oncol* (2004) 71(3):251–8. doi: 10.1016/j.radonc.2004.02.011

49. Halasz LM, Bussière MR, Dennis ER, Niemierko A, Chapman PH, Loeffler JS, et al. Proton stereotactic radiosurgery for the treatment of benign meningiomas. *Int J Radiat Oncol Biol Phys* (2011) 81(5):1428–35. doi: 10.1016/j.ijrobp.2010.07.1991

50. Weber DC, Schneider R, Goitein G, Koch T, Ares C, Geismar JH, et al. Spot scanning-based proton therapy for intracranial meningioma: long-term results from the Paul scherrer institute. *Int J Radiat Oncol Biol Phys* (2012) 83(3):865–71. doi: 10.1016/j.ijrobp.2011.08.027

51. Combs SE, Kessel K, Habermehl D, Haberer T, Jäkel O, Debus J. Proton and carbon ion radiotherapy for primary brain tumors and tumors of the skull base. *Acta Oncol* (2013) 52(7):1504–9. doi: 10.3109/0284186X.2013.818255

52. Murray FR, Snider JW, Bolsi A, Lomax AJ, Walser M, Kliebsch U, et al. Long-term clinical outcomes of pencil beam scanning proton therapy for benign and non-benign intracranial meningiomas. *Int J Radiat Oncol Biol Phys* (2017) 99(5):1190–8. doi: 10.1016/j.ijrobp.2017.08.005

53. Vlachogiannis P, Gudjonsson O, Montelius A, Grusell E, Isacsson U, Nilsson K, et al. Hypofractionated high-energy proton-beam irradiation is an alternative treatment for WHO grade I meningiomas. *Acta Neurochir (Wien)* (2017) 159(12):2391–400. doi: 10.1007/s00701-017-3352-4

54. El Shafie RA, Czech M, Kessel KA, Habermehl D, Weber D, Rieken S, et al. Clinical outcome after particle therapy for meningiomas of the skull base: toxicity and local control in patients treated with active rasterscanning. *Radiat Oncol* (2018) 13 (1):54. doi: 10.1186/s13014-018-1002-5

55. Champeaux-Depond C, Weller J. Outcome after protontherapy for progression or recurrence of surgically treated meningioma. *Brain Tumor Res Treat* (2021) 9(2):46–57. doi: 10.14791/btrt.2021.9.e9

56. El Shafie RA, Czech M, Kessel KA, Habermehl D, Weber D, Rieken S, et al. Evaluation of particle radiotherapy for the re-irradiation of recurrent intracranial meningioma. *Radiat Oncol* (2018) 13(1):86. doi: 10.1186/s13014-018-1026-x

57. Imber BS, Neal B, Casey DL, Darwish H, AL L, Cahlon O, et al. Clinical outcomes of recurrent intracranial meningiomas treated with proton beam reirradiation. *Int J Part Ther* (2019) 5(4):11–22. doi: 10.14338/IJPT-18-00045.1. Spring.

58. Momin AA, Recinos MA, Cioffi G, Patil N, Soni P, Almeida JP, et al. Descriptive epidemiology of craniopharyngiomas in the united states. *Pituitary* (2021) 24(4):517–22. doi: 10.1007/s11102-021-01127-6

59. Sainte-Rose C, Puget S, Wray A, Zerah M, Grill J, Brauner R, et al. Craniopharyngioma: the pendulum of surgical management. *Childs Nerv Syst* (2005) 21(8-9):691–5. doi: 10.1007/s00381-005-1209-2

60. Puget S, Garnett M, Wray A, Grill J, Habrand JL, Bodaert N, et al. Pediatric craniopharyngiomas: classification and treatment according to the degree of hypothalamic involvement. *J Neurosurg* (2007) 106(1 Suppl):3–12. doi: 10.3171/ped.2007.106.1.3

61. Sterkenburg AS, Hoffmann A, Gebhardt U, Warmuth-Metz M, Daubenbüchel AM, Müller HL. Survival, hypothalamic obesity, and neuropsychological/psychosocial status after childhood-onset craniopharyngioma: newly reported long-term outcomes. *Neuro Oncol* (2015) 17(7):1029–38. doi: 10.1093/neuonc/nov044

62. Müller HL, Merchant TE, Warmuth-Metz M, Martinez-Barbera JP, Puget S. Craniopharyngioma. *Nat Rev Dis Primers* (2019) 5(1):75. doi: 10.1038/s41572-019-0125-9

63. Fouda MA, Karsten M, Staffa SJ, Scott RM, Marcus KJ, Baird LC. Management strategies for recurrent pediatric craniopharyngioma: new recommendations. *J Neurosurg Pediatr* (2021) 27(5):548–55. doi: 10.3171/2020.9.PEDS20606

64. Edmonston DY, Wu S, Li Y, Khan RB, Boop FA, Merchant TE. Limited surgery and conformal photon radiation therapy for pediatric craniopharyngioma: long-term results from the RT1 protocol. *Neuro Oncol* (2022) 24(12):2200–9. doi: 10.1093/neuonc/noac124

65. Cossu G, Jouanneau E, Cavallo LM, Elbabaa SK, Giammattei L, Starnoni D, et al. Surgical management of craniopharyngiomas in adult patients: a systematic review and consensus statement on behalf of the EANS skull base section. *Acta Neurochir (Wien)* (2020) 162(5):1159–77. doi: 10.1007/s00701-020-04265-1

66. Cavallo LM, Frank G, Cappabianca P, Solari D, Mazzatenta D, Villa A, et al. The endoscopic endonasal approach for the management of craniopharyngiomas: a series of 103 patients. *J Neurosurg* (2014) 121(1):100–13. doi: 10.3171/2014.3.JNS131521

67. Cagnazzo F, Zoli M, Mazzatenta D, Gompel JJV. Endoscopic and microscopic transsphenoidal surgery of craniopharyngiomas: a systematic review of surgical outcomes over two decades. *J Neurol Surg A Cent Eur Neurosurg* (2018) 79(3):247–56. doi: 10.1055/s-0037-1607195

68. Na MK, Jang B, Choi KS, Lim TH, Kim W, Cho Y, et al. Craniopharyngioma resection by endoscopic endonasal approach versus transcranial approach: a systematic review and meta-analysis of comparative studies. *Front Oncol* (2022) 12:1058329. doi: 10.3389/fonc.2022.1058329

69. Mazzatenta D, Zoli M, Guaraldi F, Ambrosi F, Faustini Fustini M, Pasquini E, et al. Outcome of endoscopic endonasal surgery in pediatric craniopharyngiomas. *World Neurosurg* (2020) 134:e277–88. doi: 10.1016/j.wneu.2019.10.039

70. Dandurand C, Sepehry AA, Asadi Lari MH, Akagami R, Gooderham P. Adult craniopharyngioma: case series, systematic review, and meta-analysis. *Neurosurgery* (2018) 83(4):631–41. doi: 10.1093/neuros/nyx570

71. Clark AJ, Cage TA, Aranda D, Parsa AT, Sun PP, Auguste KI, et al. A systematic review of the results of surgery and radiotherapy on tumor control for pediatric craniopharyngioma. *Childs Nerv Syst* (2013) 29(2):231–8. doi: 10.1007/s00381-012-1926-2

72. Müller HL, Tauber M, Lawson EA, Özyurt J, Bison B, Martinez-Barbera JP, et al. Hypothalamic syndrome. *Nat Rev Dis Primers* (2022) 8(1):24. doi: 10.1038/s41572-022-00351-z

73. Iannalfi A, Fragkandrea I, Brock J, Saran F. Radiotherapy in craniopharyngiomas. *Clin Oncol (R Coll Radiol)* (2013) 25(11):654–67. doi: 10.1016/j.clon.2013.07.005

74. Harrabi SB, Adeberg S, Welzel T, Rieken S, Habermehl D, Debus J, et al. Long term results after fractionated stereotactic radiotherapy (FSRT) in patients with craniopharyngioma: maximal tumor control with minimal side effects. *Radiat Oncol* (2014) 16:9:203. doi: 10.1186/1748-717X-9-203

75. Bishop AJ, Greenfield B, Mahajan A, Paulino AC, Okcu MF, Allen PK, et al. Proton beam therapy versus conformal photon radiation therapy for childhood craniopharyngioma: multi-institutional analysis of outcomes, cyst dynamics, and toxicity. *Int J Radiat Oncol Biol Phys* (2014) 90(2):354–61. doi: 10.1016/j.ijrobp.2014.05.051

76. Kamogawa M, Shuto T, Matsunaga S. Effects of two different radiotherapies for craniopharyngiomas using stereotactic radiosurgery/ stereotactic radiotherapy or fractionated stereotactic radiotherapy. *Surg Neurol Int* (2022) 13:563. doi: 10.25259/SNI_802_2022

77. Rutenberg MS, Holtzman AL, Indelicato DJ, Huh S, Rao D, Fiester PJ, et al. Disease control after radiotherapy for adult craniopharyngioma: clinical outcomes from a Large single-institution series. *J Neurooncol* (2022) 157(3):425–33. doi: 10.1007/s11060-022-03983-z

78. Niranjan A, Lunsford LD. The role of leksell radiosurgery in the management of craniopharyngiomas. *Prog Neurol Surg* (2019) 34:166–72. doi: 10.1159/000493061

79. Greenfield BJ, Okcu MF, Baxter PA, Chintagumpala M, Teh BS, Dauser RC, et al. Long-term disease control and toxicity outcomes following surgery and intensity modulated radiation therapy (IMRT) in pediatric craniopharyngioma. *Radiother Oncol* (2015) 114(2):224–9. doi: 10.1016/j.radonc.2014.11.035

80. Jimenez RB, Ahmed S, Johnson A, Thomas H, Depauw N, Horick N, et al. Proton radiation therapy for pediatric craniopharyngioma. *Int J Radiat Oncol Biol Phys* (2021) 110(5):1480–7. doi: 10.1016/j.ijrobp.2021.02.045

81. Rutenberg MS, Rotondo RL, Rao D, Holtzman AL, Indelicato DJ, Huh S, et al. Clinical outcomes following proton therapy for adult craniopharyngioma: a single-institution cohort study. *J Neurooncol* (2020) 147(2):387–95. doi: 10.1007/s11060-020-03432-9.3

82. Ajithkumar T, Mazhari AL, Stickan-Verfürth M, Kramer PH, Fuentes CS, Lambert J, et al. Proton therapy for craniopharyngioma - an early report from a single European centre. *Clin Oncol (R Coll Radiol)* (2018) 30(5):307–16. doi: 10.1016/j.clon.2018.01.012

83. Merchant TE, CH H, Shukla H, Ying X, Nill S, Oelfke U. Proton versus photon radiotherapy for common pediatric brain tumors: comparison of models of dose characteristics and their relationship to cognitive function. *Pediatr Blood Cancer* (2008) 51(1):110–7. doi: 10.1002/pbc.21530

84. . Boehling NS, Grosshans DR, Bluett JB, Palmer MT, Song X, Amos RA, et al. Dosimetric comparison of three-dimensional conformal proton radiotherapy, intensity-modulated proton therapy, and intensity-modulated radiotherapy for treatment of pediatric craniopharyngiomas. *Int J Radiat Oncol Biol Phys* (2012) 82 (2):643–52. doi: 10.1016/j.ijrobp.2010.11.027

85. Beltran C, Roca M, Merchant TE. On the benefits and risks of proton therapy in pediatric craniopharyngioma. *Int J Radiat Oncol Biol Phys* (2012) 82(2):e281–7. doi: 10.1016/j.ijrobp.2011.01.005

86. Pulsifer MB, Duncanson H, Grieco J, Evans C, Tseretopoulos ID, MacDonald S, et al. Cognitive and adaptive outcomes after proton radiation for pediatric patients with brain tumors. *Int J Radiat Oncol Biol Phys* (2018) 102(2):391–8. doi: 10.1016/j.ijrobp.2018.05.069

87. Gross JP, Powell S, Zelko F, Hartsell W, Goldman S, Fangusaro J, et al. Improved neuropsychological outcomes following proton therapy relative to X-ray therapy for pediatric brain tumor patients. *Neuro Oncol* (2019) 21(7):934–43. doi: 10.1093/neuonc/noz070

88. Kahalley LS, Peterson R, Ris MD, Janzen L, Okcu MF, Grosshans DR, et al. Superior intellectual outcomes after proton radiotherapy compared with photon radiotherapy for pediatric medulloblastoma. *J Clin Oncol* (2020) 38(5):454–61. doi: 10.1200/JCO.19.0170

89. Greenberger BA, Pulsifer MB, Ebb DH, MacDonald SM, Jones RM, Butler WE, et al. Clinical outcomes and late endocrine, neurocognitive, and visual profiles of proton radiation for pediatric low-grade gliomas. *Int J Radiat Oncol Biol Phys* (2014) 89 (5):1060–8. doi: 10.1016/j.ijrobp.2014.04.053

90. Stokkevåg CH, Indelicato DJ, Herfarth K, Magelssen H, Evensen ME, Ugland M, et al. Normal tissue complication probability models in plan evaluation of children with brain tumors referred to proton therapy. *Acta Oncol* (2019) 58(10):1416–22. doi: 10.1080/0284186X.2019.1643496

91. Huynh M, Marcu LG, Giles E, Short M, Matthews D, Bezak E. Current status of proton therapy outcome for paediatric cancers of the central nervous system - analysis of the published literature. *Cancer Treat Rev* (2018) 70:272–88. doi: 10.1016/j.ctrv.2018.10.003

92. Huynh M, Marcu LG, Giles E, Short M, Matthews D, Bezak E. Are further studies needed to justify the use of proton therapy for paediatric cancers of the central nervous system? a review of current evidence. *Radiother Oncol* (2019) 133:140–8. doi: 10.1016/j.radonc.2019.01.009

93. Indelicato DJ, Merchant T, Laperriere N, Lassen Y, Vennarini S, Wolden S, et al. Consensus report from the Stockholm pediatric proton therapy conference. *Int J Radiat Oncol Biol Phys* (2016) 96(2):387–92. doi: 10.1016/j.ijrobp.2016.06.2446

94. Uh J, Merchant TE, Li Y, Li X, Sabin ND, Indelicato DJ, et al. Effects of surgery and proton therapy on cerebral white matter of craniopharyngioma patients. *Int J Radiat Oncol Biol Phys* (2015) 93(1):64–71. doi: 10.1016/j.ijrobp.2015.05.017

95. Uh J, Merchant TE, Conklin HM, Ismael Y, Li Y, Han Y, et al. Diffusion tensor imaging-based analysis of baseline neurocognitive function and posttreatment white matter changes in pediatric patients with craniopharyngioma treated with surgery and proton therapy. *Int J Radiat Oncol Biol Phys* (2021) 109(2):515–26. doi: 10.1016/j.ijrobp.2020.08.060

96. Fitzek MM, Linggood RM, Adams J, Munzenrider JE. Combined proton and photon irradiation for craniopharyngioma: long-term results of the early cohort of patients treated at Harvard cyclotron laboratory and Massachusetts general hospital. *Int J Radiat Oncol Biol Phys* (2006) 64(5):1348–54. doi: 10.1016/j.ijrobp.2005.09.034

97. Luu QT, Loredo LN, Archambeau JO, Yonemoto LT, Slater JM, Slater JD. Fractionated proton radiation treatment for pediatric craniopharyngioma: preliminary report. *Cancer J* (2006) 12(2):155–9.

98. Hall MD, Bradley JA, Rotondo RL, Hanel R, Shah C, Morris CG, et al. Risk of radiation vasculopathy and stroke in pediatric patients treated with proton therapy for brain and skull base tumors. *Int J Radiat Oncol Biol Phys* (2018) 101(4):854–9. doi: 10.1016/j.ijrobp.2018.03.027

99. Lucas JTJr, Faught AM, Hsu CY, Wilson LJ, Guo Y, Li Y, et al. Pre- and posttherapy risk factors for vasculopathy in pediatric patients with craniopharyngioma treated with surgery and proton radiation therapy. *Int J Radiat Oncol Biol Phys* (2022) 113(1):152–60. doi: 10.1016/j.ijrobp.2021.12.172

100. Winkfield KM, Linsenmeier C, Yock TI, Grant PE, Yeap BY, Butler WE, et al. Surveillance of craniopharyngioma cyst growth in children treated with proton radiotherapy. *Int J Radiat Oncol Biol Phys* (2009) 73(3):716–21. doi: 10.1016/j.ijrobp.2008.05.010

101. Daly AF, Beckers A. The epidemiology of pituitary adenomas. *Endocrinol Metab Clin North Am* (2020) 49(3):347–55. doi: 10.1016/j.ecl.2020.04.002

102. Molitch ME. Diagnosis and treatment of pituitary adenomas: a review. *JAMA* (2017) 317(5):516–24. doi: 10.1001/jama.2016.19699

103. Asa SL, Mete O, Perry A, Osamura RY. Overview of the 2022 WHO classification of pituitary tumors. *Endocr Pathol* (2022) 33(1):6–26. doi: 10.1007/s12022-022-09703-7

104. Li A, Liu W, Cao P, Zheng Y, Bu Z, Zhou T. Endoscopic versus microscopic transsphenoidal surgery in the treatment of pituitary adenoma: a systematic review and meta-analysis. *World Neurosurg* (2017) 101:236–46. doi: 10.1016/j.wneu.2017.01.022

105. Minniti G, Clarke E, Scaringi C, Enrici RM. Stereotactic radiotherapy and radiosurgery for non-functioning and secreting pituitary adenomas. *Rep Pract Oncol Radiother* (2016) 21(4):370–8. doi: 10.1016/j.rpor.2014.09.004

106. Adler JRJr, Gibbs IC, Puataweepong P, Chang SD. Visual field preservation after multisession cyberknife radiosurgery for perioptic lesions. *Neurosurgery* (2006) 59 (2):244–54. doi: 10.1227/01.NEU.0000223512.09115.3E

107. Roberts BK, Ouyang DL, Lad SP, Chang SD, Harsh GR4, Adler JRJr, et al. Efficacy and safety of CyberKnife radiosurgery for acromegaly. *Pituitary* (2007) 10 (1):19–25. doi: 10.1007/s11102-007-0004-3

108. Iwata H, Sato K, Tatewaki K, Yokota N, Inoue M, Baba Y, et al. Hypofractionated stereotactic radiotherapy with CyberKnife for nonfunctioning pituitary adenoma: high local control with low toxicity. *Neuro Oncol* (2011) 13 (8):916–22. doi: 10.1093/neuonc/nor055

109. Liao HI, Wang CC, Wei KC, Chang CN, Hsu YH, Lee ST, et al. Fractionated stereotactic radiosurgery using the novalis system for the management of pituitary adenomas close to the optic apparatus. *J Clin Neurosci* (2014) 21(1):111–5. doi: 10.1016/j.jocn.2013.03.024

110. Kotecha R, Sahgal A, Rubens M, De Salles A, Fariselli L, Pollock BE, et al. Stereotactic radiosurgery for non-functioning pituitary adenomas: meta-analysis and international stereotactic radiosurgery society practice opinion. *Neuro Oncol* (2020) 22 (3):318–32. doi: 10.1093/neuonc/noz225

111. Mathieu D, Kotecha R, Sahgal A, De Salles A, Fariselli L, Pollock BE, et al. Stereotactic radiosurgery for secretory pituitary adenomas: systematic review and international stereotactic radiosurgery society practice recommendations. *J Neurosurg* (2021) 136(3):801–12. doi: 10.3171/2021.2.JNS204440

112. Zhang N, Pan L, Wang EM, Dai JZ, Wang BJ, Cai PW. Radiosurgery for growth hormone-producing pituitary adenomas. *J Neurosurg* (2000) 93 Suppl 3:6–9. doi: 10.3171/jns.2000.93.supplement

113. Pan L, Zhang N, Wang EM, Wang BJ, Dai JZ, Cai PW. Gamma knife radiosurgery as a primary treatment for prolactinomas. *J Neurosurg* (2000) 93 Suppl 3:10–3. doi: 10.3171/jns.2000.93.supplement

114. Jezková J, Hána V, Krsek M, Weiss V, Vladyka V, Liscák R, et al. Use of the leksell gamma knife in the treatment of prolactinoma patients. *Clin Endocrinol (Oxf)* (2009) 70(5):732–41. doi: 10.1111/j.1365-2265.2008.03384.x

115. Petit JH, Biller BM, Yock TI, Swearingen B, Coen JJ, Chapman P, et al. Proton stereotactic radiotherapy for persistent adrenocorticotropin-producing adenomas. *J Clin Endocrinol Metab* (2008) 93(2):393–9. doi: 10.1210/jc.2007-1220

116. Petit JH, Biller BM, Coen JJ, Swearingen B, Ancukiewicz M, Bussiere M, et al. Proton stereotactic radiosurgery in management of persistent acromegaly. *Endocr Pract* (2007) 13(7):726–34. doi: 10.4158/EP.13.7.726

117. Wattson DA, Tanguturi SK, Spiegel DY, Niemierko A, Biller BM, Nachtigall LB, et al. Outcomes of proton therapy for patients with functional pituitary adenomas. *Int J Radiat Oncol Biol Phys* (2014) 90(3):532–9. doi: 10.1016/j.ijrobp.2014.06.068

118. Ronson BB, Schulte RW, Han KP, Loredo LN, Slater JM, Slater JD. Fractionated proton beam irradiation of pituitary adenomas. *Int J Radiat Oncol Biol Phys* (2006) 64(2):425–34. doi: 10.1016/j.ijrobp.2005.07.978

119. Küchler M, El Shafie RA, Adeberg S, Herfarth K, König L, Lang K, et al. Outcome after radiotherapy for vestibular schwannomas (VS)-differences in tumor control, symptoms and quality of life after radiotherapy with photon versus proton therapy. *Cancers (Basel)* (2022) 14(8):1916. doi: 10.3390/cancers14081916

120. Goldbrunner R, Weller M, Regis J, Lund-Johansen M, Stavrinou P, Reuss D, et al. EANO guideline on the diagnosis and treatment of vestibular schwannoma. *Neuro Oncol* (2020) 22(1):31–45. doi: 10.1093/neuonc/noz153

121. Lehrer EJ, Prabhu AV, Sindhu KK, Lazarev S, Ruiz-Garcia H, Peterson JL, et al. Proton and heavy particle intracranial radiosurgery. *Biomedicines* (2021) 9(1):31. doi: 10.3390/biomedicines9010031

122. Erickson NJ, Schmalz PGR, Agee BS, Fort M, Walters BC, McGrew BM, et al. Koos classification of vestibular schwannomas: a reliability study. *Neurosurgery* (2019) 85(3):409–14. doi: 10.1093/neuros/nyy409

123. Koos WT, Day JD, Matula C, Levy DI. Neurotopographic considerations in the microsurgical treatment of small acoustic neurinomas. *J Neurosurg* (1998) 88(3):506–12. doi: 10.3171/jns.1998.88.3.0506

124. Zhu S, Rotondo R, Mendenhall WM, Dagan R, Lewis D, Huh S, et al. Long-term outcomes of fractionated stereotactic proton therapy for vestibular schwannoma: a case series. *Int J Part Ther* (2018) 4(4):37–46. doi: 10.14338/IJPT-17-00032.1

125. Barnes CJ, Bush DA, Grove RI, Loredo LN, Slater JD. Fractionated proton beam therapy for acoustic neuromas: tumor control and hearing preservation. *Int J Part Ther* (2018) 4(4):28–36. doi: 10.14338/IJPT-14-00014.1

126. Weber DC, Chan AW, Bussiere MR, Harsh GR4, Ancukiewicz M, Barker FG2nd, et al. Proton beam radiosurgery for vestibular schwannoma: tumor control and cranial nerve toxicity. *Neurosurgery* (2003) 53(3):577–86. doi: 10.1227/01.neu.0000079369.59219.c0

127. Eichkorn T, Regnery S, Held T, Kronsteiner D, Hörner-Rieber J, El Shafie RA, et al. Effectiveness and toxicity of fractionated proton beam radiotherapy for cranial nerve schwannoma unsuitable for stereotactic radiosurgery. *Front Oncol* (2021) 11:772831. doi: 10.3389/fonc.2021.772831

128. Apicella G, Paolini M, Deantonio L, Masini L, Krengli M. Radiotherapy for vestibular schwannoma: review of recent literature results. *Rep Pract Oncol Radiother* (2016) 21(4):399–406. doi: 10.1016/j.rpor.2016.02.002

129. Combs SE, Farzin M, Boehmer J, Oehlke O, Molls M, Debus J, et al. Clinical outcome after high-precision radiotherapy for skull base meningiomas: pooled data from three large German centers for radiation oncology. *Radiother Oncol* (2018) 127 (2):274–9. doi: 10.1016/j.radonc.2018.03.006

130. Combs SE, Adeberg S, Dittmar JO, Welzel T, Rieken S, Habermehl D, et al. Skull base meningiomas: long-term results and patient self-reported outcome in 507 patients treated with fractionated stereotactic radiotherapy (FSRT) or intensity modulated radiotherapy (IMRT). *Radiother Oncol* (2013) 106(2):186–91. doi: 10.1016/j.radonc.2012.07.008

131. Bachtiary B, Veraguth D, Roos N, Pfiffner F, Leiser D, Pica A, et al. Hearing loss in cancer patients with skull base tumors undergoing pencil beam scanning proton therapy: a retrospective cohort study. *Cancers (Basel)* (2022) 14(16):3853. doi: 10.3390/cancers14163853

132. Seidensaal K, Harrabi SB, Uhl M, Debus J. Re-irradiation with protons or heavy ions with focus on head and neck, skull base and brain malignancies. *Br J Radiol* (2020) 93(1107):20190516. doi: 10.1259/bjr.20190516

133. Gamez ME, Patel SH, McGee LA, Sio TT, McDonald M, Phan J, et al. A systematic review on re-irradiation with charged particle beam therapy in the management of locally recurrent skull base and head and neck tumors. *Int J Part Ther* (2021) 8(1):131–54. doi: 10.14338/IJPT-20-00064.1

134. Combs SE, Baumert BG, Bendszus M, Bozzao A, Brada M, Fariselli L, et al. ESTRO ACROP guideline for target volume delineation of skull base tumors. *Radiother Oncol* (2021) 156:80–94. doi: 10.1016/j.radonc.2020.11.014

135. Combs SE, Ganswindt U, RL F, Kondziolka D, Tonn JC. State-of-the-art treatment alternatives for base of skull meningiomas: complementing and controversial indications for neurosurgery, stereotactic and robotic based radiosurgery or modern fractionated radiation techniques. *Radiat Oncol* (2012) 7:226. doi: 10.1186/1748-717X-7-226

136. Conti A, Senger C, Acker G, Kluge A, Pontoriero A, Cacciola A, et al. Correction to: normofractionated stereotactic radiotherapy versus CyberKnife-based hypofractionation in skull base meningioma: a German and Italian pooled cohort analysis. *Radiat Oncol* (2020) 15(1):279. doi: 10.1186/s13014-020-01707-z

137. Mayo C, Martel MK, Marks LB, Flickinger J, Nam J, Kirkpatrick J. Radiation dose-volume effects of optic nerves and chiasm. *Int J Radiat Oncol Biol Phys* (2010) 76 (3 Suppl):S28–35. doi: 10.1016/j.ijrobp.2009.07.1753

138. Mayo C, Yorke E, Merchant TE. Radiation associated brainstem injury. *Int J Radiat Oncol Biol Phys* (2010) 76(3 Suppl):S36–41. doi: 10.1016/j.ijrobp.2009.08.078

139. Shen X, Andrews DW, Sergott RC, Evans JJ, Curran WJ, Machtay M, et al. Fractionated stereotactic radiation therapy improves cranial neuropathies in patients with skull base meningiomas: a retrospective cohort study. *Radiat Oncol* (2012) 7:225. doi: 10.1186/1748-717X-7-225

140. Li PC, Liebsch NJ, Niemierko A, Giantsoudi D, Lessell S, Fullerton BC, et al. Radiation tolerance of the optic pathway in patients treated with proton and photon radiotherapy. *Radiother Oncol* (2019) 131:112–9. doi: 10.1016/j.radonc.2018.12.007

141. Florijn MA, Sharfo AWM, Wiggenraad RGJ, van Santvoort JPC, Petoukhova AL, Hoogeman MS, et al. Lower doses to hippocampi and other brain structures for skull-base meningiomas with intensity modulated proton therapy compared to photon therapy. *Radiother Oncol* (2020) 142:147–53. doi: 10.1016/j.radonc.2019.08.019

142. Arvold ND, Niemierko A, Broussard GP, Adams J, Fullerton B, Loeffler JS, et al. Projected second tumor risk and dose to neurocognitive structures after proton versus photon radiotherapy for benign meningioma. *Int J Radiat Oncol Biol Phys* (2012) 83(4): e495–500. doi: 10.1016/j.ijrobp.2011.10.056

143. Hall EJ. Intensity-modulated radiation therapy, protons, and the risk of second cancers. *Int J Radiat Oncol Biol Phys* (2006) 65(1):1–7. doi: 10.1016/j.ijrobp.2006.01.027

144. Scoccianti S, Detti B, Cipressi S, Iannalfi A, Franzese C, Biti G. Changes in neurocognitive functioning and quality of life in adult patients with brain tumors treated with radiotherapy. *J Neurooncol* (2012) 108(2):291–308. doi: 10.1007/s11060-012-0821-8

145. Jacob J, Durand T, Feuvret L, Mazeron JJ, Delattre JY, Hoang-Xuan K, et al. Cognitive impairment and morphological changes after radiation therapy in brain tumors: a review. *Radiother Oncol* (2018) 128(2):221–8. doi: 10.1016/j.radonc.2018.05.027

146. Kotecha R, Hall MD. Impact of radiotherapy dosimetric parameters on neurocognitive function in brain tumor patients. *Neuro Oncol* (2020) 22(11):1559–61. doi: 10.1093/neuonc/noaa208

147. Makale MT, McDonald CR, Hattangadi-Gluth JA, Kesari S. Mechanisms of radiotherapy-associated cognitive disability in patients with brain tumours. *Nat Rev Neurol* (2017) 13(1):52–64. doi: 10.1038/nrneurol.2016.185

148. Balentova S, Adamkov M. Molecular, cellular and functional effects of radiation-induced brain injury: a review. *Int J Mol Sci* (2015) 16(11):27796–815. doi: 10.3390/ijms161126068

149. Gibson E, Monje M. Effect of cancer therapy on neural stem cells: implications for cognitive function. *Curr Opin Oncol* (2012) 24(6):672–8. doi: 10.1097/CCO.0b013e3283571a8e

150. Schmal Z, Isermann A, Hladik D, von Toerne C, Tapio S, Rübe CE. DNA Damage accumulation during fractionated low-dose radiation compromises hippocampal neurogenesis. *Radiother Oncol* (2019) 137:45–54. doi: 10.1016/j.radonc.2019.04.021

151. Goda JS, Dutta D, Krishna U, Goswami S, Kothavade V, Kannan S, et al. Hippocampal radiotherapy dose constraints for predicting long-term neurocognitive outcomes: mature data from a prospective trial in young patients with brain tumors. *Neuro Oncol* (2020) 22(11):1677–85. doi: 10.1093/neuonc/noaa076.5

152. Lambrecht M, Eekers DBP, Alapetite C, Burnet NG, Calugaru V, Coremans IEM, et al. Radiation dose constraints for organs at risk in neuro-oncology; the European particle therapy network consensus. *Radiother Oncol* (2018) 128(1):26–36. doi: 10.1016/j.radonc.2018.05.001

153. Brown PD, Jaeckle K, Ballman KV, Farace E, Cerhan JH, Anderson SK, et al. Effect of radiosurgery alone vs radiosurgery with whole brain radiation therapy on cognitive function in patients with 1 to 3 brain metastases: a randomized clinical trial. *JAMA* (2016) 316(4):401–9. doi: 10.1001/jama.2016.9839

154. Jalali R, Gupta T, JS G, Goswami S, Shah N, Dutta D, et al. Efficacy of stereotactic conformal radiotherapy vs conventional radiotherapy on benign and low-grade brain tumors: a randomized clinical trial. *JAMA Oncol* (2017) 3(10):1368–76. doi: 10.1001/jamaoncol.2017.0997

155. Tsai PF, Yang CC, Chuang CC, Huang TY, Wu YM, Pai PC, et al. Hippocampal dosimetry correlates with the change in neurocognitive function after hippocampal sparing during whole brain radiotherapy: a prospective study. *Radiat Oncol* (2015) 10:253. doi: 10.1186/s13014-015-0562-x

156. Brown PD, Gondi V, Pugh S, Tome WA, Wefel JS, Armstrong TS, et al. Hippocampal avoidance during whole-brain radiotherapy plus memantine for patients

with brain metastases: phase III trial NRG oncology CC001. *J Clin Oncol* (2020) 38 (10):1019–29. doi: 10.1200/JCO.19.02767

157. Gondi V, Hermann BP, Mehta MP, Tomé WA. Hippocampal dosimetry predicts neurocognitive function impairment after fractionated stereotactic radiotherapy for benign or low-grade adult brain tumors. *Int J Radiat Oncol Biol Phys* (2012) 83(4):e487–93. doi: 10.1016/j.ijrobp.2011.10.021

158. Gondi V, Tomé WA, Mehta MP. Why avoid the hippocampus? a comprehensive review. *Radiother Oncol* (2010) 97(3):370–6. doi: 10.1016/j.radonc.2010.09.013

159. Kazda T, Jancalek R, Pospisil P, Sevela O, Prochazka T, Vrzal M, et al. Why and how to spare the hippocampus during brain radiotherapy: the developing role of hippocampal avoidance in cranial radiotherapy. *Radiat Oncol* (2014) 9:139. doi: 10.1186/1748-717X-9-139

160. Tabrizi S, Yeap BY, Sherman JC, Nachtigall LB, Colvin MK, Dworkin M, et al. Long-term outcomes and late adverse effects of a prospective study on proton radiotherapy for patients with low-grade glioma. *Radiother Oncol* (2019) 137:95–101. doi: 10.1016/j.radonc.2019.04.027

161. Harrabi SB, Bougatf N, Mohr A, Haberer T, Herfarth K, Combs SE, et al. Dosimetric advantages of proton therapy over conventional radiotherapy with photons in young patients and adults with low-grade glioma. *Strahlenther Onkol* (2016) 192 (11):759–69. doi: 10.1007/s00066-016-1005-9

162. Adeberg S, Harrabi SB, Bougatf N, Verma V, Windisch P, Bernhardt D, et al. Dosimetric comparison of proton radiation therapy, volumetric modulated arc therapy, and three-dimensional conformal radiotherapy based on intracranial tumor location. *Cancers (Basel)* (2018) 10(11):401. doi: 10.3390/cancers10110401

163. Dutz A, Lühr A, Troost EGC, Agolli L, Bütof R, Valentini C, et al. Identification of patient benefit from proton beam therapy in brain tumour patients based on dosimetric and NTCP analyses. *Radiother Oncol* (2021) 160:69–77. doi: 10.1016/j.radonc.2021.04.008

164. van der Weide HL, Kramer MCA, Scandurra D, Eekers DBP, Klaver YLB, Wiggenraad RGJ, et al. Proton therapy for selected low grade glioma patients in the Netherlands. *Radiother Oncol* (2021) 154:283–90. doi: 10.1016/j.radonc.2020.11.004

165. Kaur G, Sayegh ET, Larson A, Bloch O, Madden M, Sun MZ, et al. Adjuvant radiotherapy for atypical and malignant meningiomas: a systematic review. *Neuro Oncol* (2014) 16(5):628–36. doi: 10.1093/neuonc/nou025

166. Wu A, MC J, Meola A, HN W, Chang SD. Efficacy and toxicity of particle radiotherapy in WHO grade II and grade III meningiomas: a systematic review. *Neurosurg Focus* (2019) 46(6):E12. doi: 10.3171/2019.3.FOCUS1967

167. Coggins WS, Pham NK, Nguyen AV, Branch DW, Guillet JY, Korst G, et al. A systematic review of ion radiotherapy in maintaining local control regarding atypical and anaplastic meningiomas. *World Neurosurg* (2019) 132:282–91. doi: 10.1016/j.wneu.2019.08.149

frontiers | Frontiers in Oncology

TYPE Original Research
PUBLISHED 12 June 2023
DOI 10.3389/fonc.2023.1153662

OPEN ACCESS

EDITED BY
Arianna Rustici,
University of Bologna, Italy

REVIEWED BY
Bharat Guthikonda,
Louisiana State University Health Shreveport, United States
Mario Zuccarello,
University of Cincinnati, United States

*CORRESPONDENCE
Raffaele De Marco
r_dema@outlook.it;
raffaele.demarco@unito.it

RECEIVED 29 January 2023
ACCEPTED 19 May 2023
PUBLISHED 12 June 2023

CITATION
Di Perna G, De Marco R, Baldassarre BM, Lo Bue E, Cofano F, Zeppa P, Ceroni L, Penner F, Melcarne A, Garbossa D, Lanotte MM and Zenga F (2023) Facial nerve outcome score: a new score to predict long-term facial nerve function after vestibular schwannoma surgery. *Front. Oncol.* 13:1153662. doi: 10.3389/fonc.2023.1153662

Facial nerve outcome score: a new score to predict long-term facial nerve function after vestibular schwannoma surgery

Giuseppe Di Perna[1,2,3], Raffaele De Marco[1,2*], Bianca Maria Baldassarre[1,2], Enrico Lo Bue[1,2], Fabio Cofano[1,4], Pietro Zeppa[1], Luca Ceroni[5], Federica Penner[1,2], Antonio Melcarne[1,6], Diego Garbossa[1,6], Michele Maria Lanotte[1,7] and Francesco Zenga[2,6]

[1]Department of Neuroscience "Rita Levi Montalcini", University of Turin, Turin, Italy, [2]Skull Base and Pituitary Surgery Unit, "Città della Salute e della Scienza" University Hospital, Turin, Italy, [3]Spine Surgery Unit, Casa di Cura "Città di Bra", Bra, Cuneo, Italy, [4]Spine Surgery Unit, Humanitas Gradenigo Hospital, Turin, Italy, [5]Department of Psychology, University of Turin, Turin, Italy, [6]Neurosurgery Unit, "Città della Salute e della Scienza" University Hospital, Turin, Italy, [7]Functional, Oncological and Stereotactic Neurosurgery Unit, "Città della Salute e delle Scienza" University Hospital, Turin, Italy

Introduction: Patients' quality of life (QoL), facial nerve (FN), and cochlear nerve (CN) (if conserved) functions should be pursued as final outcomes of vestibular schwannoma (VS) surgery. In regard to FN function, different morphologic and neurophysiological factors have been related to postoperative outcomes. The aim of the current retrospective study was to investigate the impact of these factors on the short- and long-term FN function after VS resection. The combination of preoperative and intraoperative factors resulted in designing and validating a multiparametric score to predict short- and long-term FN function.

Methods: A single-center retrospective analysis was performed for patients harboring non-syndromic VS who underwent surgical resection in the period 2015–2020. A minimum follow-up period of 12 months was considered among the inclusion criteria. Morphological tumor characteristics, intraoperative neurophysiological parameters, and postoperative clinical factors, namely, House–Brackmann (HB) scale, were retrieved in the study. A statistical analysis was conducted to investigate any relationships with FN outcome and to assess the reliability of the score.

Results: Seventy-two patients with solitary primary VS were treated in the period of the study. A total of 59.8% of patients showed an HB value < 3 in the immediate postoperative period (T1), reaching to 76.4% at the last follow-up evaluation. A multiparametric score, Facial Nerve Outcome Score (FNOS), was built. The totality of patients with FNOS grade A showed an HB value < 3 at 12 months, decreasing to 70% for those with FNOS grade B, whereas 100% of patients with FNOS grade C showed an HB value ≥ 3. The ordinal logistic regression showed three times increasing probability to see an HB value ≥ 3 at 3-month follow-up

for each worsening point in FNOS score [Exp(B), 2,999; $p < 0.001$] that was even more probable [Exp(B), 5.486; $p < 0.001$] at 12 months.

Conclusion: The FNOS score resulted to be a reliable score, showing high associations with FN function both at short- and long-term follow-up. Although multicenter studies would be able to increase its reproducibility, it could be used to predict the FN damage after surgery and the potential of restoring its function on the long-term period.

KEYWORDS

vestibular schwannoma, restrosigmoid approach, facial nerve, facial nerve function, intraoperative neuromonitoring, outcome score

1 Introduction

Facial nerve (FN) function after surgery for vestibular schwannoma (VS) highly influences the quality of life (QoL) of the patients (1–7). More than gross total resection (GTR), preserving FN function is a primary concern along with hearing, if did not affect, during VS surgery. Although optimal percentages of anatomical preservation of the FN (reaching 95%) have been described, functional preservation rates are still lower, varying from 70 to 90% in different series (8, 9).

To preserve this function, surgical strategy has been moved from GTR to near-total (NTR) or subtotal resection (STR) balancing functional integrity preservation with disease's control and respecting the concept of "maximal safe resection", which is broadly diffused in skull base surgery (10, 11).

However, despite surgical strategy to preserve FN function (12) and the introduction of this "sparing surgery policy" (13), FN palsy still continues to represent the main source of morbidity related to VS surgery.

The possibility to predict long-term outcome of FN function could anticipate the patient that can benefit from an early procedure of facial-hypoglossal anastomosis (14).

Different factors resulted to be associated to postoperative FN function, independently or in association, but only few studies have proposed specific practical tools to anticipate FN function (15–18).

Therefore, the aim of this study is to evaluate the effect of morphological and neurophysiological factors on short- and long-term FN function. In addition, by combining factors significantly capable of influencing nerve function, the current study aims to build a new multi-parametric score defining its validity and association with short- and long-term FN function.

2 Materials and methods

This is a retrospective study analyzing prospectively collected data of patients undergoing surgery for VS removal by a team of experienced surgeons composed of neurosurgeons and otolaryngologists, at the authors' institution from 2015 to 2020.

Adult patients (age ≥ 18 years) with primary diagnosis of non-syndromic vestibular schwannoma were included in the study. Conversely, patients with preoperative FN deficiency and patients undergoing facial-hypoglossal anastomosis were excluded from the study. Finally, unavailability of clinical, radiological, and intra- and postoperative data, and a minimum 12-month follow-up resulted in exclusion from the study. All inclusion and exclusion criteria were summarized in (Supplementary Table 1).

The following data were collected for the study: biographical data, age, sex, tumor type, tumor size, tumor morphology, preoperative neurological status, type of surgical approach, intraoperative FN stimulation data, extent of resection, complications, length of surgery, histological examination, and clinical data regarding FN function assessed both postoperatively and during follow-up.

2.1 Neuroimaging

Tumor size and its relationships with surrounding CPA (Cerebellopontine angle) structures were analyzed using T1-weighted (T1w) sequences with gadolinium and FIESTA (fast imaging employing steady-state acquisition) or CISS (constructive interference in steady state) nuclear magnetic resonance imaging (MRI) sequences. Specifically, tumor size was measured in

Abbreviations: VS, vestibular schwannoma; ST, stimulation threshold; FN, facial nerve; NF2, neurofibromatosis 2; CPA, cerebellopontine angle; CSF, cerebrospinal fluid; MRI, magnetic resonance imaging; FIESTA, fast imaging employing steady-state acquisition; CISS, constructive interference in steady state; TIVA-TCI, total intravenous anesthesia– target controlled infusion; IONM, intraoperative neurophysiological monitoring; LD, lumbar drain; MEPs, motor evoked potentials; SEPs, sensory evoked potentials; BAEPs, brainstem acoustic evoked potentials; f-MEPs, corticobulbar evoked potentials for the facial nerve; FT-0, facial nerve threshold T0; FT-1, facial nerve threshold T1; DT, delta threshold; GTR, gross total resection; NTR, near total resection; STR, sub total resection; HB, House–Brackmann.

millimeters, using the largest diameter of the extra-meatal portion of the tumor measured on axial cuts of T1w sequences with gadolinium, according to the international measurement criteria (19, 20). Tumors with diameters greater than 30 mm were classified as large tumors, whereas tumors with diameters less than 30 mm were classified as small tumors.

On the basis of the presence or absence of the cystic component, either central or peripheral, tumors were classified morphologically as cystic and non-cystic (21).

VS relationships with the internal acoustic meatus and CPA structures was assessed by using two of the most used classification systems, namely, the Koos and the Samii classifications (22–24).

2.2 Surgical technique and intraoperative neurophysiological monitoring

A retrosigmoid approach to the CPA was performed in all cases. Patient was positioned in lateral position with the head fixed to a Mayfield headrest, slightly flexed and rotated so that the mastoid tip resulted to be the highest point. A lumbar drain was placed in all patients to facilitate intraoperative brain relaxation and to facilitate surgical wound closure in the postoperative period.

Once the CPA was exposed, direct stimulation of the VS surface was performed routinely by using a monopolar stimulator, to identify any posterior dislocation of the VII cranial nerve. Subsequently, the tumor capsule was opened, and intralesional debulking was performed to reduce tumor size to identify the FN along its cisternal course. Debulking was performed with the use of ultrasonic aspirator (Sonopet®, Stryker) by constant direct stimulation of the FN to promptly identify the nerve close to the tumor. Once the tumor volume in the CPA was reduced, the FN was identified at its origin from the brainstem. At this point, a search for the FN proximal ST was performed by direct stimulation (*see section IONM*).

After identifying the FN at its origin, lesion debulking proceeded, and the tumor was dissected from the FN following the plane previously identified on the brainstem.

In cases where the plane of dissection was not identifiable and in cases of infiltration of the nerve by the tumor, a residual tumor was left attached to the nerve to preserve both its anatomical and functional integrity.

At the end of resection, direct stimulation of the nerve at its emergence to the brainstem was repeated and the new ST was recorded.

2.2.1 IONM

All the procedures were performed using a neurophysiological monitoring system including motor evoked potentials (MEPs), sensory evoked potentials (SEPs), brainstem acoustic evoked potentials (BAEPs), free running-electromyography (EMG), and direct stimulation. In patients undergoing surgery in the last 2 years of the series, monitoring of corticobulbar evoked potentials for FN (f-MEPs) was also introduced; however, because of the heterogeneity of the available data, information on such monitoring was not included in this study.

Data were collected for direct stimulation performed with NIM 3.0 (*Nerve Monitoring System*, *Medtronic*) that allowed to record the activity of selected muscle groups by EMG monitoring. Electrodes for FN monitoring were inserted at the level of the orbicularis muscle of the eye and the orbicularis of the mouth of the side corresponding to the nerve of interest for two-channel monitoring.

Monitoring was performed by associating continuous monitoring of free-running EMG activity and by direct stimulation with a monopolar stimulator, to identify, in the different phases of the surgery, both the nerve stimulation thresholds (STs) and the course of the dislocated nerve during tumor removal.

The stimulation phases were performed as follows: (1) identification of the FN ST at its emergence from the brainstem (proximal ST); (2) direct supra-threshold stimulation during tumor debulking to identify and map the nerve along its course; (3) check of proximal ST before starting the intra-meatal removal phases; (4) check of proximal ST at the end of tumor removal.

Intraoperative neurophysiological monitoring (IONM) data collected and evaluated in the study were as follows:

-*Facial nerve threshold T0 (FT-0)*: The minimum amplitude (milliamperes) required to obtain an EMG response of the nerve at its proximal emergence at the brainstem level before tumor removal;

-*Facial nerve threshold T1 (FT-1)*: The minimum amplitude (milliampere) required to obtain an EMG response of the nerve at its proximal emergence at brainstem level after tumor removal;

-*Delta threshold (DT)*: The difference in absolute value between FT-1 and FT-0.

2.3 Extent of resection

The extent of resection was defined by evaluating gadolinium-enhanced T1w MRI sequences performed at 3 months after surgery. GTR was defined as the complete absence of residual detectable on T1w MRI with gadolinium, NTR was defined as the presence of residual with a diameter ≤ 2 mm often not visible on MRI but left *in situ* during surgery to functionally preserve the nerve, and STR was defined as the presence of residual not attributable to NTR.

2.4 Outcome definition and classification

The primary outcome of the study was FN function after surgery and was assessed using the HB clinical scale (25). In this study, House–Brackmann (HB) scale values were used as the primary outcome and were grouped into two categories so that the analytic evaluation could be based on nominal variables. The categories used were "good" including patients with HB 1 and/or 2 and "poor" including patients with HB values of 3, 4, 5, and 6.

Clinical evaluation of FN function was performed by a team of three experienced neurosurgeons (RDM, ELB, and FZ) at different times during the postoperative period and was done by direct clinical interview and/or video call. Specifically, HB grade was assigned at postoperative day 4 (T1), at 3 months after surgery

(T2), 12 months after surgery (T3), and during clinical evaluation at the last available follow-up (T4). Given the inherent subjectivity of the adopted scale, if there was discordance between the values assigned by the different examiners, then the worst score was considered.

2.5 Statistical analysis

Descriptive statistics were reported with mean and standard deviation for cardinal variables and with frequency and percentage for categorical variables. A Shapiro–Wilk Test was used to assess the normality of the distribution of quantitative variables and a Spearman's Rho test to assess the concordance of scores for quantitative variables. The existence of a model with statistically significant predictive ability toward the dichotomized HB grade was assessed using the binary logistic regression model. Statistical significance was set at $p \leq 0.05$. All the analysis was conducted on SPSS (version 26.0; IBM Corp., Armonk, NY).

3 Results

After a thorough evaluation of the inclusion and exclusion criteria, a total number of 72 patients were considered eligible for the study. Twenty-eight patients were not included because of the lack of facial function data at 1 year (15 patients), realization of facial-hypoglossal anastomosis (five patients), and a positive history of previous surgery and/or radiosurgery (eight patients).

Most of patients were women with a ratio of 2.4:1 [51 F (70.8%) and 21 M (29.2%)]. The mean age was 59.9 ± 8.76 years ($p = 0.159$). Regarding neuroimaging data, the mean largest tumor diameter was 27.4 ± 18.59 mm ($p < 0.001$), and most tumors did not have the cystic component [51 (70.8%) vs. 21 (29.2%)]. In accordance with Samii's classification, the most represented type was T4A [25 patients (34.7%)]. The mean duration of surgery was 324.16 ± 89.3 min ($p < 0.001$), and the extent of resection was 32 GTR (44.4%), 30 NTR (41.6%), and 10 STR (13.9%). Mean follow-up was 22.4 ± 18.4 months. As for complications, four patients (5.5%) developed a CSF (Cerebrospinal fluid) fistula, which was subsequently surgically repaired, one patient (1.3%) developed hydrocephalus undergoing peritoneal ventricular shunt placement, and one patient (1.3%) developed transverse and sigmoid sinus thrombosis that was subsequently solved with heparin therapy.

Analyzing FN function according to HB, 43 patients belonged to the HB "good" group on postoperative day 4, 49 patients at 3 months, and 53 patients at 12 months. At the last follow-up, 76.4% of patients showed "good" HB versus 23.6% of patients with "poor" HB. Specifically, 43 patients (59.7%) had HB value of 1 at 12 months and at the last follow-up, whereas patients with HB value of 2 were 10 (13.9%) at 12 months and 12 (16.7%) at the last follow-up (Figure 1).

All population characteristics were reported in Table 1.

3.1 Statistical analysis

First, a direct statistical association was investigated between variables, and, thereafter, a logistic regression model was built to analyze the relationships of these variables with the FN functionality during the follow-up. All the variables that had been found to be significantly correlated in the multivariate analysis models were merged to build a score (see section FNOS) after defining statistically significant cutoffs for continuous variables. Age, surgical time, and the extent of resection did not result to be significantly associated to postoperative HB grade.

Finally, the value resulting from the FNOS was assigned to all patients, and univariate and multivariate analyses were performed to validate the score, demonstrating a significant association with the outcome measure (FN function).

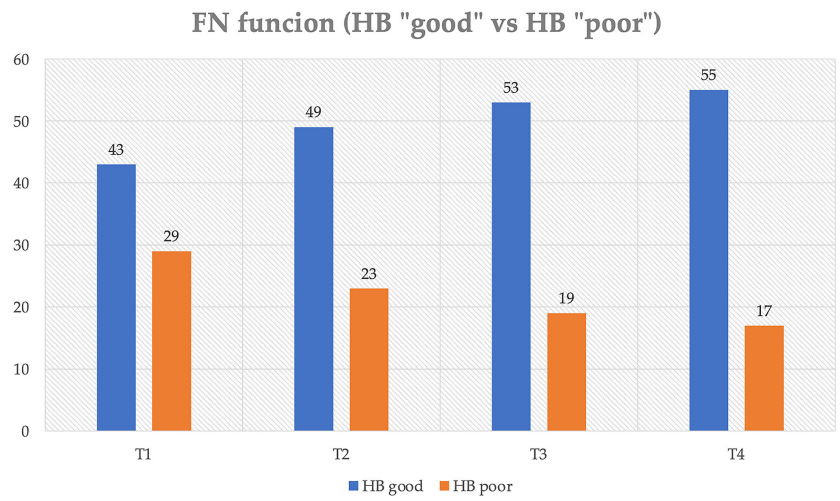

FIGURE 1
Distribution of postoperative FN function (House–Brackmann scale) over time. T1, IV postoperative day; T2, 3-month follow-up; T3, 1-year follow-up; T4, last follow-up.

10.3389/fonc.2023.1153662

TABLE 1 Demographics: quantitative and qualitative variables.

Variable	Mean	SD	Shapiro–Wilk Test
Age	59.91	8.76	p = 0.159
Tumor major diameter	27.44	18.59	p < 0.001
Facial nerve stimulation T1 (mA)	0.20	0.35	p < 0.001
Delta threshold (mA)	0.18	0.35	p < 0.001
Surgical time (min)	324.16	89.33	p = 0.049
Variables		**Frequencies**	**%**
Sex	F	51	70.8
	M	21	29.2
Cystic	Yes	21	29.2
	No	51	70.8
Samii grade	T1	2	2.8
	T2	5	6.9
	T3a	16	22.2
	T3b	20	27.8
	T4a	25	34.7
	T4b	4	5.6
Koos	1	3	4.2
	2	23	31.9
	3	19	26.4
	4	27	37.5
HB T1 (IV postop day)	1	22	30.6
	2	21	29.2
	3	14	19.4
	4	10	13.9
	5	5	6.9
HB T2 (3 months)	1	33	45.8
	2	16	22.2
	3	9	12.5
	4	8	11.1
	5	6	8.3
HB T3 (12 months)	1	43	59.7
	2	10	13.9
	3	8	11.1
	4	6	8.3
	5	5	6.9
HB T4 (last follow-up)	1	43	59.7
	2	12	16.7
	3	9	12.5
	4	4	5.6

(Continued)

TABLE 1 Continued

Variables		Frequencies	%
	5	4	5.6
Extent of resection	GTR	32	44.4
	NTR	30	41.6
	STR	10	13.9
Complications	CSF Leak	4	5.5
	Hydrocephalus	1	1.3
	Sinus thrombosis	1	1.3

A Shapiro–Wilk test was used to assess normality of distribution of quantitative variables.

Initially, a statistically significant linear correlation was observed between HB scale values and different assessment timings ($p < 0.01$). As shown in Supplementary Table 2, there was a strong statistically significant association ($V = 0.774$, $p < 0.01$) between the HB grade recorded at IV postoperative day (T1) and 3-month follow-up (T2). Only 2.3% of patients in the group of "good" HB (HB < 3) at T1 experienced a worsening at T2, whereas the 24.1% of "poor" HB subjects at T1 had an improvement at T2. Similarly, these associations were confirmed between the degree of HB at T1 and T4 ($V = 0.677$, $p < 0.01$). None of the "good" HB subjects at T1 had a worsening at T4; 41.4% of the "poor" HB subjects at T1 had an improvement at T4.

An ordinal logistic regression model using the degree of HB (HB < 3 vs. ≥ 3, "good" vs. "poor") showed a statistically significant association with the maximum tumor diameter, Samii grade, the FT1, and the DT.

Specifically, the absence of a cystic component was found to be a protective factor. Indeed, the likelihood of observing an elevated HB value was, respectively, −2.6- and −1.3- fold lower in solid tumors both in the medium and long terms [T2: Nagelkerke R-square, 0. 603 with $p < 0.05$; Exp(B), 2.60; $p < 0.001$; T3: R-square Nagelkerke, 0.645 with $p < 0.05$; Exp(B), 1.28; $p < 0.001$; T4: R-square Nagelkerke, 0.598 with $p < 0.05$; Exp(B), 1.29; $p < 0.001$]. Similarly, DT appeared to be a worsening factor with an approximately seven-fold greater likelihood at T2 and T3 and approximately six-fold greater likelihood at T4 of observing an elevated HB value [T2: R-square Nagelkerke, 0. 603 with $p < 0.05$; Exp(B), 7.03; $p < 0.001$; T3: R-square Nagelkerke, 0.645 with $p < 0.05$; Exp(B), 7.10; $p < 0.001$; T4: R-square Nagelkerke, 0.598 with $p < 0.05$; Exp(B), 5.79; $p < 0.001$]. Last, FT-1 showed a strong relationship in the logistic regression analysis, resulting in a seven-fold increase at T2 and a five-fold increase at T3 in the risk of obtaining a "poor" HB for each increase in FT-1 (Table 2).

The univariate (Supplementary Table 3) and the multivariate analyses with binary logistic regression using as dependent variable the HB "good" and HB "poor" groups confirmed the statistical significance of the independent variables found to be associated in the previous model.

As next step, cutoffs were identified by descriptive analysis of statistically significant associations. Although association analysis was performed at various times, because of the high association value identified at 12 months ($p < 0.001$), cutoffs were identified at T3 for both the DT and FT-1 variables (Supplementary Table 4).

Indeed, 100% of patients with DT ≤ 0.07 and 66.7% of patients with DT between 0.07 and 0.19 were HB "good" at 3 months, whereas 100% of patients with DT > 0.19 had HB "poor" at the same time (Cramer's V, 0.896; $p < 0.001$). Similarly, statistically significant associations between FT-1 value and HB grade group were reported in (Supplementary Table 3). Specifically, 100% of patients with FT-1 ≤ 0.08 and 70% of patients with FT between 0.08 and 0.20 were HB "good" at 3 months, whereas 100% of patients with FT > 0.20 had HB "poor" (Cramer's V, 0.892; $p < 0.001$).

Once cutoffs of continuous variables and significantly associated categorical variables were identified, the relationship between FNOS and HB groups ("good" vs. "poor", < 3 vs. ≥ 3) was assessed.

3.2 Facial Nerve Outcome Score

Building the score was based on the idea of being able to interpolate the statistically correlated independent variables with the postoperative FN function. Tumor size, Samii classification, solid or cystic radiological aspect, FT-1, DT, and FT-1 * DT all showed a statistical significance in the logistic regression and were retrieved as independent variable of the score (Figure 2).

In terms of cutoff, an arbitrary threshold of 30 mm was defined considering the average value of study population (27 ± 18 mm) and the results in terms of FN function obtained for tumors with a maximum diameter greater than 30 mm (21, 22, 26–30).

The Samii grade and dimensions appeared to be related statistically to the FN function at FU. T3a Samii grade, namely, a tumor extending in the CPA cistern and in contact with the trunk, causes a more important dislocation of the FN, making its surgical dissection more difficult and at higher risk of postoperative deficit (22, 27, 31, 32). For this reason, one point was given in case of tumor presenting as Samii T3b or T4.

One point was given for the presence of intratumor cystic component, because of its absence resulted to be a protective factor, reducing by about two times the probability of observing a deficit of FN HB "poor".

TABLE 2 Multivariate analysis showing the role of different variables influencing FN outcome at different time (T2–T4).

T2			
Nagelkerke R^2	Model's Fit	Goodness of Model	
		Pearson	Variance
0.603	p < 0.05	p > 0.05	p > 0.05
Variable		Exp(B)	p-Value
Samii Grade		17.18	**0.000**
Cystic		−2.60	**0.001**
DT		7.035	**0.000**
FT-1		7.0	**0.001**
T3			
Nagelkerke R^2	Model's Fit	Goodness of Model	
		Pearson	Variance
0.645	p < 0.05	p > 0.05	p > 0.05
Variable		Exp(B)	p-Value
Samii grade			–
Cystic		−1.28	**0.001**
DT		7.10	**0.000**
FT-1		5.0	**0.007**
T4			
Nagelkerke R^2	Model's Fit	Goodness of Model	
		Pearson	Variance
0.603	p < 0.05	p > 0.05	p > 0.05
Variable		Exp(B)	p-Value
Samii grade			–
Cystic		−1.287	**0.001**
DT		5.79	**0.000**
FT-1		1.7	**0.01**

The bold values denote statistical significance a P < 0.05 level.

Three ranges were identified for the maximum nerve ST at its brainstem emergence recorded at the end of surgery (FT-1), assigning one point for values of FT-1 < 0.08 mA, two points for values of FT-1 between 0.09 mA and 0.20 mA, and three points for values of FT-1 > 0.20 mA.

Similarly, the difference between FT-1 (at the end) and FT-0 (at the beginning) (DT) was divided in values < 0.07 mA (one point), values between 0.08 and 0.19 mA (two points), and values > 0.19 mA (three points).

Given the close mathematical correlation of the parameters DT and FT-1, the value considered by the score for the calculation of the final score did not take into account the individual values but the product of both, reported in the score as FT-1 * DT.

The final score was the result of the sum of the individual scores assigned to the following four items: tumor size (< 30 mm and ≥ 30 mm), Samii classification (≤ T3a and > T3b), morphology (solid and cystic), and FT-1 * DT.

According to the result, ranging from 1 to 12, three groups of patients can be identified:

-FNOS-A for scores ≤ to 4;

-FNOS-B for scores between 5 and 6;

-FNOS-C for scores ≥ to 7.

Three cases illustrating score calculation are reported in Figure 3.

At this point, an association was investigated between the FNOS grade the HB group at different moments of the FU. A strong and increasing positive association between FNOS grade and HB grade was observed at both T1, T2, T3, and T4 (Tables 3A-D; Figure 4).

10.3389/fonc.2023.1153662

TABLE 3 Association between FNOS class and FN function (HB grade) at different time (T1–T4).

a			
Variable		HB T1	
	Modality	HB "good"	HB "poor"
FNOS	A ≤ 4	42	5
	%	89.4	10.6
	B = 5–6	1	9
	%	10	90.0
	C ≥ 7	0	15
	%	0	100
Chi-Squared		Cramer's V	p-Value
49.684		0.831	**0.000**
b			
Variable		HB T2	
	Modality	HB "good"	HB "poor"
FNOS	A ≤ 4	45	2
	%	95.7	4.3
	B = 5–6	4	6
	%	40	60
	C ≥ 7	0	15
	%	0	100
Chi-Squared		Cramer's V	p-Value
60.800		0.851	**0.000**
c			
Variable		HB T3	
	Modality	HB "good"	HB "poor"
FNOS	A ≤ 4	47	0
	%	100	0
	B = 5–6	8	2
	%	80	20
	C ≥ 7	0	15
	%	0	100
Chi-Squared		Cramer's V	p-Value
60.364		0.919	**0.000**
d			
Variable		HB T4	
	Modality	HB "good"	HB "poor"
FNOS	A ≤ 4	47	0
	%	100	0
	B = 5–6	9	4

(Continued)

TABLE 3 Continued

d			
Variable		HB T4	
	%	81.8	18.2
	C ≥ 7	0	15
	%	0	100
Chi-Squared		Cramer's V	p-Value
63.129		0.936	**0.000**

Patients were divided in "good" and "poor" HB outcome (< 3 and ≥ 3, respectively).
The bold values denote statistical significance a P < 0.05 level.

However, this association was more evident at 12 months and at the last follow-up (T1 Cramer's V, 0.831; T2 Cramer's V, 0.851; T3 Cramer's V, 0.919; T4 Cramer's V, 0.936; p < 0.001). Specifically, 100% of patients with FNOS-A belonged to HB "good" group at 12 months after surgery, whereas decreasing at 70% for those with FNOS-B and 100% of patients with FNOS-C presented an HB ≥ 3 at 12 months (Table 3).

Finally, a binary logistic regression confirmed the existence of this statistically significant association of the score with the HB group with a model with good reliability at 3 and 12 months, whereas losing statistical significance at the last follow- up for the violation of the assumptions of logistic regression, given the high strength of association (Supplementary Table 5). On an in-depth view, the unitary increase of FNOS value showed an increase by about three times the probability of observing a "poor" HB value at 3 months [R-square Nagelkerke, 0.798; Exp(B), 2.999; p < 0.001] and by about five times at 12 months [R-square Nagelkerke, 0.891; Exp(B), 5.486; p < 0.001].

Similarly, the binary logistic regression analysis performed using the categorical FNOS variable to assess the probability of observing a "good" or "poor" HB value at T2, T3, and T4 lost statistical significance because the high precision of the model violated the regression axioms (see percentages of model accuracy in Supplementary Table 5).

4 Discussion

Important advances in the treatment of VS have been registered in recent years due to technological development and the growth of surgical technique. This improvement has increasingly highlighted the importance of functional preservation of the FN and overall neurological status (30, 33–35).

Several studies reported percentages ranging from 60% to 90% of patients with HB 1 or 2 at 12 months after surgery, emphasizing the importance of several clinical, morphological, and functional factors significantly correlated with this outcome (21, 29, 30, 36).

In the present study, the percentage of patients with FN function classifiable as "good", HB < 3, resulted 73.7% at 12 months after surgery, reaching 76.4% at the last follow-up (mean, 24 months). Tumor size, tumor morphology, the grade according to the Samii classification, and FT-1 and DT, among IONM parameters, were found to be significantly related to the long-term FN function. Meanwhile, unlike other studies, the extent of resection was not statistically significant. These factors represent the structural pillars of the FNOS, a score that combines the importance of neurophysiological parameters of FN function with tumor characteristics and was found to be strongly associated with long-term FN function.

4.1 Tumor size

Since the first studies concerning VS surgery, tumor size, predominantly assessed as the largest diameter of the cisternal component of the tumor, has been found to be a prognostic factor related to postoperative FN function (22, 26–28), although there is no homogeneity in the definition of a true size cutoff (20).

A grater diameter means often a pre-existing nerve suffering due to compressing and stretching forces exerted by large tumors and the need for more aggressive and repeated surgical maneuvers. Those were the explanation of the higher 1-year incidence of patients with HB greater than 3 among stage IV tumors (45% HB value of 3–6) reported by Rinaldi et al. (28). In the present study, tumor size was not significantly associated with HB grade in the long term (p = 0.100) but maintained significance of the association until T2 (p = 0.05). The latter was a result that it is not too different from another one registered in 256 patients (30) although the maximum diameter of involved tumors was 15 mm.

4.2 Grade according to Samii

Samii et al. in 1997, reporting their experience on the treatment of 1,000 VSs, proposed a grading scale and demonstrated how it correlated with facial nerve function (22). The important role of this grading system in predicting FN outcome was more recently confirmed in 212 patients as well (32); the percentage of patients with HB 1 to 3 was 90% for Samii grade 2–3 tumors (T2–T3) versus 70% of tumors classified as T4 (p < 0.001). Moreover, in addition to the relationship between Samii grade and the anatomical and functional preservation of the facial nerve, the FN outcome could rely on the type of nerve displacement. Indeed, the anterior dislocation of the nerve led to significantly better results (HB I and II: 76%) compared to antero-lateral or antero-medial dislocation (HB I and II: 60%).

10.3389/fonc.2023.1153662

FNOS SCORE	
ITEMS	**VALUES**
Dimensions	
< 30 mm	0
≥ 30 mm	1
Samii Grade	
≤ T3a	0
≥ T3b	1
Morphology	
Solid	0
Cystic	1
FT-1 Group	
A (≤ 0.08 mA)	1
B (0.09 - 0.20 mA)	2
C (> 0.20 mA)	3
DT Group	
A (≤ 0.07 mA)	1
B (0.08 - 0.19 mA)	2
C (> 0.19 mA)	3
FT-1 * DT	
Total	*

***FNOS Total: Dimensions + Samii grade + Morphology + (FT-1 * DT)**

FNOS Grade	Value
FNOS-A	≤ 4
FNOS-B	5 – 6
FNOS-C	≥ 7

FIGURE 2
Facial Nerve Outcome Score (FNOS). Each item of the score is showed: dimensions, Samii grade, morphology, facial nerve threshold T1 (FT-1) (the minimum amplitude (mA) required to obtain an EMG response of the nerve at its proximal emergence at brainstem level after tumor removal), and delta threshold (DT) (the difference in absolute value between FT-1 and FT-0). The final score is the result of dimensions + Samii grade + morphology + (FT-1 * DT).

This aspect, replicated in the literature (21), could be related to the type of relationship that the tumor develops with the trunk, considering that the dislocation of the trunk can alter the position of the nerve emergence in regard to its entrance in the internal auditory meatus, causing its rotation along its major axis in the cisternal tract, where, together with fibers splitting induced by the tumor, it could lead to the presence of greater antero-superior and antero-inferior displacement in the Samii T4 grades.

In the present study, although nerve dislocation pattern was not considered, the percentage of patients with "good" HB in Samii T4 tumors was significantly lower than in patients with Samii T2 and T3 tumors both in the short and long terms (HB "good" at 12 months: 93%, Samii T2–T3; 67%, Samii T4; Figure 5). Moreover, this difference is even more marked in the short-term (HB "good": 17% postoperatively and 8% at 3 months in Samii T4 tumors), confirming that may be an effect strictly connected to surgical maneuvers but not exclusively relied on them, giving the presence of other factors that can affect the long-term outcome (i.e., functional status of the nerve and type of nerve damage).

4.3 Morphology

Several studies in the literature highlighted the importance of the presence of a cystic component within the VS and the influence that this component may have on the FN function (21, 37–40).

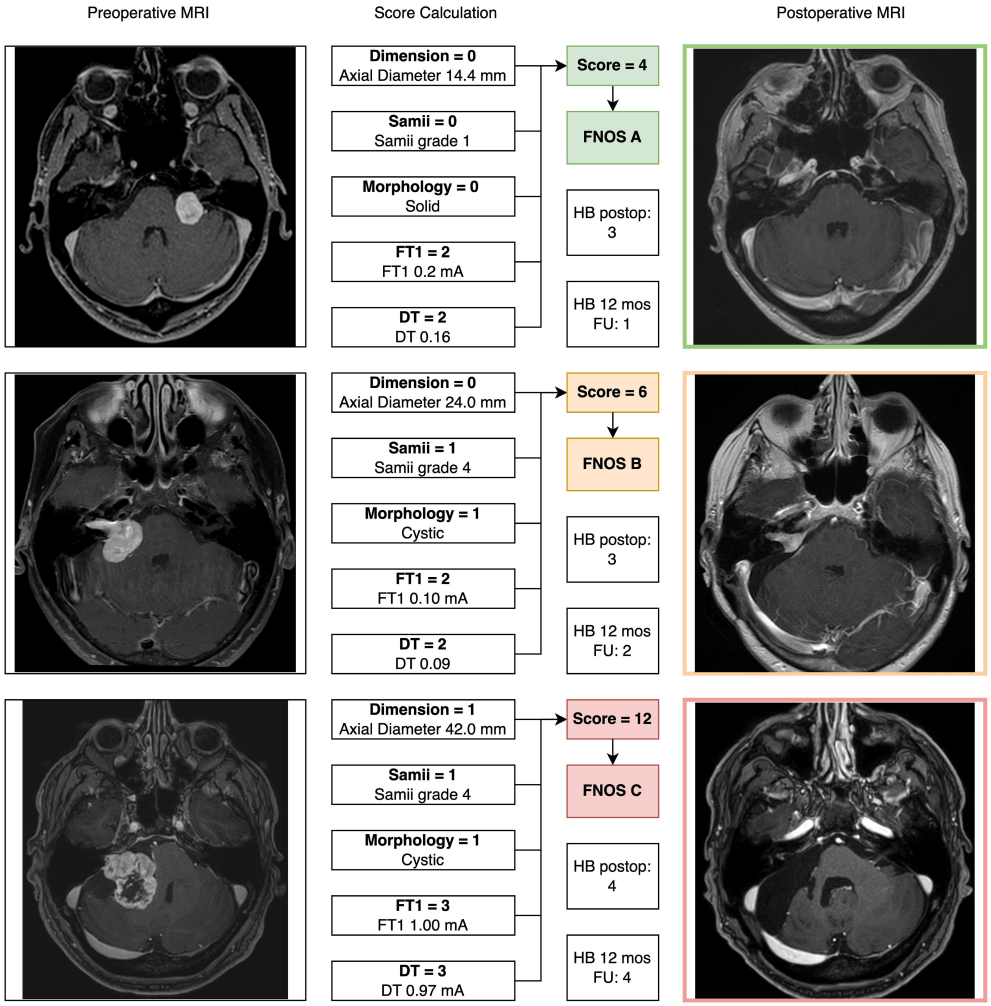

FIGURE 3
Three exemplary cases of patients with vestibular schwannoma were reported illustrating the "Facial Nerve Outcome Score" calculation. In all cases, a 12-month postoperative brain MRI (axial cut of T1-weigthed contrast enhanced MRI) showed the extent of resection.

Moon et al., analyzing 106 VSs (24 cystic and 82 solids), reported a higher incidence of nerve sections and worse function according to HB grade in patients with cystic VSs. The authors also hypothesized the role played by the expression of matrix metallo proteases (MMPs). In particular, the high expression of MMP-2 within the cyst fluid and the inner layer of the cyst wall would seem to be responsible for the tumor size enlargement and the marked adhesion of cystic VS to the nerve, also emphasizing the role that the proteolytic activity of MMP-2 may play on the integrity of the blood-liquid barrier at the nerve surface (39).

Although many works in the literature agree on the increased risk of nerve damage and recommend the observance of some technical expedients such as blunt dissection, considering the absence of a true arachnoid plane with the cyst wall, some authors did not find a statistically significant difference on FN function between solid and cystic VSs (32, 41).

In the present study, the presence of a cystic component was significantly correlated with FN function in logistic regression analysis. Specifically, the absence of a cystic component results in an approximately two-fold reduced probability of having a "poor" HB at postoperative and at 3 months. When evaluated at 12 months and at the last follow-up, this correlation— always significant —is reduced to a probability of having a "poor" HB grade about one time lower. This aspect underlines once again how the impact of factors related to the morphology of the tumor seems to have a greater predictive power in the short term than in the long term, probably because of surgical maneuvers.

4.4 FT-1 * DT

In the increasingly demonstrated surgical perspective of favoring FN preservation over the extent of resection of VSs, shifting the goal from maximal resection to maximal "safe" resection, scientific interest in IONM and various techniques for intraoperative monitoring of FN function has exponentially grown (15, 17, 18, 24, 30, 32, 34, 36, 41–46).

Since the important experience of Goldbrunner et al. reporting an increase from 1.6% to 75% in the probability of having a significant facial deficit at 6 months for patients with proximal-

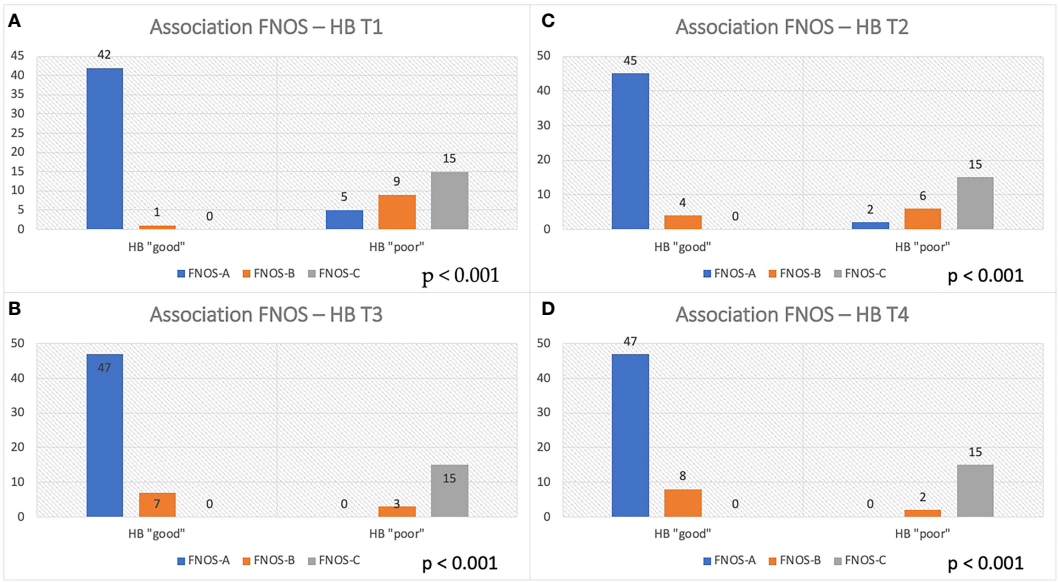

FIGURE 4
Association between FNOS and FN function (HB grade) at different time (T1-T4, **A–D**). Patients are divided in "good" and "poor" HB outcome < 3 and ≥ 3, respectively, considering the result of the score FNOS (FNOS-A, -B and -C).

distal EMG ratios < 0.8 and < 0.128, respectively (16), different parameters of IONM have been investigated obtaining good results. Indeed, Prell et al. found a "poor" FN outcome for A-train times greater than 10 s (44), Lin et al. found a positive predictive value in stimulating the nerve emergence at level of the brainstem and evaluating the EMG response in microV (18), and others found a predictive value even more significant combining two or more variables (43).

More recently, the use of FN cortico-bulbar evoked potentials (f-MEPs) has been introduced to increase the predictive power of the IONM (9, 47). A statistically significant correlation was found between f-MEPs with HB grade at 6 weeks, 6 months, and 12 months after surgery (78% and 73% of HB I or II, respectively) (36, 46).

A strong association between intraoperative FN stimulation parameters and short- and long-term postoperative HB grade in

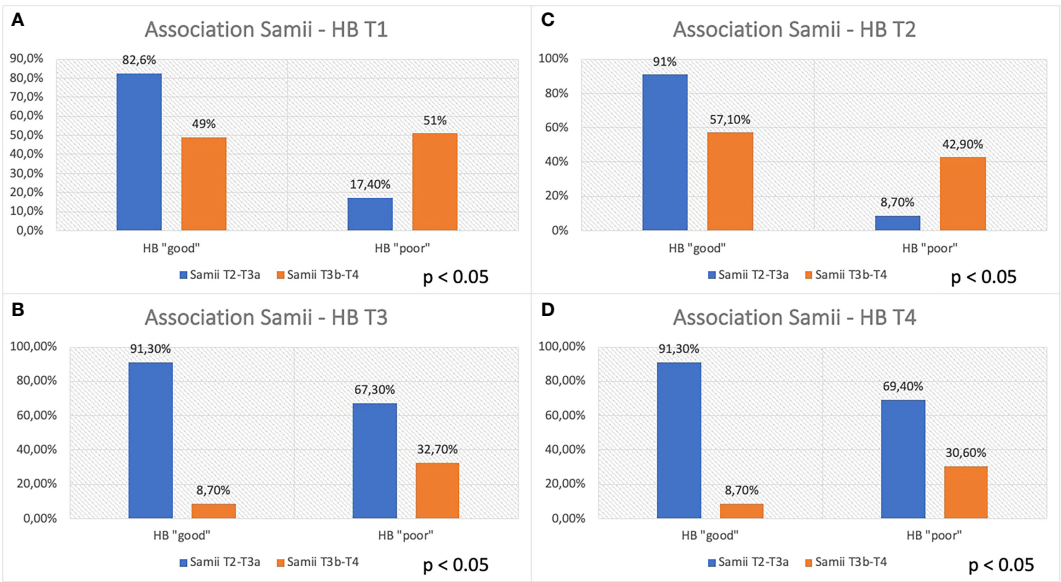

FIGURE 5
Association between Samii grade and FN function at different time (T1–T4, **A–D**). Patients are divided, considering the Samii grade (T2–T3a vs. T3b–T4), in "good" and "poor" HB outcome, < 3 and ≥ 3, respectively.

both univariate and multivariate analyses was confirmed in the current results (Supplementary Table 4). A total of 100% of patients with FT-1 ≤ 0.8 mA and DT ≤ 0.7 mA reported "good" HB at 12-month follow-up and conversely at the same time 100% of patients with FT-1 > 0.20 mA and DT > 0.19 mA reported "poor" HB, whereas, for intermediate values of FT-1 (0.09–0.20 mA) and DT (0.08–0.19 mA), the percentages of "good" HB at 12 months were 69.2% and 66.7%, respectively.

4.5 Score strength and gray zone

The FNOS was found to be a reliable tool with a strong statistical association with postoperative FN function in both the short- and long-term. Ordinal logistic regression analysis showed that, for each one-point increase in the score, there was a significant approximately five-fold increase in the risk of obtaining a "poor" HB outcome at 1-year after surgery, underscoring the importance of the parameters that constitute the score.

A total of 100% of FNOS-A patients (scores 1–4) have "good" HB at 12 months and at last follow-up. Conversely, 100% of FNOS-C patients (scores 7–12) have "poor" HB at 12 months and at last follow-up. Although the strength of association of the score remains high even in the short term, it was lower than in the long term (Cramer's V T3/T4 of 0.919/0.936 vs. Cramer's V T1/T2 of 0.831/0.851), being, indeed, significantly lower the percentages of patients with HB "good" in the postoperative and at 3 months for FNOS-A patients (T1, 89.4%; T2, 95.7%). The reason behind could be two-fold: The stimulation parameters have demonstrated a greater influence on the FN function on the long-term, whereas the morphological parameters have shown a greater strength on the short term. Probably, this aspect could be related to the fact that, in the first 3 months after surgery, the surgical maneuvers related to the size, morphology, and relationships of the nerve with adjacent structures play a more important role on the nerve damage. Furthermore, it could be hypothesized that the nerve damage in these patients is predominantly neuropraxic, considering the percentage of FNOS-A patients with "good" HB grade on the long-term follow-up (Figure 4).

The latter aspect is more stressed in patients who fall into a "gray zone" of the score, namely, FNOS-B patients.

As shown in Figure 4, these patients show higher percentages of "HB poor" up to 3 months after surgery and then show satisfactory percentages of "good" HB in the long-term, underlining the ability of the score to intercept the extent of FN damage and consequently the potential for recovery (HB "poor" FNOS B: T1, 90%; T2, 60%; T3, 20%; and T4, 18.2%). These data represent an important aspect regarding the fact of being able to expect a long-term improvement in patients with postoperative FNOS-B who present a grade HB "poor" in the short-term follow- up. In these patients, it is likely that the nerve damage is predominantly in the sphere of axonotmesis or that there may be factors —already described in the literature— not strictly related to surgery, that may affect the short-term nerve function (e.g., neuroinflammation, vasospasm, and herpes simplex virus reactivation) (22, 48, 49). Nevertheless, although strong association was found, the small size of this sample did not allow to adequately assess the predictive value of the gray zone.

5 Limitations

One of the main limitations of the study is linked to its retrospective nature, although the prospectively collected data allow for adequate statistical analysis. Unfortunately, the small size of the cohort decreases the statistical power of the result and of the predictive value of the score. Furthermore, the IONM parameters used are only direct nerve stimulation parameters, and this represents a limitation, given the increasingly use of f-MEPs and their scientific validation, associated with the possibility of overcoming limitations arising from EMG alone (i.e., the repeatability of f-MEPs during tumor removal even without direct nerve exposure).

Another important aspect is the violation of regression assumptions for the analysis of the categorical variable FNOS. This violation, due to the high association obtained from the score with the outcome on the HB scale, represents a statistical limitation to the possibility of building a probabilistic predictive model that allows to estimate the exact likelihood of having a "good" or a "poor HB" on the basis of belonging to each FNOS group. However, binary logistic regression analysis with the FNOS scores on an ordinal scale allows us to significantly estimate the probability of having a more or less good outcome for each one-point change in the score. This seems to be mainly related, in part, to the relatively small number of patients but mainly to the discrepancy between the higher number of patients with a good outcome compared with those with a bad outcome. Thus, because of the low variance, it was impossible to obtain a statistically significant predictive model of the FNOS score, although the association of the score with HB class in the long term was well established. On the other hand, a higher percentage of favorable outcomes represents the goal of surgery, and the statistical need to analyze more negative outcomes would create a problem from an ethical point of view.

Therefore, if, on the one hand, statistically speaking, this represents the major limitation of the study; on the other hand, from a clinical and research point of view, it could represent a solid and concrete starting point for further research. Indeed, by increasing the number of patients and considering the multicentric extension of the analysis, it is expected that the predictivity of the individual classes of the score could reach statistical significance due to the greater number of variables included and the proportional increase of unfavorable outcomes.

6 Conclusions

The FNOS represents a reliable score and resulted to be strongly associated with long- term FN function. A one-point score increase showed to possibility to predict a five-fold increase of the risk of "poor" HB at 12 months after surgery. Direct nerve stimulation parameters play a crucial role in predicting long-term facial function. The percentage of patients belonging to the gray zone (FNOS-B) with a FN function classifiable as HB "poor" in the short term significantly decreases in the long term, suggesting the

potential ability to catch patients with higher chance for recovery that should be better assessed with larger and multicentric series.

Data availability statement

The original contributions presented in the study are included in the article/Supplementary Material. Further inquiries can be directed to the corresponding author.

Ethics statement

An informed consent was signed for clinical and surgical procedures. Ethical review and approval was not required due to the retrospective nature of the study.

Author contributions

GDP: conceptualization, methodology, writing (original draft), and supervision; RDM: investigation, visualization and writing (review and editing); BMB: investigation and writing (review and editing); ELB: data collection; FC: writing (review and editing) and supervision; PZ: data collection; LC: formal analysis; FP: data collection; AM: writing (review and editing); DG: supervision; MML: supervision; FZ: supervision and conceptualization. All authors contributed to the article and approved the submitted version.

Conflict of interest

The authors declare that the research was conducted in the absence of any commercial or financial relationships that could be construed as a potential conflict of interest.

Publisher's note

All claims expressed in this article are solely those of the authors and do not necessarily represent those of their affiliated organizations, or those of the publisher, the editors and the reviewers. Any product that may be evaluated in this article, or claim that may be made by its manufacturer, is not guaranteed or endorsed by the publisher.

Supplementary material

The Supplementary Material for this article can be found online at: https://www.frontiersin.org/articles/10.3389/fonc.2023.1153662/full#supplementary-material

References

1. Parving A, Tos M, Thomsen J, Møller H, Buchwald C. Some aspects of life quality after surgery for acoustic neuroma. *Arch Otolaryngol Head Neck Surg* (1992) 118:1061–4. doi: 10.1001/ARCHOTOL.1992.01880100053013

2. Samii M, Matthies C. Management of 1000 vestibular schwannomas (acoustic neuromas): the facial nerve–preservation and restitution of function. *Neurosurgery* (1997) 40:684–95. doi: 10.1097/00006123-199704000-00006

3. Betchen SA, Walsh J, Post KD. Self-assessed quality of life after acoustic neuroma surgery. *J Neurosurg* (2003) 99:818–23. doi: 10.3171/JNS.2003.99.5.0818

4. Nicoucar K, Momjian S, Vader JP, De Tribolet N. Surgery for large vestibular schwannomas: how patients and surgeons perceive quality of life. *J Neurosurg* (2006) 105:205–12. doi: 10.3171/JNS.2006.105.2.205

5. Li MKK, Niles N, Gore S, Ebrahimi A, McGuinness J, Clark JR. Social perception of morbidity in facial nerve paralysis. *Head Neck* (2016) 38:1158–63. doi: 10.1002/HED.24299

6. Papatsoutsos E, Spielmann PM. Self-evaluated quality of life and functional outcomes after microsurgery, stereotactic radiation or observation-only for vestibular schwannoma of the adult patient: a systematic review. *Otol Neurotol* (2018) 39:232–41. doi: 10.1097/MAO.0000000000001664

7. Bender M, Tatagiba M, Gharabaghi A. Quality of life after vestibular schwannoma surgery: a question of perspective. *Front Oncol* (2022) 11:770789/FULL. doi: 10.3389/FONC.2021.770789/FULL

8. Acioly MA, Liebsch M, De Aguiar PHP, Tatagiba M. Facial nerve monitoring during cerebellopontine angle and skull base tumor surgery: a systematic review from description to current success on function prediction. *World Neurosurg* (2013) 80(6): e271–300. doi: 10.1016/J.WNEU.2011.09.026

9. Bhimrao SK, Le TN, Dong CC, Makarenko S, Wongprasartsuk S, Westerberg BD, et al. Role of facial nerve motor-evoked potential ratio in predicting facial nerve function in vestibular schwannoma surgery both immediate and at 1 year. *Otol Neurotol* (2016) 37:1162–7. doi: 10.1097/MAO.0000000000001137

10. Goldbrunner R, Minniti G, Preusser M, Jenkinson MD, Sallabanda K, Houdart E, et al. EANO guidelines for the diagnosis and treatment of meningiomas. *Lancet Oncol* (2016) 17:e383–91. doi: 10.1016/S1470-2045(16)30321-7

11. Goldbrunner R, Weller M, Regis J, Lund-Johansen M, Stavrinou P, Reuss D, et al. EANO guideline on the diagnosis and treatment of vestibular schwannoma. *Neuro Oncol* (2020) 22:31–45. doi: 10.1093/NEUONC/NOZ153

12. Sampath P, Holliday MJ, Brem H, Niparko JK, Long DM. Facial nerve injury in acoustic neuroma (vestibular schwannoma) surgery: etiology and prevention. *J Neurosurg* (1997) 87:60–6. doi: 10.3171/JNS.1997.87.1.0060

13. Van De Langenberg R, Hanssens PEJ, Van Overbeeke JJ, Verheul JB, Nelemans PJ, De Bondt BJ, et al. Management of large vestibular schwannoma. part i. planned subtotal resection followed by gamma knife surgery: radiological and clinical aspects: clinical article. *J Neurosurg* (2011) 115:875–84. doi: 10.3171/2011.6.JNS101958

14. Yetiser S, Karapinar U. Hypoglossal-facial nerve anastomosis: a meta-analytic study. *Ann Otol Rhinol Laryngol* (2007) 116:542–9. doi: 10.1177/000348940711600710

15. Fenton JE, Chin RYK, Shirazi A, Atlas MD, Fagan PA. Prediction of postoperative facial nerve function in acoustic neuroma surgery. *Clin Otolaryngol Allied Sci* (1999) 24:483–6. doi: 10.1046/J.1365-2273.1999.00287.X

16. Goldbrunner RH, Schlake HP, Milewski C, Tonn JC, Helms J, Roosen K. Quantitative parameters of intraoperative electromyography predict facial nerve outcomes for vestibular schwannoma surgery. *Neurosurgery* (2000) 46:1140–8. doi: 10.1097/00006123-200005000-00023

17. Fenton JE, Chin RY, Fagan PA, Sterkers O, Sterkers JM. Predictive factors of long-term facial nerve function after vestibular schwannoma surgery. *Otol Neurotol* (2002) 23:388–92. doi: 10.1097/00129492-200205000-00027

18. Lin VYW, Houlden D, Bethune A, Nolan M, Pirouzmand F, Rowed D, et al. A novel method in predicting immediate postoperative facial nerve function post acoustic neuroma excision. *Otol Neurotol* (2006) 27:1017–22. doi: 10.1097/01.MAO.0000235308.87689.35

19. Kanzaki J, Tos M, Sanna M, Moffat DA. New and modified reporting systems from the consensus meeting on systems for reporting results in vestibular schwannoma. *Otol Neurotol* (2003) 24:642–8. doi: 10.1097/00129492-200307000-00019

20. Starnoni D, Giammattei L, Cossu G, Link MJ, Roche PH, Chacko AG, et al. Surgical management for large vestibular schwannomas: a systematic review, meta-analysis, and consensus statement on behalf of the EANS skull base section. *Acta Neurochir (Wien)* (2020) 162:2595–617. doi: 10.1007/S00701-020-04491-7

21. Mastronardi L, Gazzeri R, Barbieri FR, Roperto R, Cacciotti G, Sufianov A. Postoperative functional preservation of facial nerve in cystic vestibular schwannoma. *World Neurosurg* (2020) 143:e36–43. doi: 10.1016/J.WNEU.2020.04.018

22. Samii M, Matthies C. Management of 1000 vestibular schwannomas (acoustic neuromas): surgical management and results with an emphasis on complications and how to avoid them. *Neurosurgery* (1997) 40:11–23. doi: 10.1097/00006123-199701000-00002

23. Koos WT, Day JD, Matula C, Levy DI. Neurotopographic considerations in the microsurgical treatment of small acoustic neurinomas. *J Neurosurg* (1998) 88:506–12. doi: 10.3171/JNS.1998.88.3.0506

24. Wu H, Zhang L, Han D, Mao Y, Yang J, Wang Z, et al. Summary and consensus in 7th international conference on acoustic neuroma: an update for the management of sporadic acoustic neuromas. *World J Otorhinolaryngol - Head Neck Surg* (2016) 2:234. doi: 10.1016/J.WJORL.2016.10.002

25. House JW, Brackmann DE. Facial nerve grading system. *Otolaryngol Head Neck Surg* (1985) 93:146–7. doi: 10.1177/019459988509300202

26. Hardy DG, MacFarlane R, Baguley D, Moffat DA. Surgery for acoustic neurinoma. an analysis of 100 translabyrinthine operations. *J Neurosurg* (1989) 71:799–804. doi: 10.3171/JNS.1989.71.6.0799

27. Brackmann DE, Cullen RD, Fisher LM. Facial nerve function after translabyrinthine vestibular schwannoma surgery. *Otolaryngol - Head Neck Surg* (2007) 136:773–7. doi: 10.1016/J.OTOHNS.2006.10.009

28. Rinaldi V, Casale M, Bressi F, Potena M, Vesperini E, De Franco A, et al. Facial nerve outcome after vestibular schwannoma surgery: our experience. *J Neurol Surg B Skull Base* (2012) 73:21–7. doi: 10.1055/S-0032-1304559

29. Killeen DE, Barnett SL, Mickey BE, Hunter JB, Isaacson B, Kutz JW. The association of vestibular schwannoma volume with facial nerve outcomes after surgical resection. *Laryngoscope* (2021) 131:E1328–34. doi: 10.1002/LARY.29141

30. Ren Y, MacDonald BV, Tawfik KO, Schwartz MS, Friedman RA. Clinical predictors of facial nerve outcomes after surgical resection of vestibular schwannoma. *Otolaryngol Head Neck Surg* (2021) 164:1085–93. doi: 10.1177/0194599820961389

31. Samii M, Gerganov VM, Samii A. Functional outcome after complete surgical removal of giant vestibular schwannomas. *J Neurosurg* (2010) 112:860–7. doi: 10.3171/2009.7.JNS0989

32. Kunert P, Dziedzic T, Podgórska A, Nowak A, Czernicki T, Marchel A. Surgery for sporadic vestibular schwannoma. part IV. predictive factors influencing facial nerve function after surgery. *Neurol Neurochir Pol* (2016) 50:36–44. doi: 10.1016/J.PJNNS.2015.11.006

33. Ben Ammar M, Piccirillo E, Topsakal V, Taibah A, Sanna M. Surgical results and technical refinements in translabyrinthine excision of vestibular schwannomas: the gruppo otologico experience. *Neurosurgery* (2012) 70:1481–91. doi: 10.1227/NEU.0B013E31824C010F

34. Lee S, Seol HJ, Park K, Lee J, Nam DH, Kong DS, et al. Functional outcome of the facial nerve after surgery for vestibular schwannoma: prediction of acceptable long-term facial nerve function based on immediate postoperative facial palsy. *World Neurosurg* (2016) 89:215–22. doi: 10.1016/J.WNEU.2016.01.038

35. Syed MI, Wolf A, Ilan O, Hughes CO, Chung J, Tymianski M, et al. The behaviour of residual tumour after the intentional incomplete excision of a vestibular schwannoma: is it such a bad thing to leave some behind? *Clin Otolaryngol* (2017) 42:92–7. doi: 10.1111/COA.12670

36. Liu SW, Jiang W, Zhang HQ, Li XP, Wan XY, Emmanuel B, et al. Intraoperative neuromonitoring for removal of large vestibular schwannoma: facial nerve outcome and predictive factors. *Clin Neurol Neurosurg* (2015) 133:83–9. doi: 10.1016/J.CLINEURO.2015.03.016

37. Lunardi P, Missori P, Mastronardi L, Fortuna A. Cystic acoustic schwannomas. *Acta Neurochir (Wien)* (1991) 110:120–3. doi: 10.1007/BF01400678

38. Benech F, Perez R, Fontanella MM, Morra B, Albera R, Ducati A. Cystic versus solid vestibular schwannomas: a series of 80 grade III-IV patients. *Neurosurg Rev* (2005) 28:209–13. doi: 10.1007/S10143-005-0380-Y/TABLES/7

39. Moon KS, Jung S, Seo SK, Jung TY, Kim IY, Ryu HH, et al. Cystic vestibular schwannomas: a possible role of matrix metalloproteinase-2 in cyst development and unfavorable surgical outcome. *J Neurosurg* (2007) 106:866–71. doi: 10.3171/JNS.2007.106.5.866

40. Huo Z, Zhang Z, Huang Q, Yang J, Wang Z, Jia H, et al. Clinical comparison of two subtypes of cystic vestibular schwannoma: surgical considerations and outcomes. *Eur Arch Otorhinolaryngol* (2016) 273:4215–23. doi: 10.1007/S00405-016-4149-4

41. Troude L, Boucekine M, Montava M, Lavieille JP, Régis JM, Roche PH. Predictive factors of early postoperative and long-term facial nerve function after Large vestibular schwannoma surgery. *World Neurosurg* (2019) 127:e599–608. doi: 10.1016/J.WNEU.2019.03.218

42. Axon PR, Ramsden RT. Intraoperative electromyography for predicting facial function in vestibular schwannoma surgery. *Laryngoscope* (1999) 109:922–6. doi: 10.1097/00005537-199906000-00015

43. Neff BA, Ting J, Dickinson SL, Welling DB. Facial nerve monitoring parameters as a predictor of postoperative facial nerve outcomes after vestibular schwannoma resection. *Otol Neurotol* (2005) 26:728–32. doi: 10.1097/01.MAO.0000178137.81729.35

44. Prell J, Rampp S, Romstöck J, Fahlbusch R, Strauss C. Train time as a quantitative electromyographic parameter for facial nerve function in patients undergoing surgery for vestibular schwannoma. *J Neurosurg* (2007) 106:826–32. doi: 10.3171/JNS.2007.106.5.826

45. Duarte-Costa S, Vaz R, Pinto D, Silveira F, Cerejo A. Predictive value of intraoperative neurophysiologic monitoring in assessing long-term facial function in grade IV vestibular schwannoma removal. *Acta Neurochir (Wien)* (2015) 157:1991–8. doi: 10.1007/S00701-015-2571-9

46. Hendriks T, Kunst HPM, Huppelschoten M, Doorduin J, Ter Laan M. TcMEP threshold change is superior to a-train detection when predicting facial nerve outcome in CPA tumour surgery. *Acta Neurochir (Wien)* (2020) 162:1197–203. doi: 10.1007/S00701-020-04275-Z

47. Ling M, Tao X, Ma S, Yang X, Liu L, Fan X, et al. Predictive value of intraoperative facial motor evoked potentials in vestibular schwannoma surgery under 2 anesthesia protocols. *World Neurosurg* (2018) 111:e267–76. doi: 10.1016/J.WNEU.2017.12.029

48. Tos M, Thomsen J, Youssef M, Turgut S. Causes of facial nerve paresis after translabyrinthine surgery for acoustic neuroma. *Ann Otol Rhinol Laryngol* (1992) 101:821–6. doi: 10.1177/000348949210101004

49. Carlstrom LP, Copeland WR, Neff BA, Castner ML, Driscoll CLW, Link MJ. Incidence and risk factors of delayed facial palsy after vestibular schwannoma resection. *Neurosurgery* (2016) 78:251–5. doi: 10.1227/NEU.0000000000001015

frontiers | Frontiers in Oncology

TYPE Original Research
PUBLISHED 26 June 2023
DOI 10.3389/fonc.2023.1152833

OPEN ACCESS

EDITED BY
Arianna Rustici,
University of Bologna, Italy

REVIEWED BY
Daniele Bagatto,
University Hospital of Udine, Italy
Luciano Mastronardi,
Ospedale San Filippo Neri, Italy
Giulia Cossu,
Centre Hospitalier Universitaire Vaudois (CHUV), Switzerland

*CORRESPONDENCE
Georgios Naros
georgios.naros@med.uni-tuebingen.de

RECEIVED 28 January 2023
ACCEPTED 08 June 2023
PUBLISHED 26 June 2023

CITATION
Machetanz K, Lee L, Wang SS, Tatagiba M and Naros G (2023) Trading mental and physical health in vestibular schwannoma treatment decision. *Front. Oncol.* 13:1152833. doi: 10.3389/fonc.2023.1152833

Trading mental and physical health in vestibular schwannoma treatment decision

Kathrin Machetanz, Larissa Lee, Sophie S. Wang, Marcos Tatagiba and Georgios Naros*

Neurosurgical Clinic, Department of Neurosurgery and Neurotechnology, Eberhard Karls University, Tuebingen, Germany

Objective: Observation, radiotherapy and surgery are treatment options in vestibular schwannomas (VS). Decision making differs between centers and is usually based on tumor characteristics (e.g., size) and the expected physical health (PH) outcome (i.e., hearing and facial function). However, mental health (MH) is often under-reported. The objective of the present study was to ascertain the impact of VS treatment on PH and MH.

Methods: PH and MH were assessed in a prospective cross-sectional study including 226 patients with unilateral sporadic VS before and after surgical removal (SURG). Quality-of-life (QoL) was estimated by self-rating questionnaires: general Short-Form Health Survey (SF-36), Penn Acoustic Neuroma Quality-of-Life Scale (PANQOL), Dizziness Handicap Inventory (DHI), Hearing Handicap Inventory (HHI), Tinnitus Handicap Inventory (THI), and Facial Disability Index (FDI). QoL changes over time as well as predictive factors were accessed by multivariate analyses of covariance (MANCOVA).

Results: In total, 173 preoperative and 80 postoperative questionnaires were analyzed. There was a significant PH deterioration related to facial function (FDI, PANQOL-face) after surgery. In line with facial rehabilitation, however, FDI improved within the first five years after surgery and did not differ compared to the preoperative patient cohort, eventually. In contrast, MH (i.e., PANQOL-anxiety) and general health (i.e., PANQOL-GH) improved with surgery and correlated with the extent-of-resection.

Conclusion: Physical and mental health is significantly influenced by VS surgery. While PH might decrease after surgery, MH potentially increases when patient is cured. Practitioners should take MH into account before advising an incompletely VS treatment (e.g., subtotal resection, observation or radiosurgery).

KEYWORDS

vestibular schwannoma (VS), quality of life, mental health, physical health, extent of resection (EOR)

Introduction

Vestibular schwannomas (VS) are characterized by a progressive loss of cranial nerve (CN) functions (e.g., hearing, balance), affecting patient's quality of life (QoL) (1–3). Total surgical removal of the tumor is usually providing a definite cure (4, 5). Concurrently, VS surgery implies an increased risk of additional harm to the CN (e.g., facial palsy) (5–10). Observation or radiosurgery are further treatment strategies and in recent years complete VS resection has been discouraged in large VS (11). Instead, current guidelines recommend partial resection (PR) with subsequent radiotherapy in these cases (11). The underlying rationale for this recommendation is to preserve CN function and QoL assuming a linear relationship between them. In fact, several studies report a deterioration of QoL by VS surgery (12–14) relating to hearing, vestibular and facial function (6–8). Radiosurgery or observation has been suggested to affect CN function and QoL to a lesser extent. However, there is increasing evidence that neither radiosurgery nor observation can preserve CN function (in particular hearing) on a long-term (2, 3, 15, 16). Furthermore, some symptoms might be accentuated in comparison to microsurgery (15, 16). Recent studies do not detect any QoL differences when comparing patients following different treatment strategies (14, 17, 18). However, most studies mainly relate to physical health (PH) aspects of QoL. Mental health (MH) referring to the emotional and psychological well-being is often under-reported (17, 19).

An important feature of treatment strategies avoiding a complete VS resection is that it turns a potentially curable disease into a chronic disease with a higher risk of recurrence. It is well known that chronic diseases (e.g., Parkinson's, cancer) affect patient's MH independent of their PH (20, 21). In line, two recent studies demonstrated that a gross total resection (GTR) in VS is associated with a better MH compared to partial VS resection (PR) (19). It has been hypothesized that microsurgery may confer an advantage with regard to patient's MH, relating to the psychological benefit of "cure" from tumor removal (17). In general, however, QoL data in VS treatment differentiating between PH and MH is scarce (14, 17, 18, 22).

The present study aims to investigate the physical and mental health-related QoL in patients with non-treated (before surgery), incompletely (subtotal resection, STR) and completely treated VS (GTR).

Methods

Patient characteristics

This prospective cross-sectional study included 226 patients (Table 1) with an unilateral VS who answered standardized questionnaires on QoL during their treatment at our Neurosurgical Department between 11/2019 and 09/2021. A total of 141/226 (62.5%) underwent surgical resection of the VS *via* a retrosigmoidal approach in a semi-sitting or supine position in that period (Figure 1). Patients with neurofibromatosis, previous VS surgery and incomplete questionnaires were excluded. The study was approved by the local Hospital Ethics Committee and conducted in accordance with the declaration of Helsinki.

Quality of life questionnaires

Several QoL questionnaires were completed during the treatment period: the general Short-Form Health Survey (SF-36), Penn Acoustic Neuroma Quality-of-Life Scale (PANQOL), Dizziness Handicap Inventory (DHI), Hearing Handicap Inventory (HHI), Tinnitus Handicap Inventory (THI), and Facial Disability Index (FDI) (Table 2) (23–25).

The SF-36 is the most common health-related QoL questionnaire. Its 36 items can be divided into physical and mental classes with 4 domains each: physical function (SF36-PF), role-physical (SF36-RP), bodily pain (SF36-BP), general health (SF36-GH), vitality (SF36-VT), social functioning (SF36-SF), role-emotional (SF36-RE) and mental health (SF36-MH). Each domain is scored from 0-100, with a higher score corresponding to a better QoL.

The PANQOL is a disease-specific questionnaire containing 26 questions which are divided into the domains anxiety (PAN-ANX), facial function (PAN-FACE), general health (PAN-GH), balance (PAN-BAL), hearing (PAN-HEAR), energy (PAN-ENGY) and pain (PAN-PAIN). A total score (PAN-TTL) is calculated from the individual scores. The response options are classified on a Likert scale from strong disagreement (1) to strong agreement (5), whereby the values are normalized to a scale of 0-100 points to determine the domain scores. A score of 100 corresponds to the best possible QoL, a score of 0 to the lowest QoL.

The HHI, THI and DHI are symptom-specific questionnaires for dizziness, hearing function and tinnitus. Each questionnaire contains 25 self-assessment items, which can be answered by yes (2), sometimes (1) or no (0). Item scores result in a total score of 0-100, whereby a higher score corresponds to greater impairment by the symptom. The FDI were administered to all patients with facial paresis. The FDI contains 10 questions, which are divided into the domains *physical function* (-25=worst to 100=best function; FDI-PF) and *social function* (0=worst to 100=best function; FDI-SF).

Disease-specific data

In addition, we analyzed numerous disease specific information. Magnetic resonance images (MRI) were retrospectively analyzed to determine the tumor size according to Koos classification (1: purely intrameatal, 2: intra- and extrameatal, 3: filling the cerebellopontine cistern, 4: compressing or shifting the brainstem) (26) and tumor side. The extent of resection (EOR) after surgery (GTR: complete resection; STR: minimal residual tumor on the facial nerve or

Abbreviations: CN, cranial nerve; DHI, Dizziness Handicap Inventory; FDI, Facial Disability Index; GH, general health; GTR, gross total resection; HHI, Hearing Handicap Inventory; MCID, minimal clinically important difference; MH, mental health; PANQOL, Penn Acoustic Neuroma Quality-of-Life Scale; PH, physical health; TBS, time before surgery; TSD, time since diagnosis; TSS, time since surgery, PR, partial resection; QoL, quality of life; STR, sub-total resection; THI, Tinnitus Handicap Inventory; VS, vestibular schwannoma.

TABLE 1 Patient characteristics.

	total	Preoperative	Postoperative	
	n=226 patients	n=173 question.	n=80 question.	
Gender				
male/	103/123	84/89	35/45	X^2 = 0.507
female	(46.6%/54.45%)	(48.6%/51.4%)	(43.85%/56.3%)	p=0.476
Age	53.2 ± 12.4	53.7 ± 12.2	50.4 ± 12.1	p=0.092
Koos				
T1	35 (15.5%)	35 (20.2%)	1 (1.3%)	H=37.99
T2	68 (30.1%)	59 (34.1%)	14 (17.5%)	**p<0.001***
T3	73 (32.3%)	55 (31.8%)	32 (40%)	
T4	50 (22.2%)	24 (13.8%)	33 (41.3%)	
Side				
Left/	122/104	99/74	36/44	X^2 = 3.29
Right	(54%/46%)	(57.2%/42.8%)	(45%/55%)	p=0.07
Operation				
Yes	141 (62.4%)	88 (50.9%)	80 (100%)	X^2 = 59.19
No	85 (37.6%)	85 (49.1%)	0 (0%)	**p<0.001***
Extent of resection				
GTR			56 (70%)	
STR			19 (23.7%)	
PR			5 (6.3%)	
H&B				
I		170 (98.3%)	45 (56.3%)	H=76.2
II		3 (1.7%)	17 (21.3%)	**p<0.001***
III			9 (11.3%)	
IV			7 (8.8%)	
V			2 (2.5%)	
TSD/TSS		1.28 ± 2.2 y	2.16 ± 3 y	
SF36				
physical function		84.6 ± 22.2	83.6 ± 17.9	p=0.073
role physical		69.9 ± 40.0	65.3 ± 38.9	p=0.206
bodily pain		71.8 ± 29.9	76.0 ± 29.3	p=0.273
general health		61.1 ± 18.1	65.1 ± 19.5	p=0.137
vitality		55.6 ± 21.3	57.3 ± 21.0	p=0.563
social function		75.0 ± 25.7	77.3 ± 24.0	p=0.679
role emotional		71.5 ± 40.3	78.3 ± 37.5	p=0.121
mental health		68.0 ± 18.2	73.3 ± 37.5	**p=0.028***
PANQOL				
anxiety		66.1 ± 22.5	73.9 ± 21.8	**p=0.011***
facial		89.5 ± 14.6	75.2 ± 23.8	**p<0.001***
general health		55.0 ± 17.3	63.9 ± 19.5	**p=0.001***
balance		70.9 ± 24.8	67.4 ± 22.5	p=0.150
hearing		64.0 ± 22.0	60.1 ± 22.4	p=0.215
energy		67.5 ± 23.7	68.1 ± 23.9	p=0.821
pain		66.9 ± 29.2	70.4 ± 31.9	p=0.238
Total		68.6 ± 15.4	68.2 ± 16.9	p=0.89
DHI		14.4 ± 20.1	19.1 ± 20.9	**p=0.032***
THI		20.6 ± 21.4	18.2 ± 20.9	p=0.266
HHI		20.5 ± 22.4	28.6 ± 22.0	**p=0.001***
FDI				
physical function		98.8 ± 8.40	86.8 ± 17.6	**p<0.001***
social function		97.7 ± 11.2	86.9 ± 17.9	**p<0.001***

*bold-marked p-values indicate significance comparing pre- and postoperative patients by a Chi-square (X2) or Kruskal-Wallis test (H).

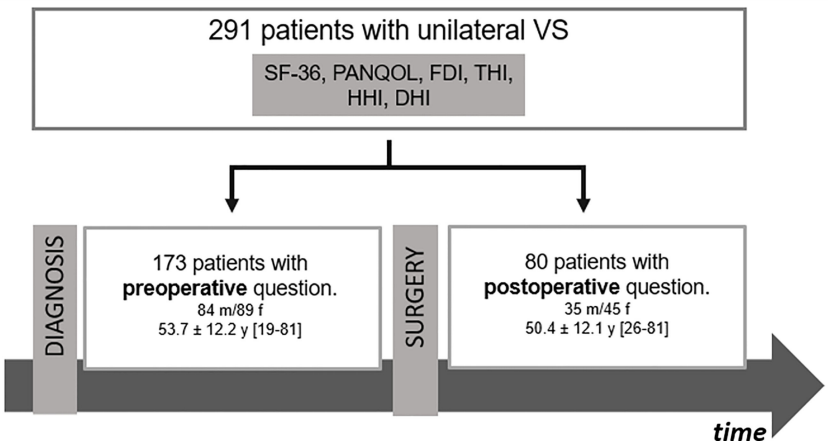

FIGURE 1
Flow chart of patients' cohort. DHI, Dizziness Handicap Inventory; FDI, Facial Disability Index; HHI, Hearing Handicap Inventory; PANQOL, Penn Acoustic Neuroma Quality-of-Life Scale; SF-36: Short-Form Health Survey 36.

exclusively in the internal auditory canal; PR: great tumor volume) was determined by MRI and the surgical record. Medical records of patients were reviewed to define the time between diagnosis and QoL survey (time since diagnosis, TSD; preoperatively), time between preoperative QoL survey and surgery (time before surgery, TBS; preoperatively; only patients who answered the preoperative survey and underwent VS resection at a later time during the evaluation period), time between surgery and postoperative survey (time since surgery, TSS; postoperatively) as well as the facial function according to the House-Brackmann scale (H&B) (27). The H&B classifies overall facial function into ranges from 1 (normal) to 6 (total paralysis) based on the assessment of e.g. eye closure and mouth movement.

Statistics

Statistical tests were performed using SPSS (IBM SPSS Statistics for Windows, Version 26.0. Armonk, NY: IBM Corp.). Group differences in distribution of clinical characteristics (e.g., EOR) were determined by Chi-squared or Kruskal-Wallis tests. In a first step, (multivariate) analyses of covariance ((M)ANCOVAs) were performed to evaluate the effects of surgery (SURG) and gender (SEX) on QoL scores. Secondary, a (M)ANCOVA-based evaluation of the impact of TSD, TSS and EOR on QoL was performed. In order to ensure that results were not influenced by assumption violations, data were checked for outliers, homogeneity of variance–covariance matrices (Box's M test) and homogeneity of variances (Levene's test). In this context, a MANCOVA is a two-step process. In the first step, the overall hypothesis is tested, i.e. whether there is a difference between different groups. If this test is significant, in the second step the MANCOVA was followed by *post-hoc* tests (i.e. univariate ANOVAs) to explain the group differences. Furthermore, we performed a secondary subcohort analysis of patients who completed the questionnaires in both the pre- and postoperative period. To estimate differences in QoL scores before and after surgery we performed a repeated measures ANOVA. Statistical significance was considered at $p < 0.05$ for all statistical tests.

Results

Patient cohort

A total of 226 patients (53.2 ± 12.4 years; 123 female) completed all QoL questionnaires. 103/226 (45.6%) of the VS corresponded to a tumor size Koos 1/2 and 123/226 (54.4%) to a grade 3/4 (Table 1). VS were resected in 141/226 (62.4%) of the patients, while 85/226 (37.6%) had not undergone surgery at the time of evaluation (Figure 1). In summary, 27/226 (11.9%) patients completed questionnaires pre- and postoperatively (Supplementary Table 1), whereas 146/226 (64.6%) and 53/226 (23.5%) were surveyed only pre- or postoperatively, respectively.

Common health-related QoL: SF36

A MANCOVA was applied to SF36 subdomains in order to determine the effect of surgery (SURG) on QoL while controlling for SEX, AGE and tumor size (SIZE) (Figure 2A). Neither SURG ($F_{(8,240)}=1.09$, $p=0.374$) nor SEX ($F_{(8,240)}=1.37$, $p=0.21$) had a significance effect on QoL. In contrast, MANOVA depicted a significant effect of AGE on SF36 ($F_{(8,240)}=3.72$, $p<0.001$). Follow-up ANOVAs confirmed a significant impact of AGE on PH as depicted by SF36-PF ($F_{(1,247)}=12.74$, $p<0.001$) and SF36-GH ($F_{(1,247)}=5.50$, $p=0.020$). Independent of the other covariates, PH items (SF36-PF and SF36-GH) decreased with age ($r=-0.2$, $p=0.001$ and $r=-0.15$, $p=0.016$).

TABLE 2 General health, disease- and symptom-specific QoL questionnaires.

	Name	Abbr.	Description	No. of items	Best/ worst value	MCID
SF36					100/0	
	Physical:					8
	Physical function	SF36-PF	- Extent to which the health condition affects physical activities such as self-care, walking, climbing stairs, lifting	10		
	Role physical	SF36-RP	- Extent to which the health condition affects work or other daily activities, e.g. being able to do less than usual, limitations in the type of activities, or difficulty in performing certain activities	4		
	Bodily pain	SF36-BP	- Level of pain and impact of pain on normal work	2		
	General health	SF36-GH	- Personal health assessment, including current health status and resistance to illness	5		
	Mental:					7
	Vitality	SF36-VT	- Feeling energetic and full of drive vs. tired and exhausted	4		
	Social functioning	SF36-SF	- Extent to which physical health or emotional problems interfere with normal social activities	2		
	Role-emotional	SF36-RE	- Extent to which emotional problems interfere with work, or other daily activities, including spending less time, getting less done and not working as diligently as usual	3		
	Mental health	SF36-MH	- General mental health, including depression, anxiety emotional and behavioral control, general positive mood	5		
	(Reported health transition)		- Assessment of expected health transition	1		
PANQOL					100/0	
	Physical:					
	Facial function	PAN-FACE	- Level of facial weakness and dysfunction	3		10
	Balance	PAN-BAL	- Level of balance and dizziness complaints	6		16 (14-19)
	Hearing	PAN-HEAR	- Level of hearing problems	4		6 (5-8)
	Pain	PAN-PAIN	- Impact of headache on health related quality of life	1		11 (10-13)
	Mental:					
	Anxiety	PAN-ANX	- Level of anxiety and pain due to the VS	4		11 (5-22)
	Energy	PAN-ENGY	- Level of energy, vitality and the ability to concentrate	6		13 (10-17)
	General health	PAN-GH	- Assessment of general health and expected health transition	2		15 (11-19)
HI	Hearing HI	HHI	- Assessment for self-perceived hearing handicap	25	0/100	12
	Tinnitus HI	THI	- Assessment for self-perceived tinnitus handicap	25	0/100	7
	Dizziness HI	DHI	- Assessment for self-perceived dizziness handicap	25	0/100/0	18
FDI				5	100	
	Physical function	FDI-PF	- Level of limitations in physical disability, e.g. problems with instrumental activities of daily living and difficulty with producing appropriate facial expressions			
	Social function	FDI-SF	- Social and emotional problems experienced due to facial dysfunction	5		

SF36: 36-item Short-Form Health Survey, PANQOL, Penn Acoustic Neuroma Quality-of-Life Scale; HI, Handicap Inventory; FDI, Facial Disability Inde; literature-based minimal clinically important differences (MCID) [Carlson et al., 2015 (23); Newman et al., 1991 (24); Zeman et al., 20 (25)].

Disease-specific QoL: PANQOL

A MANCOVA was performed to estimate the effect of SURG on PANQOL subdomains while controlling for SEX, AGE and SIZE. There was a significant multivariate main effect of SURG ($F_{(7,241)}$=7.75, p<0.001; Figure 2B). SURG improved mental and general health in the subdomains PAN-GH (63.9 ± 19.5 vs 55.0 ± 17.3; $F_{(1,247)}$=4.86, p=0.028) and PAN-ANX (73.9 ± 21.8 vs 66.1 ± 22.5; $F_{(1,247)}$=5.68, p=0.018). In contrast, PH relating to facial function (PAN-FACE) decreased postoperatively on a group level (75.2 ± 23.8 and 89.5 ± 14.6; $F_{(1,247)}$=27.35, p<0.001) (Figure 3A).

MANCOVA also proved a significant main effect of SEX on PANQOL ($F_{(7,241)}$=3.49, p=0.001; Figure 2C). Females had significant worse PAN-ANX (64.9 ± 22.0 vs 72.6 ± 22.5; $F_{(1,247)}$=7.44, p=0.007), PAN-BAL (65.3 ± 24.8 vs 74.9 ± 22.4; $F_{(1,247)}$=9.47, p=0.002) and PAN-PAIN (64.6 ± 31.3 vs 71.9 ± 28.1; $F_{(1,247)}$=7.56, p=0.006) scores independent of the actual VS treatment. Furthermore, both covariates AGE ($F_{(7,241)}$=5.93, p<0.001) and SIZE ($F_{(7,241)}$=2.13, p=0.04) had significant impact on PANQOL. Increasing AGE had a negative effect on facial function (PAN-FACE; r=-0.18, p=0.005; Spearman's), balance (PAN-BAL; r=-0.15, p=0.001; Spearman's) and hearing (PAN-HEAR; r=-0.15, p=0.016; Spearman's). PAN-GH was significantly impacted by the SIZE ($F_{(1,247)}$=5.47, p = 0.02) with better values in Koos 3/4 compared to Koos 1/2 tumors (H=14.75, p=0.001; Kruskal-Wallis) (Figure 2D).

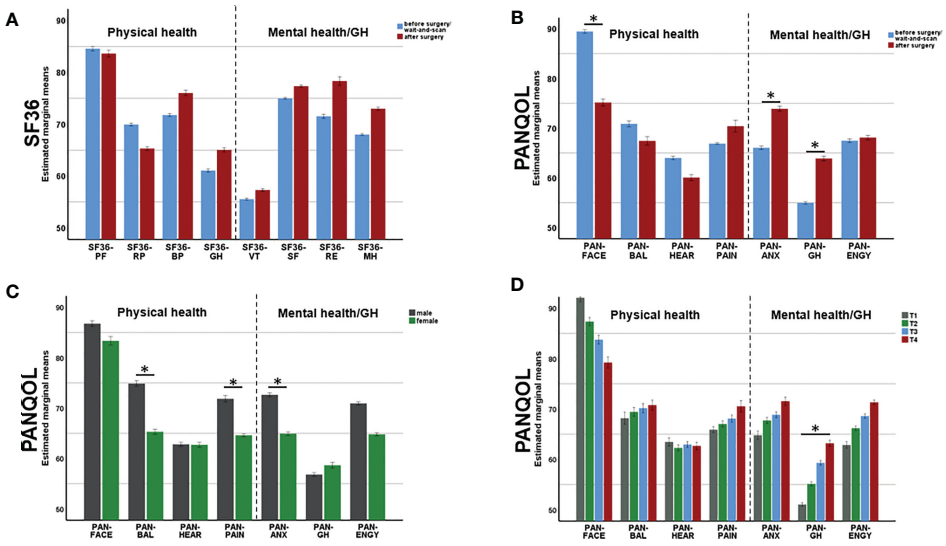

FIGURE 2
Changes of physical (PH) mental health (MH) after surgery. While SF36 **(A)** did not depict any surgery-related changes in QoL, PANQOL **(B)** showed a decline of PH (related to the facial function, PAN-FACE) after surgery. At the same time, surgery improved MH related to anxiety (PAN-ANX) and general health (PAN-GH). Multivariate analysis also depicted an effect of gender **(C)** and tumor size **(D)** on QoL. Bars in **(C, D)** demonstrate data from both, pre- and postoperatively. PANQOL, Penn Acoustic Neuroma Quality-of-Life Scale; PAN-ANX, PANQOL anxiety; PAN-ENGY, PANQOL energy; PANQOL-GH, PANQOL general health; PAN-FACE, PANQOL facial; PAN-BAL, PANQOL balance; PAN-HEAR, PANQOL hearing; PAN-PAIN, PANQOL pain; SF36-PF: SF36 physical function; SF36-RP: SF36 role physical; SF36-BP: SF36 bodily pain; SF36-GH: SF36 general health; SF36-VT: SF36 vitality; SF36-SF: SF36 social functioning; SF36-RE: SF36 role emotional; SF36-MH: SF36 mental health. Significance is indicated by an asterisk (*; $p<0.05$, MANOVA).

Symptom-specific QoL: HHI, THI, DHI and FDI

In the MANCOVA, there was a significant effect of SURG ($F_{(3,245)}=4.96$, $p=0.002$), SEX ($F_{(3,245)}=7.55$, $p<0.001$) and AGE ($F_{(3,245)}=3.94$, $p=0.009$) on the handicap inventories (i.e., DHI, HHI and THI). In the follow-up ANOVAs, both SURG (20.5 ± 22.4 vs 28.6 ± 22.0; $F_{(1,247)}=7.55$, $p=0.006$) and AGE ($F_{(1,247)}=3.89$, $p=0.05$) had negative impact on hearing perception (HHI). In contrast, females suffered from dizziness (DHI) more frequently than males regardless of VS treatment (20.4 ± 22.4 and 10.8 ± 16.6; $F_{(1,247)}=13.47$, $p<0.001$). Tinnitus perception (THI) was unaffected by SURG, SEX or AGE in the present cohort.

Both FDI subscores representing the physical (FDI-PH) and social handicap (FDI-SH) of a facial palsy were negatively affected by SURG ($F_{(1,247)}=36.9$, $p<0.001$ and $F_{(1,247)}=23.25$, $p<0.001$). The covariate SIZE had impact only on FDI-PH ($F_{(1,\ 247)}=4.51$, $p=0.035$). FDI-PF and FDI-SF correlated significantly with H&B ($r=-0.88$, $p<0.001$ and $r=-0.85$, $p<0.001$; Spearman's.

Impact of time since diagnosis, time before/since surgery as and extent of resection on patients' QoL

In order to evaluate the impact of timing of the survey after VS diagnosis and before surgery on mental health, the association between PAN-GH and PAN-ANX as well as TSD and TBS was analyzed. Among the 173 preoperative questionnaires, there was no significant correlation between TSD and PAN-ANX or PAN-GH. Furthermore, in the 88/173 patients who completed a questionnaire in the observation phase and underwent surgery later during the evaluation period, no correlation between TBS and mental health was found either (PAN-ANX: $r=0.021$, $p=0.843$; PAN-GH: $r=-0.18$, $p= 0.093$; Spearman's).

As the functional status after surgery is constantly changing due to rehabilitation mechanisms, we ought to evaluate health-related QoL depending on the TSS. In fact, for both FDI-PF ($H=56.65$, $p<0.001$; Kruskal Wallis) and FDI-SF($H=53.93$, $p<0.001$; Kruskal Wallis) there was a significant decline of QoL directly after surgery which improved during the postoperative course in line with facial rehabilitation (Figure 3B). After a TSS of approx. 5 years, there was no significant difference in neither FDI-PF ($H=36.16$, $p=0.122$; Kruskal Wallis) nor FDI-SF ($H=33.17$, $p=0.240$; Kruskal Wallis) when compared to the preoperative situation (Figure 3B). There was no comparable effect for the disability inventories THI, HHI, DHI or PAN-ANX and PAN-GH (Figures 3C, D). In contrast, postoperative mental and general health parameters (PAN-ANX and PAN-GH) were associated with the EOR. Kruskal-Wallis test revealed a significant better PAN-ANX ($H=6.81$, $p=0.033$) and PAN-GH ($H=10.63$, $p=0.005$) in GTR and STR in comparison to PR (Figures 4A, B).

Discussion

The present study evaluated main determinants of physical and mental health in patients with VS. While PH and MH did not change after diagnosis, deterioration of PH was detected postoperatively - mainly caused by an occurrence of facial nerve

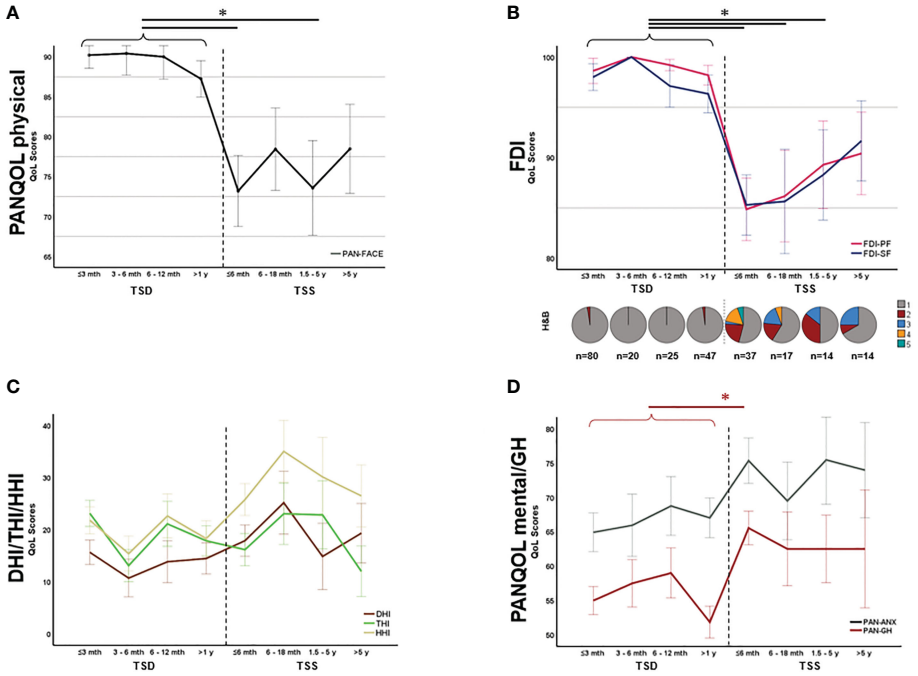

FIGURE 3
Symptom-specific quality of life (QoL) over time. PAN-FACE **(A)** and FDI scores **(B)** improved after surgery in line with the facial rehabilitation (see distribution of H&B scores in the inlay). After 5 years, PAN-FACE and FDI differed significant in comparison to the preoperative patient cohort. In contrast, neither DHI, THI and HHI **(C)** nor PAN-ANX/PAN-GH **(D)** changed during follow-up. The numbers under the pie charts in **(B)** indicate the total number of patients in each time period. DHI, dizziness handicap inventory; THI, tinnitus handicap inventory; HHI, hearing handicap inventory; FDI-PF, Facial disability index - physical function; FDI-SF, Facial disability index – social function; TSD, time-since-diagnosis; TSS, time-since-surgery. Significance is highlighted by an asterisk (*; p<0.05, Dunn's test, corrected).

palsy and the deterioration of hearing function. However, PH related to facial function improved within the first years after surgery. Furthermore, mental and general health improved postoperatively and correlated with the EOR. The decision on therapy is therefore a consideration between MH and PH and must be made on a patient-specific basis.

Current guidelines for VS advise observation or radiotherapy and discourage complete VS resection to preserve CN function (11). The present study documents a significant postoperatively deterioration of facial and hearing QoL scores with a similar or even less pronounced extent compared to previous studies (13, 28). The retrosigmoid approach in this context may have resulted in less hearing loss compared to studies applying a translabyrinthine approach. However, physical limitations should not only be compared pre- and postoperatively, but also functional recovery after surgery should be considered when deciding on treatment. Our findings elicit an improvement of FDI-PF and FDI-SF over time after microsurgery. Nevertheless, our study could not detect a significant effect of TSS alone on facial function. This could be attributed to a data bias, since patients without physical complaints usually no longer present themselves in our outpatient clinic after approx. 3 years. Thus, an overrepresentation of patients with impairing facial palsy must be assumed in our postoperative cohort. In fact, previous studies show heterogenous results regarding longitudinal facial palsy-specific QoL (29, 30). Further longitudinal studies are necessary to assess the frequency, course of recovery and subjective limitation of facial palsies after VS resection.

Tinnitus and dizziness are symptoms often associated with VS. Nevertheless, they are often underrated when deciding on the treatment strategy. Tinnitus and vertigo, however, can significantly worsen QoL in VS patients (23, 31). Thus, we determined tinnitus-related QoL by the THI. Tinnitus-related discomfort tended to improve slightly although previous reported "minimal clinically important difference" (MCID) could not be reached (25). This is concordant with previous studies demonstrating postoperative improvement in patients with preoperative tinnitus, while patients without preoperative tinnitus can develop a new-onset tinnitus after surgery in ~20% (32–34). Consequently, patients with preoperative severe tinnitus could be offered microsurgical resection of the VS, as radiotherapy may worsen tinnitus-related discomfort (35). The results of studies investigating pre- and postoperative dizziness in VS are ambiguous (36). Our study could not reveal pre- and postoperative differences of DHI and PAN-BAL. Instead, more dizziness was associated with female gender and higher age.

The relevance of MH on overall health is often underestimated in the treatment of benign tumors. While there are numerous studies on MH in meningiomas (37–39), data on MH in VS are scarce. The present study could not demonstrate an effect of surgery on mental or physical SF-36 scores, confirming the assumption about low predictability of QoL in VS by the SF-36 (40, 41). However, despite the deterioration in PH the PANQOL findings demonstrated a significant increase of mental and general health post-surgically. In contrast, during the preoperative observational phase there was a deterioration of mental scores over time. This suggests that patients

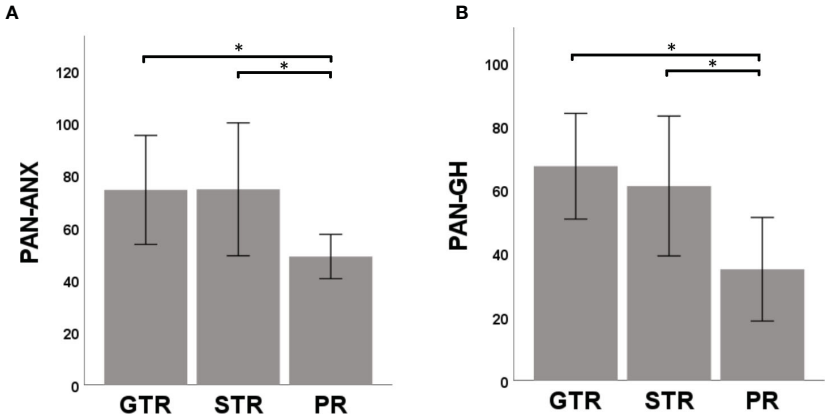

FIGURE 4
Relationship between mental health and extent-of-resection (EOR). Both PAN-ANX **(A)** and PAN-GH **(B)** correlated with EOR. Patients with significant residual tumor (partial resection, PR) claimed higher level of anxiety and a reduced level of general health in comparison to patients undergoing a gross total resection (GTR) or subtotal resection (STR). Significance is highlighted by an asterisk (*; p<0.05, Dunn's test, corrected).

experience relief from treatment, whereas knowledge of the presence of a VS without treatment leads to a state of anxiety. These result supports the hypothesis of Carlson et al. which suggests that microsurgery may improve patient's MH when the tumor is "cured" after complete surgical removal (17). While previous studies could demonstrate a reduced QoL of VS patients in comparison to age and sex matched normative data already before surgery, conversely, they could not prove a significant difference of MH between observational, microsurgery and radiotherapy groups (14, 17, 18, 28, 42–44). However, factors affecting the results (e.g., EOR, gender) are not taken into account in these studies. While multivariate statistics could not demonstrate an effect of EOR on MH scores, univariate analysis demonstrated a significantly worse PAN-GH in partial resections compared to STR and GTR. This is concordant with studies comparing GTR with incomplete resection or combined radio- and microsurgery (19, 28). Since other studies furthermore demonstrated a significant regrowth rate with a tumor residue of >0.7 cm^3 and a higher MIB-1 index (45, 46), general recommendation for PR in large VS should be avoided. Instead, multicenter studies, that prospectively assign patients to different intention-to-treat groups (i.e. intended GTR, intended PR), are necessary.

Limitations

The present study is limited due to the lack of comparison with radiosurgery or other surgical procedures (e.g., translabyrinthine surgery), a non-tumor cohort and the absence of longitudinality. The small number of postoperative controls can lead to a selection bias of the health status, since at long-term, patients with persistent complaints continue to present themselves in the consultation, while patients with good health no longer present themselves.

Conclusion

In VS patients, the trading of MH and PH is essential for treatment decision making. While mental health in particular is impaired preoperatively, patients are impaired postoperatively, especially due to physical problems related to cranial nerve dysfunction. Attending physicians should take this into account during treatment decision making.

Data availability statement

The raw data that support the findings of this study are available from the corresponding author upon reasonable request.

Ethics statement

The studies involving human participants were reviewed and approved by Ethics committee of the medical faculty of Eberhard Karls University Tübingen and conducted in accordance with the declaration of Helsinki.

Author contributions

Study conception and design: KM, GN. Data acquisition: KM, LL, SW. Data analysis: GN, KM. Data interpretation: KM, SW, MT, GN. Statistical analysis: KM, GN. writing of the first draft: KM, GN. Review of the final manuscript: KM, MT, GN. All authors contributed to the article and approved the submitted version.

Conflict of interest

The authors declare that the research was conducted in the absence of any commercial or financial relationships that could be construed as a potential conflict of interest.

Publisher's note

All claims expressed in this article are solely those of the authors and do not necessarily represent those of their affiliated organizations, or those of the publisher, the editors and the reviewers. Any product that may be evaluated in this article, or claim that may be made by its manufacturer, is not guaranteed or endorsed by the publisher.

Supplementary material

The Supplementary Material for this article can be found online at: https://www.frontiersin.org/articles/10.3389/fonc.2023.1152833/full#supplementary-material

SUPPLEMENTARY TABLE 1
QoL values of patients who completed the questionnaires both in the pre- and postoperative period. *p-values indicate significance pre-and postoperatively by a repeated measures ANOVA.

References

1. Nilsen KS, Lund-Johansen M, Nordahl SHG, Finnkirk M, Goplen FK. Long-term effects of conservative management of vestibular schwannoma on dizziness, balance, and caloric function. *Otolaryngol - Head Neck Surg (United States)* (2019) 161:846–51. doi: 10.1177/0194599819860831

2. Sughrue ME, Yang I, Aranda D, Lobo K, Pitts LH, Cheung SW, et al. The natural history of untreated sporadic vestibular schwannomas: a comprehensive review of hearing outcomes - clinical article. *J Neurosurg* (2010) 112:163–7. doi: 10.3171/2009.4.JNS08895

3. Sughrue ME, Kane AJ, Kaur R, Barry JJ, Rutkowski MJ, Pitts LH, et al. A prospective study of hearing preservation in untreated vestibular schwannomas: clinical article. *J Neurosurg* (2011) 114:381–5. doi: 10.3171/2010.4.JNS091962

4. Nakatomi H, Jacob JT, Carlson ML, Tanaka S, Tanaka M, Saito N, et al. Long-term risk of recurrence and regrowth after gross-total and subtotal resection of sporadic vestibular schwannoma. *J Neurosurg* (2020) 133:1052–8. doi: 10.3171/2016.11.JNS16498

5. Tatagiba M, Ebner FH, Nakamura T, Naros G. Evolution in surgical treatment of vestibular schwannomas. *Curr Otorhinolaryngol Rep* (2021) 9:467–76. doi: 10.1007/s40136-021-00366-2

6. Falcioni M, Fois P, Taibah A, Sanna M. Facial nerve function after vestibular schwannoma surgery: clinical article. *J Neurosurg* (2011) 115:820–6. doi: 10.3171/2011.5.JNS101597

7. Matthies C, Samii M. Management of 1000 vestibular schwannomas (acoustic neuromas): clinical presentation. *Neurosurgery* (1997) 40:1–9. doi: 10.1097/00006123-199701000-00001

8. Ebner FH, Tatagiba M. Update on diagnostics and microsurgical treatment of vestibular schwannoma. *Nervenarzt* (2019) 90:578–86. doi: 10.1007/s00115-019-0721-7

9. Acioly MA, Gharabaghi A, Liebsch M, Carvalho CH, Aguiar PH, Tatagiba M. Quantitative parameters of facial motor evoked potential during vestibular schwannoma surgery predict postoperative facial nerve function. *Acta Neurochir (Wien)* (2011) 153:1169–79. doi: 10.1007/s00701-011-0995-4

10. Rizk AR, Adam A, Gugel I, Schittenhelm J, Tatagiba M, Ebner FH. Implications of vestibular schwannoma consistency: analysis of 140 cases regarding radiologic and clinical features. *World Neurosurg* (2017) 99:159–63. doi: 10.1016/j.wneu.2016.11.082

11. Goldbrunner R, Weller M, Regis J, Lund-Johansen M, Stavrinou P, Reuss D, et al. Eano guideline on the diagnosis and treatment of vestibular schwannoma. *Neuro Oncol* (2020) 22:31–45. doi: 10.1093/neuonc/noz153

12. Soulier G, van Leeuwen BM, Putter H, Jansen JC, Malessy MJA, van Benthem PPG, et al. Quality of life in 807 patients with vestibular schwannoma: comparing treatment modalities. *Otolaryngol - Head Neck Surg (United States)* (2017) 157:92–8. doi: 10.1177/0194599817695800

13. Pruijn IMJ, Kievit W, Hentschel MA, Mulder JJS, Kunst HPM. What determines quality of life in patients with vestibular schwannoma? *Clin Otolaryngol* (2021) 46:412–20. doi: 10.1111/coa.13691

14. Miller LE, Brant JA, Naples JG, Bigelow DC, Lee JYK, Ruckenstein MJ. Quality of life in vestibular schwannoma patients: a longitudinal study. *Otol Neurotol* (2020) 41:e256–61. doi: 10.1097/MAO.0000000000002445

15. Murphy ES, Barnett GH, Vogelbaum MA, Neyman G, Stevens GHJ, Cohen BH, et al. Long-term outcomes of gamma knife radiosurgery in patients with vestibular schwannomas: clinical article. *J Neurosurg* (2011) 114:432–40. doi: 10.3171/2009.12.JNS091339

16. Boari N, Bailo M, Gagliardi F, Franzin A, Gemma M, del Vecchio A, et al. Gamma knife radiosurgery for vestibular schwannoma: clinical results at long-term follow-up in a series of 379 patients. *J Neurosurg* (2014) 121:123–42. doi: 10.3171/2014.8.GKS141506

17. Carlson ML, Barnes JH, Nassiri A, Patel NS, Tombers NM, Lohse CM, et al. Prospective study of disease-specific quality-of-Life in sporadic vestibular schwannoma comparing observation, radiosurgery, and microsurgery. *Otol Neurotol* (2021) 42:e199–208. doi: 10.1097/MAO.0000000000002863

18. Neve OM, Jansen JC, Koot RW, de RM, Paul G. van Benthem P, AM S, et al. Long-term quality of life of vestibular schwannoma patients: a longitudinal analysis. *Otolaryngol - Head Neck Surg (United States)* (2022) 168(2):210–7. doi: 10.1177/01945998221088565

19. Link MJ, Lund-Johansen M, Lohse CM, Driscoll CLW, Myrseth E, Tveiten OV, et al. Quality of life in patients with vestibular schwannomas following gross total or less than gross total microsurgical resection: shouldwe be taking the entire tumor out? *Clin Neurosurg* (2018) 82:541–7. doi: 10.1093/neuros/nyx245

20. Voinov B, Richie WD, Bailey RK. Depression and chronic diseases: it is time for a synergistic mental health and primary care approach. *Prim Care Companion J Clin Psychiatry* (2013) 15(2):PCC.12r01468. doi: 10.4088/PCC.12r01468

21. Chen CM, Mullan J, Su YY, Griffiths D, Kreis IA, Chiu HC. The longitudinal relationship between depressive symptoms and disability for older adults: a population-based study. *Journals Gerontol - Ser A Biol Sci Med Sci* (2012) 67:A:1059–1067. doi: 10.1093/gerona/gls074

22. Windisch P, Tonn JC, Fürweger C, Ehret F, Wowra B, Kufeld M, et al. Longitudinal changes of quality of life and hearing following radiosurgery for vestibular schwannoma. *Cancers (Basel)* (2021) 13:1–10. doi: 10.3390/cancers13061315

23. Carlson ML, Tveiten OV, Driscoll CL, Goplen FK, Neff BA, Pollock BE, et al. Long-term quality of life in patients with vestibular schwannoma: an international multicenter cross-sectional study comparing microsurgery, stereotactic radiosurgery, observation, and nontumor controls. *J Neurosurg* (2015) 122:833–42. doi: 10.3171/2014.11.JNS14594

24. Newman CW, Weinstein BE, Jacobson GP, Hug GA. Test-retest reliability of the hearing handicap inventory for adults. *Ear Hear* (1991) 12:355–7. doi: 10.1097/00003446-199110000-00009

25. Zeman F, Koller M, Figueiredo R, Aazevedo A, Rates M, Coelho C, et al. Tinnitus handicap inventory for evaluating treatment effects: which changes are clinically relevant? *Otolaryngol - Head Neck Surg* (2011) 145:282–7. doi: 10.1177/0194599811403882

26. Erickson NJ, Schmalz PGR, Agee BS, Fort M, Walters BC, McGrew BM, et al. Koos classification of vestibular schwannomas: a reliability study. *Clin Neurosurg* (2019) 85:409–14. doi: 10.1093/neuros/nyy409

27. House JW, Brackmann DE. Facial nerve grading system. *Otolaryngol - Head Neck Surg* (1985) 93:146–7. doi: 10.1177/019459988509300202

28. Carlson ML, Tombers NM, Kerezoudis P, Celda MP, Lohse CM, Link MJ. Quality of life within the first 6 months of vestibular schwannoma diagnosis with implications for patient counseling. *Otol Neurotol* (2018) 39:e1129–36. doi: 10.1097/MAO.0000000000001999

29. Lee J, Fung K, Lownie SP, Parnes LS. Assessing impairment and disability of facial paralysis in patients with vestibular schwannoma. *Arch Otolaryngol Head Neck Surg* (2007) 133(1):56–60. doi: 10.1001/archotol.133.1.56

30. Lee S, Seol HJ, Park K, Lee J, Nam DH, Kong DS, et al. Functional outcome of the facial nerve after surgery for vestibular schwannoma: prediction of acceptable long-term facial nerve function based on immediate postoperative facial palsy. *World Neurosurg* (2016) 89:215–22. doi: 10.1016/j.wneu.2016.01.038

31. Kojima T, Oishi N, Nishiyama T, Ogawa K. Severity of tinnitus distress negatively impacts quality of life in patients with vestibular schwannoma and mimics primary tinnitus. *Front Neurol* (2019) 10:389. doi: 10.3389/fneur.2019.00389

32. Wang JJ, Feng YM, Wang H, Wu YQ, Shi HB, Chen ZN, et al. Changes in tinnitus after vestibular schwannoma surgery. *Sci Rep* (2019) 9:1–12. doi: 10.1038/s41598-019-38582-y

33. Trakolis L, Ebner FH, Machetanz K, Sandritter J, Tatagiba M, Naros G. Postoperative tinnitus after vestibular schwannoma surgery depends on preoperative tinnitus and both pre- and postoperative hearing function. *Front Neurol* (2018) 9:136. doi: 10.3389/fneur.2018.00136

34. Trakolis L, Bender B, Ebner FH, Ernemann U, Tatagiba M, Naros G. Cortical and subcortical gray matter changes in patients with chronic tinnitus sustaining after vestibular schwannoma surgery. *Sci Rep* (2021) 11:8411. doi: 10.1038/s41598-021-87915-3

35. Park SH, Oh HS, Jeon JH, Lee YJ, Moon IS, Lee W-SS. Change in tinnitus after treatment of vestibular schwannoma: microsurgery vs. *Gamma knife radiosurgery. Yonsei Med J* (2014) 55:19–24. doi: 10.3349/ymj.2014.55.1.19

36. Inoue Y, Ogawa K, Kanzaki J. Quality of life of vestibular schwannoma patients after surgery. *Acta Otolaryngol* (2001) 121:59–61. doi: 10.1080/000164801300006281

37. Maurer R, Daggubati L, Ba DM, Liu G, Leslie D, Goyal N, et al. Mental health disorders in patients with untreated meningiomas: an observational cohort study using the nationwide marketscan database. *Neuro-Oncology Pract* (2020) 7:507–13. doi: 10.1093/nop/npaa025

38. Wagner A, Shiban Y, Lange N, Joerger AK, Hoffmann U, Meyer B, et al. The relevant psychological burden of having a benign brain tumor: a prospective study of patients undergoing surgical treatment of cranial meningiomas. *J Neurosurg* (2019) 131:1840–7. doi: 10.3171/2018.8.JNS181343

39. Kalasauskas D, Keric N, Ajaj SA, von CL, Ringel F, Renovanz M. Psychological burden in meningioma patients under a wait-and-watch strategy and after complete resection is high–results of a prospective single center study. *Cancers (Basel)* (2020) 12:1–13. doi: 10.3390/cancers12123503

40. Godefroy WP, Kaptein AA, Vogel JJ, van der Mey AGL. Conservative treatment of vestibular schwannoma. *Otol Neurotol* (2009) 30:968–74. doi: 10.1097/MAO.0b013e3181b4e3c9

41. Adegboyega G, Jordan C, Kawka M, Chisvo N, Toescu SM, Hill C. Quality of life reporting in the management of posterior fossa tumours: a systematic review. *Front Surg* (2022) 9:970889. doi: 10.3389/fsurg.2022.970889

42. McLaughlin EJ, Bigelow DC, Lee JYK, Ruckenstein MJ. Quality of life in acoustic neuroma patients. *Otol Neurotol* (2015) 36:653–6. doi: 10.1097/MAO.0000000000000674

43. Chweya CM, Tombers NM, Lohse CM, Link MJ, Carlson ML. Disease-specific quality of life in vestibular schwannoma: a national cross-sectional study comparing microsurgery, radiosurgery, and observation. *Otolaryngol - Head Neck Surg (United States)* (2021) 164:639–44. doi: 10.1177/0194599820941012

44. Bender M, Tatagiba M, Gharabaghi A. Quality of life after vestibular schwannoma surgery: a question of perspective. *Front Oncol* (2022) 11:770789. doi: 10.3389/fonc.2021.770789

45. Fukuda M, Oishi M, Hiraishi T, Natsumeda M, Fujii Y. Clinicopathological factors related to regrowth of vestibular schwannoma after incomplete resection: clinical article. *J Neurosurg* (2011) 114:1224–31. doi: 10.3171/2010.11.JNS101041

46. Park HH, Park SH, Oh HC, Jung HH, Chang JH, Lee KS, et al. The behavior of residual tumors following incomplete surgical resection for vestibular schwannomas. *Sci Rep* (2021) 11(1):4665. doi: 10.1038/s41598-021-84319-1

frontiers | Frontiers in Oncology

TYPE Original Research
PUBLISHED 30 June 2023
DOI 10.3389/fonc.2023.1160764

OPEN ACCESS

EDITED BY
Haotian Zhao,
New York Institute of Technology,
United States

REVIEWED BY
Kamil Krystkiewicz,
Copernicus Memorial Hospital, Poland
Christopher M. Heaphy,
Boston University, United States
Jiwei Bai,
Capital Medical University, China

*CORRESPONDENCE
Sofia Asioli
sofia.asioli3@unibo.it

RECEIVED 07 February 2023
ACCEPTED 20 June 2023
PUBLISHED 30 June 2023

CITATION
Righi A, Cocchi S, Maioli M, Zoli M, Guaraldi F, Carretta E, Magagnoli G, Pasquini E, Melotti S, Vornetti G, Tonon C, Mazzatenta D and Asioli S (2023) SMARCB1/INI1 loss in skull base conventional chordomas: a clinicopathological and molecular analysis.
Front. Oncol. 13:1160764.
doi: 10.3389/fonc.2023.1160764

SMARCB1/INI1 loss in skull base conventional chordomas: a clinicopathological and molecular analysis

Alberto Righi[1], Stefania Cocchi[1], Margherita Maioli[1], Matteo Zoli[2,3], Federica Guaraldi[2], Elisa Carretta[1], Giovanna Magagnoli[1], Ernesto Pasquini[2], Sofia Melotti[3], Gianfranco Vornetti[2], Caterina Tonon[2,3], Diego Mazzatenta[2,3] and Sofia Asioli[2,3]*

[1]IRCCS Istituto Ortopedico Rizzoli, Bologna, Italy, [2]IRCCS Istituto delle Scienze Neurologiche di Bologna, Bologna, Italy, [3]Department of Biomedical and Neuromotor Sciences (DIBINEM), University of Bologna, Bologna, Italy

Introduction: The loss of SMARCB1/INI1 protein has been recently described in poorly differentiated chordoma, an aggressive and rare disease variant typically arising from the skull base.

Methods: Retrospective study aimed at 1) examining the differential immunohistochemical expression of SMARCB1/INI1 in conventional skull base chordomas, including the chondroid subtype; 2) evaluating SMARCB1 gene deletions/copy number gain; and 3) analyzing the association of SMARCB1/INI1 expression with clinicopathological parameters and patient survival.

Results: 65 patients (35 men and 30 women) affected by conventional skull base chordoma, 15 with chondroid subtype, followed for >48 months after surgery were collected. Median age at surgery was 50 years old (range 9-79). Mean tumor size was 3.6 cm (range 2-9.5). At immunohistochemical evaluation, a partial loss of SMARCB1/INI1 (>10% of neoplastic examined cells) was observed in 21 (32.3%) cases; the remaining 43 showed a strong nuclear expression. Fluorescence *in situ* hybridization (FISH) analysis was performed in 15/21 (71.4%) cases of the chordomas with partial SMARCB1/INI1 loss of expression. Heterozygous deletion of SMARCB1 was identified in 9/15 (60%) cases and was associated to copy number gain in one case; no deletion was found in the other 6 (40%) cases, 3 of which presenting with a copy number gain. No correlations were found between partial loss of SMARCB1/INI1 and the clinicopathological parameters evaluated (i.e., age, tumor size, gender, tumor size and histotype). Overall 5-year survival and 5-year disease-free rates were 82% and 59%, respectively. According to log-rank test analysis the various clinico-pathological parameters and SMARCB1/INI1 expression did not impact on overall and disease free-survival.

Discussion: Partial loss of SMARCB1/INI1, secondary to heterozygous deletion and/or copy number gain of SMARCB1, is not peculiar of aggressive forms, but can be identified by immunohistochemistry in a significant portion of

conventional skull base chordomas, including the chondroid subtype. The variable protein expression does not appear to correlate with clinicopathological parameters, nor survival outcomes, but still, it could have therapeutic implications.

KEYWORDS

skull base, chordoma, prognosis, SMARCB1/INI1, FISH analysis

Introduction

Skull base chordomas represent a heterogeneous group of tumors, including different histotypes (i.e., conventional, chondroid, poorly differentiated and dedifferentiated types) with different clinical behavior (1–5).

SWI/SNF-related matrix-associated actin-dependent regulator of chromatin subfamily B member 1 (SMARCB1), also known as integrase interactor 1 (INI1), is a critical component of a chromatin-remodeling protein complex (4, 6). Recent studies have described the immunohistochemical loss of SMARCB1/INI1 protein in poorly differentiated chordoma associated with *SMARCB1* gene deletions at fluorescence *in situ* hybridization (FISH) examination, mainly deriving from large, homozygous deletions at 22q11 locus (4, 6–8). The loss of SMARCB1/INI1 protein could potentially serve as theoretical basis for evaluating the efficacy of new targeted therapies, i.e., Enhancer of Zeste homologue 2 (EZH2) inhibitors (Tazemetostat), histone deacetylase inhibitors, and CDK4 inhibitors (4, 7, 9–11).

Some studies have recently suggested the partial loss of SMARCB1/INI1 expression at immunohistochemistry as a poor prognostic marker of outcome, being associated with higher recurrence rates and shorter survival in patients with other tumor types, including colorectal, pancreatic, uterine and sinonasal carcinomas (12–16).

Genetic studies have demonstrated that conventional chordomas are characterized by very low to modest mutation burden, and are mainly characterized by large copy number loss, typically involving chromosomes 1p, 3, 9q, 10, 13, and 14, and a small number of copy number gains on chromosome 7 and 1q (4, 9). Loss of chromosome 22 and/or heterozygous deletion of *SMARCB1* seems to be a rare event in conventional chordomas, although data are referred to small series (4, 17–19).

This study aimed at evaluating the differential immunohistochemical expression of SMARCB1/INI1 in conventional skull base chordoma, including chondroid subtype, and the presence of *SMARCB1* gene deletion/copy number gain by FISH. Potential associations of SMARCB1/INI1 expression with different clinicopathological parameters and survival outcomes were then analyzed.

Materials and methods

Patient selection

Patients with conventional - including chondroid variant - and with poorly differentiated chordoma (1, 2), naïve for surgery and radiation therapy, operated via endoscopic endonasal approach from 1998 to 2017 in a tertiary care center (Programma Neurochirurgia Ipofisi - Pituitary Unit, IRCCS Istituto delle Scienze Neurologiche di Bologna, Italy), followed by Radiation-therapy, and with a clinico-radiological follow-up ≥48 months. Formalin-fixed paraffin-embedded (FFPE) tumor tissue of adequate size and quality was required to perform morphologic, immunohistochemical and molecular evaluations. The pathologist selected the most representative tumor fragments for size and quality (i.e., maximum representation of neoplastic cells and lowest portions of extra-chordoma tissues and necrosis). All the original tumor slides were reviewed, and the diagnosis was confirmed independently by two pathologists (SA and AR) with a confirmation of immunohistochemical expression of brachyury and pan-cytokeratin AE1/AE3. Three cases of poorly differentiated chordomas diagnosed at the Programma Neurochirurgia Ipofisi-Pituitary Unit, IRCCS Istituto delle Scienze Neurologiche di Bologna, Italy, for which FFPE tissue was available, were also included. Ethical committee approval was obtained from the Comitato Etico di Area Vasta Emilia Centro on 01/04/2019 (protocol # CE-AVEC: 184/2019/OSS/AUSLBO).

Immunohistochemical analysis

The tissue was fixed in 4% buffered formalin, processed and embedded in paraffin; 4µm-thick tissue sections were then cut and heated at 58°C for 2 h. Immunohistochemical staining was performed using an automated immunostainer following the manufacturer's guidelines (Ventana BenchMark -Ventana Medical Systems, Tucson AZ, USA) using an antibody anti-INI-1 (MRQ-27; Cell Marque), a mouse monoclonal antibody ready to use at the concentration of 0,4 µg/ml (MRQ-27; Cell Marque). Antibody detection was performed using UltraView DAB Detection Kit (Ventana Medical Systems, Tucson AZ, USA).

Immunohistochemical evaluation was performed as previously described (20). The percentage of cells stained was determined evaluating all neoplastic areas in the whole of the obtained slides in each case, independently assessed by two pathologists (AR, SA). This evaluation was done visually and a comparison between immunohistochemical expression of SMARCB1/INI1 and the signals of FISH analysis was done. Immunohistochemical staining grades were defined as intact (strong nuclear staining in malignant cells), deficient (completely unstained nuclei in malignant cells), and reduced (very weak but still noticeable nuclear staining in malignant cells), using the strong staining of normal background cells as reference (20, 21). Strong homogeneous nuclear staining in the background (including inflammatory cells, stromal fibroblasts, vascular endothelial cells, and/or normal epithelial cells) served as an internal control and was considered a prerequisite for immunohistochemical interpretation. Only unequivocal staining of the nuclei in viable tumor tissue (necrotic areas were excluded) was analyzed. The evaluations were performed on 200X of magnification, evaluating the mean of SMARCB1/INI1 loss, when present, for each mm^2.

FISH analysis

FISH was performed to assess *SMARCB1* gene deletion using a commercial SPEC SMARCB1/22q12 Dual colour Probe (ZytoVision, Bremerhaven, Germany), according to manufacturer's instructions. The probe included a 545 kb sequence mapping in 22q11.23 region (ZyGreen fluorochrome labeled) harboring *SMARCB1* gene, and a 335 kb sequence mapping in 22q12.1-q12.2 region (ZyOrange fluorochrome labelled) harboring *KREMEN1* gene, used as internal control probe, to help in detecting chromosome 22q large deletions. As previously described (22), FISH was performed on interphase nuclei using the Histology FISH accessory kit (Dako, Glostrup, Denmark), according to the manufacturers' protocol. Briefly, 3 µm-thick FFPE tissue sections were mounted on positively charged slides. Slides were heated overnight at 60°C, deparaffinized with xylene, and dehydrated with ethanol. Samples and probes were co-denaturated in a Dako Hybridizer (Dako, Glostrup, Denmark) at 75°C for 10 minutes and incubated overnight at 37°C. Slides were then washed in stringent solution for 10 minutes at 63°C and stained with DAPI (Vector Laboratories, Inc. Burlingame CA, USA). Signal analysis was performed in combination with SMARCB1/INI1 nuclear expression correlation. For each slide, a minimum of 100 nuclei within the marked tumor area with intact morphology were scored using an Olympus BX41 fluorescent microscope (Tokyo, Japan) at 100X of magnification. Nuclei with no signal and signals in overlapped nuclei were considered non-informative and were not analyzed to avoid truncation or overlapping artifact. The presence of two copies of the *SMARCB1* gene with a 1:1 ratio with the control probe was considered as the normal copy number pattern. A heterozygous co-deletion pattern (or large deletion) was defined if one allele copy of both *SMARCB1* gene and control probe were lost, with a ratio of 1:1. Copy number gain was defined as the presence of extra copies of both *SMARCB1* and control probe. A Color View III CCD camera soft imaging system (Olympus) was used to capture images, then analyzed with a CytoVision imaging software version 7.5 (Leica Biosystem Richmond Inc, USA).

Statistical analysis

Disease-free Survival (DFS) was defined as the time between treatment completion and first disease relapse. Patients free from disease were censored at last follow up. Overall Survival (OS) was defined as the time between treatment completion and death or last follow-up. Descriptive statistic was used to report patient and clinical characteristics. T-test or Wilcoxon Mann-Whiney test were used to analyze continuous variables; chi-squared test or Fisher's exact test to analyze categorical variables. Kolmogorov-Smirnov and Shapiro-Wilk test were used to verify normal distribution of continuous variables. Time-to event measures were estimated using Kaplan–Meier method, and log-rank test was used to compare different parameters. All p-values were two-sided and a $p<0.05$ was considered as statistically significant. All statistical analyses were performed using SAS software 9.4 (SAS Institute Inc., Cary, NC).

Results

Sixty-five patients with conventional skull base chordoma, including 35 (53.8%) men and 30 (46.2%) women, with a median age at first surgery of 50 years old (range 9-79), were enrolled. Mean tumor size at presentation was 3.6 cm (range 2-9.5 cm) (see Table 1). Histologically, 50 (76.9%) were conventional chordomas, while 15 (23.1%) were chordomas of chondroid subtype, characterized by extracellular matrix mimicking hyaline cartilage inside physalifourous neoplastic cell proliferation in the majority of the neoplastic evaluated areas (1, 2). The mean of Ki-67 labeling index was 4% (range 1-25).

At immunohistochemical evaluation, a partial loss of SMARCB1/INI1 (between 10% and 40% of neoplastic cells evaluated) was observed in 21 (32.3%) cases; the remaining 44 (67.7%) cases showed a strong nuclear expression in all neoplastic cells (see Supplementary File Table 1). None of conventional/chondroid chordoma cases displayed complete loss of SMARCB1/INI1 loss. Poorly differentiated chordomas presented loss of SMARCB1/INI1 in all evaluated neoplastic cells.

Conventional chordomas with focal loss of SMARCB1/INI1 displayed two different staining patterns in neoplastic areas: 13 cases showed a mosaic pattern of protein loss, with isolated single/small foci of negative cells closed to other foci of cells that retained SMARCB1/INI1 (Figure 1A); 8 cases showed protein loss in large areas, looking like 'subclonal' foci within the tumor (Figure 1B). No differences in clinicopathological factors between the two different staining patterns were observed. Regardless to the pattern of SMARCB1/INI1 expression, no association could be established between SMARCB1/INI1 expression and gender, age, tumor size, Ki67 and histological subtype (see Table 1). FISH analysis could be performed with a readable signal in 15/21 (71.4%) cases of conventional chordomas with a partial immunohistochemical loss of SMARCB1/INI1

10.3389/fonc.2023.1160764

TABLE 1 Main clinicopathological characteristics and distribution according to SMARCB1/INI1 immunohistochemical expression.

Parameters	All samples (n=65)	SMARCB1/INI1 + (n=44)	SMARCB1/INI +/- (n=21)	P value
Age (median, range; years)	50 (9-79)	51.6 (17-79)	49.2 (9-73)	0.5956
Age (N, %)				
≤ 50 years	34 (52.3)	23 (52.3)	11 (52.4)	0.9935
>50 years	31 (47.7)	21 (47.7)	10 (47.6)	
Gender (N, %)				
Male	35 (53.8)	21 (47.7)	14 (66.7)	0.1520
Female	30 (46.2)	23 (52.3)	7 (33.3)	
Tumor size (N, %)				
< 3cm	10 (15.4)	5 (11.4)	5 (23.8)	0.2714
≥ 3cm	55 (84.6)	39 (88.6)	16 (76.2)	
Histological subtype (N, %)				
conventional	50 (76.9)	34 (77.3)	16 (76.2)	1.000
chondroid	15 (23.1)	10 (22.7)	5 (23.8)	
Ki-67 (N, %)				
≤ 3%	36 (55.4)	24 (54.6)	12 (57.1)	0.8438
>3%	29 (44.6)	20 (45.4)	9 (42.9)	

expression. Six cases did not show hybridized signal due to poor tissue quality, and were thus considered inadequate for FISH scoring. FISH analysis demonstrated the presence of heterozygous deletion of *SMARCB1* in 9/15 (60%) cases in over 10% of tumors cells (range 10% to 80%, Figure 2), and was associated with a copy number gain in one case. No deletion was observed in the other 6 (40%) cases, 3 of which presenting with a copy number gain of *SMARCB1* (Figure 2). FISH identified homozygous *SMARCB1* deletions in all 3 cases of poorly differentiated chordoma.

Follow-up duration after treatment completion was 80 months (range, 51-127). Overall 5-year survival and 5-year disease-free rates were 83% (95%CI: 69.9-90.5) and 59% (95% CI:44.5-71.3), respectively. Univariate analysis showed that the risk of recurrence/metastases was higher for conventional than

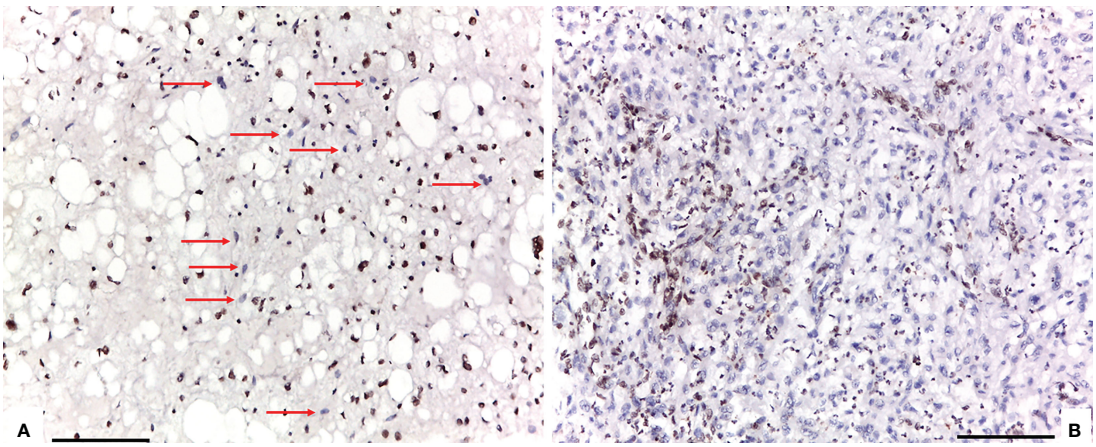

FIGURE 1
Two different staining patterns in neoplastic areas of focal loss of SMARCB1/INI1: **(A)** an example of a case that showed a mosaic pattern of protein loss, with isolated single/small foci of negative cells (red arrows) closed to other foci of cells that retained SMARCB1/INI1; **(B)** an example of a case that showed protein loss in large areas, looking like 'subclonal' foci within the tumor (A, B: 100X of magnification, Scale bar=75 µm).

10.3389/fonc.2023.1160764

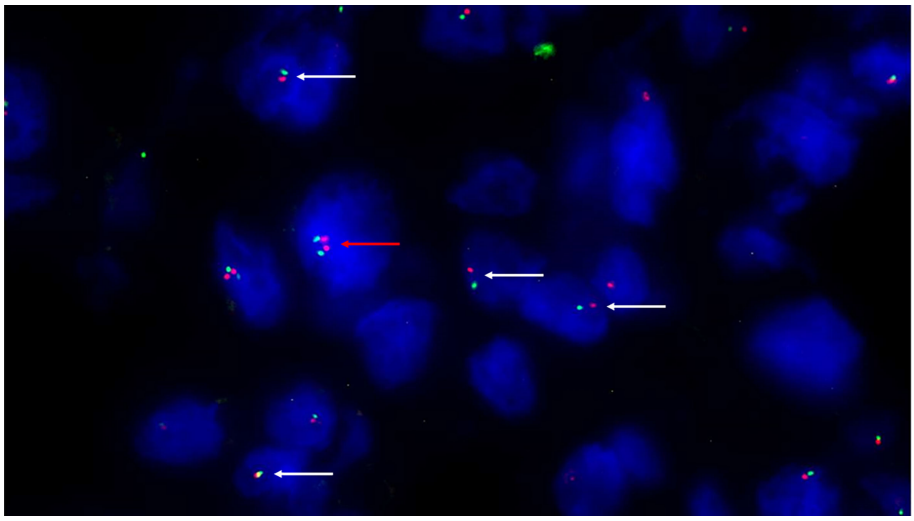

FIGURE 2
Fluorescence *in situ* hybridization (FISH) with SPEC SMARCB1/22q12 Dual Color Probe detected, in a representative tumoral area. Monoallelic co-deletion pattern: only one copy of SMARCB1/INI1 (green signal) and one copy of 22q12 (red signal) were observed in most tumor cells (white arrows). A cell without deletion is shown in the field as internal control (red arrow). (200X of magnification).

chondroid chordoma (p=0.0281). Among all considered parameters, only the histological subtype impacted on DFS, while no predictor of OS was identified (see Tables 2, 3; Figures 3, 4).

Discussion

Skull base chordomas represent a heterogeneous group of neoplasia, extremely difficult to be eradicated by surgical and

TABLE 2 Results from univariate Kaplan-Meier models for OS and DFS.

	5 years-OS % (95%CI)	p-value	5 years-DFS % (95%CI)	p-value
Entire sample	82.6 (69.9-90.5)		59.2 (44.5-71.3)	
Age (N, %)				
≤50 years	81.3 (62.8-91.1)	0.6248	61.8 (41.1-77.0)	0.7148
>50 years	84.1 (62.7-93.8)		56.1 (34.1-73.3)	
Gender (N, %)				
Male	75.3 (56.4-86.8)	0.1200	56.8 (36.8-72.6)	0.4467
Female	92.7 (73.7-98.1)		61.2 (38.2-77.8)	
Tumor size (N, %)				
< 3cm	80.0 (40.9-94.6)	0.8875	68.6 (30.5-88.7)	0.5574
≥ 3cm	83.6 (69.7-91.5)		57.4 (41.1-70.7)	
Histological subtype (N, %)				
conventional	80.5 (65.7-89.4)	0.3733	50.8 (34.7-64.9)	0.0281
chondroid	90.9 (50.8-98.7)		91.7 (53.9-98.8)	
Ki-67 (N, %)				
≤ 3%	79.4 (59.4-90.3)	0.6194	60.4 (39.1-76.3)	0.6474
>3%	85.6 (66.0-94.4)		57.4 (36.0-73.9)	
SMARCB1/INI1 immunohistochemical expression (N, %)				
positive	84.0 (67.5-92.5)	0.6860	59.1 (40.3-73.8)	0.6105
negative	79.9 (54.8-92.0)		58.4 (33.6-76.8)	

TABLE 3 Results from univariate Kaplan-Meier models for OS and DFS according the different pattern of partial loss of SMARCB1/INI1 by immunohistochemistry.

	5 years-OS % (95%CI)	p-value overall	p-value subclonal vs mosaic
Pattern		0.7246	0.5671
Subclonal	75.0 (31.5-93.1)		
Mosaic	83.3 (48.2-95.6)		
Positive	84.0 (67.5-92.5)		
	5 years-DFS % (95%CI)		
Pattern		0.1859	0.1785
Subclonal	42.9 (9.8-73.4)		
Mosaic	67.7 (34.9-86.5)		
Positive	59.1 (40.3-73.8)		

adjuvant means, although typically slow-growing. New therapeutic targeted therapies are currently under investigation, including EZH2 inhibitors (Tazemetostat) (4, 10, 11, 23). EZH2 is a catalytic subunit of the histone methyltransferase PCR2 polycomb repressive complex whose overexpression promotes oncogenesis (24). Agents targeting EZH2 have shown to induce tumor regression and promote radiation sensitivity in models of SMARCB1/INI1-deficient tumors, including poorly differentiated chordomas, malignant rhabdoid tumors and epithelioid sarcomas (4, 10, 11). Differently from most of atypical teratoid/rhabdoid tumors, in chordomas, loss of SMARCB1/INI1 expression at immunohistochemistry results from a homozygous deletion of the SMARCB1 gene (4, 9, 25), and has been reported not only in poorly differentiated variants (in which it represents a diagnostic hallmark) (4, 6, 9, 26, 27), but also in a case of conventional chordoma with transformation to poorly differentiated chordoma (17), and in another case of conventional chordoma with dedifferentiated sarcomatous components (28).

Based on literature data, total loss of SMARCB1/INI1 immunohistochemical expression associated with the presence of a homozygous deletion of the *SMARCB1* gene is correlated with aggressive clinical behavior of chordomas (8, 17, 27–29). Only few series have evaluated SMARCB1/INI1 immunohistochemical expression in association with FISH analysis in conventional chordoma. Overall, the study by Mobley et al. (30) and by Hassellbatt et al. (4) found the retention of SMARCB1/INI1 without a recurrent deletion of *SMARCB1* region in 14 out of 24 cases. Conversely, Yadav et al. (27) described 2 cases of conventional chordomas with loss of immunohistochemical expression of SMARCB1/INI1 associated with loss of *SMARCB1* locus, and Wen reported a single case of extra-axial conventional chordoma with a partial loss of SMARCB1/INI1 at immunohistochemistry despite no deletion of *SMARCB1* detected by FISH analysis (9). Therefore, to best of our knowledge, this is the largest study aimed at investigation the incidence of SMARCB1/INI1 loss in of conventional skull base chordomas, accounting for >95% of chordomas (1, 2, 8). Immunohistochemical analysis demonstrated a partial loss of SMARCB1/INI1 in 10 to 40% of neoplastic cells in 21/65 (32.3%) cases, and no correlations between partial SMARCB1/INI1 loss and clinicopathological parameters. Furthermore, unlike poorly differentiated chordoma and other types of carcinomas (8, 12, 13, 21, 31), log-rank test analysis showed no impact of SMARCB1/INI1 expression on overall and disease free-survival.

From a molecular point of view, SMARCB1/INI1 loss of function may be caused by gene deletions, inactivating mutations, or epigenetic modifications. *SMARCB1* heterozygosity is considered the main underlying mechanism and can be revealed by FISH analysis with very high sensitivity (7, 9, 32). FISH analysis on FFPE tissue in SMARCB1-deficient tumors has been proven to be a reliable test to investigate large homozygous or heterozygous deletions at 22q11.12 (33). Due to cross-hybridizations of chromosome 22 alpha satellites to other centromeric regions, probes specific for 22q12.1-q12.2 region are frequently used as control for chromosome 22 copy number detection. However, since the SMARCB1 gene and the control probe used are only 5.5 Mb away (chromosome bands 22q11.23 and 22q12.1-q12.2, respectively), secondary regional deletions may occur in SMARCB1-deleted tumors. Many studies have stated that in SMARCB1-deficient tumors large deletions covering also the EWSR1 gene locus (chromosome band 22q12.2) can occur (7, 30, 33–35), so demonstrating the deletion of a large portion of the long arm of chromosome 22. More advanced genomics and epigenetics sequencing approaches should be used in future in depth studies of chromatin modifier SMARCB1/INI1. In our series, 21 cases of conventional chordoma displayed partial loss of SMARCB1/INI1 expression at immunohistochemistry; 6 (28.6%) showed no readable signal at FISH analysis, due to the poor tissue quality. Of the remaining 15, 9 showed heterozygous large 22q deletion encompassing the entire *SMARCB1* gene locus, while 6 cases had no deletion, confirming a previous observation (9). Consistent with previous studies (4, 9),

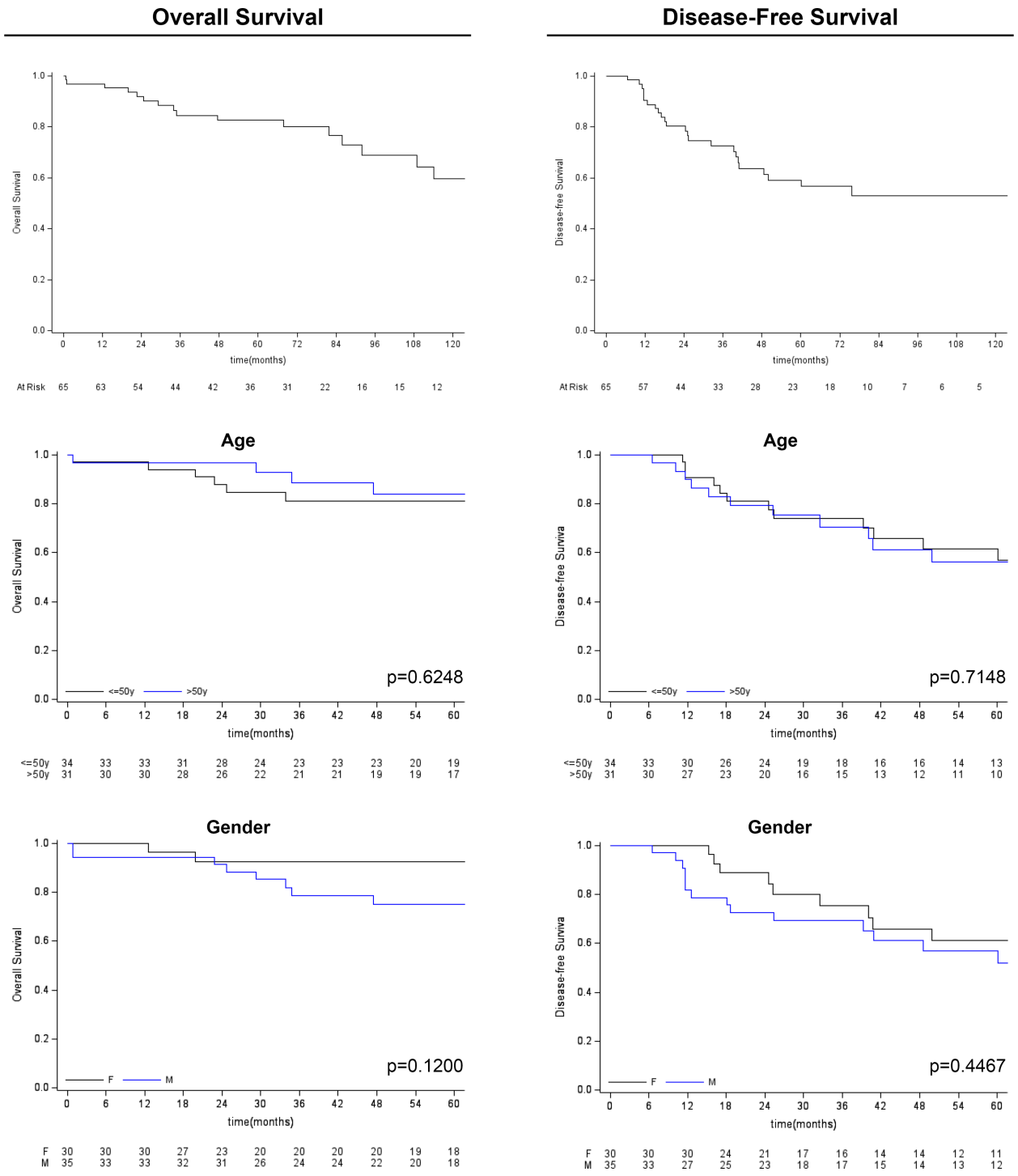

FIGURE 3
Kaplan-Meier survival analysis (overall survival and disease-free survival) for age and gender variables.

homozygous *SMARCB1* loss was observed in the 3 cases of poorly differentiated, but not in conventional chordoma. Interestingly, one case with *SMARCB1* heterozygous deletion showed copy number gain of *SMARCB1*; control probe suggested a gain in the 22q region. This pattern was observed also in 3 cases without *SMARCB1* deletion. Anyway, since the 12 patients with heterozygous 22q deletion and/or a copy number gain of *SMARCB1* showed reduced expression of SMARCB1/INI1 at immunohistochemistry, it is possible that this partial loss of SMARCB1/INI1 is a marker of the accumulation of additional mutations as suggested by Bai et al., who reported complex copy number alterations, including also the deletion of 22q, without apparent recurrent oncogene mutations in conventional

10.3389/fonc.2023.1160764

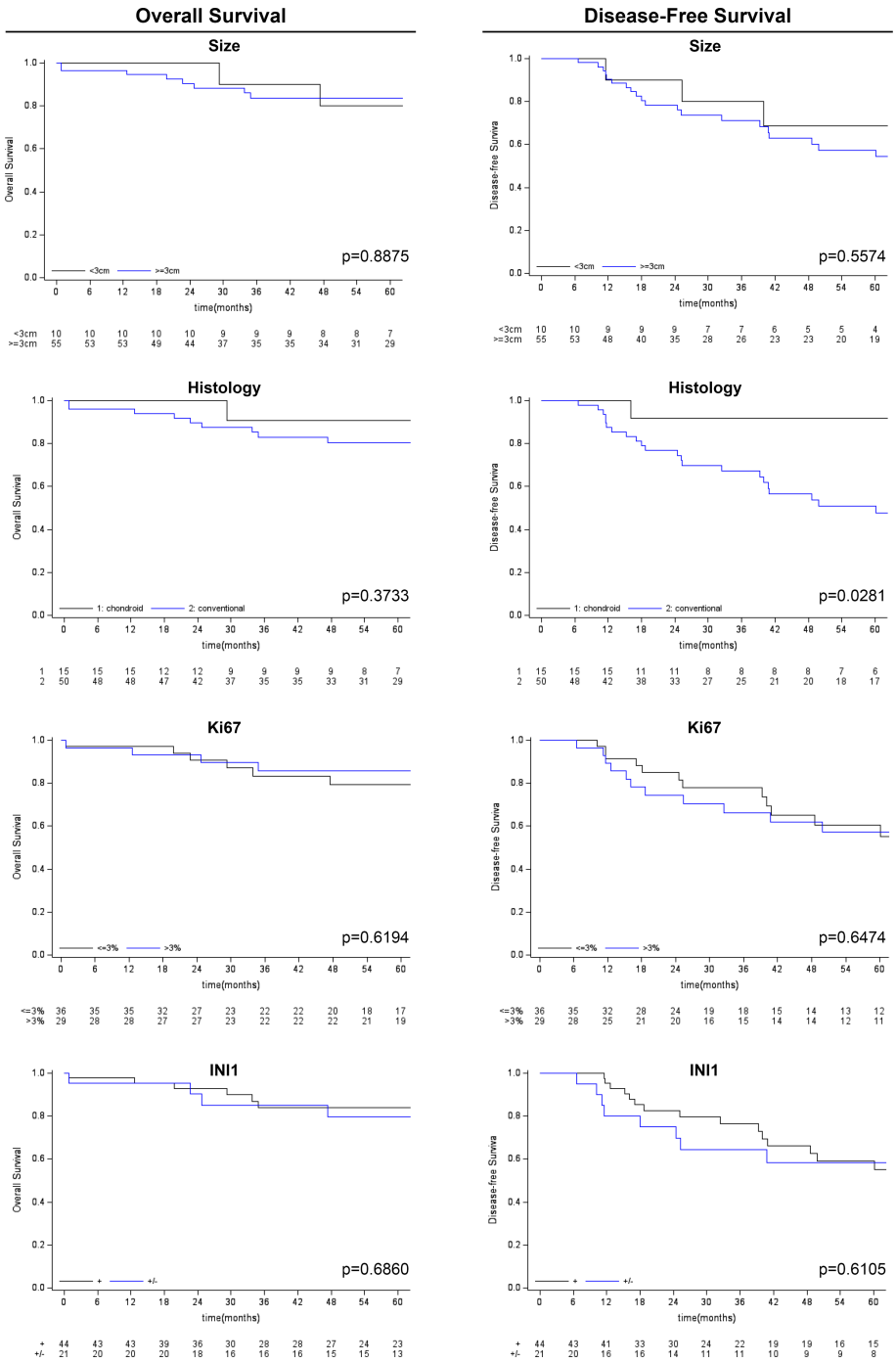

FIGURE 4
Kaplan-Meier survival analysis (overall survival and disease-free survival) for other clinico-pathological variables considered (tumor size, histological subtype, Ki-67 and SMARCB1/INI1 immunohistochemical expression).

chordoma (29). Therefore, EZH2 inhibitors (Tazemetostat) may prove to be beneficial in treating conventional chordoma, as recently demonstrated *in vitro* and *in vivo* studies and in patient-derived xenograft model (23, 36). Although promising, these data are preliminary and collected retrospectively, thus need to be confirmed by larger prospective studies, possibly multicentric because of the rarity of the disease.

In conclusion, the partial loss of SMARCB1/INI1, secondary to heterozygous deletion and/or copy number gain of SMARCB1, can be identified by immunohistochemistry in a significant portion of conventional chordomas, and is not peculiar of aggressive cases. The different protein expression does not appear to correlate with clinicopathological parameters, nor survival outcomes. However, it could still have therapeutic implications.

Author's note

This work was partially presented as platform presentation at the 112th Meeting of the United States and Canadian Academy of Pathology in New Orleans, Louisiana, USA, 11-16 March, 2023.

Data availability statement

The original contributions presented in the study are included in the article/Supplementary Material. Further inquiries can be directed to the corresponding author.

Ethics statement

The studies involving human participants were reviewed and approved by Comitato Etico di Area Vasta Emilia Centro on 01/04/2019 (protocol # CE-AVEC: 184/2019/OSS/AUSLBO). Written informed consent to participate in this study was provided by the participants' legal guardian/next of kin.

Author contributions

All authors contributed to the study conception and design. Material preparation, data collection and analysis were performed by AR, SC, MM, MZ, GM, EP, SM, GV, CT, DM, and SA. EC performed statistical analysis. The draft of the manuscript was written by AR, FG, SC, and SA. All authors read and approved the final manuscript.

Funding

The publication of this article was supported by the "Ricerca Corrente" funding from the Italian Ministry of Health. This work was supported by funds for selected research topics from the Fondazione CARISBO Project (#19344).

Conflict of interest

The authors declare that the research was conducted in the absence of any commercial or financial relationships that could be construed as a potential conflict of interest.

Publisher's note

Supplementary material

The Supplementary Material for this article can be found online at: https://www.frontiersin.org/articles/10.3389/fonc.2023.1160764/full#supplementary-material

References

1. WHO Classification of Tumours Editorial Board. WHO classification of tumours. In: *Soft tissue and bone tumours, 5th Edition*. Lyon, France: WHO Press (2020).

2. WHO Classification of Tumours Editorial Board. Central nervous system tumours. Lyon (France): International Agency for Research on Cancer (2021). (WHO classification of tumours series, 5th ed.; vol. 6). Available at: https://publications.iarc.fr/601.

3. Asioli S, Zoli M, Guaraldi F, Sollini G, Bacci A, Gibertoni D, et al. Peculiar pathological, radiological and clinical features of skull-base de-differentiated chordomas. results from a referral centre case-series and literature review. *Histopathology* (2020) 76(5):731–9. doi: 10.1111/his.14024

4. Hasselblatt M, Thomas C, Hovestadt V, Schrimpf D, Johann P, Bens S, et al. Poorly differentiated chordoma with SMARCB1/INI1 loss: a distinct molecular entity with dismal prognosis. *Acta Neuropathol* (2016) 132(1):149–51. doi: 10.1007/s00401-016-1574-9

5. Yoneoka Y, Tsumanuma I, Fukuda M, Tamura T, Morii K, Tanaka R, et al. Cranial base chordoma–long term outcome and review of the literature. *Acta Neurochir (Wien)* (2008) 150(8):773–8. doi: 10.1007/s00701-008-1600-3

6. Antonelli M, Raso A, Mascelli S, Gessi M, Nozza P, Coli A, et al. SMARCB1/INI1 involvement in pediatric chordoma: a mutational and immunohistochemical analysis. *Am J Surg Pathol* (2017) 41(1):56–61. doi: 10.1097/PAS.0000000000000741

7. Owosho AA, Zhang L, Rosenblum MK, Antonescu CR. High sensitivity of FISH analysis in detecting homozygous SMARCB1 deletions in poorly differentiated chordoma: a clinicopathologic and molecular study of nine cases. *Genes Chromosomes Cancer* (2018) 57(2):89–95. doi: 10.1002/gcc.22511

8. Shih AR, Cote GM, Chebib I, Choy E, DeLaney T, Deshpande V, et al. Clinicopathologic characteristics of poorly differentiated chordoma. *Mod Pathol* (2018) 31(8):1237–1245. doi: 10.1038/s41379-018-0002-1

9. Wen X, Cimera R, Aryeequaye R, Abhinta M, Athanasian E, Healey J, et al. Recurrent loss of chromosome 22 and SMARCB1 deletion in extra-axial chordoma: a clinicopathological and molecular analysis. *Genes Chromosomes Cancer* (2021) 60(12):796–807. doi: 10.1002/gcc.22992

10. Kalimuthu SN, Chetty R. Gene of the month: SMARCB1. *J Clin Pathol* (2016) 69(06):484–9. doi: 10.1136/jclinpath-2016-203650

11. Tarpey PS, Behjati S, Young MD, Martincorena I, Alexandrov LB, Farndon SJ, et al. The driver landscape of sporadic chordoma. *Nat Commun* (2017) 8(1):890. doi: 10.1038/s41467-017-01026-0

12. Agaimy A, Rau TT, Hartmann A, Stoehr R. SMARCB1 (INI1)-negative rhabdoid carcinomas of the gastrointestinal tract: clinicopathologic and molecular study of a highly aggressive variant with literature review. *Am J Surg Pathol* (2014) 38(07):910–20. doi: 10.1097/PAS0000000000000173

13. Agaimy A, Haller F, Frohnauer J, Schaefer I-M, Ströbel P, Hartmann A, et al. Pancreatic undifferentiated rhabdoid carcinoma: KRAS alterations and SMARCB1 expression status define two subtypes. *Mod Pathol* (2015) 28:248–60. doi: 10.1038/modpathol.2014.100

14. Chitguppi C, Rabinowitz MR, Johnson J, Bar-Ad V, Fastenberg JH, Molligan J, et al. Loss of SMARCB1 expression confers poor prognosis to sinonasal undifferentiated carcinoma. *J Neurol Surg B Skull Base* (2020) 81(6):610–9. doi: 10.1055/s-0039-1693659

15. Donner LR, Wainwright LM, Zhang F, Biegel JA. Mutation of the INI1 gene in composite rhabdoid tumor of the endometrium. *Hum Pathol* (2007) 38:935–9. doi: 10.1016/j.humpath.2016.12.003

16. Wang J, Andrici J, Sioson L, Clarkson A, Sheen A, Farzin M, et al. Loss of INI1 expression in colorectal carcinoma is associated with high tumor grade, poor survival, BRAFV600E mutation, and mismatch repair deficiency. *Hum Pathol* (2016) 55:83–90. doi: 10.1016/j.humpath.2016.04.018

17. Curcio C, Cimera R, Aryeequaye R, Rao M, Fabbri N, Zhang Y, et al. Poorly differentiated chordoma with whole-genome doubling evolving from a SMARCB1-

deficient conventional chordoma: a case report. *Genes Chromosomes Cancer* (2021) 60 (1):43–8. doi: 10.1002/gcc.22895

18. Choy E, MacConaill LE, Cote GM, Le LP, Shen JK, Nielsen GP, et al. Genotyping cancer-associated genes in chordoma identifies mutations in oncogenes and areas of chromosomal loss involving CDKN2A, PTEN, and SMARCB1. *PloS One* (2014) 9: e101283. doi: 10.1371/journal.pone.0101283

19. Wang L, Zehir A, Nafa K, Zhou N, Berger MF, Casanova J, et al. Genomic aberrations frequently alter chromatin regulatory genes in chordoma. *Genes Chromosomes Cancer* (2016) 55(7):591–600. doi: 10.1002/gcc.22362

20. Strehl JD, Wachter DL, Fiedler J, Heimerl E, Beckmann MW, Hartmann A, et al. Pattern of SMARCB1 (INI1) and SMARCA4 (BRG1) in poorly differentiated endometrioid adenocarcinoma of the uterus: analysis of a series with emphasis on a novel SMARCA4-deficient dedifferentiated rhabdoid variant. *Ann Diagn Pathol* (2015) 19(04):198–202. doi: 10.1016/j.anndiagpath.2015.04.001

21. Agaimy A, Hartmann A, Antonescu CR, Chiosea SI, El-Mofty SK, Geddert H, et al. SMARCB1 (INI-1)-deficient sinonasal carcinoma: a series of 39 cases expanding the morphologic and clinicopathologic spectrum of a recently described entity. *Am J Surg Pathol* (2017) 41(04):458–71. doi: 10.1097/PAS0000000000000797

22. Cocchi S, Gamberi G, Magagnoli G, Maioli M, Righi A, Frisoni T, et al. CIC rearranged sarcomas: a single institution experience of the potential pitfalls in interpreting CIC FISH results. *Pathol Res Pract* (2022) 231:153773. doi: 10.1016/j.prp.2022.153773

23. Passeri T, Dahmani A, Masliah-Planchon J, Naguez A, Michou M, El Botty R, et al. Dramatic *In vivo* efficacy of the EZH2-inhibitor tazemetostat in PBRM1-mutated human chordoma xenograft. *Cancers (Basel)* (2022) 14(6):1486. doi: 10.3390/cancers14061486

24. Wilson BG, Wang X, Shen X, McKenna ES, Lemieux ME, Cho Y-J, et al. Epigenetic antagonism between polycomb and SWI/SNF complexes during oncogenic transformation. *Cancer Cell* (2010) 18(4):316–28. doi: 10.1016/j.ccr.2010.09.006

25. Walhart TA, Vacca B, Hepperla JA, Hamad SH, Petrongelli J, Wang Y, et al. SMARCB1 loss in poorly differentiated chordomas drives tumor progression. *Am J Pathol* (2023) 16:S0002–9440(23)00028-7. doi: 10.1016/j.ajpath.2022.12.012

26. Rekhi B, Michal M, Ergen FB, Roy P, Puls F, Haugland HK, et al. Poorly differentiated chordoma showing loss of SMARCB1/INI1: clinicopathological and radiological spectrum of nine cases, including uncommon features of a relatively under-recognized entity. *Ann Diagn Pathol* (2021) 55:151809. doi: 10.1016/j.anndiagpath.2021.151809

27. Yadav R, Sharma MC, Malgulwar PB, Pathak P, Sigamani E, Suri V, et al. Prognostic value of MIB-1, p53, epidermal growth factor receptor, and INI1 in childhood chordomas. *Neuro Oncol* (2014) 16(3):372–81. doi: 10.1093/neuonc/not228

28. Hung YP, Diaz-Perez JA, Cote GM, Wejde J, Schwab JH, Nardi V, et al. Dedifferentiated chordoma: clinicopathologic and molecular characteristics with integrative analysis. *Am J Surg Pathol* (2020) 44(9):1213–23. doi: 10.1097/PAS.0000000000001501

29. Bai J, Shi J, Li C, Wang S, Zhang T, Hua X, et al. Whole genome sequencing of skull-base chordoma reveals genomic alterations associated with recurrence and chordoma-specific survival. *Nat Commun* (2021) 12(1):757. doi: 10.1038/s41467-021-21026-5

30. Mobley BC, McKenney JK, Bangs CD, Callahan K, Yeom KW, Schneppenheim R, et al. Loss of SMARCB1/INI1 expression in poorly differentiated chordomas. *Acta Neuropathol* (2010) 120(6):745–53. doi: 10.1007/s00401-010-0767

31. Yeter HG, Kosemehmetoglu K, Soylemezoglu F. Poorly differentiated chordoma: review of 53 cases. *APMIS* (2019) 127(9):607–15. doi: 10.1111/apm.12978

32. Dermawan JK, Singer S, Tap WD, Nacev BA, Chi P, Wexler LH, et al. The genetic landscape of SMARCB1 alterations in SMARCB1-deficient spectrum of mesenchymal neoplasms. *Mod Pathol* (2022) 35(12):1900–9. doi: 10.1038/s41379-022-01148-x

33. Huang SC, Zhang L, Sung YS, Chen CL, Kao YC, Agaram NP, et al. Secondary EWSR1 gene abnormalities in SMARCB1-deficient tumors with 22q11-12 regional deletions: potential pitfalls in interpreting EWSR1 FISH results. *Genes Chromosomes Cancer* (2016) 55(10):767–76. doi: 10.1002/gcc.22376

34. Le Loarer F, Zhang L, Fletcher CD, Ribeiro A, Singer S, Italiano A, et al. Consistent SMARCB1 homozygous deletions in epithelioid sarcoma and in a subset of myoepithelial carcinomas can be reliably detected by FISH in archival material. *Genes Chromosomes Cancer* (2014) 53(6):475–86. doi: 10.1002/gcc.22159

35. Cha YJ, Hong CK, Kim DS, Lee SK, Park HJ, Kim SH. Poorly differentiated chordoma with loss of SMARCB1/INI1 expression in pediatric patients: a report of two cases and review of the literature. *Neuropathology* (2018) 38(1):47–53. doi: 10.1111/neup.12407

36. Li M, Shen Y, Xiong Y, Wang S, Li C, Bai J, et al. Loss of SMARCB1 promotes autophagy and facilitates tumour progression in chordoma by transcriptionally activating ATG5. *Cell Prolif* (2021) 54(12):e13136. doi: 10.1111/cpr.13136

frontiers | Frontiers in Oncology

TYPE Review
PUBLISHED 16 October 2023
DOI 10.3389/fonc.2023.1242453

OPEN ACCESS

EDITED BY
Sharon R. Pine,
University of Colorado Anschutz Medical Campus, United States

REVIEWED BY
Georgios A. Maragkos,
University of Virginia Hospital, United States
Jamie Van Gompel,
Mayo Clinic, United States

*CORRESPONDENCE
Alicia Tosoni
a.tosoni@isnb.it

RECEIVED 19 June 2023
ACCEPTED 25 September 2023
PUBLISHED 16 October 2023

CITATION
Tosoni A, Di Nunno V, Gatto L, Corradi G, Bartolini S, Ranieri L and Franceschi E (2023) Olfactory neuroblastoma: diagnosis, management, and current treatment options.
Front. Oncol. 13:1242453.
doi: 10.3389/fonc.2023.1242453

Olfactory neuroblastoma: diagnosis, management, and current treatment options

Alicia Tosoni[1*], Vincenzo Di Nunno[1], Lidia Gatto[2], Giacomo Corradi[3], Stefania Bartolini[1], Lucia Ranieri[1] and Enrico Franceschi[1]

[1]Nervous System Medical Oncology Department, IRCCS Istituto delle Scienze Neurologiche di Bologna, Bologna, Italy, [2]Department of Oncology, Azienda Unità Sanitaria Locale (AUSL) Bologna, Bologna, Italy, [3]Department of Medical and Surgical Sciences, University of Bologna, Bologna, Italy

Olfactory neuroblastoma (ONB) is a rare neoplasm originating from the olfactory neuroepithelium representing 3-6% of tumors of the sinonasal tract. ONB require multi-disciplinary care. Historically, the gold standard surgical procedure for ONB has been open craniofacial resection. In the last years, endoscopic endonasal approaches have been largely introduced with lower complication rates, shorter hospital stay, and similar clinical outcome. Radiotherapy plays an important role in the management of ONB, however there are not generally accepted recommendations for its application. Although there is agreement that multimodal therapy is needed, the optimal use of chemotherapy is still unknown. The rarity of the disease, makes difficult to draw definitive conclusions about the role of systemic treatment in induction and concomitant setting.

KEYWORDS

esthesioneuroblastoma, olfactory neuroblastoma, chemotherapy, radiotherapy, surgery

Epidemiology

Olfactory neuroblastoma (ONB), also called esthesioneuroblastoma, is a rare neoplasm originating from the olfactory neuroepithelium with neuroblastic differentiation, representing 3-6% of tumors of the sinonasal tract. Since its initial description in 1924, more than 1000 cases of ONB have been described worldwide (1).

It most often presents in the superior nasal cavity including the lamina cribrosa of the ethmoid bone and the superior nasal concha. It is a locally aggressive neoplasm that may involve local structures such as the skull base and orbits, and has a tendency to metastasize in 20-48% of cases. The typical sites of metastasis are cervical lymph nodes (10-33% of patients), bones, and lungs (2). ONB demonstrates an unimodal distribution with a more common presentation in adulthood around the age of 50-60 years (3).

In a retrospective surveillance, epidemiology, and end results (SEER) registry analysis 636 patients were identified in the period 1977-2016, the majority being male (59.7%), and

Caucasian with a median age of 51.4 years. The highest incidence of disease onset occurred in patients between the ages of 18-39 years (17.5%) and 40-59 years at diagnosis (46.1%) and the majority of patients were diagnosed with a primary tumor involving the nasal cavity (78.3%) (4). Interestingly, another analysis on SEER data indicates that patients of the lowest socioeconomic status (SES) were almost 85% more likely to present with advanced-stage cancer than patients in the highest SES. Notably the same study reported that patients with lower SES exhibited higher mortality and a dramatic 70% worse disease specific survival (DSS) compared with the highest SES (5).

Diagnosis

Nasal obstruction followed by epistaxis are typical early manifestations (6, 7). Hyposmia and anosmia can precede the diagnosis of ONB by several years (4). Other symptoms are related to the anatomic structures affected by the local invasion. Visual or ocular disorders could be related to the extension into the orbit. Intracranial invasion can produce headache, and manifestations of inappropriate antidiuretic hormone secretion (SIADH). Because of the aspecific nature of early symptoms, delayed diagnosis is frequent with an median time of 6–12 months between symptom onset and diagnosis (8). A "dumbbell-shaped" mass extending across the cribriform plate is one of the most characteristic radiological findings of this tumor (9). Computer tomography (CT) and/or magnetic resonance imaging (MRI) of skull base, paranasal sinuses, and neck are needed for qualitative evaluation and staging. CT is an helpful initial study, and can better describe the bone involvement, whereas MRI better evaluate the orbital and intracranial infiltration On MRI ONB is most typically hypointense on T1 and could appear as a contrast enhancing lesion. T2 shows and isointense or hyperintense mass (10). Full body CT and positron emission tomography scans are indicated in the diagnostic work up to determine the systemic extent of disease (11). (Figure 1) Some reports suggest that Gallium68-DOTATOC PET could be additionally used to assess the somatostatin receptor expression, demonstrating an utility in the diagnosis, staging, and treatment-response monitoring of patients with ONB (12).

Biopsy is mandatory for diagnosis, and it is generally performed after imaging. The great variety of different histotypes occurring primarily in the sinonasal tract together with the presence of limited biopsy material, pose significant diagnostic difficulties for the pathologist requiring specific knowledge and availability of immunohistochemical and molecular techniques. In recent years, the increasingly frequent participation in work groups has favored the development of a pathologists network with specific skills in sinonasal region area as well (13). For correct diagnostic identification, several biomarkers have been identified, including: synaptophysin, chromogranin, S-100, CD-56 and neuron-specific haemolysis (NSE). These biomarkers appear to be of fundamental importance for diagnosis, but have not yet been included among the prognostic factors. Proliferation marker studies using Ki-67 reveal a high proliferative index of 10–50%. Studies are increasingly focusing on the molecular profile, even for these extremely rare diseases (14).

A disease specific grading system for ONB has been described by Hyams in 1988, in which the disease is stratified into four grades ranging from most differentiated (grade I) to least differentiated (grade IV) on the basis of mitotic activity, nuclear polymorphism, amount of fibrillary matrix, rosette formation, and amount of necrosis (Table 1). Recent evidence suggests a correlation between the Hyams grading and clinical outcome, with high-grade (grade III/IV) tumors associated with worse survival outcomes as compared with low-grade (grade I/II) tumors (5-year survival rate of 80% and 54% and a 10-year survival rate of 67% and 36% for low and high grade, respectively) (15). Similarly, the meta-analysis conducted by Dulguerov et al. confirmed that Hyams grading was significant associated with survival, showing a 5-years survival rate of 56% and 25% for low grade and high grade respectively (16). On the other hand, it is important to note that Hyams system is a subjective scale, leading to variable grading between pathologists.

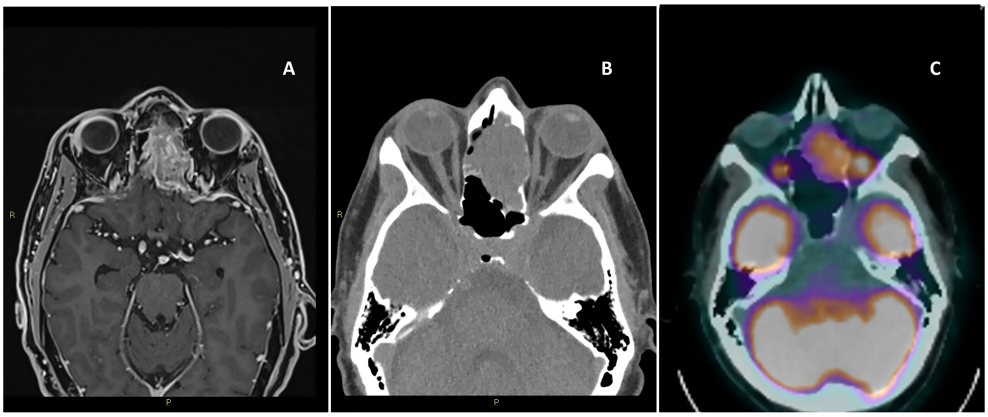

FIGURE 1
Magnetic resonance imaging of the brain T1 with contrast, axial view **(A)**, computer tomography of the brain axial view without contrast **(B)**, positron emission tomography axial view **(C)**.

10.3389/fonc.2023.1242453

TABLE 1 Hyams grade for olfactory neuroblastoma.

	Grade I	Grade II	Grade III	Grade IV
Architecture	Lobular	Lobular	Variable	Variable
Fibrillary matrix	Prominent	Present	Minimal	Absent
Mitosis	Absent	Present	Prominent	Marked
Necrosis	Absent	Absent	May present	Common
Nuclear pleomorphism	Absent	Moderate	Prominent	Marked
Rosettes	Homer Wright	Homer Wright	Flexner-Wintersteiner	Flexner-Wintersteiner

Furthermore, biopsy may also lead to sampling error when the entire tumor is not examined, as different parts of the tumor may contain different Hyams grades.

However, based on published data, Hyams grading may represent an important factor for decision making in therapeutic strategies such as induction chemotherapy and adjuvant radiotherapy (RT), and may also be considered in surveillance protocols.

Staging

Different staging systems have been proposed. The most commonly applied was proposed by Kadish and colleagues in 1976. This staging system classifies three categories: stage A, tumor restricted to the nasal cavity; stage B, tumor extending to the paranasal sinuses; stage C, tumor extending beyond the paranasal cavities. The Kadish classification was later modified by Morita et al. (17) designating the class D that includes patients with cervical lymph node metastases (18). A significant differences in clinical outcome has been showed between the four groups of the modified Kadish classification, in particular the overall survival (OS) and DSS rates at 10 years to be 83.4% and 90%, respectively, for patients with stage A disease; 49% and 68.3% for patients with stage B disease; 38.6% and 66.7% for patients with stage C disease; and 13.3% and 35.6% for patients with stage D disease (19).

Other proposed staging systems include the tumor-nodal-metastasis (TNM) system by the American Joint Committee on Cancer, and a modified TNM version by Dulguerov (20).

The Dulguerov system, uses the TNM classification including the imaging data, it separates patients with or without sphenoid sinus disease, as well as differentiates between those intracranial but extradural tumors from those with true brain involvement. (Table 2).

TABLE 2 Staging systems of olfactory neuroblastoma.

Kadish staging
A Confined to nasal cavity
B Involves nasal cavity and paranasal sinuses
C Extends beyond the nasal cavity and paranasal sinuses
Morita modification
A Confined to nasal cavity
B Involves nasal cavity and paranasal sinuses
C Extends beyond the nasal cavity and paranasal sinuses
D Regional or distant metastasis
Dulguerov Modified TNM Staging
Primary tumor
T1 Nasal cavity/paranasal sinuses (not sphenoid or superior most ethmoid)
T2 Includes sphenoid with extension to/erosion of cribriform plate
T3 Extends into orbit or anterior cranial fossa without dural invasion
T4 Tumor involving brain
Lymph nodes
N0 No cervical limph node metastasis
N1 Any cervical lymph node metastasis
Distant metastasis
M0 No metastasis
M1 Distant metastasis

Therapy

The complex anatomy of this region with proximity to vital structures such as the orbit, skull base, and brain, makes complete surgical resection with sufficient margins not often feasible.

This tumor location require multidisciplinary care that includes medical oncologists, neurosurgeons, head and neck surgeons, pathologists and radiation oncologists. Local treatment with surgery is frequently recommended for primary therapy. While a combination of surgery and postoperative RT is indicated for the management of more local advanced resectable cancers. Locally advanced disease often requires a multidisciplinary approach with surgery, radiation, and systemic therapy serving as key components of treatment (21).

Surgery

Surgery remains a fundamental step in the therapeutic process. The extent of resection (R0 and R1) has been shown to be an independent factor for overall survival and event free survival (22).

Historically, the gold standard surgical procedure for ONB has been open craniofacial resection or transfacial surgery. In the last two decades, endoscopic endonasal approaches have been introduced with lower complication rates and shorter hospital stay (23). In 2019, the International Consensus Statement on Endoscopic Skull Base Surgery suggested that Kadish stage A and B tumors should be treated endoscopically. Kadish C tumors should be performed endoscopically only if negative margins can be obtained, while Kadish C tumors involving the orbit, spread lateral to the orbital axis, hard/soft palate, or midface should be treated with an open surgery (24).

Multiple factors may be considered in choosing the optimal surgical approach, including tumor size and location, patient comorbidities, and experience of the surgical team. Notably, when selecting the optimal surgical approach, the surgeon must consider the approach that will allow for a negative margin resection and adequate reconstruction.

In patient with intracranial involvement, when anatomic barriers preclude the surgeon from gross total resection, a combined intracranial and extracranial approach could be required, and in these patients an endoscopic surgical technique may be combined with a transcranial neurosurgical approach. However, the continue evolution of endoscopic technique, that allows the visualization of the suprasellar region in a similar fashion to that of bilateral subfrontal approach, makes this combined approach less used (2).

It is difficult to compare the clinical outcome between endoscopic and open surgical approach, due to the rarity of this tumor that limits evaluation of large-scale studies. Several reviews and meta-analyses comparing outcomes between endoscopic and open surgery have shown at least equivalent survival data. A systematic review and pooled-data analysis of 226 patients demonstrated that there was no difference in survival outcomes between endoscopic and traditional open surgery for T1 and T2 sinonasal malignancies (24).

Schwart et al. (25) compared the results of endoscopic surgery (ES) with transcranial surgery (TS) for ONB over two different time periods (before 2012 and 2012-2017) to assess the evolution of results over time. In particular, before 2012, the meta-analysis showed that ES was already advantageous compared to the other surgical approaches: gross total resection (GTR) 98.1% versus 85.2% and progression free survival (PFS) 8% versus 22.1%. Major complications included meningitis, CSF leaks and infections. In particular CSF leak is one of the more important complications, being reported in 6% of patients after TS, 7.2% after ES, and 18% in combined cranionasal approach (26). However, the use of repair strategies, such as the pedicled nasoseptal flap procedure, appear to be effective, being post operative CSF leak repair failure reported in only 5.3% of patients (27).

In subsequent years, TC approach continues to be accompanied by a relatively high rate of complications of 52.9%, and purely ES continue to proliferate, demonstrating high 5-year overall survival OS (82–97%).

Studies of ES versus TS approaches for pooled groups of sinonasal malignancies, including ONB, have shown comparable GTR rates between the two (23, 24).

Spielman DB et al., reported on 339 ONB patients undergoing ES for different stages and grades of disease. Negative margins have been achieved in 86.9% of cases with an overall recurrence rate of 10.3% and 5-year survival of 91.1% (28). On the other hand, Patel et al. reported on 151 patients from 17 institutions who underwent TS, of these 77% of tumors with Kadish stage C. Overall 60% had received treatment before TS, radiation therapy or chemotherapy. Postoperative adjuvant RT and adjuvant chemotherapy were used in 60 patients. Treatment complications occurred in about 32% of patients with an OS of 78% and a recurrence free survival of 64% at 5 years (29).

The current practice appears to favor ES or combined approaches for early-stage, endoscopically accessible disease. For later-stage, more invasive disease, some can be resected successfully endoscopically, but TS could still be considered to achieve a maximal safe resection. Surgical management of the cervical lymph nodes for patients with ONB remains matter of debate. The incidence of cervical metastases at diagnosis is 5-8%, but the incidence of a later development increase to 20-25%. Despite this relative high incidence, surgical management of the neck is reserved for patients presenting with clinical or radiological evidence of neck disease (30).

Radiotherapy

RT plays an important role in the management of ONB, however there are not generally accepted recommendations for its application. Different radiation approaches have been evaluated over the years, ranging from elective RT to treat Kadish stage A and B to pre/postoperative RT plus concomitant chemotherapy (31). Concomitantly, there has been an improvement in RT techniques over the years, reducing treatment-related toxicity and allowing the preservation of nearby vital structures. In patients with early stage disease (Kadish A and B) some studies (17, 32, 33) reported no survival differences between primary RT and combination treatment with surgery plus pre or post operative RT. However, in general an increase in tumor control has been reported when surgery is combined with RT, even if no consensus exist for the timing of the RT that can be used pre or postoperatively (32, 33). With regard to postoperative RT (PORT), a retrospective study based on SEER database confirmed no impact in OS in Kadish stage A and B, whereas a significant better OS was demonstrated in patients with more advanced stages (C and D), with an OS at 5 and 10 years of 70.7% and 53.4% with PORT versus 42.6% and 29.5% without PORT (34). It is generally accepted that higher stage lesions require the combination of surgery and RT (17, 31, 32) even if some studies (35, 36) suggest a combined approach for all stages. Considering tumor grade, low grade tumors can be treated with surgery alone if there are free tumor resection margins. Whereas RT is recommended for high grade tumors and low-grade tumors

borderline resected, or residual or recurrent tumors (17, 31). In general, preoperative dose of 45 Gy and postoperatively dose of 50–60 Gy are indicated. For definitive RT, doses of 60–70 Gy should be recommended (31). Some retrospective studies analyzing the role of elective neck irradiation in patients with clinical N0 reported a significant reduced risk of cervical nodal regional recurrence, but this did not translate to a survival benefit.[33,34] The safety of intensity-modulated RT (IMRT) in the management of ONB has been evaluated retrospectively over 3 years showing the absence of acute high-grade toxicity and infrequent cases of late toxicity, including: dysosmia (3.8%), hearing loss (3.8%), brain damage (1.9%), and temporal lobe necrosis (1.9%). No late ocular toxicity was observed (37). New radiation techniques such as particle-beam radiation therapy (PBRT), typically using accelerated proton or carbon-ion, has the advantage of a dose-focusing Bragg peak, which allows the radiation to penetrate in to the depth of the target and then terminate, sparing normal tissues beyond the target from unnecessary radiation (38, 39). Furthermore, carbon-ion beam is characterized by a higher linear energy transfer and a relative biological effectiveness which enables more effective cell killing through inducing more DNA double-bond damage. Because of their rarity, no standard of care in PBRT has been established for ONB. Preliminary data on retrospective series reported that this type of approach is well tolerated and that it is acceptable in terms of OS and PFS, in the absence of acute or late toxicities greater than or equal to grade 3 (40).

Induction chemotherapy

The main goals of induction chemotherapy (IC) could be to allow in responding patients an organ preservation of critical structures like eye or brain, and to reduce the risk of distant metastasis (41). Furthermore an important advantage associated to IC is its potential role in predicting clinical outcome (42).

However, whether these goals are achieved has not been well established due to the rarity of the disease, heterogeneity of considered series, and lack of prospective studies. Data examining the utility of IC are limited to small series, reporting on Kadish C patients treated with various schemes and demonstrating a response rate (RR) of 25-100% (Table 3). The outcome reported by these series, suggests that Kadish C patients treated with a multimodality strategy including IC followed by surgery and RT could achieve similar survival of patients presenting with locally advance disease (OS at five years of 72%) (39, 40).

Concomitant chemoradiotherapy

Local recurrence remains the major issue in the management of ONB (49). With the aim to increase local control some studies and referral centers advocate the use of concurrent chemoradiation (CT-RT) with cisplatin after surgery for patients at high risk of local recurrence (30). In a recent retrospective study (50), on 931 ONB patients who received CT-RT, a greater benefit has been reported (HR 0.22, P <.01) in comparison to patients treated with RT alone. Similarly, Sun et al. (51) reported results on 138 patients with non-metastatic ONB demonstrating that surgery followed by CT-RT achieved the best prognosis compared to patients treated with surgery alone and surgery plus RT. Xiong et al. (52) compared the prognosis of patients with different treatment modalities demonstrating that surgery followed by CT-RT yielded the best survival results. On the contrary, in a retrospective study in which 797 ONB patients were considered, it was found by multivariate analysis that the use of chemotherapy in addition to RT or surgery was associated with a reduced DSS (HR 2.78) and OS (HR 2.17) (53).

TABLE 3 Neoadjuvant treatment.

Author	Number of pts	Regimen	RR
Patil (41)	12	DDP+VP-16	66.7%
Fitzek (43)	9	DDP+VP-16	60%
Zappia (44)	2	DDP+VP-16	100%
Chao (45)	8	DDP+VP-16 or VCR+EX+doxo	25%
Wade (46)	8	VCR+EX	62%
Kim (47)	11	Ifo+VP-16+DDP	82%
Bartel (48)	4	Ifo+VP-16+DDP	75%
Modesto (49)	23	HDCT or DDP+VP-16 or CBCDA+5FU	74%

DDP cisplatin, VP-16 vepesid, VCR vincristin, EX endoxan, Doxo doxorubicin, ifo ifosfamide, CBCDA carboplatin, 5FU 5 fluorouracil, HDCT, high dose chemotherapy,

Adjuvant chemotherapy

The efficacy of adjuvant chemotherapy to increase OS has been explored in some retrospective series. Miller et al. (50) compared survival among patients treated with surgery followed by RT alone to patients who underwent the same treatment followed by adjuvant chemotherapy, showing no increase in OS or recurrence free survival with the addition of adjuvant chemotherapy. In the Mayo Clinic retrospective review (54) adjuvant chemotherapy for patients with high grade, Stage C ONB was of benefit following complete resection leading to an increase in median time to relapse (35 and 10.5 months), and in OS (83 and 78 months respectively).

Treatment of advance disease

Metastatic disease could develop in 12% of ONB patients with a median time of 15 months (55). Clinical reports suggest that ONB can be considered a chemosensitive tumor (42). However, due to the rarity of the disease, no standard chemotherapy regimen exists. One of the earliest studies on chemotherapy in the palliative setting has been published by Mayo Clinic (56) in which 10 patients with advanced disease were observed retrospectively after first-line treatment with platinum-based chemotherapy. The study reported

TABLE 4 Case reports on target therapies in recurrent olfactory neuroblastoma.

Molecular target	Treatment	Outcome
PTCH1 splice site 395-1G>A (59)	Vismodegib	PFS 3 months
	Sunitinib	SD for 24 months
PIK3R2 G87fs*14 (59)	Everolimus	SD for 12 months
CTNNB1 T41I, *PTEN* splice site 210-2A>C, *ARID1A* Q1424*, *KDM5C* E375* (59)	Everolimus	PFS 3 months
	Pazopanib/ docetaxel	SD for 24 months
TP53 Loss, *KIT* amplification, *AXL-ARHGEF* fusion (59)	Sunitinib	PFS > 3 months
IHC+ *PDGFR-b* in stromal and endothelial cells (63)	Sunitinib	SD for 15 months
EGFR Mutation p.Arg521Lys exon13 (64) *KDR* Mutations p.Gln472His (exon11) and p.Val297lle (exon7) *FGFR2* Mutation p.Met186Thr exon5 *RET* Mutation p.Met1009Thr exon 18.	Cetuximab plus sunitinib	CR after 1 months
Not identified (65)	Everolimus plus cisplatin	SD > 24 months
Not identified (66)	Bevacizumab	SD for 22 months
Fumarate Hydratase Mutation Exon 10 K477dup (67)	Pazopanib	PR > 48 months

IHC+ Immunohistochemistry positivity, PFS progression free survival, SD stable disease, CR complete response, PR partial response. fs* frameshift mutation.

chemotherapy response only in two of the four patients with high-grade tumors. OS was 44.5 months and 26.5 months in patients with low and high-grade tumors respectively. The study concluded that Hyams grade was an important predictor of treatment response, but was also related to a worse outcome. Marinelli et al. (55) conducted a systematic review and meta-analysis on 118 patients metastatic ONB treated in 48 studies demonstrating that the combination of chemotherapy with surgery and/or RT exhibited the best overall survival when compared to a single treatment modality. Platinum plus etoposide chemotherapy seems to be the most used regimen, even if not provide a survival benefit when compared with all other regimens.

Treatment of recurrent disease

Recurrence has been showed in 30-60% of patients successfully (1-5 Garret) treated for the primary tumor. Recurrence tends to appear commonly after 5 years or more after initial treatment. Recurrence seems to develop before in high grade compared to low grade tumors (3.75 vs 5.7 years) (57). Patients more commonly developed a local recurrence (sinonasal 22.2%, intracranial 31.1%, cervical lymph nodes 33.3%), while metastatic recurrence has been demonstrated in only 13.3% of patients (57). No standard treatment exists for recurrent disease. Multidisciplinary discussion is needed to consider single or multimodality treatment that could comprise salvage surgery, targeted radiotherapy and/or chemotherapy based on recurrence location and previous treatments. Ni et al. (57) recent published on 64 recurrent ONB patients treated at Mayo Clinic, reporting the choice of salvage surgery in 69% (neck dissection in 51%), radiotherapy in 56%, gamma knife surgery in 20%, and chemotherapy in 26% of recurrent patients (Ni). In terms of chemotherapy, 70% of patients were treated with platinum based chemotherapy, 40% with taxanes, 50% with topoisomerase inhibitors and 30% with alkylating agents. The role of stereotactic radiosurgery to treat focal intracranial recurrence of ONB has been also evaluated in 27 recurrent patients unfit for open or endoscopic surgery, reporting a local control in 89% of tumors after a median of 36 months, without treatment complications (58). Salvage treatment seems to be effective with 63% of patients alive 5 years after recurrence. However subsequent recurrence has been reported in 20% of patients, frequently requiring additional therapy (57).

Target treatments

Identifying potentially targetable genomic alterations in rare tumors is particular intriguing because no standard of care exists, and treatment is often extrapolated. The development and improvement of new sequencing technology, next-generation sequencing (NGS) has been applied and increasingly used to identify novel and rare cancer mutations, providing a molecular rationale for appropriate targeted therapy (Table 4). A comprehensive genomic profiling (59) was performed on 41 consecutive clinical cases of ONB using NGS to identify genomic alterations that could identify potential targeted therapies. 68% of ONB harbored genetic alterations, and approximately half featured at least one genetic alteration of therapeutic relevance. The most commonly altered gene was *TP53* (17%), with genetic alterations in *PIK3CA*, *NF1*, *CDKN2A*, and *CDKN2C* occurring in 7% of samples. In this interesting analysis data on individualized target treatment have been reported: one case of disease stabilization to everolimus for a tumor with a PIK3R2 mutation; two responses to sunitinib; and one stable disease in response to pazopanib and docetaxel. Topcagic et al. (60) explored a wide range of potentially targetable biomarkers in ONB samples using multiple molecular profiling platforms including NGS. The results showed mutations in *TP53*, *CTNNB1*, *EGFR*, *APC*, *cKIT*, *cMET*, *PDGFRA*, *DCH1*, *FH* and *SMAD4* genes. Multiple genes within the Wnt/β-catenin signaling pathway including *CTNNB1*, *APC* and *CDH1* exhibited mutations within this cohort. Multiple alterations in markers such as *ERCC1, TOPO1, TUBB3* and *MRP1*, which are known to reflect sensitivity to cisplatin, irinotecan, vincristine and combination therapy, have been identified. In one study, ONB was found to have in 28% of tumors, an amplifications of the targetable receptor tyrosine kinase *FGFR3* which could be a possible therapeutic target (61). Interestingly, Gallia et al. (62) showed a high frequency of deletions in the dystrophin (*DMD*) gene (86% of tumors) This high prevalence implicates an unexpected functional role for genes causing hereditary muscular dystrophies in ONB. The authors point

to previous studies, which demonstrated the tumour-suppressive role of *DMD*, highlighting the potential utility of this specific aberration as a therapeutic target. (21) Recent case reports have shown a prolonged disease stabilization after treatment with sunitinib (63), and a partial response after treatment with the combination of sunitinb and cetuximab in one patient whose tumor harboring gene mutations in the genes encoding *EGFR, FGFR2, KDR*, and *RET* (64). Case studies have reported disease stabilization in response to treatment with everolimus (65), and imatinib (61). Dunbar et al. reported on a metastatic ONB patient achieving a stable disease for 22 months with the antiangiogenic agent bevacizumab (66). A single case of a metastatic ONB, showing at the NGS a pathogenic fumarate hydratase mutation, achieved a prolonged partial response with pazopanib for over 4 years (67). Lastly, conflicting data have been reported on PD-L1 expression in ONB, with 0-40% of PD-L1 expression in tumor cells (60, 68), suggesting that there should be further investigation into the role of immunotherapy in ONB. Unfortunately, to systematically study the efficacy of targeting these individual pathways in rare cancers like ONB would be nearly impossible. Hence, novel clinical trial designs, such as basket trials, will be required to assess these approaches. As we know unequivocally that surgical resection currently comprises the cornerstone of ONB management, a "Window of Opportunity" trial to apply these agents prior to surgery could offer a possible avenue to test this strategy.

The role of multimodality therapy

Although the majority of patients initially present with locally advance disease, the overall prognosis is high compared to other sinonasal tumors, with a 5-year overall and progression free survival estimated at 63% and 57% respectively. Nodal involvement at diagnosis, present in 21% of ONB patients, remains the major prognostic factor (49). Surgery alone has been considered as an adequate treatment only for small, low-grade tumors confined to the ethmoids when negative surgical margins can be obtain. For more advanced disease, or high grade disease a consensus has been obtained in the use of multimodality therapy including a complete surgical resection in combination with RT and/or chemotherapy (6, 36). IC could be considered for stage C tumors as a consequence of ONB chemosensivity to maximize the chance of optimal surgical resection or definitive RT, especially for high grade tumors who are known to have worse prognosis and higher chemosensivity. After surgical resection adjuvant RT must be considered in case of high grade and/or advanced stage tumors, or in presence of no clear or borderline margins. According to data from other head and neck tumors, cisplatin concurrent chemotherapy could increase radiation efficacy and decrease disease dissemination particularly in case of positive margins and nodal extension at diagnosis. RT alone or CT-RT is a possible approach for patients with low grade unresectable tumors, which could lead in case of response to a subsequent surgical approach.

Conclusions

Clinical management of these rare disease has been improved in recent years. The progressive introduction of endoscopic surgery approaches has reduced patients perioperative morbidity, and seems to give, in high volume specialized centers, similar clinical outcome in comparison to open craniofacial resection. Another challenge in endoscopic approach in patients with intracranial disease has been the improvement in skull base reconstruction techniques, that allows combined surgical approaches also in locally advance disease. Evident improvements have been demonstrated in RT techniques. The introduction of particle-beam radiation therapy is ideally suited for dose escalation in complex anatomical sites, reducing toxicity of nearby critical tissues.

On the other hand, even if an agreement that multimodal therapy is needed (69), the optimal use of chemotherapy is still unknown. Clearly, the heterogeneity and rarity of the disease, makes difficult to draw definitive conclusions about the role of systemic treatment in induction setting, and its possible role in organ preservation. Likewise limited data are available about the use of concomitant CRT. Advances in molecular profiling could lead to the identification of new target therapies with new future therapeutic scenario.

Author contributions

AT, GC wrote sections of the manuscript. All authors contributed to manuscript revision, read, and approved the submitted version. The publication of this article was supported by the "Ricerca Corrente" funding from the Italian Ministry of Health.

Conflict of interest

The authors declare that the research was conducted in the absence of any commercial or financial relationships that could be construed as a potential conflict of interest.

Publisher's note

References

1. Arnold PM, Habib A, Newell K, Anderson KK. Esthesioneuroblastoma metastatic to the thoracic intradural and extradural space. *Spine J Off J North Am Spine Soc* (2009) 9(5):e1–5. doi: 10.1016/j.spinee.2008.08.010

2. Fiani B, Quadri SA, Cathel A, Farooqui M, Ramachandran A, Siddiqi I, et al. Esthesioneuroblastoma: A comprehensive review of diagnosis, management, and current treatment options. *World Neurosurg* (2019) 126:194–211. doi: 10.1016/j.wneu.2019.03.014

3. Yin Z, Wang Y, Wu Y, Zhang X, Wang F, Wang P, et al. Age distribution and age-related outcomes of olfactory neuroblastoma: a population-based analysis. *Cancer Manag Res* (2018) 10:1359–64. doi: 10.2147/CMAR.S151945

4. Brisson RJ, Quinn TJ, Deraniyagala RL. The role of chemotherapy in the management of olfactory neuroblastoma: A 40-year surveillance, epidemiology, and end results registry study. *Health Sci Rep* (2021) 4(2):e257. doi: 10.1002/hsr2.257

5. Sharma RK, Irace AL, Overdevest JB, Turner JH, Patel ZM, Gudis DA. Association of race, ethnicity, and socioeconomic status with esthesioneuroblastoma presentation, treatment, and survival. *OTO Open* (2022) 6(1):2473974X221075210. doi: 10.1177/2473974X221075210

6. Dulguerov P, Calcaterra T. Esthesioneuroblastoma: the UCLA experience 1970-1990. *Laryngoscope* (1992) 102(8):843–9. doi: 10.1288/00005537-199208000-00001

7. Zafereo ME, Fakhri S, Prayson R, Batra PS, Lee J, Lanza DC, et al. Esthesioneuroblastoma: 25-year experience at a single institution. *Otolaryngol–Head Neck Surg Off J Am Acad Otolaryngol-Head Neck Surg* (2008) 138(4):452–8. doi: 10.1016/j.otohns.2007.12.038

8. Abdelmeguid AS. Olfactory neuroblastoma. *Curr Oncol Rep* (2018) 20(1):7. doi: 10.1007/s11912-018-0661-6

9. Thompson LDR. Olfactory neuroblastoma. *Head Neck Pathol* (2009) 3(3):252–9. doi: 10.1007/s12105-009-0125-2

10. Palejwala SK, Sharma S, Le CH, Chang E, Erman AB, Lemole GM. Complex skull base reconstructions in Kadish D esthesioneuroblastoma: case report. *J Neurol Surg Rep* (2017) 78(2):e86–92. doi: 10.1055/s-0037-1601877

11. Bradley PJ, Jones NS, Robertson I. Diagnosis and management of esthesioneuroblastoma. *Curr Opin Otolaryngol Head Neck Surg* (2003) 11(2):112–8. doi: 10.1097/00020840-200304000-00009

12. Roytman M, Tassler AB, Kacker A, Schwartz TH, Dobri GA, Strauss SB, et al. [68Ga]-DOTATATE PET/CT and PET/MRI in the diagnosis and management of esthesioneuroblastoma: illustrative cases. *J Neurosurg Case Lessons* (2021) 1(2):1–7. doi: 10.3171/CASE2058

13. Hellquist H, Agaimy A, Stenman G, Franchi A, Nadal A, Skalova A, et al. Development of head and neck pathology in Europe. *Virchows Arch Int J Pathol* (2022) 480(5):951–65. doi: 10.1007/s00428-022-03275-x

14. Capper D, Engel NW, Stichel D, Lechner M, Glöss S, Schmid S, et al. DNA methylation-based reclassification of olfactory neuroblastoma. *Acta Neuropathol (Berl)* (2018) 136(2):255–71. doi: 10.1007/s00401-018-1854-7

15. Goshtasbi K, Abiri A, Abouzari M, Sahyouni R, Wang BY, Tajudeen BA, et al. Hyams grading as a predictor of metastasis and overall survival in esthesioneuroblastoma: a meta-analysis. *Int Forum Allergy Rhinol* (2019) 9(9):1054–62. doi: 10.1002/alr.22373

16. Dulguerov P, Allal AS, Calcaterra TC. Esthesioneuroblastoma: a meta-analysis and review. *Lancet Oncol* (2001) 2(11):683–90. doi: 10.1016/S1470-2045(01)00558-7

17. Morita A, Ebersold MJ, Olsen KD, Foote RL, Lewis JE, Quast LM. Esthesioneuroblastoma: prognosis and management. *Neurosurgery* (1993) 32(5):706–14. doi: 10.1227/00006123-199305000-00002

18. Kadish S, Goodman M, Wang CC. Olfactory neuroblastoma. A clinical analysis of 17 cases. *Cancer* (1976) 37(3):1571–6.

19. Jethanamest D, Morris LG, Sikora AG, Kutler DI. Esthesioneuroblastoma: a population-based analysis of survival and prognostic factors. *Arch Otolaryngol Head Neck Surg* (2007) 133(3):276–80. doi: 10.1001/archotol.133.3.276

20. Joshi RR, Husain Q, Roman BR, Cracchiolo J, Yu Y, Tsai J, et al. Comparing Kadish, TNM, and the modified Dulguerov staging systems for esthesioneuroblastoma. *J Surg Oncol* (2019) 119(1):130–42. doi: 10.1002/jso.25293

21. Mody MD, Saba NF. Multimodal therapy for sinonasal Malignancies: updates and review of current treatment. *Curr Treat Options Oncol* (2020) 21(1):4. doi: 10.1007/s11864-019-0696-4

22. Ozsahin M, Gruber G, Olszyk O, Karakoyun-Celik O, Pehlivan B, Azria D, et al. Outcome and prognostic factors in olfactory neuroblastoma: a rare cancer network study. *Int J Radiat Oncol Biol Phys* (2010) 78(4):992–7. doi: 10.1016/j.ijrobp.2009.09.019

23. Hagemann J, Roesner J, Helling S, Jacobi C, Doescher J, Engelbarts M, et al. Long-term outcome for open and endoscopically resected sinonasal tumors. *Otolaryngol Head Neck Surg* (2019) 160(5):862–9. doi: 10.1177/0194599818815881

24. Higgins TS, Thorp B, Rawlings BA, Han JK. Outcome results of endoscopic vs craniofacial resection of sinonasal Malignancies: a systematic review and pooled-data analysis. *Int Forum Allergy Rhinol* (2011) 1(4):255–61. doi: 10.1002/alr.20051

25. Schwartz TH, Morgenstern PF, Anand VK. Lessons learned in the evolution of endoscopic skull base surgery: JNSPG 75th Anniversary Invited Review Article. *J Neurosurg* (2019) 130(2):337–46. doi: 10.3171/2018.10.JNS182154

26. Komotar RJ, Starke RM, Raper DMS, Anand VK, Schwartz TH. Endoscopic endonasal compared with anterior craniofacial and combined cranionasal resection of esthesioneuroblastomas. *World Neurosurg* (2013) 80(1–2):148–59. doi: 10.1016/j.wneu.2012.12.003

27. Shahangian A, Soler ZM, Baker A, Wise SK, Rereddy SK, Patel ZM, et al. Successful repair of intraoperative cerebrospinal fluid leaks improves outcomes in endoscopic skull base surgery. *Int Forum Allergy Rhinol* (2017) 7(1):80–6. doi: 10.1002/alr.21845

28. Spielman DB, Liebowitz A, Grewal M, Safi C, Overdevest JB, Iloreta AM, et al. Exclusively endoscopic surgical resection of esthesioneuroblastoma: A systematic review. *World J Otorhinolaryngol - Head Neck Surg* (2022) 8(1):66–72. doi: 10.1002/wjo2.10

29. Patel SG, Singh B, Stambuk HE, Carlson D, Bridger PG, Cantu G, et al. Craniofacial surgery for esthesioneuroblastoma: report of an international collaborative study. *J Neurol Surg Part B Skull Base* (2012) 73(3):208–20. doi: 10.1055/s-0032-1311754

30. Ow TJ, Bell D, Kupferman ME, Demonte F, Hanna EY. Esthesioneuroblastoma. *Neurosurg Clin N Am* (2013) 24(1):51–65. doi: 10.1016/j.nec.2012.08.005

31. Eich HT, Staar S, Micke O, Eich PD, Stützer H, Müller R. Radiotherapy of esthesioneuroblastoma. *Int J Radiat Oncol Biol Phys* (2001) 49(1):155–60. doi: 10.1016/S0360-3016(00)00811-7

32. Yin ZZ, Gao L, Luo JW, Yi JL, Huang XD, Qu Y, et al. Long-term outcomes of patients with esthesioneuroblastomas: A cohort from a single institution. *Oral Oncol* (2016) 53:48–53. doi: 10.1016/j.oraloncology.2015.11.021

33. Elkon D, Hightower SI, Lim ML, Cantrell RW, Constable WC. Esthesioneuroblastoma. *Cancer* (1979) 44(3):1087–94. doi: 10.1002/1097-0142(197909)44:3<1087::AID-CNCR2820440343>3.0.CO;2-A

34. Duo GS, Feng JL, Zhang ZY, Wang LJ. Survival impact of postoperative radiotherapy in patients with olfactory neuroblastoma: 513 cases from the SEER database. *Cancer Radiother J Soc Francaise Radiother Oncol* (2022) 26(5):663–9. doi: 10.1016/j.canrad.2021.12.006

35. Urdaneta N, Fischer JJ, Knowlton A. Olfactory neuroblastoma. Observations on seven patients treated with radiation therapy and review of the literature. *Am J Clin Oncol* (1988) 11(6):672–8.

36. Broich G, Pagliari A, Ottaviani F. Esthesioneuroblastoma: a general review of the cases published since the discovery of the tumour in 1924. *Anticancer Res* (1997) 17(4A):2683–706.

37. Bao C, Hu W, Hu J, Dong Y, Lu JJ, Kong L. Intensity-modulated radiation therapy for esthesioneuroblastoma: 10-year experience of a single institute. *Front Oncol* (2020) 10:1158. doi: 10.3389/fonc.2020.01158

38. Hu W, Hu J, Huang Q, Gao J, Yang J, Qiu X, et al. Particle beam radiation therapy for sinonasal Malignancies: Single institutional experience at the Shanghai Proton and Heavy Ion Center. *Cancer Med* (2020) 9(21):7914–24. doi: 10.1002/cam4.3393

39. McDonald MW, Liu Y, Moore MG, Johnstone PAS. Acute toxicity in comprehensive head and neck radiation for nasopharynx and paranasal sinus cancers: cohort comparison of 3D conformal proton therapy and intensity modulated radiation therapy. *Radiat Oncol Lond Engl* (2016) 11:32. doi: 10.1186/s13014-016-0600-3

40. Hu W, Hu J, Gao J, Yang J, Qiu X, Kong L, et al. Intensity-modulated particle beam radiation therapy in the management of olfactory neuroblastoma. *Ann Transl Med* (2020) 8(15):926–6. doi: 10.21037/atm-19-4790

41. Patil VM, Joshi A, Noronha V, Sharma V, Zanwar S, Dhumal S, et al. Neoadjuvant chemotherapy in locally advanced and borderline resectable nonsquamous sinonasal tumors (Esthesioneuroblastoma and sinonasal tumor with neuroendocrine differentiation). *Int J Surg Oncol* (2016) 2016:6923730. doi: 10.1155/2016/6923730

42. Sheehan JM, Sheehan JP, Jane JA, Polin RS. Chemotherapy for esthesioneuroblastomas. *Neurosurg Clin N Am* (2000) 11(4):693–701. doi: 10.1016/S1042-3680(18)30094-9

43. Fitzek MM, Thornton AF, Varvares M, Ancukiewicz M, Mcintyre J, Adams J, et al. Neuroendocrine tumors of the sinonasal tract. Results of a prospective study incorporating chemotherapy, surgery, and combined proton-photon radiotherapy. *Cancer* (2002) 94(10):2623–34. doi: 10.1002/cncr.10537

44. Zappia JJ, Carroll WR, Wolf GT, Thornton AF, Ho L, Krause CJ. Olfactory neuroblastoma: the results of modern treatment approaches at the University of Michigan. *Head Neck* (1993) 15(3):190–6. doi: 10.1002/hed.2880150303

45. Chao KS, Kaplan C, Simpson JR, Haughey B, Spector GJ, Sessions DG, et al. Esthesioneuroblastoma: the impact of treatment modality. *Head Neck* (2001) 23(9):749–57. doi: 10.1002/hed.1107

46. Wade PM, Smith RE, Johns ME. Response of esthesioneuroblastoma to chemotherapy. Report of five cases and review of the literature. *Cancer* (1984) 53 (5):1036–41.

47. Kim DW, Jo YH, Kim JH, Wu HG, Rhee CS, Lee CH, et al. Neoadjuvant etoposide, ifosfamide, and cisplatin for the treatment of olfactory neuroblastoma. *Cancer* (2004) 101(10):2257–60. doi: 10.1002/cncr.20648

48. Bartel R, Gonzalez-Compta X, Cisa E, Cruellas F, Torres A, Rovira A, et al. Importance of neoadjuvant chemotherapy in olfactory neuroblastoma treatment: Series report and literature review. *Acta Otorrinolaringol Esp* (2018) 69(4):208–13. doi: 10.1016/j.otorri.2017.07.001

49. Modesto A, Blanchard P, Tao YG, Rives M, Janot F, Serrano E, et al. Multimodal treatment and long-term outcome of patients with esthesioneuroblastoma. *Oral Oncol* (2013) 49(8):830–4. doi: 10.1016/j.oraloncology.2013.04.013

50. Orton A, Boothe D, Evans D, Lloyd S, Monroe MM, Jensen R, et al. Esthesioneuroblastoma: A patterns-of-care and outcomes analysis of the national cancer database. *Neurosurgery* (2018) 83(5):940–7. doi: 10.1093/neuros/nyx535

51. Sun M, Wang K, Qu Y, Zhang J, Zhang S, Chen X, et al. Long-term analysis of multimodality treatment outcomes and prognosis of esthesioneuroblastomas: a single center results of 138 patients. *Radiat Oncol* (2020) 15(1):219. doi: 10.1186/s13014-020-01667-4

52. Xiong L, Zeng XL, Guo CK, Liu AW, Huang L. Optimal treatment and prognostic factors for esthesioneuroblastoma: retrospective analysis of 187 Chinese patients. *BMC Cancer* (2017) 17(1):254. doi: 10.1186/s12885-017-3247-z

53. Cranmer LD, Chau B. Chemotherapy in the management of olfactory neuroblastoma/esthesioneuroblastoma: An analysis of the surveillance, epidemiology, and end results (SEER) 1973-2015 database. *J Clin Oncol* (2019) 37(15_suppl):e17573–3. doi: 10.1200/JCO.2019.37.15_suppl.e17573

54. Porter AB, Bernold DM, Giannini C, Foote RL, Link MJ, Olsen KD, et al. Retrospective review of adjuvant chemotherapy for esthesioneuroblastoma. *J Neurooncol novembre* (2008) 90(2):201–4. doi: 10.1007/s11060-008-9645-y

55. Marinelli JP, Janus JR, Van Gompel JJ, Link MJ, Foote RL, Lohse CM, et al. Esthesioneuroblastoma with distant metastases: Systematic review & meta-analysis. *Head Neck ottobre* (2018) 40(10):2295–303. doi: 10.1002/hed.25209

56. McElroy EA, Buckner JC, Lewis JE. Chemotherapy for advanced esthesioneuroblastoma: the Mayo Clinic experience. *Neurosurgery* (1998) 42 (5):1023–7. doi: 10.1097/00006123-199805000-00040

57. Ni G, Pinheiro-Neto CD, Iyoha E, Van Gompel JJ, Link MJ, Peris-Celda M, et al. Recurrent esthesioneuroblastoma: long-term outcomes of salvage therapy. *Cancers* (2023) 15(5):1506. doi: 10.3390/cancers15051506

58. Van Gompel JJ, Link MJ, Sheehan JP, Xu Z, Mathieu D, Kano H, et al. Radiosurgery is an effective treatment for recurrent esthesioneuroblastoma: A multicenter study. *J Neurol Surg Part B Skull Base* (2014) 75(6):409–14. doi: 10.1055/s-0034-1378151

59. Gay LM, Kim S, Fedorchak K, Kundranda M, Odia Y, Nangia C, et al. Comprehensive genomic profiling of esthesioneuroblastoma reveals additional treatment options. *Oncologist* (2017) 22(7):834–42. doi: 10.1634/theoncologist.2016-0287

60. Topcagic J, Feldman R, Ghazalpour A, Swensen J, Gatalica Z, Vranic S. Comprehensive molecular profiling of advanced/metastatic olfactory neuroblastomas. *PloS One* (2018) 13(1):e0191244. doi: 10.1371/journal.pone.0191244

61. Lazo de la Vega L, McHugh JB, Cani AK, Kunder K, Walocko FM, Liu CJ, et al. Comprehensive molecular profiling of olfactory neuroblastoma identifies potentially targetable FGFR3 amplifications. *Mol Cancer Res MCR* (2017) 15(11):1551–7. doi: 10.1158/1541-7786.MCR-17-0135

62. Gallia GL, Zhang M, Ning Y, Haffner MC, Batista D, Binder ZA, et al. Genomic analysis identifies frequent deletions of Dystrophin in olfactory neuroblastoma. *Nat Commun* (2018) 9:5410. doi: 10.1038/s41467-018-07578-z

63. Preusser M, Hutterer M, Sohm M, Koperek O, Elandt K, Dieckmann K, et al. Disease stabilization of progressive olfactory neuroblastoma (esthesioneuroblastoma) under treatment with sunitinib mesylate. *J Neurooncol* (2010) 97(2):305–8. doi: 10.1007/s11060-009-0027-x

64. Wang L, Ding Y, Wei L, Zhao D, Wang R, Zhang Y, et al. Recurrent olfactory neuroblastoma treated with cetuximab and sunitinib: A case report. *Med (Baltimore)* (2016) 95(18):e3536. doi: 10.1097/MD.0000000000003536

65. Fury MG, Sherman E, Haque S, Korte S, Lisa D, Shen R, et al. A phase I study of daily everolimus plus low-dose weekly cisplatin for patients with advanced solid tumors. *Cancer Chemother Pharmacol* (2012) 69(3):591–8. doi: 10.1007/s00280-011-1734-5

66. Dunbar EM, Pumphrey PK, Bidari S. Unexpectedly durable palliation of metastatic olfactory neuroblastoma using anti-angiogenic therapy with Bevacizumab. *Rare Tumors* (2012) 4(2):e33. doi: 10.4081/rt.2012.e33

67. Spengler M, Wheelden M, Mackley HB, Drabick JJ. Durable major response with pazopanib in recurrent, heavily pretreated metastatic esthesioneuroblastoma harboring a fumarate hydratase mutation. *JCO Precis Oncol* (2021) 5:664–9. doi: 10.1200/PO.20.00486

68. London NR, Rooper LM, Bishop JA, Xu H, Bernhardt LJ, Ishii M, et al. Expression of programmed cell death ligand 1 and associated lymphocyte infiltration in olfactory neuroblastoma. *World Neurosurg* (2020) 135:e187–93. doi: 10.1016/j.wneu.2019.11.112

69. Bossi P, Saba NF, Vermorken JB, Strojan P, Pala L, de Bree R, et al. The role of systemic therapy in the management of sinonasal cancer: A critical review. *Cancer Treat Rev* (2015) 41(10):836–43. doi: 10.1016/j.ctrv.2015.07.004

frontiers | Frontiers in Oncology

TYPE Original Research
PUBLISHED 17 October 2023
DOI 10.3389/fonc.2023.1191399

OPEN ACCESS

EDITED BY
Sharon R. Pine,
University of Colorado Anschutz Medical Campus, United States

REVIEWED BY
Matteo Zoli,
IRCCS Institute of Neurological Sciences of Bologna (ISNB), Italy
Matteo Martinoni,
IRCCS Institute of Neurological Sciences of Bologna (ISNB), Italy

*CORRESPONDENCE
Wei Jin
njneurosurgery@163.com
Huiying Yan
yanhuiying8888@126.com

†These authors have contributed equally to this work

RECEIVED 22 March 2023
ACCEPTED 02 October 2023
PUBLISHED 17 October 2023

CITATION
Yan C, Mao J, Yao C, Liu Y, Jin W and Yan H (2023) Application of endoport-assisted neuroendoscopic techniques in lateral ventricular tumor surgery. *Front. Oncol.* 13:1191399. doi: 10.3389/fonc.2023.1191399

Application of endoport-assisted neuroendoscopic techniques in lateral ventricular tumor surgery

Chaolong Yan[1,2†], Jiannan Mao[1†], Chenbei Yao[1], Yang Liu[1], Wei Jin[1,2*] and Huiying Yan[1*]

[1]Department of Neurosurgery, Nanjing Drum Tower Hospital, Affiliated Hospital of Medical School, Nanjing University, Nanjing, China, [2]Department of Neurosurgery, Nanjing Drum Tower Hospital, Clinical College of Nanjing Medical University, Nanjing, China

Objective: The objective of this study was to investigate the clinical experience and therapeutic efficiency of Endoport-assisted neuroendoscopic surgery for resection of lateral ventricular tumors. The key points and application value of this surgical technique were additionally discussed.

Methods: A retrospective analysis was conducted on the clinical and follow-up data of 16 patients who underwent endoport-assisted neuroendoscopic surgery for lateral ventricular tumors at the Department of Neurosurgery, Nanjing Drum Tower Hospital, the Affiliated Hospital of Nanjing University Medical School, between January 2018 and September 2020. The surgical procedures, complications and outcomes were analyzed.

Results: The study included a total of 16 patients (5 males and 11 females) with lateral ventricular tumors, with a mean age of 43.2 years (18-70 years old). The tumors were distributed as follows: 5 cases involved the body of the lateral ventricle, 3 involved the frontal horn and body, 3 involved the occipital horn, 2 involved the trigone, 2 involved the frontal horn, and 1 case involved the occipital horn and body. Perioperative complications were analyzed, revealing 1 case of intraoperative acute epidural hematoma intraoperative and 2 cases of postoperative obstructive hydrocephalus. All complications were promptly managed. Postoperative MRI revealed that 14 cases (88%) achieved total resection, while 2 cases (12%) achieved subtotal resection. During the follow-up of 6-38 months, no recurrence was observed. The patient diagnosed with glioblastoma died 16 months after surgery (GOS=1), while the remaining patients have successfully resumed to normal daily life with a GOS score of 5.

Conclusion: In conclusion, endoport-assisted neuroendoscopic surgery proved to be a minimally invasive and effective technique for resecting lateral ventricular tumors, with acceptable complications. It effectively utilizes the benefits of close observation, comprehensive exposure, and reduced tissue damage. Therefore, endoport-assisted neuroendoscopic surgery is suitable for the resection of lateral ventricular tumors.

KEYWORDS

endoport, neuroendoscopy, lateral ventricular tumor, surgical treatment, prognosis

Introduction

The lateral ventricle, is a paired C-shaped structure located deep within the cerebral hemispheres (1, 2). Lateral ventricular tumors, accounting for less than 1% of intracranial neoplasms, mostly exhibit slow growth (3, 4). Early diagnosis and complete resection of these tumors hold the potential for clinical cure. Hence, neurosurgeons managing lateral ventricular tumors must strive for maximal tumor resection while minimizing damage to nerves and blood vessels (5).

In recent years, with advancements in surgical techniques and the adoption of minimally invasive approaches, the endoport-assisted neuroendoscopic technique has emerged as a promising method for resecting lateral ventricular tumors (2, 6, 7). Furthermore, the widespread use of neuro-navigation systems and intraoperative electrophysiological monitoring has contributed to overcoming challenges such as endoscopic hemostasis and the protection of functional areas and neural nuclei. These advancements have resulted in improved efficacy of neuroendoscopy in the treatment of lateral ventricular tumors.

Materials and methods

Clinical data collection

A retrospective review was conducted, encompassing clinical and follow-up data from 16 patients who presented with lateral ventricular tumors and subsequently underwent endoport-assisted neuroendoscopic surgery between January 2018 and September 2020 in the department of neurosurgery in Nanjing Drum Tower Hospital, The Affiliated Hospital of Nanjing University Medical School. The research protocol involving human participants was approved by the Ethics Committee at Nanjing Drum Tower Hospital.

Data collection involved a comprehensive assessment of medical records, imaging data, pathological reports, and operation videos for each patient. Demographic information, initial symptoms, tumor location, pathological diagnosis, and the presence of preoperative hydrocephalus were documented. Additionally, complications that occurred during or after operation were carefully recorded for analysis. Follow-up was obtained in the clinic or by telephone and ended in March 2021.

Surgical equipment

All operations were performed using rigid Karl Storz neuroendoscopy with 0° or 30° optics, 150 mm length and 4 mm diameter (Karl Storz, Tuttlingen, Germany). An endoport with a diameter of 21 mm and length of 7 cm (Vycor Medical Inc., Boca Raton, FL, USA) was selected to handle the lesions in our institute. To facilitate the surgery, a pneumatic holding arm (Karl Storz, Tuttlingen, Germany) was utilized to stabilize the neuroendoscopy, while a snake holding arm was employed to secure the endoport. Additionally, conventional craniotomy instruments and neuroendoscopic auxiliary instruments were used during the surgical procedures.

Surgical techniques

The trans-frontal cortical approach to the frontal horns and the body of the lateral ventricle

The trans-frontal cortical approach is an effective surgical route for accessing the frontal horns and bodies of the lateral ventricle, including the anterior part of the third ventricle (Figure 1). It is particularly suitable for resecting tumors mainly limited in the frontal horns or the bodies of the lateral ventricle. The patient was placed in the supine position with the head slightly elevated. The head was turned 30° to the contralateral side and secured with a 3-pin Mayfield head holder. Neuro-navigation based on preoperative magnetic resonance imaging (MRI) was employed to guide the anatomical localization. The insertion point for endoport was approximately 3 cm from the midline and 1 cm in front of the coronal suture (Kocher's point).

Following routine disinfection, a linear incision was made centered on the insertion point. A craniotomy (approximately 3 cm diameter) was performed above the middle frontal gyrus, and the dura was opened with an arc-shaped incision. An ostomy through the middle frontal gyrus was created to insert and secure the endoport using the snake holding arm. Cerebrospinal fluid (CSF) outflow confirmed entry into the lateral ventricle. Tailed cotton strips were used to slowly release CSF while securing a 0° neuro-endoscope into the endoport using the pneumatic holding arm. Gradual identification of the anatomical landmarks of the frontal horn and body of the lateral ventricle was achieved. Under neuroendoscopic visualization, the tumors were carefully observed and removed. An ultrasonic dissector could be utilized for tumors with hard texture. For larger tumors, intratumoral decompression was performed initially to gradually reduce tumor volume. Adjustments in the directions of the endoport and neuro-endoscope may be necessary to identify the tumor boundary and achieve complete tumor removal.

Following tumor resection, bipolar coagulation and hemostatic materials were employed to ensure thorough hemostasis. Special care was taken to protect the surrounding brain tissue and vasculature, particularly the lateral wall of the lateral ventricle, where important nervous nuclei such as the thalamus and caudate nucleus, as well as the colliculus veins, are located. Damage to these structures can significantly impact patient prognosis. Finally, a drainage tube was inserted into the ventricle, and the endoport was removed under endoscopic visualization. Postoperative close monitoring is crucial to detect and manage potential complications.

The transtemporal approach to the trigone of the lateral ventricle

The trigone, located at the interface between the body of the lateral ventricle and the occipital and temporal horns (Figure 2), can be accessed directly using the transtemporal approach. This approach offers a short trajectory and provides direct access to the temporal horn and trigone of the lateral ventricle. It is particularly suitable for removing tumors located in the trigone of the lateral ventricle. The patient was positioned in the lateral decubitus position, with the head fixed using a 3-pin Mayfield

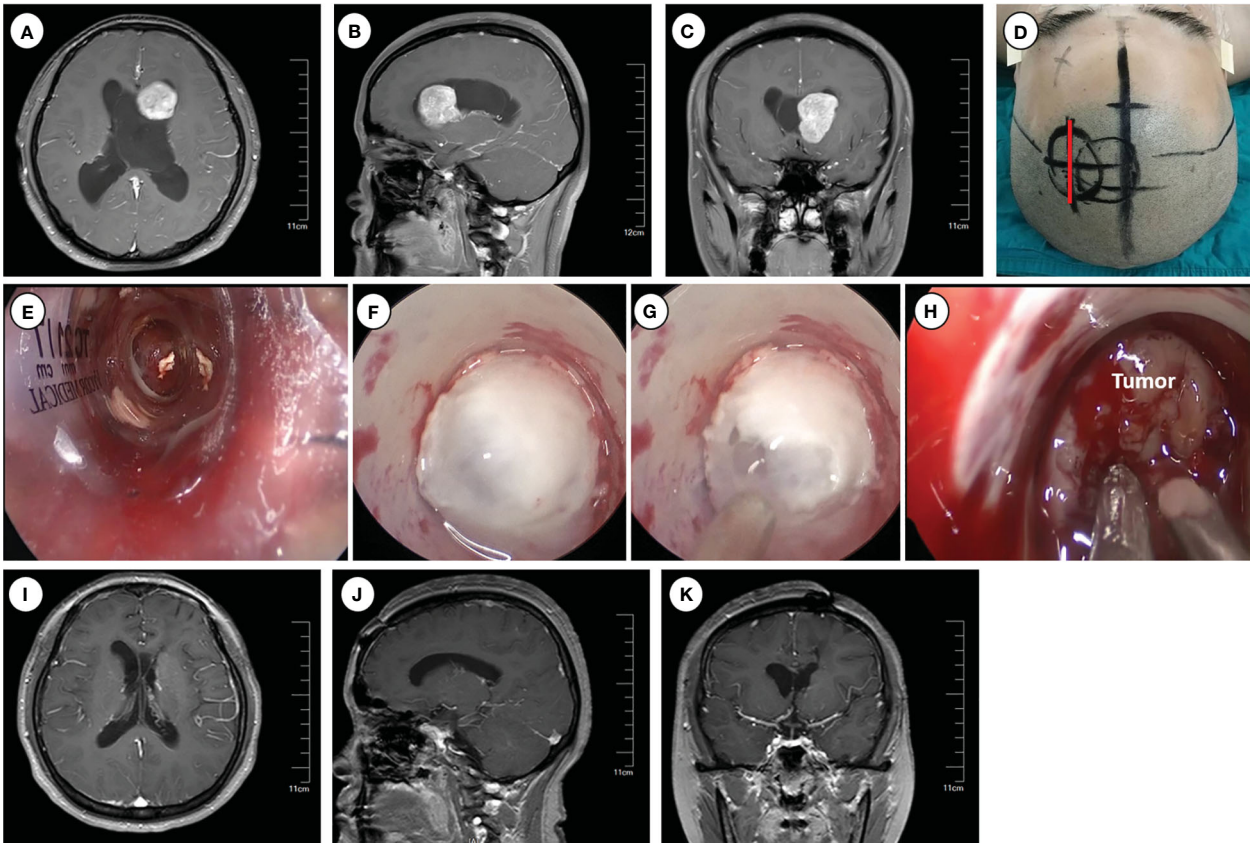

FIGURE 1
Operative approaches for the frontal horns and the body of the lateral ventricle. **(A–C)** Axial, sagittal and cronal images of preoperative enhanced magnetic resonance imaging. **(D)** Schematic diagram of surgical incision (marked with red line). **(E–H)** Intraoperative pictures for inserting Endoport **(E)**, ventriculostomy to release CSF **(F–G)**, and tumor resection **(H)**. **(I–K)** Axial, sagittal and coronal images of enhanced magnetic resonance imaging at 6 months postoperative.

head holder and rotated to the contralateral side to optimize the operative field by positioning the zygomatic process uppermost. Neuro-navigation based on preoperative magnetic resonance imaging (MRI) was employed for precise anatomical localization. The insertion point for endoport was approximately 4.5 cm above and behind the external auditory canal.

Following routine disinfection, a linear incision was made centered on the insertion point. The dura was then opened with an arc-shaped incision. The ostomy through the parietal lobe was created to insert and secure the Endoport using the snake holding arm. Once cerebrospinal fluid (CSF) outflow was observed, entry into the trigone of the lateral ventricle was confirmed. Tailed cotton strips were used to slowly release CSF while fixing a 0° neuroendoscopy into the endoport using the pneumatic holding arm. The tumors were carefully observed and removed under neuroendoscopic visualization. The subsequent tumor removal procedures were the same as described previously.

Clinical efficacy evaluation

All cases underwent a computed tomography (CT) scan within 24 hours post-surgery to rule out postoperative complications such as hemorrhage or hydrocephalus. Plain and enhanced magnetic resonance imaging (MRI) scans three days post-surgery, were performed to assess the extent of surgical resection. The need for further radiotherapy or chemotherapy was determined based on postoperative pathological analysis. Subsequently, follow-ups were conducted through outpatient visits or regular telephone interviews at 1, 3, and 6 months postoperatively, followed by annual follow-ups thereafter. During these follow-ups, tumor recurrence and the patients' ability to carry out daily activities were assessed and recorded. Clinical outcomes were evaluated with the Glasgow Outcome Scale (GOS): a score of GOS $\geq$ 4 indicates favorable prognosis, while a score of GOS < 4 indicates poor prognosis.

Results

Clinical features and histopathological types of patients with lateral ventricular tumors

A total of 16 patients (5 males, 11 females) who suffered from lateral ventricle tumors and underwent endoport-assisted neuroendoscopic surgery were included in this study. The mean

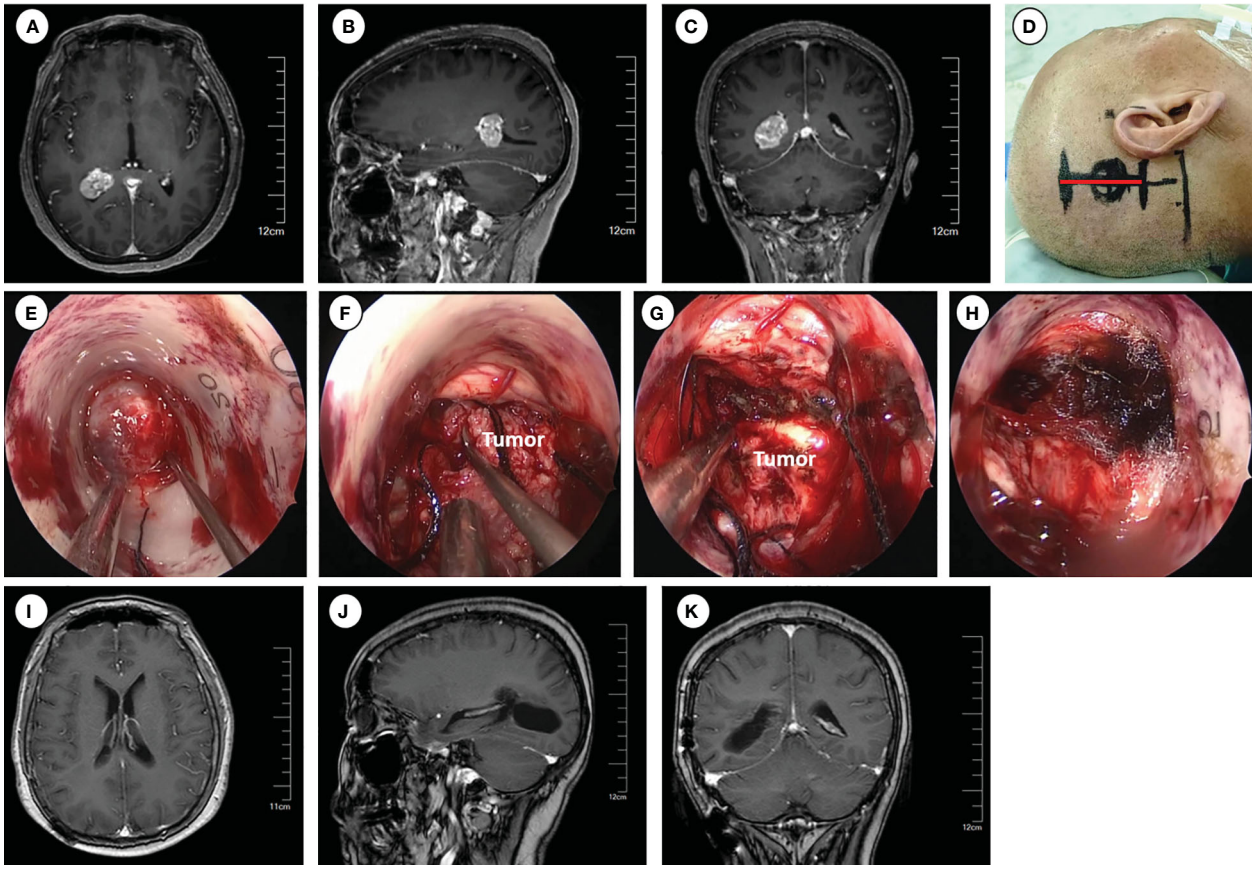

FIGURE 2
Operative approaches for the trigone of the lateral ventricle. **(A–C)** Axial, sagittal and coronal images of preoperative enhanced magnetic resonance imaging. **(D)** Schematic diagram of surgical incision (marked with red line). **(E–H)** Intraoperative pictures for exposing the tumor **(E)**, tumor removal **(F–G)**, and hemostasis of the surgical field **(H)**. **(I–K)** Axial, sagittal and coronal images of enhanced magnetic resonance imaging at 6 months postoperative.

age of the patients was 43.2 years, ranging from 18 to 70 years. Upon admission, the patients presented with various initial symptoms, including headache (8 cases), dizziness (3 cases), unconsciousness (1 cases), facial numbness (1 cases) and no apparent symptom (3 cases). The distribution of tumor locations among the cases was as follows: 7 cases in the left and 9 cases in the right, involved the lateral ventricle body (5 cases), frontal horn and body (3 cases), occipital horn (3 cases), trigone (2 cases), frontal horn (2 cases) and occipital horn and body (1 case). Additionally, 9 cases (56.25%) presented with preoperative obstructive hydrocephalus.

All the tumors were successfully removed using endoport-assisted neuroendoscopic surgery, and all the resected specimens were sent to the neuropathology department for the detailed histopathological examination. The postoperative histopathological results were as follows: central neurocytoma (WHO II) in 5 cases, meningioma (WHO I) in 5 cases, diffuse astrocytoma (WHO II) in 2 cases, astrocytoma (WHO I) in 1 case, glioblastoma (WHO IV) in 1 case, ependymoma (WHO II) in 1 case, and colloid cyst in 1 case. A summary of the clinical features and histopathological types of the patients is presented in Table 1.

Perioperative complications

Among the patients, a total of three cases experienced complications either during or after the surgery: 1 case occurred intraoperative and 2 cases occurred postoperative. During the operation, one patient developed frontal acute epidural hematoma, which was promptly addressed, without long-term adverse consequences. Postoperatively, two patients developed obstructive hydrocephalus following operation. One case was successfully alleviated through external ventricular drainage, while the other case required the implementation of a ventriculoperitoneal shunt to achieve relief. Otherwise, one patient experienced transient hemiplegia, which improved after three weeks of active treatment.

Clinical prognosis

All patients underwent regular follow-up at the outpatient clinic after discharge. The average duration of follow-up was 19.56 months, ranging from 6 to 38 months. The follow-up results revealed that 14 cases (88%) achieved total resection of tumors

TABLE 1 Clinical features, histopathological types and follow-up results of patients with lateral ventricular tumors.

No.	Gender	Age	Initial symptom	Location	Side	Hydrocephalus	Histopathology*	Surgical complication	Resection	Follow-up (Months)	GOS score
01	Female	25	Headache	Frontal horn, body	Right	Yes	Central neurocytoma (WHO II)	No	Total	38	5
02	Male	31	Asymptom	Frontal horn	Left	No	Central neurocytoma (WHO II)	No	Total	36	5
03	Female	23	Headache	Body	Right	Yes	Central neurocytoma (WHO II)	No	Total	36	5
04	Female	18	Headache	Body	Left	Yes	Astrocytoma (WHO I)	Acute epidural hematoma	Total	35	5
05	Female	37	Headache	Frontal horn, body	Left	Yes	Glioblastoma (WHO IV)	Hydrocephalus, external ventricular drainage	Subtotal	16	1
06	Male	70	Unconsciousness	Frontal horn, body	Left	Yes	Diffuse astrocytoma (WHO II)	Transient hemiplegia, improved after 3 weeks	Subtotal	26	5
07	Female	60	Dizziness	Trigone	Right	No	Meningioma (WHO I)	No	Total	23	5
08	Female	65	Dizziness	Trigone	Left	No	Ependymoma (WHO II)	No	Total	19	5
09	Male	64	Facial numbness	Body	Right	No	Diffuse astrocytoma (WHO II)	No	Total	18	5
10	Male	59	Asymptom	Frontal horn	Right	No	Colloid cyst	No	Total	18	5
11	Female	36	Headache	Occipital horn	Right	Yes	Meningioma (WHO I)	No	Total	9	5
12	Female	20	Headache	Occipital horn, body	Right	No	Meningioma (WHO I)	No	Total	7	5
13	Female	62	Headache	Occipital horn	Right	Yes	Meningioma (WHO I)	No	Total	7	5
14	Female	25	Headache	Body	Left	Yes	Central neurocytoma (WHO II)	No	Total	6	5
15	Male	34	Dizziness	Body	Right	Yes	Central neurocytoma (WHO II)	Hydrocephalus, ventriculo-peritoneal shunt	Total	8	5
16	Female	63	Asymptom	Occipital horn	Left	No	Meningioma (WHO I)	No	Total	11	5

*2016 WHO Classification of CNS tumors.

without residual or recurrence during the follow-up period. In the remaining 2 cases (12%), the resection was considered subtotal. Unfortunately, one of these cases was pathologically diagnosed as glioblastoma (WHO IV) and regrettably passed away 16 months after the operation. The other case was diagnosed with diffuse astrocytoma (WHO II) and is currently undergoing long-term survival with the tumor under standardized treatment in the field of oncology. Based on the long-term follow-up regarding patients' daily living activities, 15 cases exhibited a favorable prognosis, as indicated by a Glasgow Outcome Scale (GOS) score of 5. Only one case diagnosed with glioblastoma had a poor prognosis, with a GOS score of 1 (Table 1).

Discussion

The occurrence of mass lesions in the lateral ventricle is relatively rare, but it poses significant technical challenges due

to its deep location and proximity to vital anatomical structures (8). Lateral ventricular tumors are typically slow-growing and often diagnosed until they reach a large size or cause obstructive hydrocephalus (2). Surgical removal remains the preferred treatment method for these tumors due to the lack of effective drug treatments, and complete surgical resection can lead to a favorable prognosis (9, 10). Thus, surgeons must carefully consider various factors when selecting the appropriate surgical approach for each patient, including achieving effective and complete tumor resection from optimal angles, minimizing disruption and retraction of normal brain tissues, and early exposure of vital anatomical structures. In our study, we performed 16 cases of lateral ventricular tumor resection using endoport-assisted neuroendoscopic surgery. The total resection rate was 88%, which was similar to previous literature reports (Table 2) (11–16). There has been no case of recurrence in the follow-up period.

Application of endoscope in intraventricular tumor surgery

Currently, surgical resection remains the primary treatment method for lateral ventricular tumors. The traditional surgical

TABLE 2 List of Publications Reporting Resection of Lateral Ventricular Tumors with or without Neuroendoscopy.

Reference	Number of tumors	Population (Adult/ Pediatric)	Surgical methods	Gross-Total Resection (%)	Histology	Complications	Recurrent (%)
Vincenzo et al., 2005 (11)	72	Both	Without endoscopy	82% (59/72)	Anaplastic astrocytoma, glioblastoma, meningioma, ependymoma, pilocytic astrocytoma, SEGA, subependymoma, central neurocytoma, choroid plexus papilloma, choroid plexus carcinoma, choroid plexus cysts, ganglioglioma, gangliogliomeurocytoma, PNET, metastases	27.8% (20/72, 4 deep venous thrombosis, 2 respiratory distress, 3 hydrocephalus, 2 extradural hematoma, 5 small intracerebral hematoma, 4 subdural hygroma)	N/A
Jo et al., 2011 (12)	10	Adult	Endoscopy for excision	50% (5/10)	Cavernous angioma, metastasis, meningioma, paragonimus westermani, anaplastic oligodendroglioma, central neurocytoma, brain abscess, glioblastoma	N/A	N/A
Eveline et al., 2016 (13)	12	Pediatric	Endoscopy for excision	92% (11/12)	SEGA, anaplastic ependymoma, neuroepithelial tumor, ependymoma, NGGCT and pilocytic astrocytoma	8.3% (1/12, 1 ICP transitory increase)	2/12 (17%)
Chandrashekhar et al., 2021 (14)	7	N/A	Endoscopy for excision	N/A	Colloid cysts, low-grade glioma, neurocysticercosis	N/A	N/A
	31	N/A	Endoscopy-assisted excision	N/A	Colloid cysts, neurocytomas, and epidermoid cysts	N/A	N/A
Xie et al., 2021 (15)	7	Both	Endoscopy for excision	100%	SEGA, central neuroblastoma, central neuroblastoma, ependymoma, meningioma and metastatic adenocarcinoma	28.6% (2/7, 1 hematoma, 1 visual defect)	0
Suresh et al., 2023 (16)	26	Both	Endoscopy for excision	69% (18/26)	Central neurocytoma, high −grade glioma, ependymoma, colloid cysts, pilocytic astrocytoma, SEGA, PNET	30% (8/28, 4 seizures, 2 transient hemiparesis, 2 visual impairment, 2 mild disturbance in memory, 2 subdural hygroma)	N/A
Current study	16	Adult	Endoscopy for excision	88% (14/16)	central neurocytoma, meningioma, diffuse astrocytoma, astrocytoma, glioblastoma, ependymoma, and colloid cyst	18.8 % (3/16, 1 hematoma, 2 obstructive hydrocephalus)	0

N/A, not applicable; SEGA, subependymal giant cell astrocytoma; NGGCT, nongerminomatous germ cell tumors; PNET, primitive neuroectodermal tumor.

strategy primarily involves tumor removal by using a microscope through craniotomy. In the majority of cases, cortical incisions or corpus callosotomy are required during the surgery, which inevitably results in damage to normal brain tissue. Moreover, due to the limited field of view provided by the tubular vision of the microscope and the deep location of the tumor, larger incisions are often required to achieve better tumor visualization. In recent years, with advancements in surgical techniques and the evolving concept of minimally invasive surgery, the use of endoscopes in brain surgery increased greatly, from simple fenestrations for obstructive hydrocephalus and arachnoid cysts initially, to biopsy even removing complex tumors from the deeper areas of the brain gradually (5, 16–20). Compared to traditional microscopic surgery, a rigid endoscope allows for access into ventricles, providing superior magnification and illumination for enhanced inspection of regional anatomy and precise lesion dissection (12). Moreover, combined with angle endoscopy enables close observation and access of the hidden angles inside the ventricles to coagulate or clip of vascular pedicle of the tumor (21). The extensive observation range of neuroendoscopy significantly reduces the need for brain tissue traction compared to operating under a microscope, thus better protecting surrounding normal tissue. However, the endoscopic surgery also meets significant limitations, such as the thermal damage of endoscope itself, the operational damage to the blind areas behind the endoscope's field of view and the limitations of bimanual microsurgical techniques for tumor resection or hemostasis (16).

Application of Endoport in intraventricular tumors

Endoport, as a tubular retractor, can effectively help overcome the challenges and fully utilize the advantages of endoscopy. Endoport isolates the brain tissue outside the tubular retractor, providing a safe pathway for surgical instruments inserted freely under direction vision and preventing any damage to the surgical path caused by surgical procedures (7, 22). Moreover, compared with traditional retractor-assisted microsurgery, its tubular structure reduces the risk of sharp damages of sheet retractors caused by traction on brain tissue. The tubular shape of the retractor allows for the even distribution of pressure on the retracted brain tissue, minimizing damage to the greatest extent possible (20). Additionally, endoport allows for movement in multiple angles, enabling full exposure of the tumor without increasing tension on brain tissue. This not only improves the rate of complete tumor resection but also provides better protection for surrounding tissues (12, 22, 23). A study has reported that patients who underwent microsurgical procedures via a trans-cortical approach had a postoperative seizure incidence of 8% and a postoperative paralysis incidence of 12% (24). These complications were largely related to excessive traction on the functional cortical areas. In contrast, none of the cases in our group experienced postoperative complications such as seizures or persistent hemiplegia.

Application of neuro-navigation in tumors location and inserted position selection

The key to the successful endoscopic tumor surgery lies in the precise localization of the tumor and the selection of the puncture point and direction (16). Thus, the precise location of the tumors on MRI preoperative and intraoperative neuro-navigation are of great importance for brain-deep tumors localization. In a survey of neurosurgeons with experience in endoscopic surgery, the utilization rate of neuro-navigation in the biopsy and resection of intraventricular tumors was found to be 62.4% (25). In our sixteen cases, preoperative MRI and intraoperative neuro-navigation were used in all cases. Besides these, the intraoperative endoscopic ultrasonography and MRI were also reported to be helpful in real-time tumor positioning, facilitating complete tumor removal and protection of nearby structures (26).

The inserted point of Endoport lies on the position of lateral ventricular tumors. For the tumors localized in the frontal horns and the body of the lateral ventricle, we selected trans-frontal cortical approach (middle frontal gyrus). This approach facilitates the exposure of the anterior choroidal artery and is suitable for the resection of tumors in the anterior part of the lateral ventricle. For the tumors localized in the trigone of the lateral ventricle, we selected transtemporal approach. This approach provides a short trajectory and a direct access to the temporal horn and trigone of the lateral ventricle. In our 16 cases, the total resection rate of tumors was 88% through these approaches. Two subtotal resected tumors were glioblastoma and diffused astrocytoma separately. However, due to the risk of damaging the fiber tracts, there is currently ongoing debate regarding the choice between the transcortical and sulcal approaches. Further research is needed to establish reliable conclusions.

Keep the cerebrospinal fluid circulation unobstructed

Preoperative CSF circulation disturbance was common in patients with lateral ventricular tumors and it was found in 9 cases of our 16 cases. For cases of obstructive hydrocephalus due to the blockage of the foramen of Monro found intraoperative, simultaneous ventriculostomy was performed to establish drainage. Operations within ventricles commonly lead to loss of CSF and collapse of brain tissue (15). In our study, we encountered a case of acute epidural hematoma, which was considered to be caused by rapid collapse of brain tissue resulting from excessive release of cerebrospinal fluid. Thus, the slow release of CSF intraoperatively was necessary to prevent rapid brain tissue collapse and the potential development of epidural hematoma (27, 28). Early postoperative CT scan also acids in early diagnosis. Besides these, it was essential to ensure the patency of the interventricular foramen and avoid blockage by blood clots during surgery. Before completing the procedure, warm saline was perfused to inflate the collapsed brain tissue and reduce intracranial air accumulation. Otherwise, if postoperative external ventricular drainage necessary, the flow velocity and volume needed to be close controlled to prevent the occurrence of ventricular walls adhesion or isolated ventricle (16).

Postoperative complications and comprehensive treatment

Reported complication rates for resection of intraventricular tumors are between 0% and 30%, including hemorrhage, hydrocephalus, subdural hygroma, deep venous thrombosis, hemiparesis and neurological deficit (Table 2) (11–16, 29–32). In our study, 1 case experienced acute epidural hematoma, which was considered due to the following reasons (1): young patient, no adhesion between the pia mater and the dura mater (2), rapid collapse of brain tissue resulting from excessive release of cerebrospinal fluid. Thus, slow intraoperative CSF release is necessary to prevent rapid brain tissue collapse. When Endoport near the ventricular wall, using an electrical coagulation to create a small opening or a ventricular puncture needle could be helpful to release CSF slowly. Besides, tailed cotton strips could be used to plug the fistula to slow down the CSF release if CSF still flows out too quickly. Another two patients developed obstructive hydrocephalus following operation. After corresponding treatment, no permanent sequelae were left.

Additionally, specific pathological types may require further standardized treatment even after discharge. Among the cases in this group, a patient diagnosed with glioblastoma survived for 16 months after the operation, while another patient with diffuse astroglioma achieved long-term survival despite residual tumor. As both tumors originated in the thalamus, preserving the functionality of the structure as much as possible during the surgery led to incomplete tumor resection according to the standard guidelines. Comprehensive treatment is needed for every patient according to separate pathologic diagnosis.

Limitations

The number of cases in this study is relatively insufficient. There is an inherent bias in the follow-up time, which still needs to be extended. Further studies and long-term follow-up are necessary to validate the long-term therapeutic efficiency and outcomes of this surgical method. Besides, We have limited experience in utilizing other endoscopic-assisted techniques, such as CUSA and LASER. Acquiring more experience in these techniques would undoubtedly contribute to broadening the scope of indications for endoscopic resection under our care.

Conclusion

Overall, Endoport-assisted neuroendoscopic techniques offer significant advantages in managing lateral ventricular tumors. It effectively utilizes the benefits of close observation, comprehensive exposure, and reduced tissue damage. Therefore, Endoport-assisted neuroendoscopic surgery is suitable for the resection of lateral ventricular tumors. This technique is worthy to be popularized in clinical practice.

Data availability statement

The original contributions presented in the study are included in the article/supplementary material. Further inquiries can be directed to the corresponding authors.

Ethics statement

This study was conducted retrospectively from data obtained for clinical purposes. All procedures performed in studies involving human participants were approved by ethics committee at Nanjing Drum Tower Hospital and in accordance with the ethical standards of the institutional and/or national research committee and with the 1964 Helsinki declaration and its later amendments or comparable ethical standards. Informed consent was obtained from all individual participants and their close relatives included in the study. Informed consent was received from participant or legal guardian (in case of patient less than 18 years of age) for participation as well as publication of their data and photographs.

Author contributions

All authors contributed to the study conception and design. Material preparation, data collection and analysis were performed by CLY and JM. The first draft of the manuscript was written by CLY. JM, CBY and YL participated the surgery and handled the pictures. WJ and HY commented and corrected on previous versions of the manuscript. All authors read and approved the final manuscript. All authors contributed to the article and approved the submitted version.

Acknowledgments

We would like to thank Pro. Chunhua Hang for technical guidance.

Conflict of interest

The authors declare that the research was conducted in the absence of any commercial or financial relationships that could be construed as a potential conflict of interest.

Publisher's note

References

1. Deopujari CE, Karmarkar VS, Shaikh ST, Gadgil US. Developing a dynamic simulator for endoscopic intraventricular surgeries. *Childs Nerv Syst* (2019) 35(4):621–7. doi: 10.1007/s00381-019-04087-2

2. Souweidane MM. Endoscopic surgery for intraventricular brain tumors in patients without hydrocephalus. *Neurosurgery* (2008) 62(6 Suppl 3):1042–8. doi: 10.1227/01.NEU.0000333769.51069.80

3. Sayyahmelli S, Baran O, Ugurlar D, Kemerdere R, Antar V, Tanriverdi T. Intracranial intraventricular tumors: long-term surgical outcome of 25 patients. *Turk J Med Sci* (2017) 47(1):76–84. doi: 10.3906/sag-1509-119

4. Ellenbogen RG. Transcortical surgery for lateral ventricular tumors. *Neurosurg Focus* (2001) 10(6):E2. doi: 10.3171/foc.2001.10.6.3

5. Stachura K, Grzywna E, Krzyzewski RM, Kwinta BM, Adamek D, Moskala MM. Endoscopic biopsy of intra- and paraventricular brain tumors. *Wideochir Inne Tech Maloinwazyjne* (2019) 14(1):107–13. doi: 10.5114/wiitm.2018.76117

6. Cappabianca P, Cinalli G, Gangemi M, Brunori A, Cavallo LM, de Divitiis E, et al. Application of neuroendoscopy to intraventricular lesions. *Neurosurgery* (2008) 62 Suppl 2:575–97; discussion 97-8. doi: 10.1227/01.neu.0000316262.74843.dd

7. Moosa S, Ding D, Mastorakos P, Sheehan JP, Liu KC, Starke RM. Endoport-assisted surgical evacuation of a deep-seated cerebral abscess. *J Clin Neurosci* (2018) 53:269–72. doi: 10.1016/j.jocn.2018.04.028

8. Ahmad F, Sandberg DI. Endoscopic management of intraventricular brain tumors in pediatric patients: a review of indications, techniques, and outcomes. *J Child Neurol* (2010) 25(3):359–67. doi: 10.1177/0883073809340318

9. Souweidane MM. Endoscopic management of pediatric brain tumors. *Neurosurg Focus* (2005) 18(6A):E1. doi: 10.3171/foc.2005.18.6.2

10. Tirado-Caballero J, Rivero-Garvía M, González-Pombo M, Cárdenas-Ruiz-Valdepeñas E, Kaen A, Márquez-Rivas J. Fully Endoscopic Transforaminal-Transchoroidal Approach for Tectal Area Tumor Removal. *World neurosurgery* (2020) 137:164–72. doi: 10.1016/j.wneu.2019.12.106

11. D'Angelo VA, Galarza M, Catapano D, Monte V, Bisceglia M, Carosi I. Lateral ventricle tumors: surgical strategies according to tumor origin and development–a series of 72 cases. *Neurosurgery* (2005) 56(1 Suppl):36–45; discussion 36-45. doi: 10.1227/01.neu.0000144778.37256.ef

12. Jo K-W, Shin HJ, Nam D-H, Lee J-I, Park K, Kim JH, et al. Efficacy of endoport-guided endoscopic resection for deep-seated brain lesions. *Neurosurg Rev* (2011) 34 (4):457–63. doi: 10.1007/s10143-011-0319-4

13. Hidalgo ET, Ali A, Weiner HL, Harter DH. Resection of Intraventricular Tumors in Children by Purely Endoscopic Means. *World Neurosurg* (2016) 87:372–80. doi: 10.1016/j.wneu.2015.11.052

14. Deopujari CE, Karmarkar VS, Shaikh ST, Mohanty CB, Sharma V, Tadghare J, et al. Neuroendoscopy in the Surgical Management of Lateral and Third Ventricular Tumors: Looking Beyond Microneurosurgery. *Neurol India* (2021) 69(6):1571–8. doi: 10.4103/0028-3886.333458

15. Xie S, Xu L, Wang K, Sun FJ, Xie MX, Wang P, et al. Endoport-assisted Neuroendoscopic Techniques Used in the Resection of Intraventricular Lesions. *Turk Neurosurg* (2021). doi: 10.5137/1019-5149.JTN.32824-20.5

16. Sankhla SK, Warade A, Khan GM. Endoport-Assisted Endoscopic Surgery for Removal of Lateral Ventricular Tumors: Our Experience and Review of the Literature. *Neurol India* (2023) 71(1):99–106. doi: 10.4103/0028-3886.370438

17. Guiot J, Rougerie J, Fourestier M, Fournier A, Comoy C, Vulmiere J, et al. [Intracranial endoscopic explorations. *Presse Med (1893)* (1963) 71:1225–8.

18. Hsu W, Li KW, Bookland M, Jallo GI. Keyhole to the brain: Walter Dandy and neuroendoscopy. *J Neurosurg Pediatr* (2009) 3(5):439–42. doi: 10.3171/2009.1.PEDS08342

19. Apuzzo ML, Heifetz MD, Weiss MH, Kurze T. Neurosurgical endoscopy using the side-viewing telescope. *J Neurosurg* (1977) 46(3):398–400. doi: 10.3171/jns.1977.46.3.0398

20. Shapiro SZ, Sabacinski KA, Mansour SA, Echeverry NB, Shah SS, Stein AA, et al. Use of Vycor Tubular Retractors in the Management of Deep Brain Lesions: A Review of Current Studies. *World Neurosurgery* (2020) 133:283–90. doi: 10.1016/j.wneu.2019.08.217

21. Gaab MR, Schroeder HW. Neuroendoscopic approach to intraventricular lesions. *Neurosurgical Focus* (1999) 6(4):e5. doi: 10.3171/foc.1999.6.4.8

22. Ding D, Starke RM, Crowley RW, Liu KC. Endoport-assisted microsurgical resection of cerebral cavernous malformations. *J Clin Neurosci* (2015) 22(6):1025–9. doi: 10.1016/j.jocn.2015.01.004

23. Przybylowski CJ, Ding D, Starke RM, Webster Crowley R, Liu KC. Endoport-assisted surgery for the management of spontaneous intracerebral hemorrhage. *J Clin Neurosci* (2015) 22(11):1727–32. doi: 10.1016/j.jocn.2015.05.015

24. Milligan BD, Meyer FB. Morbidity of transcallosal and transcortical approaches to lesions in and around the lateral and third ventricles: a single-institution experience. *Neurosurgery* (2010) 67(6):1483–96. doi: 10.1227/NEU.0b013e3181f7eb68

25. Esposito F, Di Rocco F, Zada G, Cinalli G, Schroeder HWS, Mallucci C, et al. Intraventricular and Skull Base Neuroendoscopy in 2012: A Global Survey of Usage Patterns and the Role of Intraoperative Neuronavigation. *World Neurosurgery* (2013) 80(6):709–16. doi: 10.1016/j.wneu.2013.05.011

26. Motegi H, Kobayashi H, Terasaka S, Yamaguchi S, Ishi Y, Ito Y, et al. Application of endoscopic ultrasonography to intraventricular lesions. *Acta Neurochir (Wien)* (2016) 158(1):87–92. doi: 10.1007/s00701-015-2617-z

27. Abraham AP, Moorthy RK, Jeyaseelan L, Rajshekhar V. Postoperative intraventricular blood: a new modifiable risk factor for early postoperative symptomatic hydrocephalus in children with posterior fossa tumors. *Childs Nerv Syst* (2019) 35(7):1137–46. doi: 10.1007/s00381-019-04195-z

28. Torres-Corzo J, Vinas-Rios JM, Viana Rojas JA, Cervantes D, Sánchez-Aguilar M, Chalita-Williams JC, et al. Endoscopic transventricular exploration with biopsy of the basal cisterns and the role of endoscopic third ventriculostomy in patients suffering with basal cistern meningitis and consecutive hydrocephalus. *Neurol Res* (2016) 38 (7):593–9. doi: 10.1080/01616412.2016.1190120

29. Souweidane MM, Luther N. Endoscopic resection of solid intraventricular brain tumors. *J Neurosurg* (2006) 105(2):271–8. doi: 10.3171/jns.2006.105.2.271

30. Oertel JMK, Baldauf J, Schroeder HWS, Gaab MR. Endoscopic options in children: experience with 134 procedures. *J Neurosurg Pediatr* (2009) 3(2):81–9. doi: 10.3171/2008.11.PEDS0887

31. Cinalli G, Spennato P, Ruggiero C, Aliberti F, Trischitta V, Buonocore MC, et al. Complications following endoscopic intracranial procedures in children. *Childs Nerv Syst* (2007) 23(6):633–44. doi: 10.1007/s00381-007-0333-6

32. Barber SM, Rangel-Castilla L, Baskin D. Neuroendoscopic resection of intraventricular tumors: a systematic outcomes analysis. *Minim Invasive Surg* (2013) 2013:898753. doi: 10.1155/2013/898753

Frontiers in Oncology

Advances knowledge of carcinogenesis and tumor progression for better treatment and management

The third most-cited oncology journal, which highlights research in carcinogenesis and tumor progression, bridging the gap between basic research and applications to imrpove diagnosis, therapeutics and management strategies.

Discover the latest Research Topics

See more →

Frontiers

Avenue du Tribunal-Fédéral 34
1005 Lausanne, Switzerland
frontiersin.org

Contact us

+41 (0)21 510 17 00
frontiersin.org/about/contact